MAX-PLANCK-INSTITUT FÜR KOHLENFORSCHUNG

technische universität dortmund

Asymmetric Nickel-Catalyzed Coupling Reactions of Electrophiles and 1,3-Dienes: Inter- and Intramolecular Approaches

Dissertation

Zur Erlangung des akademischen Grades eines

Doktors der Naturwissenschaften

(Dr. rer. nat.)

der Fakultät für Chemie und Chemische Biologie

der Technischen Universität Dortmund

vorgelegt von

Thilo Bender

geboren am 27.09.1996 in Speyer

Mülheim an der Ruhr, August 2026

Eidesstattliche Versicherung (Affidavit)

Bender, Thilo

Name, Vorname
(Surname, first name)

Matrikel-Nr.
(Enrolment number)

Belehrung:

Wer vorsätzlich gegen eine die Täuschung über Prüfungsleistungen betreffende Regelung einer Hochschulprüfungsordnung verstößt, handelt ordnungswidrig. Die Ordnungswidrigkeit kann mit einer Geldbuße von bis zu 50.000,00 € geahndet werden. Zuständige Verwaltungsbehörde für die Verfolgung und Ahndung von Ordnungswidrigkeiten ist der Kanzler/die Kanzlerin der Technischen Universität Dortmund. Im Falle eines mehrfachen oder sonstigen schwerwiegenden Täuschungsversuches kann der Prüfling zudem exmatrikuliert werden, § 63 Abs. 5 Hochschulgesetz NRW.

Die Abgabe einer falschen Versicherung an Eides statt ist strafbar.

Wer vorsätzlich eine falsche Versicherung an Eides statt abgibt, kann mit einer Freiheitsstrafe bis zu drei Jahren oder mit Geldstrafe bestraft werden, § 156 StGB. Die fahrlässige Abgabe einer falschen Versicherung an Eides statt kann mit einer Freiheitsstrafe bis zu einem Jahr oder Geldstrafe bestraft werden, § 161 StGB.

Die oben stehende Belehrung habe ich zur Kenntnis genommen:

Official notification:

Any person who intentionally breaches any regulation of university examination regulations relating to deception in examination performance is acting improperly. This offence can be punished with a fine of up to EUR 50,000.00. The competent administrative authority for the pursuit and prosecution of offences of this type is the chancellor of the TU Dortmund University. In the case of multiple or other serious attempts at deception, the candidate can also be unenrolled, Section 63, paragraph 5 of the Universities Act of North Rhine-Westphalia.

The submission of a false affidavit is punishable.

Any person who intentionally submits a false affidavit can be punished with a prison sentence of up to three years or a fine, Section 156 of the Criminal Code. The negligent submission of a false affidavit can be punished with a prison sentence of up to one year or a fine, Section 161 of the Criminal Code.

I have taken note of the above official notification.

Ort, Datum
(Place, date)

Unterschrift
(Signature)

Titel der Dissertation:
(Title of the thesis):

Asymmetric Nickel-Catalyzed Coupling Reactions of Electrophiles and 1,3-Dienes:

Inter- and Intramolecular Approaches

Ich versichere hiermit an Eides statt, dass ich die vorliegende Dissertation mit dem Titel selbstständig und ohne unzulässige fremde Hilfe angefertigt habe. Ich habe keine anderen als die angegebenen Quellen und Hilfsmittel benutzt sowie wörtliche und sinngemäße Zitate kenntlich gemacht.
Die Arbeit hat in gegenwärtiger oder in einer anderen Fassung weder der TU Dortmund noch einer anderen Hochschule im Zusammenhang mit einer staatlichen oder akademischen Prüfung vorgelegen.

I hereby swear that I have completed the present dissertation independently and without inadmissible external support. I have not used any sources or tools other than those indicated and have identified literal and analogous quotations.

The thesis in its current version or another version has not been presented to the TU Dortmund University or another university in connection with a state or academic examination.*

*Please be aware that solely the German version of the affidavit ("Eidesstattliche Versicherung") for the PhD thesis is the official and legally binding version.

Ort, Datum
(Place, date)

Unterschrift
(Signature)

1. Berichterstatter: Prof. Dr. Alois Fürstner

2. Berichterstatter: Prof. Dr. Martin Hiersemann

Die vorliegende Arbeit entstand unter der Anleitung von Prof. Dr. Alois Fürstner in der Zeit von Juli 2022 bis August 2026 am Max-Planck-Institut für Kohlenforschung in Mülheim an der Ruhr. Teile dieser Arbeit wurden bereits veröffentlicht:

T. Bender, A. Fürstner, *J. Am. Chem. Soc.* **2024**, *146*, *49*, 33295–33301.

Die praktischen Arbeiten erfolgten teilweise in Zusammenarbeit mit Yannik Sell. NMR spektroskopische Messungen wurden in Kooperation mit Dr. Markus Leutzsch durchgeführt, welcher zudem unterstützende DFT-Rechnungen durchgeführt hat. Einkristallstrukturanalysen wurden von Dr. Nils Nöthling oder Jörg Rust vorgenommen. Die beschriebenen Ergebnisse bilden eine vollständige Übersicht über diese gemeinsamen Arbeiten. Die von diesen Mitarbeitern alleinverantwortlich erzielten Ergebnisse wurden als solche an entsprechender Stelle gekennzeichnet.

Danksagung

Zunächst möchte ich meinem Doktorvater, Prof. Dr. Alois Fürstner, herzlich dafür danken, dass er mir die Möglichkeit gegeben hat, meine Doktorarbeit in seinem Arbeitskreis anzufertigen. Besonders danke ich ihm für das große Vertrauen, den Freiraum zur eigenständigen Gestaltung meiner Forschungsprojekte sowie die zahlreichen Gespräche, aus denen ich fachlich wie persönlich viel lernen konnte.

Prof. Dr. Martin Hiersemann danke ich herzlich für die Übernahme des Koreferats.

Ein großer Dank gilt Dr. Thomas Q. Davies, der mich zu Beginn meiner Doktorarbeit in die Nickel-Dien-Chemie eingearbeitet und mir wertvolles Feedback zu meinen eigenen Ideen gegeben hat.

Christian Wille danke ich für die Synthese exorbitanter Mengen VAPOL, seine stetige Hilfsbereitschaft und die tolle Zusammenarbeit in Box 1. Yannik Sell danke ich für die angenehme und erfolgreiche Zusammenarbeit bei den Substratsynthesen, die wesentlich zum schnellen Projektfortschritt beigetragen hat. Zudem danke ich Christian Wille, Saskia Schulthoff, Christopher Rustemeier, Yannik Sell, Roswitha Leichtweiß und Andrea Bosserhoff für ihren Einsatz, der sowohl innerhalb als auch außerhalb des Labors zu einem reibungslosen Arbeitsalltag beigetragen hat.

Für die herausragenden NMR-Analysen teilweise äußerst komplexer Proben sowie die stets hilfreichen wissenschaftlichen Diskussionen möchte ich Dr. Markus Leutzsch danken. Des Weiteren danke ich den Mitarbeitern aller Analytikabteilungen des Instituts für ihre exzellente Arbeit. Insbesondere möchte ich mich bei Conny Wirtz, Markus Kochius und Dr. Nils Nöthling bedanken. Außerdem danke ich Roswitha Leichtweiß für das Messen und Analysieren zahlreicher HPLC-Proben.

Für die zügige und gründliche Korrektur dieser Arbeit möchte ich Noah Richter, Dr. Nepomuk Korber, Dr. Nikolai Rossouw und Dr. Soumyadeep Chakrabortty danken.

Meinen Senior-PhD-Kollegen Dr. Daniel Rütter, Dr. Nepomuk Korber und Dr. Simon Spohr möchte ich für die freundliche Aufnahme in die Fürstner-Gruppe und die Unterstützung zu Beginn meiner Promotion danken. Für zahlreiche wissenschaftliche Diskussionen und wertvolles Feedback danke ich außerdem meinen Postdoc-Kollegen Dr. Thomas Varlet, Dr. Jack Sutro, Dr. Jae Yeon Kim, Dr. Soumyadeep Chakrabortty, Dr. Guanghao Huang und Dr. Minxu Cui. Allen aktuellen und ehemaligen Mitarbeitern der Fürstner-Gruppe möchte ich für die hervorragende Arbeitsatmosphäre danken. Besonders hervorheben möchte ich hierbei: Dr. Peter Chapple, Dr. Ricardo Molina Betancourt, Dr. Juan Carlos Babón Molina, Dr. Nikolai Rossouw, Dr. Anne Zimmer, Alexander Schwalenberg, Albert Hermann, Andrea Tomio, Paul Moths, Noah Richter, Luis Renken, Clément Rein, Djung Sue Jeon, Julius Steidele und Quentin Riedl.

Ein ganz besonderer Dank gilt meinem Kollegen Daniel Isak, den ich bereits seit Kindertagen kenne, mit dem ich während dieser Promotion viele Höhen und Tiefen erlebt habe und der mich

bei wissenschaftlichen und persönlichen Fragen oft beraten hat. Ich bin sehr dankbar, dass mich diese langjährige Freundschaft auch durch diese Zeit begleitet hat.

Mein größter Dank gilt meiner Familie, die mich bei all meinen Entscheidungen stets unterstützt, mir während des Studiums und der Promotion wichtigen Rückhalt gegeben und vor allem immer an mich geglaubt hat. Besonders danken möchte ich meiner Partnerin Diana, die nicht nur nach dem Studium mit mir nach Mülheim gezogen ist, sondern mir auch in allen Phasen meiner Promotion viel Verständnis und Unterstützung entgegengebracht hat. Besonders in den herausfordernden Phasen dieser Zeit war sie stets an meiner Seite, hat mir den Rücken freigehalten, mich ermutigt und mir immer wieder die nötige Motivation und Zuversicht gegeben. Dafür bin ich ihr von Herzen dankbar und freue mich auf unsere weitere gemeinsame Zukunft.

Inhalt

Nickel-katalysierte intermolekulare reduktive Kupplungsreaktionen zwischen Aldehyden und 1,3-Dienen wurden erstmals vor fast drei Jahrzehnten untersucht. Trotz ihrer Vielseitigkeit wurden enantioselektive Varianten dieser Transformationen lange Zeit als ungelöste Herausforderung angesehen und haben erst vor Kurzem zunehmend an Aufmerksamkeit gewonnen. Ein von VAPOL abgeleiteter Phosphoramidit-Ligand erweist sich bisher als einzigartig effektiv darin, den regiochemischen Verlauf dieser Kupplungsreaktionen zu verändern und gleichzeitig eine hervorragende Enantiokontrolle auszuüben. Diese regioinvertierte reduktive Kupplung begünstigt die Reaktion am weniger nukleophilen Dien-Terminus und erwies sich bereits als geeignet für elektronenreiche Silyl-Dienolether und elektronenarme Sorbat-Derivate.

Im ersten Teil dieser Arbeit wurde diese Methodik durch den Einsatz von geschützten 5-Amino-2,4-pentadienoaten erweitert, einer neuartigen Klasse von 1,3-Dienen mit Push-Pull-Charakter. In Gegenwart des chiralen Liganden verläuft die Kupplung am amino-substituierten Terminus des Diens, wodurch vicinale *anti*-konfigurierte Aminoalkohole mit hervorragender Diastereo- und Enantioselektivität entstehen. Ein stereoselektiver Zugang zu diesem Strukturmotiv ist aufgrund seines weit verbreiteten Vorkommens in Naturstoffen, pharmazeutischen Wirkstoffen und chiralen Katalysatoren von großem Interesse.

Eine Reihe von Faktoren, die die Regio- und Enantioselektivität der Reaktion beeinflussen, wurde untersucht, darunter Lösungsmitteleffekte sowie elektronische und sterische Eigenschaften der Reaktionspartner. Darüber hinaus wurde der synthetische Nutzen der Methodik durch die Diversifizierung der resultierenden Aminoalkohol-Produkte in eine Reihe pharmazeutisch relevanter Motive unterstrichen.

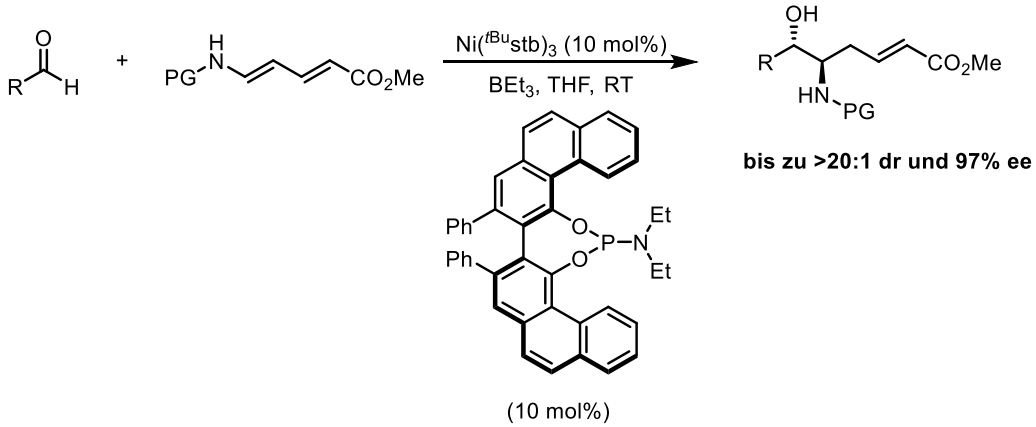

Nach der erfolgreichen Entwicklung dieser asymmetrischen intermolekularen reduktiven Kupplungsreaktion konzentrierte sich der zweite Teil dieser Arbeit auf die Entwicklung einer analogen intramolekularen Variante dieses Reaktionsmodus. Geeignete Substrate für die angestrebte Transformation wurden durch N-Substitution des Amino-pentadienoat-Gerüsts mit einem vorfunktionalisierten Aldehydderivat synthetisiert. Nach umfassender Untersuchung der Reaktionsbedingungen und Ligandenkandidaten wurde der kommerziell erhältliche P-chirale (*S*)-

AntPhos als idealer Ligand identifiziert, wodurch die diastereo- und enantioselektive Synthese verschiedener hydroxylierter Tetrahydroisochinolin-Derivate mit *anti*-konfiguriertem Aminoalkohol-Motiv sowie weiterer verwandter N-Heterozyklen ermöglicht wurde.

Zusätzlich zu diesen synthetischen Studien wurden reaktive Metallazyklen erfolgreich hergestellt und charakterisiert, was seltene experimentelle Belege für ihre Rolle im katalytischen Zyklus lieferte. Solche Allyl-Nickelazyklen werden allgemein als Schlüsselintermediate in reduktiven Kupplungsreaktionen zwischen 1,3-Dienen und Elektrophilen angesehen. Dies motivierte Untersuchungen dazu, ob ihre Reaktivität in Reaktionsmodi jenseits der konventionellen reduktiven Kupplungschemie genutzt werden kann.

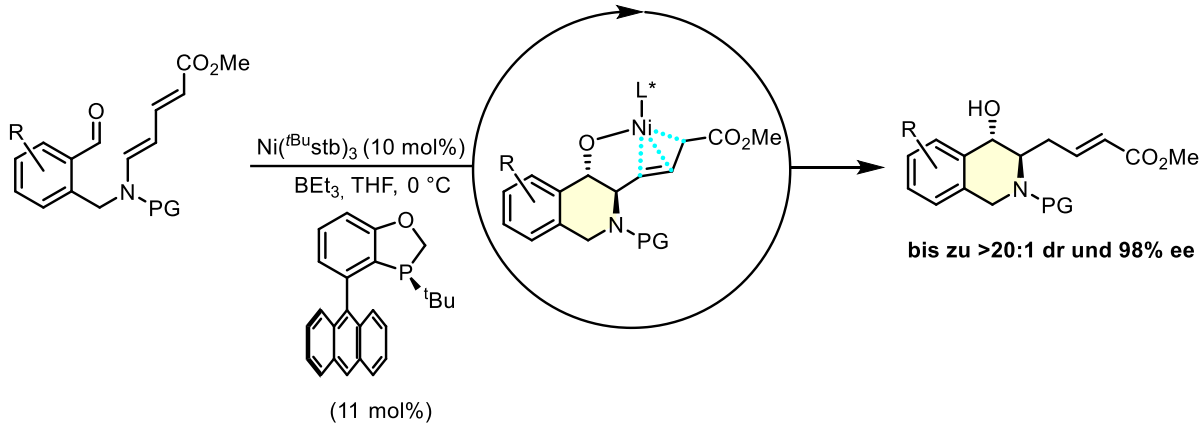

Im dritten Teil dieser Arbeit wurde daher ein vollständig neuer Reaktionsmodus verfolgt. Es wurde versucht, die Reaktivität dieser Zwischenstufen durch Abfangreaktionen mit einem externen Nukleophil zu nutzen, das in der Lage ist, das Allylfragment anzugreifen. Zu diesem Zweck wurde ein verknüpfter nukleophiler Arm in ein Imin-Substrat eingeführt, das anschließend einer Kupplung mit einem silylierten Dienolether unterzogen wurde. Die geplante redoxneutrale Tandem-Reaktion erwies sich als unerwartet komplex. Eine Reihe von Kontrollversuchen deutete darauf hin, dass die *in situ*-Bildung einer Nickel(III)-Amido-Spezies für die reduktive Eliminierung entscheidend sein könnte. Zu diesem Zweck lieferte ein katalytisches System aus $NiCl_2$(dme) und Zinkpulver zur Katalysatoraktivierung die vielversprechendsten Ergebnisse und ermöglichte katalytische Umsatzraten in mehreren Modellreaktionen. Dennoch behinderten Probleme bei der Reproduzierbarkeit die weitere Entwicklung dieser neuartigen Transformation. Mögliche Ursachen für diese Einschränkungen sowie Optimierungsstrategien werden diskutiert.

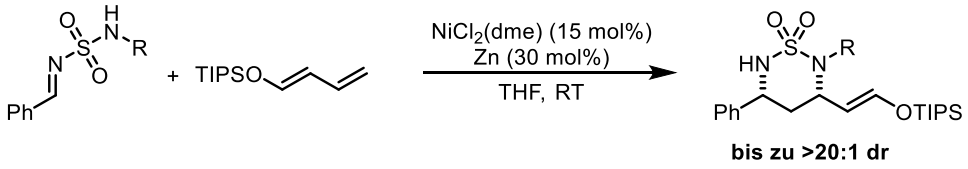

Abstract

Nickel-catalyzed intermolecular reductive coupling reactions between aldehydes and 1,3-dienes were first investigated almost three decades ago. Despite their versatility, asymmetric variants of these transformations have long been viewed as an unresolved challenge and have only recently gained increasing attention. A VAPOL-derived phosphoramidite ligand is, so far, uniquely effective in altering the regiochemical course of these coupling reactions while exerting excellent enantiocontrol. This regioinverted reductive coupling favors reaction at the least nucleophilic diene terminus and has been shown to accommodate both electron-rich silyl dienol ethers and electron-poor sorbate derivatives.

In the first part of the present thesis, this methodology was extended through the use of 5-amino-2,4-pentadienoates, a novel class of 1,3-dienes with a push-pull character. In the presence of the chiral ligand, the reaction proceeds at the amine-substituted terminus of the diene, affording vicinal *anti*-configured amino alcohols with excellent diastereo- and enantioselectivity. Selective approaches to this structural motif are highly desirable given its widespread occurrence in natural products, pharmaceuticals, and chiral catalysts.

A number of factors influencing the regio- and enantioselectivity of the reaction were investigated, including solvent effects as well as the electronic and steric properties of the reaction partners. Moreover, the synthetic utility of the methodology was underscored by the diversification of the resulting amino alcohol products into a range of pharmaceutically relevant motifs.

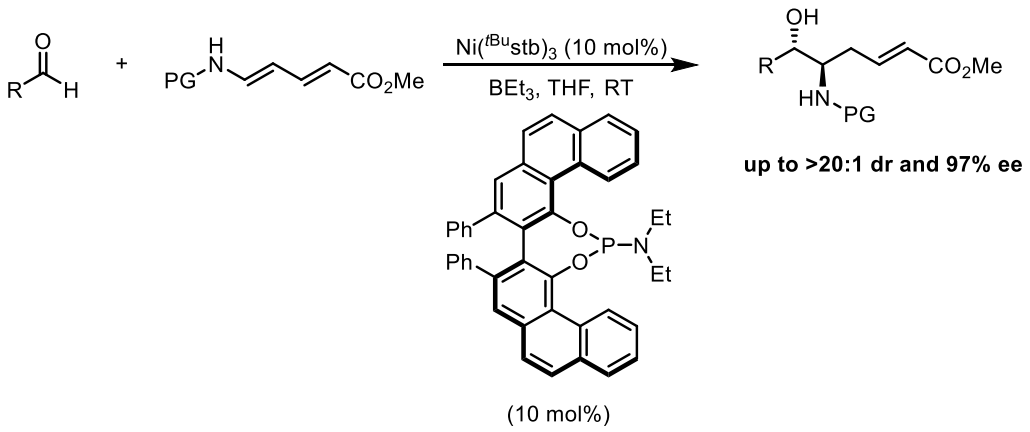

Following the successful development of this asymmetric intermolecular reductive coupling reaction between protected amino-pentadienoates and aldehydes, the second part of this work focused on the development of an analogous intramolecular version of this reaction mode. Suitable substrates were obtained by N-substitution of the amino-pentadienoate scaffold with a pre-functionalized aldehyde derivative. Following extensive screening of reaction conditions and ligand candidates, commercially available P-chiral (*S*)-AntPhos was identified as the ideal ligand, enabling the diastereo- and enantioselective synthesis of various hydroxylated tetrahydroisoquinoline derivatives bearing an *anti*-configured amino alcohol motif, as well as several related N-heterocycles.

In addition to these synthetic studies, reactive metallacycles were successfully prepared and characterized, providing rare experimental evidence for their role in the catalytic cycle. Such allyl-nickelacycles are generally assumed to be key intermediates in reductive coupling reactions between 1,3-dienes and electrophiles. This prompted investigations into whether their reactivity could be harnessed in reaction modes beyond conventional reductive coupling chemistry.

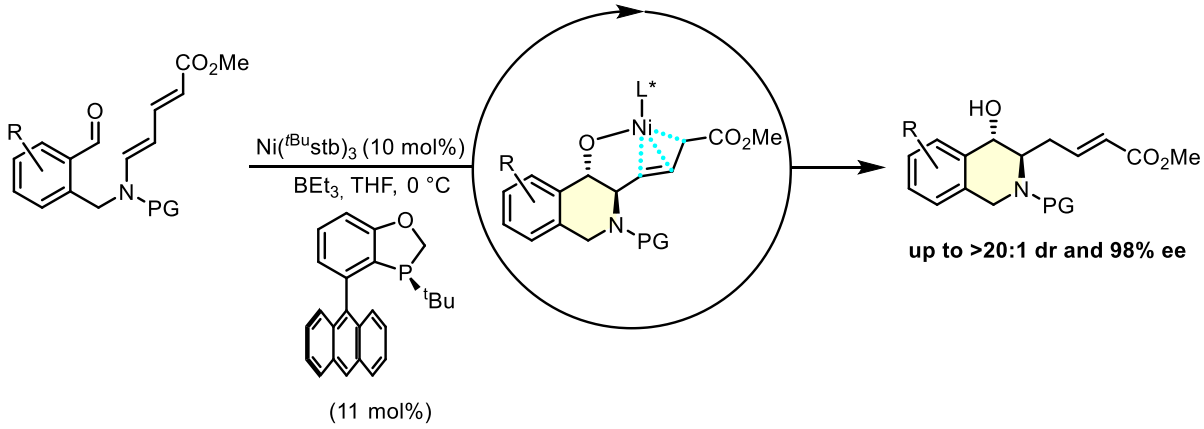

In the third part of this work, an entirely new reaction mode was pursued. It was attempted to harness the reactivity of these intermediates through interception with an external nucleophile capable of attacking the allyl unit. To this end, a tethered nucleophilic handle was incorporated into an imine substrate which was subsequently subjected to coupling with a silyl dienol ether.

The envisaged redox-neutral tandem reaction proved less straightforward than anticipated. A series of control experiments suggested that *in situ* generation of a nickel(III) amido species may be essential for the reductive elimination step. To this end, a catalytic system consisting of $NiCl_2$(dme) and zinc powder for catalyst activation provided the most promising results and enabled catalytic turnover in several model reactions. Nevertheless, reproducibility issues hampered further development of this novel transformation. Potential causes of these limitations and optimization strategies are therefore discussed.

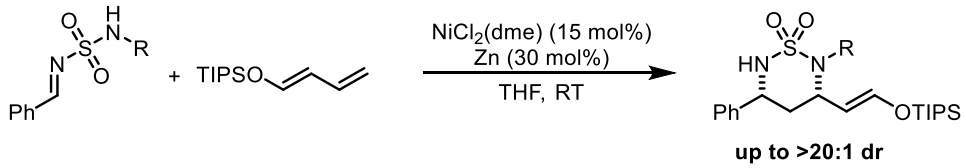

Table of Contents

Inhalt I

Abstract III

1 Introduction ..... - 1 -

1.1 Nickel(0) Complexes and Their Reactivity toward 1,3-Dienes: A Brief History ..... - 1 -

1.2 Nickel-Catalyzed Reductive Coupling Reactions Involving 1,3-Dienes ..... - 4 -

1.2.1 Intramolecular Reductive Couplings ..... - 4 -

1.2.2 Intermolecular Reductive Couplings ..... - 9 -

1.2.3 Enantioselective Intermolecular Reductive Couplings ..... - 15 -

1.2.4 Enantioselective Regioinverted Reductive Couplings ..... - 19 -

1.3 Occurrence, Application and Enantioselective Synthesis of Vicinal Amino Alcohols - 26 -

2 Regioinverted Nickel-Catalyzed Reductive Coupling Reactions for the Enantioselective Synthesis of Vicinal Amino Alcohol Derivatives ..... - 31 -

2.1 Aim ..... - 31 -

2.2 Preliminary Results and Rationale for Substrate Design ..... - 32 -

2.3 Reaction Optimization for Aromatic Aldehydes ..... - 35 -

2.4 Reaction Scope with Aromatic Aldehydes ..... - 39 -

2.5 Effects on Regioselectivity and Enantioselectivity ..... - 44 -

2.6 Reaction Optimization for Aliphatic Aldehydes ..... - 48 -

2.7 Reaction Scope with Aliphatic Aldehydes ..... - 51 -

2.8 Synthesis and Application of Modified Dienes ..... - 53 -

2.9 Scale-Up and Derivatization ..... - 58 -

2.10 Mechanistic Considerations ..... - 60 -

2.11 Summary ..... - 63 -

3 Enantioselective Synthesis of Tetrahydroisoquinolines and Related Heterocycles *via* Intramolecular Nickel-Catalyzed Reductive Coupling Reactions ..... - 67 -

3.1 Aim ..... - 67 -

3.2 Preliminary Experiments and Reaction Optimization ..... - 69 -

3.3 Substrate Synthesis ..... - 74 -

3.4 Reaction Scope ..... - 76 -

3.5 Downstream Functionalization ..... - 81 -

3.6 Synthesis and Characterization of Allyl-Oxanickelacycle Intermediates and Their Mechanistic Implications ..... - 84 -
3.7 Summary ..... - 93 -
4 Studies Toward Nickel-Catalyzed Redox-Neutral Tandem Reactions between Silyl Dienol Ethers and Functionalized Imines ..... - 98 -
4.1 Introduction ..... - 98 -
4.2 Aim ..... - 102 -
4.3 Preliminary Experiments ..... - 104 -
4.4 Mechanistic Considerations and Rationale for Reaction Design ..... - 106 -
4.5 Studies on Catalytic Reaction Conditions and Reproducibility ..... - 110 -
4.6 Summary and Outlook ..... - 114 -
5 Experimental Section ..... - 119 -
5.1 General Information ..... - 119 -
5.2 Preparation of Precursors, Substrates and Ligands ..... - 121 -
5.3 Enantioselective Nickel-Catalyzed Intermolecular Reductive Couplings ..... - 147 -
5.3.1 Experimental Procedure, Work-up and Notes ..... - 147 -
5.3.2 Control Experiments ..... - 150 -
5.3.3 Determination of the Regioisomeric Ratio (rr) ..... - 152 -
5.3.4 Enantioselective Synthesis of Vicinal Amino Alcohol Derivatives ..... - 155 -
5.3.5 Downstream Derivatization ..... - 198 -
5.4 Enantioselective Nickel-Catalyzed Intramolecular Reductive Couplings ..... - 202 -
5.4.1 Experimental Procedure and Work-up ..... - 202 -
5.4.2 Enantioselective Synthesis of Tetrahydroisoquinoline Derivatives and Related Heterocycles ..... - 204 -
5.4.3 Downstream Derivatization ..... - 230 -
5.4.4 Rotamer Formation ..... - 236 -
5.4.5 Preliminary Data on Nickel-Catalyzed Synthesis of Chromanol Derivatives ..... - 239 -
5.4.6 Preparation and Analysis of Allyl-Oxanickelacycle Complexes ..... - 242 -
5.4.7 Kinetic Reaction Profile of a Reductive Cyclization Reaction and Speciation of the Crude Reaction Mixture ..... - 263 -
5.4.8 Determination of the Relative and Absolute Configuration of the Reductive Cyclization Products ..... - 269 -
5.5 Nickel-Catalyzed Redox-Neutral Tandem Reactions ..... - 277 -

6 Bibliography ..... - 280 -
7 Appendix ..... - 287 -
7.1 List of Abbreviations ..... - 287 -
7.2 Overview of Tools ..... - 290 -
7.3 Supporting Crystallographic Information ..... - 290 -

1 Introduction

1.1 Nickel(0) Complexes and Their Reactivity toward 1,3-Dienes: A Brief History

Nickel has played a central role in transition-metal catalysis for more than a century. In 1922, Nobel laureate Paul Sabatier described nickel as a "spirited horse" of "excessive activity" and "maximum alterability", which, given proper catalyst preparation "can do all kinds of work and maintain its activity for a long time".[1, 2] In modern terms, this versatility arises from the ability of nickel to access multiple oxidation states (0, I, II, and III), enabling both two-electron and single-electron pathways. As a result, nickel promotes a wide range of catalytic transformations and serves not only as an earth-abundant, cost-efficient alternative to palladium, but often exhibits complementary reactivity (*e.g.* in cross-coupling reactions)[3] or even entirely distinct catalytic behavior.

In 1953, Ziegler and co-workers made a serendipitous discovery when unintentionally performing their "Aufbau-reaction"[4] for the synthesis of higher aluminum alkyls from triethylaluminum and ethylene gas in the presence of residual nickel salts.[5] Instead of the expected products, they observed quantitative formation of 1-butene. This "nickel effect" prompted systematic studies on the influence of other transition metals on the "Aufbau-reaction", ultimately leading to the discovery of zirconium- and titanium-based catalysts for polyethylene synthesis and earning Ziegler the Nobel Prize in Chemistry in 1963.[6] In addition, these studies inadvertently established a general protocol for the reduction of nickel(II) salts with trialkylaluminum reagents, thereby providing a blueprint for the synthesis of nickel(0) π-complexes.

In the following years, Wilke and co-workers adopted this approach and developed a general protocol for the synthesis of nickel(0)-π-complexes *via* reduction of nickel(II) salts (*e.g.* $Ni(acac)_2$) to nickel(0) in the presence of olefins.[7] This strategy provided access to well-defined species such as Ni(cdt) **1** or $Ni(cod)_2$ **2**, while highly reactive tris(ethylene)nickel **3** was prepared *via* ligand displacement from Ni(cdt) with ethylene gas.[8] The ability of these complexes to undergo rapid ligand exchange with external ligands or substrates led to the term "naked nickel" and underlines their utility as versatile precatalysts. Notably, more than 80 years after its discovery, $Ni(cod)_2$ remains the most widely used nickel(0)-precatalyst, even as air- and bench-stable alternatives have gained increasing attention in recent years.[9-15]

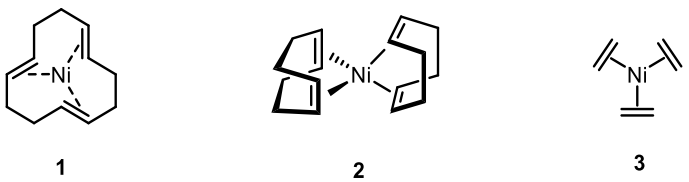

1 2 3

Figure 1: Representative examples of nickel(0) π-complexes developed by Wilke *et al.*

The pronounced affinity of nickel towards π-systems was not only explored in the synthesis of metal complexes, but also in stoichiometric reactions. 1,3-Dienes were of particular interest, given their significance as key feedstocks for polymer and fine chemical production.

Following initial studies on the reactivity of *in situ* generated nickel(0)-species toward 1,3-butadiene,[16] Wilke and co-workers investigated the reactivity of $Ni(cod)_2$ with 1,3-butadiene in the presence of exogenous phosphine ligands. They showed that $Ni(cod)_2$ reacts with two equivalents of 1,3-butadiene *via* an oxidative cyclization to form two types of complexes **5** and **6**, depending on the cone angle of the ligand (Scheme 1).[17] Above −10 °C, irreversible rearrangement of **5** to **6** was observed, whereas decomposition to the starting materials took place at room temperature.

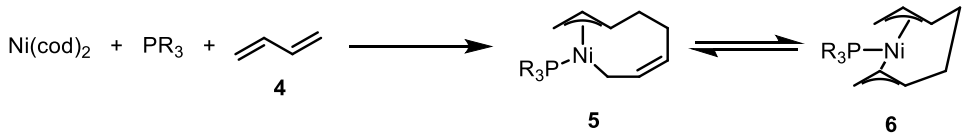

Scheme 1: Formation of η^1,η^3 and η^3,η^3 bis(allyl)-nickel complexes from $Ni(cod)_2$ and 1,3-butadiene in presence of a phosphine ligand.

Treatment of these bis(allyl)-nickel-complexes with carbon monoxide resulted in reductive elimination, yielding cyclodimerization products such as 4-vinylcyclohex-1-ene **8**, 1,2-divinylcyclobutane **9** and (1,5)-cycloocta-1,5-diene **10** (Scheme 2). Notably, this reactivity extends beyond simple butadiene to other 1,3-dienes such as isoprene.[18]

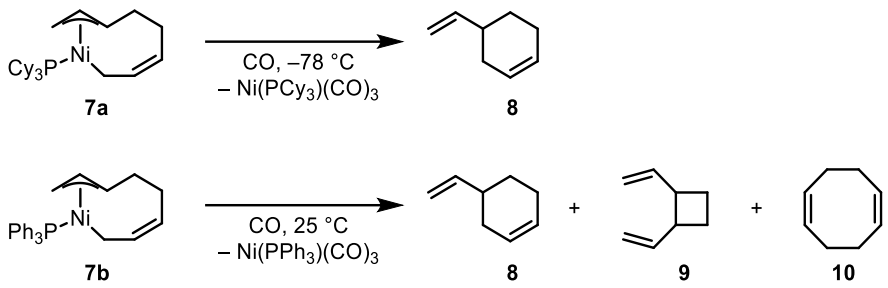

Scheme 2: Reactivity of $Ni(PR_3)(\eta^1,\eta^3$-octadiene) complexes under CO-atmosphere at different temperatures.

Importantly, the bis(allyl)nickel(II) intermediates formed during these reactions displayed pronounced nucleophilicity towards carbonyl compounds, distinguishing them from analogous palladium or platinum allyl species.[18]

This unique reactivity was first exploited by Baker *et al.* in the 1970s, who conducted stoichiometric reactions between aldehydes and simple 1,3-dienes in the presence of a Ni(0)-precatalyst and phosphine ligand.[19, 20] The reaction featuring acetaldehyde resulted in the formation of a set of four different 2:1 adducts, **12a**-**12d**. The product distribution was shown to be highly ligand-dependent (Scheme 3). The formation of **12a** and **12b** can be rationalized through β-hydride-elimination following addition of the bis-allyl-species into the aldehyde. Subsequent reductive elimination of the resulting nickel-hydride can then complete the redox-neutral coupling reaction and furnish the respective product. In contrast, formation of the dienyl

alcohols **12c** and **12d** proceeds *via* a reductive coupling. In the absence of an external reductant, catalytic turnover is not possible, hence these products are only formed upon protonation during work-up with aqueous potassium cyanide.[20]

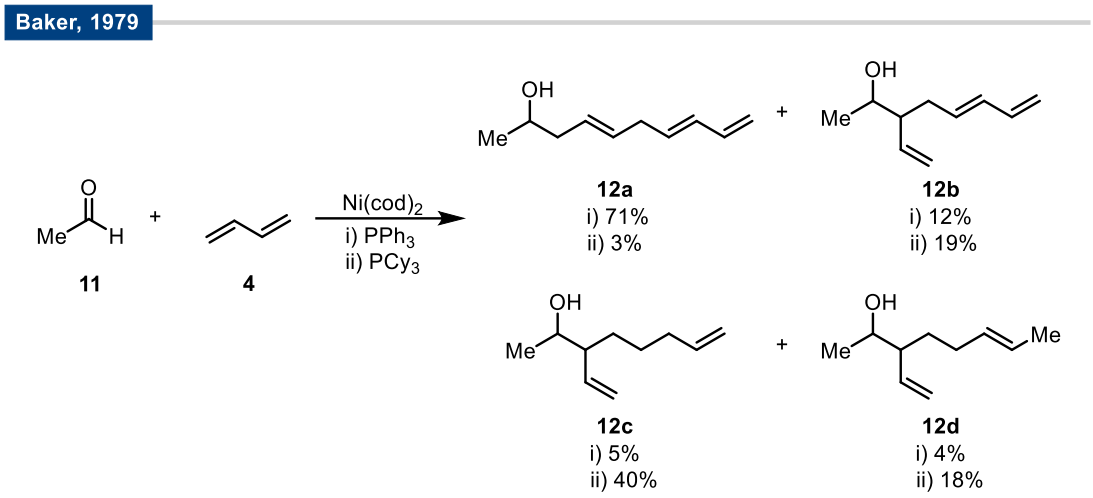

Scheme 3: Nickel-catalyzed coupling of acetaldehyde and 1,3-butadiene.

When the reaction was performed with isoprene, a complex product mixture, including 1:1 diene-aldehyde adducts **15a** and **15b** was observed. Notably, more reactive Ni(cdt) was required instead of $Ni(cod)_2$ to efficiently promote the coupling reaction (Scheme 4).

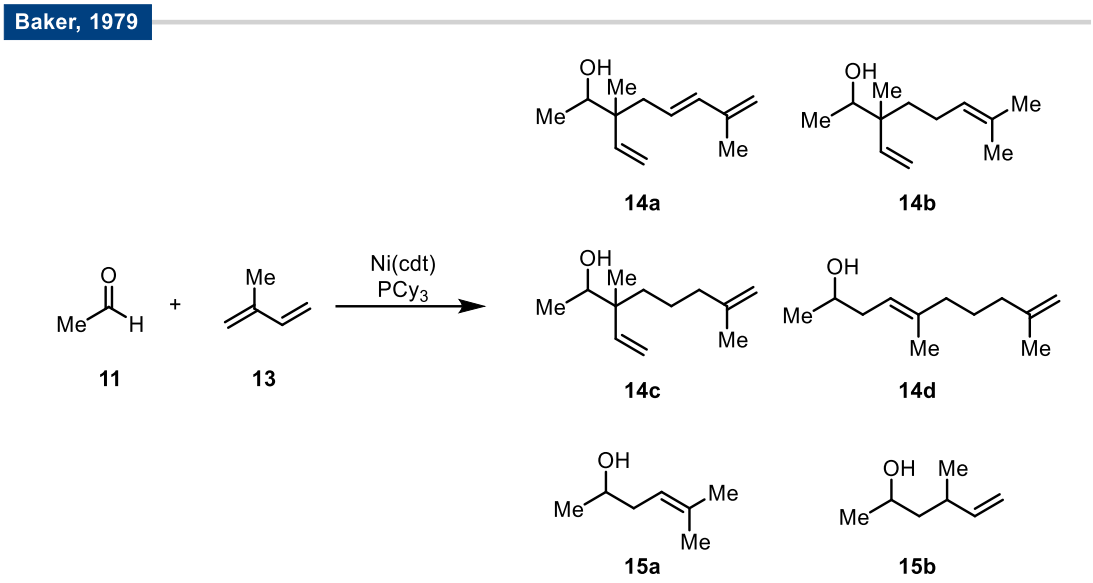

Scheme 4: Reported products for the nickel-catalyzed coupling of acetaldehyde and isoprene.

While these early studies did not yield synthetically practical methods due to low selectivity and the stoichiometric use of nickel, they provided the first proof of concept for both reductive and redox-neutral couplings of 1,3-dienes and aldehydes and highlighted the utility of allyl-nickel intermediates.

1.2 Nickel-Catalyzed Reductive Coupling Reactions Involving 1,3-Dienes

1.2.1 Intramolecular Reductive Couplings

In the early 1990s, the group of Miwako Mori started investigating stoichiometric reductive cyclization reactions of ω-dienyl aldehydes and ketones catalyzed by a nickel(0) species (formed *in situ* by reduction of $Ni(acac)_2$ with DIBAL–H).[21] Control experiments suggested that the formation of a Ni–H species during the catalytic cycle is essential, as reactions lacking a hydride source did not proceed efficiently.

With these considerations in mind, the group developed the first catalytic reductive coupling reaction of aldehydes with 1,3-dienes, utilizing $Ni(cod)_2$ as a well-defined nickel(0) source, PPh_3 as an ancillary ligand, and triethylsilane as a stoichiometric reductant (Scheme 5).[21] This approach enabled the highly diastereoselective reductive cyclization of three different substrates, providing access to the corresponding silyl-protected cyclic alcohols.

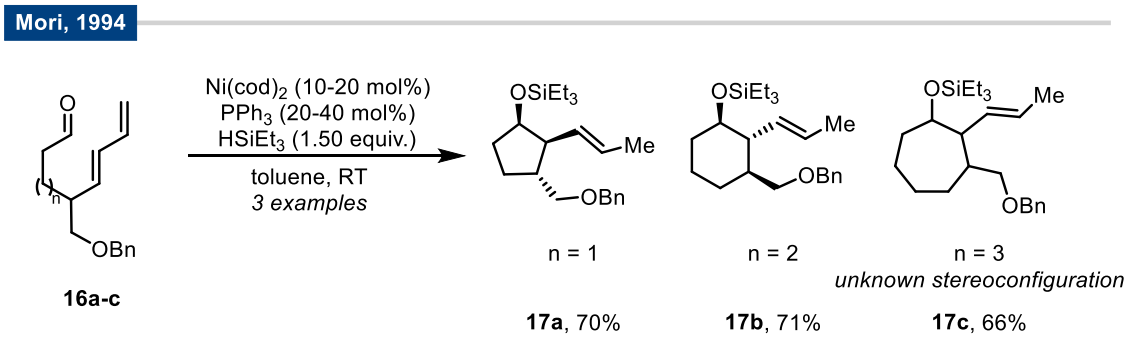

Scheme 5: Diastereoselective nickel-catalyzed reductive coupling reactions of ω-dienyl aldehydes by Mori *et al.*

The catalytic cycle (Scheme 6) is initiated by oxidative addition of the silane to the nickel(0) species, resulting in the formation of a Ni(II)–H intermediate **Int-A**. Coordination of the ω-dienyl aldehyde to the nickel center then enables migratory insertion into the Ni–H bond, leading to the formation of an allyl-nickel intermediate, which can be described as an η^1- (**Int-B**) or η^3-species (**Int-C**). Subsequent C–C bond formation generates the alkoxy-nickel intermediate **Int-D** which undergoes reductive elimination to release the silyl-protected cyclic alcohol product **17a** and regenerate the nickel(0) catalyst, thereby completing the catalytic cycle.

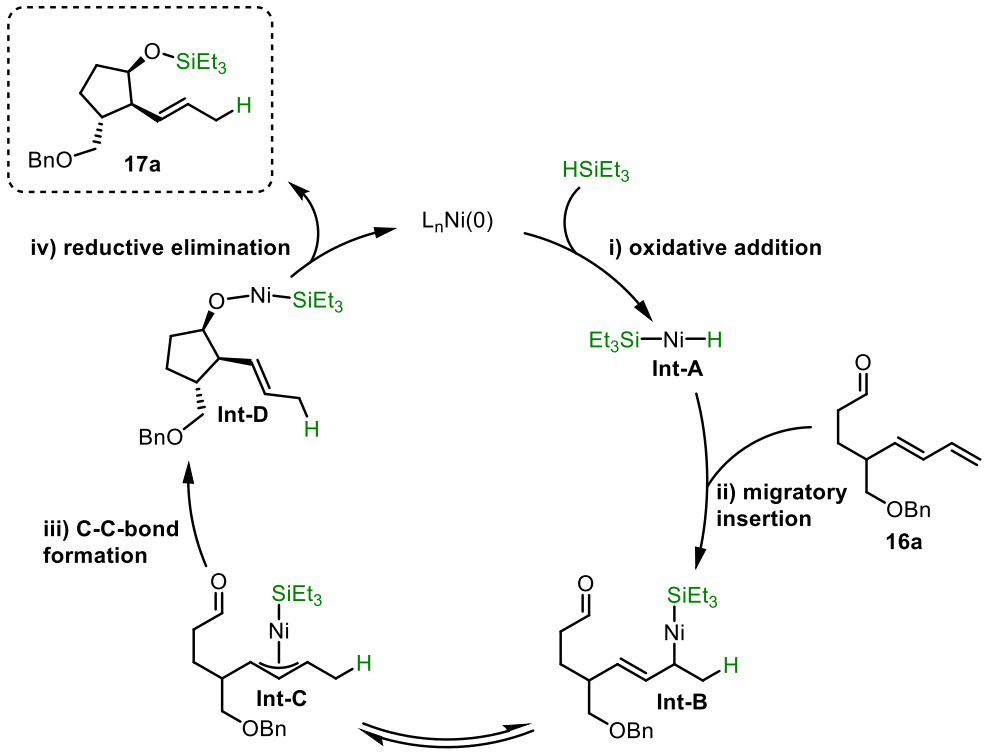

Scheme 6: Proposed catalytic cycle for the nickel-catalyzed reductive cyclization promoted by $HSiEt_3$.

In the following years various extensions and modifications of this reactivity were reported. These included expansion of the substrate scope to cyclic dienes,[22] as well as the development of silastannylative,[23, 24] disilylative,[24] and ligand-free protocols.[25] Furthermore, the use of a chiral amino acid-derived substrate enabled the formal total synthesis of the Elaeocarpus alkaloid (–)-Elaeokanine C, demonstrating the utility of this methodology in natural product synthesis (Scheme 7).[26]

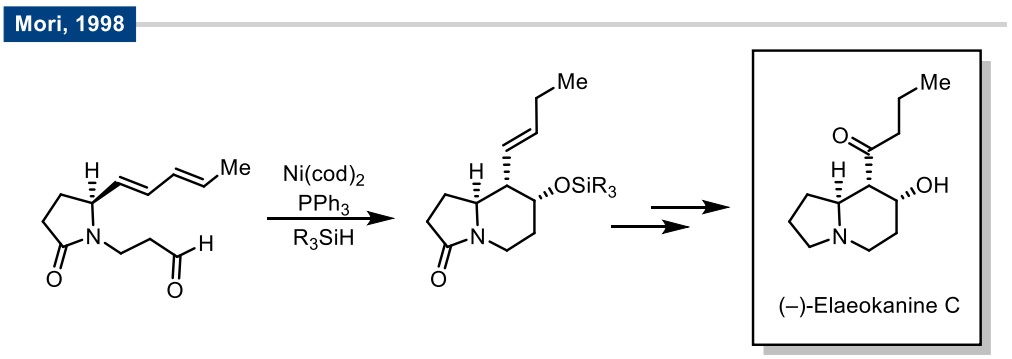

Scheme 7: Synthesis of (–)-Elaeokanine C *via* a nickel-catalyzed reductive cyclization approach.

Efforts were also directed towards the development of an asymmetric version of the reductive cyclization. To this end, Mori *et al.* modified their previously reported racemic procedure by replacing PPh_3 with the chiral phosphorane ligand **L1** and investigated a variety of sterically and electronically modified silanes as reductants (Scheme 8).[27-29] Although moderate enantioselectivities were observed, the scope of the reaction was very limited and a general protocol for the reaction could not be established.

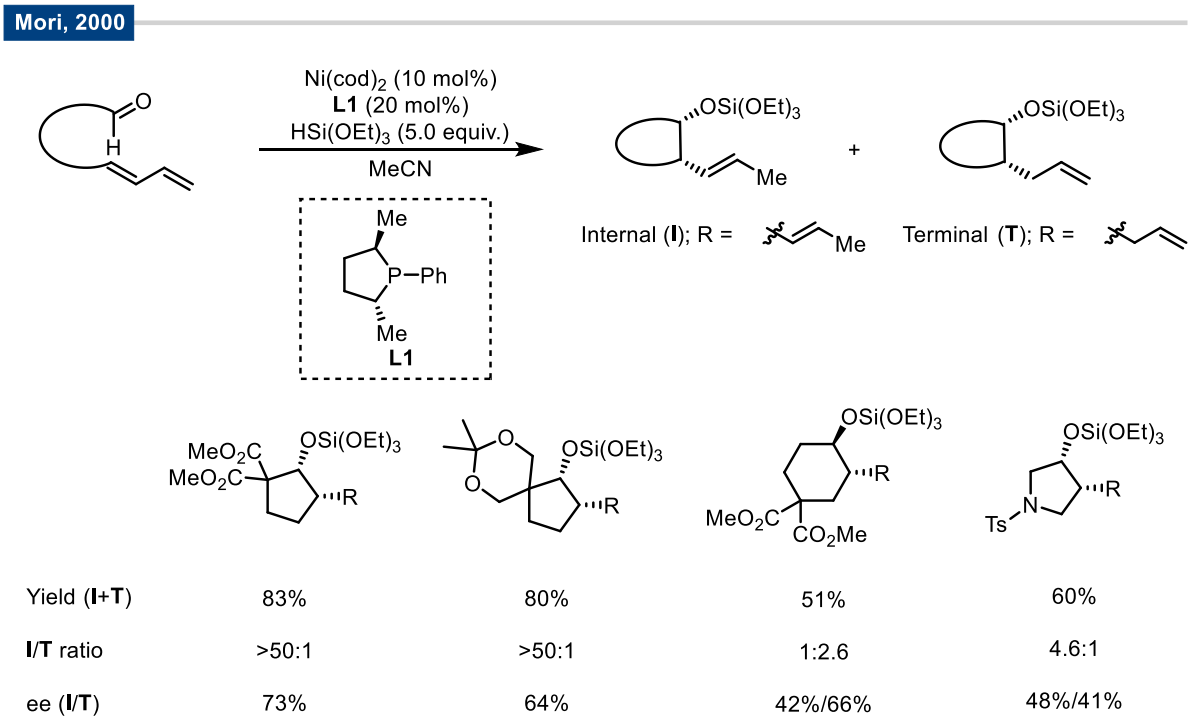

Scheme 8: Selected examples of the nickel-catalyzed asymmetric cyclization of ω-dienyl aldehydes.

Moreover, in some cases, significant amounts of an inseparable regioisomer bearing a terminal double bond were formed. While this undesired side reaction could occasionally be suppressed by careful choice of solvent and silane reducing agent, its occurrence appeared to be substrate-dependent, and no general solution was achieved.

Since the formation of this regioisomer could not be explained by the previously established catalytic cycle, Mori *et al.* proposed that a second, competing pathway might be operative. This alternative catalytic cycle (Scheme 9) proceeds *via* oxidative cyclization of the substrate at the nickel(0) center, resulting in the formation of the allyl-alkoxy-nickel complex **Int-A**. This species then undergoes σ-bond metathesis with the silane reducing agent to form the nickel-hydride species **Int-B**. Reductive elimination then releases the observed regioisomer and recovers the catalyst, thus completing the catalytic cycle.[27, 28]

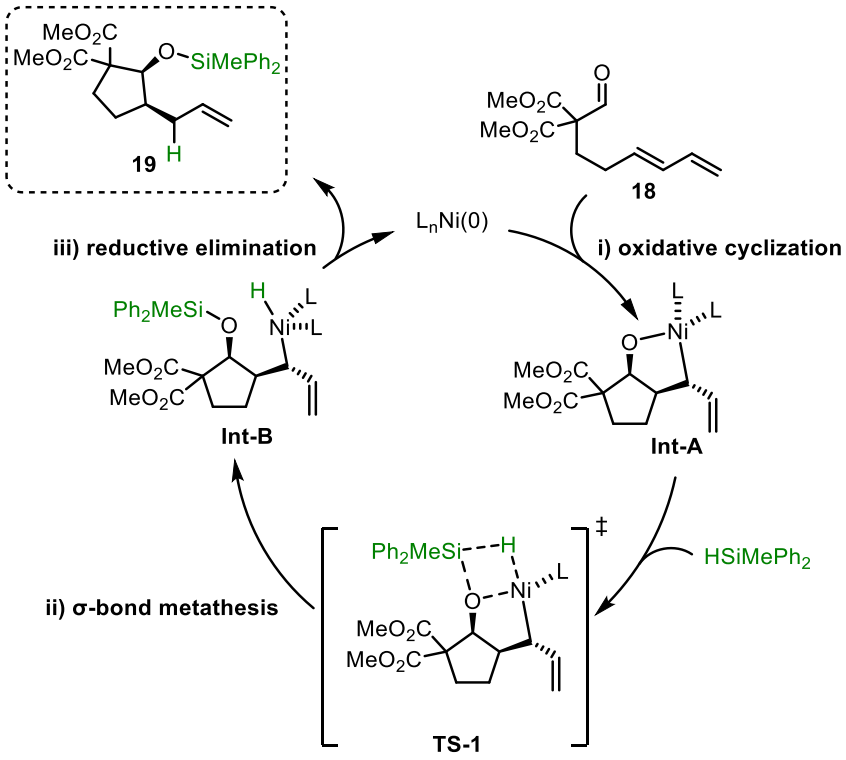

Scheme 9: Alternative catalytic cycle explaining the formation of regioisomers with terminal double bonds.

Overall, these pioneering works represent some of the earliest examples of nickel-catalyzed reductive coupling reactions involving 1,3-dienes and established key mechanistic principles that continue to influence modern research in the field to this day. However, major challenges such as competing side reactions and limited enantioselectivity remained unresolved. Furthermore, limited substrate diversity and scope, particularly by modern standards, hampered further developments. Therefore, attention ultimately shifted to the more broadly applicable intermolecular variants of reductive couplings of 1,3-dienes and electrophiles.

A similar trend could be observed in the realm of nickel-catalyzed reductive coupling reactions involving alkynes. While initial studies by Montgomery *et al.*[30, 31] in the late 1990s focused on intramolecular cyclizations of alkynes tethered to aldehydes, intermolecular coupling reactions quickly became the central focus of this growing research field.[32-38] Almost 20 years after its initial discovery, the intramolecular reaction mode recently regained attention, as Tang and Liu achieved the enantioselective syntheses of tetrahydrofurans, pyrrolidines, and piperidines, important scaffolds frequently encountered in natural products and drugs.[39-41]

Furthermore, new protocols enabling diastereoselective and enantioselective syntheses of various carbo- and heterocycles *via* reductive cyclization of alkenes have recently been developed.[42-47] While these methods represent valuable and synthetically useful additions to the arsenal of nickel-catalyzed reductive cyclization reactions, they all rely on simple alkenes rather than 1,3-dienes. This not only eliminates an important functional handle in the corresponding products but also circumvents some of the long-standing challenges associated with the original transformation.

In conclusion, nickel-catalyzed reductive cyclization reactions, particularly those involving 1,3-dienes, remain underexplored compared to their intermolecular counterparts. The development of new strategies enabling precise control over regio-, diastereo-, and enantioselectivity, is therefore highly desirable.

1.2.2 Intermolecular Reductive Couplings

In 1998, approximately four years after the initial discovery of nickel-catalyzed intramolecular reductive cyclization reactions with ω-dienyl aldehydes, the groups of Miwako Mori and Yoshinao Tamaru independently shed light on the intermolecular variant of this methodology.

Mori *et al.* demonstrated that their initial protocol could serve as a blueprint for an analogous intermolecular reaction involving aldehydes and terminal 1,3-dienes, yielding homoallylic alcohol derivatives (Scheme 10, top).[48] Additions to aromatic aldehydes proceeded with uniformly high regioselectivity and complete (*E*:*Z*) olefin control, whereas reactions with aliphatic aldehydes suffered from low control over the double bond geometry.

Subsequently, the group demonstrated that, in reductive couplings of aldehydes with silyl-substituted dienes, the choice of ligand strongly influences the stereochemical outcome of the reaction. While PPh_3-ligated nickel catalysts afforded (*E*)-configured allylation products, N-heterocyclic carbene (NHC)-ligated systems furnished the corresponding (*Z*)-configured products (Scheme 10, bottom) exclusively.[49]

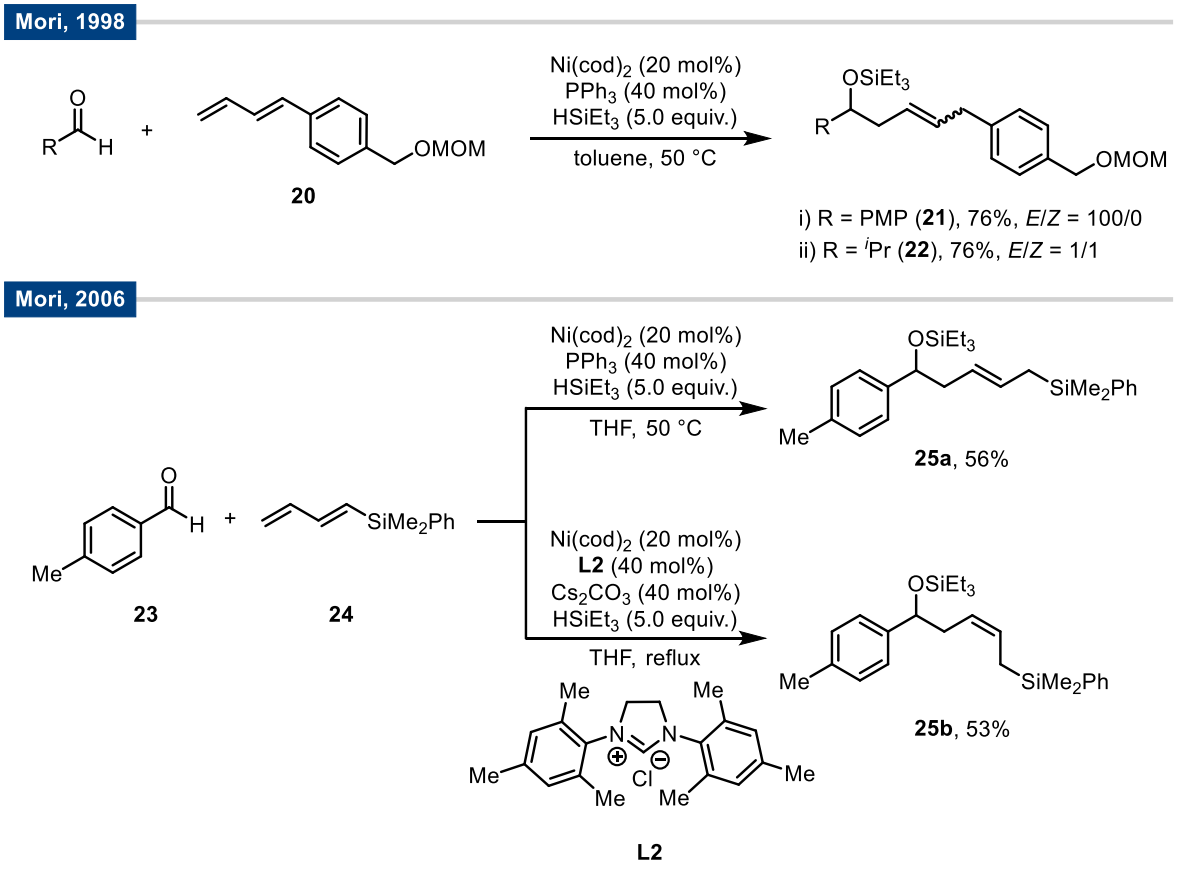

Scheme 10: Nickel-catalyzed intermolecular coupling reactions of aldehydes and 1,3-dienes promoted by $HSiEt_3$.

In the same year, Tamaru *et al.* published their seminal work on nickel-catalyzed homoallylation reactions[50] which they later expanded into an in-depth study.[51] A key distinction from previous reports was the choice of reductant; instead of commonly employed silanes, triethylborane was used to promote the reaction. Moreover, the reactions were performed in the absence of

exogenous ligands, employing $Ni(acac)_2$ as a convenient precatalyst that was reduced *in situ* to catalytically active nickel(0).

Notably, the more sensitive $Ni(cod)_2$ gave comparable yields but significantly shorter reaction times, as the slow *in situ* catalyst activation could be bypassed.[50] These homoallylation reactions displayed high versatility, enabling the coupling of benzaldehyde with a diverse set of dienes and even trienes, including feedstock chemicals such as isoprene, myrcene and butadiene. The reactions proceeded at ambient temperature, typically with high regiocontrol and excellent diastereoselectivity.

While 1,3-butadiene displayed good reactivity and gave the expected product **27a** in appreciable yield, a regioisomeric byproduct **27b** was formed due to double bond isomerization (Scheme 11, A). In contrast, substituted 1,3-dienes did not undergo this isomerization. However, their unsymmetrical structures allowed for reaction at different termini, again opening up the possibility of regioisomer formation.

In this context, Tamaru and co-workers found that the regioselectivity of the reaction was strongly dictated by the substitution pattern of the butadiene-framework. Introduction of a methyl substituent at one of the terminal positions (Scheme 11, B) induced a preference for addition at the opposing unsubstituted terminal double bond to yield product **29a**, although a considerable amount of regioisomer **29b** was still observed. Placement of the methyl-substituent on the adjacent internal C-atom led to complete regiocontrol with isoprene **13** reacting exclusively at the terminal C1-position to afford the corresponding alcohol **30** with excellent 1,3-*anti* diastereoselectivity (Scheme 11, C).

Siloxy-groups exerted even stronger regiocontrolling effects than methyl groups, as silyl dienol ether **31** reacted exclusively at the unsubstituted terminus (Scheme 11, D). This outcome can be rationalized by the reduced nucleophilicity and increased steric shielding at the siloxy-substituted C-atom. This trend was further validated using the di-substituted derivative **33**, which again gave a single regioisomer **34** in excellent 1,3-*anti* diastereoselectivity (Scheme 11, E).

Use of (*E*,*E*)-methyl sorbate **35** furnished the corresponding aldol-type product **36** in excellent 1,2-*anti* diastereoselectivity, demonstrating that even electron-deficient dienes are competent substrates (Scheme 11, F). Notably, even 1,3,5-triene **37** was compatible with the transformation. The coupling proceeded exclusively at the *Z*-configured double bond, affording 1,2-*syn* product **38**, containing three stereocenters, as a single diastereomer (Scheme 11, G).

Tamaru, 1998 & 2006

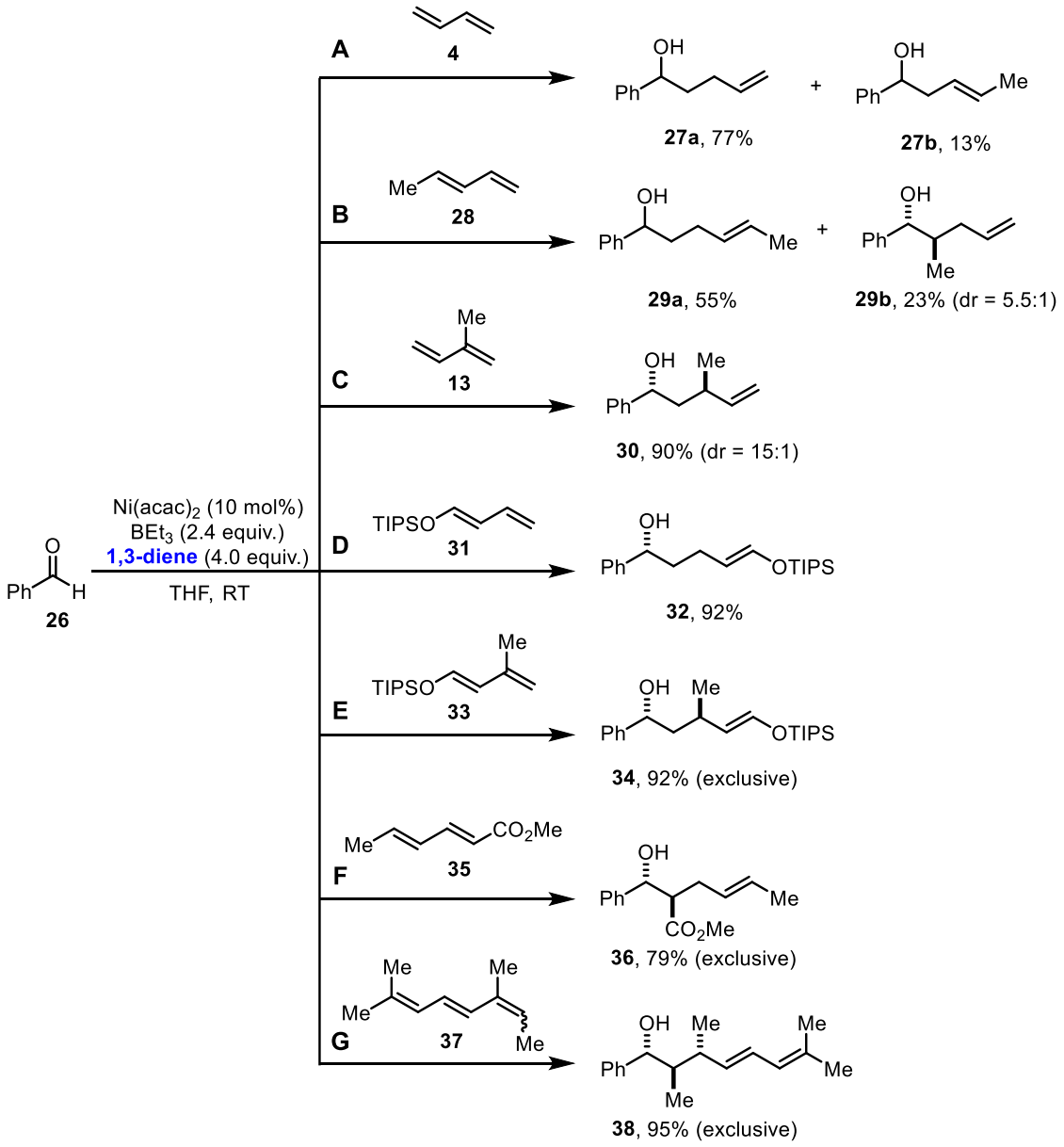

Scheme 11: Selected examples of the intermolecular reductive coupling reactions developed by Tamaru *et al.*

By performing a series of competition experiments, Tamaru *et al.* established a relative reactivity order for different classes of dienes (Figure 2).[51]

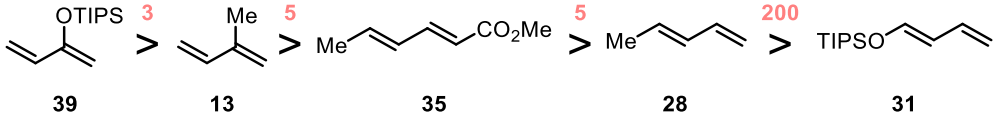

Figure 2: Relative order of reactivity of selected 1,3-dienes in the homoallylation reaction determined by Tamaru *et al.* (red numbers indicate the factor by which the reactivity differs).

Similar to regioselectivity, the substitution pattern of the diene significantly affected its reactivity. Siloxydiene **39** and isoprene **13** bearing substituents at an internal position showed the highest reactivity. In contrast, the methyl substituent at the terminal position of the butadiene framework in 1,3-pentadiene **28** resulted in a decrease in reactivity by a factor of ~25 compared to isoprene,

whereas silyl dienol ether **31** was ~15,000 times less reactive than its sibling **39**. Interestingly, no correlation between the observed reactivity and the nucleophilicity of the dienes was found. This is illustrated by the superior reactivity of methyl sorbate **35** compared to 1,3-pentadiene **28**, despite the former possessing a lower-lying HOMO.

The synthetic protocol was successfully applied to homoallylation reactions of isoprene with a variety of aldehydes. Aromatic aldehydes and α,β-unsaturated aldehydes could be used, affording the corresponding products in excellent 1,3-*anti* diastereoselectivity. Linear aliphatic aldehydes also reacted smoothly, whereas more sterically hindered secondary and tertiary aldehydes exhibited low reactivity under the standard conditions. To address this limitation, Tamaru *et al.* employed diethylzinc as an alternative reductant.[51, 52] Although incompatible with more reactive aldehydes due to competing ethylation of the aldehyde, its use significantly improved the yields of the desired homoallylation product for both linear and branched aliphatic aldehydes. Furthermore, diethylzinc even enabled the homoallylation of ketones with various 1,3-dienes, albeit partial loss of regioselectivity was observed.[51, 52]

Based on their experimental findings, Tamaru and co-workers proposed a mechanism for the triethylborane mediated nickel-catalyzed homoallylation reaction between aldehydes and 1,3-dienes (Scheme 12).[51]

First, the precatalyst $Ni(acac)_2$ gets reduced *in situ* by BEt_3 to generate a catalytically active nickel(0) species. The catalytic cycle then proceeds *via* coordination of both the diene and the aldehyde to the nickel center. Coordination of the diene in an *s-trans* conformation was proposed based on observed differences in reactivity between open-chain and cyclic 1,3-dienes.[51, 53] Subsequent oxidative cyclization affords the allyl-oxanickelacycle **Int-B**. At this stage, the stereochemical outcome is determined, with diaxial repulsion likely being the primary factor responsible for the high diastereoselectivity. Although this step might occur under ambient conditions in the absence of a Lewis acid, computational studies by Houk *et al.* on related couplings suggest that LUMO-lowering effects induced by triethylborane binding to the aldehyde can accelerate this step.[54]

In the following step, transfer of an ethyl group by transmetalation leads to formation of allyl-nickel-species **Int-C**. This step simultaneously generates a vacant coordination site, enabling β-hydride elimination to occur. The resulting nickel-hydride species **Int-D** then undergoes reductive elimination, releasing ethylene gas and the borinate ester of the reductive coupling product, which upon aqueous work-up affords the corresponding free alcohol.

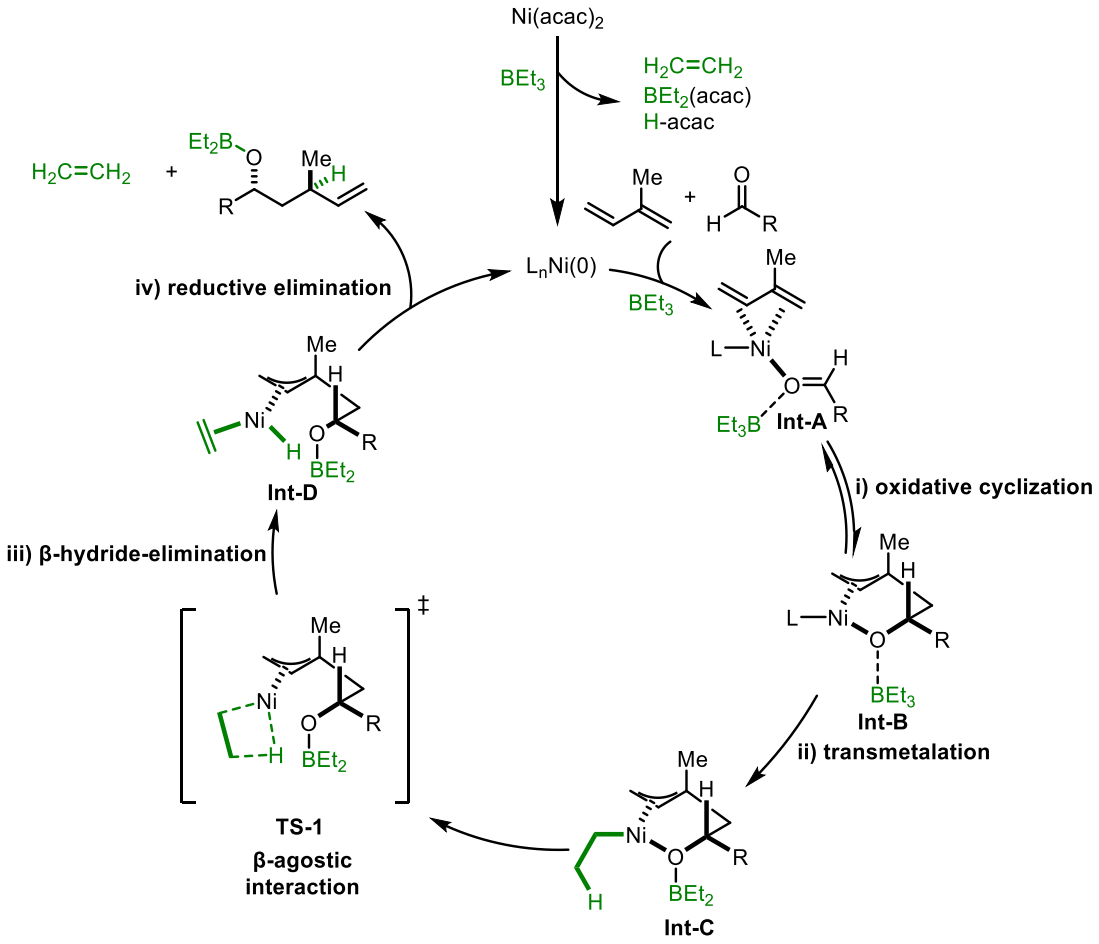

Scheme 12: Proposed catalytic cycle for the BEt_3-promoted nickel-catalyzed reductive coupling reaction of 1,3-dienes and aldehydes.

Further experimental evidence for the proposed mechanistic rationale was provided by Ogoshi *et al.* who succeeded in isolating and characterizing several allyl-alkoxy-nickel complexes, representing key intermediates in the catalytic cycle.[55] To this end, stoichiometric reactions between benzaldehyde, a diene (*e.g.* 2,3-dimethylbuta-1,3-diene) and PCy_3 were performed, enabling the isolation of single crystals suitable for X-ray crystallographic analysis (Scheme 13).

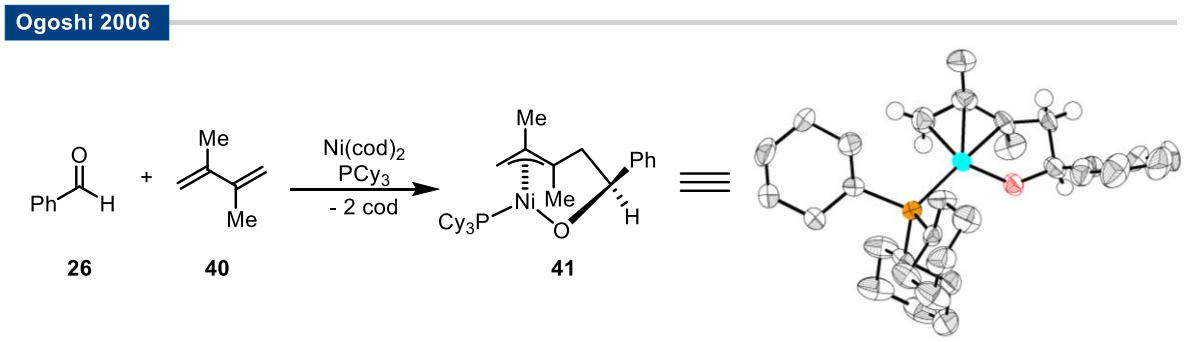

Scheme 13: Preparation and X-ray crystal structure of an allyl-alkoxy-nickel complex by Ogoshi *et al.* (majority of H-atoms omitted for clarity).

Further studies on these homoallylation reactions revealed that diisobutylaluminum acetylacetonate is also an effective reductant in the coupling of dienes bearing terminal aryl

substituents. However, mixtures of linear and branched regioisomers were observed, which limited the utility of this approach.[56] Moreover, the scope of electrophiles was expanded to lactols, aqueous glutaraldehyde and imines.[57-59] Remarkably, these transformations could be carried out in the presence of stoichiometric amounts of water, despite the use of reductants that are typically highly susceptible to hydrolysis, while still affording excellent results.

Over time, several closely related reaction modes have been developed. The established system comprising low-valent nickel, 1,3-dienes and alkylborane or alkylzinc reagents has been successfully applied in multicomponent couplings, enabling the efficient construction of complex molecular architectures.[60-65] More recently, ligand-controlled diene-coupling reactions employing alternative promoters such as diboranes,[66, 67] silylboranes,[68] or aryl-boronic acids,[69-71] as well as reductant-free protocols[72] have emerged.

1.2.3 Enantioselective Intermolecular Reductive Couplings

Despite the versatility of nickel-catalyzed reductive coupling reactions of 1,3-dienes, asymmetric versions remain rare and have been described as a "largely unresolved challenge" in a recent review.[73]

A first breakthrough was reported in 2007 by Zhou *et al.* who utilized the spirobiindane phosphoramidite ligand **L3** to achieve the first example of an enantioselective "Tamaru-type" homoallylation reaction (Scheme 14).[74] Although excellent enantiomeric excesses were obtained, the scope of the reaction remained very limited, as only diene **42** was compatible with the asymmetric reaction mode and only a narrow range of aromatic aldehydes was investigated.

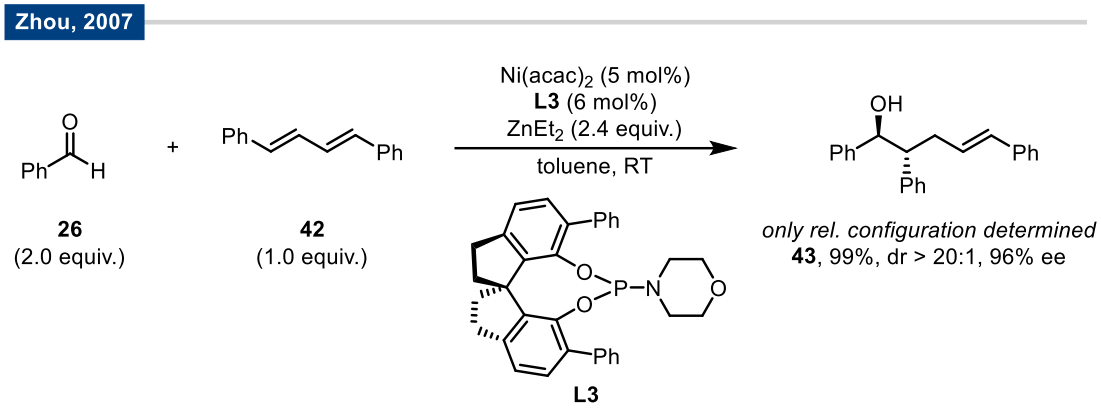

Scheme 14: First example of an enantioselective "Tamaru-type" coupling reported by Zhou *et al.*

In the same year, Saito and co-workers reported the first asymmetric silane-promoted "Mori-type" coupling of 1,3-dienes and aldehydes (Scheme 15).[75] Instead of phosphorus-based ligands, the chiral NHC-ligand **L4** was employed, enabling high enantioselectivities, while maintaining precise control over the alkene geometry, in analogy to the racemic variant reported by Mori *et al.*[49] Although aliphatic aldehydes could be used, high enantioselectivities were again restricted to diene **42**, while utilization of alternative dienes resulted in a marked decrease in selectivity.

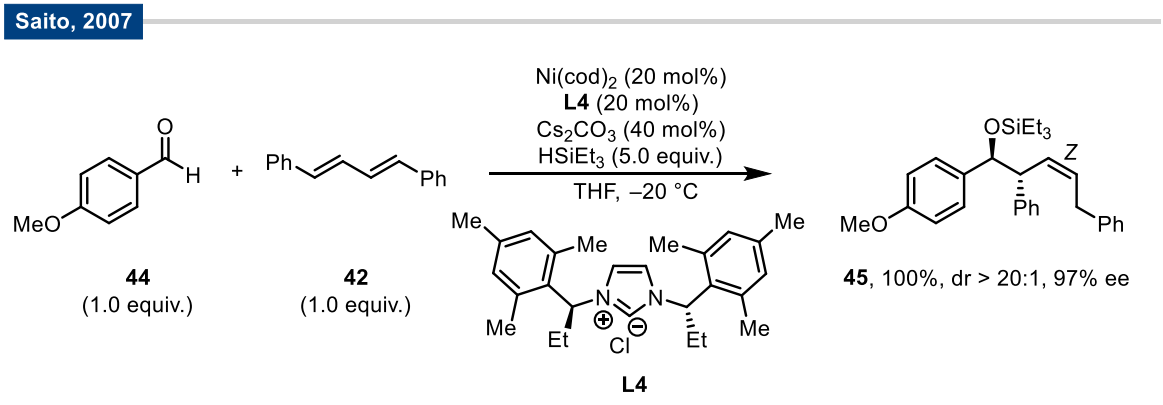

Scheme 15: First example of an enantioselective "Mori-type" coupling reported by Saito *et al.*

More recently, Xiao and co-workers have addressed some of these limitations by developing an enantioselective and stereoconvergent silane-promoted coupling of (*Z*,*E*)-1,3-dienes with aldehydes, providing access to chiral *Z*-homoallylic alcohols (Scheme 16).[76] Using a modified

chiral NHC ligand, the method tolerates a broader range of terminally substituted dienes, including not only aryl-derivatives, but also aliphatic, ester- and amide-substituted analogs.

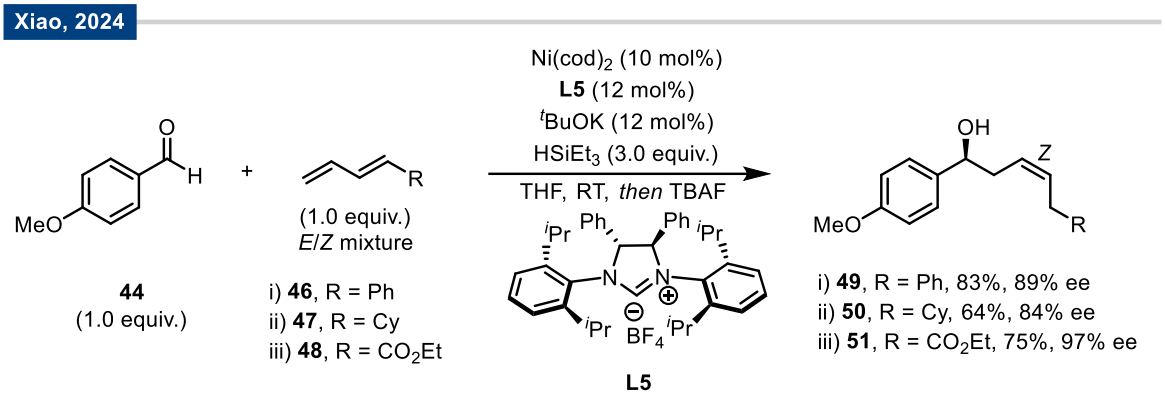

Scheme 16: Enantioselective stereoconvergent "Mori-type" coupling reported by Xiao *et al.*

Almost identical reaction conditions were also utilized by Wang *et al.* for the reductive coupling reactions with oxetane-fused dienes, although in that case, the position of the double bond was retained (Scheme 17).[77]

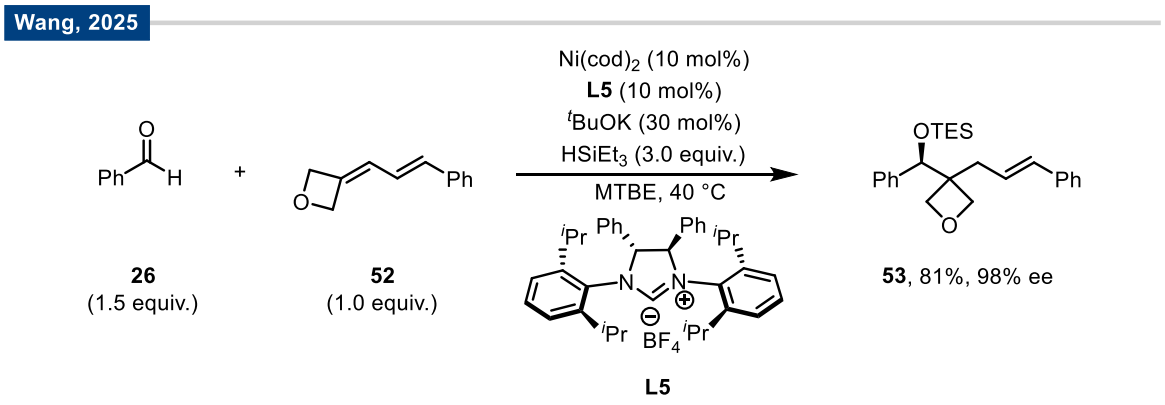

Scheme 17: Enantioselective "Mori-type" coupling of oxetane-fused dienes reported by Wang *et al.*

In addition to these developments, asymmetric reductive coupling reactions employing alternative promoters have been explored. In 2012, Sato *et al.* reported a three-component coupling of 1,3-dienes and aldehydes using silylboranes (Scheme 18).[78] While excellent enantioselectivities and exclusive 1,3-*syn* diastereoselectivity were achieved for the resulting allylsilane derivatives, the substrate scope remained limited, as only diene **20** was well compatible with the asymmetric reaction mode.

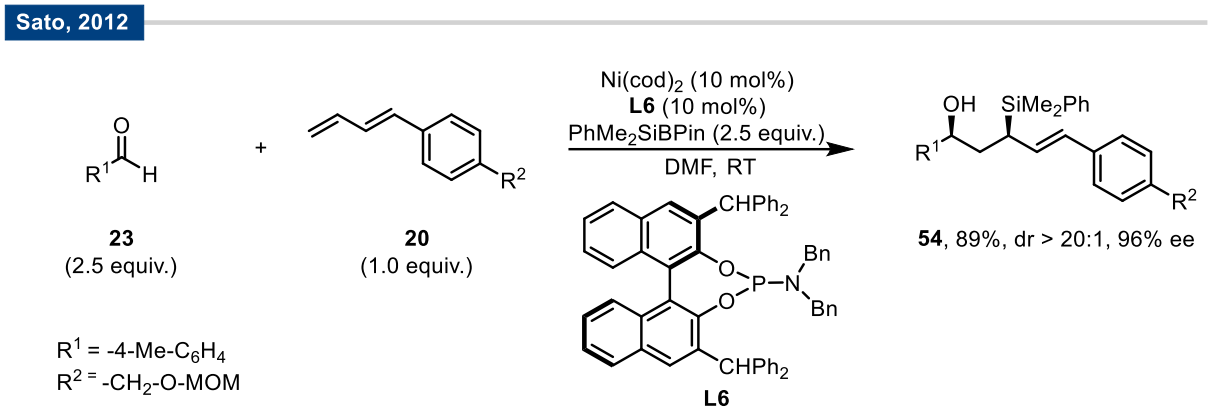

Scheme 18: Enantioselective silylative coupling between aldehydes and dienes reported by Sato *et al.*

Following the initial discovery of diborylative coupling reactions by Morken *et al.*,[66, 67] Xiao and co-workers recently revisited this transformation with the aim of developing an asymmetric variant. By employing the chiral spiro phosphine-oxazoline ligand **L7**, the group was able to obtain the corresponding diol products after oxidative work-up with excellent stereocontrol (Scheme 19).[79]

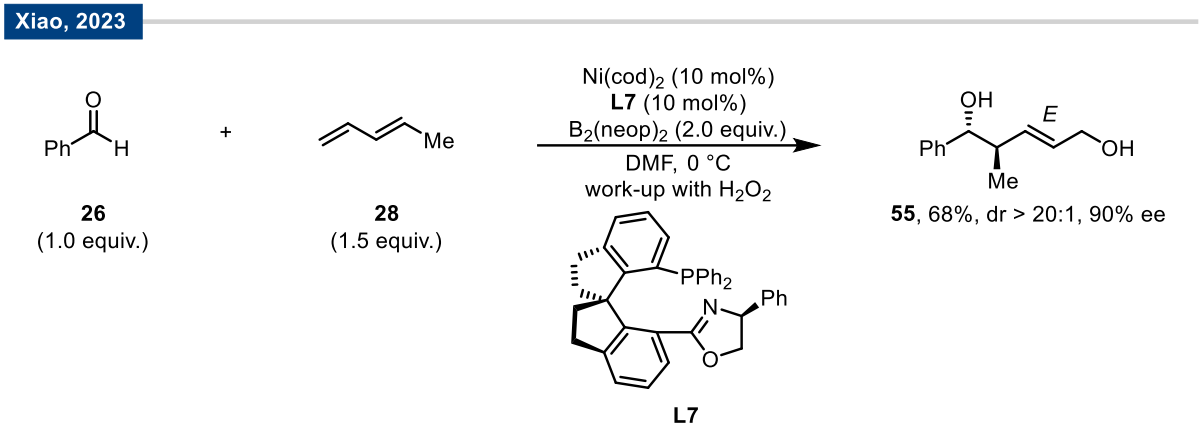

Scheme 19: Enantioselective borylative coupling between aldehydes and dienes reported by Xiao *et al.*

The method exhibits a broad substrate scope with respect to both the aldehyde and the diene. In addition to (*E*)-1,3-pentadiene **28**, a variety of mono-substituted dienes was well compatible, affording the corresponding products in excellent 1,2-*anti* selectivity. Utilization of (*Z*)-1,3-pentadiene resulted in the formation of the complementary 1,2-*syn* product, successfully demonstrating that the inherent diastereospecificity of nickel-catalyzed diene couplings can be translated into the asymmetric realm. Notably, the addition of an exogenous ligand provides effective regiocontrol, as in contrast to the ligand-free reductive coupling reported by Tamaru (see Chapter 1.2.2), selective reaction at the substituted terminus of the diene was observed in the presence of PCy_3 or chiral ligand **L7**.

Shortly thereafter, the utility of **L7** was extended to three-component couplings with boronic acids, building on earlier reports.[69-71, 80, 81] This approach enables a modular and efficient synthesis of polyketide motifs from readily available starting materials while maintaining broad substrate scope with respect to both the diene and the aldehyde (Scheme 20).[81]

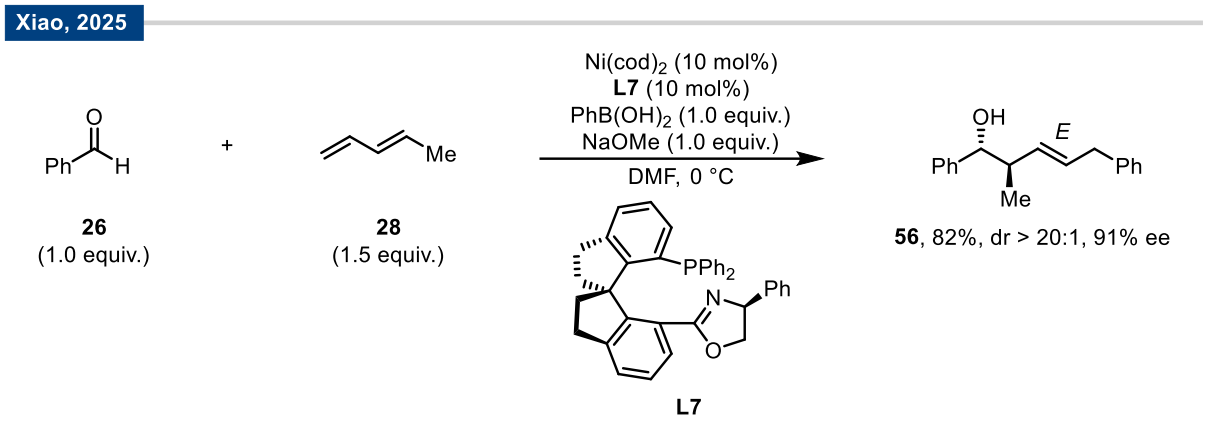

Scheme 20: Enantioselective three-component coupling between aldehydes, dienes and boronic acids reported by Xiao *et al.*

Most recently, Xiao *et al.* reported the first asymmetric, redox-neutral nickel-catalyzed coupling of 1,3-dienes and aldehydes utilizing the novel diamidophosphite ligand **L8** (Scheme 21).[82] Importantly, methanol not only serves as the cosolvent in this transformation, but also promotes ring-opening of the allyl-oxanickelacycle intermediate formed after oxidative cyclization. Subsequent ligand-to-ligand hydrogen transfer regenerates the diene moiety in the product, while simultaneously eliminating the need for an external reductant to close the catalytic cycle. This method provides access to a wide variety of chiral dienols with excellent enantioselectivity, representing an efficient and atom-economical alternative to the use of preformed dienylmetal reagents.

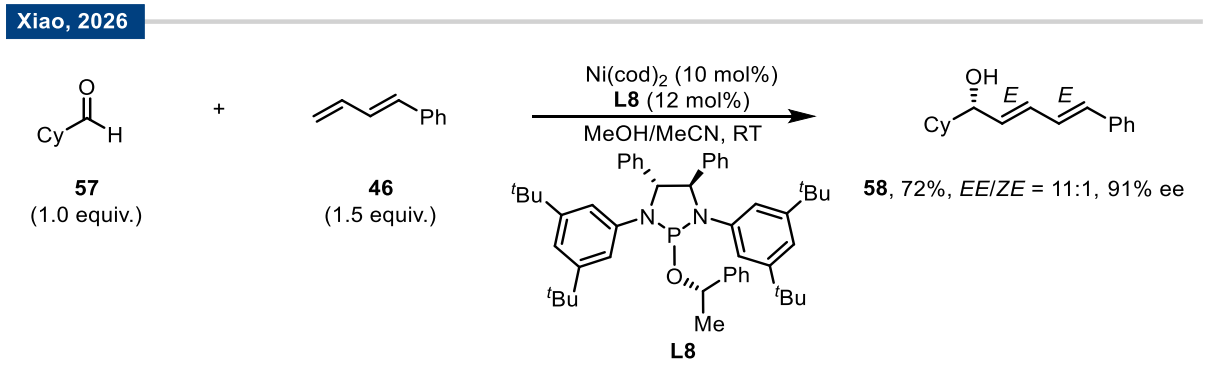

Scheme 21: Enantioselective redox-neutral coupling between aldehydes and dienes reported by Xiao *et al.*

Despite these significant advances, most methodologies for the enantioselective nickel-catalyzed coupling of 1,3-dienes and aldehydes remain limited to relatively simple dienes bearing one or two alkyl or aryl substituents. The incorporation of heteroatom-containing functional groups typically leads to diminished reactivity and reduced enantioselectivity or has simply not been explored at all. Consequently, the development and application of new diene substrates bearing synthetically relevant functional groups, particularly those applicable to natural product synthesis and pharmaceutical development, remains an important and largely unmet challenge. Addressing these limitations is expected to substantially enhance the synthetic utility and enable a broader applicability of nickel-catalyzed diene coupling reactions.

1.2.4 Enantioselective Regioinverted Reductive Couplings

During a total synthesis campaign of the natural product Chagosensine,[83, 84] our group successfully utilized the "Tamaru homoallylation reaction", despite its limited application in natural product synthesis.[85] In particular, the coupling of D-ribose-derived aldehyde **59a** with isoprene **13** was performed under modified conditions in the presence of phosphoramidite ligand **L9a** to enhance both the reactivity and diastereoselectivity of the reaction (Scheme 22).[84] Despite extensive ligand screening, catalyst control remained minimal, and the stereochemical outcome was dominated by intrinsic substrate bias favoring "Felkin-Ahn" addition. This observation contrasts with Tamaru's report that "the homoallylation does not follow the Cram model (or Felkin-Ahn model)".[51]

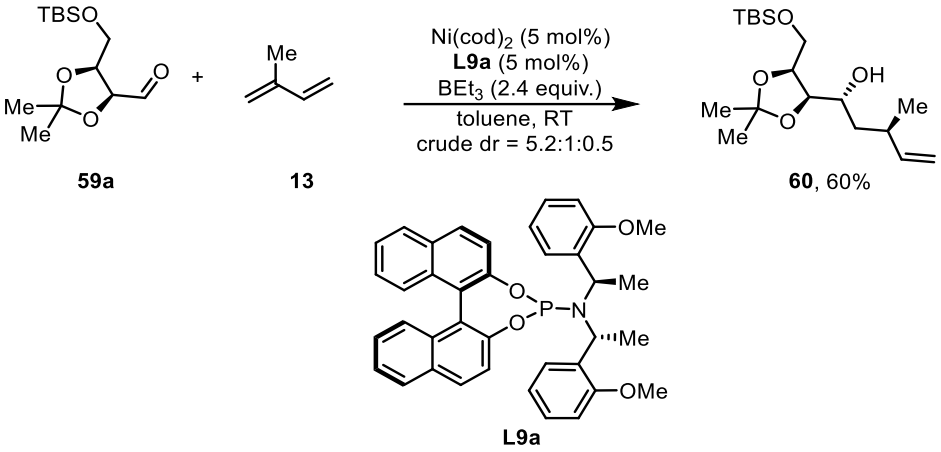

Scheme 22: Utilization of a "Tamaru-type" homoallylation reaction during the total synthesis of Chagosensine.[84]

Importantly, an unexpected observation was made during the optimization of the modified, ligand-assisted homoallylation. When chiral aldehyde **59b** was subjected to coupling with silyl dienol ether **33** in presence of phosphoramidite ligand **L9b**, the expected product resulting from reaction at the unsubstituted diene terminus was not observed. Instead, small amounts of an unexpected regioisomer **61**, arising from reaction at the siloxy-substituted end of the diene, were isolated as a single diastereomer (Scheme 23).

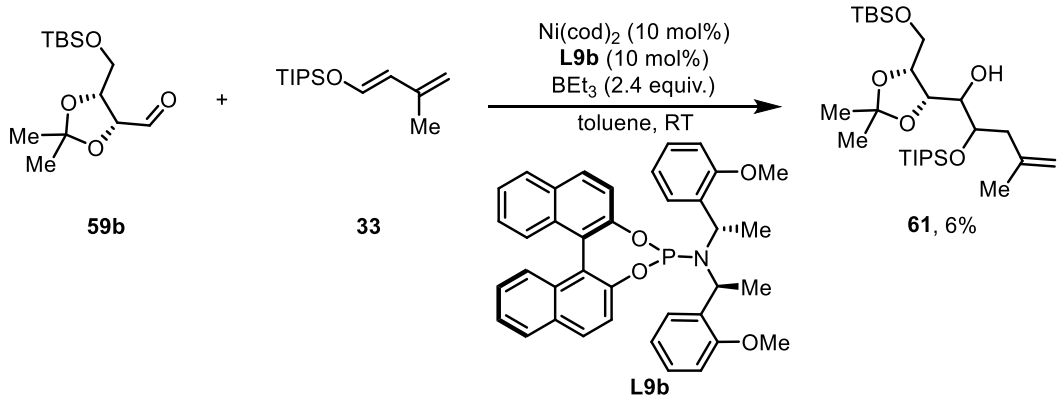

Scheme 23: Unexpected regioisomer formation in a reductive coupling involving a silyl dienol ether.[86]

Although silyl dienol ethers such as **33** represent the least reactive class of dienes investigated by Tamaru *et al.* in their initial studies (see Chapter 1.2.2), they typically react selectively at the unsubstituted terminus due to its higher electron density and steric accessibility. While the observed regiochemical outcome was unexpected, the value of such an "*iso*-Tamaru reaction", arising from the isomeric nature of the product, was immediately apparent. Further investigation of this reactivity therefore appeared highly worthwhile. A general method for the enantioselective synthesis of pre-differentiated 1,2-diols was deemed highly attractive, as access to such compounds is limited and largely relies on glycolate aldol reactions based on chiral auxiliary systems or related reactions.[84, 86-89]

In order to establish this desired reactivity, a more systematic ligand screening was undertaken.[90] Using hydrocinnamaldehyde as a model substrate, a range of sterically and electronically diverse ligands was evaluated. Many of these candidates had already been tested during the earlier optimization of the "Tamaru homoallylation" in the Chagosensine synthesis. Notably, the reaction did not proceed under the ligand-free "Tamaru-type" conditions, likely owing to the relatively low reactivity of both hydrocinnamaldehyde and silyl dienol ethers, as previously reported.[51, 52]

In many cases, however, the addition of an exogenous ligand did not only significantly enhance reactivity but also consistently led to preferential reaction at the siloxy-substituted-terminus of the diene. This effect was not limited to sophisticated ligand systems, but was also observed with simple ligands such as PPh_3, which had already been employed in the earliest works in the field by Mori and co-workers. These findings suggested that ligand effects in nickel-catalyzed homoallylation reactions had largely been overlooked and could offer substantial opportunities if systematically explored.

During ligand optimization, cyclodiphosphazane ligands were identified as particularly effective in inverting the regiochemical outcome of the reaction. These bis-monodentate ligands had previously been successfully employed by Gade *et al.* in the nickel-catalyzed reductive coupling of benzaldehyde and 1,4-diphenylbutadiene **42**, achieving enantiomeric excesses of up to 84%.[91]

However, despite screening approximately 40 different chiral cyclodiphosphazanes for the coupling of hydrocinnamaldehyde and silyl dienol ether **33**, the enantioselectivity remained moderate. No ligand was identified that simultaneously provided high regio-, diastereo-, and enantioselectivity along with full conversion. Cyclodiphosphazane **L10** fulfilled three of these four key criteria, enabling full conversion in the model reaction and affording the desired coupling product **63a** as a single regioisomer with excellent diastereoselectivity (Scheme 24, top). Unfortunately, enantioselectivity remained limited, as the homoallylation product was obtained with merely 36% ee.

Using the racemic version of ligand **L10**, the reaction scope was explored. The transformation performed exceptionally well with a range of silyl protecting groups of varying steric demand and diverse aliphatic, aromatic, and even α,β-unsaturated aldehydes could be used (Scheme 24, bottom).[86]

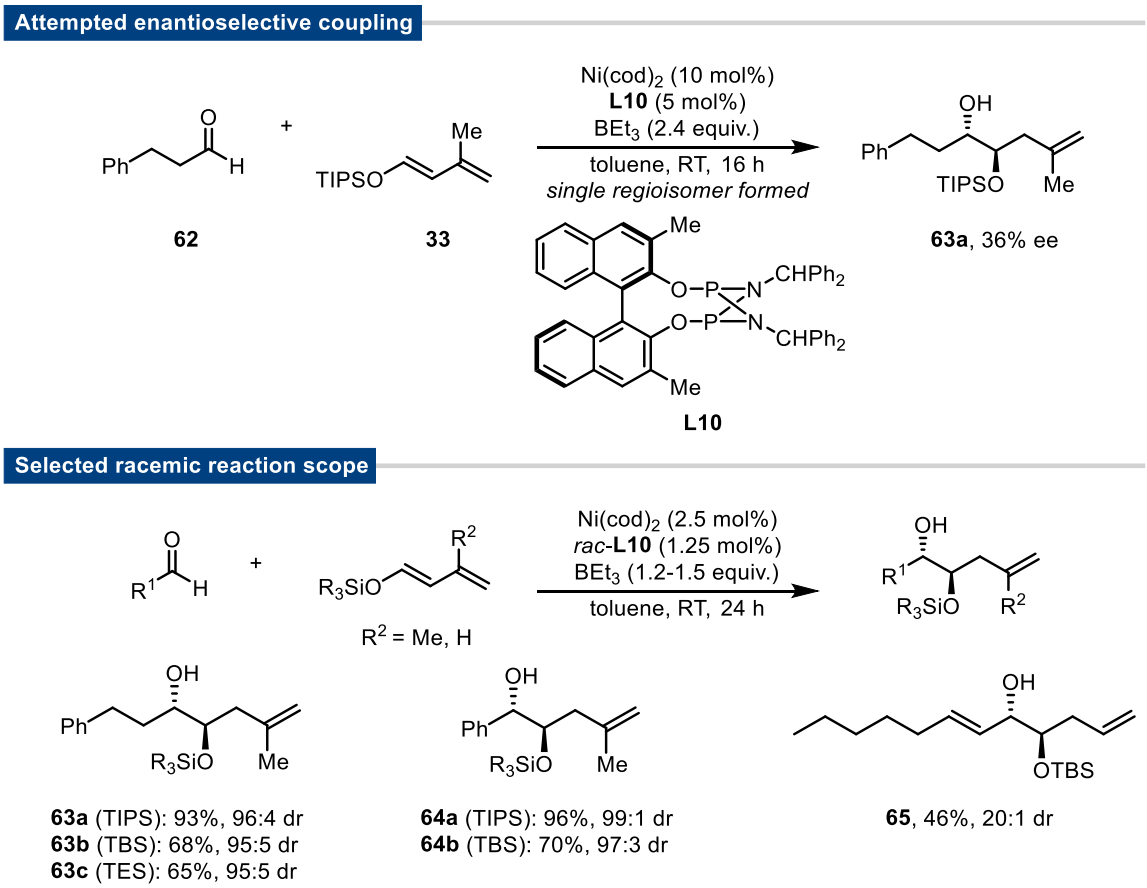

Scheme 24: Selected examples for the enantioselective and racemic nickel-catalyzed coupling of silyl dienol ethers with aldehydes in the presence of a cyclodiphosphazane ligand.

Convinced by the scope and utility of the reaction, our group revisited the ligand design to develop an asymmetric variant. To this end, phosphoramidite ligands with different chiral backbones were evaluated in a model reaction. Despite their track-record in nickel-catalyzed asymmetric reductive couplings of dienes and aldehydes, ligands based on SPINOL[74] and BINOL[78] backbones exhibited low yields as well as poor diastereo- and enantioselectivities.

It was hypothesized, that the location of the chiral cleft on the backside of these ligands was responsible for the low level of enantioinduction. Enlarging the major groove on the front side of the ligand could hence be beneficial (Figure 3). Such a modification was expected to create a helically chiral environment around the nickel center, potentially enhancing enantioselectivity.

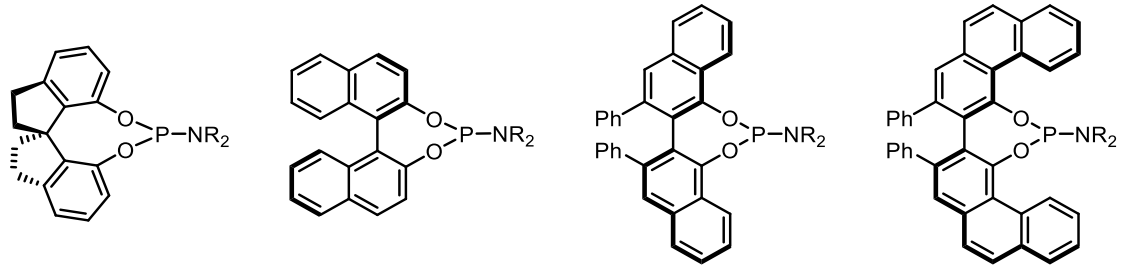

Figure 3: Structural comparison of phosphoramidite ligands derived from different diol backbones (corresponding diol backbones from left to right: SPINOL, BINOL, VANOL, VAPOL).

To test this hypothesis, analogous ligand candidates derived from axially chiral VANOL and VAPOL were prepared.[92, 93] Both ligands improved enantioselectivities compared to the SPINOL- and BINOL-based candidates, but only the VAPOL-derived ligand addressed all the issues associated with the reaction and achieved the highest enantioselectivity. This represents one of the few examples of a VAPOL-derived phosphoramidite in homogeneous catalysis and the first reported use in nickel catalysis.[94-96] Further screening of the amine moiety identified the Et_2N-derivative **L11** as the most effective ligand for the reductive coupling. After additional optimization of the reaction temperature and catalyst loading, a general reaction protocol was established (Scheme 25).

The asymmetric reaction proved compatible with a variety of aldehydes, achieving up to >90% ee for both aliphatic and aromatic substrates. Furthermore, the reaction exhibited complete regiocontrol and excellent diastereoselectivity. Moreover, it was highly diastereospecific: *E*-configured dienol ethers afforded *anti*-1,2-diols, whereas *Z*-configured analogs resulted in the formation of *syn*-1,2-diols, while maintaining excellent enantioselectivities. Notably, this methodology has recently been utilized by Chen and co-workers in the total synthesis of the proposed structure of the macrolide Neaumycin B, highlighting its applicability for the preparation of complex target structures.[97]

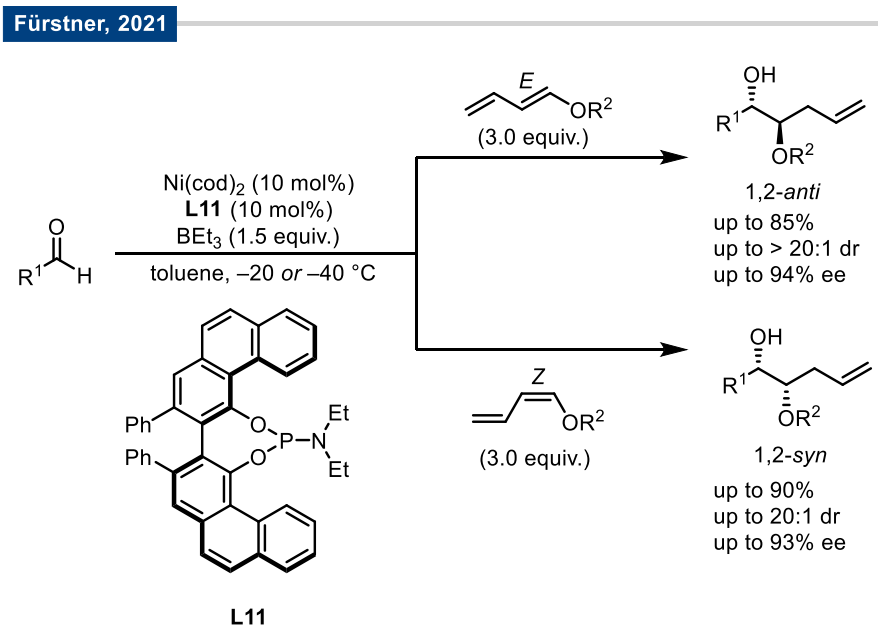

Scheme 25: Nickel-catalyzed enantioselective synthesis of pre-differentiated homoallylic *syn*- or *anti*-1,2-diols from aldehydes and dienol ethers.

It was hypothesized why the addition of an exogenous ligand has such a drastic impact on the reaction outcome.[86, 90] The catalytic cycle is believed to follow the elementary steps previously proposed by Tamaru *et al.* (see Chapter 1.2.2). Accordingly, the reaction proceeds through coordination of the aldehyde, diene and an additional ligand **L** to the nickel center, forming a (pseudo)tetrahedral 18e$^-$ complex. The relative orientation of the diene with respect to the aldehyde is largely controlled by the steric demand of the ligand.

Under Tamaru's conditions, the additional ligand **L** at the nickel center is a small solvent molecule (*e.g.* THF, toluene). In this case, no significant steric interaction between the bulky siloxy-group of the diene and **L** is expected. Therefore, both orientations – siloxy group facing toward **L** (Scheme 26, top) or away from **L** (Scheme 26, bottom) – are possible. Oxidative cyclization, however, proceeds significantly faster when the unsubstituted diene terminus faces the aldehyde, as this terminus is more electron-rich and dienes strongly prefer reaction at this position under ligand-free conditions.[51] Addition at the substituted terminus may not be kinetically feasible under Tamaru's ligand-free conditions, hence the reaction proceeds exclusively along the usual regiochemical course.

Addition of an exogenous ligand introduces steric bulk at the metal center and has been shown to significantly increase reactivity, enabling reaction at the least nucleophilic position of the diene.[86, 90] Relatively slim ligands such as PPh_3 resulted in mixtures of regioisomers, whereas bulkier ligands led to full inversion of the regiochemical outcome. This is presumably due to the diene orienting the siloxy-group away from **L** to reduce steric clashing (Scheme 26, bottom). Following oxidative cyclization, the catalytic cycle would then proceed, yielding the regioisomeric "*iso*-Tamaru product". Nonetheless these arguments remain purely speculative.

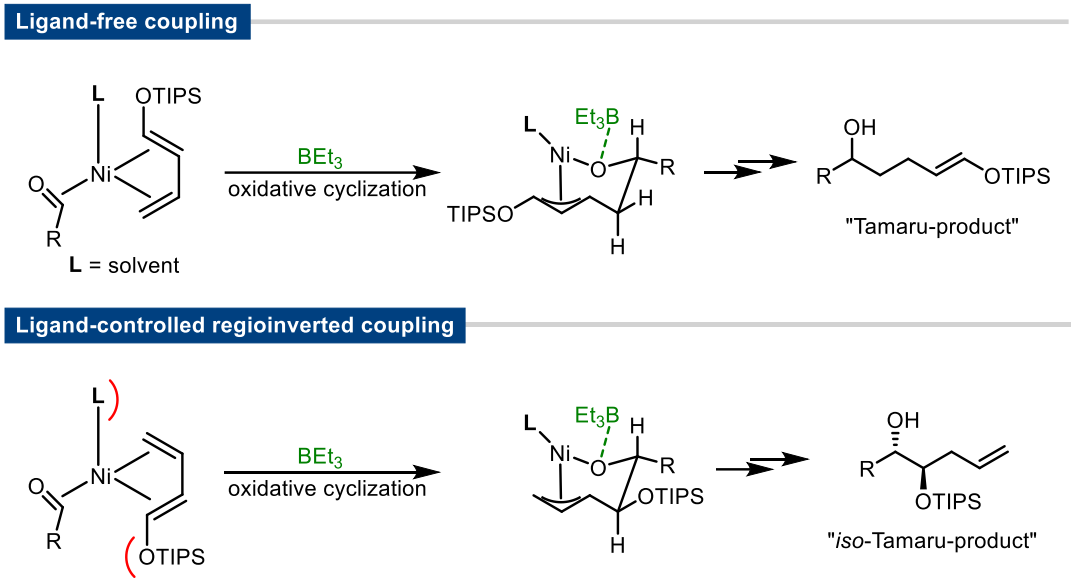

Scheme 26: Simplified model explaining steric effects of the ligand on the regiochemical course of the reductive coupling.

As Tamaru and co-workers had already shown that imines can undergo reductive coupling reactions with isoprene and related 1,3-dienes,[58] our group investigated whether this reactivity could be extended to silyl dienol ethers. Gratifyingly, a synthetic protocol for the reductive coupling of tosyl-protected imines with silyl dienol ethers was established.[98]

In analogy to the coupling with aldehydes, the reaction proceeded under an inverted regiochemical course in the presence of VAPOL-derived phosphoramidite ligand **L11**. While reactions involving aliphatic imines exhibited slightly diminished enantioselectivities, aromatic imines were fully compatible with the method and the corresponding *syn*-configured vicinal

amino alcohol derivatives were obtained in excellent diastereo- and enantioselectivity (Scheme 27).

Interestingly, the addition of stoichiometric amounts of degassed water proved essential, significantly increasing reactivity while also suppressing double-bond isomerization and thereby preventing the formation of the corresponding regioisomer. While it has been shown previously, that related reductive couplings can tolerate water,[57-59] the precise reason for its pronounced effect on the reaction outcome remains unknown.

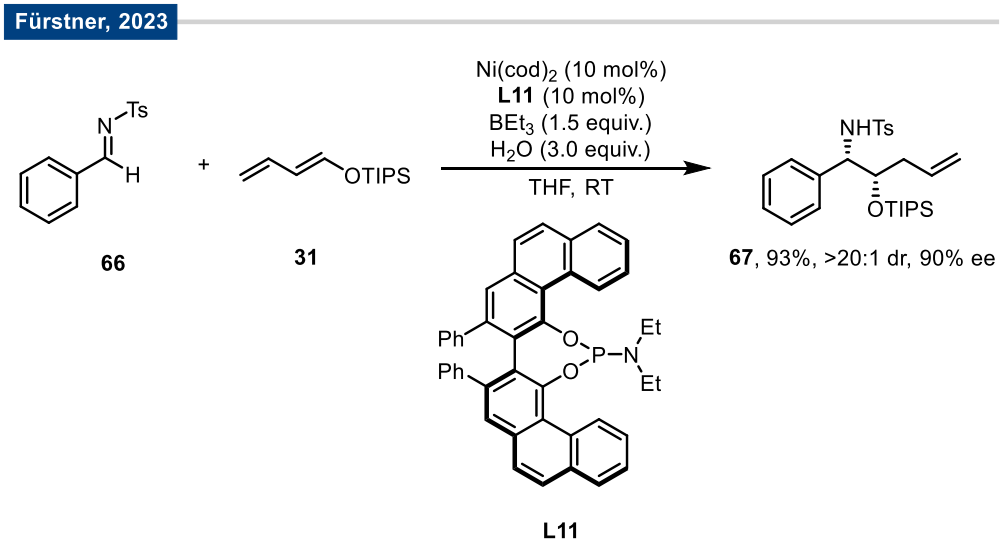

Scheme 27: Nickel-catalyzed enantioselective coupling of protected imines and silyl dienol ethers.

In addition to variation of the electrophile, alternative dienes were explored to further investigate the scope of the asymmetric, regioinverted nickel-catalyzed coupling reactions. A variety of dienes previously employed in the racemic "Tamaru homoallylation" were examined, revealing that electron-deficient methyl sorbate was exceptionally well-suited to the novel reaction conditions. As with silyl dienol ethers, the regiochemical course was completely inverted in the presence of chiral ligand **L11**, with the diene reacting at the least nucleophilic site to yield deoxypropionate-type products in excellent yield and enantioselectivity (Scheme 28).[99]

In contrast to the couplings of aldehydes and dienol ethers, this reaction could typically be performed at ambient temperature with reduced catalyst loading, owing to the higher reactivity of methyl sorbate. Moreover, the highly sensitive $Ni(cod)_2$ could be replaced with bench-stable nickel-stilbene precatalysts developed by Cornella and co-workers,[9, 10] allowing for a more convenient setup.

The reaction showed broad scope with respect to both aldehydes and dienes: (*E*,*E*)-methyl sorbate gave excellent 1,2-*anti* selectivity, whereas (*E*,*Z*)-methyl sorbate afforded *syn*-configured products selectively. Other diene derivatives bearing ester, amide, or pinacolboronate (BPin) groups at the distal end also provided satisfactory results. Furthermore, the methyl group at the reacting diene terminus could even be replaced with a CF_3-group without compromising enantioselectivity or regiocontrol.

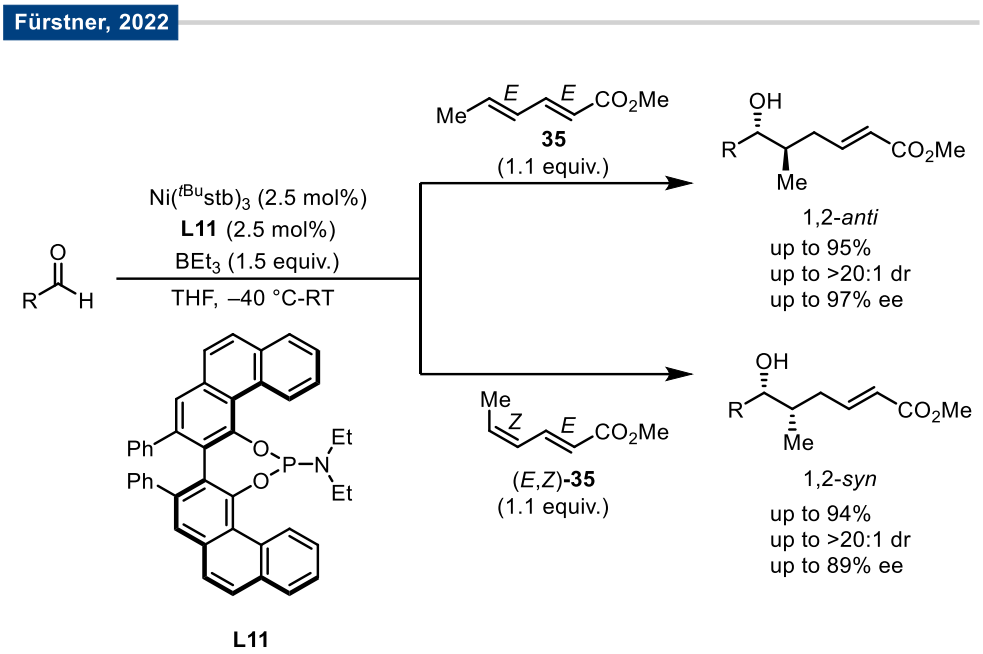

Scheme 28: Nickel-catalyzed enantioselective coupling of aldehydes and methyl sorbate.

Overall, these studies on asymmetric nickel-catalyzed reductive couplings between 1,3-dienes and aldehydes or imines highlight the broad applicability and synthetic utility of this novel reaction mode. The VAPOL-derived ligand **L11** is uniquely effective in altering the regiochemical outcome and exerting enantiocontrol among a wide set of ligand candidates. The combination of nickel(0) and **L11** accommodates a variety of substitution patterns on the butadiene framework, effectively coupling both electron-rich and electron-deficient dienes. Future efforts should focus on further broadening the scope of this transformation, which already shows promising generality with respect to the substrate.

1.3 Occurrence, Application and Enantioselective Synthesis of Vicinal Amino Alcohols

Vicinal amino alcohols, also referred to as 1,2-amino alcohols or β-amino alcohols, represent an important class of bifunctional molecules featuring vicinal amino (-NH_2, -NHR, -NR_2) and hydroxy (-OH) groups. This structural motif is highly prevalent, occurring in more than 300,000 known compounds,[100] and is of central importance in the fields of natural products, pharmaceuticals, and ligand/catalyst design (Figure 4).[101, 102]

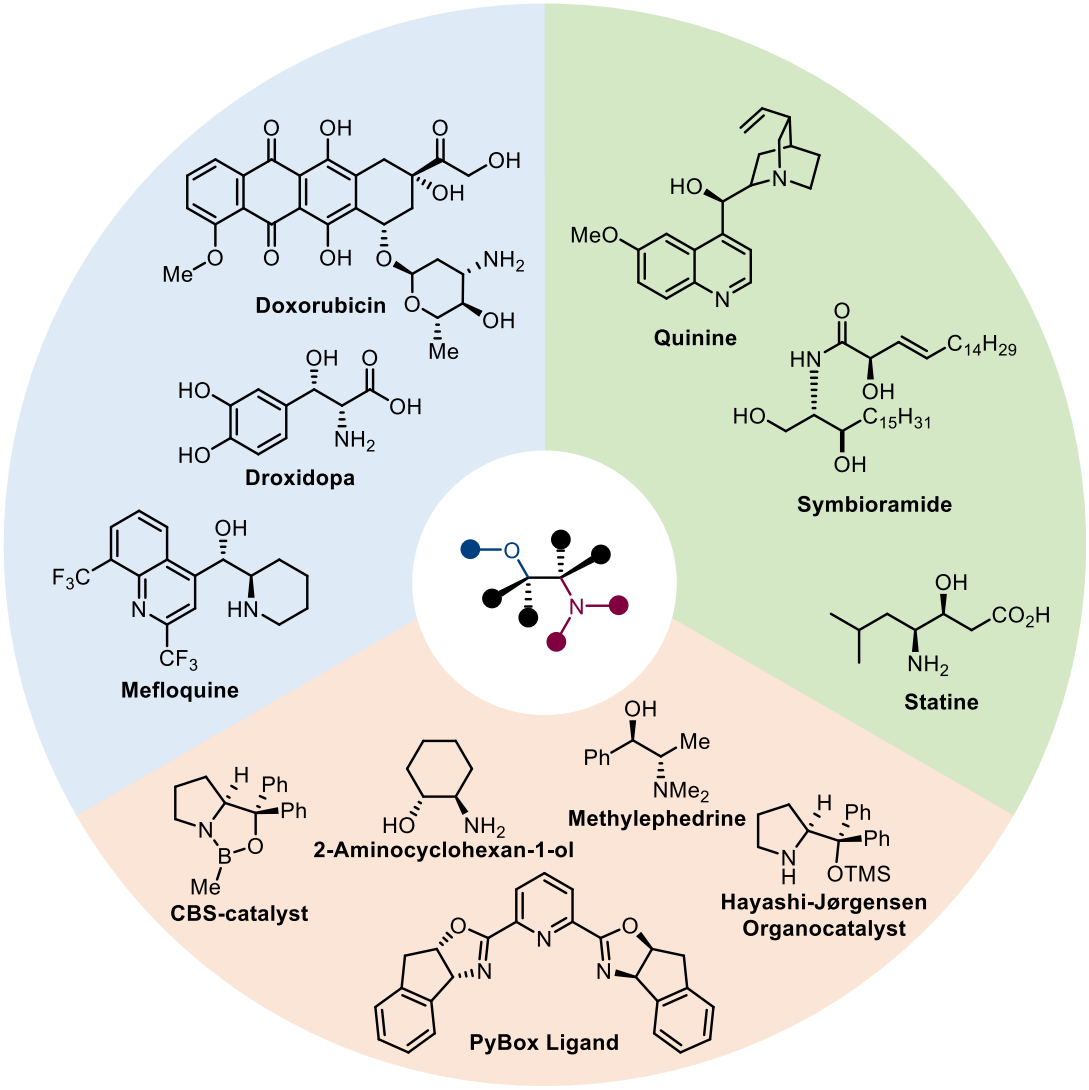

Figure 4: Representative examples for natural products (green), synthetic pharmaceuticals (blue) and ligands/catalysts (orange) containing structural motifs derived from chiral vicinal amino alcohols.

More than 10,000 structures featuring this motif have been isolated from natural sources, underscoring both its structural diversity and functional relevance in biological system.[103]

Representative examples include the alkaloid Quinine, which bears a tertiary amine within a rigid quinuclidine framework. It can be isolated from the bark of the cinchona tree, and has been widely used as a drug for the treatment of Malaria.[104] Sphingolipids, such as Symbioramide, which contain secondary amines, are key constituents of the plasma membrane lipid bilayer of all

eukaryotic cells,[105-108] whereas the natural amino acid Statine bearing a primary amine, is a key structural element responsible for the biological activity of the potent aspartyl protease inhibitor pepstatin.[109, 110]

The pronounced biological activity associated with this motif, has driven its incorporation into novel drugs and drug candidates. For example, Doxorubicin contains a vicinal amino alcohol moiety within its amino sugar subunit Daunosamine and represents one of the most widely used chemotherapeutic drugs for treating various forms of cancer.[111] The synthetic amino acid Droxidopa is a prodrug that is enzymatically converted into norepinephrine in the brain for the treatment of Parkinson's disease,[112] while Mefloquine is a synthetic analog of naturally occurring Quinine used for the prophylaxis and treatment of Malaria.[113]

The spatial proximity of the nitrogen and oxygen containing functional groups in vicinal amino alcohols not only affects their physical properties and conformational behavior[114] but also qualifies them as bidentate ligands, as both the nitrogen- and oxygen-atom exhibit coordinating properties. This has been extensively exploited over the last decades for the development of novel ligands and catalysts based on this motif. Applications range from methylephedrine-mediated asymmetric alkynylation of aldehydes,[115] to the use of 2-aminocyclohexan-1-ol in Suzuki coupling reactions[116] and the development of polydentate PyBox ligands, for homogeneous transition metal catalysis.[117] Moreover, their utility extends to organocatalysis, as exemplified by the versatile Hayashi-Jørgensen catalyst,[118-120] and to reactions based on main-group catalysis, such as the borane-mediated "Corey-Bakshi-Shibata" (CBS) reduction, which employs a chiral amino alcohol-derived oxazaborolidine catalyst.[121]

Given their broad application and relevance, the development of stereoselective methods for the synthesis of vicinal amino alcohols has been a long-standing objective in organic synthesis. Apart from biocatalytic approaches,[122] several transition-metal-catalyzed transformations have been developed since the 1990s. These include, but are not limited to: (i) asymmetric (transfer) hydrogenation, (ii) asymmetric borrowing hydrogen, (iii) asymmetric aminohydroxylation of alkenes, (iv) asymmetric ring-opening of epoxides and aziridines, (v) asymmetric nucleophilic addition to carbonyls/imines, (vi) asymmetric radical coupling, (vii) asymmetric C–H amination through a metal-nitrene and (viii) asymmetric kinetic resolution and desymmetrization. These diverse synthetic strategies have been thoroughly discussed in a recent review.[100]

In addition to this arsenal, asymmetric transition-metal-catalyzed redox-neutral and reductive coupling reactions between electrophiles and π-compounds have recently emerged as alternative, highly effective strategies to access chiral vicinal amino alcohol derivatives in an atom-efficient manner.

In 2019, Krische *et al.* reported an iridium-catalyzed redox-neutral enantioselective allylation of primary alcohols with phthalimido allene **69** (Scheme 29).[123] The method provided access to an array of *anti*-configured vicinal amino alcohols in a highly diastereo- and enantioselective manner. Notably, either primary alcohols or aldehydes can be used, with the former undergoing

irreversible dehydrogenation during the catalytic cycle, forming the corresponding electrophilic aldehyde *in situ*.[123]

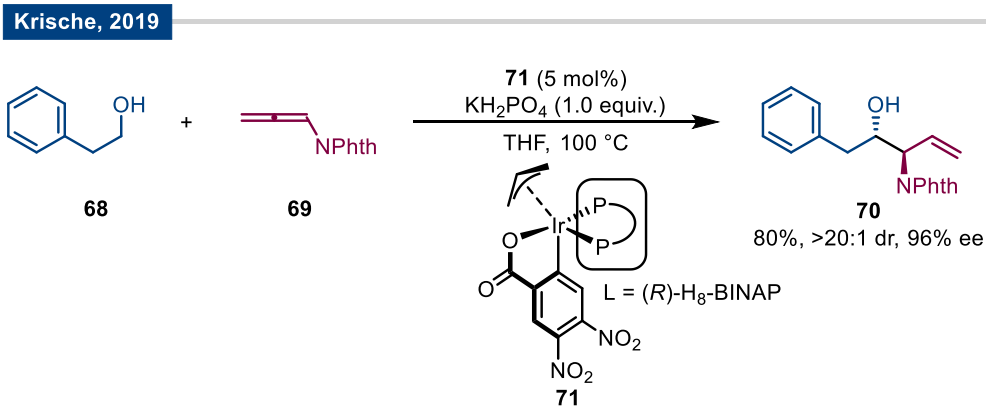

Scheme 29: Iridium-catalyzed enantioselective redox-neutral allylation of a primary alcohol with a phthalimido allene.

In the same year, Sieber and co-workers reported the use of closely related N-protected amino allenes in copper-catalyzed reductive couplings with ketones. Following an initial study employing chiral auxiliary-based allenes in combination with a racemic NHC-ligand,[124] they established improved enantioselective protocols employing achiral allenes.[125, 126] The optimized system, based on $Cu(OAc)_2$/JosiPhos **L12** and methyl-dimethoxysilane as the reductant, afforded chiral amino alcohols with high stereocontrol (Scheme 30, top).[126] More recently, limitations arising from the incompatibility of the *in situ* generated Cu–H species with aldehydes were addressed, enabling their use as electrophiles.[127] In addition, a related borylative coupling of aldehydes with phthalimido allenes further expanded the scope of this methodology.[128]

The utility of copper-hydride chemistry in this area extends beyond protocols involving amino allene derivatives. In 2018, Malcolmson and co-workers reported the enantioselective synthesis of vicinal amino alcohols *via* copper-catalyzed reductive coupling reactions between ketones and 2-azadienes. The reaction proceeds through regioselective hydrometallation of the 2-azadiene, followed by enantioselective addition into the ketone in the presence of chiral phenyl-bisphospholanoethane (Ph-BPE) ligand **L13**.[129] Following imine reduction and alcohol deprotection, the desired *anti*-configured products were obtained with good to excellent levels of diastereo- and enantioselectivity (Scheme 30, middle). Subsequently, the group extended this strategy to related 2-azatrienes in (*Z*)-selective reductive aminoallylation reactions. The established $Cu(OAc)_2$/Ph-BPE system again provided high levels of stereocontrol and a broad variety of *anti*-configured vicinal amino alcohol derivatives was successfully accessed.[130]

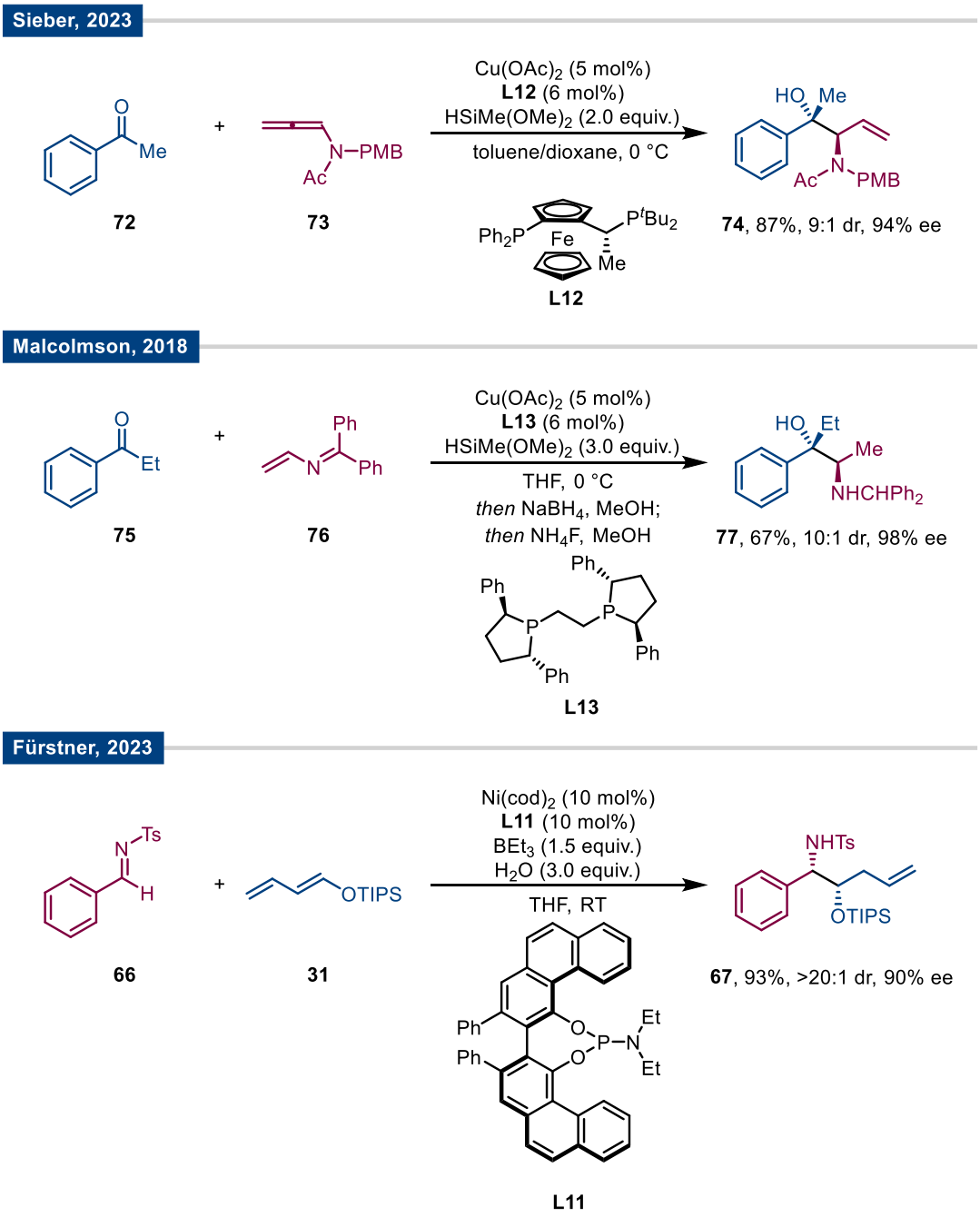

Scheme 30: Representative examples of state-of-the-art reductive couplings for the enantioselective synthesis of vicinal amino alcohol derivatives.

Complementary to these developments, our group has recently established a nickel-catalyzed reductive coupling of N-tosyl imines with silyl dienol ethers, providing regio-, diastereo-, and enantioselective access to a range of *syn*-configured vicinal amino alcohol derivatives in presence of chiral VAPOL-derived phosphoramidite ligand **L11** and triethylborane as reductant (Scheme 30, bottom; also see Chapter 1.2.4).[98] Importantly, the synthetic utility of this novel transformation was demonstrated by the enantioselective synthesis of a key building block for non-peptidic neurokinin NK1 receptor antagonists as well the γ-amino acid Statine.[98]

In conclusion, these redox-neutral and reductive coupling strategies have significantly expanded the synthetic toolbox for accessing vicinal amino alcohols and offer atom-economical alternatives

to classical approaches. Nonetheless, this area remains largely underexplored, with initial reports only appearing in 2018. At the same time, the predominant reliance of these protocols on earth-abundant metals such as copper and nickel illustrates their potential for sustainable stereoselective synthesis of vicinal amino alcohols. Continued advances in this field will be essential to further broaden the scope and applicability of these transformations to access this privileged structural motif.

2 Regioinverted Nickel-Catalyzed Reductive Coupling Reactions for the Enantioselective Synthesis of Vicinal Amino Alcohol Derivatives

2.1 Aim

During recent studies in our group, the combination of nickel(0) and phosphoramidite ligand **L11** has been shown to be uniquely effective in inverting the regiochemical course of reductive coupling reactions while exerting exceptional diastereo- and enantiocontrol. Following the demonstrated compatibility of dienol ethers and sorbate derivatives, it was hypothesized that this novel methodology could be further extended.

Given their prevalence in natural products, pharmaceuticals, and ligands/catalysts, the enantioselective synthesis of vicinal amino alcohols appeared worthwhile to pursue. A first possible approach – the coupling of imines with dienol ether derivatives – had already been investigated by our group. However, several limitations were identified, including restrictions regarding the N-protecting group, diminished enantioselectivities in reactions involving aliphatic imines, and the inability to access *anti*-configured products.[98]

A second, regiocomplementary strategy, was therefore envisaged in which the amine moiety is installed on the diene fragment (Scheme 31). Coupling of such amine-substituted dienes with aldehydes would result in the formation of vicinal amino alcohols with an alternative constitution and potentially also complementary configuration.

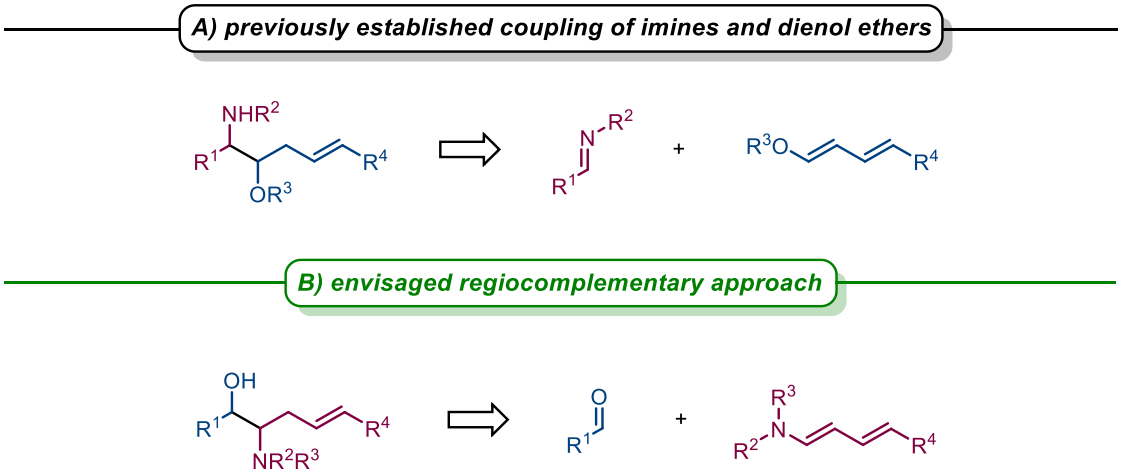

Scheme 31: Complementary approaches for the synthesis of vicinal amino alcohols *via* reductive coupling reactions.

While in related iridium- or copper-catalyzed coupling reactions, the amine moiety/nitrogen-atom is typically located on the π-compound (see Chapter 1.3), an analogous approach had not been reported for nickel. Consequently, the successful implementation of such previously unexplored dienes would not only provide access to the desired amino alcohol products, but also introduce an entirely distinct class of 1,3-dienes into the realm of nickel-catalyzed reductive couplings, an aspect that has been largely overlooked since the seminal work of Tamaru.

2.2 Preliminary Results and Rationale for Substrate Design

In this chapter a preliminary catalytic reaction by Dr. Jae Yeon Kim as well as results from a diene screening from a previous project by Dr. Thomas Q. Davies were included, as they provide a better understanding for the early-stage development of this project.

The investigations began by designing the envisaged amine-substituted dienes for the synthesis of the targeted vicinal amino alcohol derivatives. To this end, previous observations regarding the reactivity of silyl dienol ethers were used as a basis (Figure 5). Under ligand-free "Tamaru-type" conditions, these dienes reacted exclusively at the unsubstituted terminus,[51] whereas in the presence of phosphoramidite ligand **L11**, the regiochemical course was reversed and the coupling occurred at the siloxy-substituted end of the diene.[90] Based on the hypothesis that this reversal is primarily governed by steric clashing of the bulky ligand and the silyl protecting group (see Chapter 1.2.4), the structural design of the silyl dienol ethers was extrapolated to literature-known N-Boc-substituted diene **78**.[131]

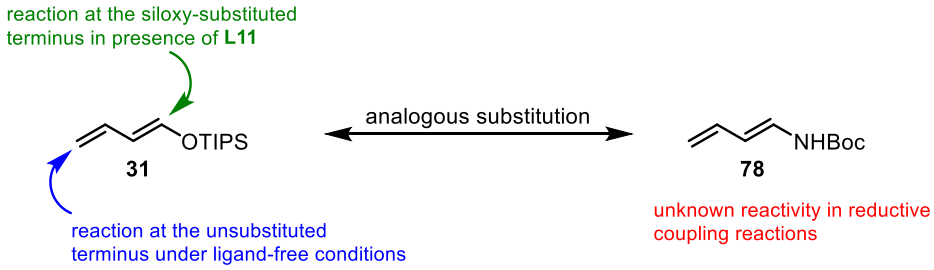

Figure 5: Rationale for the initial substrate design.

In analogy to silyl dienol ether **31**, dienecarbamate **78** is only substituted at one terminus, resulting in markedly different steric accessibility of the two ends of the diene. Although the Boc-protecting group is partially sp^2-hybridized, it was still expected to exert effective control over the regioselectivity due to its sterically demanding *tert*-butyl substituent. To test this hypothesis, the asymmetric regioinverted reductive coupling reaction between benzaldehyde and diene **78** was attempted under the previously established conditions (Scheme 32).

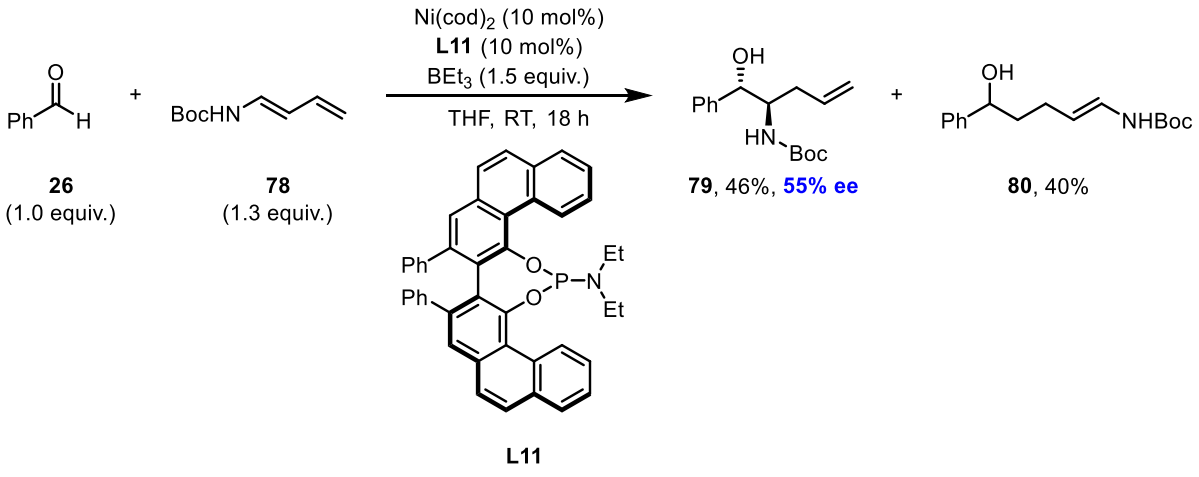

Scheme 32: Reductive coupling of benzaldehyde and dienecarbamate **78** (initial test reaction carried out by Dr. J. Y. Kim; later repeated by the author).

The N-Boc-substituted diene, which had not been employed in comparable transformations before, exhibited good reactivity, and full conversion of benzaldehyde was observed within 18 hours. However, the reaction displayed low regiocontrol, affording both the desired vicinal amino alcohol **79** and its regioisomer **80** in almost equal yields. Furthermore, the enantioselectivity of the reaction was limited as **79** was obtained in a moderate enantiomeric excess of 55%.

Notwithstanding, the experiment demonstrated that N-carbamate substituted dienes are generally compatible with nickel-catalyzed reductive couplings, prompting further efforts toward reaction optimization. At the same time, it became apparent that the current mechanistic picture (see Chapter 1.2.4) is oversimplified and that the observed regioselectivity cannot be rationalized solely by steric effects. To avoid a second, time- and labor-intensive ligand screening campaign aimed at identifying a ligand capable of addressing the multiple selectivity challenges associated with this transformation, the design of the diene was modified to improve its compatibility with phosphoramidite ligand **L11**.

Previous screenings of suitable diene candidates in our group had revealed important effects of the substrate design on both regio- and enantioselectivity (Scheme 33).[99, 132] For instance, reaction of hydrocinnamaldehyde with 1,3-pentadiene **28** afforded the corresponding product **82** with moderate regioselectivity (rr = 4:1) and enantioselectivity (78% ee). In contrast, formal introduction of a methyl ester group, through replacement of 1,3-pentadiene **28** with methyl sorbate **35**, resulted in exclusive formation of the desired product **83** (rr > 20:1) with excellent enantioselectivity (96% ee). Phenyl-substituted dienes **46** and **81** exhibited invariably poor regioselectivity but demonstrated a similarly pronounced effect on enantioselectivity, as introduction of a methyl ester group increased the enantiomeric excess of product **85** by more than 30% compared to the unsubstituted analog **84**.

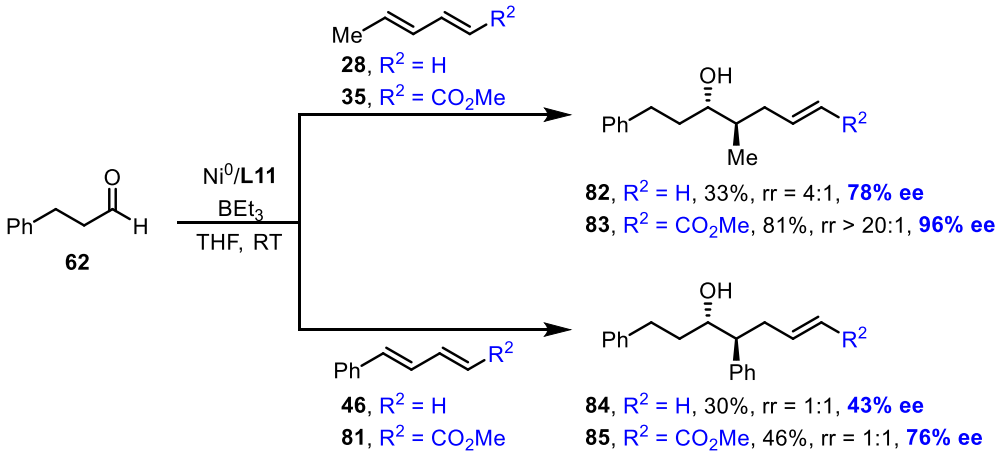

Scheme 33: Effect of CO_2Me-groups on regio- and enantioselectivity observed by Dr. Thomas Q. Davies.[132]

Based on these prior observations, an improved substrate design was devised (Figure 6). It was sought to incorporate a readily cleavable carbamate protecting group, while introduction of an ester-group on the opposing end of the diene was expected to enhance control over regio- and

enantioselectivity of the reaction. Such protected 5-amino-2,4-pentadienoates had rarely been reported in the literature and their reactivity was only briefly explored in "Diels-Alder-type" reactions.[133]

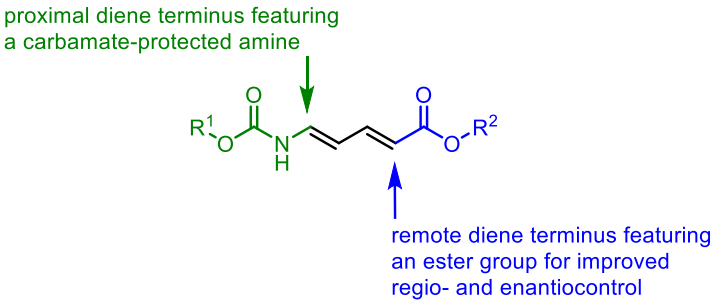

Figure 6: Envisaged improved substrate design.

An efficient, scalable and modular synthesis of the desired protected 5-amino-2,4-pentadienoates was developed (Scheme 34). Dimethyl muconate **86**, obtained from commercial muconic acid,[134] was selectively saponified at one terminus to yield monocarboxylic acid **87**.[135] Subsequent treatment with neat thionyl chloride, followed by reaction with sodium azide in analogy to a protocol of Varlet *et al.*[136] afforded the corresponding acyl azide. Notably this acyl azide exhibited good stability, likely due to a favorable ratio of carbon and oxygen atoms relative to nitrogen atoms in the molecule (*note:* organic azides are typically stable if $(N_{Carbon} + N_{Oxygen})/N_{Nitrogen} \geq 3$).[137] Although the acyl azide was successfully isolated during early-stage development (<100 mg scale), it was typically handled in solution and directly subjected to the subsequent "Curtius rearrangement" for safety reasons and convenience.

Importantly, the choice of alcohol in the final step determines the nature of the carbamate in the resulting diene and enables introduction of a range of synthetically useful and orthogonal protecting groups. Furthermore, the reaction proved to be readily scalable and Boc-protected diene **88a** was successfully prepared several times on a multi-gram scale in a highly reproducible manner.

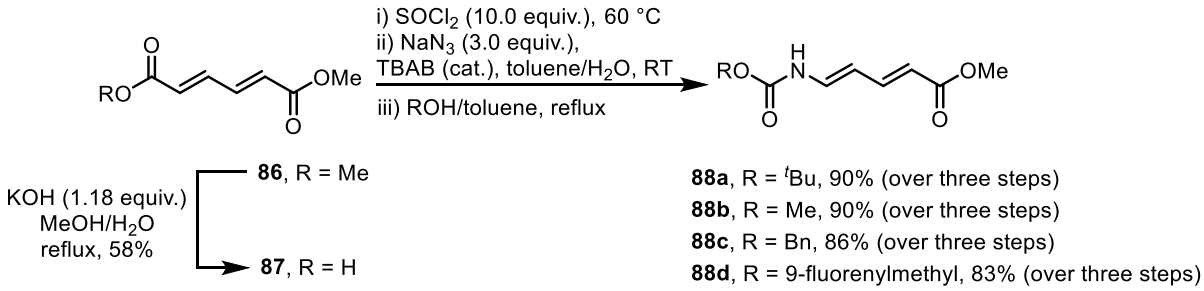

Scheme 34: Optimized modular synthesis of protected 5-amino-2,4-pentadienoates.

While these dienes could be purified by flash column chromatography on silica gel, they showed signs of partial hydrolysis upon storage in air over extended periods (2-3 days). In contrast, storage in Schlenk flasks under an argon atmosphere at –18 °C enabled their use for periods exceeding one year without any noticeable decomposition.

2.3 Reaction Optimization for Aromatic Aldehydes

After establishing a synthetic protocol for the preparation of the protected amino-pentadienoates, the reductive coupling of benzaldehyde with the Boc-protected diene **88a** was selected as a model reaction to evaluate the reactivity of this novel class of substrates. The reaction was conducted using the bench-stable nickel stilbene complex **89** developed by Cornella *et al.*,[9, 10] in both the presence of phosphoramidite ligand **L11** and under ligand-free conditions (Scheme 35).

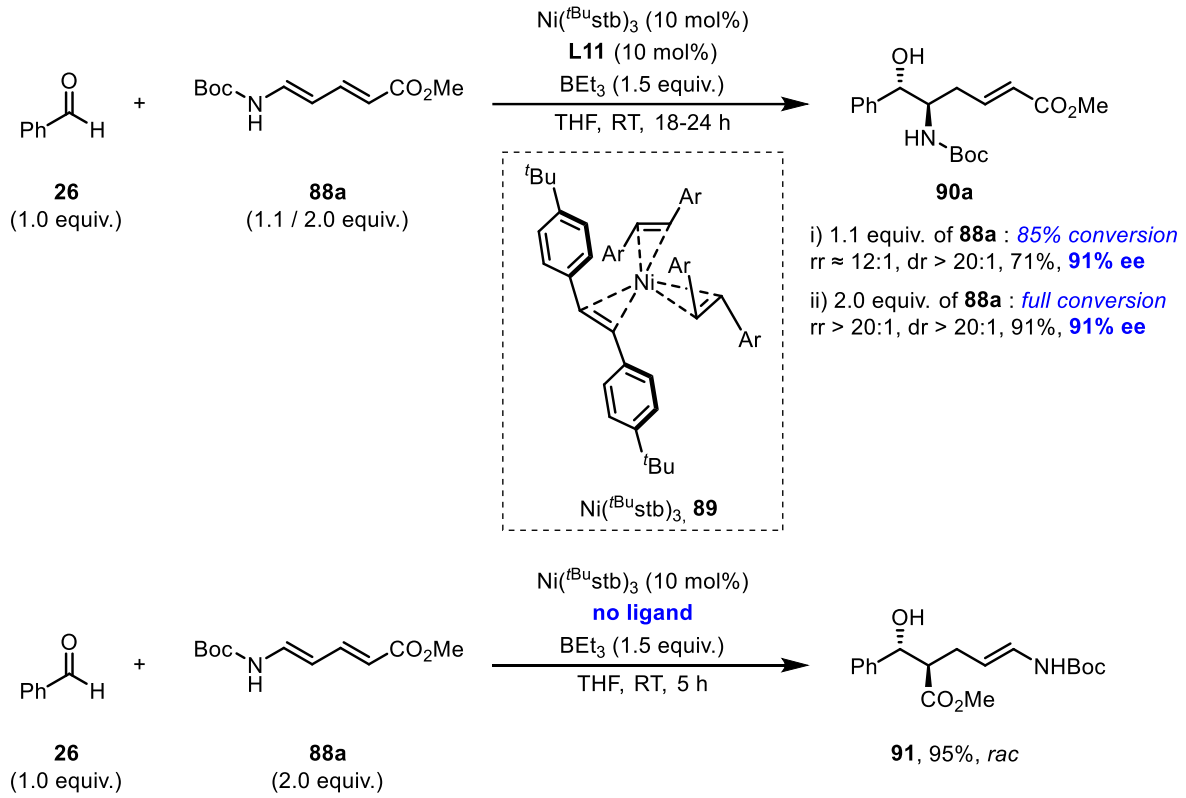

Scheme 35: Reductive coupling of benzaldehyde and N-Boc-protected amino-pentadienoate **88a** in the presence of phosphoramidite ligand **L11** and under ligand-free conditions.

The initial ligand-controlled test reaction was performed with 1.1 equivalents of diene and displayed incomplete conversion after 18 hours. Extending the reaction time did not result in any improvement, with conversions remaining at ≤ 85% as judged by ^{1}H NMR, likely indicating catalyst deactivation. Despite these shortcomings in reactivity, the effects on regio- and enantioselectivity sought through the optimized substrate design were achieved, as the corresponding vicinal amino alcohol **90a** was formed with markedly improved regiocontrol (rr ≈ 12:1) and could be isolated as a single regioisomer in excellent enantioselectivity (91% ee) following flash chromatography.

Since the catalyst loading of 10 mol% was already relatively high, it was decided to perform the reductive coupling with 2.0 equivalents of diene to push the reaction to completion. Gratifyingly, full conversion of benzaldehyde as well as an improved regioselectivity of > 20:1 were observed within 24 hours, presumably due to stabilization of the catalytically active nickel species by coordination of the diene in solution.

In a control experiment, the reductive coupling was performed under ligand-free conditions. Notably, significant nickel black formation was observed in the absence of an exogenous ligand. The ligand-free reaction mixture turned deep black upon addition of the reactants to the precatalyst solution, accompanied by the precipitation of black particles over time. This strongly contrasts the observations made for the ligand-controlled regioinverted coupling, which remained intensely orange throughout the entire course of the reaction. Nonetheless, the ligand-free reaction proceeded well and full conversion of the aldehyde was observed within 5 hours. As expected, under these "Tamaru-type" conditions, aldol-type product **91** was exclusively observed, resulting from reaction at the more nucleophilic ester-substituted end of the diene.

This control experiment confirmed that phosphoramidite ligand **L11**, as in the reactions with silyl dienol ethers and sorbate derivatives, indeed inverts the regioselective course of the reaction and promotes coupling at the least nucleophilic terminus of the diene. At the same time, the experiment made clear, that a precise ratio of nickel(0) to ligand must be maintained to suppress a ligand-free background reaction resulting in the formation of racemic regioisomer **91**. This aspect is especially important since the ligand-free reaction exhibited a shorter reaction time than the ligand-controlled reaction.

Following these initial results, the ligand-controlled reductive coupling was further investigated. Solvent effects were revealed by screening of a small selection of solvents (Table 1). Drawing on insights from the previous projects, different ethereal solvents were evaluated as they are typically well compatible with the asymmetric reductive coupling reaction. Apart from THF (Table 1, entry 1), the reaction was compatible with *tert*-butyl methyl ether (MTBE) (Table 1, entry 2), diethyl ether (Table 1, entry 3), and 1,4-dioxane (Table 1, entry 4). However, in all cases a slight loss of yield and enantioselectivity was observed compared to the reaction in THF. Surprisingly, toluene, which served as solvent in the previously reported enantioselective coupling reactions of aldehydes and silyl dienol ethers, was not well suited for the present system. The reaction suffered from incomplete conversion, and, more importantly, a drastic decrease in enantioselectivity, as **90a** was obtained with merely 41% ee.

Table 1: Solvent screening for the model coupling reaction of benzaldehyde and diene **88a**.

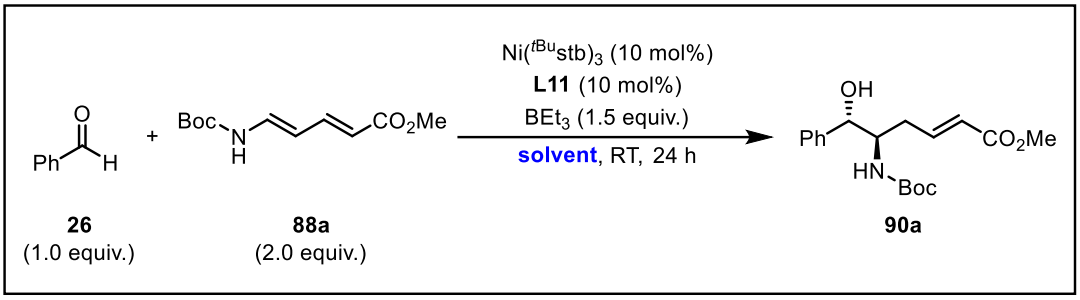

Entry	Solvent	rr	Isolated Yield	ee
1	**THF**	**> 20:1**	**91%**	**91%**
2	MTBE	> 20:1	84%	86%
3	Et_2O	> 20:1	81%	85%
4	1,4-dioxane	> 20:1	88%	87%
5	toluene	> 20:1	67%[a]	41%

[a] = 85% conversion

The previous research of our group on coupling reactions involving silyl dienol ethers and sorbate derivatives had illustrated the remarkable ability of phosphoramidite ligand **L11** to invert the regiochemical outcome of the reductive coupling, while exerting excellent enantiocontrol. Based on these results, **L11** was initially employed in the enantioselective coupling of benzaldehyde and Boc-protected amino-pentadienoate **88a**, which provided outstanding results. However, due to the marked difference in electronic and steric properties of this novel diene compared to the previous diene substrates, a variety of other ligand candidates was investigated. The aim of this screening was to determine whether **L11** would retain its superior performance or whether an alternative ligand candidate would be better suited for this transformation.

For this purpose, the model reaction was performed with a set of phosphoramidite ligands featuring varying chiral backbones. Despite their track-record in nickel-catalyzed asymmetric reductive couplings of dienes and aldehydes, both BINOL-derived phosphoramidite ligand **L14** (Table 2, entry 2) and SPINOL-derived analog **L15** (Table 2, entry 3) showed low compatibility with the regioinverted reaction mode. Instead of the desired vicinal amino alcohol **90a**, regioisomer **91** was observed almost exclusively. In contrast, TADDOL-based phosphoramidite **L16** displayed partial regiocontrol (Table 2, entry 4) as a regioisomeric ratio of 4:1 favoring the desired product was observed. Nonetheless, ligand **L16** showed insufficient enantioinduction, as the target compound was obtained in a low enantiomeric excess of 22%.

During the initial ligand screening for the coupling of aldehydes and silyl dienol ethers in our group, it was found that location and enlargement of the chiral cleft on the front side of the ligand was essential to enantioinduction (see Chapter 1.2.4). As modified analogs of VAPOL have not been reported, it was attempted to employ a VANOL-derivative to investigate a candidate that is structurally more related to **L11**. In particular, 7,7′-disubstituted VANOL ligands had been reported as favorable substitutes for regular VANOL- or VAPOL-derived catalyst systems in the literature.[138, 139] This motivated the preparation of phosphoramidite ligand **L17** and the

investigation of its ability to govern the asymmetric regioinverted coupling. Unfortunately, **L17** was shown to be completely inadequate in this context, as only traces of the desired amino alcohol product could be observed in the crude reaction mixture and regioisomer **91** was isolated as the sole product (Table 2, entry 5). Moreover, **91** was basically obtained as a racemate (1% ee), showing insufficient enantioinduction by the ligand.

Table 2: Screening of phosphoramidite ligands with different chiral backbones for the model coupling reaction of benzaldehyde and diene **88a**.

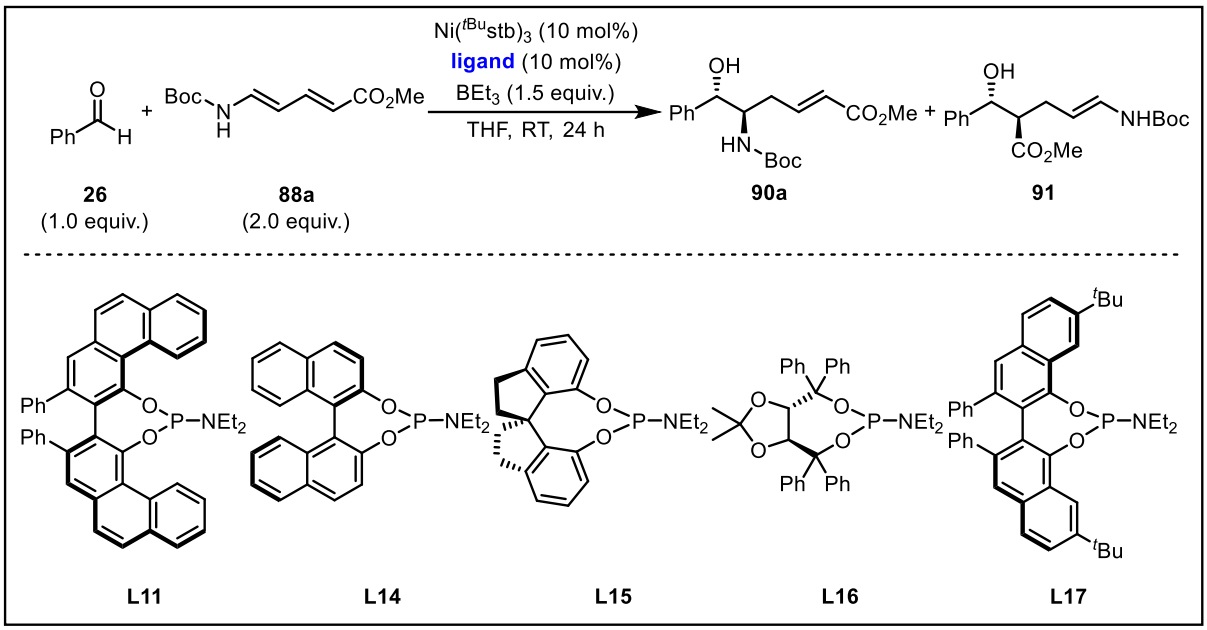

Entry	Ligand	rr (90a:91)	Isolated Yield	ee
1	**L11**	**> 20:1**	**91%**	**91%**
2	**L14**	< 1:20	n.d.[a]	n.d.
3	**L15**	1:11	n.d.	n.d.
4	**L16**	4:1	71%	22%
5	**L17**	< 1:20	85[b]	1%

[a] = 50% conversion; [b] = yield and ee refer to regioisomer **91**; n.d. = not determined

Overall, these experiments further highlighted the distinct ability of VAPOL-derived phosphoramidite **L11** to promote the reductive coupling of 1,3-dienes at their least nucleophilic terminus. Remarkably, this still holds true when employing a push-pull diene in the form of N-Boc-protected amino-pentadienoate **88a**, which markedly differs from the diene classes previously employed in this reaction, both in terms of sterics and electronics.

2.4 Reaction Scope with Aromatic Aldehydes

Following the establishment of the reaction conditions, the scope of the transformation was explored. First, the reaction was carried out using the various carbamate-protected amino-pentadienoates, which were prepared as part of the modular substrate synthesis (see Chapter 2.2). In addition to the Boc-protected amino alcohol derivative **90a** discussed before, methylcarbamate-(**90b**), Cbz-(**90c**), and Fmoc-protected (**90d**) analogs were obtained in a highly enantioselective manner and were isolated as single regioisomers in excellent yield (Scheme 36).

The steric and electronic properties of the respective diene had little impact on the selectivity of the reaction, as only minor differences in regio- and enantioselectivity and yield were observed for the formation of the corresponding amino alcohol products. Furthermore, the fact that both Cbz- and Fmoc-protecting groups were well tolerated indicates that possible interactions between the aromatic moiety of the protecting group and the extended π-system of the VAPOL-backbone of the phosphoramidite ligand do not significantly affect the regio- and enantioselectivity of the reaction, if present at all.

Qualitative differences in reactivity became apparent when the reactions were performed on a preparative scale. The methylcarbamate- and Cbz-protected analogs **88b** and **88c** showed the highest reactivity, as full conversion of benzaldehyde was observed within 16 hours. In contrast, the Boc-protected analog **88a** required up to 24 hours to achieve full conversion, as indicated by thin layer chromatography. The Fmoc-protected analog **88d** exhibited the lowest reactivity, requiring three days for complete consumption of the aldehyde.

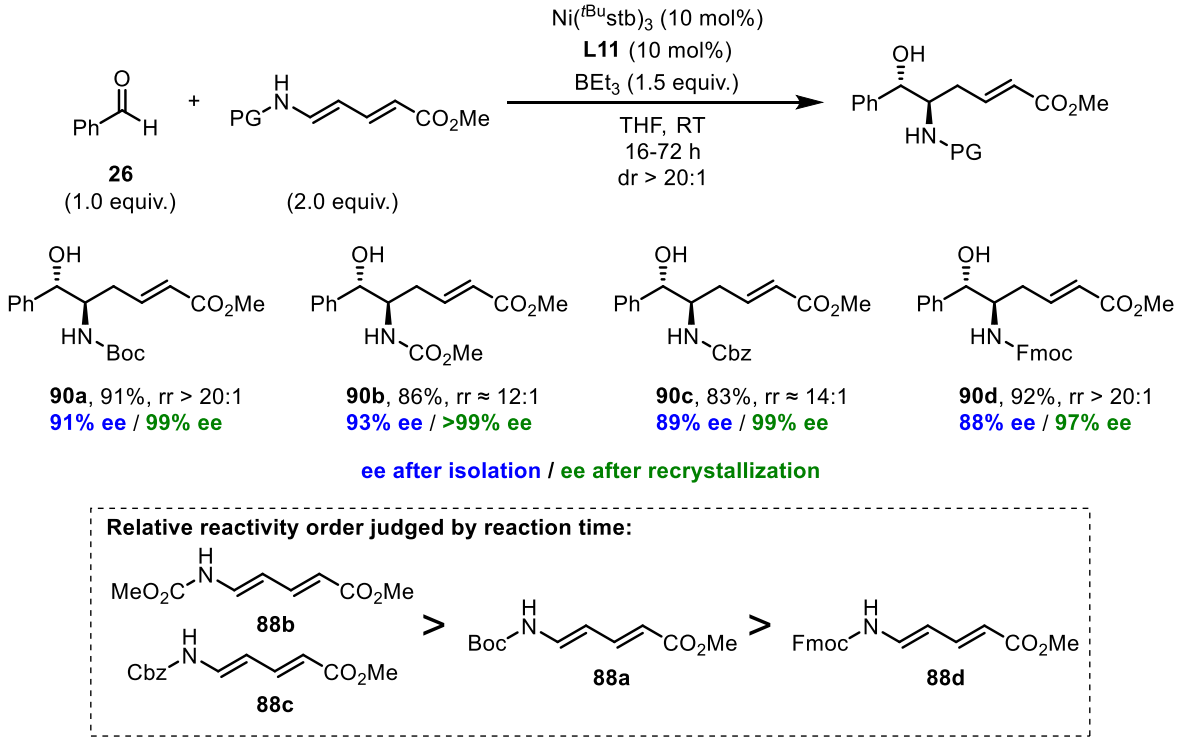

Scheme 36: Synthesis of vicinal amino alcohol derivatives with varying protecting and relative reactivity of the different dienes judged by reaction time.

All products were obtained as crystalline solids. This property was exploited, as single recrystallization of the respective amino alcohols enabled further enrichment of the major enantiomer, affording optically pure material (up to >99% ee).

Furthermore, the crystalline nature of the products allowed single crystals suitable for X-ray diffraction analysis to be grown. This enabled the reliable determination of both relative and absolute configurations of the amino alcohol derivatives (see representative example in Figure 7). These structural assignments served as the basis for assigning the configuration of related products in the reaction scope.

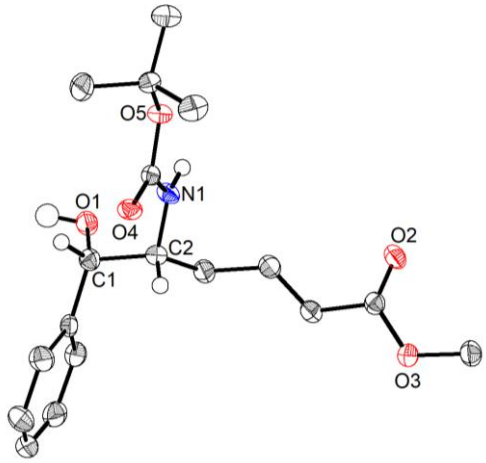

Figure 7: Single-crystal X-ray structure of amino alcohol **90a** (majority of H-atoms omitted for clarity).

Next, the compatibility of different aromatic aldehydes with this reaction mode was investigated. To this end, catalytic reactions were carried out with Boc-protected diene **88a** as it provided the best overall combination of regioselectivity, enantioselectivity, and reactivity in the model reaction, along with the synthetic utility of the protecting group.

An assortment of aldehydes were reacted under the optimized conditions with diene **88a** (Scheme 37). Both aldehydes bearing electron-withdrawing groups (*e.g.* CO_2Me, CF_3) and electron-donating groups (*e.g.* OMe) were well tolerated, affording the corresponding products **92**, **93** and **94** in high yield with excellent enantioselectivity. Notably, electron-rich aldehydes such as *para*-anisaldehyde exhibited markedly lower reactivity than their electron-deficient counterparts, thus requiring a higher excess of diene and an increased reaction time to achieve full conversion.

Excellent results were also observed for the *para*-fluoro and *para*-chloro analog, which granted selective excess to the corresponding amino alcohols **95** and **96**. The compatibility of the latter with a low-valent nickel complex is particularly noteworthy, as no reactivity issues arising from competitive oxidative addition into the C–Cl bond were observed. The retained aryl chloride offers a useful synthetic handle for potential downstream functionalization of the aryl moiety. An alternative functional handle was also incorporated in product **97** bearing a pinacolboronate substituent (BPin). Importantly, the reaction work-up had to be conducted under mild, basic conditions to isolate the desired amino alcohol in good yield (see Experimental Section).

Introduction of substituents in the *meta*- and *ortho*-position of the aldehyde was also tolerated as products **98** and **99** were isolated in satisfying yield and enantioselectivity. However, substituents in closer proximity to the aldehyde led to a slightly diminished regioselectivity in these two cases.

Extension of the aromatic π-system was likewise well tolerated without significant loss in selectivity or yield, as demonstrated by amino alcohol **100**. In addition, heteroaromatic aldehydes were successfully employed, as furan-2-carbaldehyde and N-Boc-pyrrole-2-carbaldehyde afforded the corresponding products **101** and **102** selectively. Thiophene-2-carbaldehyde gave compound **103** with diminished, yet still appreciable, enantioselectivity despite the known thiophilicity of low-valent nickel-species.

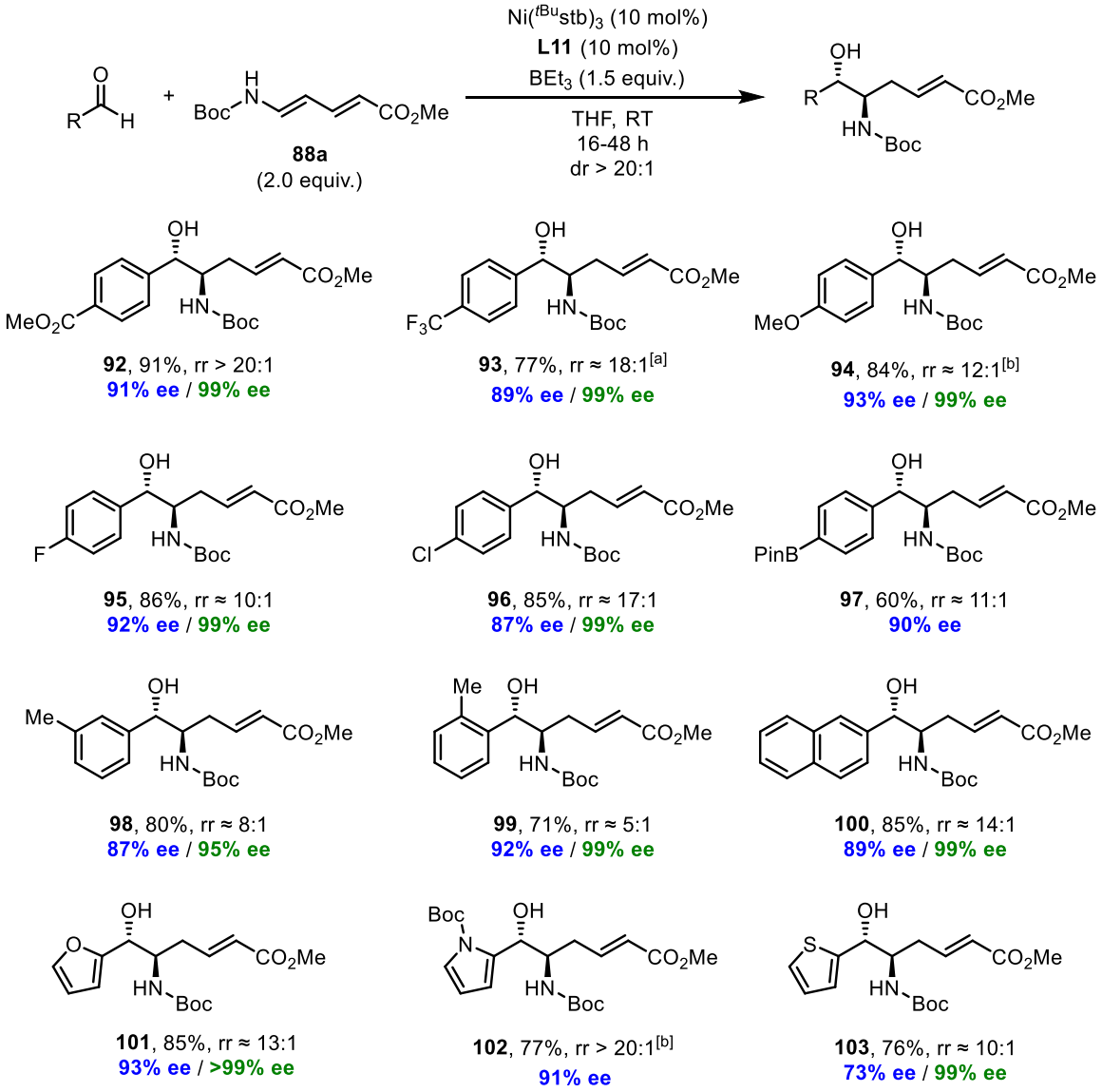

Scheme 37: Scope of the enantioselective reductive coupling of diene **88a** with aromatic aldehydes; [a] = reaction performed at −10 °C; [b] = 3.0 equiv. of **88a** used.

Most of the products were obtained as crystalline solids. A single recrystallization of the respective amino alcohols enabled substantial enantioenrichment, typically affording samples with excellent

enantiomeric excess of up to >99%, even when the initially obtained material exhibited only moderate enantiomeric purity (*e.g.* amino alcohol **103**). Moreover, these recrystallizations could be conveniently set up in vials at room temperature and typically gave the recrystallized products with only minor losses of material after storage in the freezer overnight (see Experimental Section).

During the investigation of the reaction scope, certain limitations of the method with respect to functional group compatibility were identified (Scheme 38).

Introduction of a *para*-cyano group led to a significant decrease in regio- and enantioselectivity. In addition, incomplete conversion of the aldehyde was observed, resulting in a moderate isolated yield of amino alcohol **104**. The strongly coordinating cyano group could potentially compete with ligand **L11** for coordination to the nickel center, thereby inhibiting productive catalysis or even promoting a ligand-free racemic background reaction.

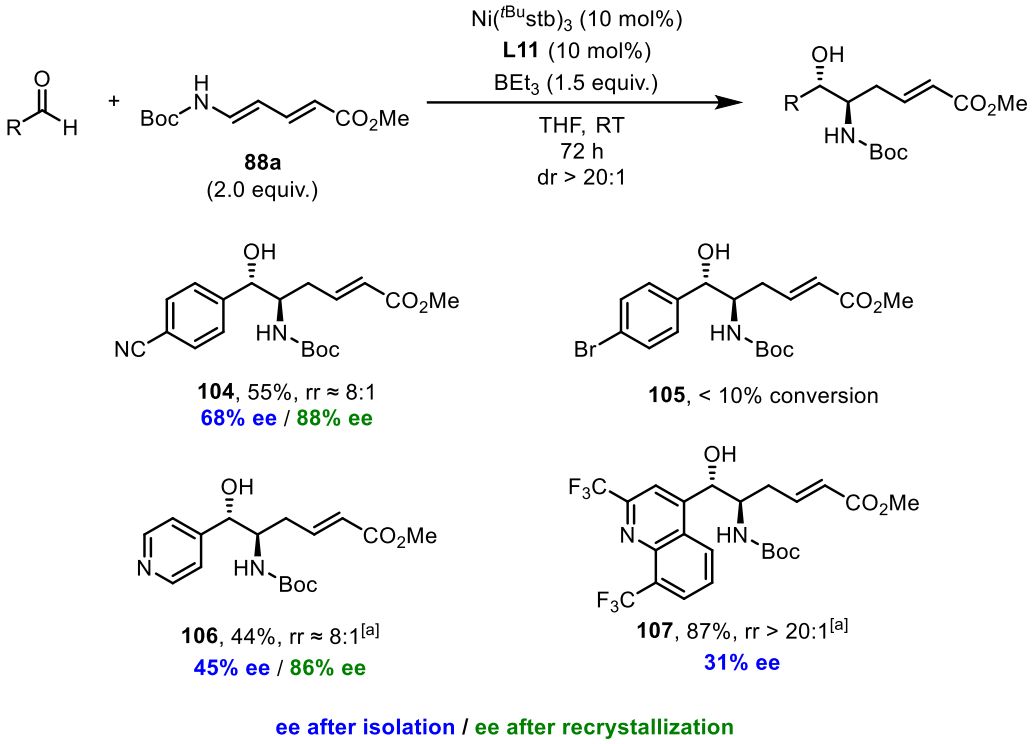

Scheme 38: Aromatic aldehydes exhibiting limited reactivity and selectivity in the reductive coupling; [a] = 3.0 equiv. of BEt_3 used.

Aryl bromides were found to be incompatible with the reaction, as *para*-bromobenzaldehyde exhibited low conversion. This is presumably due to catalyst deactivation *via* oxidative addition of nickel(0) into the C–Br bond. This observation is somewhat surprising, as aryl bromides had passed uncompromised in inverse coupling reactions with sorbate esters. The difference is likely kinetic in origin, as sorbate esters exhibit significantly higher reactivity than protected amino-pentadienoates, hence outcompeting undesired oxidative addition pathways.

Furthermore, amino alcohol **106** was obtained from isonicotinaldehyde with insufficient selectivity in the reductive coupling. The diminished isolated yield is mainly attributed to a

competing side reaction, as formation of 4-pyridinemethanol was observed, likely resulting from direct reduction of 4-pyridinecarbaldehyde by a nickel-hydride species. Furthermore, an increased amount of triethylborane was required to initiate the reaction, as no conversion was observed under standard conditions (confirmed by a repetition experiment). This behavior may arise from formation of a pyridine–BEt_3 Lewis adduct, which effectively quenches the reductant. The limited enantioselectivity might originate from the coordinating ability of the pyridine nitrogen atom, potentially affecting the enantiodetermining transition state.

Subsequently, a bis(trifluoromethyl)-substituted quinoline aldehyde was investigated as an alternative, modified heterocyclic substrate.[140] It was hypothesized that reducing the σ-donating ability and steric accessibility of the nitrogen atom *via* the adjacent CF_3-groups could improve substrate compatibility with the transformation. In addition, the corresponding amino alcohol was envisioned as a key derivative for planned downstream functionalization toward the enantioselective synthesis of antimalarial agent Mefloquine.[141-144] Although the desired amino alcohol **107** was obtained in excellent yield and with exquisite regiocontrol, the reaction again suffered from poor enantioselectivity. These findings underscore the limited compatibility of such N-heteroaromatic aldehydes with the methodology and ultimately impeded the development of a novel enantioselective synthesis of Mefloquine.

2.5 Effects on Regioselectivity and Enantioselectivity

During the investigation of the reaction scope, variations in selectivity were observed under certain conditions. Although overall reproducibility was ensured, several observations made during reaction screening and optimization are considered noteworthy.

In particular, the reductive coupling of methyl 4-formylbenzoate **108** and diene **88a** exhibited varying results regarding regioselectivity and isolated yield depending on the batch and nature of the precatalyst used (Scheme 39).

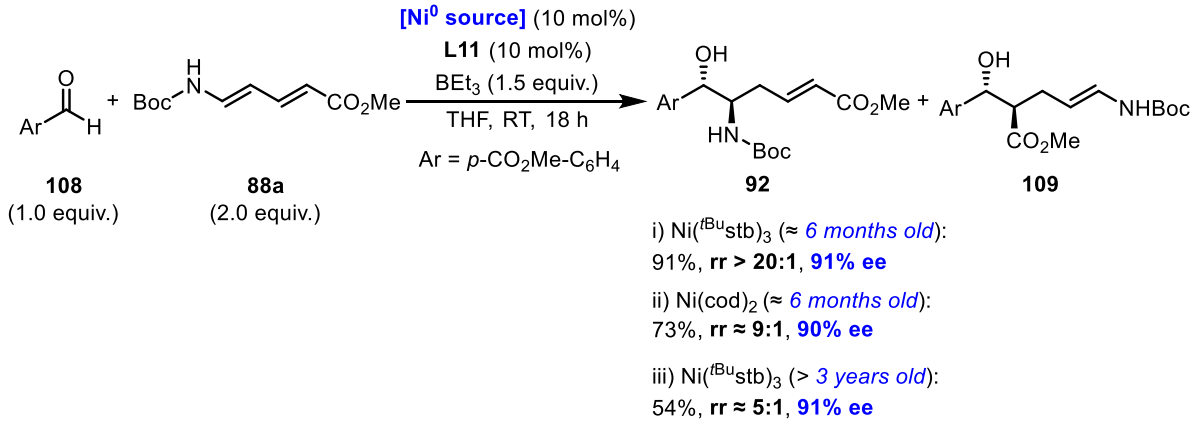

Scheme 39: Effect of precatalyst choice on the regioselectivity of a reductive coupling reaction.

Under the standard conditions employed throughout the study of the reaction scope, a commercial batch of tris-[*trans*-1,2-bis-(4-*tert*-butylphenyl)-ethene]-nickel(0) Ni($^{t\text{Bu}}$stb)$_3$ obtained from STREM chemicals was used. These conditions provided reproducible results with consistently high selectivity as confirmed by a series of repetition experiments.

In contrast, switching the precatalyst to bis(1,5-cyclooctadiene)nickel(0) Ni(cod)$_2$, resulted in a drop in regioselectivity and yield, while the enantioselectivity remained unaffected. Notably, the formation of nickel black was observed over the course of the reaction when using Ni(cod)$_2$, whereas the mixture remained homogeneous under the standard conditions.

An even more pronounced decrease in regioselectivity and yield was observed when a more than three-year-old batch of Ni($^{t\text{Bu}}$stb)$_3$ (provided by Dr. R. Saeb of the Cornella group) was employed. As in the previous experiments, enantioselectivity was retained. Interestingly, the formation of the undesired regioisomer **109** proceeded in an essentially non-enantioselective manner, as demonstrated by its isolation in merely 3% ee.

Ligand **L11** evidently exhibits little to no enantioinduction along the alternative "Tamaru-type" regiochemical pathway. Nonetheless, the observed discrepancies in selectivity, together with the nearly racemic nature of the regioisomer, suggests that a ligand-free, racemic background reaction might be operative. In this context, it has recently been reported by Arisawa and co-workers that even ppm-amounts of colloidal nickel can efficiently promote "Tamaru homoallylation reactions" with a diverse set of dienes.[145]

Based on these observations, it is proposed that the variations in regioselectivity are related to the integrity of the nickel species present in solution. Although Ni($^{t\text{Bu}}$stb)$_3$ is commonly described as "bench-stable" and can be stored under air in the freezer for extended periods, gradual decomposition over time has been reported.[10] Ni(cod)$_2$ is typically stored under argon in the freezer but is significantly more sensitive both in the solid state and in solution.

The formation of even small amounts of colloidal nickel[146] or other ill-defined nickel species, resulting from prolonged storage or *in situ* decomposition during the reaction, may have a significant impact on the reaction outcome. Such species could promote a competing, racemic "Tamaru homoallylation" as an undesired background reaction. This is further corroborated by the previously observed differences in reaction rates between the ligand-free and ligand-controlled reductive coupling reactions. Consequently, the integrity of the nickel source and proper reaction setup have to be considered in order to ensure consistent regioselectivity.

In this context, it was hypothesized that increasing the ratio of ligand **L11** to nickel(0) could have a beneficial effect. By ensuring that no unligated nickel species capable of performing a racemic background reaction remain in solution, improved regiocontrol might be achieved. To test this hypothesis, the coupling of methyl 4-formylbenzoate **108** and diene **88a** was repeated with an increased ligand loading of 20 mol% (Scheme 40).

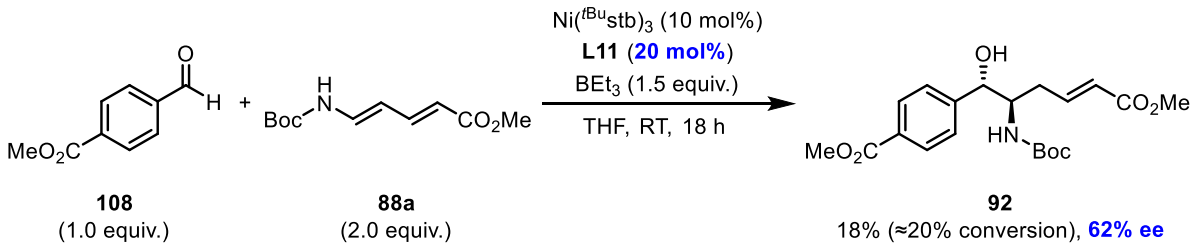

Scheme 40: Effect of increasing ligand-to-metal ratio on the outcome of the reductive coupling reaction.

However, this modification shut down the reaction almost completely, as only approximately 20% conversion of the aldehyde was observed (confirmed by a repetition experiment). Remarkably, this decrease in reactivity was accompanied by a drastically reduced enantioselectivity, as amino alcohol **92** was obtained in merely 62% ee. These observations suggest that an increased ligand-to-metal ratio impairs catalytic turnover, likely due to blocking an additional coordination site required for productive catalysis.

At the same time, the loss of enantiocontrol upon increasing the ligand loading may indicate that a non-linear effect is operative in the catalytic system. From a practical perspective, these findings demonstrate that an excess of ligand should be avoided, as it leads to diminished reactivity and enantioselectivity. Conversely, reducing the ligand loading would result in the presence of unligated nickel species, which may promote the formation of the undesired regioisomer. Consequently, a 1:1 ratio of ligand to metal is deemed necessary to enable an ideal reaction outcome and should be meticulously ensured.

Lastly, the influence of water on the reaction outcome was examined. This was motivated by previous findings from our group, where the addition of stoichiometric amounts of water significantly suppressed regioisomer formation in the asymmetric reductive coupling of tosyl-protected imines with silyl dienol ethers (see Chapter 1.2.4).[98] Although the mechanistic basis for this effect remains unclear, it raised the question of whether a similarly beneficial effect could be observed for the present system. This strategy, if successful, was thought to be particularly useful for more challenging substrates such as *ortho*-substituted benzaldehyde derivatives which exhibited diminished regioselectivity during exploration of the reaction scope under the standard reaction conditions.

To test this hypothesis, the model reaction between methyl 4-formylbenzoate **108** and diene **88a** was repeated under the standard reaction conditions in the presence of three equivalents of degassed water (Scheme 41). However, contrary to expectations, the opposite effect was observed. While full conversion of the aldehyde was achieved, a complex mixture of four different isomers was obtained. In addition to the desired amino alcohol **92** and the known regioisomer **109**, further double-bond positional isomers were detected. Despite this pronounced change in product distribution, the enantiomeric excess of the desired vicinal amino alcohol **92** remained unaffected.

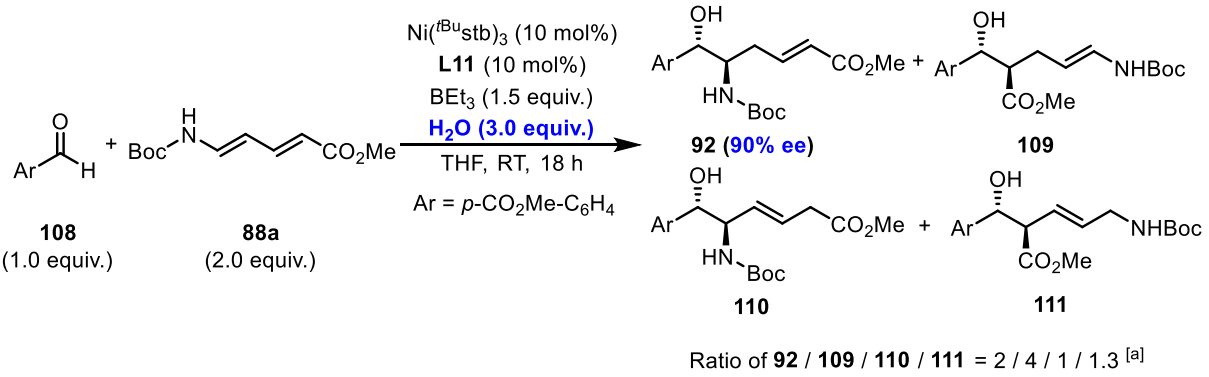

Scheme 41: Effect of stoichiometric amounts of water on the regioselectivity of a reductive coupling reaction; [a] = determined by ^{1}H NMR analysis of the crude reaction mixture.

As the catalytic reactions were typically performed under rigorously dry and inert conditions, it can be concluded that water does not negatively influence the reaction under standard reaction conditions. This is further supported by the fact that positional isomers such as **110** and **111** were not observed in any other experiment.

Overall, these results emphasize the sensitivity of the present reaction system and the importance of maintaining a well-defined and selective catalytic system. In order to achieve highly reproducible results, the quality of both precatalyst and ligand was carefully controlled. Importantly, Ni($^{t\text{Bu}}$stb)$_3$ was the nickel(0)source of choice, as it consistently provided superior results than highly sensitive Ni(cod)$_2$, despite performing the reductive coupling reactions under rigorously inert conditions using Schlenk techniques. Nonetheless, prolonged storage of the precatalyst can have a detrimental effect on regioselectivity, as demonstrated by the diminished regioselectivity obtained with a >3 years old batch of Ni($^{t\text{Bu}}$stb)$_3$. As there were indications that

non-linear effects might be operative in the reaction, the enantiopurity of **L11** was meticulously ensured to be >99% ee, as even minor deviations could exert a more pronounced effect on the ee of the amino alcohol products than initially anticipated. Under these optimized conditions, reproducible results with consistently high selectivity were obtained, as confirmed by a series of repetition experiments.

2.6 Reaction Optimization for Aliphatic Aldehydes

In addition to aromatic aldehydes, the coupling reaction with protected amino-pentadienoates was investigated using aliphatic aldehydes. To this end, preliminary experiments employing hydrocinnamaldehyde, *n*-octanal and isobutyraldehyde were performed (Scheme 42). Although the reactions exhibited promising enantioselectivities, in all three cases, poor conversion and low regiocontrol was observed.

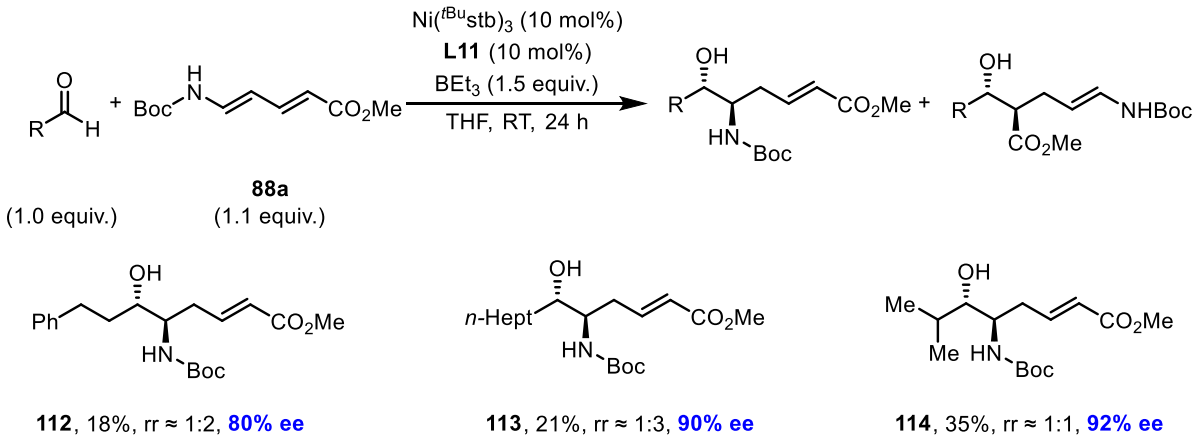

Scheme 42: Initial results for the reductive coupling of aliphatic aldehydes with diene **88a**.

Consequently, reaction optimization studies were initiated using hydrocinnamaldehyde **62** as a model substrate (Table 3).

Table 3: Selected optimization experiments for the reductive coupling of hydrocinnamaldehyde and diene **88a**.

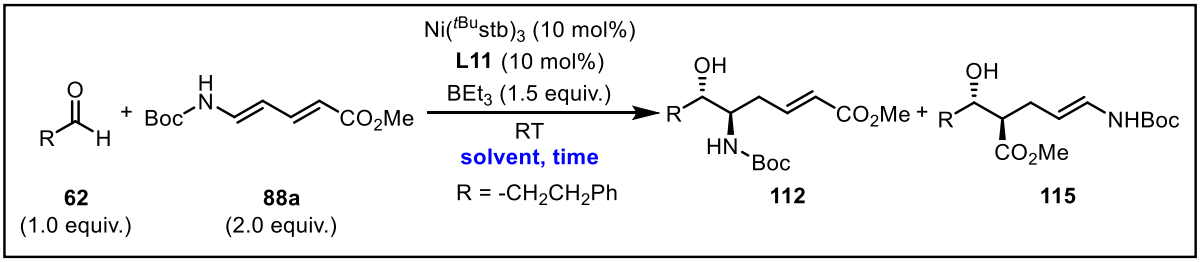

Entry	Solvent	Time	rr (112:115)	Conversion	Isolated Yield	ee
1	THF	18 h	1:2	≈ 50%[a]	18%	80%
2	toluene	72 h	4:1	≈ 70%[a]	46%	n.d.
3	toluene	72 h	4:1	≈ 75%	51%	92%
4	$C_6H_5CF_3$	48 h	3:1	≈ 30%	n.d.	n.d.
5	toluene	72 h	4:1	≈ 70%[b]	n.d.	n.d.
6	toluene	135 h	n.d.	< 5%[c]	n.d.	n.d.
7	toluene	18 h	n.d.	< 5%[d]	n.d.	n.d.
8	toluene	72 h	4:1	≈ 75%[e]	n.d.	n.d.
9	**toluene**	**72 h**	**4:1**	**100%[f]**	**72%**	**95%**

[a] = 1.1 equiv. of **88a** used; [b] = aldehyde/diene ratio = 2:1; [c] = aldehyde/diene ratio = 5:1; [d] = $ZnEt_2$ (1 M in hexane) used as reducing agent instead of BEt_3; [e] = 20 mol% of precatalyst and ligand used; [f] = BEt_3 (1 M in toluene, 3.0 equiv.) used; n.d. = not determined

To improve the initial outcome (Table 3, entry 1), the reaction conditions were modified. It was hypothesized, that the choice of solvent might affect both regioselectivity and reactivity. Hence, THF was replaced by toluene, and a stock solution of triethylborane in *n*-hexane was used instead of the corresponding solution in THF (Table 3, entry 2). In addition, the reaction time was increased to 72 hours to address the low conversion. Gratifyingly, these modifications led to a substantial improvement in reaction performance. Aldehyde conversion increased to approximately 70%, and the desired amino alcohol **112** was now formed as the major regioisomer, owing to a pronounced solvent effect.

Increasing the amount of diene was examined to further improve both conversion and regioselectivity (Table 3, entry 3). Although only a marginal increase in conversion was observed and the regioselectivity remained essentially unchanged, product **112** could be isolated as a single regioisomer in a moderate yield of 51%. Importantly, replacing THF with a toluene/*n*-hexane solvent mixture also resulted in a significant increase in enantioselectivity, with the ee of **112** improving from 80% to 92%. This finding strongly contrasts with the diminished enantiocontrol previously observed in analogous couplings involving aromatic aldehydes conducted in toluene (see Chapter 2.3). Consequently, direct comparison between coupling reactions involving aromatic and aliphatic aldehydes should be made with caution, as distinct enantiodetermining transition states may be operative in the respective transformations. An attempt to employ α,α,α-trifluorotoluene as an alternative aromatic solvent (Table 3, entry 4) was unpromising, as the diene showed low solubility under these conditions and the reaction proceeded with poor conversion.

Following these first significant improvements, the remaining issue of incomplete conversion was addressed (experiments mentioned in this segment are not shown in Table 3). Due to the comparatively high polarity of the carbamate-protected amino-pentadienoates, increasing the amount of triethylborane (in *n*-hexane) to improve conversion resulted in partial precipitation of the diene. Conversely, increasing both the loading of triethylborane and the solvent volume to maintain solubility, resulted in excessive dilution of the reaction mixture and again hampered aldehyde conversion. Notably, the methylcarbamate-(**88b**), Cbz-(**88c**), and Fmoc-protected (**88d**) analogs of diene **88a** are even more polar and thus showed low compatibility with the toluene/*n*-hexane solvent system. Elevating the reaction temperature to 50 °C resulted in a substantially more complex crude mixture as judged by ^{1}H NMR analysis, underlining the importance of conducting the reaction under ambient conditions.

Given these limitations, several other strategies were explored to improve conversion. Reversal of the reaction stoichiometry seemed plausible, as aliphatic aldehydes typically display good to excellent solubility in *n*-hexane and toluene. This approach initially appeared promising, as a 2:1 ratio of aldehyde to diene resulted in similar conversion and regioselectivity compared to the previous result (Table 3, entry 5). However, further increasing the amount of aldehyde to 5.0 equivalents completely shut down the reaction (Table 3, entry 6). Likewise, the use of diethylzinc as the ultimate reducing agent also resulted in no significant product formation,

despite its track-record in nickel-catalyzed reductive couplings of aldehydes and dienes (Table 3, entry 7). Surprisingly, increasing the catalyst/ligand loading was similarly unsuccessful (Table 3, entry 8).

Finally, the strategy of increasing the amount of reducing agent was revisited. Since commercially available solutions of triethylborane are typically supplied in THF or *n*-hexane, a stock solution in toluene was prepared from neat triethylborane. This approach enabled the use of 3.0 equivalents of reductant without inducing diene precipitation associated with *n*-hexane or the diminished regio- and enantioselectivity observed in the presence of THF. Gratifyingly, under these conditions full conversion of the aldehyde was achieved and the desired product **112** was isolated as a single regioisomer in 72% yield and 95% ee (Table 3, entry 9).

2.7 Reaction Scope with Aliphatic Aldehydes

After suitable reaction conditions for the nickel-catalyzed reductive coupling between aliphatic aldehydes and protected amino-pentadienoates had been established using the model coupling of hydrocinnamaldehyde and diene **88a**, the reaction scope was explored with respect to the aldehyde component (Scheme 43). Although the regiocontrol exerted by phosphoramidite ligand **L11** was less stringent than in the coupling with aromatic aldehydes, the corresponding amino alcohol products were isolated as single regioisomers in all cases.

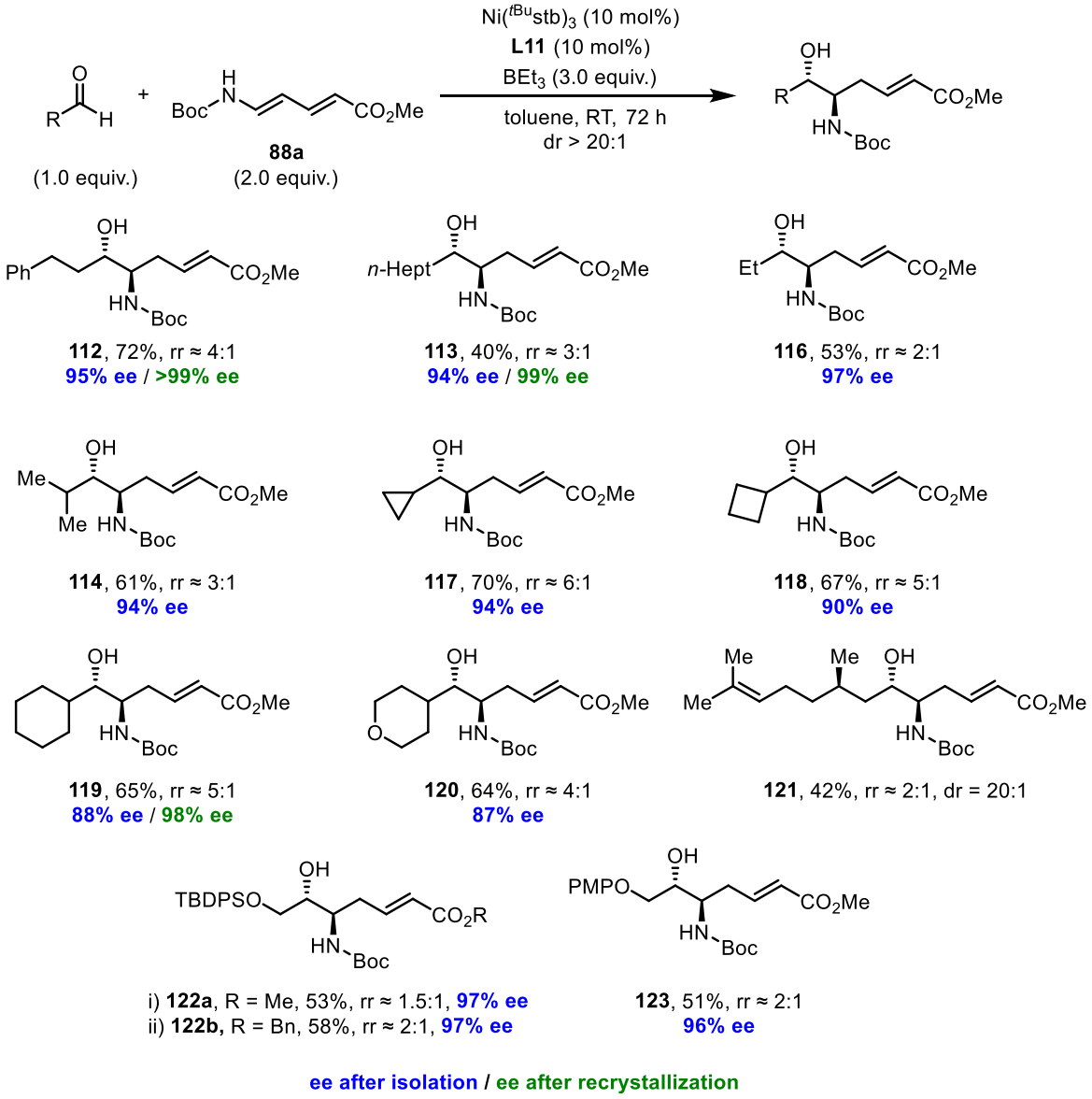

Scheme 43: Scope of the enantioselective reductive coupling of diene **88a** with aliphatic aldehydes.

Linear aliphatic aldehydes such as *n*-octanal and propionaldehyde were converted into the corresponding amino alcohols **113** and **116** with high levels of enantioselectivity, although the diminished regioselectivities translated into moderate isolated yields. Compatibility with α-branched aldehydes was demonstrated by the highly enantioselective synthesis of amino alcohol **114** from isobutyraldehyde. In addition, several cyclic aliphatic aldehydes were shown to

be competent coupling partners and generally exhibited slightly improved regiocontrol compared to the acyclic congeners. Interestingly, smaller ring sizes appeared to correlate with enhanced enantioselectivity, as illustrated by the trend observed when comparing products **117**, **118**, **119** and **120**. Furthermore, (*R*)-Citronellal, bearing a stereogenic center at the β-position relative to the aldehyde was well tolerated, affording the corresponding product **121** in excellent diastereoselectivity.

In contrast to aromatic aldehydes, the overall lower level of regiocontrol observed in couplings involving aliphatic aldehydes suggests that these substrates lack favorable secondary interactions with the extended π-system of the ligand backbone in the regiodetermining transition state.

To test this hypothesis and potentially improve regiocontrol, the effects of placing aromatic substituents on either the aldehyde or the diene partner were investigated. Protected 2-hydroxyacetaldehyde derivatives bearing arene-containing TBDPS- or PMP-protecting groups afforded the corresponding products **122a** and **123** with similarly limited regioisomeric ratios. Initial control experiments revealed that replacement of diene **88a** with the corresponding Cbz-protected analog **88c** did not improve regiocontrol. Consequently, rather than modifying the reactive terminus, the remote methyl ester was exchanged for a benzyl ester. However, this substrate modification likewise failed to significantly improve the outcome in the synthesis of the corresponding amino alcohol **122b**. Notably, excellent enantioselectivities were maintained in all cases, implying that neither modification had substantial impact on the enantiodetermining transition state. Collectively, these observations indicate that a more rational strategy for addressing the regiocontrol issue will likely require a more detailed understanding of substrate binding within the catalytically active complex.

Several limitations with respect to the aldehyde component were observed during the scope investigation (Scheme 44). Pivalaldehyde failed to undergo productive conversion, potentially due to the sterically demanding *tert*-butyl group in the α-position to the aldehyde. Additionally, α,β-unsaturated aldehydes such as myrtenal or cinnamaldehyde proved incompatible with the reductive coupling conditions.

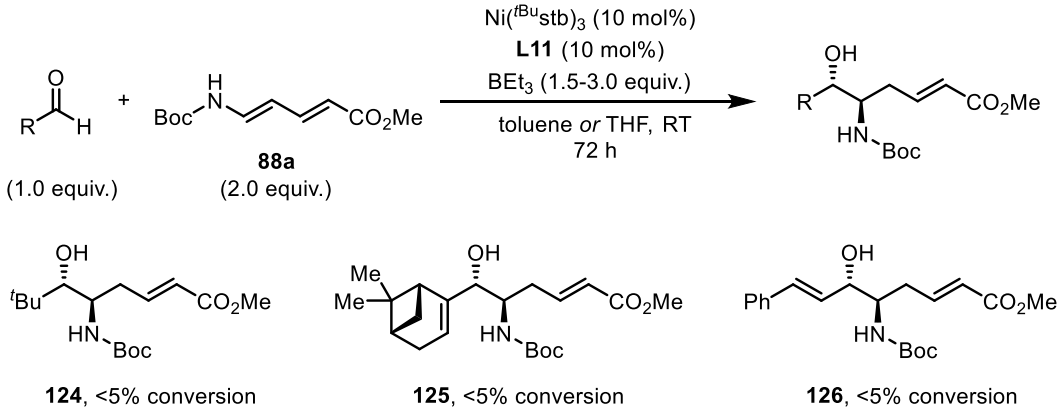

Scheme 44: Aliphatic and α,β-unsaturated aldehydes incompatible with the reductive coupling.

2.8 Synthesis and Application of Modified Dienes

A variety of modifications of the diene framework were investigated to evaluate the substrate scope of the nickel-catalyzed reductive coupling with respect to the diene component. First, modifications of the proximal amine moiety and the remote directing electron withdrawing group were explored (Scheme 45). N-methylated and N-benzylated analogs **127a** and **127b** were prepared from parent diene **88a** by treatment with sodium hydride and the respective organohalide. In addition, the ester group at the other terminus could be converted into either a dimethylamide in **128a** or a Weinreb-amide in **128b** using the corresponding amine hydrochloride salts and trimethylaluminum.

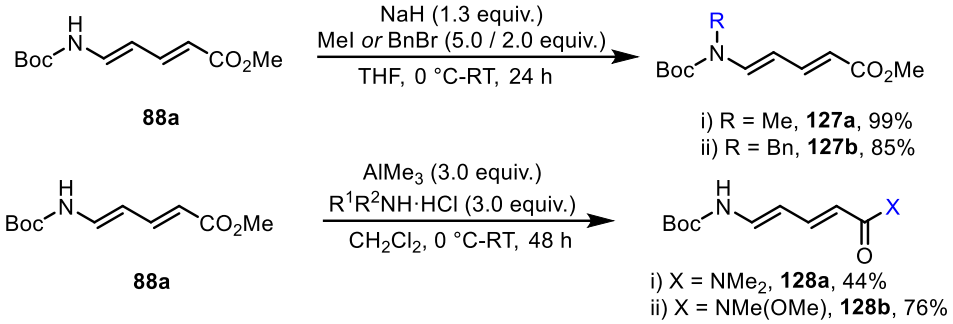

Scheme 45: Modification of the proximal and the remote terminus of diene **88a**.

All of these dienes performed well in the nickel-catalyzed reductive coupling under the established conditions and afforded the corresponding products as virtually single regioisomers. To ensure complete aldehyde conversion, increased amounts of diene and reductant were employed (Scheme 46).

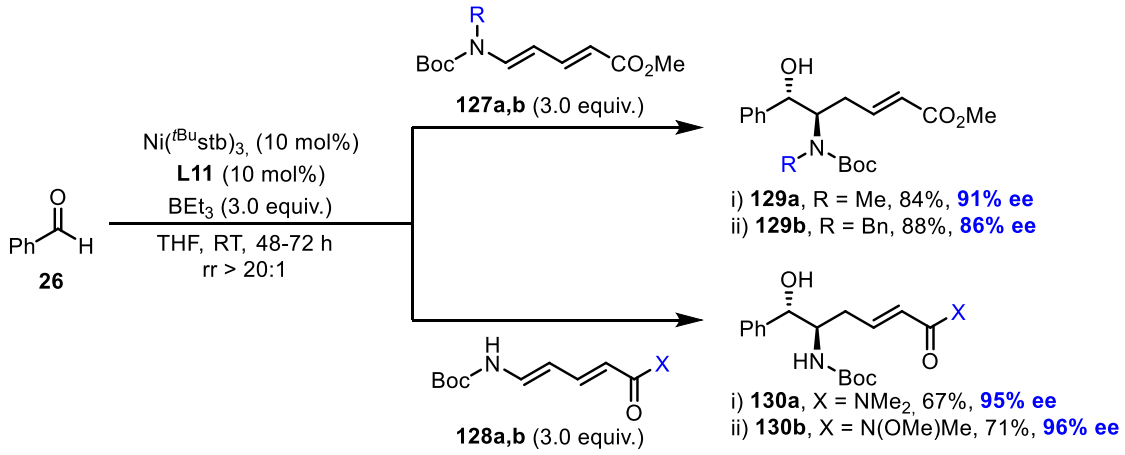

Scheme 46: Reductive coupling reactions featuring modified amino-pentadienoates.

The N-alkylated amino alcohols **129a** and **129b** were obtained in excellent yield and with similarly high optical purity. Given the operationally simple and modular synthesis of the corresponding N-alkylated dienes, these results indicate broad accessibility of structurally related amino alcohol derivatives. This pre-functionalization strategy avoids multi-step derivatization sequences for N-substitution of the reductive coupling products, but also enables orthogonal,

stepwise functionalization of the amino and alcohol groups. Moreover, the consistently high regio-, diastereo-, and enantiocontrol imparted by phosphoramidite ligand **L11** suggests that possible hydrogen-bonding interactions involving the N–H-bond do not play a significant role for the outcome of the reductive coupling.

The coupling reactions involving amide-substituted dienes **128a** and **128b** proceeded well, and the corresponding amino alcohol products **130a** and **130b** were obtained in good yields with even higher enantioselectivities than their methylester analog. The compatibility of the Weinreb-amide functionality bearing a reducible N–O bond with a nickel(0) catalyst is particularly noteworthy and offers a versatile handle for downstream functionalization.[147]

Next, the necessity of an N-protecting group was probed. Since an unprotected version of amino-pentadienoate **88a** was expected to be unstable due to facile tautomerization and subsequent hydrolysis, N,N-dimethylamino analog **131**[148] was employed as an alternative (Scheme 47, top). Although significant aldehyde conversion was observed under the standard conditions and the reaction mixture was subjected to a mild, non-oxidative work-up, the desired product **132** could not be detected and only unconverted diene **131** was observed.

The compatibility of alternative non-carbonyl electron-withdrawing groups with the transformation was also explored. Since cyano-groups are often poorly compatible with low-valent nickel species due to their strong coordinating ability, and nitro-groups are prone to reduction *via* single electron transfer reactions,[149] phenylsulfone-substituted diene **133**[150] was employed instead (Scheme 47, bottom). However, this diene displayed significantly lower reactivity than its ester- and amide-substituted congeners. Even at an increased catalyst loading of 15 mol%, the reaction stalled at approximately 85% conversion. Nonetheless, the phenylsulfone group provided excellent regiocontrol, enabling isolation of product **134** in good yield. However, a pronounced decrease in enantioselectivity and slightly diminished diastereoselectivity were observed, thus highlighting the superior compatibility of carbonyl-based electron-withdrawing groups with this methodology.

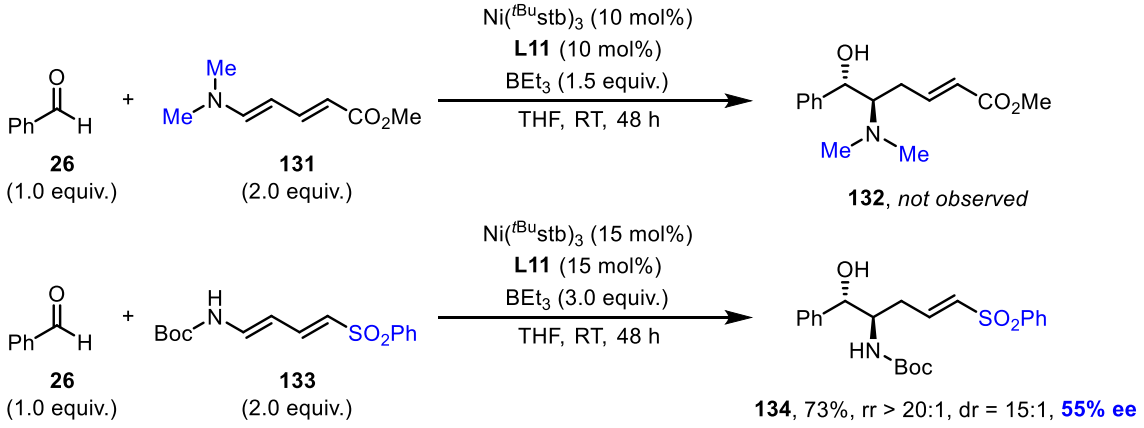

Scheme 47: Reactivity of alternative diene candidates in the nickel-catalyzed reductive coupling.

In addition to carbamate-protected dienes, a phthalimido-substituted analog was investigated. Although phthalimides are generally less attractive than carbamate-protected amines in terms of deprotection and overall preparative value, the fully sp^2-hybridized nature of the phthalimide moiety was considered potentially relevant to the reaction outcome, particularly with respect to regioselectivity. This aspect appeared worthwhile to examine, as the formation of undesired regioisomers had previously resulted in diminished isolated yields in several reductive coupling reactions (see Chapters 2.4 and 2.7).

To access the envisioned phthalimido analog, commercially available N-vinyl-phthalimide **135** was converted to α,β-unsaturated aldehyde **136** *via* a "Vilsmeier-Haack reaction". Subsequent „Horner-Wadsworth-Emmons olefination" afforded diene **138** as a single alkene isomer (Scheme 48).

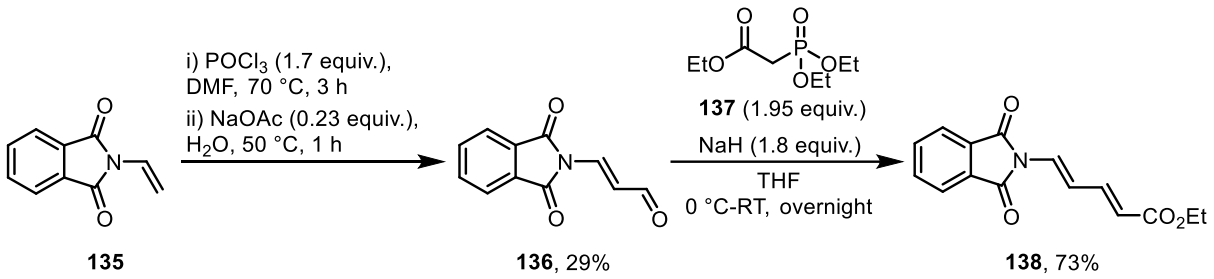

Scheme 48: Synthesis of a phthalimido-protected diene.

The compatibility of diene **138** with the reductive coupling was then evaluated. When the reaction with hydrocinnamaldehyde was attempted to probe potential regioselectivity effects, no significant conversion of either the diene or the aldehyde was observed. Even upon switching to activated *para*-CF_3-substituted benzaldehyde **139**, only small amounts of the desired product were detected (Scheme 49). This pronounced decrease in reactivity is likely due to the strongly electron-withdrawing character of the phthalimide moiety, which substantially deactivates the diene. Additionally, increased structural rigidification may impede diene coordination and contribute to the observed lack of reactivity.

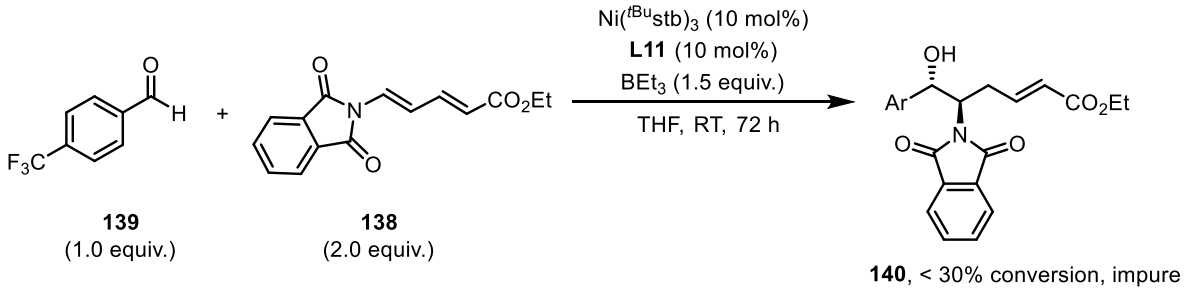

Scheme 49: Unsuccessful application of diene **138** in the nickel-catalyzed reductive coupling reaction.

Since nickel-catalyzed reductive coupling reactions are known to proceed with high diastereospecificity, the synthesis of an *E,Z*-configured amino-pentadienoate derivative was pursued to enable access to *syn*-configured vicinal amino alcohols. However, such a substrate

proved inaccessible *via* the previously established synthetic route (see Chapter 2.2), prompting the development of an alternative strategy.

First, formylation of *tert*-butyl carbamate **141** according to a procedure by Pollack *et al.*[151] afforded N-formyl-carbamate **143** (Scheme 50). Related compounds have been shown to behave as pseudo-aldehydes due to the presence of a second carbonyl unit (in this case Boc-group), which "effectively ties up the nitrogen lone pair".[152] Furthermore, analogous substrates have been reported to undergo "Wittig olefinations" with moderate to excellent *Z*-selectivity.[151-153]

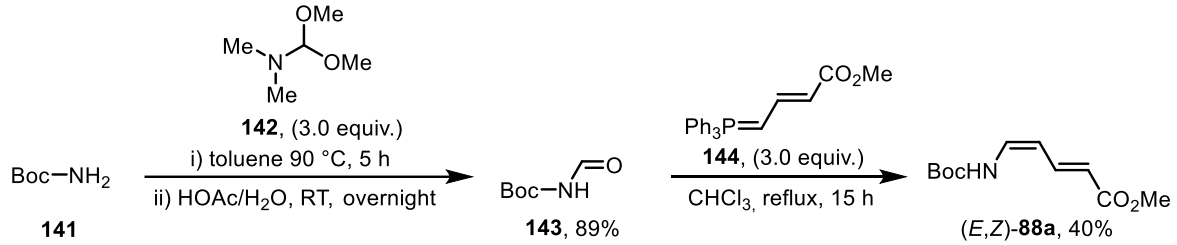

Scheme 50: Synthesis of (*E*,*Z*)-**88a** *via* an olefination approach.

Inspired by these reports, N-formyl-carbamate **143** was subjected to "Wittig olefination" using separately prepared dienyl Wittig-reagent **144**, affording desired (*E*,*Z*)-**88a** in 40% yield as a single alkene isomer. Solvent choice proved crucial, as the desired *Z*-selectivity was observed only in dichloromethane and chloroform. However, dichloromethane underwent nucleophilic substitution with two equivalents of **143**, resulting in substantial amounts of an inseparable byproduct. Therefore, chloroform remained the only suitable solvent.

After establishing a selective synthesis of the *E*,*Z*-configured 5-amino-2,4-pentadienoate, the substrate was evaluated in representative reductive coupling reactions involving aromatic and aliphatic aldehyde candidates (Scheme 51).

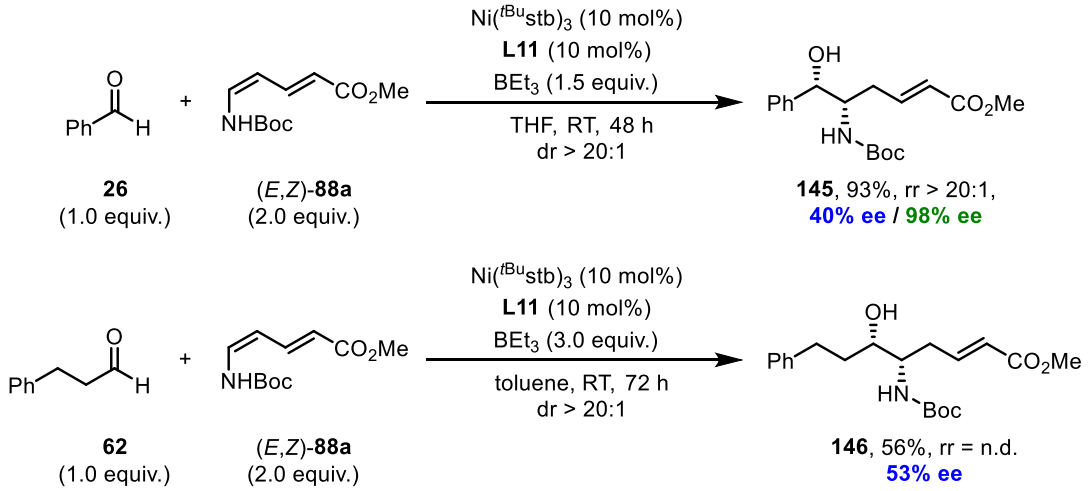

Scheme 51: Synthesis of *syn*-configured vicinal amino alcohols from diene (*E*,*Z*)-**88a** (blue = ee after isolation / green = ee after recrystallization); n.d. = not determined.

The coupling with benzaldehyde proceeded well and furnished the desired *syn*-amino alcohol with high regio- and diastereoselectivity. However, alteration of the diene geometry significantly

diminished the enantioselectivity, as product **145** was obtained with merely 40% ee. Despite the low enantiomeric excess, a single recrystallization afforded the amino alcohol in excellent optical purity and enabled confirmation of the absolute configuration by Mosher Ester analysis.[154]

The reaction with hydrocinnamaldehyde afforded the corresponding *syn*-configured product **146** in moderate yield. Although the regioisomeric ratio could not be reliably determined *via* NMR analysis of the crude reaction mixture, the generally lower regiocontrol observed for aliphatic aldehydes is presumed to be the main factor causing the reduced yield. Again, enantiocontrol induced by phosphoramidite ligand **L11** in the formation of *syn*-amino alcohol **146** appeared to be less stringent, resulting in merely 53% ee.

2.9 Scale-Up and Derivatization

The scalability of the nickel-catalyzed reductive coupling was demonstrated by the gram-scale synthesis of amino alcohol **90a** from benzaldehyde and diene **88a** (Scheme 52). Although regioselectivity was slightly diminished, the isolated yield and optical purity of the product remained essentially unchanged. Moreover, excess diene was largely recovered by flash chromatography, avoiding unnecessary loss of the valuable compound. Again, single recrystallization afforded **90a** in exceptional enantiopurity.

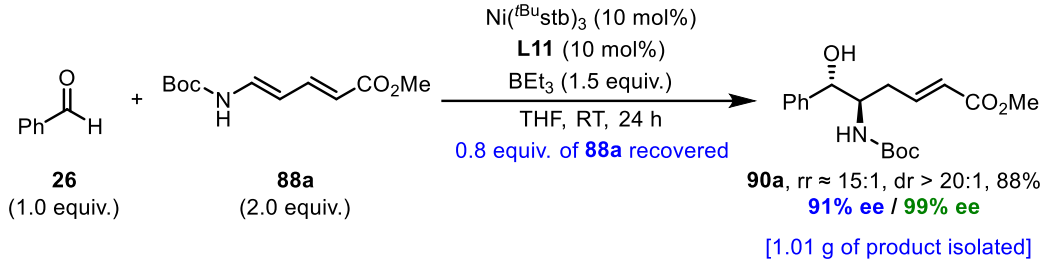

Scheme 52: Gram-scale synthesis of amino alcohol **90a** (blue = ee after isolation / green = ee after recrystallization).

Although the relevance of vicinal amino alcohols as valuable structural motifs (see Chapter 1.3) does not need any particular illustration, a variety of product derivatizations was performed with the enantioenriched material, highlighting the synthetic potential arising from the functional group arrangement of this scaffold.

First, the relative positioning of the protected amine and the ester group was exploited (Scheme 53). Hydrogenation of the double bond followed by acid-catalyzed Boc-deprotection and base-mediated cyclization afforded chiral δ-lactam **147** in excellent yield over three steps. Subsequent reduction of the lactam furnished the corresponding piperidine **148** in quantitative yield. Heterocycles of this type are found in numerous pharmaceutically relevant structures and have been isolated from natural sources.[155-158]

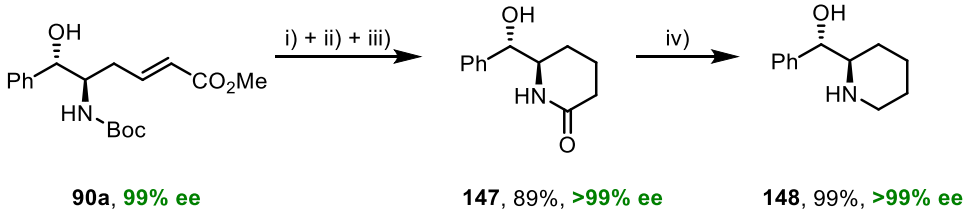

Scheme 53: Multistep derivatization of amino alcohol **90a** into δ-lactam **147** and piperidine derivative **148**; i) H_2 (1 atm), Pd/C (cat.), EtOAc, RT, 30 min; ii) HCl (20 equiv.), 1,4-dioxane, 50 °C, overnight; iii) NEt_3 (4.0 equiv.), EtOH, reflux, overnight; iv) $LiAlH_4$ (3.0 equiv.), THF, 0 °C-65 °C, 90 min.

In addition, the arrangement of the free alcohol and the α,β-unsaturated ester in **90a** enabled an "oxa-Michael addition", affording tri-substituted tetrahydrofuran **149** in essentially quantitative yield (Scheme 54).

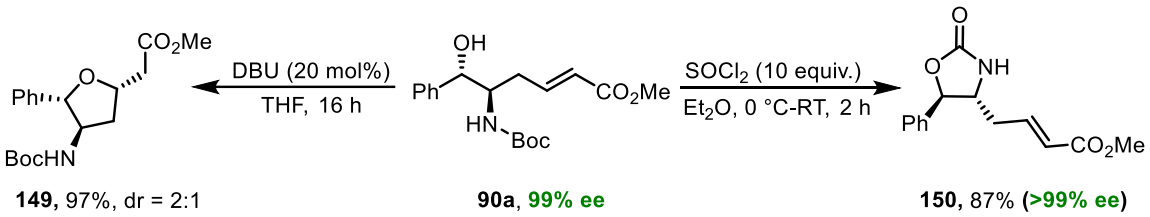

Scheme 54: Intramolecular downstream derivatizations of amino alcohol **90a**.

The close proximity of the free alcohol and the Boc-protected amine was also taken advantage of, as treatment of **90a** with thionyl chloride resulted in formation of oxazolidinone **150** (Scheme 54).

Formation of cyclic carbamates *via* this strategy generally proceeds with inversion at the alcohol-bearing stereocenter for both aliphatic and aromatic amino alcohol derivatives,[159] which was further confirmed by single-crystal X-ray analysis, establishing both the relative and absolute configuration of **150** (Figure 8).

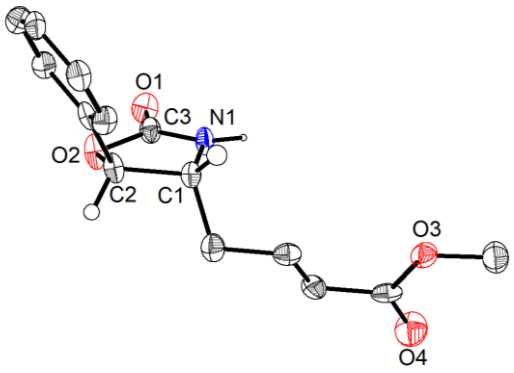

Figure 8: Single-crystal X-ray structure of oxazolidinone **150** (majority of H-atoms omitted for clarity).

Consequently, this approach provides indirect access to the *syn*-series and partially compensates for the lack of enantioselectivity observed in the direct synthesis of *syn*-configured amino alcohols from *E,Z*-configured amino-pentadienoates and aldehydes (see Chapter 2.8).

2.10 Mechanistic Considerations

Although 5-amino-2,4-pentadienoates constitute a novel substrate class for nickel-catalyzed reductive couplings with aldehydes, the available experimental evidence does not suggest fundamental deviations from the generally accepted catalytic cycle established for related couplings of unsaturated compounds with carbonyl derivatives.[160, 161] Accordingly, the reaction is proposed to proceed through initial coordination of the chiral phosphoramidite ligand **L11**, the diene and the aldehyde to the nickel center, followed by reversible oxidative cyclization to generate an allyl-oxanickelacycle intermediate (Scheme 55). Triethylborane may facilitate this step through Lewis-acid activation of the aldehyde, thereby lowering its LUMO and increasing its susceptibility toward oxidative cyclization. Whether such activation is operative or even required for the present substrate class, however, remains unclear. In the presence of triethylborane, transmetalation and β-hydride-elimination occur and generate an allyl-nickel-hydride species. Subsequent reductive elimination releases the corresponding borinate ester of the amino alcohol as the primary reaction product prior to hydrolytic work-up and simultaneously regenerates the nickel(0) catalyst, thereby completing the catalytic cycle.

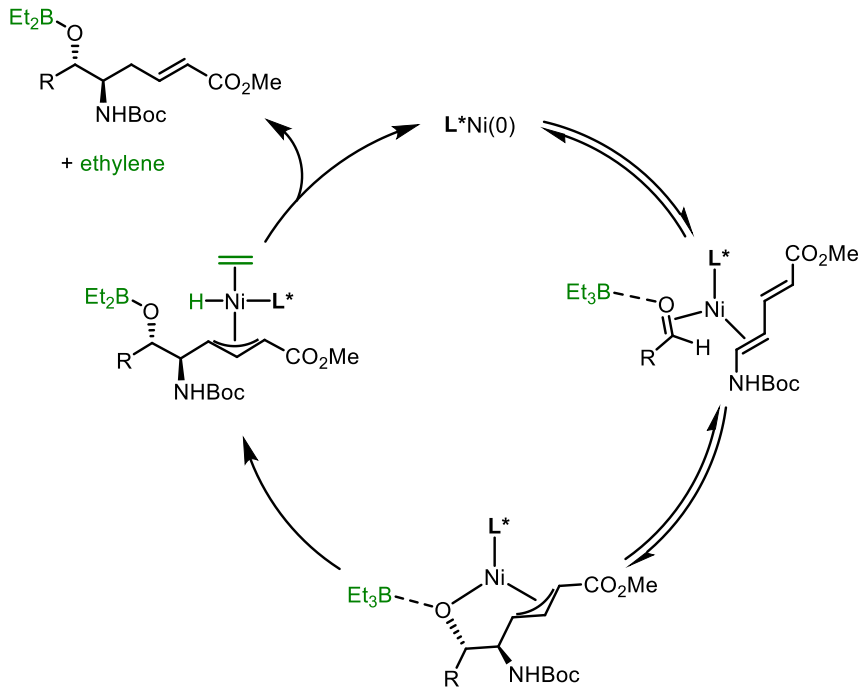

Scheme 55: Simplified presumed catalytic cycle for the reductive coupling of aldehydes and amino-pentadienoates.

Despite this seemingly straightforward reaction mechanism, several aspects of the transformation remain poorly understood. One fundamental uncertainty concerns the mode of substrate binding in the π-complex formed prior to oxidative cyclization. At present, it is unclear which of the two conjugated double bonds preferentially coordinates to the metal center and whether such a regiochemical preference in complexation influences the subsequent course of the reaction. Furthermore, early studies by Tamaru and co-workers proposed an η^4-coordination of dienes in an s-*trans* conformation, although this assumption has never been substantiated. Since the geometry of the nickel(0) π-complex is expected to determine the structure of the resulting allyl-

oxanickelacycle, uncertainties at this early stage of the catalytic cycle inevitably complicate any detailed mechanistic interpretation.

A second major unresolved question concerns the origin of the remarkable ligand effects observed with ligand **L11**. Among the ligands examined in this study and in related regioinverted reductive coupling reactions developed in our group, VAPOL-derived phosphoramidite **L11** remains so far uniquely capable of promoting reaction at the least nucleophilic terminus of the respective diene, while simultaneously providing high levels of enantiocontrol. One structural feature that distinguishes **L11** from most of the ligand candidates investigated is the location of the major groove of the chiral backbone on the front side of the ligand framework. This arrangement may position the extended π-system in close proximity to the coordinated substrates, potentially enabling secondary attractive interactions that influence substrate orientation within the chiral catalyst pocket and thereby impact the regio- and stereochemical outcome of the coupling. However, this explanation alone appears insufficient to account for the observed selectivity. Most notably, vaulted sibling **L17** essentially failed to offer any regio- or enantiocontrol (see Chapter 2.3), despite sharing many of the same architectural features. Consequently, the precise structural and electronic factors responsible for the exceptional performance of ligand **L11** remain elusive at this point.

Further insight into these questions would require detailed information about the structure of catalytically relevant intermediates. In the presence of an amino-pentadienoate, an aldehyde and ligand **L11**, formation of either a substrate-bound π-complex or an allyl-oxanickelacycle intermediate would be expected. However, attempts to crystallize any such nickel species with the aim of gaining a better understanding of the binding poses within the loaded catalyst, were unfruitful. As a result, direct experimental information regarding substrate orientation and catalyst geometry is currently unavailable. This limitation is corroborated by previous studies on related reductive couplings of sorbate derivatives in our group, which had shown "unusually complex speciation in solution" as judged by NMR analysis.[99, 162] Therefore, the possibility that multiple catalytically competent nickel species, as well as catalytically inactive reservoir species, coexist under the reaction conditions cannot be excluded.

Beyond uncertainties regarding catalyst structure and substrate binding, several experimental observations made for the coupling of amino-pentadienoate derivatives indicate that additional factors influence the selectivity-determining events of the reaction. These include but are not limited to (i) pronounced solvent effects on both regio- and enantioselectivity, (ii) the presence of a competing racemic and regiocomplementary background reaction, (iii) possible non-linear effects, (iv) drastic impact of water on regioisomer formation, and (v) substrate-dependent selectivity trends that cannot yet be rationalized in a consistent manner. Collectively, these findings suggest that the observed selectivity arises from a delicate interplay of multiple contributing factors rather than from a single dominant stereocontrolling interaction.

Overall, the currently available experimental data do not permit the development of a comprehensive mechanistic model for this transformation. Uncertainties regarding substrate

binding, catalyst speciation, and the origin of ligand-controlled selectivity continue to limit any mechanistic interpretation. Future progress will likely require the identification of a more experimentally tractable model system, ideally involving highly crystalline intermediates. In addition, extensive computational investigations may prove indispensable for elucidating the reaction pathway and identifying transient intermediates that are difficult or impossible to access through conventional spectroscopic methods.

2.11 Summary

Nickel-catalyzed intermolecular reductive coupling reactions between aldehydes and 1,3-dienes have first been investigated in the late 1990s by the groups of Mori and Tamaru in the form of silane- and borane-mediated allylation and homoallylation reactions (Scheme 56).

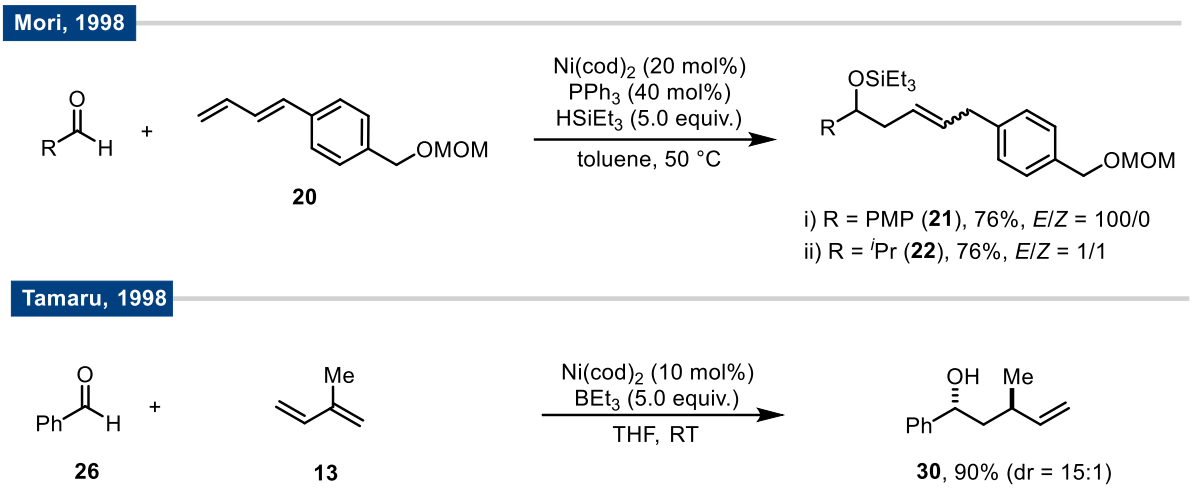

Scheme 56: Representative examples of silane-mediated "Mori-type" and borane-mediated "Tamaru-type" couplings between aldehydes and 1,3-dienes.

Despite their considerable synthetic potential, enantioselective versions of these transformations remained scarce and only recently gained increased attention. However, most asymmetric methodologies remain restricted to relatively simple dienes containing alkyl or aryl substituents. The incorporation of heteroatom-containing functional groups is typically unexplored or associated with limited substrate compatibility.

Interestingly, ligand effects had largely been overlooked in classical "Tamaru-type" reductive coupling reactions. During the total synthesis of the natural product Chagosensine in our group, it was discovered that addition of an exogenous ligand can alter the regiochemical course of the reaction, promoting coupling at the least nucleophilic site of the diene. The VAPOL-derived phosphoramidite ligand **L11** proved particularly well suited for this novel reaction mode, enabling stringent regio-, diastereo- and enantiocontrol. These asymmetric, regioinverted reductive coupling reactions had been shown to be compatible with both dienol ethers and sorbate derivatives (Scheme 57).

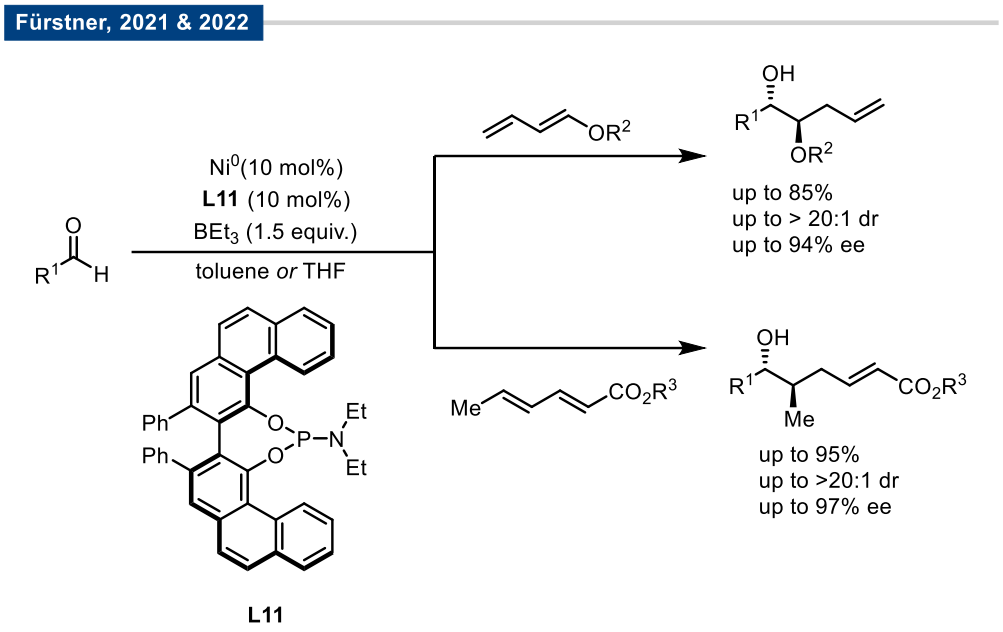

Scheme 57: Regioinverted coupling reactions between aldehydes and dienol ethers or sorbate derivatives previously developed in our group.

Given their importance across diverse fields, ranging from natural product synthesis and pharmaceuticals to chiral ligands and catalysts, vicinal amino alcohols represented attractive synthetic targets for further expanding the scope and applicability of this emerging transformation. Initial attempts to extend this reaction mode to dienecarbamates revealed limitations of the existing catalytic system featuring VAPOL-derived phosphoramidite ligand **L11** and highlighted the need for substrate redesign. The formal introduction of an electron-withdrawing ester-group at the remote terminus of the diene proved essential, as the resulting N-protected 5-amino-2,4-pentadienoates exhibited substantially improved regio- and enantioselectivity in the reductive coupling with aldehydes.

An efficient, modular and scalable synthesis of these previously unexplored push-pull dienes was developed, providing concise and practical access to a versatile family of coupling partners for the nickel-catalyzed reductive coupling. Their behavior in the reductive coupling reaction was investigated in detail. Under ligand-free conditions, these dienes react at the more nucleophilic terminus resulting in the formation of racemic aldol-type products. Remarkably, in the presence of **L11**, the intrinsic regioselectivity of the nickel-catalyzed coupling is overwritten, enabling bond formation at the least nucleophilic site of the diene and affording vicinal amino alcohol products with excellent stereocontrol (Scheme 58). Notably, modification of the ligand backbone led to pronounced decreases in both regio- and enantioselectivity, underscoring the unique ability of phosphoramidite **L11** to promote these asymmetric regioinverted coupling reactions.

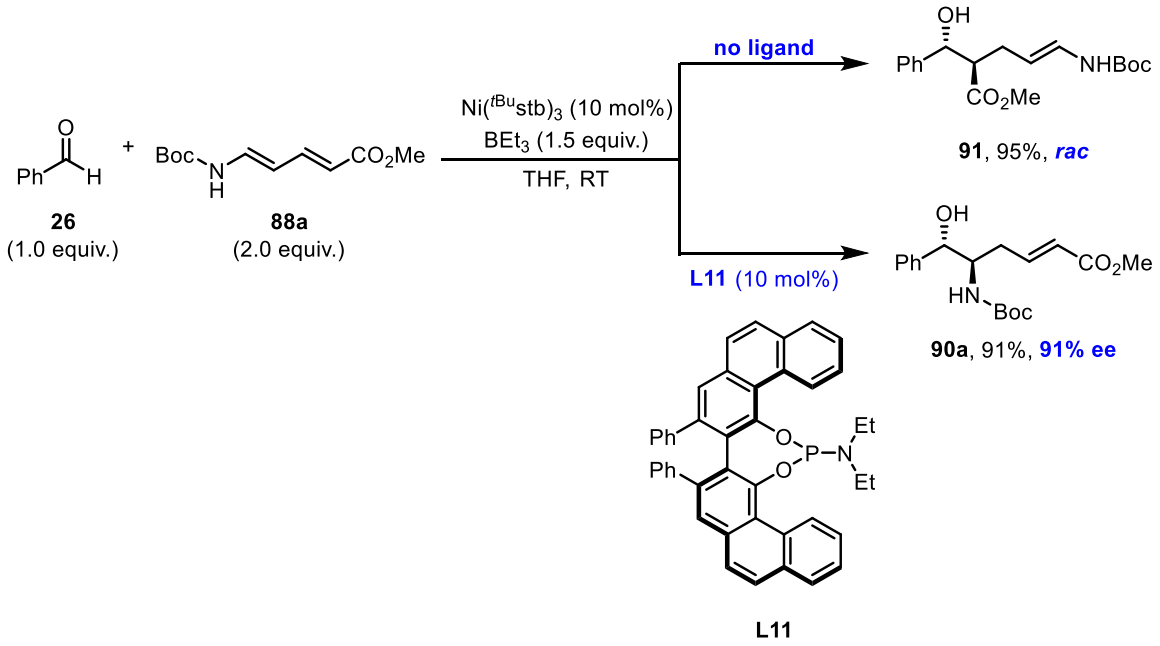

Scheme 58: Representative reactions illustrating the reactivity of an N-protected 5-amino-2,4-pentadienoate in the nickel-catalyzed reductive coupling under ligand-free conditions and in the presence of ligand **L11**.

Systematic screening of reaction conditions identified key-parameters governing catalyst performance and selectivity, providing an important guideline for the practical application of this catalytic system. Moreover, aromatic and aliphatic aldehydes were found to exhibit markedly different behavior in the reductive coupling. Therefore, separate reaction protocols had to be developed for each substrate class. Optimization studies identified pronounced solvent effects and ultimately led to two complementary reaction protocols tailored to aromatic and aliphatic aldehydes, respectively. The methodology proved broadly applicable, providing highly selective access to a diverse range of vicinal amino alcohols derived from both (hetero)aromatic and aliphatic aldehydes. Most products were obtained as crystalline solids and, following a single recrystallization, were isolated as virtually single enantiomers.

The scope of the reaction was also examined with regard to the diene component. Numerous synthetically useful and orthogonal N-protecting groups were well tolerated. Additional modifications of both the amine substituent and the electron-withdrawing directing group not only demonstrated the versatility and synthetic utility of the method but also revealed certain limitations regarding substrate design.

The practical utility of the reductive coupling was further highlighted by a gram-scale experiment without any notable loss in selectivity or yield, as well as through a variety of intramolecular derivatization reactions, enabling access to valuable structural motifs including a chiral piperidine, a tetrahydrofuran-derivative and an oxazolidinone.

Throughout this study, numerous factors influencing reactivity and selectivity with respect to both reaction conditions and substrate design were identified. Nevertheless, the exact reasons why VAPOL-derived phosphoramidite ligand **L11** is uniquely effective in altering the regiochemical

pathway and exerting high levels of enantiocontrol remain unclear. Further experimental and computational studies will therefore be required to develop a more detailed mechanistic picture.

Nevertheless, the present transformation displays significant synthetic utility, as it enables the regio-, diastereo- and enantioselective synthesis of vicinal amino alcohols, while simultaneously establishing two stereogenic centers from prochiral starting materials. This approach significantly expands the still limited repertoire of transition-metal-catalyzed reductive coupling strategies for the synthesis of these highly valuable structural motifs and provides an atom-economical alternative to established synthetic approaches. Furthermore, this study demonstrates that regioinverted nickel-catalyzed coupling reactions constitute a broadly applicable catalytic concept. Following electron-rich dienol ethers and electron-deficient sorbate derivatives, push-pull dienes now represent a third, electronically distinct class of dienes compatible with this reaction mode. This significant expansion of the substrate scope highlights the increasing generality of this methodology and further establishes it as a powerful strategy for the asymmetric synthesis of complex structural motifs.

3 Enantioselective Synthesis of Tetrahydroisoquinolines and Related Heterocycles *via* Intramolecular Nickel-Catalyzed Reductive Coupling Reactions

3.1 Aim

Following the successful development of the nickel-catalyzed enantioselective reductive coupling of protected 5-amino-2,4-pentadienoate derivatives with aldehydes, the question arose whether this transformation could be extended to an intramolecular reaction setting (Scheme 59). Notably, previous control experiments had demonstrated that N-alkylation of the diene does not adversely affect either the reactivity or the selectivity of the enantioselective regioinverted intermolecular coupling reaction (see Chapter 2.8). This observation suggested that an intramolecular variant may be realized by introducing an N-substituent bearing a suitably positioned aldehyde.

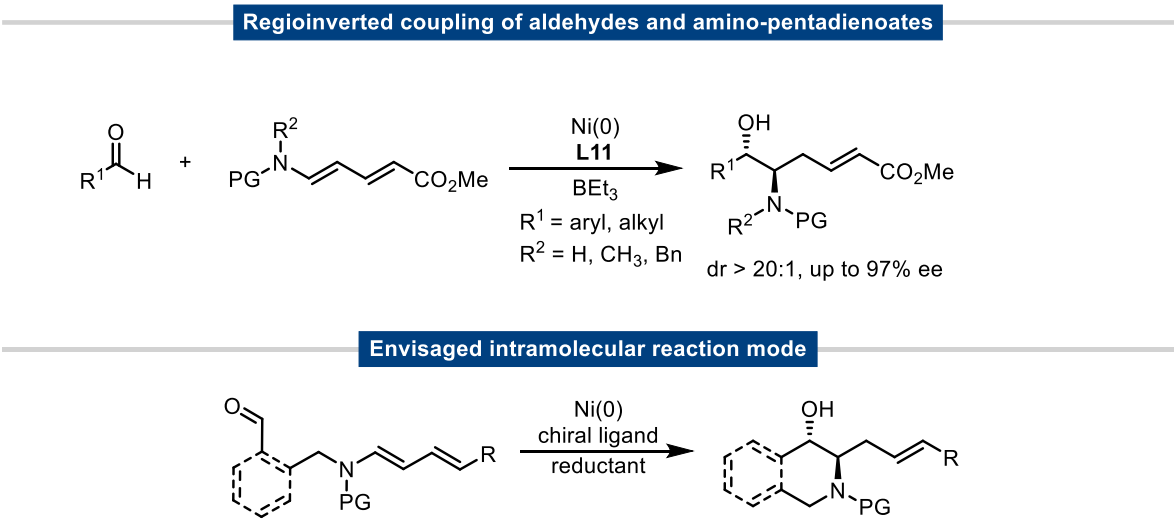

Scheme 59: Envisaged enantioselective intramolecular reductive cyclization of N-substituted amino-pentadienoates.

Such an approach to N-heterocyclic ring systems was particularly intriguing, given that intramolecular diene-aldehyde reductive coupling reactions represent the earliest examples of this particular type of nickel catalysis, predating the turn of the millennium (see Chapter 1.2.1). However, these intramolecular transformations typically suffer from poor double-bond regiocontrol, often resulting in mixtures of alkene isomers, which consequently limits both substrate scope and applicability. Moreover, only a single pioneering report describing an asymmetric diene cyclization reaction has appeared to date, featuring merely one heterocyclic example. Importantly, the limitations observed in the racemic reaction mode could not be overcome and the enantioselectivities achieved were also mostly insufficient by modern standards. Remarkably, no subsequent efforts to improve or generalize this methodology have been reported in the more than 25 years since its publication. As a result, intramolecular reductive cyclization reactions have largely remained of conceptual interest, whereas research in the field has focused predominantly on the development of more versatile asymmetric intermolecular variants (see Chapter 1.2.3 and 1.2.4).

On this basis, the development of an asymmetric nickel-catalyzed intramolecular reductive coupling reaction for heterocycle synthesis appeared highly worthwhile. Such a transformation would further extend the concept of regioinverted couplings and provide efficient access to valuable chiral N-heterocycles, thereby advancing asymmetric intramolecular reductive cyclizations from proof-of-concept demonstrations to a synthetically useful methodology.

3.2 Preliminary Experiments and Reaction Optimization

The investigations on the envisaged asymmetric intramolecular reductive coupling reaction commenced with the preparation of a suitable model substrate. Given their ease of synthesis and previously demonstrated excellent compatibility in the intermolecular reaction mode, protected amino-pentadienoates were again employed. An operationally simple base-mediated nucleophilic substitution reaction between diene **88a** and 2-(bromomethyl)benzaldehyde **151** in the presence of tetrabutylammonium iodide afforded the desired product **152** in excellent yield (Scheme 60).

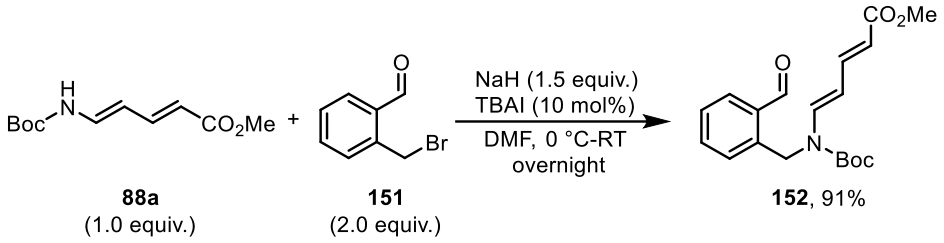

Scheme 60: Synthesis of a model substrate for the envisaged asymmetric nickel-catalyzed reductive cyclization.

This precursor was considered an ideal candidate for the nickel-catalyzed asymmetric reductive cyclization in the presence of VAPOL-derived phosphoramidite ligand **L11**. As described in the first part of this work, this ligand had proven highly effective in inverting the regiochemical course of intermolecular couplings between protected amino-pentadienoates and aldehydes, favoring reaction at the least nucleophilic, amine-substituted diene terminus. Additionally, N-benzylation of the diene had shown little impact on the enantioselectivity of the intermolecular reductive coupling, hence it was assumed that **152** might be able to cyclize in a similarly selective fashion. By tethering the diene to the aldehyde-containing moiety, the substrate was locked in a constitution that should highly favor reaction at the amine-substituted diene terminus. This design aligns with the inherent regiochemical preference induced by **L11** and was anticipated to enable a strong asymmetric induction. In addition, as observed in the intermolecular variant, the remote ester group was expected to further improve enantiocontrol.

To test this hypothesis, model substrate **152** was subjected to the reductive coupling conditions in presence of ligand **L11** (Scheme 61). The reaction proceeded smoothly and exhibited great diastereoselectivity, allowing the desired product **153** to be obtained as a single diastereomer in excellent yield. Moreover, no alkene isomer formation was observed. However, the enantiomeric excess of 13% was far off the excellent optical purity attained in the intermolecular coupling.

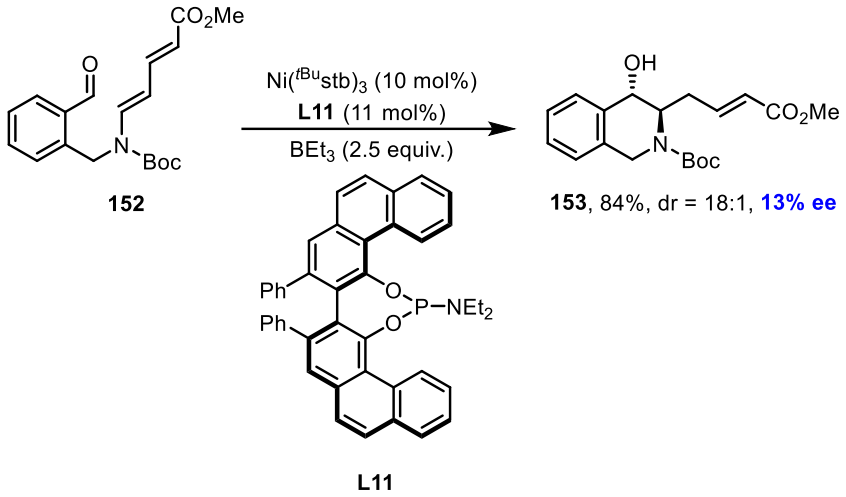

Scheme 61: Initial result for the enantioselective intramolecular reductive coupling.

Similar to the preliminary studies on the intermolecular reductive coupling reaction (see Chapter 2.2), these results emphasize that substrate design principles established for one class of nickel-catalyzed reductive couplings cannot per se be extrapolated to closely related transformations. Rather, each transformation appears to be governed by its own delicate balance of steric and electronic effects and even minor structural modifications can lead to substantial changes in reaction outcome. Nonetheless, the fact that the desired reactivity was observed and the cyclization proceeded smoothly under ambient conditions provided a strong incentive to further investigate this novel reaction mode.

To determine whether a competing racemic background reaction might account for the unexpectedly low enantioselectivity observed in the model reaction with phosphoramidite **L11**, the reaction was performed in the absence of any exogenous ligand. Under these conditions, *rac*-**153** was obtained in respectable yield (Table 4, entry 1). This result suggests that the substrate connectivity itself dictates the regiochemical course of the cyclization. Evidently, the ligand is not required to suppress coupling at the proximal double bond of the dienoate subunit, as formation of the corresponding nine-membered aldol-type product is not kinetically competitive.

Consistent with this interpretation, reactions featuring simple phosphine ligands such as PPh_3 (Table 4, entry 2) and PCy_3 (Table 4, entry 3) also resulted in formation of *rac*-**153**. In contrast, bidentate 1,2-bis(diphenylphosphino)ethane (dppe) resulted in strongly diminished reactivity (Table 4, entry 4), likely because chelation blocks a coordination site required for transmetalation and β-hydride elimination during the catalytic cycle.

Importantly, the diastereomeric ratios observed in the crude reaction mixtures varied with the choice of ligand. This observation indicates that the ligand remains coordinated to the nickel center during the stereodetermining step. Consequently, a ligand-free racemic background reaction is unlikely to be operative to a significant extent and the low enantioselectivity observed with phosphoramidite **L11** most likely results from weak enantioinduction in this transformation. At the same time, these results suggested that identification of a more suitable chiral ligand should enable substantially improved enantiocontrol.

Table 4: Control experiments for the racemic intramolecular reductive cyclization of substrate **152**.

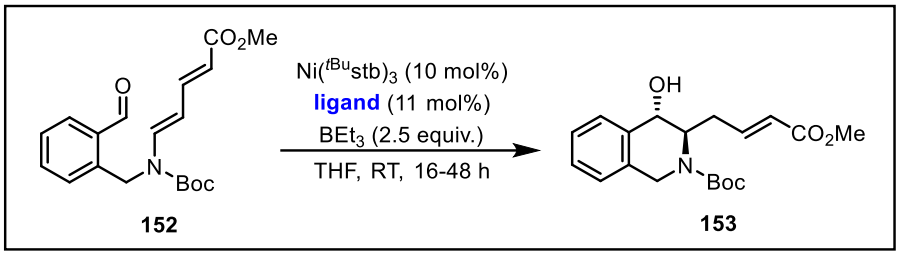

Entry	Solvent	Ligand	dr	Conversion	Isolated Yield
1	THF	---	4:1	quant.	50%
2	THF	PPh_3	4:1	quant.	n.d.
3	THF	PCy_3	11:1	quant.	80%
4	THF	dppe	n.d.	< 20%	n.d.

n.d. = not determined

To this end, a variety of monodentate phosphorous-based chiral ligands was evaluated in the model reaction (Figure 9 and Table 5). As previously observed in the intermolecular reductive coupling, BINOL- and SPINOL-derived phosphoramidite ligands displayed limited compatibility with the reaction and did not achieve meaningful conversions (Table 5, entries 1 and 2). In contrast, TADDOL-based phosphoramidites and phosphonites provided substantially improved levels of enantioinduction (Table 5, entries 3 to 12). However, despite the systematic variation of both the steric and electronic properties of the flanking aryl substituents and the phosphorus-bound headgroup, only moderate optical purities were obtained, with ee values ranging from 52% to 77%.

Inspired by the successful application of P-chiral ligands containing a 1,3-oxaphosphole motif in nickel-catalyzed enantioselective intramolecular reductive cyclization reactions of alkynes,[39-41] a number of commercially available representatives were investigated. Application of (*S*)-BIDIME **L26** improved both the diastereo- and enantioselectivity (Table 5, entry 13). In contrast, the structurally related bidentate BIBOP-ligand **L27** exhibited low conversion, marginal enantioinduction and a surprising inversion in diastereoselectivity (Table 5, entry 14). Likewise, increasing the steric bulk around the phosphorous-atom, as in **L28**, proved detrimental with respect to enantiocontrol (Table 5, entry 15). Gratifyingly, formal replacement of the 2,6-dimethoxyphenyl substituent with an anthracenyl group in (*S*)-AntPhos **L29** resulted in significant improvements in both diastereo- and enantioselectivity (Table 5, entry 16).

Although triethylborane remained the reductant of choice due to its low intrinsic reactivity toward aldehydes, diethylzinc proved to be a viable alternative, furnishing product **153** with virtually identical yield and selectivity (Table 5, entry 17). In contrast, triethylsilane proved unsuitable (Table 5, entry 18), despite its track-record in both inter- and intramolecular reductive coupling reactions between aldehydes and 1,3-dienes. The choice of solvent had a comparably small impact on the reaction outcome (Table 5, entries 19 to 21). Optimal results were obtained in THF at 0 °C

(Table 5, entry 22), while further lowering the temperature to –20 °C resulted in incomplete conversion without improving enantioselectivity.

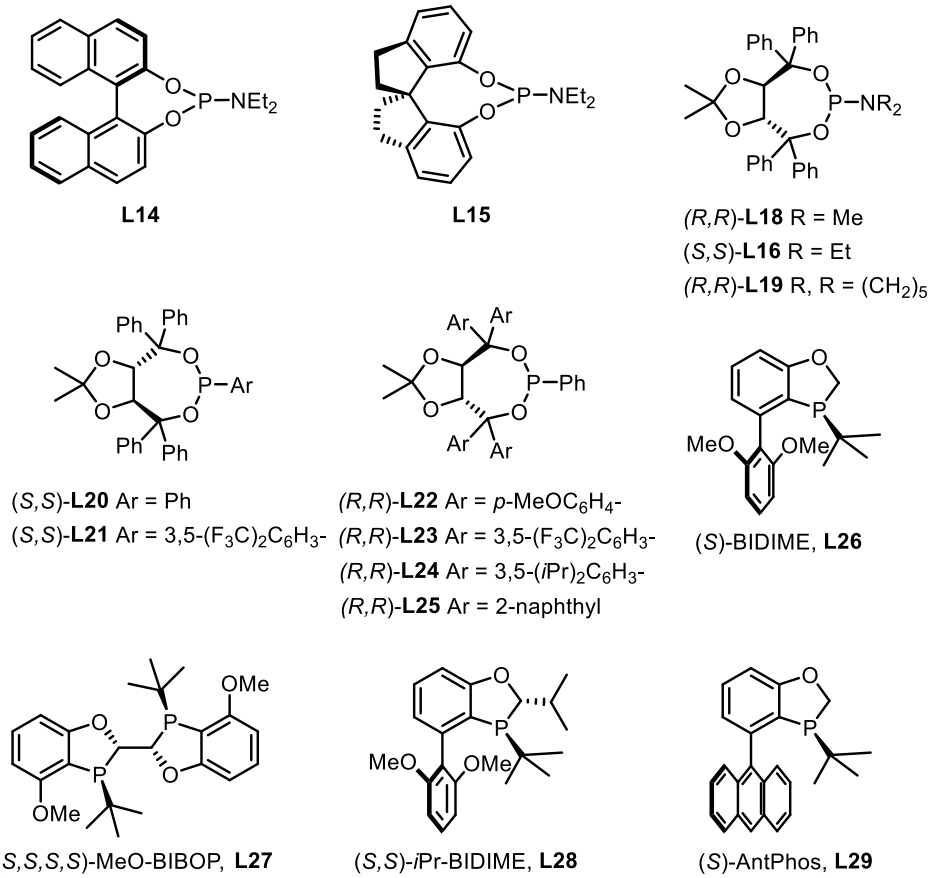

Figure 9: Ligand candidates for the nickel-catalyzed enantioselective intramolecular reductive cyclization reaction.

One particularly noteworthy observation emerged from the ligand screening. Although (*S*)-BIDIME **L26** and (*S*)-AntPhos **L29** both comprise equally configured stereogenic phosphorus centers, they furnish the antipodal products (–)-**153** and (+)-**153**, respectively. Evidently, the steric profile of the lateral biaryl substituents constitutes a critical determinant of the stereochemical outcome. In particular, the extended π-system of the anthracenyl substituent in **L29** may engage in attractive non-covalent interactions with the substrate in the enantiodetermining transition state. These interactions appear sufficiently influential to override the stereochemical bias imposed by the phosphorus stereocenter itself, thereby altering not only the degree but even the sense of asymmetric induction.

Table 5: Selected optimization experiments for the intramolecular reductive cyclization of substrate **152**.

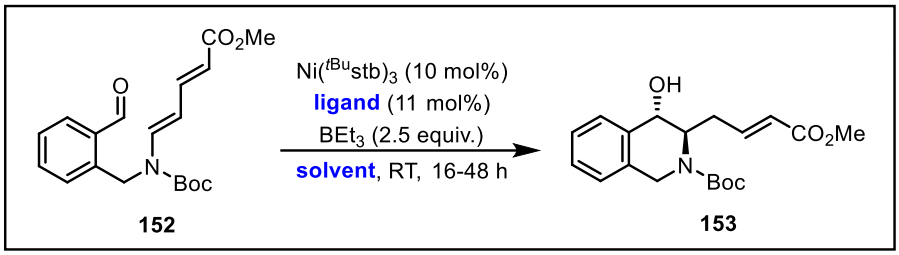

Entry	Solvent	Ligand	dr	ee	Conversion	Isolated Yield
1	THF	**L14**	n.d.	n.d.	< 30%	n.d.
2	THF	**L15**	n.d.	n.d.	< 5%	n.d.
3	THF	(*R*,*R*)-**L18**	6:1	77%	quant.	n.d.
4	THF	(*S*,*S*)-**L16**	5:1	(–)-77%	quant.	71%
5	toluene	(*S*,*S*)-**L16**	2:1	(–)-59%	quant.	n.d.
6	THF	(*R*,*R*)-**L19**	6:1	77%	quant.	n.d.
7	THF	(*S*,*S*)-**L20**	3:1	(–)-72%	quant.	29%
8	THF	(*S*,*S*)-**L21**	n.d.	(–)-66%	<50%	n.d.
9	THF	(*R*,*R*)-**L22**	6:1	54%	quant.	72%
10	THF	(*R*,*R*)-**L23**	8:1	53%	quant.	72%
11	THF	(*R*,*R*)-**L24**	11:1	67%	quant.	92%
12	THF	(*R*,*R*)-**L25**	11:1	54%	quant.	92%
13	THF	**L26**	8:1	(–)-82%	quant.	71%
14	THF	**L27**	1:20	2%	50%	40%
15	THF	**L28**	6:1	(–)-22%	quant.	n.d.
16	THF	**L29**	>20:1	90%	quant.	86%
17	THF	**L29**[a]	>20:1	90%	quant.	87%
18	THF	**L29**[b]	---	---	---	---
19	1,4-dioxane	**L29**	>20:1	87%	quant.	n.d.
20	Et_2O	**L29**	>20:1	88%	quant.	n.d.
21	2-Me-THF	**L29**	>20:1	89%	quant.	n.d.
22	**THF**	**L29**[c]	**>20:1**	**92%**	**quant.**	**88%**

[a] = $ZnEt_2$ (1 M in hexane) used as reducing agent instead of BEt_3, the reaction was complete within 1 h; [b] = neat $HSiEt_3$ used as reducing agent instead of BEt_3, no conversion was observed after 7 d; [c] = performed at 0 °C; n. d. = not determined

3.3 Substrate Synthesis

Assistance with the substrate syntheses by Yannik Sell is gratefully acknowledged.

Once reaction conditions for the enantioselective intramolecular reductive cyclization reaction were established, novel substrates containing an aldehyde and amino-pentadienoate moiety were prepared to investigate their compatibility with the newly developed reaction mode. The required amino-pentadienoates were readily prepared on multigram scale according to the previously developed "Curtius rearrangement" approach (see Chapter 2.2). Consequently, the substrate syntheses in this project largely focused on the preparation and incorporation of the corresponding aldehyde-containing fragments.

Most substrates could be assigned to one of three categories and were prepared according to the retrosynthetic strategies outlined in Scheme 62.

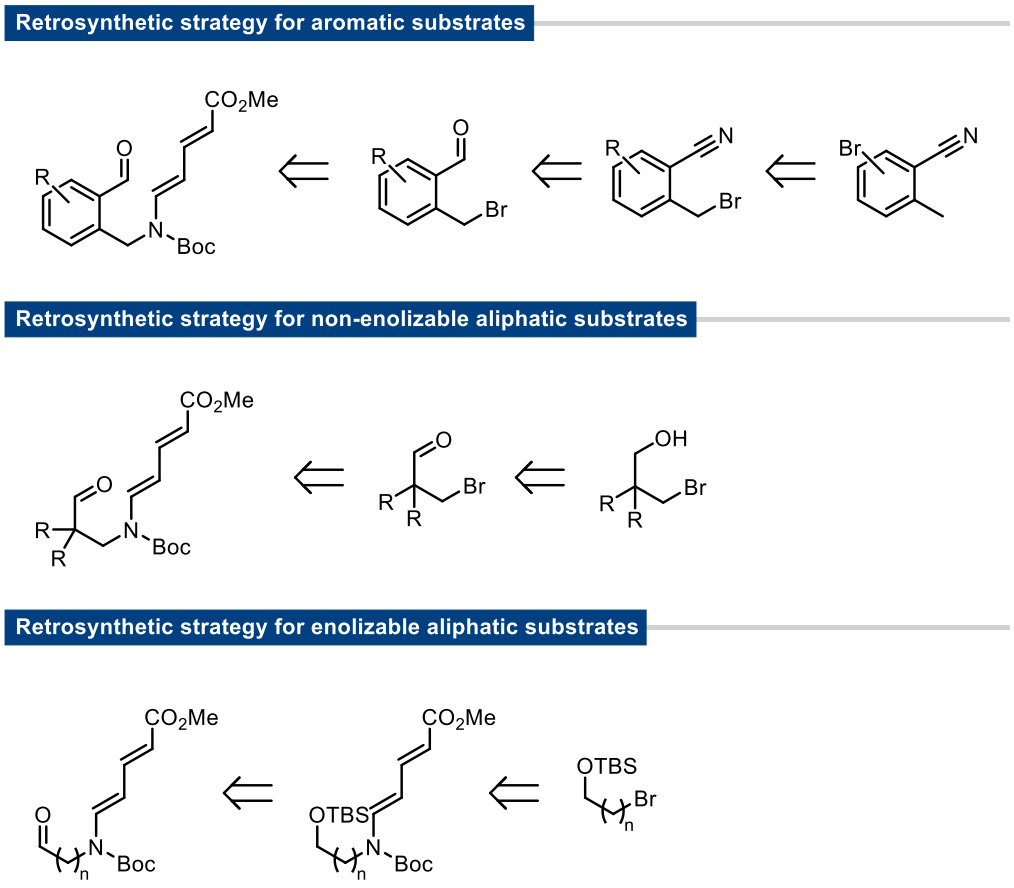

Scheme 62: General retrosynthetic strategies for the synthesis of the substrates used in the reductive cyclization studies.

The largest group was comprised of aromatic aldehyde derivatives, which were assembled by tethering a suitably substituted 2-(bromomethyl)benzaldehyde derivative to the corresponding amino-diene through a base-mediated nucleophilic substitution, analogous to the synthesis of the model substrate (see Chapter 3.2). The required bromomethylbenzaldehydes were in most cases prepared from substituted 2-methylbenzonitriles precursors. While certain substituents (*e.g.* Ph, SO_2Ph, BPin) had to be introduced by Pd-catalyzed cross-coupling reactions, the majority of the

nitrile precursors were commercially available. Subsequent "Wohl-Ziegler bromination", followed by reduction of the nitrile and hydrolysis of the resulting imine, furnished the desired 2-(bromomethyl)benzaldehydes.

For aliphatic substrates, two complementary approaches were employed depending on the nature of the aldehyde. Non-enolizable aldehydes bearing an alkyl bromide handle were obtained by oxidation of the corresponding commercially available bromoalkanols. Subsequent nucleophilic substitution then allowed attachment of the aldehyde-containing fragment to the protected amino-pentadienoate. Pleasingly, even neopentyl bromides were well compatible with this strategy. In contrast, enolizable aldehydes proved incompatible with the basic substitution conditions. Therefore, the corresponding TBS-protected bromoalkanols were first coupled to the diene scaffold. Subsequent desilylation and oxidation of the liberated alcohol then afforded the desired aldehyde substrates.

3.4 Reaction Scope

With suitable substrates in hand, the reaction scope of the enantioselective intramolecular reductive cyclization was explored (Scheme 63).

In line with observations from the intermolecular reductive coupling, the carbamate protecting group on the nitrogen atom had little influence on the reaction outcome, as both Boc- and Cbz-protected tetrahydroisoquinolines **153** and **154** were obtained in comparable yields and enantioselectivities. Moreover, the model reaction could be conveniently scaled to 1 mmol without any loss in yield or selectivity. Given the modular synthesis of the amino-pentadienoates, differently protected analogs could likely be accessed with similar efficiency if required.

Next, a "fluoride scan" was performed to assess whether substituents on the aromatic ring influence the reaction outcome and, if so, to what extent. Substituents in *ortho*-, *meta*-, and *para*-position relative to the tethered diene were well tolerated and the corresponding products **155**, **156** and **157** were obtained in excellent yields with consistently high enantioselectivities. However, introduction of the fluoride in *ortho*-position relative to the aldehyde led to partial loss of regiocontrol, as the desired product **158a** was accompanied by the inseparable, deconjugated alkene isomer **158b** (rr ≈ 4:1, determined by ^{1}H NMR). Together with the notably reduced enantioselectivities observed for both isomers, this suggests that substitution at the "*peri*-position" perturbs the otherwise highly ordered transition state and hence represents a certain limitation of this methodology.

Notwithstanding, a broad range of functional groups proved compatible with the reaction conditions. Substituents with varying electronic properties were tolerated, including a strongly electron-withdrawing phenylsulfone in **159** as well as a weakly electron-donating phenyl group in **160**. Additionally, the transformation tolerated an aryl bromide in **161**, an aryl chloride in **165** and a pinacolboronate-group in **162**, all of which are of high value for potential downstream functionalizations. The tolerance of aryl bromides is particularly noteworthy, as such substrates failed to undergo meaningful conversion in the intermolecular reductive coupling (see Chapter 2.4). In the present case, the use of diethylzinc as terminal reductant significantly increased the reaction rate, likely allowing cyclization to outcompete catalyst deactivation associated with oxidative addition to nickel(0).

Notably, substituents with strong +M-effects seem to be less compatible with the asymmetric reaction mode, as methoxy-substituted tetrahydroisoquinoline **163** was obtained in significantly lower enantiomeric excess than its trifluoromethoxy-substituted sibling **166**. Gratifyingly, oxidative quench of the pinacolboronate-substituted product **162** enabled conversion to the corresponding phenol **164**, which retained the excellent optical purity of the borylated precursor, thereby compensating for the lower enantioselectivity observed for tetrahydroisoquinoline **163**.

Heteroaromatic substrates were also briefly explored. Despite the pronounced thiophilicity of low-valent nickel, the thiophene-derived product **167** was obtained in acceptable yield and optical purity. A related furane-derived substrate required more forcing conditions to reach full

conversion. Interestingly, although enantioselectivity remained high for the formation of the corresponding product **168**, this was the only case in which diastereoselectivity favored the *cis*-configured amino alcohol subunit; in all other cases, the *anti*-configured product was formed exclusively (dr > 20:1).

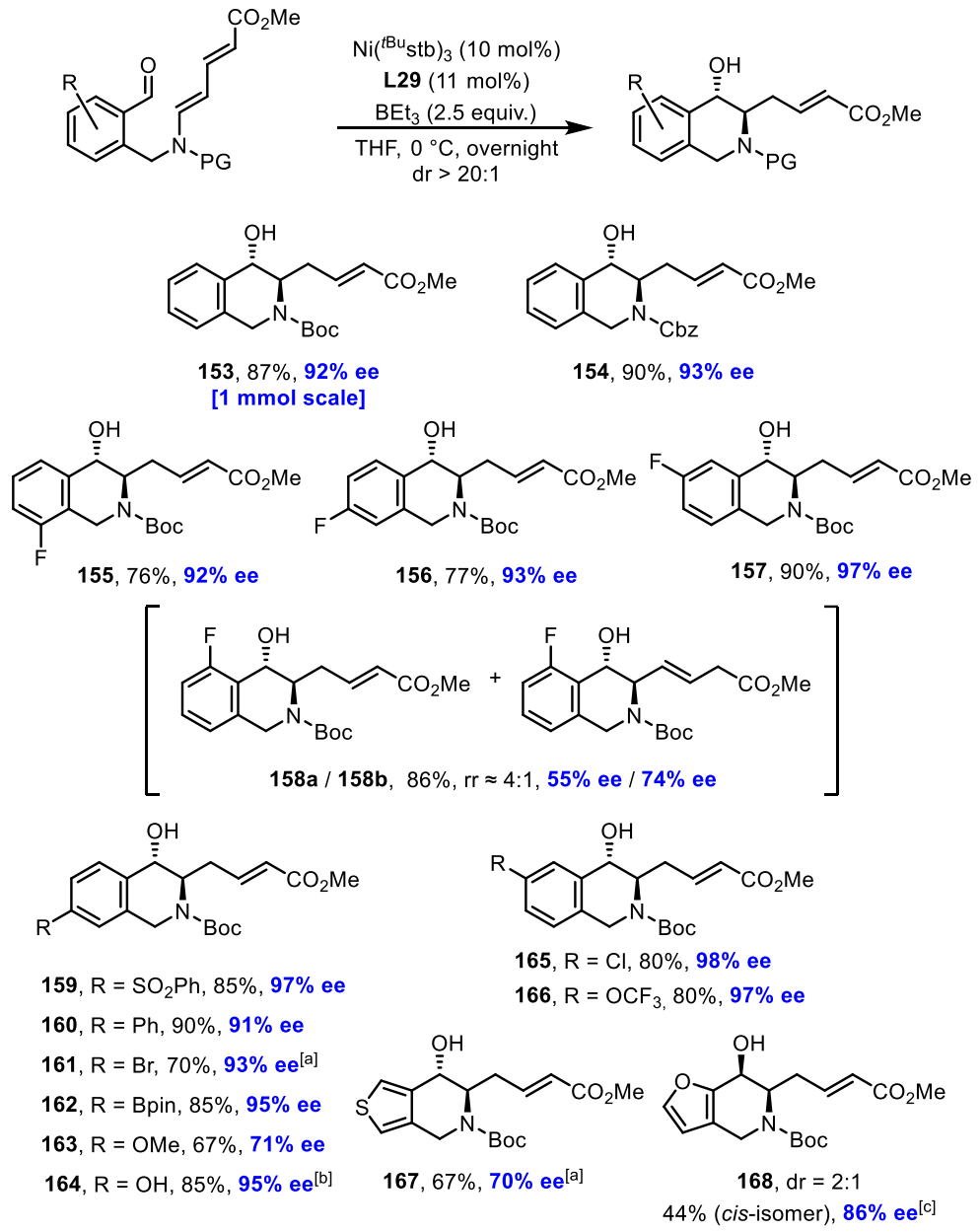

Scheme 63: Scope of the enantioselective synthesis of tetrahydroisoquinolines by nickel-catalyzed reductive cyclization; [a] = synthesized using $ZnEt_2$ as reductant; [b] = obtained by oxidative work-up of compound **162** with aq. H_2O_2, see text; [c] = performed with [Ni(tBustb)3] (20 mol%), **L29** (22 mol%) and BEt_3 (2.5 equiv.) in THF at 60 °C.

The crystalline sulfone derivative **159** enabled the determination of the relative and absolute configuration by single-crystal X-ray diffraction analysis (Figure 10). The heterocyclic ring adopts a distorted boat-like conformation, in which the N-Boc group is equatorially oriented, whereas the C7–OH substituent and the side chain branching off C6 are both axially disposed. This arrangement results in a dihedral angle of –67.4(3)° between the oxygen and nitrogen atoms of the *anti*-configured amino alcohol subunit. The corresponding hydrogen atoms at these

stereogenic centers consistently adopt a *gauche* relationship (H6–C6–C7–H7: –67.8(3)°), which explains the observed coupling constant ($^3J_{H6,H7}$ = 2.8 Hz). A comparable diagnostic coupling constant (2.7-2.8 Hz) is observed in the ^{1}H NMR spectra of all other products shown in Scheme 63 (with the exception of the major isomer of **168**), along with a similarly characteristic pattern of NOE effects (for details, see the Experimental Section). On this basis, all compounds could be confidently assigned by analogy.

Due to the presence of slowly interconverting rotamers at room temperature, caused by the presence of the carbamate protecting group, all reductive cyclization products and their derivatives exhibited multiple strongly broadened NMR signals. To address this issue, all compounds had to be characterized in [D_6]-DMSO at elevated temperatures (typically 353-383 K). Fortunately, the compounds displayed good thermal stability under these conditions and afforded well-resolved spectra with readily interpretable, diagnostic coupling patterns (for representative spectra illustrating rotamer formation and signal coalescence at elevated temperature, see the Experimental Section).

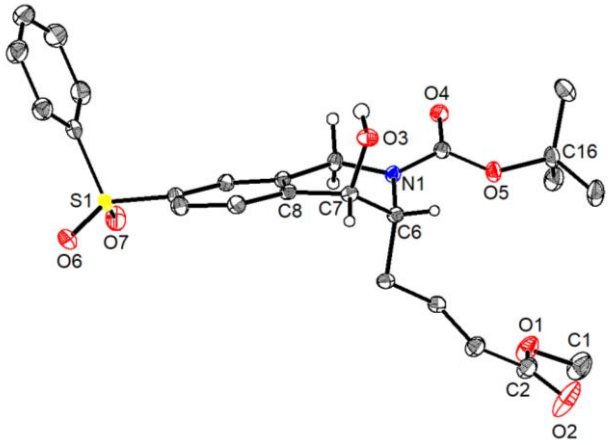

Figure 10: Single-crystal X-ray structure of tetrahydroisoquinoline derivative **159** (majority of H-atoms omitted for clarity).

In addition to chiral tetrahydroisoquinoline derivatives, a variety of aliphatic N-heterocyclic products could be accessed through the nickel-catalyzed reductive cyclization (Figure 11). Interestingly, formal removal of the aryl moiety in **169** resulted in significantly diminished diastereoselectivity, with the *cis*-configured diastereomer being formed as the main product. In the case of the pyrrolidine derivatives **170**, **171** and **172** the reversal of stereochemical preference was even more pronounced, as the products bearing *cis*-configured amino alcohol motifs were formed exclusively.

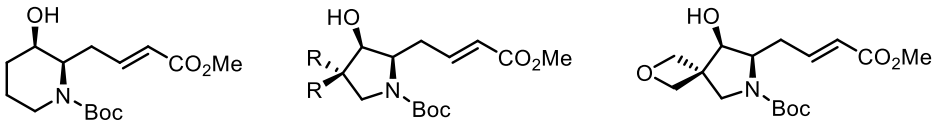

169, dr ≈ 1.5:1
34%, **90% ee**[a]

170, R = H, 50%, **96% ee**[a]
171, R = Me, 71%, **86% ee**

172, 67%, **95% ee**

Figure 11: Scope of the enantioselective synthesis of aliphatic N-heterocycles by nickel-catalyzed reductive cyclization; unless stated otherwise all products were synthesized under the conditions shown in Scheme 63; [a] = synthesized using $ZnEt_2$ as reductant.

The relevant proton resonances of the resulting saturated heterocycles displayed ^3J coupling constants in the range of 5.5-6.3 Hz, consistent with a *syn*-orientation and thus in agreement with the assigned *cis*-configuration. The altered stereochemical outcome was additionally confirmed by Mosher ester and NOE analyses,[154] which established an (*R*)-configuration at the hydroxyl-bearing stereogenic center, opposite to that observed for the corresponding tetrahydroisoquinoline derivatives (for details, see the Experimental Section).

Nonetheless, excellent enantioselectivities were obtained in all cases. It should be noted, that the enolizable cyclization precursors leading to **169** and **170** reacted poorly under the standard conditions and predominantly underwent undefined decomposition in the presence of the catalyst and reductant. However, slow addition of the substrates (over 5 hours) to the reaction mixture in combination with the use of the more reactive reductant diethylzinc resulted in a significantly cleaner reaction profile and enabled productive turnover.

Introduction of two substituents at the α-position of the aldehyde, as exemplified by the *gem*-dimethyl-substituted pyrrolidine **171** and the spirocyclic analog **172**, was well tolerated and led to a pronounced increase in reactivity. As a result, these substrates reacted efficiently under the standard conditions with triethylborane as the reductant and provided good yields. Although one might attribute this reactivity enhancement to angle compression associated with the "Thorpe-Ingold-effect",[163] the fact that incorporation of a highly (angle)-strained oxetane unit[164] had a comparable effect in the synthesis of **172** argues against such an interpretation. Instead, the observation is more consistent with a reactive rotamer effect, in which the substituents favor the conformations predisposed toward cyclization.[165]

Despite the broad compatibility of the enantioselective reaction mode with electronically and sterically diverse substrates, several limitations were identified (Figure 12). Although the reductive cyclization is highly diastereospecific, as exemplified by the formation of *cis*-configured tetrahydroisoquinoline **173** from (*E*,*Z*)-**152**, alteration of the diene geometry at the amine-substituted terminus resulted in a pronounced loss of enantiocontrol, mirroring the behavior observed in the intermolecular coupling (see Chapter 2.8).

Another similarity was found with respect to the electronic properties of the diene moiety. Modification of its push-pull character through removal of the ester group or its formal replacement with a phenyl substituent resulted in substantial erosion of the optical purity of products **174** and **175**. Likewise, introduction of an intervening methylene unit had a drastic

impact on the reaction outcome. Such a modification electronically decouples the heteroatom from the 1,3-diene system while simultaneously placing it directly at the aromatic ring. This change in substrate design resulted in an almost complete loss of enantioselectivity and a marked decrease in diastereoselectivity, as demonstrated by the synthesis of **176** and **177**.

Given that the corresponding tetrahydroquinoline and chromanol derivatives also represent attractive classes of chiral heterocycles, a dedicated ligand screening was conducted for these constitutional isomers (for details, see the Experimental Section). However, the pronounced differences in reactivity and selectivity compared to the amino-pentadienoate-derived substrates revealed that the development of an effective catalytic system for these substrate classes is far from straightforward and will require further investigation. At the same time, these findings further highlight the unique suitability of amino-pentadienoate-derived substrates for the intramolecular reaction mode.

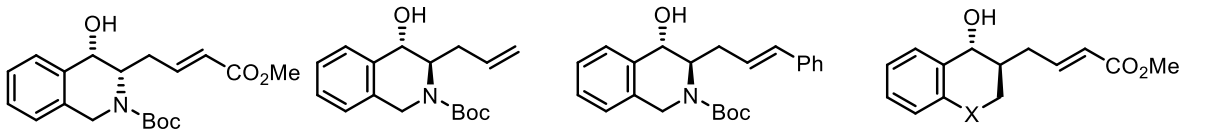

173, 72%, **41% ee** from (*E*,*Z*)-**152**

174, 87%, rr ≈ 11:1, **28% ee**

175, 78%, **14% ee**

176, X = NBoc, 58%, dr ≈ 3:1, **5% ee**
177, X = O, 81%, dr ≈ 5:1, **2% ee**

Figure 12: Selection of substrates displaying limited compatibility with the enantioselective reaction mode; all products were synthesized under the conditions shown in Scheme 63.

3.5 Downstream Functionalization

The value of the methodology becomes clear when considering the broad relevance of enantiomerically enriched heterocycles, in particular tetrahydroisoquinoline derivatives. These structural motifs are frequently encountered in alkaloids and have attracted sustained interest owing to their diverse biological and pharmacological activities.[166] While numerous stereoselective strategies for the synthesis of tetrahydroisoquinolines have been reported, including approaches based on chiral pool synthesis and asymmetric catalysis,[167-171] efficient routes to hydroxylated derivatives bearing an *anti*-configured vicinal amino alcohol motif remain comparatively scarce.[172, 173] Beyond their intrinsic synthetic value, the products obtained in this study offer multiple opportunities for further derivatization, as they contain a variety of versatile functional handles for downstream functionalization.

Motivated by the increasing importance of fluorinated heterocycles in medicinal chemistry, compound **153** was converted into the corresponding fluorinated derivative **178**.[174-176] Treatment with diethylaminosulfur trifluoride (DAST) at −78 °C afforded the desired product with retention of configuration at the stereogenic center. This stereochemical outcome can be rationalized by the formation of an N-acyl aziridinium intermediate, which directs the nucleophilic attack (Scheme 64, top).[177] Importantly, this result contrasts with the stereochemical outcome observed in iridium-catalyzed asymmetric hydrogenations of fluorinated isoquinolines reported in the literature, where *syn*-addition of hydrogen to the heteroaromatic precursor gives rise to *cis*-configured fluorinated tetrahydroisoquinolines (Scheme 64, bottom).[178, 179] Hence, the present strategy complements existing approaches for the stereoselective synthesis of fluorinated tetrahydroisoquinolines.

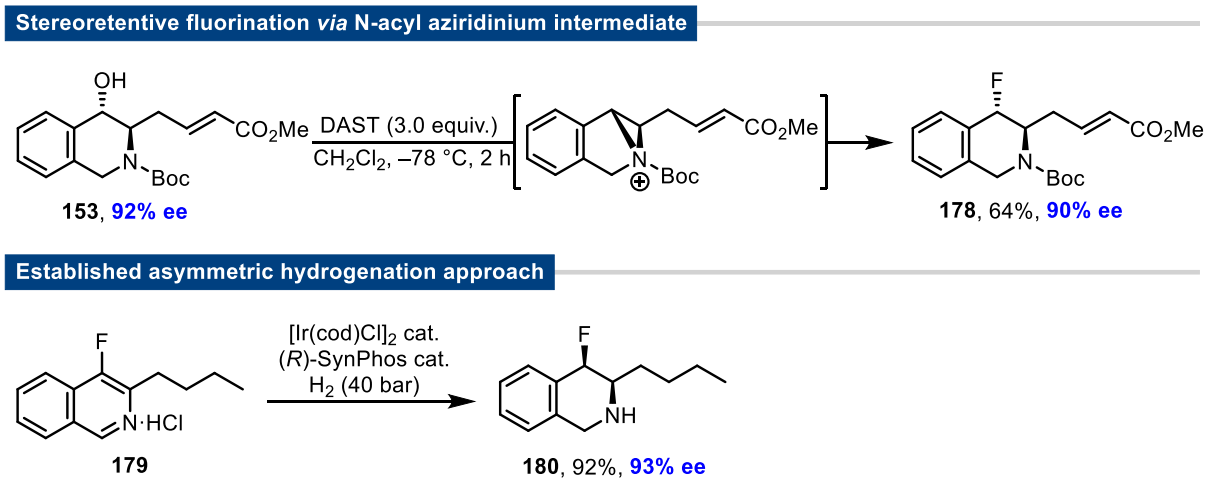

Scheme 64: Fluorination of a tetrahydroisoquinoline derivative and comparison with a complementary hydrogenation approach.

The proximity of the alcohol relative to the α,β-unsaturated ester functionality enabled a base-promoted intramolecular "oxa-Michael addition". In the presence of catalytic amounts of DBU, pyrrolidine **172** was transformed into the corresponding tricyclic product **181** in good yield (Scheme 65). Although this transformation primarily served as a proof-of-concept demonstration

of the synthetic flexibility of the obtained heterocycles, such conformationally restricted spirocyclic scaffolds are nonetheless of considerable interest as building blocks in medicinal chemistry.[180-182]

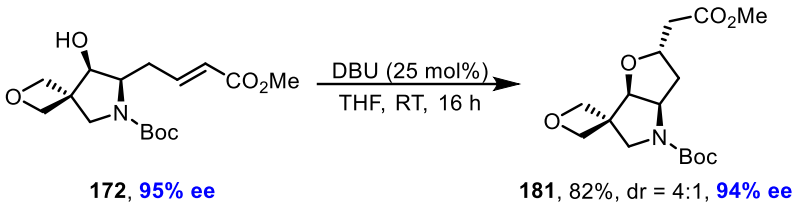

172, **95% ee** **181**, 82%, dr = 4:1, **94% ee**

Scheme 65: Base-mediated intramolecular "oxa-Michael addition" of a spirocyclic pyrrolidine.

Next, the relationship between the protected amine and the ester was exploited to construct an additional ring fused to the tetrahydroisoquinoline framework (Scheme 66). To this end, the Cbz-protected derivative **154** was selected, as catalytic hydrogenation over Pd/C enabled simultaneous removal of the protecting group and reduction of the olefin. Treatment of the obtained crude product with triethylamine in refluxing ethanol afforded the corresponding δ-lactam **182**, which was subsequently reduced with $LiAlH_4$ to the tricyclic amine **183** without any loss of optical purity. The resulting heterocyclic scaffold constitutes the central framework of phenanthroquinolizidine alkaloids, an important family of natural products known for a wide range of biological activities, including pronounced antitumor properties.[183-186] In particular, hydroxylated representatives such as 15-hydroxycryptopleurine have attracted considerable attention because of their exceptionally high potency in the sub-nanomolar range.[187, 188]

The efficient access to benzoquinolizidinol derivatives such as **183** provided by the present approach may facilitate future studies on structurally simplified analogs of these alkaloids. In this context, the broad functional group tolerance displayed in the intramolecular reductive coupling may enable decoration of the aromatic ring with a diverse range of substituents, thereby allowing the modular synthesis and investigation of structural analogs. Such investigations appear especially relevant given that even subtle modifications of the molecular framework have been shown to influence their mode of action.[189-192]

Another aspect worth considering relates to the pharmacological limitations encountered with the closely related phenanthroindolizidine alkaloid tylocrebrine. Clinical evaluation of this compound was discontinued due to severe central nervous system side effects.[193] Importantly, it has been suggested that more polar analogs might not be able to cross the blood/brain barrier and could therefore allow cyto- and CNS-toxicity to be uncoupled.[194]

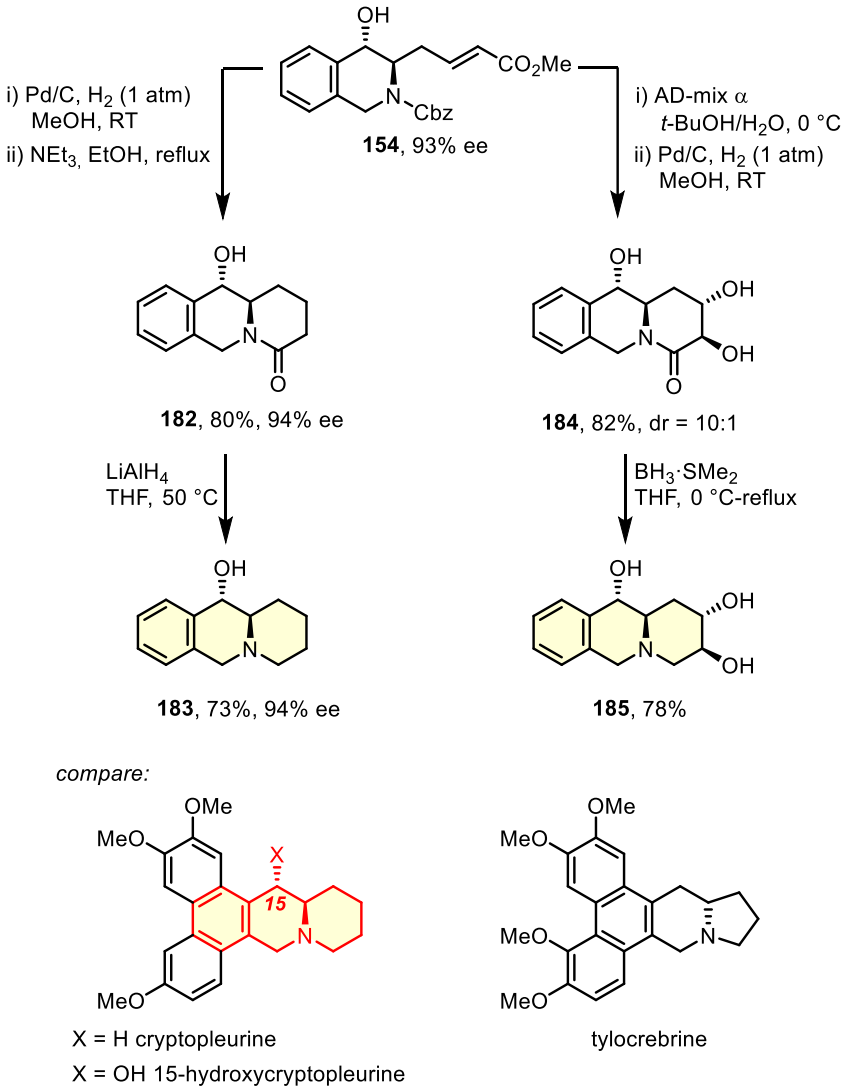

Scheme 66: Synthesis of benzoquinolizidinol derivatives and comparison with phenanthroquinolizidine alkaloids.

One possible route towards such functionalized, yet downsized analogs is illustrated by the synthesis of compound **185** from precursor **154**. Instead of direct hydrogenation, the double bond was first subjected to Sharpless asymmetric dihydroxylation,[195] followed by deprotection of the amine. Unlike its unsubstituted analog, the dihydroxylated intermediate readily underwent cyclization to the corresponding δ-lactam **184** without the need for an external base or heating. This difference in reactivity may arise from conformational effects induced by the vicinal hydroxy groups, which could facilitate intramolecular attack of the free amine on the ester. Subsequent reduction with $BH_3{\cdot}SMe_2$ furnished the corresponding tricyclic amine **185**. This sequence demonstrates how the functional groups embedded within compounds of type **184** can be leveraged for late-stage diversification. Many related strategies for downstream functionalization and synthesis of structurally and electronically differentiated analogs can be envisaged and might empower drug development campaigns.

3.6 Synthesis and Characterization of Allyl-Oxanickelacycle Intermediates and Their Mechanistic Implications

The stoichiometric NMR experiments presented herein were conducted in collaboration with Dr. Markus Leutzsch. DFT calculations supporting the experimental data were carried out by Dr. Markus Leutzsch.

There is a general consensus in the literature regarding the underlying mechanism of couplings between π-compounds (*e.g.* alkynes, alkenes, 1,3-dienes) and carbonyl derivatives. Nevertheless, the current mechanistic understanding is largely based on computational studies,[68, 81, 82, 160, 161] whereas relevant experimental studies are notably rare. This imbalance reflects the inherent complexity of these transformations, which frequently involve multiple competing regio- and stereoselective pathways as well as complex catalyst speciation under the reaction conditions. The difficulty of isolating and characterizing well-defined catalytic intermediates further impedes direct experimental interrogation of the catalytic cycle. This has ultimately also limited the development of a more detailed mechanistic understanding of the previously developed intermolecular, regioinverted coupling of amino-pentadienoates with aldehydes (see Chapter 2.10).

In the present case, however, both the aldehyde and diene functionality are incorporated into a single substrate. This results in a preorganized system that may enforce a chelating coordination mode. Accordingly, a pre-equilibrium arising from competition between aldehyde coordination and binding of a second molecule of the ancillary ligand, as proposed by computational studies by Houk *et al.*,[54] may become irrelevant. As a result, catalyst speciation in solution may become less complex. Additionally, the issue of regiocontrol is eliminated, since the tethered diene reacts exclusively at the amine-substituted terminus. This improved reaction profile may result from a similarly simplified coordination mode of the diene moiety to the metal center.

These potential advantages associated with the intramolecular reaction mode motivated stoichiometric studies aimed at identifying catalytically relevant intermediates. To this end, co-crystallization experiments employing a 1:1:1 mixture of the model substrate **152**, (*S*)-AntPhos **L29** and $Ni(cod)_2$ were conducted with the goal of either isolating a loaded nickel(0) π-complex or the corresponding nickel(II) metallacycle. However, despite the good crystallinity of the individual components, all attempts proved unsuccessful. Since (*S*)-AntPhos **L29** is required solely to impose enantioselectivity and, in contrast to phosphoramidite **L11** in the intermolecular coupling, is not involved in controlling the regiochemical course of the reaction, the system could be simplified by employing PCy_3 instead. Although achiral, this ligand proved fully compatible with the model reaction and afforded tetrahydroisoquinoline *rac*-**153** with excellent diastereoselectivity in the model reaction (see Chapter 3.2).

Following extensive efforts directed towards crystallization, single crystals suitable for X-ray diffraction analysis were successfully isolated. Structural analysis revealed these crystals to consist of the corresponding allyl-oxanickelacycle **190** (see the Experimental Section for the

structure). The quality of the crystallographic data was further improved by performing the complexation with fluorinated substrate **186**, resulting in the formation of the corresponding allyl-oxanickelacycle **187** (Scheme 67). Importantly, in both cases the complexation was carried out in the absence of any reducing agent. This precaution was taken to suppress productive catalytic turnover and thereby permit direct observation of intermediates formed upon substrate coordination. The successful isolation of complexes **187** and **190** therefore demonstrates that oxidative cyclization can indeed occur without the assistance of an external Lewis acid. It remains unknown whether this observation is a consequence of the entropically favorable intramolecular nature of the present system or whether it also applies to the intermolecular reaction featuring protected 5-amino-2,4-pentadienoates.

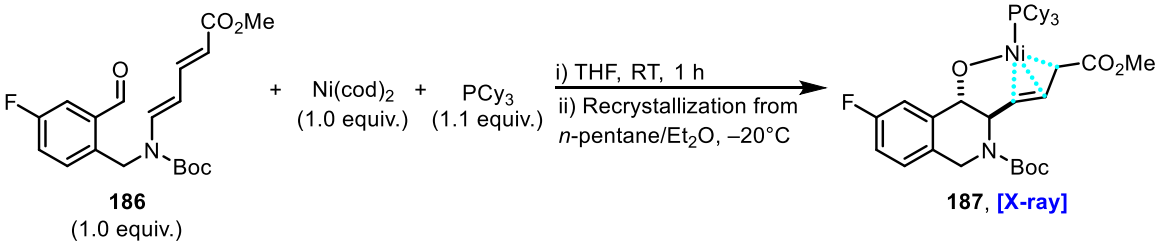

Scheme 67: Preparation of an allyl-oxanickelacycle intermediate.

Examination of the molecular structure of metallacycle **187** (Figure 13) reveals significant interaction of all three C-atoms of the allyl fragment with the nickel(II) center. Notably, the Ni–C3 and Ni–C5 distances are nearly identical, indicating substantial bonding contributions from both termini of the allyl unit. Inspection of the C–C-bonding situation within the allyl fragment however reveals a distinctly asymmetric electronic structure. In particular, the C3–C4 bond (1.3909(14) Å) is notably shorter than the adjacent C4–C5 bond (1.4257(14) Å). This difference in bond lengths speaks against an extensive delocalization within the π-system and indicates that the actual bonding mode is an η^3:η^1-hybrid between a canonical π-allylnickel species and the corresponding σ-complex.

Further structural insight is obtained from analysis of the conformation adopted by the core region of the fused heterocyclic framework. Similar to the corresponding tetrahydroisoquinoline product **153** (and by analogy **157**), the six-membered heterocycle assumes a distorted boat conformation. Nevertheless, substantial differences become apparent when the metallacycle intermediate is compared with the final reductive coupling products. Within the metallacycle, the nickel-containing ring enforces an arrangement, in which the C1–O1 alkoxide entity, the N-Boc group, as well as the allyl side chain (C3–C4–C5) are oriented equatorially. This disposition strongly contrasts the conformational preference observed in the tetrahydroisoquinoline products, where the oxygen substituent and the side chain are both axially disposed (see Chapter 3.4). This change in inherent conformational preference also affects the orientation of the substituents attached to the stereogenic centers formed upon oxidative cyclization. In metallacycle **187** the heteroatoms O1 and N1 adopt an antiperiplanar arrangement. Consequently, the hydrogen atoms attached to C1 and C2 are likewise positioned antiperiplanar to one another, as manifested in the

corresponding torsion angle of –177.6°. Release of the organic product from the metal center following reductive elimination in the catalytic cycle removes these conformational constraints. As a result, the tetrahydroisoquinoline framework adopts its preferred conformation, featuring a *gauche* relationship between the hydrogen atoms at the stereogenic centers (compare Figure 10 for single-crystal X-ray structure of a representative tetrahydroisoquinoline derivative).

The coordination geometry around the nickel(II) center is essentially square planar when the interaction with the central allylic carbon atom is disregarded. The observed distortions can largely be attributed to the differing bond lengths associated with the coordinated carbon, oxygen,

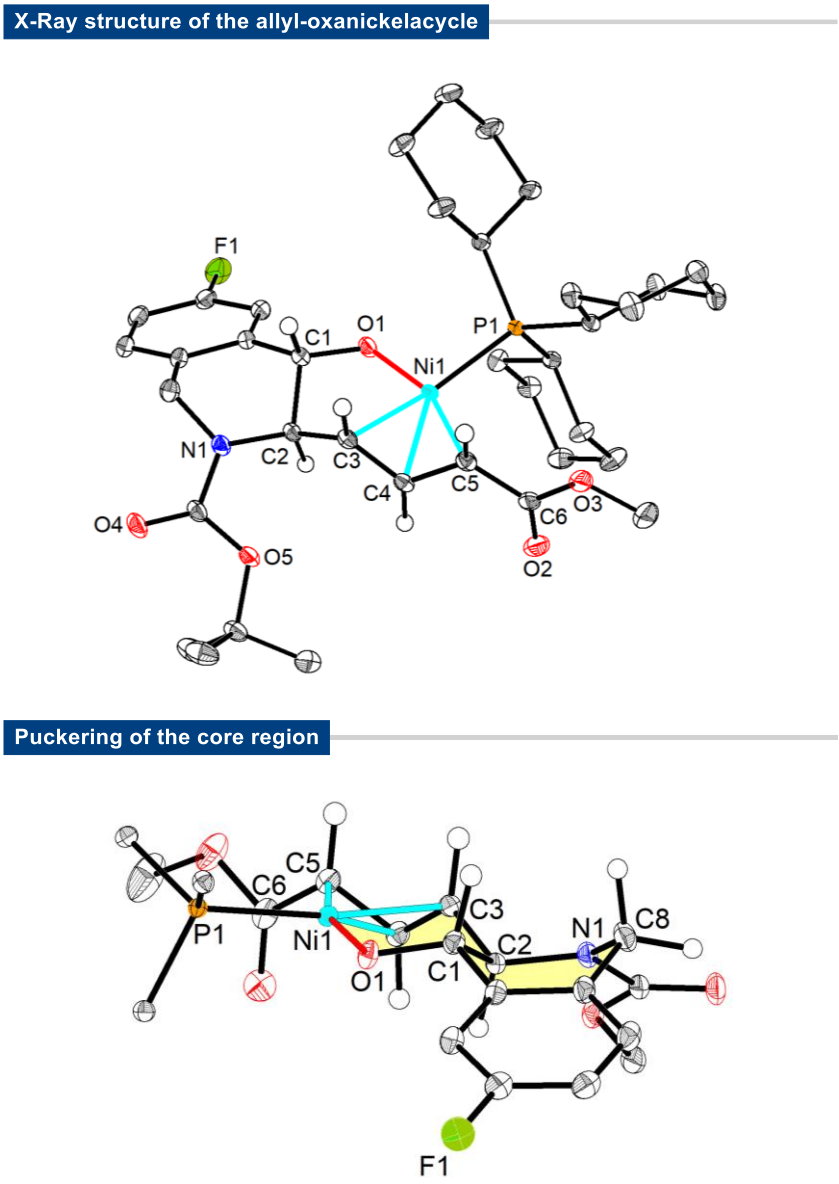

Figure 13: top) Structure of the allyl-oxanickelacycle **187** in the solid state; solute pentane and majority of H-atoms not shown for clarity; crystallographic numbering scheme. Selected bond lengths (Å) and angles (°): Ni1–P1 2.2019(3), Ni1–O1 1.8581(7), Ni1–C3 2.0301(9), Ni1–C4 1.9682(19), Ni1–C5 2.0314(10), C1–C2 1.5531(13), C3–C4 1.3909(14), C4–C5 1.4257(14), O1–Ni1–P1 91.98(2), O1–Ni1–C3 87.02(3), C3–Ni1–C5 72.63(4), C5–Ni1–P1 108.83(3), O1–C1–C2–N1 –177.53(3); bottom) truncated structure of the same complex showing the puckering of the core region: the chair-configured oxanickelacycle is annulated to a boat-configured aza-heterocycle.

and phosphorus atoms. Importantly, the Ni–O bond is located *cis* to the Ni–C3 bond. Under the catalytic reaction conditions, the presence of triethylborane enables transmetalation of

allyl-oxanickelacycle **187** and subsequent β-hydride elimination. This sequence likely results in the formation of the proposed nickel-hydride species **188**, which adopts an arrangement that is highly favorable for regioselective hydride delivery to the C3-position of the allylnickel fragment (Scheme 68).

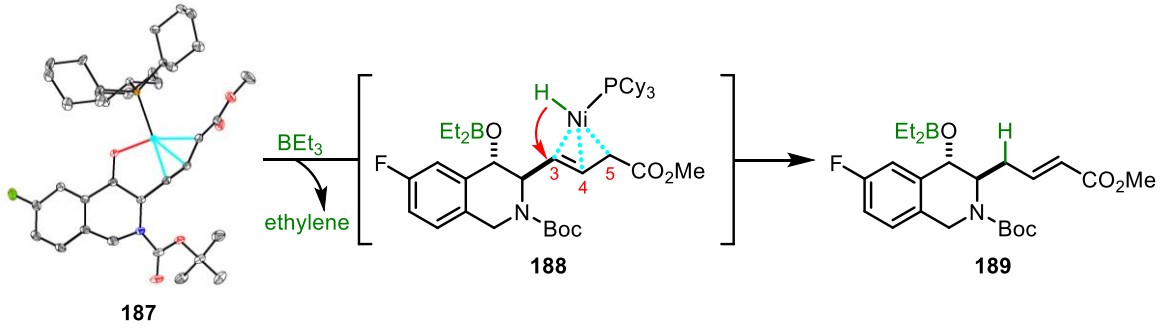

Scheme 68: Proposed reaction sequence leading to the product following allyl-oxanickelacycle formation.

The exclusively formed borinate ester **189** is thus expected to represent not only the thermodynamically preferred olefin isomer but potentially also the kinetically favored product of the reductive cyclization (a representative kinetic reaction profile is provided in the Experimental Section).

Substituents at the "*peri*-position" may, however, interfere with this final step of the catalytic cycle. Steric repulsion, potentially resulting from a "*syn*-pentane-type" interaction between the substituent and the C1–O1 bond, may alter the puckering of the core structure. If such an interaction additionally influences the geometry of the derived Ni–H intermediate, competing hydride delivery to C5 may become possible, resulting in the formation of the corresponding deconjugated olefin isomer. Experimental observations are consistent with this hypothesis, as such behavior is observed exclusively for tetrahydroisoquinolines **158a**/**158b** (see Chapter 3.4).

Following the successful isolation of complexes **187** and **190**, the nickel speciation in solution was investigated by NMR spectroscopy. To this end, a reaction mixture containing $Ni(cod)_2$, PCy_3, and substrate **152** (1:1:1) was prepared in [D_8]-THF (Scheme 69) and analyzed under ambient conditions in the absence of any reducing agent. Metallacycle **190** was readily identified as the only observable nickel-containing species. Importantly, no spectroscopic evidence was obtained for the presence of a preceding nickel(0) π-complex bearing the uncyclized substrate.

These observations suggest that oxidative cyclization and concomitant C–C bond formation occur efficiently at room temperature and proceed essentially quantitatively under the conditions employed. Furthermore, the results provide additional support for the conclusion that triethylborane is not required to promote the cyclization step. Nevertheless, coordination of triethylborane to the aldehyde may accelerate oxidative cyclization through a LUMO-lowering effect. Alternatively, the reductant may be involved exclusively in subsequent stages of the catalytic cycle.

Several characteristic spectroscopic features provide further insight into the electronic structure of the isolated metallacycle. Most notably, the protons located at the stereogenic centers display a

large vicinal coupling constant of ^3J = 9.5 Hz. This observation is fully consistent with their diaxial arrangement in the crystal structures of **187** and **190**. Additional information is obtained from the diagnostic resonances associated with the allylnickel fragment. The distal terminus C5/H5 appears considerably more shielded (δ_C = 36.9 ppm, δ_H = 1.88 ppm) than C3/H3 (δ_C = 103.8 ppm, δ_H = 4.72 ppm). The pronounced differentiation between these positions indicates substantial electronic inequivalence between the termini. The downfield shifted signals of C3/H3 are consistent with an increased sp²-character at this position, whereas the comparatively shielded signals associated with C5/H5 indicate an aliphatic electronic environment. These findings closely mirror the previously observed bonding situation of the allyl-fragment in the X-ray analysis.

Related allyl-oxanickelacycle species have previously been characterized by Ogoshi and co-workers[55] (also see Chapter 1.2.2). However, in contrast to the present system, those complexes were generated from electronically unbiased dienes (*e.g.* 1,3-butadiene). Despite the pronounced differences regarding the electronic properties of the diene moiety, the overall bonding mode of the two systems is closely related. In particular, both systems display limited delocalization within the π-system of their respective allyl fragment. The absence of an electron-withdrawing ester substituent and the associated lack of C-enolate character in **191**, lead to an even more pronounced bond alternation within the allyl unit. Consistent with this picture, the reported NMR resonances of **191** appear in similar but slightly more shielded regions (δ_C/δ_H = 31.3 ppm/0.99 ppm and 97.4 ppm/4.14 ppm, respectively; Scheme 69). Notably, neither the ester nor the carbamate functionality appears to participate in coordination to the metal center at this stage of the reaction.

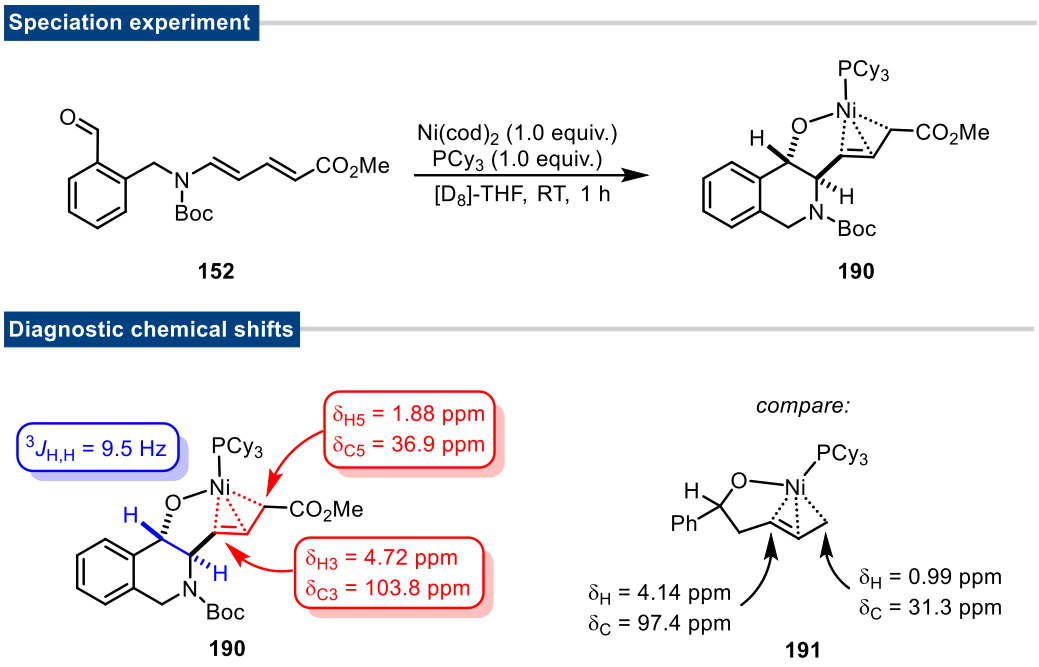

Scheme 69: Speciation NMR experiment of allyl-oxanickelacycle **190** and comparison with electronically unbiased literature-known analog **191**.

Overall, the spectroscopic data obtained in solution are fully consistent with the structural information derived from single-crystal X-ray diffraction analysis. The large vicinal coupling

constant between the protons at C1 and C2 reflects the antiperiplanar arrangement observed in the solid-state structure, while the pronounced differentiation between C3 and C5 mirrors the unequal bond lengths within the allyl fragment. The close correspondence between the crystallographic and spectroscopic observations therefore indicates that the fundamental structural features of the metallacycle are largely preserved in solution.

The characterization of these metallacycle intermediates and the mechanistic insights derived from them, prompted a more detailed investigation of the corresponding chiral reaction system employing (*S*)-AntPhos **L29**. Since repeated attempts to obtain single crystals of the relevant nickel complexes suitable for X-ray diffraction analysis were unsuccessful, the speciation studies were instead pursued by means of stoichiometric NMR experiments.

While experiments in the presence of PCy_3 at room temperature resulted in clean formation of the corresponding allyl-oxanickelacycle intermediates, the use of **L29** under analogous conditions resulted in highly complex and uninterpretable data. Gratifyingly, conducting both the complexation and NMR measurements at –40 °C significantly improved the quality of the data and allowed the identification of several relevant nickel-containing species. Nevertheless, spectral analysis remained challenging owing to the presence of numerous species in solution, resulting in substantial signal overlap. To address these issues, 1D selective TOCSY and various 2D NMR correlation experiments (see Experimental Section for details; performed in collaboration with Dr. M. Leutzsch) were employed, which allowed for reliable spectral assignment.

The spectra recorded approximately 30 minutes after mixing of the components at –40 °C revealed a mixture of unreacted starting material (≈ 80 mol%), residual free (*S*)-AntPhos (≈ 25 mol%), a nickel complex of type Ni(**L29**)$_2$ (≈ 30 mol%), as well as the corresponding oxanickelacycle (≈ 20 mol%) (Figure 14). In analogy to the corresponding experiment with PCy_3, no evidence for a nickel(0) π-complex bearing the intact, uncyclized substrate could be detected, even at this reduced temperature. Over the course of twelve hours at –40 °C, the concentration of substrate **152** gradually decreased to ≈ 30 mol% accompanied by a corresponding accumulation of the metallacycle intermediate. However, the imperfect mass balance suggested the presence of additional nickel-containing species that could not be conclusively identified.

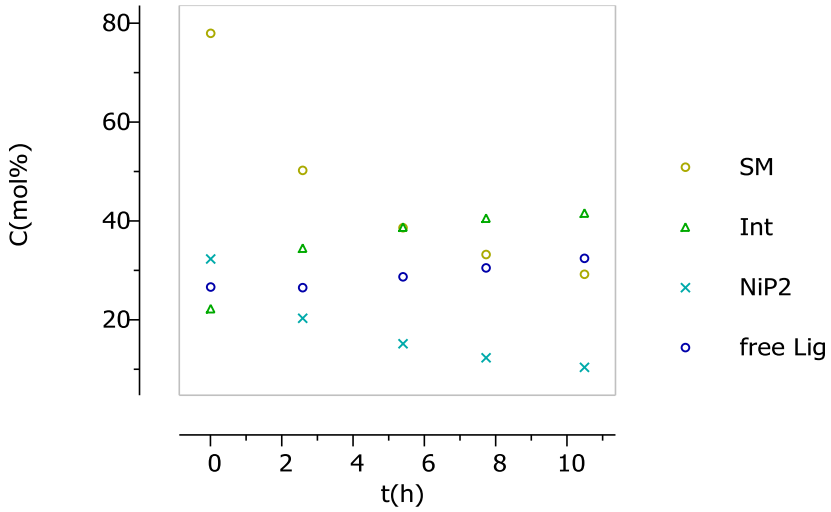

Figure 14: Time-dependent concentration profiles of different species observed in the NMR experiment (SM = substrate **152**, Int = allyl-oxanickelacycle (**192**+**193**), NiP_2 = Ni(**L29**)$_2$, free Lig = **L29**).

Importantly, the allyl-oxanickelacycle based on (*S*)-AntPhos **L29** was found to exist as two distinct diastereomeric forms **192** and **193** in solution (dr ≈ 3:1, Scheme 70). Building on the structural information previously obtained for the racemic PCy_3-based systems **187**/**190**, it was concluded that the bonding situation within the allyl unit of both isomers is essentially identical and closely resembles that observed in these systems. In this context, the large coupling constant between the protons H8 and H9 on the stereocenters ($^3J_{H,H}$ = 9.8 Hz) again indicates a diaxial arrangement of these protons in both species. The observed diastereomerism therefore cannot originate from *cis*/*trans*-isomerism of the tetrahydroisoquinoline core. This finding is in line with the outstanding diastereoselectivity observed for ligand **L29** under catalytic reaction conditions.

Instead, the spectroscopic data point toward an atropisomerism arising from different orientations of the anthracenyl substituent of ligand **L29** relative to the coordinated allyl fragment (Scheme 70). In the major atropisomer **192**, the anthracenyl unit is positioned directly above the allyl-oxanickelacycle. As a consequence, proton H12 of the allyl unit experiences massive shielding due to the aromatic ring current and therefore resonates at an unusually high-field chemical shift (δ_H = –0.44 ppm). In the minor atropisomer **193**, the anthracenyl substituent is rotated so that proton H6 located in the "*peri*-position" of the bicyclic tetrahydroisoquinoline scaffold is in close spatial proximity to the extended π-system of the ligand and consequently experiences a noticeable, albeit less pronounced, shielding effect (δ_H = 6.25 ppm versus 7.26 ppm in **192**), whereas H12 remains unaffected and resonates at δ_H = 1.90 ppm.

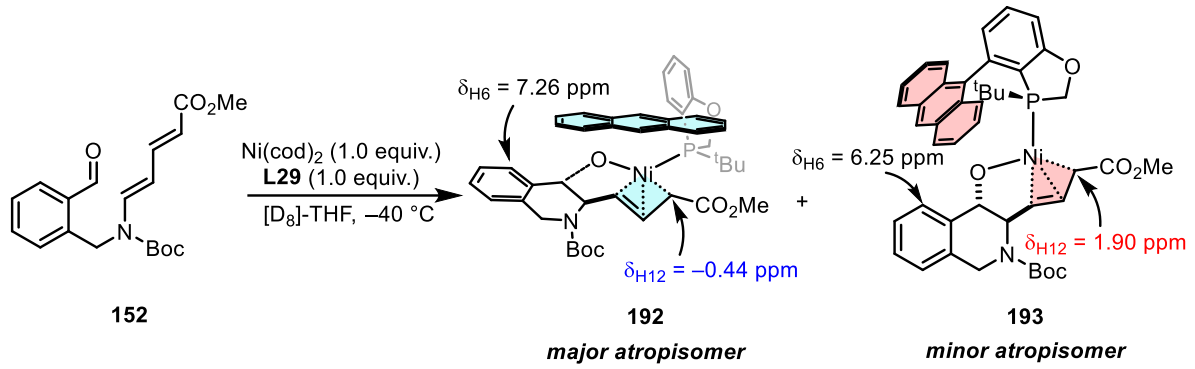

Scheme 70: Formation of atropisomers in the presence of the (*S*)-AntPhos ligand.

To obtain a more detailed structural picture, the experimental observations were complemented by DFT calculations at the B3LYP/D3BJ/def2-TZVP/CPCM(THF) level of theory (performed by Dr. M. Leutzsch). The crystallographically determined structure of complex **190** was used as the starting point, with the PCy_3 ligand being replaced by (*S*)-AntPhos **L29**. The optimized structures are in excellent agreement with all the experimentally observed spectral features of both atropisomers, as well as a number of diagnostic ROESY cross peaks between specific atoms of the allyl-oxanickelacycle and the chiral ligand (Figure 15).

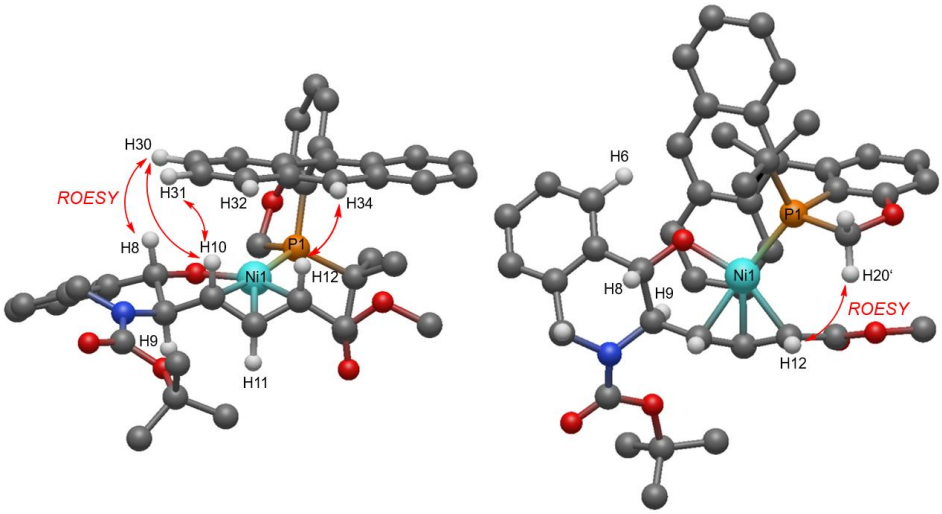

Figure 15: Computed structures of the atropisomeric allyl-oxanickelacycle intermediates formed upon intramolecular reductive coupling of **152** in the presence of the (*S*)-AntPhos ligand; left: major isomer (**192**); H12 and, to a minor degree, H10 reside under the umbrella of the anthracenyl substituent of the ligand and hence experience notable shielding by virtue of the aromatic ring current; right: minor isomer (**193**), in which the aromatic *peri*-proton H6 is close to the anthracenyl group and hence experiences shielding.

The existence of atropisomers inevitably complicates the formulation of a plausible model for the stereochemical course of the oxidative cyclization step. However, the structure of the major atropisomer **192** provided valuable insights into factors that could govern stereocontrol during the catalytic cycle and served as basis for a putative model (Figure 16). Following substrate coordination to the nickel(0) center, formation of a π-complex is proposed, in accordance with the generally accepted mechanistic picture for related nickel-catalyzed reductive coupling reactions. Notably, this species appears to be transient in nature, as neither this intermediate nor any related π-complex preceding oxidative cyclization could be detected spectroscopically. Within the sterically confined environment created by the umbrella-like anthracenyl unit, only the protons as

the smallest substituents of the substrate, can be accommodated in the upward-oriented position without causing significant steric repulsion. The resulting H···π interactions are directly reflected in the pronounced shielding effects observed for the corresponding allyl-oxanickelacycle and, importantly, provide a plausible explanation for the trends identified during the initial ligand screening. Specifically, non-covalent interactions involving the anthracenyl substituent contribute significantly to both the magnitude and even the sense of asymmetric induction imposed by the P-chiral ligand **L29** (see Chapter 3.2).

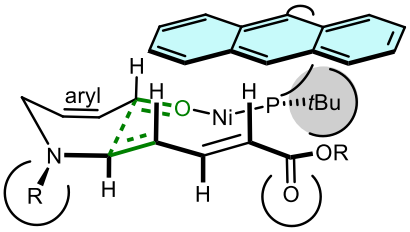

Figure 16: Putative model explaining the stereochemical course of the oxidative cyclization; aryl ring of the substrate only schematically indicated for clarity; nickel-diene bonding and parts of the ligand framework not illustrated for clarity.

In addition, the sterically demanding *tert*-butyl group on the stereogenic phosphorous atom effectively shields the backside of the complex, directing the substrate backbone toward the front-facing region of the coordination sphere. This orientation leaves sufficient space for the comparatively slim methyl ester substituent adjacent to the *tert*-butyl group, whereas placement of the aryl substituent in the same region would result in unfavorable steric interactions. As shown before, removal of the ester group or formal replacement by a phenyl-substituent resulted in a pronounced decrease in enantioselectivity (see Chapter 3.4). This indicates that the ester plays a crucial role in the enantiodetermining step of the reaction, likely *via* non-covalent interactions that are not reflected in the current stereochemical model. Accordingly, additional computational studies on the mechanism of the asymmetric reductive cyclization will be required to provide a more detailed explanation for the observed stereochemical outcome.

3.7 Summary

Nickel-catalyzed reductive coupling reactions between aldehydes and 1,3-dienes have attracted considerable attention since their initial discovery more than 30 years ago. Recently, an increasing number of asymmetric variants of these transformations have been reported, highlighting the versatility and synthetic potential of this particular type of nickel catalysis. However, these studies have exclusively focused on intermolecular reductive coupling reactions. In contrast, asymmetric intramolecular variants remain largely unexplored, despite reductive cyclization reactions representing the earliest examples in the field. In fact, only a single pioneering report describing an asymmetric cyclization reaction of ω-dienyl aldehydes has been disclosed. Due to poor control over alkene geometry, insufficient enantioselectivities, and a highly restricted substrate scope, asymmetric reductive cyclization reactions have remained at a largely conceptual stage. Furthermore, the reported products were predominantly simple carbocycles of limited synthetic value, with only a single heterocyclic example described (Scheme 71).

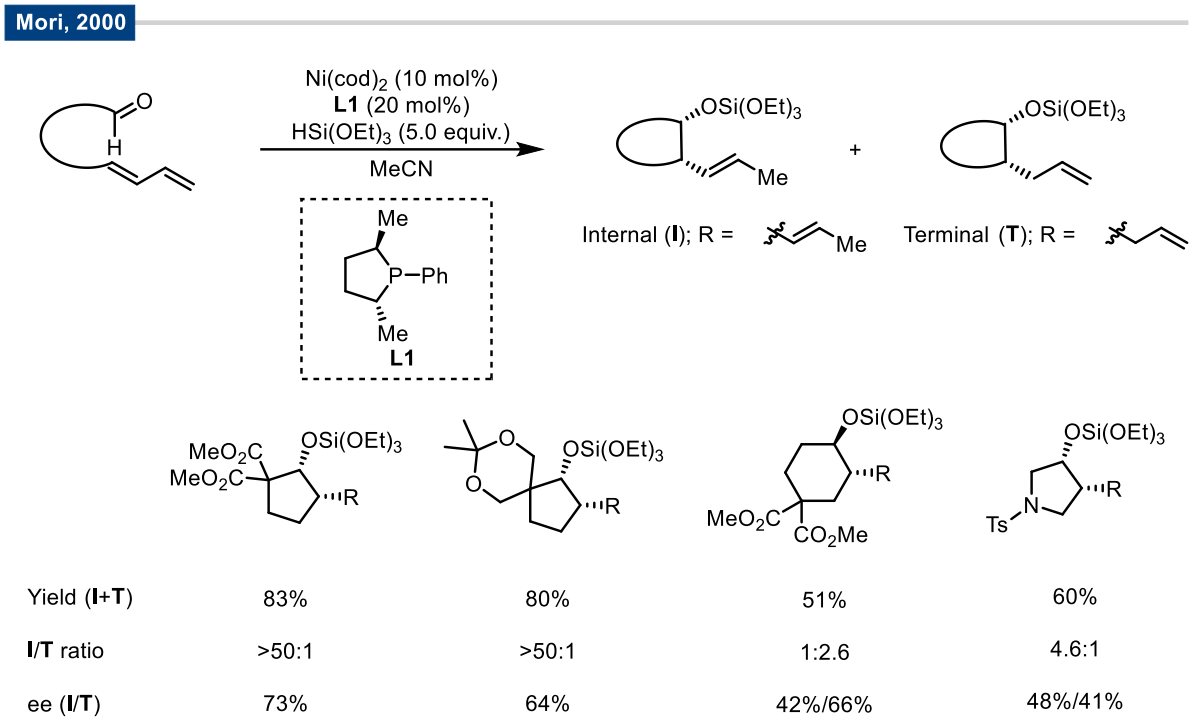

Scheme 71: Pioneering report on asymmetric intramolecular reductive cyclizations of aldehydes and 1,3-dienes by Mori *et al.*

This apparent gap motivated the development of an enantioselective reductive cyclization approach for heterocycle synthesis. Based on the previously established regioinverted coupling of aldehydes with amino-pentadienoates, it was envisioned that this reaction mode could be extended to an intramolecular setting. Incorporation of an N-substituent bearing a suitably positioned aldehyde functionality into the diene framework was therefore pursued as a strategy to enable cyclization (Scheme 72). As the tethered substrate design enforces a relative orientation of the diene and aldehyde moiety analogous to that of the previously investigated regioinverted

reductive coupling, VAPOL-derived phosphoramidite ligand **L11** was hypothesized to be well suited for promoting the desired cyclization.

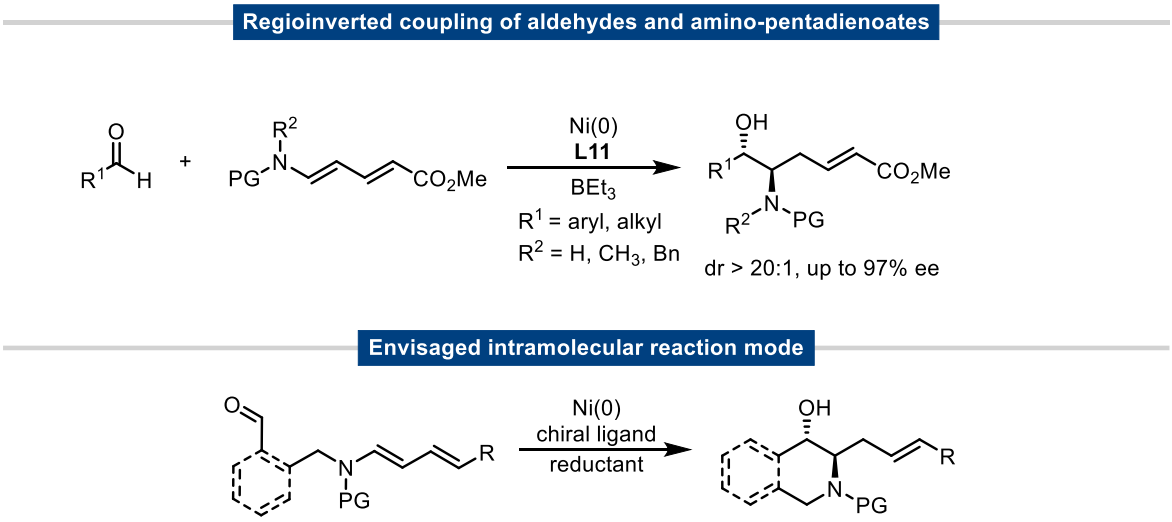

Scheme 72: Envisaged enantioselective intramolecular reductive cyclization of N-substituted amino-pentadienoates.

To evaluate the feasibility of this concept, a model substrate was prepared from Boc-protected amino-pentadienoate **88a** and 2-(bromomethyl)benzaldehyde and was subsequently investigated in the reductive cyclization reaction. Under ligand-free conditions, complete conversion to the corresponding tetrahydroisoquinoline product was observed. Notably, no formation of the corresponding nine-membered aldol product resulting from reaction at the more nucleophilic ester terminus of the diene was detected. This observation suggested that the regiochemical course of the reaction is primarily dictated by the substrate connectivity. Although exogenous ligands were not required for regiocontrol, they proved beneficial for improving diastereoselectivity. In the racemic reaction, monodentate PCy_3 afforded excellent diastereoselectivity, whereas bidentate ligands such as dppe inhibited reactivity.

Despite matching the substrate's inherent regiochemical preference, **L11** failed to induce synthetically meaningful levels of enantioselectivity in the intramolecular reaction mode. Instead, extensive screening of phosphorus-based ligands identified the P-chiral ligand (*S*)-AntPhos **L29** as the optimal ligand, enabling the first highly diastereo- and enantioselective nickel-catalyzed reductive cyclization of an aldehyde and a 1,3-diene since the pioneering report on such transformations at the beginning of the millennium.

Following establishment of the general reaction conditions, a broad range of substrates was prepared through nucleophilic substitution between amino-pentadienoates and appropriately functionalized aldehyde precursors bearing alkyl bromide handles.

The novel intramolecular reaction mode enabled highly efficient access to hydroxylated tetrahydroisoquinoline derivatives bearing an *anti*-configured amino alcohol motif, as well as related *syn*-configured aliphatic heterocycles, with excellent diastereo- and enantioselectivities (Scheme 73).

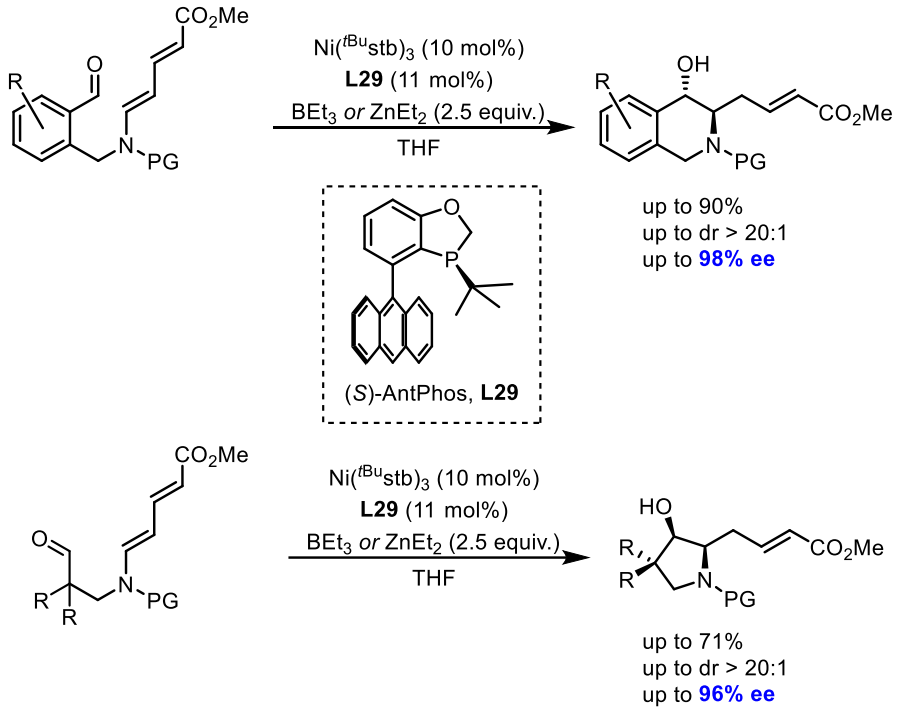

Scheme 73: Asymmetric nickel-catalyzed reductive cyclization affording hydroxylated N-heterocycles diastereo- and enantioselectively.

The reductive cyclization proved broadly applicable and tolerated a variety of functional groups relevant for potential downstream functionalization, while retaining excellent stereocontrol. Beyond the relevance to the field of nickel-catalyzed diene couplings, this transformation establishes an innovative and complementary catalytic strategy for the asymmetric synthesis of tetrahydroisoquinoline derivatives, expanding the current portfolio of synthetic approaches. In contrast to chiral-pool-based strategies, the developed methodology offers a highly modular substrate design. At the same time, it employs an earth-abundant nickel catalyst rather than the precious metals commonly required for established asymmetric hydrogenation protocols.

Despite the distinct characteristics of the intramolecular reaction mode compared to the previously developed intermolecular coupling, several notable parallels were observed. Modification of the diene's push-pull character through removal of the ester group or its formal replacement by a phenyl substituent resulted in substantial erosion of enantioselectivity. Likewise, electronically decoupling the heteroatom from the conjugated 1,3-diene system and relocating it directly to the aromatic ring led to a pronounced decrease in diastereoselectivity. Further investigations of related substrate classes revealed additional challenges and underscored the unique suitability of the amino-pentadienoate scaffold for the enantioselective intramolecular reaction mode.

The tetrahydroisoquinoline products serve as versatile building blocks, allowing access to fluorinated analogs through stereoretentive derivatization, as demonstrated by treatment with DAST. This derivatization strategy provides access to *anti*-configured products, thereby complementing the stereochemical outcomes accessible through asymmetric hydrogenation of fluorinated isoquinoline derivatives. Moreover, intramolecular downstream derivatization

provided access to the core structure of potently cytotoxic phenanthroquinolizidine alkaloids with different functionalization patterns (Figure 17).

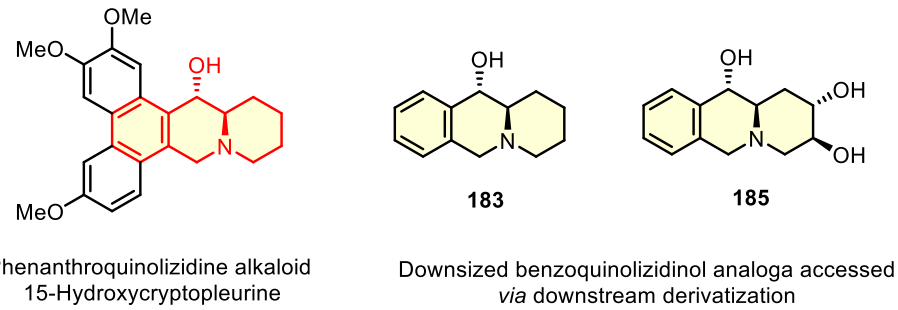

Figure 17: Structural comparison of 15-Hydroxycryptopleurine with downsized benzoquinolizidinol analoga accessed by downstream derivatization of a tetrahydroisoquinoline derivative.

Beyond the development of a novel synthetic methodology and product diversification into pharmaceutically relevant motifs, the study also provided rare experimental evidence for key intermediates of the catalytic cycle. In particular, reactive allyl-oxanickelacycle intermediates were successfully prepared and characterized despite the inherent challenges associated with their isolation. The preorganized structure of the substrates and their chelating binding mode may have facilitated controlled speciation and thereby mitigated some of the difficulties typically associated with the isolation of such species.

Stoichiometric speciation experiments involving representative substrates, $Ni(cod)_2$ and PCy_3 enabled detailed characterization of the corresponding allyl-oxanickelacycle intermediates by NMR spectroscopy and X-ray crystallographic analysis (Figure 18). These data allowed elucidation of the bonding mode of the allylnickel subunit, which proved to be an η^3:η^1-hybrid between a canonical π-allylnickel species and the corresponding σ-complex. Furthermore, distinct conformational preferences of the ligated species compared to those of the corresponding products after release from the nickel coordination sphere were illustrated.

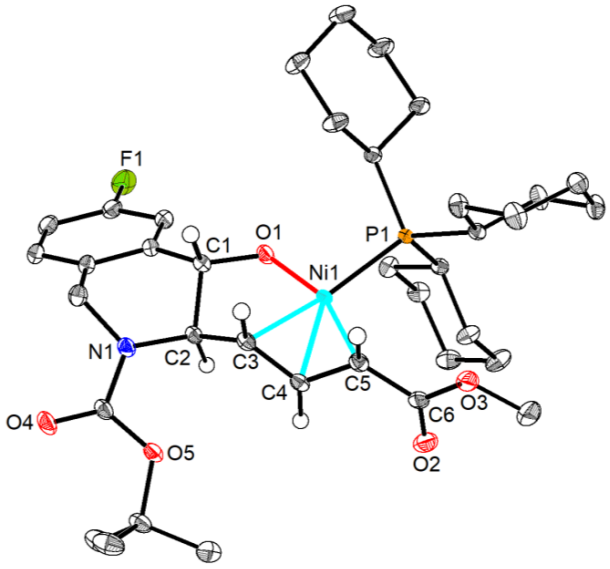

Figure 18: Single-crystal X-ray structure of an allyl-oxanickelacycle intermediate.

Speciation experiments employing the P-chiral (*S*)-AntPhos **L29** were complicated by the formation of atropisomeric species in solution. Nevertheless, shielding effects arising from the relative positioning of the anthracenyl substituent with respect to the metallacycle generated characteristic spectroscopic fingerprints that enabled assignment of two atropisomers. These experimental observations, supported by DFT calculations, provided valuable insights into potentially relevant non-covalent interactions operating in the transition state of the oxidative cyclization step and enabled, for the first time, the development of a plausible stereochemical model for the reaction.

4 Studies Toward Nickel-Catalyzed Redox-Neutral Tandem Reactions between Silyl Dienol Ethers and Functionalized Imines

4.1 Introduction

Following the development of nickel-catalyzed homoallylation reactions by Tamaru and co-workers in the late 1990s, numerous variations of this methodology have been developed (see Chapters 1.2.2, 1.2.3 and 1.2.4). While these studies have focused on the use of alternative electrophiles and reducing agents, as well as on novel dienes and the development of asymmetric reaction modes, one particularly intriguing question remained unanswered: is this transformation limited to nickel?

To address this question, the group of Masanari Kimura, a former co-worker of Yoshinao Tamaru, adopted the reaction conditions for the nickel-catalyzed isoprenylation reaction and investigated the behavior of other transition metals under the established conditions (Scheme 74).

In contrast to the nickel-catalyzed reductive coupling, which selectively afforded 1,3-*anti* configured homoallylation product **30** (Scheme 74, a), an analogous rhodium-catalyzed protocol favored reaction at the internal position, affording 1,2-*syn*-configured alcohol **194** as the major product (Scheme 74, b).[196] This difference in regioselectivity is attributed to mechanistic divergence between the two transformations. In contrast to the nickel-mediated catalytic cycle (see Chapter 1.2.2), the rhodium-catalyzed reaction presumably proceeds *via* formation of a rhodium-hydride species. Subsequent hydrorhodation generates a π-allylrhodium intermediate, which can be regarded as an allylic carbanion equivalent that undergoes addition to the aldehyde, ultimately furnishing the corresponding product.[196]

Kimura and co-workers also explored the compatibility of palladium with the reductive coupling conditions. While the coupling proceeds at the same diene terminus as in the analogous nickel-mediated process, palladium instead promotes a redox-neutral carbonyl-ene reaction, resulting in the formation of dienyl alcohol **195** (Scheme 74, c).[197] In contrast to the nickel-catalyzed coupling, triethylborane acts solely as an activating Lewis acid and does not take the role of a terminal reductant. However, the requirement for a *trans*-spanning bidentate ligand such as XantPhos limited further development of this reactivity and asymmetric variants have not been reported to date.

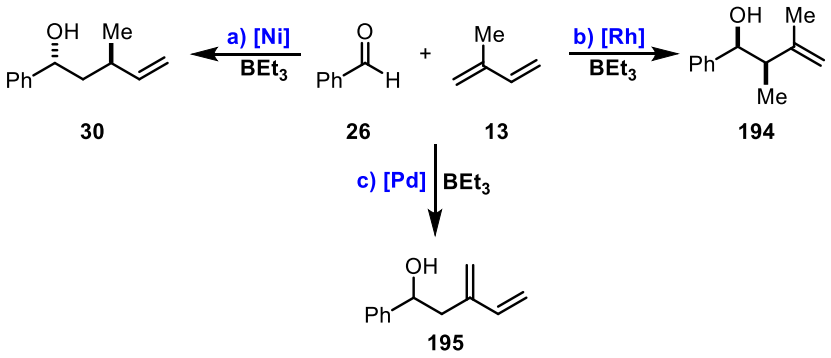

Scheme 74: BEt_3-mediated coupling between benzaldehyde and isoprene with different transition metal catalysts; reaction conditions: a) $Ni(acac)_2$ (10 mol%), benzaldehyde (1.0 equiv.), isoprene (4.0 equiv.), BEt_3 (2.4 equiv.), THF, RT; b) $[Rh(OH)(cod)]_2$ (5 mol%), benzaldehyde (1.0 equiv.), isoprene (1.0 equiv.), BEt_3 (1.0 equiv.), THF, 50 °C; c) $Pd(OAc)_2$ (10 mol%), XantPhos (10 mol%), benzaldehyde (1.0 equiv.), isoprene (4.0 equiv.), BEt_3 (2.0 equiv.), THF, RT.

Despite the limitations associated with this first-generation system, palladium-based catalyst systems have become increasingly important in redox-neutral coupling reactions between dienes and electrophiles. In particular, the ability of palladium(0) to engage in strong π-backbonding with 1,3-dienes and thereby raise their HOMO energies has been exploited, enabling reactions with suitable electrophiles even in the absence of an activating Lewis acid (Scheme 75).[198]

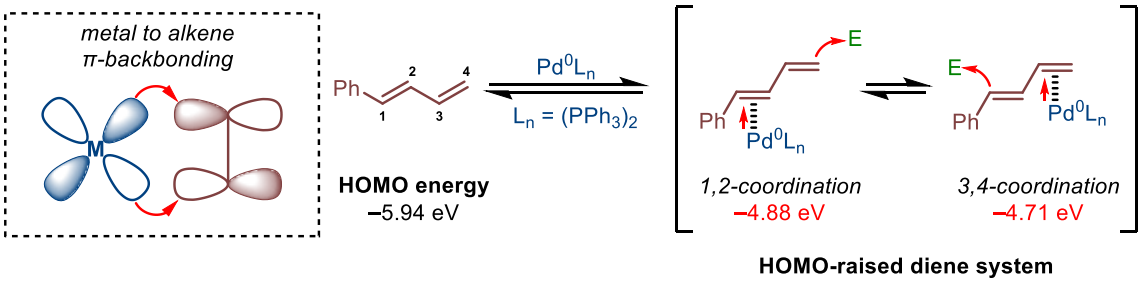

Scheme 75: HOMO-raising effects caused by metal to diene π-backbonding enable coupling reactions with electrophiles.

In recent years, the research group of Ying-Chun Chen has made significant advancements in this underexplored field of π-base catalysis. In 2021, the group reported an asymmetric redox-neutral coupling reaction between protected imines and aryl-substituted dienes.[199] The HOMO-raising effect enables addition of the diene to the imine at elevated temperature, while acid-induced β-hydride elimination during the catalytic cycle restores the 1,3-diene moiety. In the presence of phosphoramidite ligand **L30** the corresponding dienyl amine products were obtained in remarkable enantioselectivity and with good to excellent control over the double bond geometry (Scheme 76).

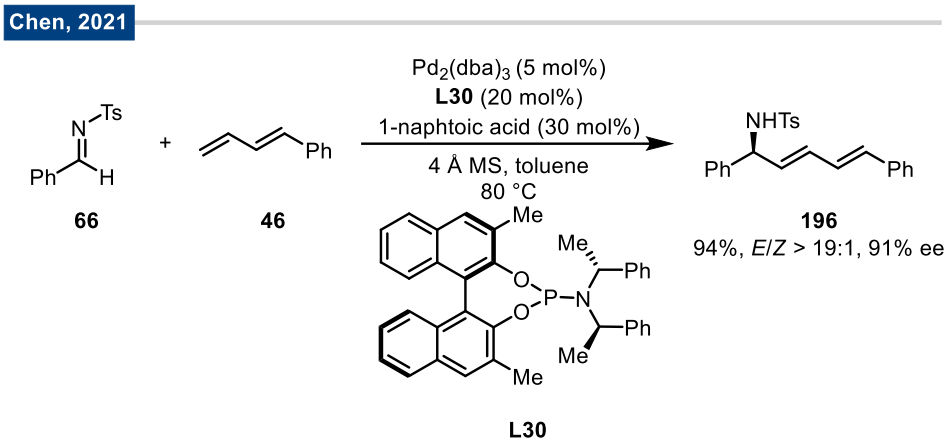

Scheme 76: Example of an asymmetric palladium-catalyzed redox-neutral coupling of protected imines and 1,3-dienes.

Recent studies have shown that nickel, when combined with suitable ligands, solvents, and additives, can mediate similar reactivities, resulting in the development of various redox-neutral couplings of aldehydes or imines with alkenes and dienes.[72, 82, 200-204] However, a comparison of palladium- and nickel-catalyzed redox-neutral coupling reactions reveals that palladium offers a significantly broader range of pathways involving the corresponding π-allyl metal intermediates. In addition to β-hydride elimination and subsequent regeneration of the π-bond in the corresponding product, nucleophilic attack on the π-allyl species, in analogy to the "Tsuji-Trost reaction", provides an alternative catalytic pathway. To this end, Chen and co-workers coupled 1,3-dienes with imines bearing a nucleophilic handle capable of attacking the π-allyl-intermediate. Both protected amines and free alcohols were compatible, enabling redox-neutral cyclization *via* tandem reactions with excellent diastereo- and enantioselectivity (Scheme 77).[199]

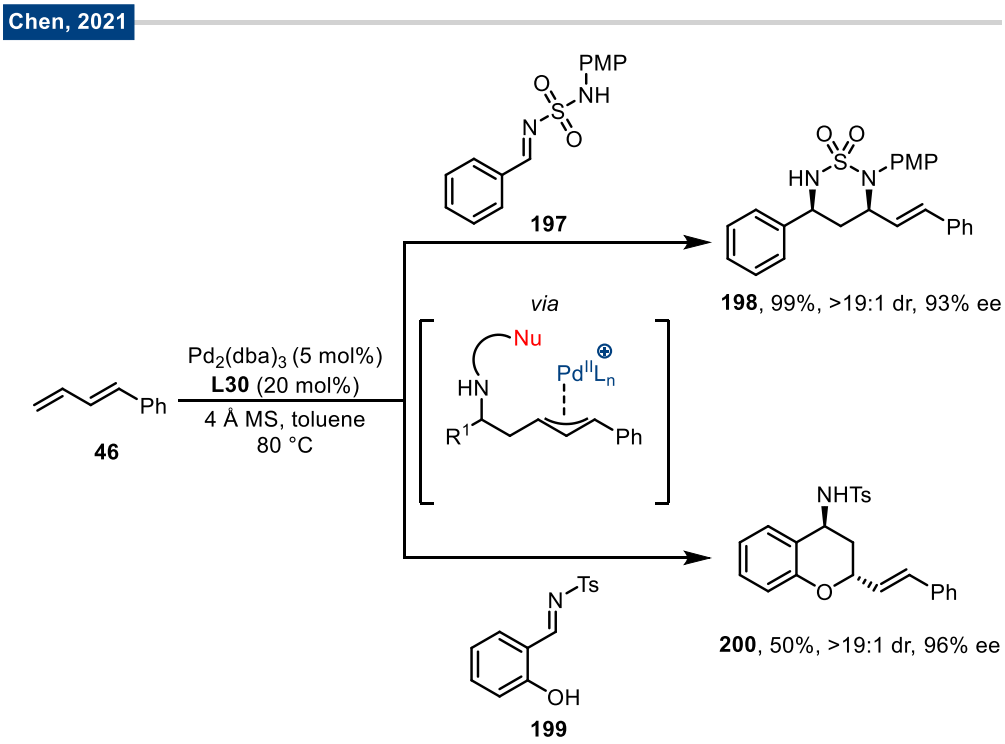

Scheme 77: Examples for palladium-catalyzed tandem reactions resulting in redox-neutral cyclization.

The considerable synthetic potential of this reaction mode has quickly inspired the development of both intra- and intermolecular modifications, enabling enantioselective access to a broad range of heteroatom-containing polycyclic scaffolds.[205-209]

In comparison, analogous nickel-catalyzed transformations have not been explored to the same extent. Although the use of alternative reductants and the development of redox-neutral protocols have gained increasing attention (see Chapters 1.2.2 and 1.2.3), the application of nucleophiles to harness the reactivity of nickel-π-allyl species through a tandem reaction has rarely been investigated. Only in 2026 (after the work presented in the following chapters had been performed), did Sauthier and co-workers, to the best of current knowledge, report a nickel-catalyzed three-component coupling employing amines as external nucleophiles (Scheme 78).[210]

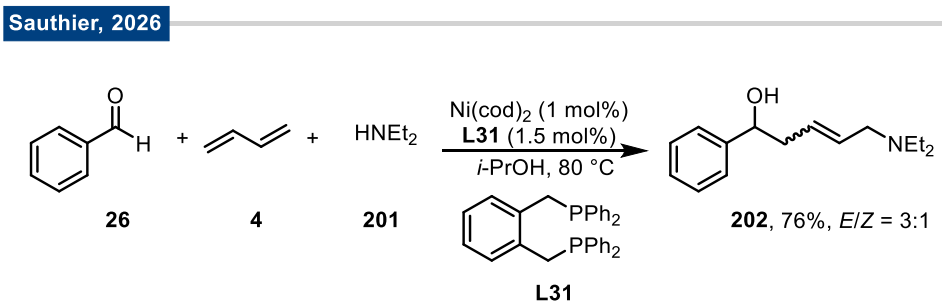

Scheme 78: Example of a nickel-catalyzed three-component coupling between benzaldehyde, butadiene and diethylamine.

Although this work presents an important milestone in expanding the scope of nickel-catalyzed couplings involving 1,3-dienes, the synthetic utility remains limited. In addition to its restriction to 1,3-butadiene as a coupling partner, the reaction exhibits poor control over the double bond geometry and suffers from competing hydroamination.

Nonetheless, given the compatibility of nickel-based catalytic systems with a broad variety of 1,3-dienes and electrophiles, further development of related reaction modes is highly desirable. Such advances could provide sustainable alternatives to established palladium-based protocols and may also complement the synthetic scope of these transformations due to the distinct catalytic behavior of nickel and palladium.

4.2 Aim

The utilization of alternative reducing agents in "Mori- and Tamaru-type" reductive coupling reactions has been crucial for increasing the applicability and overall scope of these transformations in recent years. In addition, redox-neutral protocols that rely on β-hydride elimination to regenerate the diene π-bond during the catalytic cycle have recently been developed for the synthesis of allylic alcohols and amines, thereby further expanding the scope of such nickel-catalyzed coupling reactions.

All of these transformations are believed to proceed through an allyl-nickelacycle that serves as key intermediate within the catalytic cycle. It was envisaged that, beyond these established approaches, the reactivity of these intermediates could be harnessed through interception by an external nucleophile, capable of attacking the allyl unit of the metallacycle. Comparable strategies are well established in the realm of palladium π-base catalysis and have been successfully employed in redox-neutral tandem reactions for the enantioselective synthesis of heterocyclic motifs. In contrast, analogous nickel-catalyzed approaches have not been reported to date.

It was therefore envisaged that a redox-neutral tandem reaction based on the established system of nickel(0) and VAPOL-derived phosphoramidite ligand **L11** could be developed. This catalytic system efficiently promotes the regioinverted coupling of protected imines with silyl dienol ethers, selectively affording chiral vicinal amino alcohols (see Chapters 1.2.4 and 1.3). It was hypothesized that incorporation of a tethered nucleophilic handle into the imine substrate would enable intramolecular attack on the π-allyl intermediate, thereby furnishing the corresponding cyclization product (Scheme 79).

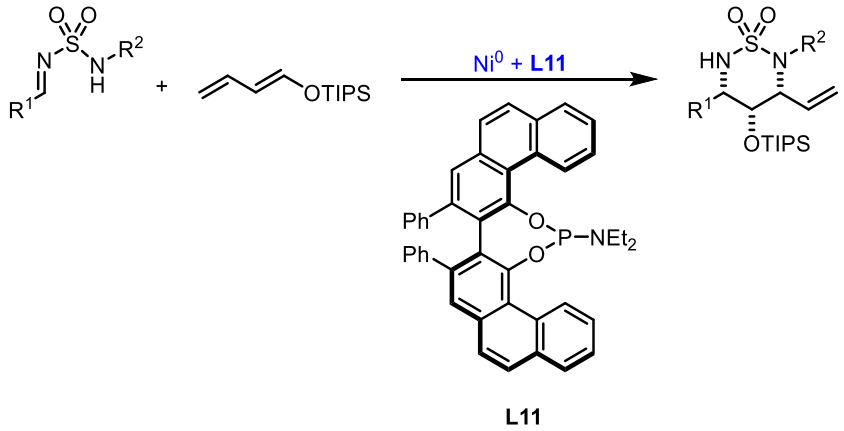

Scheme 79: Envisaged nickel-catalyzed redox-neutral tandem reaction.

Such reactivity would be highly attractive from both synthetic and conceptual perspectives. First, this transformation would provide atom-economical access to a rare structural motif combining two 1,2-amino alcohol motifs with a 1,3-diamine motif. Furthermore, a conceptual understanding of how to enable such processes could establish the foundation for an entirely new mode of nickel-catalyzed coupling reactions involving 1,3-dienes. Nickel-based systems have been shown to be compatible with a large portfolio of 1,3-dienes. This may prove particularly advantageous, given

that established palladium-based protocols are often restricted to aryl-substituted dienes. Consequently, related nickel-catalyzed reactions could not only provide a more sustainable alternative but also offer complementary reactivity patterns and access to novel, valuable chiral structural motifs.

4.3 Preliminary Experiments

The investigation of the envisaged nickel-catalyzed tandem reaction commenced with an evaluation of the compatibility of sulfamide-derived imines with the regioinverted reductive coupling reaction. Previous studies in our group had shown that the transformation is highly sensitive to the nature of the N-protecting group and consequently largely restricted to tosyl-protected substrates, while alternatives such as carbamates led to markedly reduced reactivity.[98, 162]

Gratifyingly, a model coupling between the functionalized imine **197** and silyl dienol ether **31** proceeded smoothly under the established reaction conditions and was compatible with both $Ni(cod)_2$ and bench-stable $Ni(^{tBu}stb)_3$ (Scheme 80). In analogy to previous studies, stoichiometric amounts of degassed water were essential for promoting the reaction, as almost no conversion was observed under rigorously anhydrous conditions. Once again, the regioinverted reductive coupling proceeded with high levels of regio- and enantiocontrol, underscoring the effectiveness of phosphoramidite ligand **L11** in this reaction mode. Small amounts of alkene isomer **204** were removed by flash chromatography, affording the desired compound **203** in good yield.

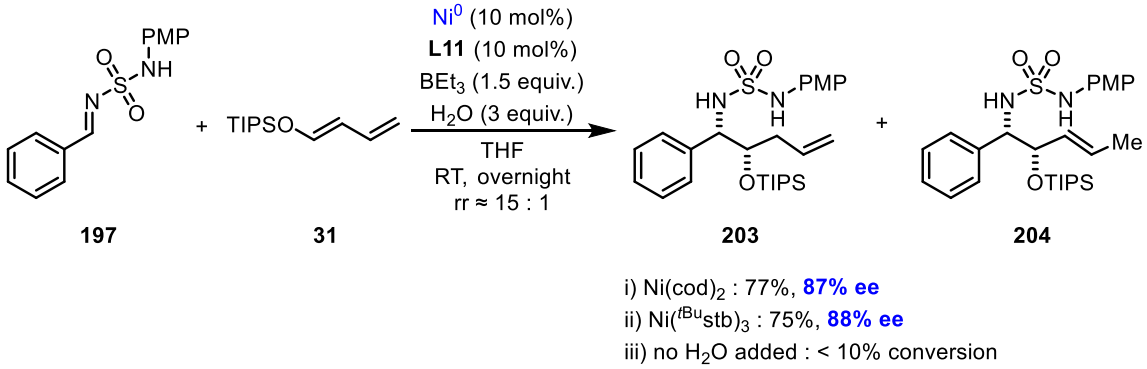

Scheme 80: Exploring the compatibility of a sulfamide-derived imine with the nickel-catalyzed regioinverted reductive coupling.

Additionally, imine analog **205** was subjected to the reductive coupling, as it was considered potentially better suited for the envisaged tandem reaction due to the increased nucleophilicity and steric accessibility of the nucleophilic handle. Fortunately, formal removal of the PMP-group did not adversely affect reactivity and full conversion to the desired product **206** was observed (Scheme 81). However, isolation could not be achieved due to the co-elution of residual oxidized ligand. Nonetheless, determination of the ee by HPLC analysis of the impure product was possible and revealed a significant loss in enantioselectivity.

Importantly, no cyclization product could be detected in either of these initial test reactions. These results indicated that, although the envisaged reaction appeared feasible in principle, cyclization was potentially kinetically outcompeted by reductive coupling in the presence of triethylborane.

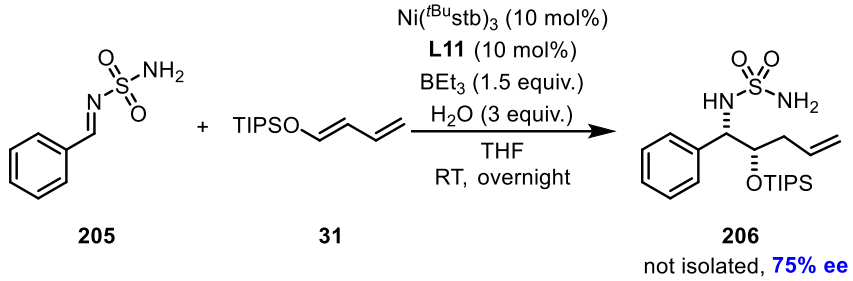

Scheme 81: Exploring the necessity and influence of the N-protecting group.

Consequently, the reaction was conducted in the absence of triethylborane and various reaction parameters were systematically modified to promote the desired redox-neutral pathway (Table 6).

Table 6: Initial screening of reaction conditions for the redox-neutral tandem reaction.

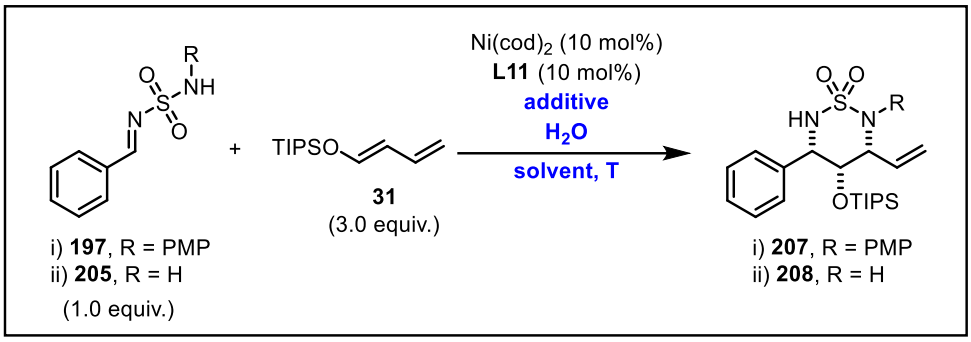

Entry	Solvent	H_2O	Additive	Temperature	Conversion
1[a]	THF	---	---	RT/reflux	0%
2[a]	THF	3.0 equiv.	---	RT/reflux	0%
3[a]	THF	---	DIPEA (1.2 equiv.)	RT/reflux	0%
4[a]	THF	3.0 equiv.	DIPEA (1.2 equiv.)	RT/reflux	0%
5[a]	toluene	---	---	100 °C	0%
6[a]	toluene	3.0 equiv.	---	100 °C	0%
7[b]	THF	3.0 equiv.	---	50 °C	0%
8[b]	THF	3.0 equiv.	K_3PO_4 (1.0 equiv.)	50 °C	0%
9[b]	DMA	3.0 equiv.	---	135 °C	0%

[a] = using imine **197**; [b] = using imine **205**

In the absence of triethylborane, no conversion of the PMP-protected imine **197** was observed, even upon heating the mixture to reflux (Table 6, entry 1). The addition of stoichiometric amounts of degassed water did not improve the outcome, despite its crucial role in the reductive coupling (Table 6, entry 2). Similarly, addition of diisopropylethylamine (DIPEA) proved ineffective (Table 6, entries 3 and 4) and no product formation was observed even at 100 °C in toluene (Table 6, entries 5 and 6). Likewise, formal removal of the PMP-group did not result in any improvement, as imine **205** failed to undergo cyclization at elevated temperature in THF (Table 6, entries 7 and 8). Notably, no conversion to the desired product was observed even at 135 °C in N,N-dimethylacetamide (DMA) (Table 6, entry 9), despite a control experiment confirming the compatibility of this solvent with the reductive coupling mode.

4.4 Mechanistic Considerations and Rationale for Reaction Design

In light of the complete lack of reactivity in the initial screening, the reaction design and possible underlying limitations were re-evaluated. The absence of triethylborane, which not only serves as a reductant but likely also as an activating Lewis acid, was recognized as a potential drawback. Nonetheless, it was assumed, that despite imines being weaker electrophiles than aldehydes, oxidative cyclization should be possible under ambient conditions or at least at elevated temperature, even in the absence of any Lewis acid.

Consequently, one of the subsequent steps in the catalytic cycle was assumed to be the cause of the lack of reactivity. Oxidative cyclization of the imine and diene with nickel(0) would likely result in formation of azanickelacycle intermediates that are in equilibrium with each other (Scheme 82). Next, attack of the nucleophilic handle at the allyl unit, either *via* an outer-sphere mechanism from **Int-A** or *via* an inner-sphere mechanism from **Int-B** would result in reductive elimination, releasing the cyclization product and a nickel(0) species, thereby completing the catalytic cycle. Although the mechanistic details of this step in the catalytic cycle are purely speculative at this point, the C–N bond formation step was believed to be the major problem.

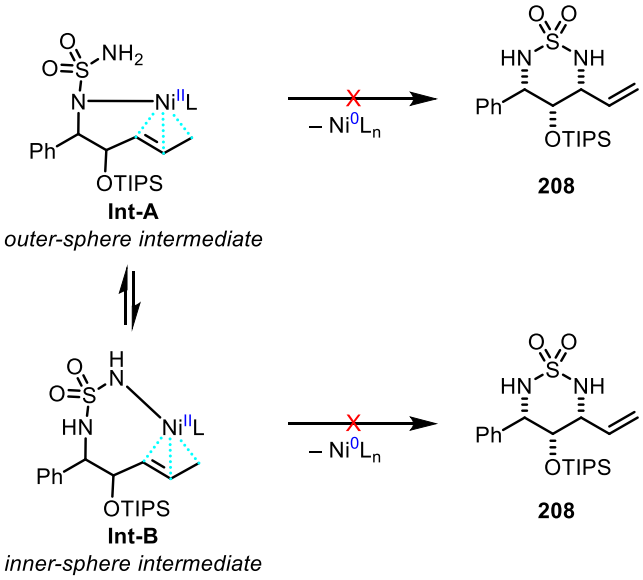

Scheme 82: Plausible intermediates formed following oxidative cyclization of the substrates.

While tandem reactions of this type are unprecedented for nickel-based systems, C–N bond-forming processes have been extensively studied in the context of nickel catalysis over the past >10 years. A longstanding challenge has proven to be the reluctance of nickel(II) alkyl amido complexes to undergo reductive elimination under ambient conditions. Computational studies suggest that, in contrast to analogous palladium-catalyzed reactions, C–N reductive elimination from nickel(II) complexes is thermodynamically disfavored, whereas palladium-based systems benefit from the exothermic nature of this step.[211] Importantly, the generation of reactive nickel(III) amido species can significantly facilitate C–N bond formation, and has been essential for the development of various synthetic protocols.

In particular, this strategy was successfully employed by MacMillan *et al.* who developed photoredox-based approaches using iridium photocatalysts to generate nickel(III) amido species *in situ*, thereby enabling the coupling of aryl bromides with primary and secondary amines (Scheme 83).[212]

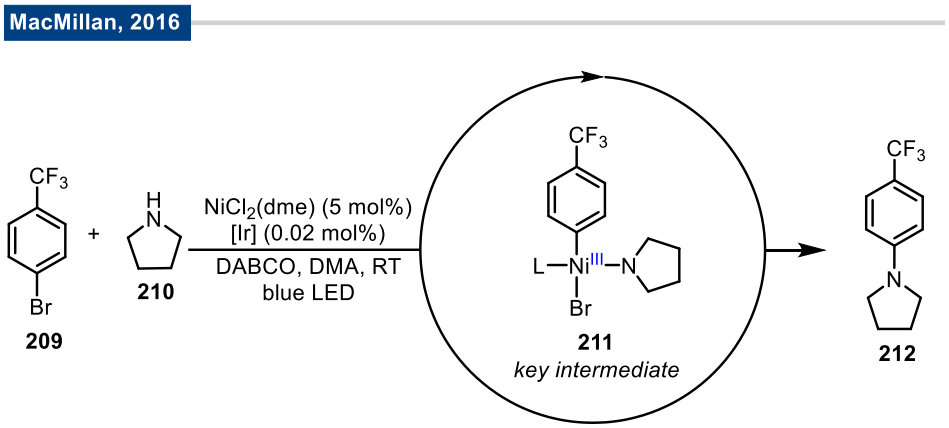

Scheme 83: Proposed nickel(III) amido key intermediate for productive C–N bond formation in photoredox aryl amination.

Inspired by these findings, the envisioned redox-neutral coupling was attempted under established photoredox conditions (Scheme 84) both in the presence and in the absence of ligand **L11**. Unfortunately, no formation of the desired product was observed and the reaction only led to partial isomerization of the diene.

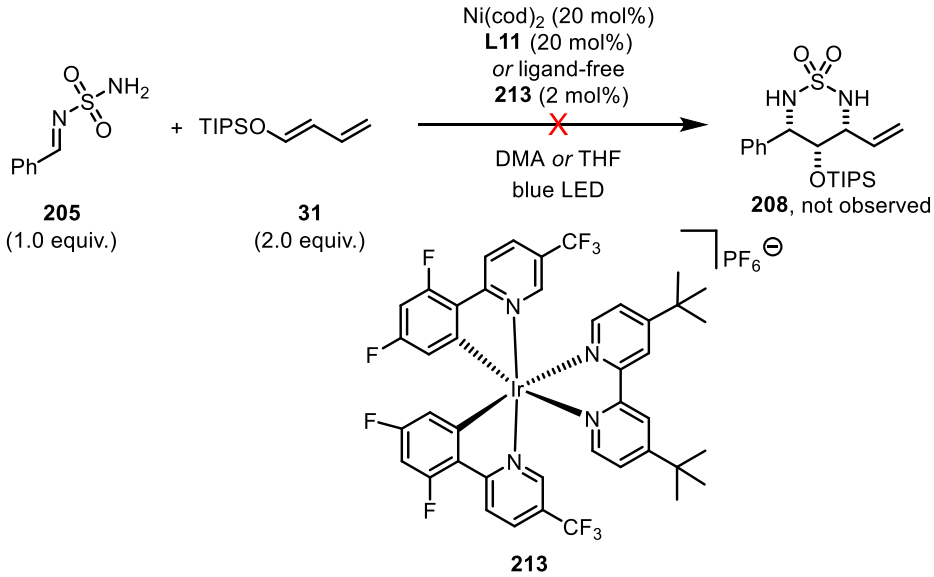

Scheme 84: Attempted photo-redox approach for the redox-neutral tandem reaction.

Consequently, alternative strategies for accessing a reactive nickel(III) amido species were explored. Drawing inspiration from earlier studies by Hillhouse *et al.*, it was attempted to promote the C–N bond formation by addition of a one-electron-oxidant.[213, 214] To this end, the reaction was conducted in the presence of ferrocenium tetrafluoroborate ($FcBF_4$) using sub-stoichiometric amounts of nickel(0) and *rac*-**L11** (Scheme 85). Under these conditions, significant albeit

incomplete conversion of the imine substrate was observed. Cyclization product **214**, resulting from coupling at the unsubstituted diene terminus, was isolated in 44% yield as a single diastereomer, suggesting that at least a single catalytic turnover had occurred. Notably, the envisaged product **208** resulting from the regioinverted coupling, was not detected.

Attempts to reproduce these results with enantiomerically pure ligand **L11** to evaluate potential asymmetric induction were unsuccessful. In four independent repetition experiments, no conversion was observed, even when stoichiometric amounts of precatalyst and ligand were employed. Consequently, despite the initial experimental support for the proposed mechanistic rationale, the reaction conditions required further revision.

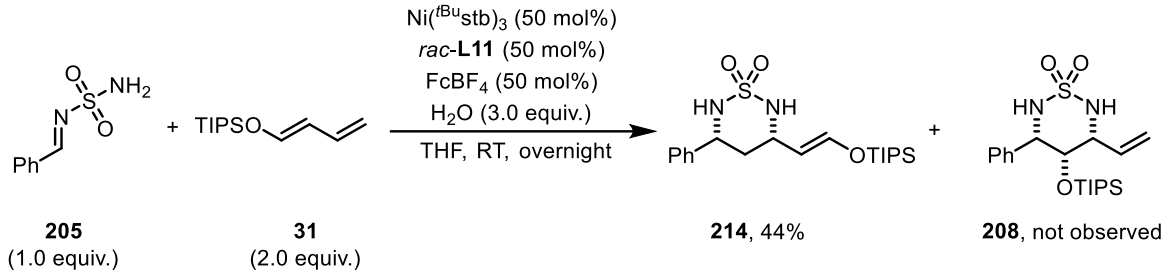

Scheme 85: Ferrocenium-mediated single-electron-transfer enables productive C–N bond formation.

Again, inspiration for reaction development was found in nickel-catalyzed Buchwald-Hartwig couplings. In particular, Nocera and co-workers recently reported a protocol enabling C–N bond formation under ambient conditions.[215] Similar to the photoredox strategy developed by MacMillan, a nickel(III) amido species was proposed as the key intermediate responsible for productive coupling. Mechanistically, the catalytically active nickel(I) species was presumed to form *via* slow single-electron reduction of a nickel(II) precatalyst by zinc powder. Subsequent oxidative addition of the aryl halide to the *in situ* generated nickel(I) complex was proposed to furnish a nickel(III) intermediate, which upon reaction with the amine and an external base would generate the reactive nickel(III)amido species (Scheme 86).

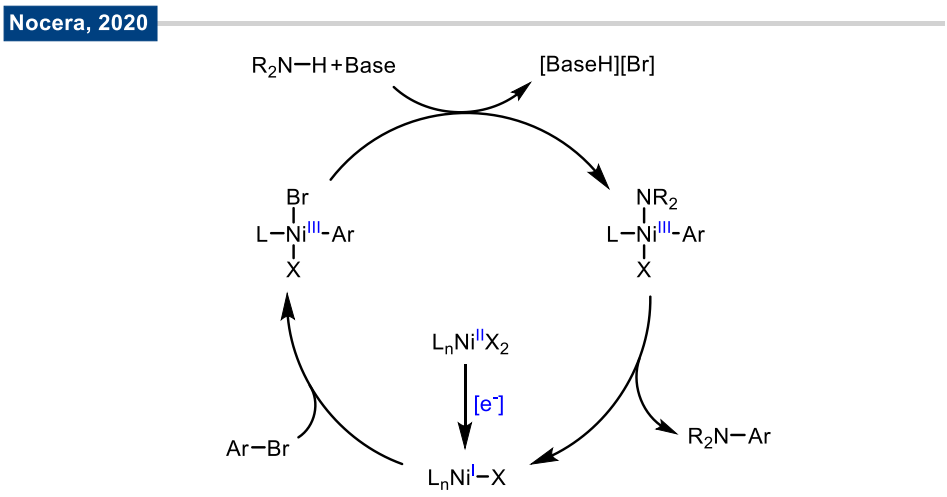

Scheme 86: Thermal nickel-mediated C–N coupling *via* a Ni(I/III) catalytic cycle.

It was hypothesized that this approach could provide an alternative strategy of generating a reactive nickel(III) species in the targeted redox-neutral tandem reaction. Following *in situ* generation of a nickel(I) species, oxidative cyclization with the imine and diene could potentially furnish a reactive nickel(III) amido complex capable of undergoing reductive elimination, thereby completing the catalytic cycle.

To test this hypothesis, the model coupling of imine **205** and dienol ether **31** was performed in the presence of (sub)stoichiometric amounts of bench-stable $NiCl_2$(dme) and activated zinc powder (Scheme 87). In analogy to the work of Nocera *et al.*, a 2:1 ratio of precatalyst to reductant was employed. Gratifyingly, the protocol was successful and afforded cyclization product **214** in 28% yield as a single diastereomer. Performing the reaction under rigorously anhydrous conditions further improved the outcome, increasing the yield to 60% by avoiding competing hydrolysis of the imine.

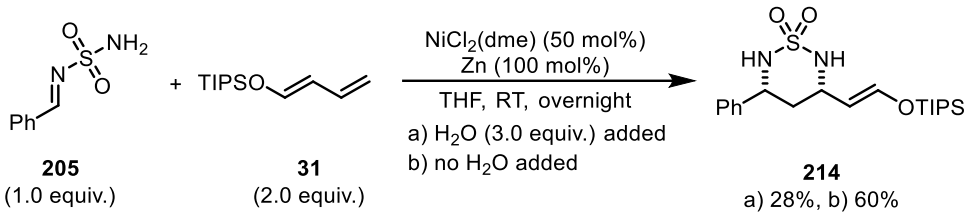

Scheme 87: Ni(II)/Zn system enables redox-neutral tandem reaction.

Although conversion of the imine was still incomplete, the observation of a turnover number greater than one suggested that the transformation could, in principle, operate catalytically. This appeared mechanistically plausible, as reductive elimination would furnish product **214** while simultaneously releasing a nickel(I) species capable of re-entering the catalytic cycle through oxidative cyclization of the starting materials. Encouraged by these findings, catalyst and reductant loadings were reduced, while the reaction time was extended in an effort to achieve full conversion under catalytic conditions. Under these optimized conditions, conversion increased to 85%, allowing product **214** to be isolated in 71% yield, motivating further investigations into this novel reaction mode (Scheme 88).

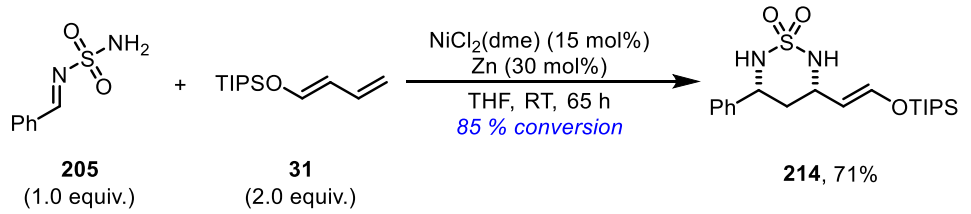

Scheme 88: Redox-neutral tandem reaction under catalytic conditions.

4.5 Studies on Catalytic Reaction Conditions and Reproducibility

Next, efforts were made toward achieving full conversion of the imine and thereby further improving the isolated yield of the product in the model reaction. To this end, a series of modified reaction conditions was evaluated, and conversions were determined by ^{1}H NMR analysis of the crude reaction mixtures using 1,3,5-trimethoxybenzene as an internal standard.

Initial screening focused on the influence of catalyst loading and temperature on the reaction outcome. Performing the catalysis at elevated temperatures resulted in diminished conversion (Table 7, entries 2 and 3). Likewise, varying the ratio of zinc to nickel(II) did not have any beneficial effect on conversion (Table 7, entries 4 and 5). Reverting to the initial reaction conditions again afforded good, albeit incomplete, conversion (Table 7, entry 6) and product **214** was isolated in a slightly improved yield of 77%. During this screening campaign, however, the poor reproducibility of the novel transformation became apparent. This was particularly evident from a set of control experiments, in which the reaction was conducted in parallel in two separate flasks (Table 7, entries 7 and 8). Despite virtually identical setups, markedly different reaction outcomes were observed, with conversions of 10% and 70%, respectively. Numerous additional control experiments were subsequently performed. Although product formation was consistently observed, conversions typically fluctuated within the range illustrated in Table 7.

Table 7: Selected screening results for the optimization of the model reaction.

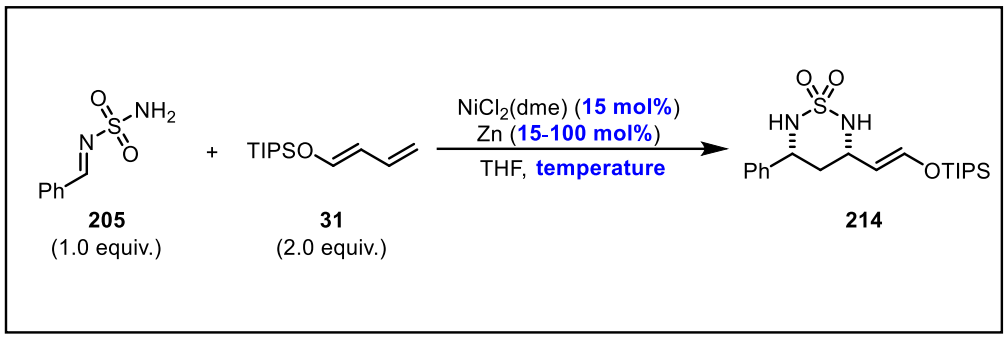

Entry	Ni/Zn	Temperature	Time	Conversion	Isolated Yield
1[a]	15/30	RT	65 h	85%	71%
2	15/30	60 °C	14 h	35%	n.d.
3	15 30	60 °C	42 h	20%	n.d.
4	15/100	RT	88 h	50%	31%
5	15/15	RT	20 h	30%	n.d.
6	**15/30**	**RT**	**65 h**	**85%**	**77%**
7[b]	15/30	RT	65 h	10%	n.d.
8[b]	15/30	RT	65 h	70%	n.d.

[a] = result of the initial catalytic coupling reaction; [b] = these reactions were performed in parallel with identical reaction setup; n.d. = not determined

The heterogeneous nature of the reaction mixture, arising from the limited solubility of $NiCl_2$(dme) in THF and the suspension of zinc, was considered a likely source of these fluctuations. Consequently, the *in situ* reduction of nickel(II) to nickel(I) may proceed in an uncontrolled and

poorly reproducible manner, potentially resulting in ill-defined nickel species in solution. To address this issue, a variety of additional parameters was investigated. These included the duration of prestirring of the nickel precursor with zinc prior to substrate addition, as well as factors such as stirring rate, concentration and systematic exclusion of light. However, none of these control series revealed any systematic correlations with reaction performance, prompting exploration of alternative approaches to improve the reproducibility and robustness of the transformation.

As the limited solubility of the precatalyst had been identified as a potential cause of the observed irreproducibility, a solvent screening was performed. Dimethylacetamide (DMA) and dimethylformamide (DMF) effectively dissolved $NiCl_2$(dme), however, no product formation was observed in either solvent (Table 8, entries 2 and 3). Similarly, performing the reaction in a THF/DMF mixture (Table 8, entry 4) or in acetonitrile (Table 8, entry 5) completely shut down reactivity. Only 1,2-dimethoxyethane (DME) (Table 8, entry 6) and ethanol (Table 8, entry 7) exhibited partial compatibility with the model reaction. However, in light of the pronounced fluctuations in reactivity previously observed, direct comparison of individual experiments remains difficult, and any apparent trends should therefore be interpreted with caution. Nonetheless, the results suggested that alternative solvents do not resolve the underlying reproducibility issues.

Table 8: Solvent screening for the model reaction.

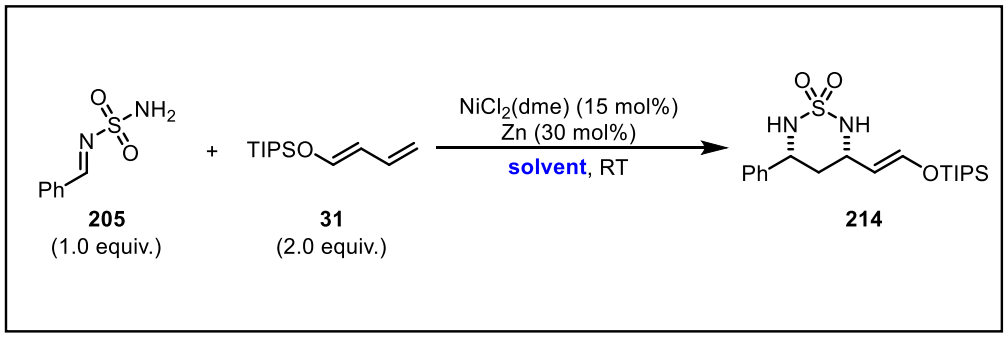

Entry	Solvent	Precatalyst dissolved at reaction start	Time	Conversion	Isolated Yield
1	**THF**	**no**	**65 h**	**85%**	**77%**
2	DMA	yes	68 h	0%	n.d.
3	DMF	yes	16 h	0%	n.d.
4	THF/DMF (9:1)	no	90 h	0%	n.d.
5	MeCN	no	19 h	0%	n.d.
6	DME	no	45 h	n.d.	27%
7	EtOH	yes	42 h	10%	n.d.

n.d. = not determined

Attention was therefore shifted to the reductant required for the generation of the catalytically active nickel species. Since zinc powder is insoluble in organic solvents, the reduction process is inherently heterogeneous and the physical properties of the zinc powder may severely influence this step. However, neither preactivation of the zinc with HCl prior to use[216] (Table 9, entry 2) nor

variation of the mesh size (Table 9, entries 3, 4 and 5) resulted in improved reactivity. Replacing zinc with manganese shut down the reaction entirely (Table 9, entry 6), likely due to the greater reducing power of manganese compared to zinc ($E^0(Mn^{2+}/Mn) = -1.18$ V; $E^0(Zn^{2+}/Zn) = -0.76$ V).[217] This may promote rapid reduction of nickel(II) to nickel(0), thereby preventing formation of the required catalytically active nickel(I) species. Tetrakis(dimethylamino)ethylene (TDAE) was also investigated as an alternative organic reductant (Table 9, entries 7 and 8) due to its proven track-record as a reductant in nickel catalysis.[218-220] Despite its excellent solubility in organic solvents and reducing properties comparable to those of zinc,[220] TDAE likewise proved incompatible with the present reaction system.

As a final attempt to address both the conversion and reproducibility issues of the model reaction, a brief screening of precatalysts was conducted. Bis(chloro)nickel phosphine complexes were evaluated in the hope that strongly σ-donating ligands might stabilize the catalytically active nickel species in solution (Table 9, entries 9 and 10). However, potentially due to their low solubility in THF, these complexes did not promote any notable substrate conversion. Surprisingly, even simple nickel(II)halide salts seemed incompatible with the transformation (Table 9, entry 11), suggesting that the 1,2-dimethoxyethane ligand may play a more crucial role than initially assumed. Furthermore, addition of exogenous ligands (*e.g.* PCy_3, bipyridine, phosphoramidite **L11**) or stoichiometric amounts of external bases (*e.g.* DABCO, *tert*-butyl amine) adversely affected the reaction and completely suppressed product formation.

Table 9: Screening of reductants and precatalysts for the model reaction.

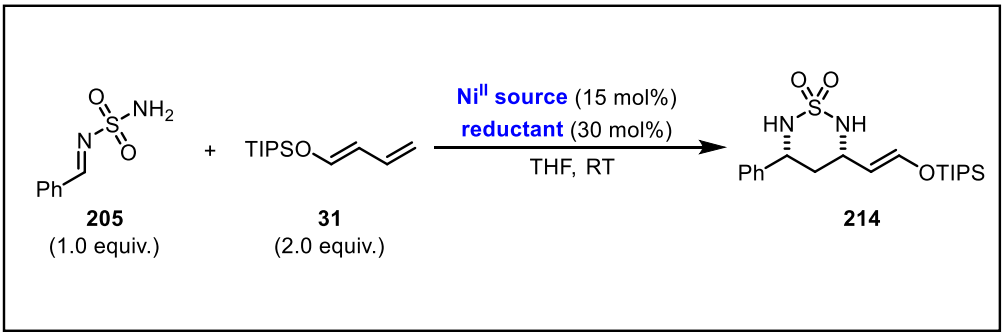

Entry	Precatalyst	Reductant	Time	Conversion	Isolated Yield
1	**$NiCl_2$(dme)**	**Zn dust**	**65 h**	**85%**	**77%**
2	$NiCl_2$(dme)	Zn dust[a]	42-120 h	45%	n.d.
3	$NiCl_2$(dme)	Zn (< 60 µm)	65 h	22%	n.d.
4	$NiCl_2$(dme)	Zn (< 10 µm)	65 h	55%	n.d.
5	$NiCl_2$(dme)	Zn (60 nm)	65 h	<5%	n.d.
6	$NiCl_2$(dme)	Mn	90 h	0%	n.d.
7	$NiCl_2$(dme)	TDAE	15 h	0%	n.d.
8	$NiCl_2$(dme)	TDAE[b]	15 h	0%	n.d.
9	$NiCl_2(PPh_3)_2$[c]	Zn dust	65 h	0%	n.d.
10	$NiCl_2$(dppp)[c]	Zn dust	65 h	0%	n.d.
11	$NiCl_2$ or NiI_2	Zn dust	40 h	0%	n.d.

[a] = freshly activated prior to use; [b] = 7.5 mol% of reductant used; [c] = low solubility of precatalyst observed; n.d. = not determined;

Although severe fluctuations in conversion were observed, product formation was detected in every single experiment conducted under the established standard conditions. In contrast, most modified conditions resulted in complete loss of reactivity, strongly suggesting that the reaction mode is highly sensitive to subtle changes in reaction parameters and that many of the tested conditions are fundamentally incompatible with the transformation. Nonetheless, it cannot be ruled out that the observed conversions do not necessarily reflect the best achievable performance and could very well be significantly improved.

Considering the complexity of the present system, further optimization studies were temporarily put on hold, and attention was shifted to preliminary evaluation of potential substrate modification. To this end, additional substituents were introduced into both the imine and the diene moiety (Scheme 89). Introduction of an additional propyl group at the nucleophilic handle was tolerated in the synthesis of compound **216**, although formation of diastereomers was observed, which could only partially be separated by flash chromatography, resulting in a diminished isolated yield. Likewise, placement of a methyl-substituent at the reactive diene terminus was tolerated, enabling access to the corresponding product **218** bearing three stereocenters. However, introduction of the additional stereocenter resulted in a substantial drop in diastereoselectivity to almost 1:1. Notably, the diastereomers could not be separated. Moreover, both reactions continued to suffer from incomplete conversion despite the use of an increased catalyst loading, indicating that the reactivity limitations persist.

Nevertheless, these experiments demonstrate that the transformation may possess considerable synthetic scope. This further highlights the potential of this novel methodology, provided that the current reactivity and reproducibility issues can ultimately be overcome.

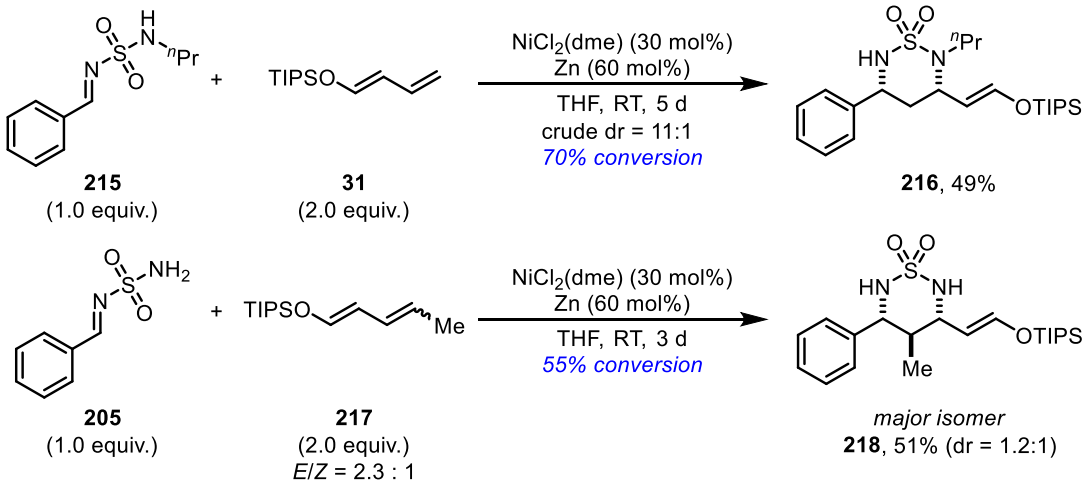

Scheme 89: Redox-neutral tandem reaction with modified imine and diene components.

4.6 Summary and Outlook

Nickel-catalyzed "Mori- and Tamaru-type" coupling reactions between electrophiles and 1,3-dienes have been developed in numerous variants, including protocols employing different promoters as well as reductant-free approaches. Since all of these transformations are believed to proceed through allyl-nickelacycle intermediates, the question arose whether the inherent reactivity of these intermediates could be harnessed through interception by an external nucleophile capable of attacking the allyl unit of the metallacycle. Such redox-neutral tandem reactions have been reported before in the field of asymmetric palladium π-base catalysis (Scheme 90). However, an analogous reaction mode with nickel, despite its ability to promote the coupling of a diverse range of 1,3-dienes, has not been reported to date.

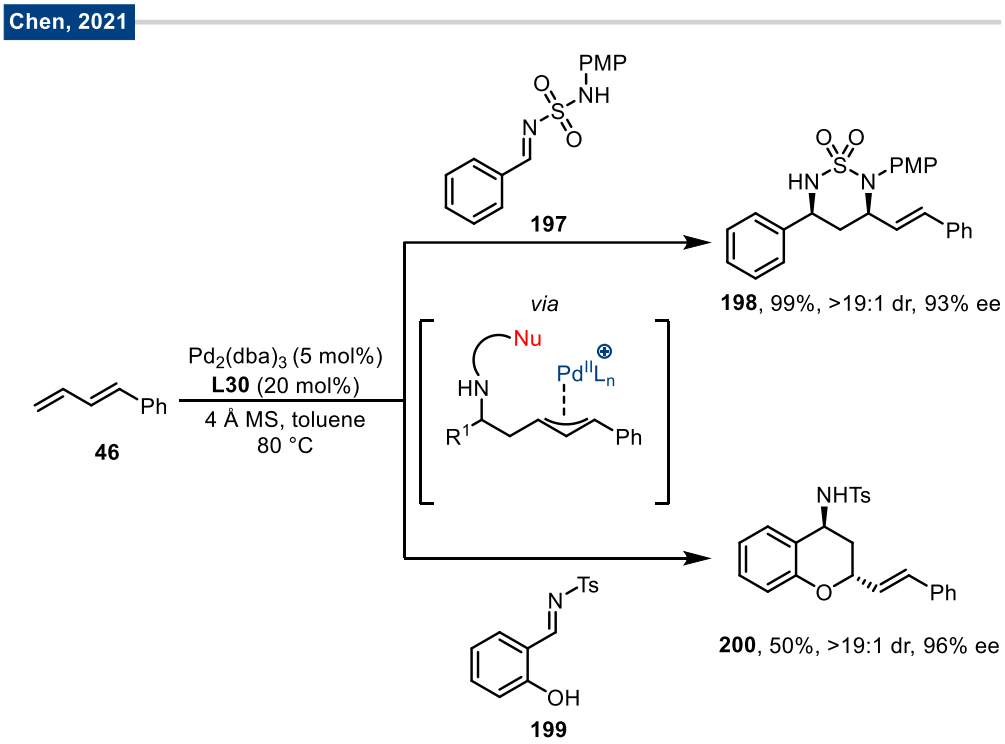

Scheme 90: Examples for palladium-catalyzed tandem reactions resulting in redox-neutral cyclization.

It was envisioned that such a transformation could be achieved by coupling functionalized imines bearing a nucleophilic handle with silyl dienol ethers in the presence of VAPOL-derived phosphoramidite ligand **L11** (Scheme 91).

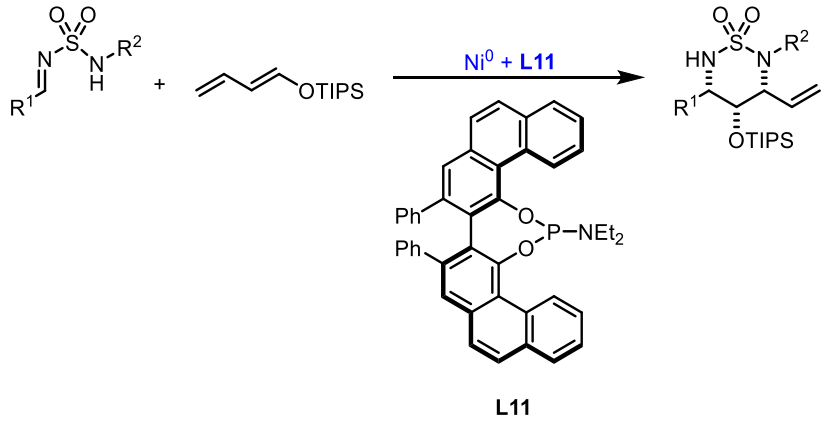

Scheme 91: Envisaged asymmetric nickel-catalyzed redox-neutral tandem reaction.

However, realizing this concept proved challenging, as no conversion to the desired cyclic sulfamide products was observed under a variety of reaction conditions. The attack of the nucleophilic handle at the allyl unit of the *in situ* generated allyl-azanickelacycle intermediate was identified as the key challenge within the catalytic cycle. It was hypothesized that formation of a nickel(III) amido species is essential to enable productive C–N bond formation in this step. After initial stoichiometric control experiments supported this hypothesis, a simple catalytic system involving $NiCl_2$(dme) and zinc powder was developed. Although the transformation is redox-neutral with respect to the substrates, the zinc is likely required for *in situ* generation of a nickel(I) species capable of productively engaging with the coupling partners.

Despite significant advances in the development of a representative model reaction and the isolation of the corresponding product in good yield and excellent diastereoselectivity (Scheme 92), the transformation still requires substantial optimization. In particular, incomplete substrate conversion and pronounced reproducibility issues were noticed. Despite extensive screening of a broad range of reaction parameters, neither issue could be satisfactorily resolved, and both currently remain limiting factors in the development of the methodology. Nonetheless, preliminary investigations into the substrate scope indicated that the reaction may tolerate structural modifications of both coupling partners. Consequently, this reaction mode could possess considerable synthetic potential and may therefore warrant further investigation.

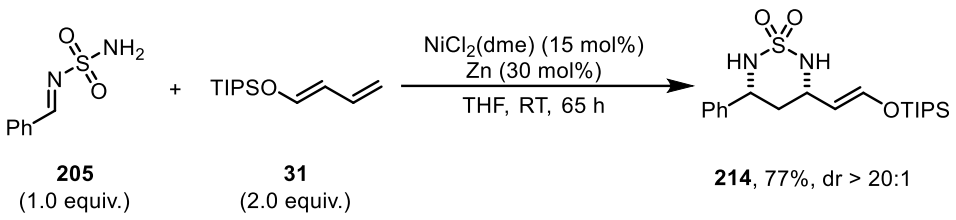

Scheme 92: Diastereoselective nickel-catalyzed redox-neutral tandem reaction between a functionalized imine and a silyl dienol ether.

At the same time, a critical re-evaluation of the current state of the project appears necessary. The original aim was the development of an enantioselective, regioinverted redox-neutral tandem

reaction between imines bearing a nucleophilic handle and silyl dienol ethers. However, both the initial control experiment employing the VAPOL-derived phosphoramidite ligand **L11** and the established ligand-free protocol followed the typical "Tamaru-type" regiochemical course, thereby affording the regioisomer of the initially targeted product in racemic fashion.

Although this outcome differs from the initial project vision, the obtained products nevertheless represent potentially valuable structures and offer diverse opportunities for downstream functionalization (Scheme 93). Most importantly, desulfonylation of the cyclic sulfamide could provide access to primary and pre-differentiated 1,3-diamines, depending on the nature of the substrate.[221-225] Furthermore, both the protected dienol ether and the alkene moieties constitute synthetic handles that enable introduction of aldehyde functionalities at different positions relative to the sulfamide core. Such intermediates could serve as useful platforms for olefination reactions, enabling installation of diverse functional groups, or alternatively participate in intramolecular downstream derivatization.

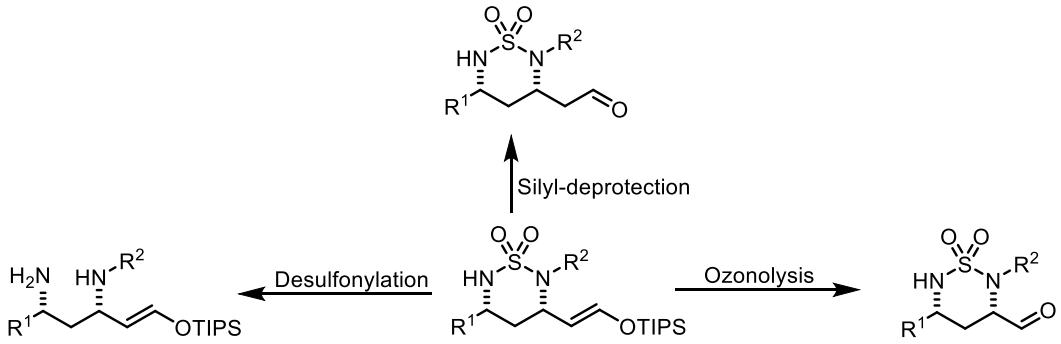

Scheme 93: Envisaged derivatization opportunities for the cyclic sulfamide products.

Given both the potential synthetic value of these products and the mechanistic novelty of the transformation, further investigation of this redox-neutral reaction mode appears worthwhile. However, the central question that remains is how the aspects of limited reactivity and reproducibility can be addressed.

At present, both these problems are assumed to arise from the ill-defined nature of the catalytically active species in solution. This may result from the sluggish and heterogeneous reduction of the precatalyst, as well as from undesired disproportionation processes that could affect the concentration of the catalytically active nickel species in solution.[226] Consequently, it is possible that only a small fraction of the precatalyst is actually converted into the catalytically active species under the current conditions and that the employed catalyst loading would otherwise be sufficient if a more controlled reduction process could be achieved.

Further optimization of the current system, including alternatives to activation with zinc, may still be possible. However, the pronounced variability in reaction performance and the incomplete conversions observed across a broad range of conditions suggest that intrinsic limitations of the present catalytic system are likely causing the issues. Consequently, the direct use of isolable, well-

defined nickel(I) precatalysts may represent a promising alternative to the currently employed *in situ* reduction strategy.

In recent years, the library of reported nickel(I) complexes, many of which exhibit considerable stability in the solid state, has steadily expanded.[227] The structural spectrum spans from halide-bridged nickel(I) dimer complexes[228, 229] over systems bearing redox-active ligands[230] to sources of "naked" nickel(I) in the form of cationic complexes with weakly coordinating counterions (Figure 19).[231]

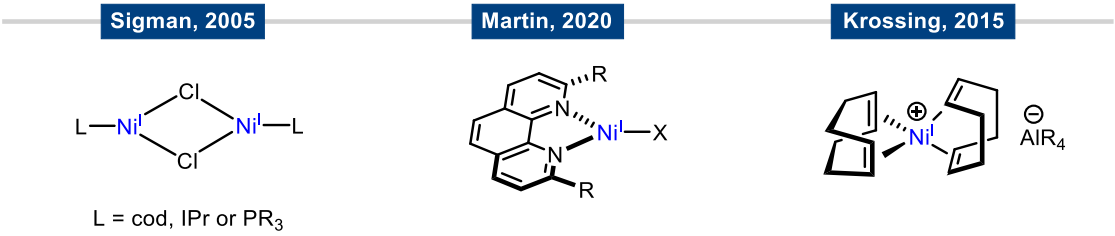

Figure 19: Selected examples of nickel(I) complexes.

Recently, Morandi *et al.* have reported a modular family of nickel(I) complexes bearing a sterically demanding phenolate ligand (Figure 20).[232, 233] These complexes can be conveniently accessed from $Ni(cod)_2$ and are accessible in various forms through ligand exchange with mono-, bi-, or tridentate donors. Importantly, they exhibit improved stability in solution compared to related systems and have already been successfully applied as well-defined alternatives to nickel(II)/zinc based catalytic systems in nickel(I/III) catalysis.[234]

The use of such well-defined nickel(I) precatalysts may therefore offer a promising strategy to overcome the challenges associated with sluggish *in situ* reduction of nickel(II) and the resulting ill-defined catalyst speciation in solution. Whether the resulting catalytically active species remain sufficiently stable after substrate coordination and throughout the catalytic cycle remains to be determined. Nevertheless, exploring such nickel(I) sources appears worthwhile.

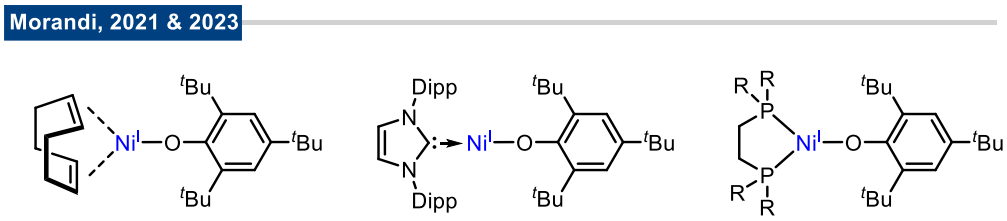

Figure 20: Representative examples from a modular family of nickel(I) complexes.

An alternative strategy may involve increasing the intrinsic reactivity of the coupling partners. While the sulfamide-derived imines employed in this study displayed encouraging reactivity, replacement of the imine with a more electrophilic aldehyde could potentially enhance the reaction rate. Consequently, the nucleophilic amine would have to be positioned adjacent to the aldehyde,[235] enabling cyclization through attack at the allyl fragment of the allyl-oxanickelacycle intermediate to afford six-membered heterocyclic products (Scheme 94).

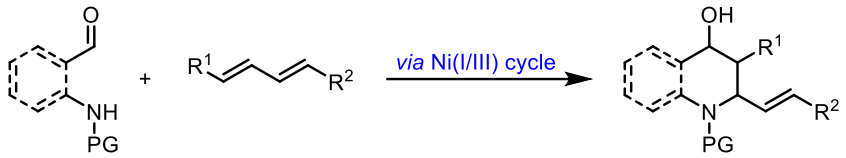

Scheme 94: Alternative substrate design for a redox-neutral cyclization reaction.

Furthermore, aldehydes are generally associated with broader substrate scope with regard to the diene component in related reductive coupling reactions. This consideration may be particularly relevant in the present case, as the employed silyl dienol ethers represent the least reactive class of dienes in intermolecular reductive coupling reactions (see Chapter 1.2.2). The use of an aldehyde substrate could therefore expand the range of viable coupling partners while simultaneously increasing the rate of productive turnover. The resulting increase in overall reaction rate may allow the tandem reaction to outcompete catalyst deactivation pathways, ultimately enabling complete substrate conversion.

Overall, the results provide a proof-of-concept for a new redox-neutral transformation that grants diastereoselective access to cyclic sulfamide derivatives. Although significant challenges remain, several plausible strategies for further development have been identified. Addressing these limitations may not only transform the present reaction into a practical synthetic method but also provide further insight into the role of nickel(I/III) catalysis in diene coupling chemistry, which may be transferable to related transformations. Furthermore, successful resolution of these challenges may ultimately reopen the possibility of pursuing an asymmetric variant of the transformation.

5 Experimental Section

5.1 General Information

Unless stated otherwise, all reactions were carried out under argon atmosphere in flame-dried Schlenk glassware.

Solvents were purified by distillation over the indicated drying agents under argon: toluene ($NaAlEt_4$), THF (Mg/anthracene), Et_2O (Mg/anthracene), *tert*-butyl methyl ether (CaH_2), pentane (Na/K), CH_2Cl_2 (CaH_2), $CHCl_3$ ($CaCl_2$), methanol (Mg). DMF and NEt_3 were dried by an absorption solvent purification system based on molecular sieves. *tert*-Butanol was dried over 3 Å molecular sieves. Dry benzyl alcohol was purchased from Sigma Aldrich and used as received. Degassed water was prepared *via* three freeze-pump-thaw cycles.

Flash chromatography: Merck silica gel 60 (40-63 µm or 15-40 µm). Thin layer chromatography (TLC): Macherey-Nagel precoated plates (POLYGRAM®SIL/UV254); visualization by UV light (254 nm) or by staining with solutions of *p*-anisaldeyhde, ninhydrin, ceric ammonium nitrate, or $KMnO_4$.

NMR: Spectra were recorded on Bruker Avance III 300, 400 MHz or Avance Neo 600 MHz (equipped with a Bruker BBO CryoProbe) NMR spectrometers in the solvents indicated; chemical shifts are given in ppm relative to TMS, coupling constants (J) in Hz. The solvent signals were used as references and the chemical shifts converted to the TMS scale ($CDCl_3$: δ_C = 77.16 ppm; residual $CHCl_3$ in $CDCl_3$: δ_H = 7.26 ppm; [D_6]-DMSO: δ_C = 39.52 ppm; residual D_2HSOCD_3 in [D_6]-DMSO: δ_H = 2.50 ppm; CD_2Cl_2: δ_C = 53.84 ppm; residual $CDHCl_2$ in CD_2Cl_2: δ_H = 5.32 ppm; residual CHD_2OD in CD_3OD: δ_H = 3.31 ppm; CD_3OD: δ_C = 49.0 ppm). All spectra were recorded at 298 K unless stated otherwise. Peak multiplicities are indicated by the following abbreviations: s: singlet, d: doublet, t: triplet, q: quartet, p: pentet, h: hextet, hept: heptet, m: multiplet, dd: double doublet, dt: double triplet, and so on; "br" indicates a broad peak, where the width is large enough to eclipse small coupling constants, which might otherwise be expected.

IR: Spectra were recorded on an Alpha Platinum ATR instrument (Bruker); wavenumbers ($\tilde{\nu}$) are reported in cm^{-1}.

MS (EI): Finnigan MAT 8200 (70 eV), ESI-MS: ESQ3000 (Bruker), Thermo Scientific LTQ-FT, or Thermo Scientific Exactive. HRMS: Bruker APEX III FT-MS (7T magnet), MAT 95 (Finnigan), Thermo Scientific LTQ-FT, or Thermo Scientific Exactive. GC-MS: Shimadzu GCMS-QP2010 Ultra instrument, GC-MS (CI): Q Exactive GC Orbitrap.

HPLC analyses for the determination of the enantiomeric excess (ee) of the individual compounds were conducted on a Shimadzu LC 20 instrument equipped with a Shimadzu SPD-M20A UV/VIS detector, or on a Shimadzu LC 40xR instrument equipped with a Shimadzu SPD-40 UV/VIS detector. Solvents (HPLC grade) were purchased and used as received. The exact conditions are specified for each compound.

Optical rotations were measured with an A-Krüss Otronic Model P8000-t polarimeter at a wavelength of 589 nm. The values are given as specific optical rotation with exact temperature, concentration (c (10 mg/mL)) and solvent.

Melting points were determined using a BÜCHI B-540 melting point apparatus.

Aldehydes were purchased from commercial suppliers with the exception of TBDPS- and PMP-protected 2-hydroxyacetaldehyde, which were prepared following literature procedures.[236, 237] Liquid aldehydes were distilled and degassed before use, solid aldehydes were recrystallized depending on the purity which was determined by ^{1}H NMR. (*E*,*E*)-Muconic acid was purchased from Fisher Scientific or BLDpharm, (Ni($^{t\text{Bu}}$stb)$_3$) was purchased from STREM chemicals. The ligand precursor VAPOL[93] and the phosphoramidite ligand **L11**[90] were prepared following previously established synthetic routes. Triethylborane solutions were prepared from neat triethylborane and the respective solvent. Unless stated otherwise, all other commercially available compounds (TCI Chemicals, Fisher Scientific, Sigma Aldrich, abcr, BLDpharm) were used as received.

5.2 Preparation of Precursors, Substrates and Ligands

(*E*,*E*)-Dimethyl muconate 86. HCl (4 M in dioxane, 19.0 mL, 67.8 mmol) was added to a stirred suspension of (*E,E*)-muconic acid (2.41 g, 17.0 mmol) in methanol (60 mL). The suspension was stirred at room temperature for 48 h. The white precipitate was filtered off and dissolved in ethyl acetate (400 mL). The solution was washed with sat. aq. $NaHCO_3$ (150 mL) and brine (150 mL). The organic layer was separated, dried over $MgSO_4$ and filtered. The solvent was removed *in vacuo* and to give the title compound as a colorless crystalline solid (2.70 g, 94%). ^{1}H NMR (400 MHz, $CDCl_3$): δ = 7.38 – 7.27 (m, 1H), 6.27 – 6.12 (m, 1H), 3.78 (s, 3H). ^{1}H NMR data matched those reported in the literature.[238]

Carboxylic acid 87. A solution of KOH (977 mg, 17.4 mmol) in methanol (9 mL) and water (3 mL) was added dropwise over 2 h to a solution of dimethyl ester **86** (2.51 g, 14.8 mmol) in methanol (150 mL) at 60 °C (bath temperature). Once the addition was complete, stirring was continued for another 2 h at 60 °C. The solvent was evaporated and the residue was dissolved in sat. aq. $NaHCO_3$ (100 mL). The aqueous layer was washed with ethyl acetate (3 x 50 mL) before it was acidified with HCl (6 M) until the product precipitated. Ethyl acetate (100 mL) was added until the precipitate was fully dissolved, the organic layer was separated and the aqueous phase extracted with ethyl acetate (100 mL). The combined organic layers were dried over $MgSO_4$, and filtered, and the solvent was removed *in vacuo*. The crude material was purified by recrystallization from *iso*-hexane/ethyl acetate to give the title compound as a crystalline colorless solid (1.35 g, 58%). mp: 162-163 °C; ^{1}H NMR (400 MHz, CD_2Cl_2): δ = 7.49 – 7.24 (m, 2H), 6.24 (td, *J* = 14.8, 1.2 Hz, 2H), 3.76 (s, 3H); ^{13}C NMR (101 MHz, CD_2Cl_2): δ = 170.6, 166.4, 143.4, 140.8, 129.4, 127.6, 52.3; IR (ATR): $\tilde{\nu}$ = 2845, 1724, 1668, 1643, 1428, 1309, 1226, 1171, 1139, 997, 856, 692, 566 cm^{-1}; HRMS (ESI$^-$): *m/z*: calcd. for $C_7H_7O_4$ [M-H]$^-$: 155.03498, found: 155.03509.

Diene 88a. A flame dried Schlenk flask was charged with carboxylic acid **87** (1.24 g, 7.94 mmol) and $SOCl_2$ (5.75 mL, 79.4 mmol) and the resulting mixture was stirred at 60 °C (bath temperature) for 3 h. The excess $SOCl_2$ was removed *in vacuo* to leave the acid chloride as a colorless solid, which was directly used in the next step.

This crude material was dissolved in toluene (18 mL) and a solution of NaN_3 (1.55 g, 23.8 mmol) and tetrabutylammonium bromide (128 mg, 0.40 mmol) in water (18 mL) was added. The mixture was vigorously stirred for 30 min at room temperature. The organic phase was separated and the aqueous layer was extracted with toluene (3 x 15 mL). The combined organic phases were washed with sat. aq. $NaHCO_3$ (20 mL) and brine (20 mL) and were then dried over $MgSO_4$ and filtered.

The volume of the solution was reduced to ca. 20 mL (***Note***: *do not dry completely*!). Dry *tert*-butanol (7.60 mL, 79.4 mmol) was added and the mixture stirred at 100 °C (bath temperature) for 2 h. The solvent was evaporated and the residue was purified by flash chromatography (SiO_2, *iso*-hexane/ethyl acetate, 4:1) to give title compound as a pale yellow solid (1.62 g, 90%). mp = 116-117 °C; ^{1}H NMR (400 MHz, CD_2Cl_2): δ = 7.28 (dd, *J* = 15.2, 11.4 Hz, 1H), 7.06 (t, *J* = 12.6 Hz, 1H), 6.80 (br, 1H), 5.78 (t, *J* = 12.6 Hz, 1H), 5.70 (dd, *J* = 15.2, 0.7 Hz, 1H), 3.68 (s, 3H), 1.47 (s,

9H); ^{13}C NMR (101 MHz, CD_2Cl_2): δ = 168.1, 152.3, 144.5, 135.6, 116.1, 107.8, 82.0, 51.5, 28.3; IR (ATR): $\tilde{\nu}$ = 3312, 2972, 1720, 1709, 1637, 1611, 1498, 1258, 1234, 1133, 992, 860, 681 cm^{-1}; HRMS (EI): *m/z*: calcd. for $C_{11}H_{17}NO_4$ [M]$^{+\cdot}$: 227.11521, found: 227.11478.

Diene 88b. A flame dried Schlenk flask was charged with carboxylic acid **87** (250 mg, 1.60 mmol)

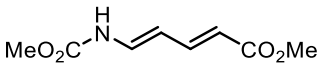

and $SOCl_2$ (1.20 mL, 16.5 mmol) and the resulting mixture stirred at 60 °C (bath temperature) for 3 h. The excess $SOCl_2$ was removed *in vacuo* to leave the acid chloride as a colorless solid, which was directly used in the next step.

This crude material was dissolved in toluene (5 mL) and a solution of NaN_3 (312 mg, 4.80 mmol) and tetrabutylammonium bromide (25.8 mg, 0.08 mmol) in water (5 mL) was added. The mixture was vigorously stirred for 30 min at room temperature. The organic phase was separated and the aqueous layer was extracted with toluene (3 x 10 mL). The combined organic phases were washed with sat. aq. $NaHCO_3$ (10 mL) and brine (10 mL), dried over $MgSO_4$ and filtered.

The volume of the solution was reduced to ca. 10 mL (***Note***: *do not dry completely*!). Dry methanol (2.60 mL, 64.2 mmol) was added and the mixture was stirred at 100 °C (bath temperature) for 2 h. The solvent was evaporated and the crude product was purified by flash chromatography (SiO_2, *iso*-hexane/ethyl acetate, 2:1 → 1:1) to give the title compound as a colorless solid (267 mg, 90%). mp = 169-171 °C; ^{1}H NMR (400 MHz, [D_6]-DMSO): δ = 10.09 (s, 1H), 7.32 (dd, *J* = 15.2, 11.5 Hz, 1H), 7.17 (dd, *J* = 13.7, 10.6 Hz, 1H), 5.89 (t, *J* = 12.7 Hz, 1H), 5.73 (d, *J* = 15.2 Hz, 1H), 3.67 (s, 3H), 3.62 (s, 3H); ^{13}C NMR (101 MHz, [D_6]-DMSO): δ = 167.0, 153.9, 145.0, 136.9, 114.7, 108.0, 52.5, 50.9; IR (ATR): $\tilde{\nu}$ = 3225, 1728, 1680, 1625, 1513, 1434, 1231, 1169, 1014, 737, 603 cm^{-1}; HRMS (EI): *m/z*: calcd. for $C_8H_{11}NO_4$ [M]$^{+\cdot}$: 185.06826, found: 185.06858.

Diene 88c. A flame dried Schlenk flask was charged with carboxylic acid **87** (782 mg, 5.01 mmol)

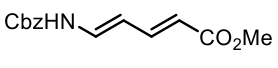

and $SOCl_2$ (3.63 mL, 50.1 mmol) and the resulting mixture was stirred at 60 °C (bath temperature) for 3 h. The excess $SOCl_2$ was removed *in vacuo* to leave the acid chloride as a colorless solid, which was directly used in the next step.

This crude material was dissolved in toluene (12 mL) and a solution of NaN_3 (979 mg, 15.1 mmol) and tetrabutylammonium bromide (83.0 mg, 0.26 mmol) in water (12 mL) was added. The mixture was vigorously stirred for 30 min at room temperature. The organic phase was separated and the aqueous layer was extracted with toluene (3 x 10 mL). The combined organic phases were washed with sat. aq. $NaHCO_3$ (15 mL) and brine (15 mL) and were then dried over $MgSO_4$ and filtered.

The volume of the solution was reduced to ca. 15 mL (***Note***: *do not dry completely*!). Dry benzyl alcohol (1.56 mL, 15.0 mmol) was added and the mixture stirred at 100 °C (bath temperature) for 3 h. The solvent was evaporated and the residue purified by recrystallization from *iso*-hexane/ethyl acetate to give title compound as colorless needles (1.12 g, 86%). mp = 132-133 °C, ^{1}H NMR (400 MHz, CD_2Cl_2): δ = 7.39 – 7.32 (m, 5H), 7.28 (dd, *J* = 15.2, 11.3 Hz, 1H), 7.12 – 7.06 (m, 1H), 7.00 (br, 1H), 5.84 (t, *J* = 12.6 Hz, 1H), 5.73 (dt, *J* = 15.2, 0.7 Hz, 1H), 5.18 (s, 2H), 3.69 (s, 3H); ^{13}C NMR (101 MHz, CD_2Cl_2): δ = 167.9, 153.3, 143.9, 136.1, 134.8, 129.0, 128.9, 128.6, 117.0, 109.0,

68.2, 51.6; IR (ATR): $\tilde{\nu}$ = 3264, 1729, 1696, 1636, 1611, 1521, 1256, 1217, 1148, 993, 694 cm^{-1}; HRMS (EI): *m/z*: calcd. for $C_{14}H_{15}NO_4$ $[M]^{+\cdot}$: 261.09956, found: 261.09958.

Diene 88d. A flame dried Schlenk flask was charged with carboxylic acid **87** (1.20 g, 7.69 mmol) and $SOCl_2$ (5.58 mL, 76.9 mmol) and the mixture stirred at 60 °C (bath temperature) for 3 h. The excess $SOCl_2$ was removed *in vacuo* to leave the acid chloride as a colorless solid, which was directly used in the next step.

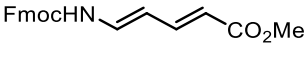

This crude material was dissolved in toluene (18 mL) and a solution of NaN_3 (1.50 g, 23.1 mmol) and tetrabutylammonium bromide (124 mg, 0.38 mmol) in water (18 mL) was added. The mixture was vigorously stirred for 30 min at room temperature. The organic phase was separated and the aqueous layer was extracted with toluene (3 x 15 mL). The combined organic phases were washed with sat. aq. $NaHCO_3$ solution (20 mL) and brine (20 mL) and were then dried over $MgSO_4$ and filtered.

The volume of the solution was reduced to ca. 20 mL (***Note***: *do not dry completely*!). 9-Fluorenylmethanol (1.37 g, 6.99 mmol) was added and the mixture was stirred at 100 °C (bath temperature) for 2 h. The solvent was evaporated and the residue was purified by recrystallization from toluene to give the title compound as a pale yellow solid (2.02 g, 83%). mp = 177-178 °C, ^{1}H NMR (400 MHz, CD_2Cl_2): δ = 7.79 (dt, *J* = 7.6, 1.0 Hz, 2H), 7.60 (dd, *J* = 7.5, 1.0 Hz, 2H), 7.42 (tt, *J* = 7.4, 1.0 Hz, 2H), 7.33 (td, *J* = 7.5, 1.2 Hz, 2H), 7.27 (dd, *J* = 14.9, 11.1 Hz, 1H), 7.06 (t, *J* = 12.5 Hz, 1H), 6.93 (br, 1H), 5.83 (t, *J* = 12.5 Hz, 1H), 5.74 (dt, *J* = 15.2, 0.7 Hz, 1H), 4.52 (d, *J* = 6.6 Hz, 2H), 4.26 (t, *J* = 6.6 Hz, 1H), 3.69 (s, 3H); ^{13}C NMR (101 MHz, CD_2Cl_2): δ = 167.9, 153.2, 144.0, 143.9, 141.7, 134.6, 128.2, 127.5, 125.3, 120.4, 117.1, 109.1, 67.9, 51.6, 47.4; IR (ATR): $\tilde{\nu}$ = 3295, 1710, 1645, 1620, 1520, 1448, 1264, 1144, 986, 736 cm^{-1}; HRMS (ESI$^+$): *m/z*: calcd. for $C_{21}H_{19}NO_4Na$ $[M+Na]^+$: 372.12063, found: 372.12064.

Diene 127a. In a flame dried Schlenk flask, sodium hydride (41.2 mg, 1.72 mmol) was suspended in THF (10 mL). A solution of diene **88a** (300 mg, 1.32 mmol) in THF (5 mL) was added dropwise at 0 °C, causing a color change to intense yellow. Methyl iodide (0.41 mL, 6.60 mmol) was added and the mixture was allowed to warm to room temperature and stirred for 1 h. The mixture was diluted with ethyl acetate (10 mL) and the reaction carefully quenched with sat. aq. $NaHCO_3$ solution (5 mL). The aqueous phase was extracted with ethyl acetate (3 x 10 mL). The combined organic phases were washed with brine (15 mL), dried over $MgSO_4$, and filtered, and the solvent was removed under reduced pressure to furnish the title compound as a yellow oil (308 mg, 97%). ^{1}H NMR (600 MHz, CD_2Cl_2): δ = 7.54 (d, *J* = 14.0 Hz, 1H), 7.34 (ddd, *J* = 15.1, 11.2, 0.7 Hz, 1H), 5.74 (d, *J* = 15.1 Hz, 1H), 5.62 (dd, *J* = 13.8, 11.3 Hz, 1H), 3.68 (s, 3H), 3.06 (s, 3H), 1.50 (s, 9H); ^{13}C NMR (151 MHz, CD_2Cl_2): δ = 168.1, 152.6, 145.3, 139.9, 115.8, 106.4, 82.7, 51.4, 31.1, 28.2; ***Note:*** *the signals at 152.6 ppm and 31.1 ppm have very low intensity.* IR (ATR): $\tilde{\nu}$ = 2978, 1707, 1618, 1432, 1370, 1321, 1239, 1121, 1051, 991, 860 cm^{-1}; HRMS (EI): *m/z*: calcd. for $C_{12}H_{19}NO_4$ $[M]^{+\cdot}$: 241.13086, found: 241.13086.

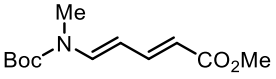

Diene 127b. In a flame dried Schlenk flask, sodium hydride (37.0 mg, 1.54 mmol) was suspended 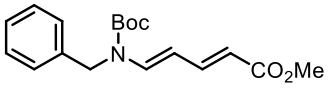 in THF (10 mL). A solution of diene **88a** (250 mg, 1.10 mmol) in THF (5 mL) was added dropwise at 0 °C, causing a color change to intense yellow. Benzyl bromide (0.26 mL, 2.20 mmol) was added and stirring continued at room temperature for 24 h. The mixture was diluted with ethyl acetate (10 mL) and the reaction carefully quenched with sat. aq. $NaHCO_3$ solution (5 mL). The organic phase was separated and the aqueous layer extracted with ethyl acetate (3 x 10 mL). The combined organic phases were washed with brine (15 mL), dried over $MgSO_4$, and filtered, and the solvent was removed under reduced pressure. The residue was purified by flash chromatography (*n*-pentane/ethyl acetate, 10:1 → 1:1) to give the product as a pale yellow solid (297 mg, 85%). mp = 94-96 °C; ^{1}H NMR (400 MHz, CD_2Cl_2): δ = 7.58 (d, *J* = 14.1 Hz, 1H), 7.36 – 7.24 (m, 4H), 7.20 – 7.17 (m, 2H), 5.63 (d, *J* = 15.1 Hz, 1H) 5.59 (t, *J* = 13.2 Hz, 1H) , 4.78 (s, 2H), 3.66 (s, 3H), 1.50 (s, 9H); ^{13}C NMR (151 MHz, CD_2Cl_2): δ = 168.0, 152.9, 145.0, 138.9, 137.2, 129.0, 127.6, 126.7, 116.1, 107.4, 83.2, 51.5, 48.0, 28.2; IR (ATR): $\tilde{\nu}$ = 1711, 1622, 1386, 1240, 1133 cm^{-1}; HRMS (EI): *m/z*: calcd. for $C_{18}H_{23}NO_4$ $[M]^{+\cdot}$: 317.16216, found: 317.16173.

Diene 128a. Trimethyl-aluminum (2.0 M in hexane, 1.45 mL, 2.90 mmol) was added dropwise to 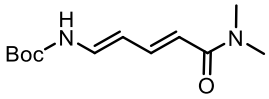 a solution of dimethylamine hydrochloride (236 mg, 2.90 mmol) in dichloromethane (5 mL) at 0 °C (***Caution***: CH_4 formation!). The mixture was allowed to warm to room temperature and stirred for 30 min. A solution of diene **88a** (219 mg, 0.96 mmol) in dichloromethane (5 mL) was added and the resulting orange mixture was stirred at room temperature for 48 h.

The mixture was cooled to 0 °C before the reaction was carefully quenched by dropwise addition of sat. aq. NH_4Cl solution (10 mL) followed by sat. aq. Rochelle's salt solution (15 mL). The mixture was diluted with dichloromethane (20 mL) and vigorously stirred for 1 h. The organic phase was separated and the aqueous layer extracted with dichloromethane (3 x 30 mL). The combined organic phases were washed with water (30 mL), dried over $MgSO_4$, and filtered, and the solvent was removed under reduced pressure. The residue was purified by flash chromatography (*n*-pentane/ethyl acetate, 1:1 → ethyl acetate) to furnish the title compound as a pale yellow solid (102 mg, 44%). mp = 199-201 °C, ^{1}H NMR (400 MHz, $CDCl_3$): δ = 7.28 (dd, *J* = 14.6, 11.4 Hz, 1H), 6.99 (t, *J* = 12.2 Hz, 1H), 6.69 (br, 1H), 6.15 (d, *J* = 14.6 Hz, 1H), 5.79 (t, *J* = 11.8 Hz, 1H), 3.03 (s, 6H), 1.47 (s, 9H); ^{13}C NMR (101 MHz, $CDCl_3$): δ = 167.3, 152.1, 141.7, 133.5, 115.9, 108.5, 81.6, 36.5, 28.3; IR (ATR): $\tilde{\nu}$ = 3203, 2979, 1725, 1646, 1504, 1255, 1158, 1124 cm^{-1}; HRMS (EI): *m/z*: calcd. for $C_{12}H_{20}N_2O_3$ $[M]^{+\cdot}$: 240.14684, found: 240.14684.

Diene 128b. Trimethyl aluminum (2.0 M in hexane, 1.65 mL, 3.30 mmol) was added dropwise to 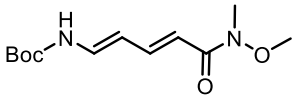 a solution of *N*,*O*-dimethylhydroxylamine hydrochloride (322 mg, 3.30 mmol) in anhydrous dichloromethane (6 mL) at 0 °C (***Caution***: CH_4 formation!). The mixture was warmed to room temperature and stirred for 30 min. A solution of diene **88a** (250 mg, 1.10 mmol) in dichloromethane (6 mL) was added and the resulting yellow solution was stirred at room temperature for 48 h. The mixture was

cooled to 0 °C before the reaction was carefully quenched by dropwise addition of sat. aq. NH_4Cl solution (10 mL), followed by the addition of sat. aq. Rochelle's salt solution (15 mL). The mixture was diluted with dichloromethane (20 mL) and vigorously stirred for 1 h. The organic layer was separated and the aqueous phase extracted with dichloromethane (3 x 30 mL). The combined organic phases were washed with water (30 mL), dried over $MgSO_4$, and filtered, and the solvent was removed under reduced pressure. The residue was purified by flash chromatography (*n*-pentane/*tert*-butyl methyl ether, 3:1 + 1% NEt_3 → 1:3 + 1% NEt_3) to give the title compound as a colorless solid (215 mg, 76%). mp = 178-180 °C, ^{1}H NMR (400 MHz, CD_2Cl_2): δ = 7.27 (ddd, *J* = 15.0, 11.4, 0.7 Hz, 1H), 7.05 (dd, *J* = 13.8, 11.5 Hz, 1H), 6.84 (br, 1H), 6.31 (d, *J* = 15.0 Hz, 1H), 5.85 (t, *J* = 12.7 Hz, 1H), 3.68 (s, 3H), 3.19 (s, 3H), 1.47 (s, 9H); ^{13}C NMR (101 MHz, CD_2Cl_2): δ = 167.9, 152.3, 142.6, 134.7, 114.8, 108.6, 81.8, 62.0, 32.6, 28.3; IR (ATR): $\tilde{\nu}$ = 3241, 2976, 1726, 1648, 1586, 1503, 1251, 1147, 1090, 999 cm^{-1}; HRMS (ESI$^+$): *m/z*: calcd. for $C_{12}H_{20}N_2O_4Na$ [M+Na]$^+$: 279.13153, found: 279.13157.

Diene 133. *m*-Chloroperoxybenzoic acid (297 mg, 1.32 mmol) was added to a solution of *tert*-butyl ((1*E*,3*E*)-4-(phenylthio)buta-1,3-dien-1-yl)carbamate[150] (175 mg, 0.63 mmol) in dichloromethane (15 mL) at –15 °C. The resulting solution was allowed to warm to room temperature and was stirred for 2 h. The mixture was diluted with sat. aq. $NaHCO_3$ solution (10 mL), was allowed to warm to room temperature and was vigorously stirred for 10 min. The organic phase was separated and the aqueous phase was extracted with dichloromethane (3 x 15 mL). The combined organic phases were washed with brine (15 mL), dried over $MgSO_4$, and filtered, and the solvent was removed under reduced pressure. The crude product was purified by flash chromatography (SiO_2, *n*-pentane/ethyl acetate, 4:1 + 1% NEt_3 → 2.5:1 + 1% NEt_3) and the obtained solid was obtained as an off-white solid (111 mg, 57%). ^{1}H NMR (400 MHz, CD_2Cl_2): δ = 7.84 (d, *J* = 7.7 Hz, 2H), 7.56 (dt, *J* = 28.4, 7.6 Hz, 3H), 7.37 – 7.05 (m, 2H), 6.83 (d, *J* = 11.9 Hz, 1H), 6.14 (d, *J* = 14.6 Hz, 1H), 5.70 (t, *J* = 12.5 Hz, 1H), 1.47 (s, 9H); ^{13}C NMR (101 MHz, CD_2Cl_2): δ = 151.9, 142.8, 142.3, 137.7, 133.3, 129.6, 127.5, 124.4, 105.3, 82.5, 28.2; IR (ATR): $\tilde{\nu}$ = 3308, 1731, 1637, 1497, 1301, 1234, 1136, 1083, 835 cm^{-1}, HRMS (ESI$^+$): *m/z*: calcd. for $C_{15}H_{19}NO_4SNa$ [M+Na]$^+$: 332.09270, found: 332.09278.

Aldehyde 136. A flame dried Schlenk flask under argon was charged with DMF (4 mL). $POCl_3$ (0.46 mL, 4.91 mmol) was added dropwise at 0 °C before the resulting mixture was allowed to warm to room temperature. N-Vinyl-phtalimide (500 mg, 2.89 mmol) in DMF (2 mL) was added and the resulting solution was stirred at 70 °C (bath temperature) for 3 h. The mixture was cooled to 0 °C for 2 h, causing the precipitation of a yellow solid. The solvent was decanted and the residual solid was washed with cold chloroform (3 x 1 mL). The obtained pale-yellow solid was dried *in vacuo* before it was used in the next step.

A solution of sodium acetate (31.3 mg, 0.38 mmol) in water (2 mL) was added to the solid material and the resulting mixture was stirred at 50 °C (bath temperature) for 1 h. After cooling to room

temperature, chloroform (10 mL) was added to the suspension and the mixture was stirred until a clear two-phase system had formed. The organic layer was separated and washed with water (2 mL), dried over $MgSO_4$ and filtered. The solvent was removed under reduced pressure to afford a pale-yellow solid, which was purified by flash chromatography (SiO_2, toluene/*tert*-butyl methyl ether, 10:1) to give the title compound as an off-white solid (169 mg, 29%). mp = 151-152 °C, ^{1}H NMR (400 MHz, $CDCl_3$): δ = 9.61 (d, *J* = 7.9 Hz, 1H), 8.01 – 7.96 (m, 2H), 7.88 – 7.84 (m, 2H), 7.72 (d, *J* = 14.8 Hz, 1H), 7.22 (dd, *J* = 14.8, 7.9 Hz, 1H); ^{13}C NMR (101 MHz, $CDCl_3$): δ = 193.1, 165.1, 138.2, 135.7, 131.5, 124.7, 119.0; IR (ATR): $\tilde{\nu}$ = 1728, 1676, 1629, 1364, 1139, 1065, 976, 715 cm^{-1}; HRMS (ESI$^+$): *m/z*: calcd. for $C_{11}H_7NO_3Na$ [M+Na]$^+$: 224.03181, found: 224.03188.

Diene 138. A flame dried Schlenk flask was charged with sodium hydride (25.5 mg, 1.06 mmol) and THF (1 mL). The suspension was cooled to 0 °C and triethyl phosphonoacetate (0.23 mL, 1.16 mmol) was added dropwise. After stirring at 0 °C for 10 min, a solution of aldehyde **136** (120 mg, 0.60 mmol) in THF (3 mL) was added dropwise, causing an immediate color change to yellow. Upon complete addition of the aldehyde, the mixture was allowed to warm to room temperature and stirring was continued for 18 h. The mixture was diluted with *tert*-butyl methyl ether (20 mL) and the reaction quenched upon addition of sat. aq. NH_4Cl (20 mL). The aqueous layer was extracted with *tert*-butyl methyl ether (2 x 30 mL). The combined organic phases were washed with brine (20 mL), dried over $MgSO_4$, and filtered, and the solvent was removed under reduced pressure. The residue was purified by flash chromatography (SiO_2, *iso*-hexane/ethyl acetate, 3:1 → 2:1) to furnish the title compound as a neon yellow solid (119 mg, 73%). mp = 149-150 °C, ^{1}H NMR (400 MHz, $CDCl_3$): δ = 7.95 – 7.88 (m, 2H), 7.81 – 7.76 (m, 2H), 7.43 – 7.31 (m, 2H), 7.23 – 7.15 (m, 1H), 6.07 – 5.99 (m, 1H), 4.23 (q, *J* = 7.1 Hz, 2H), 1.31 (t, *J* = 7.1 Hz, 3H); ^{13}C NMR (101 MHz, $CDCl_3$): δ = 167.0, 165.9, 143.3, 135.1, 131.7, 126.4, 124.1, 121.9, 117.5, 60.5, 14.5; IR (ATR): $\tilde{\nu}$ = 1717, 1698, 1622, 1367, 1203, 1130, 1075, 1015, 866, 711 cm^{-1}; HRMS (EI): *m/z*: calcd. for $C_{15}H_{13}NO_4$ [M]$^{+\cdot}$: 271.08391, found: 271.08422.

***tert*-Butyl formylcarbamate 143.**[151] A flame dried pressure Schlenk was charged with *tert*-butyl carbamate (4.11 g, 35.1 mmol), toluene (35 mL) and dimethylformamide dimethylacetal (14.0 mL, 105 mmol). The mixture was stirred at 90 °C (bath temperature) for 3 h. After cooling to room temperature, the solvent was removed under reduced pressure to give a pale yellow oil, which solidified on standing. The solid was dissolved in water (6 mL) and acetic acid (17 mL) and the mixture stirred at room temperature overnight. The mixture was diluted with *tert*-butyl methyl ether (50 mL), washed with water (6 x 25 mL) and brine (25 mL), dried over $MgSO_4$, and concentrated under reduced pressure. The obtained colorless oil was re-dissolved in the minimum amount of *n*-heptane (20 mL), which was then evaporated to give *tert*-butyl formylcarbamate as a colorless solid (4.55 g, 89%). ^{1}H NMR (400 MHz, $CDCl_3$): δ = 8.91 (d, J = 10.4 Hz, 1H), 7.30 (br, 1H), 1.53 (s, 9H). ^{1}H NMR data matched those reported in the literature.[151]

Wittig Reagent 144. A flame dried Schlenk flask was charged with triphenylphosphine (5.36 g, 20.4 mmol), toluene (30 mL) and methyl-*trans*-4-brom-2-butenoate (3.13 g, 18.5 mmol). The solution was stirred at room temperature for 24 h leading to the precipitation of a white solid. The solid was filtered off, washed with *tert*-butyl methyl ether (100 mL) and dried in air for 1 h. The solid was finely ground to give a powder that was further dried *in vacuo* to yield the corresponding triphenylphosphonium bromide (8.16 g, quant.).

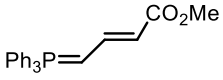

This compound was suspended in water (800 mL) and NaOH (1 M, 18.6 mL, 18.6 mmol) was added dropwise, causing the formation of a yellow-orange precipitate. After stirring the suspension at room temperature for 20 min, the solid was filtered off and dissolved in dichloromethane (150 mL). The organic phase was washed with brine (50 mL), dried over $MgSO_4$, filtered and the solvent was removed under reduced pressure to afford the title compound as an orange solid, which was directly used in the next step (5.77 g, 87%).

Diene (*E,Z*)-88a. A flame dried pressure Schlenk flask was charged with *tert*-butyl formylcarbamate **143** (649 mg, 4.47 mmol), Wittig reagent **144** (4.84 g, 13.4 mmol), and chloroform (40 mL). The mixture was stirred at reflux temperature for 17 h. The solvent was removed under reduced pressure and the residue was purified by flash chromatography (SiO_2, *iso*-hexane/ethyl acetate, 7:1 + 1% NEt_3 → *iso*-hexane/ethyl acetate, 5:1 + 1% NEt_3) to afford the title compound as a colorless viscous oil (410 mg, 40%). ^{1}H NMR (400 MHz, CD_2Cl_2): δ = 7.56 – 7.49 (m, 1H), 7.29 (d, *J* = 11.3 Hz, 1H), 6.75 (t, *J* = 10.6 Hz, 1H), 5.81 (dt, *J* = 14.9, 0.8 Hz, 1H), 5.37 (t, *J* = 10.8 Hz, 1H), 3.71 (s, 3H), 1.47 (s, 9H); ^{13}C NMR (101 MHz, CD_2Cl_2): δ = 168.1, 152.4, 137.6, 130.8, 118.2, 104.3, 81.8, 51.8, 28.3; IR (ATR): $\tilde{\nu}$ = 3307, 2979, 1695, 1631, 1492, 1233, 1139, 1006, 857 cm^{-1}; HRMS (EI): *m/z*: calcd. for $C_{11}H_{17}NO_4$ $[M]^{+\cdot}$: 227.11521, found: 227.11501.

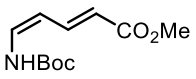

(*E,E*)-Dibenzyl muconate S1. Benzyl bromide (1.52 mL, 12.8 mmol) was added to a mixture of (*E,E*)-muconic acid (825 mg, 5.81 mmol), KOH (1.49 g, 26.6 mmol), and Bu_4NHSO_4 (4.34 g, 12.8 mmol) in dichloroethane (25 mL) and water (25 mL). The mixture was stirred at 50 °C (bath temperature) overnight. After cooling to room temperature, the organic phase was separated and the aqueous layer extracted with dichloromethane (3 x 50 mL). The combined organic phases were washed with water (100 mL), sat. aq. $NaHCO_3$ (100 mL) and brine (100 mL), and were then dried over $MgSO_4$. The solvent was removed under reduced pressure and the residue purified by flash chromatography (SiO_2, *iso*-hexane/ethyl acetate, 6:1) to give the title compound as a colorless solid (898 mg, 48%). mp = 103-104 °C; ^{1}H NMR (400 MHz, $CDCl_3$): δ = 7.40 – 7.30 (m, 12H), 6.29 – 6.20 (m, 2H), 5.22 (s, 4H); ^{13}C NMR (101 MHz, $CDCl_3$): δ = 165.8, 141.3, 135.7, 128.8, 128.6, 128.5, 128.4, 66.9; IR (ATR): $\tilde{\nu}$ = 1702, 1612, 1453, 1310, 1236, 1151, 1022, 859, 732, 692 cm^{-1}; HRMS (ESI$^+$): *m/z*: calcd. for $C_{20}H_{18}O_4Na$ $[M+Na]^+$: 345.10973, found: 345.10984.

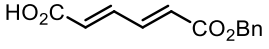

Carboxylic acid S2. A solution of KOH (138 mg, 2.46 mmol) in water (5 mL) was added dropwise over 5 h to a solution of compound **S1** (754 mg, 2.34 mmol) in THF (20 mL) at room temperature and the resulting mixture was stirred overnight. THF was removed

under reduced pressure and the remaining aqueous solution was diluted with sat. aq. $NaHCO_3$ (20 mL). The aqueous phase was washed with ethyl acetate (3 x 20 mL) before it was acidified with HCl (6 M) until a solid precipitated. Ethyl acetate (30 mL) was added until the precipitate was fully dissolved, the organic layer was separated and the aqueous phase extracted with ethyl acetate (100 mL). The organic phase was washed with brine (15 mL), dried over $MgSO_4$, and the solvent was removed under reduced pressure. The residue was purified by flash chromatography (SiO_2, *iso*-hexane/ethyl acetate 2:1 + 1% AcOH) to yield the title compound as a pale yellow solid (105 mg, 19%). ^{1}H NMR (400 MHz, $CDCl_3$): δ = 7.46 – 7.32 (m, 7H), 6.36 – 6.13 (m, 2H), 5.23 (s, 2H); ^{13}C NMR (101 MHz, $CDCl_3$): δ = 170.5, 165.7, 143.1, 140.9, 135.7, 129.2, 128.8, 128.6, 128.5, 127.6, 67.0; IR (ATR): $\tilde{\nu}$ = 2938, 1710, 1389, 1240, 1024, 989, 825, 608 cm^{-1}; HRMS (ESI$^-$): *m/z*: calcd. for $C_{13}H_{11}O_4$ [M-H]$^-$: 231.06629, found: 231.06634.

Diene S3. A flame dried Schlenk flask was charged with carboxylic acid **S2** (120 mg, 0.52 mmol) and $SOCl_2$ (1 mL, 13.8 mmol) and the resulting mixture was stirred at 60 °C (bath temperature) for 3 h. The excess $SOCl_2$ was removed *in vacuo* to leave the acid chloride as a colorless solid, which was directly used in the next step.

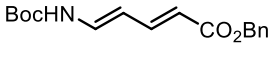

This crude material was dissolved in toluene (3 mL) and a solution of NaN_3 (101 mg, 1.55 mmol) and tetrabutylammonium bromide (8.3 mg, 0.03 mmol) in water (3 mL) was added. The mixture was vigorously stirred for 1 h at room temperature. The organic phase was separated and the aqueous phase was extracted with toluene (3 x 5 mL). The combined organic phases were washed with sat. aq. $NaHCO_3$ (5 mL) and brine (5 mL) and were then dried over $MgSO_4$.

The volume of the solution was reduced to ca. 3 mL (***Note***: *do not dry completely*!). Dry *tert*-butanol (1.00 mL, 10.7 mmol) was added and the mixture was stirred at 100 °C (bath temperature) for 2 h. The solvent was evaporated and the residue purified by flash chromatography (SiO_2, *iso*-hexane/ethyl acetate, 7:1) to give the title compound as an off-white solid (125 mg, 80%). ^{1}H NMR (400 MHz, CD_2Cl_2): δ = 7.37 – 7.30 (m, 6H), 7.08 (t, *J* = 12.7 Hz, 1H), 6.78 (d, *J* = 10.4 Hz, 1H), 5.81 – 5.73 (m, 2H), 5.15 (s, 2H), 1.47 (s, 9H); ^{13}C NMR (101 MHz, CD_2Cl_2): δ = 167.3, 152.2, 144.8, 137.1, 135.6, 128.9, 128.4, 128.4, 116.2, 107.8, 82.1, 66.1, 28.2; IR (ATR): $\tilde{\nu}$ = 3304, 1709, 1636, 1502, 1255, 1125, 998, 863 cm^{-1}; HRMS (ESI$^+$): *m/z*: calcd. for $C_{17}H_{21}NO_4Na$ [M+Na]$^+$: 326.13628, found: 326.13617.

Phosphoramidite ligand L17. An oven-dried pressure Schlenk flask was charged with (*R*)-7,7'-(*t*-Bu)$_2$-VANOL (200 mg, 0.36 mmol)[139] and toluene (2.0 mL). Tris(diethylamino)phosphine (111 μL, 0.40 mmol) was added and the mixture stirred at 110 °C (bath temperature) for 24 h. After cooling to room temperature, the solution was concentrated *in vacuo* and the residue was purified by flash chromatography (SiO_2, pentane/*tert*-butyl methyl ether 100:1 → 30:1) to give phosphoramidite **L17** as a colorless solid (215 mg, 91%). $[\alpha]_D^{20}$= +87.6 (c = 0.50, $CHCl_3$); ^{1}H NMR (400 MHz, C_6D_6): δ = 8.73 (d, *J* = 1.9 Hz, 1H), 8.63 (d, *J* = 2.0 Hz, 1H), 7.65 (d, *J* = 8.6 Hz, 1H), 7.60 (d, *J* = 8.7 Hz, 1H), 7.51 – 7.44 (m, 3H), 7.41 (s, 1H), 6.94 – 6.86 (m, 2H), 6.83 – 6.68 (m, 8H), 3.19 (ddq, *J* = 14.1, 9.5, 7.1 Hz, 2H), 2.87 (ddq,

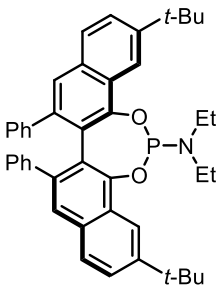

J = 14.0, 10.7, 7.0 Hz, 2H), 1.39 (d, *J* = 4.8 Hz, 18H), 0.88 (t, *J* = 7.0 Hz, 6H); ^{13}C NMR (101 MHz, C_6D_6): δ = 149.4, 149.0, 148.9, 148.8, 148.6, 141.4, 141.3, 140.9, 140.7, 133.3, 133.0, 129.7, 129.3, 128.4, 128.2, 127.42, 127.40, 127.3, 126.5, 126.4, 126.10, 126.07, 125.91, 125.86, 125.8, 124.5, 124.41, 124.38, 118.5, 117.6, 39.5, 39.3, 35.3, 35.2, 31.5, 31.3, 15.27, 15.25; ^{31}P NMR (162 MHz, C_6D_6): δ = 151.1; IR (ATR): $\tilde{\nu}$ = 2962, 2867, 2279, 1595, 1495, 1460, 1370, 1319, 1204, 1177, 1112, 1022, 929, 911, 824, 764 cm^{-1}; HRMS (CI): *m/z*: calcd. for $C_{44}H_{47}NO_2P$ $[M+H]^+$: 652.33389, found: 652.33408.

Compound S4. A 2-neck flask was charged with 4-bromo-2-methylbenzonitrile (1.37 g, 7.00 mmol), sodium benzenesulfonate (1.38 g, 8.40 mmol), tris(dibenzylidene-acetone)dipalladium(0) (160 mg, 0.18 mmol), XantPhos (203 mg, 0.35 mmol), caesium carbonate (3.42 g, 10.5 mmol) and toluene (40 mL). The mixture was stirred at reflux temperature overnight. The mixture was allowed to cool to room temperature before it was diluted with water (50 mL) and ethyl acetate (100 mL). The organic phase was separated, washed with water (50 mL) and brine (50 mL), dried over $MgSO_4$, and filtered, and the solvent was removed under reduced pressure. The residue was purified by flash chromatography (SiO_2, *n*-hexane/ethyl acetate, 4:1) to give the title compound as a red-brown solid (1.45 g, 80%). ^{1}H NMR (600 MHz, $CDCl_3$): δ = 7.97 – 7.93 (m, 2H), 7.90 (dt, *J* = 1.9, 0.7 Hz, 1H), 7.85 – 7.82 (m, 1H), 7.74 – 7.70 (m, 1H), 7.67 – 7.59 (m, 1H), 7.58 – 7.52 (m, 2H), 2.61 (s, 3H); ^{13}C NMR (151 MHz, $CDCl_3$): δ = 145.6, 143.8, 140.4, 134.1, 133.6, 129.7, 129.1, 128.1, 125.5, 117.5, 116.6, 20.8; IR (ATR): $\tilde{\nu}$ = 2230, 1447, 1323, 1288, 1155, 1095, 733 cm^{-1}; HRMS (EI): *m/z*: calcd. for $C_{14}H_{11}NO_2S$ $[M]^{+\cdot}$: 257.05050, found: 257.05052.

Compound S5. A flame-dried Schlenk flask was charged with compound **S4** (1.34 g, 5.20 mmol), N-bromosuccinimide (1.85 g, 10.4 mmol), benzoyl peroxide (420 mg (75 wt%), 1.30 mmol) and chloroform (8 mL). The mixture was stirred at reflux temperature overnight before it was allowed to cool to room temperature and all precipitates were filtered off. The solvent was removed under reduced pressure and the residue was purified by flash chromatography (SiO_2, *n*-hexane/ethyl acetate, 4:1) which also allowed for recovery of unconverted starting material. The title compound was obtained as a colorless solid (745 mg, 43% (93% brsm)). ^{1}H NMR (600 MHz, $CDCl_3$): δ = 8.13 (dd, *J* = 1.8, 0.5 Hz, 1H), 7.98 – 7.92 (m, 3H), 7.79 (dd, *J* = 8.1, 0.5 Hz, 1H), 7.67 – 7.61 (m, 1H), 7.58 – 7.53 (m, 2H), 4.64 (s, 2H); ^{13}C NMR (151 MHz, $CDCl_3$): δ = 146.5, 143.0, 140.0, 134.34, 134.32, 129.9, 129.3, 128.2, 127.9, 116.9, 115.5, 28.1; IR (ATR): $\tilde{\nu}$ = 2232, 1447, 1324, 1155, 1084, 722 cm^{-1}; HRMS (EI): *m/z*: calcd. for $C_{14}H_{10}NO_2BrS$ $[M]^{+\cdot}$: 334.96103, found: 334.96147.

Compound S6. A flame-dried Schlenk flask charged with 2-methyl-4-(4,4,5,5-tetramethyl-1,3,2-dioxaborolan-2-yl)benzonitrile (2.98 g, 11.1 mmol), N-bromo-succinimide (2.29 g, 12.9 mmol), benzoyl peroxide (152 mg (75wt%), 0.63 mmol), and chloroform (18 mL). The mixture was stirred at reflux temperature for 24 h before it was allowed to cool to room temperature and all precipitates were filtered off. The filtrate was washed with water (2 x 10 mL) and brine (10 mL), dried over $MgSO_4$,

and filtered, and the solvent was removed under reduced pressure. Recrystallization of the crude product from *n*-hexane/ethyl acetate gave the title compound as a pale yellow solid (2.02 g, 51%). ^{1}H NMR (600 MHz, $CDCl_3$): δ = 10.29 (s, 1H), 7.93 (dd, *J* = 7.5, 1.1 Hz, 1H), 7.88 – 7.86 (m, 1H), 7.83 (d, *J* = 7.5 Hz, 1H), 4.94 (s, 2H), 1.36 (s, 11H); ^{13}C NMR (151 MHz, $CDCl_3$): δ = 192.3, 138.2, 137.9, 135.5, 135.0, 132.7, 84.7, 29.7, 25.0 (the signal of C-Bpin was not detected); IR (ATR): $\tilde{\nu}$ = 2979, 2229, 1405, 1357, 1276, 1141, 965, 851 cm^{-1}; HRMS (EI): *m/z*: calcd. for $C_{14}H_{17}NO_2BrB$ $[M]^{+\cdot}$: 321.05303, found: 321.05330.

Compound S7. A flame-dried Schlenk flask was charged with 2-methyl-5-(trifluoromethoxy)-benzonitrile (1.00 g, 4.97mmol), N-bromosuccinimide (0.93 g, 5.23 mmol), benzoyl peroxide (122 mg (75wt%), 0.50 mmol) and chloroform (10 mL). The mixture was stirred at reflux temperature overnight before it was allowed to cool to room temperature and all precipitates were filtered off. The solvent was removed under reduced pressure and the residue was purified by flash chromatography (SiO_2, *n*-hexane/ethyl acetate, 99:1 → 97:3) to give the title compound as a colorless solid (712 mg, 51%). ^{1}H NMR (600 MHz, $CDCl_3$): δ = 7.62 (dd, *J* = 8.6, 0.5 Hz, 1H), 7.51 (dd, *J* = 2.5, 1.0 Hz, 1H), 7.45 (ddd, *J* = 8.6, 2.6, 1.0 Hz, 1H), 4.63 (s, 2H); ^{13}C NMR (151 MHz, $CDCl_3$): δ = 148.9 (q, *J* = 2.0 Hz), 140.0, 132.5, 125.9, 125.2, 120.3 (q, *J* = 259.8 Hz), 115.6, 114.2, 28.2; ^{19}F NMR (565 MHz, $CDCl_3$): δ = –58.1; IR (ATR): $\tilde{\nu}$ = 2235, 1611, 1581, 1496, 1254, 1215, 1173, 881, 613 cm^{-1}; HRMS (ESI^+): *m/z*: calcd. for $C_9H_5BrF_3NONa$ $[M+Na]^+$: 301.93988, found: 301.93960.

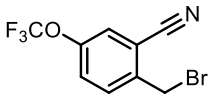

Compound S8. A flame-dried Schlenk flask was charged with 4-methylthiophene-3-carbonitrile (421 mg, 3.42 mmol), N-bromosuccinimide (639 mg, 3.59 mmol), benzoyl peroxide (82.9 mg (75wt%), 0.34 mmol) and chloroform (7 mL). The mixture was stirred at 85 °C (bath temperature) overnight before it was cooled to room temperature and all precipitates were filtered off. The solvent was removed under reduced pressure and the residue was purified by flash chromatography (SiO_2, *n*-hexane/ethyl acetate, 96:4 → 80:20). The resulting product was further purified by recrystallization from *n*-hexane/*tert*-butyl methyl ether to yield the title compound as a colorless solid (573 mg, 2.21 mmol, 65%). ^{1}H NMR (400 MHz, $CDCl_3$): δ = 7.95 (d, *J* = 3.1 Hz, 1H), 7.44 (dt, *J* = 3.2, 0.6 Hz, 1H), 4.55 (s, 2H); ^{13}C NMR (101 MHz, $CDCl_3$): δ = 139.4, 136.9, 126.6, 113.8, 111.8, 23.7; IR (ATR): $\tilde{\nu}$ = 3099, 2924, 2225, 1452, 1427, 1218, 1178, 870, 824 cm^{-1}; HRMS (EI): *m/z*: calcd. for C_6H_4NBrS $[M]^{+\cdot}$: 200.92425, found: 200.92440.

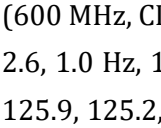

Aldehyde 151. Representative Procedure A. A solution of diisobutylaluminum hydride (1.0 M in hexane, 16.5 mL, 16.5 mmol) was added dropwise over 30 min to a solution of 2-cyanobenzylbromide (2.94 g, 15.0 mmol) in dichloromethane (60 mL) at 0 °C (bath temperature). The mixture was warmed to room temperature and stirred for another 2 h. The mixture was cooled to 0 °C before it was carefully poured into an ice-cold aq. HBr (6.0 M, 55 mL). The mixture was vigorously stirred for 1 h at 0 °C and was then extracted with dichloromethane (3 x 30 mL). The combined organic phases were washed with sat. aq. $NaHCO_3$ (2 x 30 mL) and brine (30 mL), dried over $MgSO_4$, and filtered, and the solvent was removed under reduced pressure to give the product as a dark brown oil which solidified over time (2.65 g, 89%).

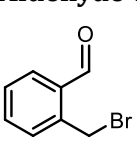

The product was used without further purification. ^{1}H NMR (400 MHz, $CDCl_3$): δ = 10.26 (s, 1H), 7.85 (dd, *J* = 7.4, 1.6 Hz, 1H), 7.61 – 7.44 (m, 3H), 4.95 (s, 2H). The data matched the literature.[239]

Aldehyde S9. The title compound was prepared by following the representative procedure **A** using 2-(bromomethyl)-3-fluorobenzonitrile (2.99 g, 14.0 mmol). The product was obtained as a dark brown oil (2.74 g, 90%), which was used without further purification. ^{1}H NMR (600 MHz, $CDCl_3$): δ = 10.23 (d, *J* = 1.4 Hz, 1H), 7.66 (ddd, *J* = 7.6, 1.2, 0.6 Hz, 1H), 7.52 (ddd, *J* = 8.3, 7.6, 5.2 Hz, 1H), 7.34 (ddd, *J* = 9.5, 8.3, 1.3 Hz, 1H), 5.00 (d, *J* = 1.6 Hz, 2H); ^{13}C NMR (151 MHz, $CDCl_3$): δ = 191.2 (d, *J* = 3.3 Hz), 161.1 (d, *J* = 252.1 Hz), 134.7 (d, *J* = 2.5 Hz), 130.5 (d, *J* = 8.7 Hz), 129.8 (d, *J* = 3.2 Hz), 126.6 (d, *J* = 15.0 Hz), 121.3 (d, *J* = 22.9 Hz), 20.0 (d, *J* = 7.1 Hz); ^{19}F NMR (565 MHz, $CDCl_3$): δ = −116.5; IR (ATR): $\tilde{\nu}$ = 1706, 1691, 1607, 1582, 1463, 1252, 1224, 793 cm^{-1}; HRMS (EI): *m/z*: calcd. for C_8H_6OFBr $[M]^{+\cdot}$: 215.95807, found: 215.95809.

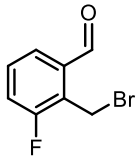

Aldehyde S10. The title compound was prepared by following the representative procedure **A** using 2-(bromomethyl)-4-fluorobenzonitrile (1.15 g, 5.37 mmol). The product was obtained as a dark brown solid (1.03 g, 88%), which was used without further purification. ^{1}H NMR (400 MHz, $CDCl_3$): δ = 10.18 (s, 1H), 7.87 (dd, *J* = 8.5, 5.7 Hz, 1H), 7.25 – 7.12 (m, 3H), 4.92 (s, 2H). The data matched the literature.[240]

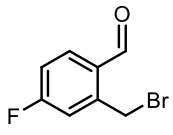

Aldehyde S11. The title compound was prepared by following the representative procedure **A** using 2-(bromomethyl)-5-fluorobenzonitrile (1.14 g, 5.34 mmol). The product was obtained as a dark brown solid (1.01 g, 87%), which was used without further purification. ^{1}H NMR (400 MHz, $CDCl_3$): δ = 10.25 (d, *J* = 1.3 Hz, 1H), 7.55 (dd, *J* = 8.4, 2.8 Hz, 1H), 7.47 (dd, *J* = 8.5, 5.1 Hz, 1H), 7.30 – 7.23 (m, 1H), 4.89 (s, 2H); ^{13}C NMR (101 MHz, $CDCl_3$): δ = 190.3 (d, *J* = 1.8 Hz), 162.9 (d, *J* = 251.5 Hz), 135.4 (d, *J* = 3.7 Hz), 135.0 (d, *J* = 6.0 Hz), 133.8 (d, *J* = 7.6 Hz), 121.2 (d, *J* = 21.6 Hz), 119.3 (d, *J* = 22.5 Hz), 28.4; ^{19}F NMR (282 MHz, $CDCl_3$): δ = −110.7; IR (ATR): $\tilde{\nu}$ = 1693, 1607, 1584, 1494, 1421, 1245, 1150, 877, 605 cm^{-1}; HRMS (EI): *m/z*: calcd. for C_8H_6OFBr $[M]^{+\cdot}$: 215.95807, found: 215.95806.

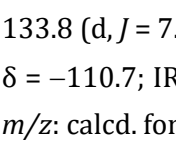

Aldehyde S12. The title compound was prepared by following the representative procedure **A** using 2-(bromomethyl)-6-fluorobenzonitrile (1.06 g, 4.95 mmol). The product was obtained as a dark brown solid (0.61 g, 57%), which was used without further purification. ^{1}H NMR (400 MHz, $CDCl_3$): δ = 10.54 (d, *J* = 0.6 Hz, 1H), 7.55 (ddd, *J* = 8.4, 7.7, 5.7 Hz, 1H), 7.28 (dd, *J* = 7.7, 1.0 Hz, 1H), 7.16 (ddd, *J* = 10.6, 8.4, 1.1 Hz, 1H), 4.93 (s, 2H); ^{13}C NMR (101 MHz, $CDCl_3$): δ = 188.5 (d, *J* = 11.6 Hz), 166.4 (d, *J* = 258.6 Hz), 140.9, 135.8 (d, *J* = 10.2 Hz), 127.8 (d, *J* = 3.3 Hz), 121.4 (d, *J* = 6.4 Hz), 116.9 (d, *J* = 22.0 Hz), 29.8 (d, *J* = 2.7 Hz); ^{19}F NMR (282 MHz, $CDCl_3$): δ = −120.0; IR (ATR): $\tilde{\nu}$ = 1687, 1606, 1571, 1471, 1450, 1254, 1186, 1154, 804 cm^{-1} HRMS (EI): *m/z*: calcd. for C_8H_6OFBr $[M]^{+\cdot}$: 215.95807, found: 215.95810.

Aldehyde S13. The title compound was prepared by following the representative procedure **A** using 2-(bromomethyl)-4-methoxybenzonitrile (1.29 g, 5.71 mmol). The product was obtained as a dark brown solid (1.14 g, 87%), which was used without further purification. ^{1}H NMR (400 MHz, $CDCl_3$): δ = 10.09 (s, 1H), 7.84 – 7.72 (m, 1H), 7.02 – 6.90 (m, 2H), 4.93 (s, 2H), 3.90 (s, 3H). The data matched the literature.[240]

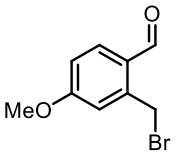

Aldehyde S14. The title compound was prepared by following the representative procedure **A** using 3-(bromomethyl)-[1,1'-biphenyl]-4-carbonitrile (600 mg, 2.20 mmol).[241] The product was obtained as a dark brown oil (523 mg, 86%), which was used without further purification. ^{1}H NMR (400 MHz, $CDCl_3$): δ = 10.28 (s, 1H), 7.90 (d, *J* = 8.0 Hz, 1H), 7.73-7.70 (m, 2H), 7.65-7.62 (m, 2H), 7.51-7.41 (m, 3H), 5.01 (s, 2H). The data matched the literature.[240]

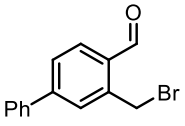

Aldehyde S15. The title compound was prepared by following the representative procedure **A** using 4-bromo-2-(bromomethyl)benzonitrile (1.00 g, 3.64 mmol). The product was obtained as a dark brown solid (650 mg, 64%), which was used without further purification. ^{1}H NMR (400 MHz, $CDCl_3$): δ = 10.20 (s, 1H), 7.95 – 7.57 (m, 3H), 4.88 (s, 2H). The data matched the literature.[240]

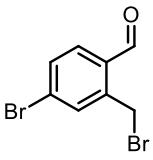

Aldehyde S16. The title compound was prepared by following the representative procedure **A** using compound **S5** (915 mg, 2.72 mmol). The product was obtained as a dark red-brown solid (754 mg, 82%), which was used without further purification. ^{1}H NMR (400 MHz, $CDCl_3$): δ = 10.31 (s, 1H), 8.10 – 8.01 (m, 2H), 8.00 – 7.91 (m, 3H), 7.68 – 7.60 (m, 1H), 7.59 – 7.50 (m, 2H), 4.91 (s, 2H); ^{13}C NMR (101 MHz, $CDCl_3$): δ = 190.6, 146.4, 140.8, 140.4, 136.1, 134.1, 133.9, 130.5, 129.8, 128.2, 128.1, 28.0; IR (ATR): $\tilde{\nu}$ = 1706, 1570, 1446, 1332, 1302, 1187, 1153, 1088, 728 cm^{-1}; HRMS (EI): *m/z*: calcd. for $C_{14}H_{11}O_3BrS$ $[M]^{+\cdot}$: 337.96069, found: 337.96087.

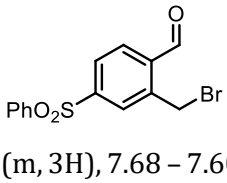

Aldehyde S17. A solution of diisobutylaluminum hydride (1.0 M in hexane, 3.40 mL, 3.40 mmol) was added dropwise over 30 min to a solution of compound **S6** (1.00 g, 3.11 mmol) in dichloromethane (10 mL) at 0 °C (bath temperature). The mixture was allowed to warm to room temperature and was stirred for another 2 h. The mixture was cooled to 0 °C and carefully poured into an ice-cold aqueous formic acid solution (8 M, 6 mL). The mixture was vigorously stirred for 2 h at 0 °C before it was extracted with dichloromethane (3 x 10 mL). The combined organic phases were washed with sat. aq. $NaHCO_3$ (2 x 10 mL) and brine (10 mL), dried over $MgSO_4$, and filtered, and the solvent was removed under reduced pressure to give the product as a dark brown solid, which was used without further purification (887 mg, 88%). ^{1}H NMR (600 MHz, $CDCl_3$): δ = 10.29 (s, 1H), 7.93 (dd, *J* = 7.5, 1.1 Hz, 1H), 7.88 – 7.86 (m, 1H), 7.83 (d, *J* = 7.5 Hz, 1H), 4.94 (s, 2H), 1.36 (s, 12H); ^{13}C NMR (151 MHz, $CDCl_3$): δ = 192.3, 138.2, 137.9, 135.5, 135.0, 132.7, 84.7, 29.7, 25.0 (the signal of C-Bpin was not detected); IR (ATR): $\tilde{\nu}$ = 2978, 1699, 1390, 1356, 1331, 1288, 1213, 1142, 1084, 852 cm^{-1}; HRMS (ESI$^+$): *m/z*: calcd. for $C_{14}H_{18}O_3BrBNa$ $[M+Na]^+$: 347.04247, found: 347.04248.

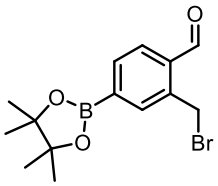

Aldehyde S18. The title compound was prepared by following the representative procedure **A** using 2-(bromomethyl)-5-chlorobenzonitrile (950 mg, 4.12 mmol). The product was obtained as a dark brown solid (745 mg, 77%), which was used without further purification. ^{1}H NMR (600 MHz, $CDCl_3$): δ = 10.22 (d, *J* = 0.5 Hz, 1H), 7.82 (dd, *J* = 2.2, 0.4 Hz, 1H), 7.54 (dd, *J* = 8.2, 2.3 Hz, 1H), 7.45 – 7.39 (m, 1H), 4.88 (s, 2H); ^{13}C NMR (151 MHz, $CDCl_3$): δ = 190.5, 137.7, 135.5, 134.4, 134.1, 133.2, 133.1, 28.5; IR (ATR): ṽ = 1736, 1447, 1372, 1233, 1043 cm^{-1}; HRMS (EI): *m/z*: calcd. for C_8H_6OClBr $[M]^{+\cdot}$: 231.92852, found: 231.92847.

Aldehyde S19. The title compound was prepared by following the representative procedure **A** using compound **S7** (709 mg, 2.53 mmol). The product was obtained as an orange-brown liquid (638 mg, 89%), which was used without further purification. ^{1}H NMR (600 MHz, $CDCl_3$): δ = 10.26 (s, 1H), 7.69 (dd, *J* = 2.7, 1.0 Hz, 1H), 7.54 (dt, *J* = 8.4, 0.5 Hz, 1H), 7.46 – 7.37 (m, 1H), 4.90 (s, 2H); ^{13}C NMR (151 MHz, $CDCl_3$): δ = 190.2, 149.7 (q, *J* = 2.0 Hz), 137.9, 134.7, 133.5, 126.2, 124.7, 120.4 (q, *J* = 259.0 Hz), 28.1; ^{19}F NMR (585 MHz, $CDCl_3$): δ = –58.0; IR (ATR): ṽ = 1699, 1580, 1494, 1254, 1211, 1151, 885, 841, 809 cm^{-1}; HRMS (EI): *m/z*: calcd. for $C_9H_6O_2BrF_3$ $[M]^{+\cdot}$: 281.94979, found: 281.94976.

Aldehyde S20. A solution of diisobutylaluminum hydride (1.0 M in hexane, 4.60 mL, 4.60 mmol) was added dropwise over 30 min to a solution of compound **S8** (845 mg, 4.18 mmol) in dichloromethane (12 mL) at 0 °C (bath temperature). The mixture was allowed to reach room temperature and was stirred for another 2 h. The mixture was cooled to 0 °C before it was carefully poured into an ice-cold aqueous formic acid solution (8 M, 9 mL). The mixture was vigorously stirred for 2 h at 0 °C before it was extracted with dichloromethane (3 x 10 mL). The combined organic phases were washed with sat. aq. $NaHCO_3$ (2 x 10 mL) and brine (10 mL), dried over $MgSO_4$, and filtered, and the solvent was removed under reduced pressure to give the product as a dark brown solid, which was used without further purification (808 mg, 94%). ^{1}H NMR (400 MHz, $CDCl_3$): δ = 10.01 (d, *J* = 0.8 Hz, 1H), 8.14 (d, *J* = 3.2 Hz, 1H), 7.41 (dq, *J* = 3.2, 0.8 Hz, 1H), 4.81 (s, 2H); ^{13}C NMR (101 MHz, $CDCl_3$): δ = 185.2, 140.7, 139.1, 137.8, 128.0, 26.0; IR (ATR): ṽ = 3093, 1681, 1451, 1420, 1218, 1174, 815 cm^{-1}; HRMS (EI): *m/z*: calcd. for C_6H_5OSBr $[M]^{+\cdot}$: 203.92391, found: 203.92381.

Compound S21. A flame-dried Schlenk flask was charged with methyl 3-methyl-2-furoate (1.50 g, 10.7 mmol), N-bromosuccinimide (2.00 g, 1.05 mmol), benzoyl peroxide (129 mg (75wt%), 0.53 mmol) and chloroform (22 mL). The mixture was stirred at reflux temperature overnight before it was allowed to cool to room temperature and all precipitates were filtered off. The solvent was removed under reduced pressure and the residue was purified by flash chromatography (SiO_2, *n*-hexane/ethyl acetate, 98:2 → 96:4) to give the title compound as a pale yellow liquid (1.33 g, 57%). ^{1}H NMR (400 MHz, $CDCl_3$): δ = 7.49 (d, *J* = 1.8 Hz, 1H), 6.60 (d, *J* = 1.8 Hz, 1H), 4.70 (s, 2H), 3.93 (s, 3H); ^{13}C NMR (101 MHz, $CDCl_3$): δ = 159.3, 145.5, 140.1, 131.3, 114.2, 52.2, 22.4; IR (ATR): ṽ = 1713, 1600, 1493, 1440, 1410, 1305, 1199, 1136, 1063, 894 cm^{-1}; HRMS (ESI$^+$): *m/z*: calcd. for $C_7H_7BrO_3Na$ $[M+Na]^+$: 240.94708, found: 240.94705.

Aldehyde S22. A solution of diisobutylaluminum hydride (1.0 M in hexane, 7.70 mL, 7.70 mmol) was added dropwise over 10 min to a solution of compound **S21** (844 mg, 3.85 mmol) in dichloromethane (17 mL) at −95 °C (bath temperature). The resulting mixture was then stirred at this temperature for another 2 h. The cooling bath was removed and the mixture was diluted with dichloromethane (5 mL) and aq. HBr (1 M, 10 mL). After vigorous stirring for 10 min, the organic phase was separated and the aqueous phase was extracted with dichloromethane (3 x 20 mL). The combined organic phases were washed with water (20 mL) and brine (20 mL), dried over $MgSO_4$ and filtered into a round bottom flask.

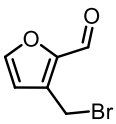

Dess-Martin periodinane (4.93 g, 11.6 mmol) and $NaHCO_3$ (1.62 g, 19.2 mmol) were added and the resulting mixture was stirred at room temperature for 2 h. The reaction was diluted with sat. aq. $Na_2S_2O_3$ solution and vigorously stirred for 20 min. The organic phase was separated and the aqueous phase extracted with dichloromethane (3 x 15 mL). The combined organic phases were washed with water (30 mL) and brine (30 mL), dried over $MgSO_4$ and filtered, and the solvent was removed under reduced pressure (***Note***: *do not dry completely! The product quickly starts decomposing once concentrated but is stable in solution even at high concentrations*). The crude mixture was purified by flash chromatography (SiO_2, *n*-pentane/diethyl ether, 95:5). Before removing the solvent, a small amount of C_6D_6 (~2 mL) and trimethoxybenzene (18.1 mg, 0.11 mmol) were added to the product solution. The volatile components were carefully removed under reduced pressure. The product was obtained as a stock solution in C_6D_6 (250 mg, 34% / determined with internal standard via ^{1}H NMR). (***Note:*** *NMR analysis of the isolated product was possible by removing the solvent and quickly redissolving the product in $CDCl_3$ to avoid decomposition. The obtained stock solution in C_6D_6 was frozen and the glass stored in the freezer; no signs of decomposition were noticed after >3 months*). ^{1}H NMR (600 MHz, $CDCl_3$): δ = 9.86 (d, *J* = 0.6 Hz, 1H), 7.59 (d, *J* = 1.8 Hz, 1H), 6.68 (dd, *J* = 1.8, 0.6 Hz, 1H), 4.68 (s, 2H); ^{13}C NMR (151 MHz, $CDCl_3$): δ = 179.4, 148.0, 147.3, 132.0, 115.0, 21.0; IR (ATR): $\tilde{\nu}$ = 1678, 1588, 1479, 1428, 1376, 1234, 1153, 764 cm^{-1}; HRMS (EI): *m/z*: calcd. for $C_6H_5O_2Br$ $[M]^{+\cdot}$: 187.94676, found: 187.94688.

Aldehyde S23. A mixture of pyridinium chlorochromate (2.59 g, 12.0 mmol) and silica gel (2.50 g) was suspended in dichloromethane (20.0 mL). 3-Bromo-2,2-dimethyl-1-propanol (1.00 g, 6.00 mmol) was added and the mixture was stirred at room temperature for 16 h. The solid was filtered off and carefully rinsed with diethylether (80 mL). The solvent was removed under reduced pressure to give the product as a light brown oil, which was used without further purification (941 mg, 95%). ^{1}H NMR (400 MHz, $CDCl_3$): δ = 9.49 (s, 1H), 3.46 (s, 2H), 1.22 (s, 6H). The data matched the literature.[242]

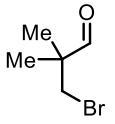

Aldehyde S24. (3-(Bromomethyl)oxetan-3-yl)methanol (1.09 g, 6.00 mmol) was added to a suspension of Dess-Martin periodinane (5.09 g, 12.0 mmol) in dichloromethane (40 mL) at 0 °C (bath temperature). The mixture was allowed to warm to room temperature and stirred for 2 h. Sat. aq. $NaHCO_3$ (20 mL) and sat. aq. $Na_2S_2O_3$ (20 mL) were added and the resulting mixture was vigorously stirred for 30 min. The organic phase was separated and the aqueous phase was extracted with dichloromethane (3 x 10 mL). The combined

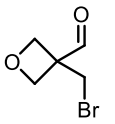

organic phases were washed with sat. aq. $Na_2S_2O_3$ (10 mL) and brine (10 mL), dried over $MgSO_4$ and filtered, and the solvent was removed under reduced pressure. The residue was purified by flash chromatography (SiO_2, *n*-hexane/ethyl acetate, 1.5:1) to give the title compound as a colorless oil (510 mg, 47%). ^{1}H NMR (400 MHz, $CDCl_3$): δ = 9.90 (s, 1H), 4.83 (d, *J* = 6.8 Hz, 2H), 4.56 (d, *J* = 6.8 Hz, 2H), 3.87 (s, 2H). The data matched the literature.[181]

Compound (S25). Diene **88a** (352 mg, 1.55 mmol) was added in portions to a suspension of

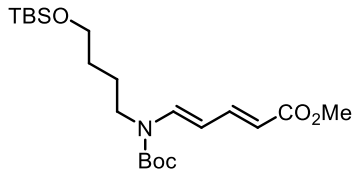

sodium hydride (56.7 mg, 2.36 mmol) in THF (9.0 mL) at 0 °C (bath temperature). After complete addition, the mixture was stirred at 0 °C for 10 min before (4-bromobutoxy)(*tert*-butyl)dimethylsilane (828 mg, 3.10 mmol) and tetrabutylammonium iodide (57.2 mg, 0.15 mmol) were added. The mixture was stirred at 65 °C (bath temperature) for 3 h. After cooling to 0 °C, sat. aq. $NaHCO_3$ (5 mL) was carefully added, followed by ethyl acetate (20 mL) and water (10 mL). The mixture was vigorously stirred for 5 min, the organic phase was separated and the aqueous layer was extracted with ethyl acetate (3 x 20 mL). The combined organic phases were washed with brine (20 mL), dried over $MgSO_4$, and filtered, and the solvent was removed under reduced pressure. The residue was purified by flash chromatography (SiO_2, *n*-hexane/ethyl acetate, 20:1 → 4:1) to give the title compound as a yellow oil (517 mg, 81%). ^{1}H NMR (400 MHz, $CDCl_3$): δ = 7.42 (d, *J* = 13.0 Hz, 1H), 7.33 (ddd, *J* = 15.2, 11.2, 0.7 Hz, 1H), 5.72 (d, *J* = 15.2 Hz, 1H), 5.60 (dd, *J* = 14.0, 11.2 Hz, 1H), 3.73 (s, 3H), 3.63 (t, *J* = 6.1 Hz, 2H), 3.56 (t, *J* = 7.5 Hz, 2H), 1.69 – 1.52 (m, 4H), 1.51 (s, 9H), 0.88 (s, 9H), 0.04 (s, 6H); ^{13}C NMR (101 MHz, $CDCl_3$): δ = 168.2, 152.4, 145.5, 138.6, 115.4, 106.2, 82.6, 62.8, 51.4, 44.2, 30.2, 28.3, 26.1, 23.9, 18.4, –5.1; IR (ATR): $\tilde{\nu}$ = 2951, 1712, 1620, 1388, 1333, 1237, 1129, 996, 836 cm^{-1} HRMS (ESI$^+$): *m/z*: calcd. for $C_{21}H_{39}NO_5SiNa$ $[M+Na]^+$: 436.24897, found: 436.24945.

Compound S26. A solution of TBAF in THF (1.0 M, 1.60 mL, 1.60 mmol) was added dropwise to a

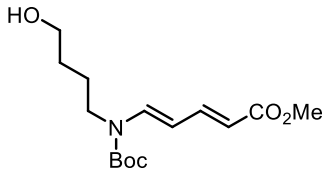

solution of compound **S25** (517 mg, 1.25 mmol) in THF (5.0 mL) at 0 °C (bath temperature). The mixture was stirred at room temperature for 30 min before water (10 mL) and *tert*-butyl methyl ether (20 mL) were added. The organic phase was separated and the aqueous layer extracted with *tert*-butyl methyl ether (2 x 20 mL). The combined organic phases were washed with brine (20 mL), dried over $MgSO_4$, and filtered, and the solvent was removed under reduced pressure. The residue was purified by flash chromatography (SiO_2, *n*-hexane/ethyl acetate, 4:1 → 1:1) to give the title compound as a pale yellow oil (315 mg, 84%). ^{1}H NMR (600 MHz, $CDCl_3$): δ = 7.40 (s, 1H), 7.33 (dd, *J* = 15.1, 11.2 Hz, 1H), 5.73 (d, *J* = 15.2 Hz, 1H), 5.61 (dd, *J* = 14.0, 11.2 Hz, 1H), 3.72 (s, 3H), 3.68 (t, *J* = 6.3 Hz, 2H), 3.58 (s, 2H), 1.70 – 1.63 (m, 2H), 1.61 – 1.56 (m, 2H), 1.51 (s, 9H); ^{13}C NMR (151 MHz, $CDCl_3$): δ = 168.2, 152.4, 145.3, 138.5, 115.6, 106.2, 82.7, 62.5, 51.5, 43.8, 29.8, 28.3, 23.7; IR (ATR): $\tilde{\nu}$ = 3464, 2947, 1711, 1619, 1390, 1242, 1134, 1071 cm^{-1} HRMS (ESI$^+$): *m/z*: calcd. for $C_{15}H_{25}NO_5Na$ $[M+Na]^+$: 322.16249, found: 322.16220.

Compound S27. Diene **88a** (217 mg, 1.00 mmol) was added in portions to a suspension of sodium hydride (36.0 mg, 1.50 mmol) in THF (5.0 mL) at 0 °C (bath temperature). After complete addition, the mixture was stirred at 0 °C for another 10 min. (3-Bromopropoxy)-*tert*-butyldimethylsilane (508 mg, 2.00 mmol) and tetrabutylammonium iodide (36.9 mg, 0.10 mmol) were added and the mixture was stirred at 65 °C (bath temperature) for 3 h. After cooling to 0 °C, sat. aq. $NaHCO_3$ (5 mL) was carefully added, followed by addition of ethyl acetate (20 mL) and water (10 mL). The mixture was vigorously stirred for 5 min, the organic phase was separated and the aqueous layer extracted with ethyl acetate (3 x 20 mL). The combined organic phases were washed with brine (20 mL), dried over $MgSO_4$, and filtered, and the solvent was removed under reduced pressure. The residue was purified by flash chromatography (SiO_2, *n*-hexane/*tert*-butyl methyl ether, 20:1 → 10:1) to give the title compound as a pale yellow oil (307 mg, 77%). ^{1}H NMR (400 MHz, $CDCl_3$): δ = 7.42 (d, *J* = 13.5 Hz, 1H), 7.34 (ddd, *J* = 15.1, 11.3, 0.6 Hz, 1H), 5.79 – 5.63 (m, 2H), 3.73 (s, 3H), 3.67 – 3.59 (m, 4H), 1.82 – 1.72 (m, 2H), 1.51 (s, 9H), 0.91 (s, 9H), 0.06 (s, 6H); ^{13}C NMR (101 MHz, $CDCl_3$): δ = 168.2, 152.4, 145.5, 138.7, 115.4, 106.3, 82.6, 60.6, 51.4, 41.6, 30.5, 28.3, 26.1, 18.4, –5.2; IR (ATR): $\tilde{\nu}$ = 2930, 1713, 1621, 1388, 1335, 1239, 1131, 836 cm^{-1} HRMS (ESI$^+$): *m/z*: calcd. for $C_{20}H_{37}NO_5SiNa$ [M+Na]$^+$: 422.23332, found: 422.23283.

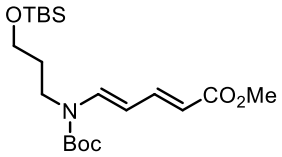

Compound S28. A solution of TBAF in THF (1.0 M, 1.15 mL, 1.15 mmol) was added dropwise to a solution of compound **S27** in THF (4.0 mL) at 0 °C (bath temperature). The mixture was stirred at room temperature for 30 min before water (10 mL) and *tert*-butyl methyl ether (20 mL) were added. The organic phase was separated and the aqueous layer extracted with *tert*-butyl methyl ether (2 x 20 mL). The combined organic phases were washed with brine (20 mL), dried over $MgSO_4$ and filtered, and the solvent was removed under reduced pressure. The residue was purified by flash chromatography (SiO_2, *n*-hexane/ethyl acetate, 2:1) to give the title compound as an orange-yellow oil (198 mg, 79%). ^{1}H NMR (400 MHz, $CDCl_3$): δ = 7.43 – 7.28 (m, 2H), 5.75 (d, *J* = 15.1 Hz, 1H), 5.67 (dd, *J* = 14.0, 11.2 Hz, 1H), 3.73 (s, 3H), 3.71 (br, 2H), 3.57 (br, 2H), 2.88 (br, 1H), 1.78 (p, *J* = 6.1 Hz, 2H), 1.52 (s, 9H); ^{13}C NMR (101 MHz, $CDCl_3$): δ = 168.1, 153.2, 145.0, 138.0, 116.1, 106.7, 83.4, 58.8, 51.5, 40.0, 29.7, 28.2; IR (ATR): $\tilde{\nu}$ = 3476, 2950, 1709, 1615, 1435, 1387, 1334, 1239, 1127, 1060, 995 cm^{-1} HRMS (ESI$^+$): *m/z*: calcd. for $C_{14}H_{23}NO_5Na$ [M+Na]$^+$: 308.14684, found: 308.14692.

Diene S29. A flame-dried Schlenk flask was charged with (2*E*,4*E*)-5-phenylpenta-2,4-dienoic acid (580 mg, 3.33 mmol) and $SOCl_2$ (2.42 mL, 33.3 mmol) and the resulting mixture was stirred at 60 °C (bath temperature) for 3 h. The excess $SOCl_2$ was removed *in vacuo* to leave the acid chloride as a colorless solid, which was directly used in the next step.

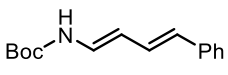

This crude material was dissolved in toluene (8 mL) and a solution of NaN_3 (650 mg, 10.0 mmol) and tetrabutylammonium bromide (53.7 mg, 0.17 mmol) in water (8 mL) was added. The mixture was vigorously stirred for 30 min at room temperature. The organic phase was separated and the

aqueous layer was extracted with toluene (3 x 15 mL). The combined organic phases were washed with sat. aq. $NaHCO_3$ (20 mL) and brine (20 mL) and were then dried over $MgSO_4$ and filtered.

The volume of the filtrate was reduced to ca. 20 mL under reduced pressure (***Caution:*** *do not dry completely!*). Dry *tert*-butanol (3.12 mL, 33.3 mmol) was added and the mixture stirred at 100 °C (bath temperature) for 2 h. The solvent was removed under reduced pressure and the residue was purified by recrystallization from *n*-hexane/ethyl acetate to give title compound as a pale yellow solid (566 mg, 69%). ^{1}H NMR (400 MHz, CD_2Cl_2): δ = 7.37 – 7.33 (m, 2H), 7.31 – 7.24 (m, 2H), 7.22 – 7.13 (m, 1H), 6.84 (t, *J* = 12.6 Hz, 1H), 6.76 (dd, *J* = 15.6, 10.7 Hz, 1H), 6.55 (d, *J* = 12.5 Hz, 1H), 6.37 (d, *J* = 15.6 Hz, 1H), 5.87 – 5.73 (m, 1H), 1.48 (s, 9H); ^{13}C NMR (101 MHz, CD_2Cl_2): δ = 152.7, 138.3, 128.9, 128.2(4), 128.1(6), 127.6, 127.1, 126.1, 110.9, 81.2, 28.4; IR (ATR): $\tilde{\nu}$ = 3311, 2979, 1669, 1648, 1503, 1368, 1252, 1148, 975 cm^{-1}; HRMS (EI): *m/z*: calcd. for $C_{15}H_{19}NO_2$ $[M]^{+\cdot}$: 245.14103, found: 245.14113.

Representative Procedure B: Substrate 152. Diene **88a** (682 mg, 3.00 mmol) was added in portions to a suspension of sodium hydride (108 mg, 4.50 mmol) in N,N-dimethylformamide (22 mL) at 0 °C (bath temperature). After complete addition, the mixture was stirred at 0 °C for another 10 min. Aldehyde **151** (1.19 g, 6.00 mmol) and tetrabutylammonium iodide (110.8 mg, 0.30 mmol) were added and the mixture was stirred at room temperature overnight. The mixture was cooled to 0 °C and sat. aq. $NaHCO_3$ (15 mL) was carefully added, followed by addition of ethyl acetate (20 mL) and water (10 mL). The mixture was vigorously stirred for 5 min, the organic phase was separated, and the aqueous phase was extracted with ethyl acetate (3 x 20 mL). The combined organic phases were washed with aq. sat. LiCl (5 x 10 mL), dried over $MgSO_4$, and filtered, and the solvent was removed under reduced pressure. The residue was purified by flash chromatography (SiO_2, *n*-hexane/ethyl acetate, 4:1) to afford the title compound as a pale brown solid (940 mg, 91%). ^{1}H NMR (400 MHz, $CDCl_3$): δ = 10.16 (d, *J* = 0.7 Hz, 1H), 7.86 (dd, *J* = 7.4, 1.7 Hz, 1H), 7.61 (br, 1H), 7.55 (td, *J* = 7.5, 1.6 Hz, 1H), 7.49 (td, *J* = 7.4, 1.3 Hz, 1H), 7.30 (dd, *J* = 15.3, 11.3 Hz, 1H), 7.10 (d, *J* = 7.6 Hz, 1H), 5.58 (d, *J* = 15.2 Hz, 1H), 5.37 (dd, *J* = 13.8, 11.3 Hz, 1H), 5.25 (s, 2H), 3.68 (s, 3H), 1.47 (br, 9H); ^{13}C NMR (101 MHz, $CDCl_3$): δ = 193.9, 167.9, 152.5, 144.6, 138.5, 138.3, 136.0, 134.3, 133.2, 127.6, 125.7, 116.3, 107.5, 83.1, 51.4, 46.4, 28.2; IR (ATR): $\tilde{\nu}$ = 2979, 1710, 1694, 1622, 1434, 1384, 1331, 1241, 1135, 996 cm^{-1} HRMS (ESI$^+$): *m/z*: calcd. for $C_{19}H_{23}NO_5Na$ $[M+Na]^+$: 368.14684, found: 368.14710.

Representative Procedure C: Substrate 186. Diene **88a** (273 mg, 1.20 mmol) was added in portions to a suspension of sodium hydride (43.2 mg, 1.80 mmol) in N,N-dimethylformamide (9.0 mL) at 0 °C (bath temperature). After complete addition, the mixture was stirred at 0 °C for another 10 min. Aldehyde **S11** (521 mg, 2.40 mmol) and tetrabutylammonium iodide (44.3 mg, 0.12 mmol) were added and the mixture was stirred at room temperature overnight. The reaction was cooled to 0 °C and more sodium hydride (14.4 mg, 0.60 mmol) was added. After stirring at 0 °C for another 10 min, additional aldehyde **S11** (130 mg, 0.60 mmol) was introduced. The

mixture was stirred at room temperature for 5 h before the reaction was carefully quenched at 0 °C with sat. aq. $NaHCO_3$ (10 mL), followed by addition of ethyl acetate (10 mL) and water (5 mL). The mixture was vigorously stirred for 5 min, the organic phase was separated, and the aqueous layer was extracted with ethyl acetate (3 x 10 mL). The combined organic phases were washed with aq. sat. LiCl (5 x 5 mL), dried over $MgSO_4$, and filtered, and the solvent was removed under reduced pressure. The residue was purified by flash chromatography (SiO_2, *n*-hexane/ethyl acetate, 4:1) to give the title compound as a pale yellow solid (376 mg, 86%). ^{1}H NMR (600 MHz, $CDCl_3$): δ = 10.12 (s, 1H), 7.60 (br, 1H), 7.56 (dd, *J* = 8.2, 2.8 Hz, 1H), 7.33 – 7.23 (m, 2H), 7.08 (dd, *J* = 8.7, 5.0 Hz, 1H), 5.60 (d, *J* = 15.3 Hz, 1H), 5.36 (t, *J* = 12.5 Hz, 1H), 5.19 (s, 2H), 3.69 (s, 3H), 1.49 (br, 9H); ^{13}C NMR (151 MHz, $CDCl_3$): δ = 192.2, 167.9, 162.0 (d, *J* = 248.9 Hz), 152.4, 144.4, 138.1, 134.6, 134.2, 127.9 (d, *J* = 7.2 Hz), 121.6 (d, *J* = 21.9 Hz), 121.3 (d, *J* = 21.1 Hz), 116.6, 107.5, 83.4, 51.5, 45.8, 28.2; ^{19}F NMR (585 MHz, $CDCl_3$): δ = –114.4; IR (ATR): ṽ = 2980, 1669, 1621, 1495, 1384, 1240, 1132, 995, 857 cm^{-1} HRMS (ESI$^+$): *m/z*: calcd. for $C_{19}H_{22}NO_5FNa$ [M+Na]$^+$: 386.13742, found: 386.13736.

Substrate S30. The title compound was prepared according to the representative procedure **B**

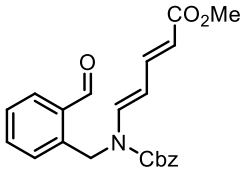

using diene **88c** (261 mg, 1.00 mmol) and aldehyde **151** (398 mg, 2.00 mmol). The crude material was purified by flash chromatography (SiO_2, *n*-hexane/ethyl acetate, 4:1) to give the product as an off-white solid (325 mg, 86%). ^{1}H NMR (600 MHz, [D_6]-DMSO, 383 K): δ = 10.23 (s, 1H), 7.95 (dd, *J* = 7.5, 1.5 Hz, 1H), 7.68 (d, *J* = 14.0 Hz, 1H), 7.59 (td, *J* = 7.6, 1.5 Hz, 1H), 7.52 (td, *J* = 7.5, 1.2 Hz, 1H), 7.47 – 7.27 (m, 6H), 7.13 (dd, *J* = 7.8, 1.4 Hz, 1H), 5.83 – 5.75 (m, 1H), 5.69 (d, *J* = 15.2 Hz, 1H), 5.32 (s, 2H), 5.26 (s, 2H), 3.63 (s, 3H); ^{13}C NMR (151 MHz, [D_6]-DMSO, 383 K): δ = 192.9, 166.0, 152.8, 143.5, 137.2, 135.2, 133.2, 133.0, 132.9, 127.8, 127.5, 127.1, 126.9, 125.1, 116.1, 108.1, 67.6, 50.1, 45.1; IR (ATR): ṽ = 2950, 1713, 1696, 1626, 1399, 1225, 1139, 994 cm^{-1}; HRMS (ESI$^+$): *m/z*: calcd. for $C_{22}H_{21}NO_5Na$ [M+Na]$^+$: 402.13119, found: 402.13104.

Substrate S31. The title compound was prepared according to the representative procedure **C**

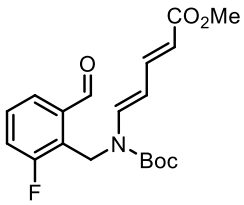

using diene **88a** (182 mg, 0.80 mmol) and aldehyde **S9** (434 mg, 2.00 mmol). The crude material was purified by flash chromatography (SiO_2, *n*-hexane/ethyl acetate, 4:1) to give the product as a yellow liquid (246 mg, 85%). ^{1}H NMR (600 MHz, $CDCl_3$): δ = 10.20 (d, *J* = 1.7 Hz, 1H), 7.66 (dd, *J* = 7.6, 1.3 Hz, 1H), 7.46 (td, *J* = 7.9, 4.9 Hz, 1H), 7.38 (d, *J* = 14.0 Hz, 1H), 7.29 – 7.26 (m, 1H), 7.23 (ddd, *J* = 15.2, 11.1, 0.7 Hz, 1H), 5.60 (dt, *J* = 15.2, 0.6 Hz, 1H), 5.55 (dd, *J* = 14.0, 11.1 Hz, 1H), 5.34 (s, 2H), 3.69 (s, 3H), 1.49 (s, 9H); ^{13}C NMR (151 MHz, $CDCl_3$): δ = 192.4 (d, *J* = 3.3 Hz), 168.0, 161.7 (d, *J* = 250.7 Hz), 152.4, 144.8, 138.0, 136.2 (d, *J* = 3.0 Hz), 129.5, 129.5, 125.5 (d, *J* = 11.7 Hz), 121.6 (d, *J* = 24.2 Hz), 116.2, 107.4 (d, *J* = 1.8 Hz), 83.3, 51.4, 39.4, 28.2; ^{19}F NMR (282 MHz, $CDCl_3$): δ = –115.1; IR (ATR): ṽ = 2980, 1698, 1621, 1465, 1385, 1330, 1242, 1132, 995 cm^{-1}; HRMS (EI): *m/z*: calcd. for $C_{19}H_{22}NO_5F$ [M]$^{+\cdot}$: 363.14765, found: 363.14788.

Substrate S32. The title compound was prepared according to the representative procedure **C** using diene **88a** (227 mg, 1.00 mmol) and aldehyde **S10** (563 mg, 2.50 mmol). The crude material was purified by flash chromatography (SiO_2, toluene/*tert*-butyl methyl ether, 30:1) to give the product as an off-white solid (187 mg, 51%). ^{1}H NMR (600 MHz, $CDCl_3$): δ = 10.10 (d, *J* = 0.7 Hz, 1H), 7.88 (dd, *J* = 8.4, 5.6 Hz, 1H), 7.58 (br, 1H), 7.30 (dd, *J* = 15.2, 11.1 Hz, 1H), 7.16 (td, *J* = 8.0, 2.5 Hz, 1H), 6.79 (d, *J* = 9.8 Hz, 1H), 5.61 (d, *J* = 15.2 Hz, 1H), 5.35 (t, *J* = 12.5 Hz, 1H), 5.25 (s, 2H), 3.70 (s, 3H), 1.50 (br, 9H); ^{13}C NMR (151 MHz, $CDCl_3$): δ = 192.1, 167.9, 166.5 (d, *J* = 257.8 Hz), 152.3, 144.3, 142.6, 138.7 (d, *J* = 9.9 Hz), 137.8, 129.8, 116.8, 114.7 (d, *J* = 22.0 Hz), 113.7 (d, *J* = 24.0 Hz), 107.6, 83.5, 51.5, 46.2, 28.2; ^{19}F NMR (585 MHz, $CDCl_3$): δ = −102.0; IR (ATR): $\tilde{\nu}$ = 2981, 1700, 1625, 1584, 1435, 1384, 1242, 1135, 966 cm^{-1}; HRMS (ESI$^+$): *m/z*: calcd. for $C_{19}H_{22}NO_5FNa$ $[M+Na]^+$: 386.13742, found: 386.13716.

Substrate S33. The title compound was prepared according to the representative procedure **C** using diene **88a** (69.0 mg, 0.30 mmol) and aldehyde **S12** (165 mg, 0.75 mmol). The crude material was purified by flash chromatography (SiO_2, *n*-hexane/ethyl acetate, 5:1) to give the product as a pale brown solid (70.0 mg, 63%). ^{1}H NMR (600 MHz, $CDCl_3$): δ = 10.59 (d, *J* = 0.7 Hz, 1H), 7.59 (br, 1H), 7.53 (td, *J* = 8.1, 5.6 Hz, 1H), 7.30 (dd, *J* = 15.2, 11.1 Hz, 1H), 7.12 (t, *J* = 9.4 Hz, 1H), 6.87 (d, *J* = 7.9 Hz, 1H), 5.60 (d, *J* = 15.2 Hz, 1H), 5.35 (t, *J* = 12.6 Hz, 1H), 5.18 (s, 2H), 3.69 (s, 3H), 1.48 (br, 9H); ^{13}C NMR (151 MHz, $CDCl_3$): δ = 189.4 (d, *J* = 11.6 Hz), 167.9, 167.0 (d, *J* = 258.7 Hz), 152.4, 144.5, 140.8, 138.1, 136.2 (d, *J* = 10.4 Hz), 121.4, 121.3 (d, *J* = 3.2 Hz), 116.6, 115.3 (d, *J* = 21.6 Hz), 107.5, 83.3, 51.5, 46.8, 28.2; ^{19}F NMR (585 MHz, $CDCl_3$): δ = −120.1; IR (ATR): $\tilde{\nu}$ = 2980, 1712, 1694, 1624, 1474, 1384, 1328, 1238, 1134, 995 cm^{-1}; HRMS (ESI$^+$): *m/z*: calcd. for $C_{19}H_{22}NO_5FNa$ $[M+Na]^+$: 386.13742, found: 386.13770.

Substrate S34. The title compound was prepared according to the representative procedure **B** using diene **88a** (182 mg, 0.80 mmol) and aldehyde **S13** (367 mg, 1.60 mmol). The crude material was purified by flash chromatography (SiO_2, *n*-hexane/ethyl acetate, 4:1) to give the product as a yellow oil which slowly solidified upon standing (220 mg, 73%). ^{1}H NMR (600 MHz, $CDCl_3$): δ = 10.00 (d, *J* = 0.7 Hz, 1H), 7.80 (d, *J* = 8.5 Hz, 1H), 7.60 (br, 1H), 7.35 – 7.27 (m, 1H), 6.92 (dd, *J* = 8.5, 2.5 Hz, 1H), 6.58 (s, 1H), 5.59 (d, *J* = 15.2 Hz, 1H), 5.37 (t, *J* = 12.6 Hz, 1H), 5.24 (s, 2H), 3.83 (s, 3H), 3.69 (s, 3H), 1.49 (s, 9H); ^{13}C NMR (151 MHz, $CDCl_3$): δ = 192.3, 168.0, 164.5, 152.5, 144.7, 141.1, 139.0, 138.1, 126.7, 116.3, 112.5, 111.4, 107.5, 83.2, 55.7, 51.4, 46.3, 28.2; IR (ATR): $\tilde{\nu}$ = 2978, 1711, 1688, 1623, 1568, 1384, 1288, 1240, 1135, 969 cm^{-1}; HRMS (ESI$^+$): *m/z*: calcd. for $C_{20}H_{25}NO_6Na$ $[M+Na]^+$: 398.15741, found: 398.15744.

Substrate S35. The title compound was prepared according to the representative procedure **C** using diene **88a** (136 mg, 0.60 mmol) and aldehyde **S14** (413 mg, 1.50 mmol). The crude material was purified by flash chromatography (SiO_2, *n*-hexane/ethyl acetate, 5:1) to give the product as a pale brown solid (185 mg, 73%). ^{1}H NMR (600 MHz, $CDCl_3$): δ = 10.19 (d, *J* = 0.6 Hz, 1H), 7.93 (d, *J* = 7.9 Hz, 1H), 7.70 (d, *J* = 7.8 Hz, 1H), 7.63 (br, 1H), 7.54 – 7.51 (m, 2H), 7.48 – 7.44 (m, 2H), 7.43 – 7.39 (m, 1H), 7.36 – 7.27 (m, 2H), 5.60 (d, *J* = 15.2 Hz, 1H), 5.48 – 5.41 (m, 1H), 5.32 (s, 2H), 3.68 (s, 3H), 1.48 (s, 9H); ^{13}C NMR (151 MHz, $CDCl_3$): δ = 193.4, 168.0, 152.6, 147.0, 144.6, 139.6, 139.0, 138.2, 136.6, 132.0, 129.2, 128.8, 127.5, 126.2, 124.5, 116.5, 107.6, 83.2, 51.4, 46.5, 28.2; IR (ATR): $\tilde{\nu}$ = 2966, 1711, 1692, 1624, 1384, 1260, 1241, 1135, 1097, 1020, 799 cm^{-1}; HRMS (ESI$^+$): *m/z*: calcd. for $C_{25}H_{27}NO_5Na$ [M+Na]$^+$: 444.17814, found: 444.17800.

Substrate S36. The title compound was synthesized according to the representative procedure **B** using diene **88a** (136 mg, 0.60 mmol) and aldehyde **S15** (334 mg, 1.20 mmol). The crude material was purified by flash chromatography (SiO_2, *n*-hexane/ethyl acetate, 5:1) to give the product as a brown solid (190 mg, 75%). ^{1}H NMR (400 MHz, $CDCl_3$): δ = 10.10 (s, 1H), 7.71 (d, *J* = 8.1 Hz, 1H), 7.64 (dd, *J* = 8.1, 1.8 Hz, 1H), 7.60 (br, 1H), 7.34 – 7.26 (m, 1H), 7.20 (s, 1H), 5.61 (d, *J* = 15.2 Hz, 1H), 5.36 (t, *J* = 12.6 Hz, 1H), 5.22 (s, 2H), 3.69 (s, 3H), 1.49 (s, 9H); ^{13}C NMR (101 MHz, $CDCl_3$): δ = 192.7, 167.8, 152.3, 144.3, 140.5, 137.8, 137.0, 131.9, 131.0, 130.1, 129.2, 116.8, 107.5, 83.5, 51.4, 45.9, 28.2; IR (ATR): $\tilde{\nu}$ = 2979, 1707, 1624, 1590, 1384, 1241, 1135, 970 cm^{-1}; HRMS (ESI$^+$): *m/z*: calcd. for $C_{19}H_{22}NO_5BrNa$ [M+Na]$^+$: 446.05736, found: 446.05727.

Substrate S37. The title compound was prepared according to the representative procedure **B** using diene **88a** (136 mg, 0.60 mmol) and aldehyde **S16** (407 mg, 1.20 mmol). The crude material was purified by flash chromatography (SiO_2, *n*-hexane/ethyl acetate, 2:1) to give the product as a yellow solid (82.5 mg, 28%). ^{1}H NMR (400 MHz, $CDCl_3$): δ = 10.21 (s, 1H), 8.07 (d, *J* = 8.0 Hz, 1H), 8.01 (d, *J* = 7.9 Hz, 1H), 7.88 – 7.81 (m, 2H), 7.64 – 7.52 (m, 3H), 7.51 – 7.40 (m, 2H), 7.32 – 7.24 (m, 1H), 5.49 (d, *J* = 15.2 Hz, 1H), 5.31 – 5.08 (m, 3H), 3.73 (s, 3H), 1.51 (s, 9H); ^{13}C NMR (101 MHz, $CDCl_3$): δ = 192.5, 167.8, 152.2, 146.6, 144.1, 140.5, 140.2, 137.7, 136.1, 136.0, 133.9, 129.7, 128.0, 126.7, 125.4, 116.9, 107.6, 83.8, 51.5, 46.2, 28.2; IR (ATR): $\tilde{\nu}$ = 2977, 1707, 1625, 1385, 1326, 1243, 1138, 728 cm^{-1}; HRMS (ESI$^+$): *m/z*: calcd. for $C_{25}H_{27}NO_7SNa$ [M+Na]$^+$: 508.14004, found: 508.14029.

Substrate S38. The title compound was prepared according to the representative procedure **C** using diene **88a** (136 mg, 0.60 mmol) and aldehyde **S17** (488 mg, 1.50 mmol). The crude material was purified by flash chromatography (SiO_2, *n*-hexane/ethyl acetate, 4:1) and subsequently recrystallized from pentane/*tert*-butyl methyl ether. ***Note:*** *The silica used for flash chromatography was treated with*

boric acid prior to use following a literature procedure.[243] The product was isolated as an off-white solid (179 mg, 63%). ^{1}H NMR (600 MHz, $CDCl_3$): δ = 10.18 (d, *J* = 0.7 Hz, 1H), 7.90 (d, *J* = 7.5 Hz, 1H), 7.84 (d, *J* = 7.5 Hz, 1H), 7.64 (br, 1H), 7.49 (br, 1H), 7.31 (dd, *J* = 15.2, 11.2 Hz, 1H), 5.58 (d, *J* = 15.2 Hz, 1H), 5.39 (t, *J* = 12.5 Hz, 1H), 5.24 (s, 2H), 3.68 (s, 3H), 1.48 (br, 9H), 1.31 (s, 12H); ^{13}C NMR (151 MHz, $CDCl_3$): δ = 194.3, 168.1, 152.8, 145.0, 138.5, 137.1, 135.7, 134.9, 134.8, 133.8, 131.9, 116.1, 107.3, 84.5, 83.1, 51.4, 46.2, 28.1, 25.0; IR (ATR): ṽ = 2979, 1712, 1699, 1624, 1385, 1368, 1240, 1137, 966, 854 cm^{-1}; HRMS (ESI$^+$): *m/z*: calcd. for $C_{25}H_{34}NO_7BNa$ [M+Na]$^+$: 494.23205, found: 494.23218.

Substrate S39. The title compound was prepared according to the representative procedure **B** using diene **88a** (136 mg, 0.60 mmol) and aldehyde **S18** (280 mg, 1.20 mmol). The crude material was purified by flash chromatography (SiO_2, *n*-hexane/ethyl acetate, 5:1) and subsequently recrystallized from *n*-hexane/ethyl acetate. The product was obtained as a pale yellow solid (100 mg, 44%). ^{1}H NMR (600 MHz, $CDCl_3$): δ = 10.11 (d, *J* = 0.7 Hz, 1H), 7.83 (d, *J* = 2.3 Hz, 1H), 7.59 (br, 1H), 7.52 (dd, *J* = 8.4, 2.3 Hz, 1H), 7.29 (dd, *J* = 15.2, 11.1 Hz, 1H), 7.05 (d, *J* = 8.3 Hz, 1H), 5.60 (d, *J* = 15.2 Hz, 1H), 5.39 – 5.30 (m, 1H), 5.20 (s, 2H), 3.69 (s, 3H), 1.48 (br, 9H); ^{13}C NMR (151 MHz, $CDCl_3$): δ = 192.3, 167.9, 152.4, 144.3, 138.0, 136.9, 135.2, 134.4, 134.2, 133.8, 127.5, 116.7, 107.5, 83.4, 51.5, 46.0, 28.2; IR (ATR): ṽ =2980, 1700, 1620, 1434, 1383, 1330, 1238, 1129, 995, 906 cm^{-1}; HRMS (ESI$^+$): *m/z*: calcd. for $C_{19}H_{22}NO_5ClNa$ [M+Na]$^+$: 402.10787, found: 402.10793.

Substrate S40. The title compound was prepared according to the representative procedure **B** using diene **88a** (182 mg, 0.80 mmol) and aldehyde **S19** (453 mg, 1.60 mmol). The crude material was purified by flash chromatography (SiO_2, *n*-hexane/ethyl acetate, 6:1) to give the product as an off-white solid (239 mg, 67%). ^{1}H NMR (400 MHz, $CDCl_3$): δ = 10.15 (d, *J* = 0.7 Hz, 1H), 7.71 (dd, *J* = 2.6, 1.1 Hz, 1H), 7.60 (br, 1H), 7.45 – 7.38 (m, 1H), 7.30 (dd, *J* = 15.2, 11.2 Hz, 1H), 7.14 (d, *J* = 8.5 Hz, 1H), 5.61 (d, *J* = 15.2 Hz, 1H), 5.36 (dd, *J* = 14.0, 11.2 Hz, 1H), 5.23 (s, 2H), 3.70 (s, 3H), 1.49 (br, 9H); ^{13}C NMR (101 MHz, $CDCl_3$): δ = 192.0, 167.9, 152.4, 148.7 (q, *J* = 2.2 Hz), 144.3, 137.9, 137.1, 134.5, 127.8, 127.2, 126.5, 120.5 (q, *J* = 258.7 Hz), 116.8, 107.5, 83.5, 51.5, 45.9, 28.2; ^{19}F NMR (282 MHz, $CDCl_3$): δ = –58.0; IR (ATR): ṽ = 2982, 1709, 1626, 1386, 1246, 1136, 995 cm^{-1}; HRMS (ESI$^+$): *m/z*: calcd. for $C_{20}H_{22}NO_6F_3Na$ [M+Na]$^+$: 452.12914, found: 452.12900.

Substrate S41. The title compound was prepared according to the representative procedure **B** using diene **88a** (182 mg, 0.80 mmol) and aldehyde **S20** (327 mg, 1.60 mmol). The crude material was purified by flash chromatography (SiO_2, *n*-hexane/ethyl acetate, 4:1) to give the product as an off-white solid (212 mg, 76%). ^{1}H NMR (400 MHz, $CDCl_3$): δ = 10.00 (d, *J* = 1.0 Hz, 1H), 8.15 (d, *J* = 3.2 Hz, 1H), 7.55 (br, 1H), 7.30 (dd, *J* = 15.2, 11.2 Hz, 1H), 6.90 (dd, *J* = 3.1, 1.2 Hz, 1H), 5.63 (d, *J* = 15.2 Hz, 1H), 5.49 (dd, *J* = 14.0, 11.2 Hz, 1H), 5.07 (s, 2H), 3.70 (s, 3H), 1.49 (br, 9H); ^{13}C NMR (101 MHz, $CDCl_3$): δ = 186.0, 168.0, 152.3, 144.7, 141.4, 139.7, 137.9, 137.2, 123.1, 116.4, 107.4,

83.2, 51.4, 44.3, 28.2; IR (ATR): $\tilde{\nu}$ = 2979, 1709, 1682, 1620, 1434, 1383, 1327, 1239, 1131, 995, 966 cm^{-1}; HRMS (ESI$^+$): *m/z*: calcd. for $C_{17}H_{21}NO_5SNa$ [M+Na]$^+$: 374.10326, found: 374.10352.

Substrate S42. The title compound was prepared according to the representative procedure **B** using diene **88a** (102 mg, 0.45 mmol) and a stock solution of aldehyde **S22** (170 mg, 0.90 mmol) in C_6D_6. The crude material was purified by flash chromatography (SiO_2, *n*-pentane/ethyl acetate, 5:1) to give the product as a pale yellow oil (93.5 mg, 62%). ^{1}H NMR (400 MHz, $CDCl_3$): δ = 9.87 (d, *J* = 0.7 Hz, 1H), 7.56 (d, *J* = 1.7 Hz, 1H), 7.43 (br, 1H), 7.33 – 7.22 (m, 1H), 6.43 (d, *J* = 1.7 Hz, 1H), 5.68 (d, *J* = 15.2 Hz, 1H), 5.60 (dd, *J* = 13.9, 11.0 Hz, 1H), 5.01 (s, 2H), 3.70 (s, 3H), 1.52 (s, 9H); ^{13}C NMR (101 MHz, $CDCl_3$): δ = 180.4, 168.0, 152.3, 148.4, 147.7, 144.4, 137.5, 131.8, 116.8, 113.2, 107.5, 83.5, 51.5, 39.2, 28.2; IR (ATR): $\tilde{\nu}$ = 2979, 1709, 1677, 1621, 1475, 1385, 1330, 1240, 1131, 996, 787 cm^{-1}; HRMS (ESI$^+$): *m/z*: calcd. for $C_{17}H_{21}NO_6Na$ [M+Na]$^+$: 358.12611, found: 358.12597.

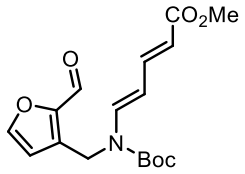

Substrate S43. A solution of compound **S26** (1.23 g, 0.97 mmol) in dichloromethane (5.0 mL) and water (19.2 µL, 1.07 mmol) was added to a suspension of Dess-Martin periodinane (357 mg, 2.90 mmol) and $NaHCO_3$ (488 mg, 5.81 mmol) in dichloromethane (5.0 mL) at 0 °C (bath temperature). The mixture was stirred at room temperature for 3 h. Dichloromethane (5 mL), sat. aq. $NaHCO_3$ (5 mL) and sat. aq. $Na_2S_2O_3$ (5 mL) were added and the mixture was vigorously stirred for 20 min. The organic phase was separated and the aqueous layer extracted with dichloromethane (3 x 10 mL). The combined organic phases were washed with sat. aq. $Na_2S_2O_3$ (10 mL) and brine (10 mL), dried over $MgSO_4$, and filtered, and the solvent was removed under reduced pressure. The residue was purified by flash chromatography (SiO_2, *n*-pentane/ethyl acetate, 5:1 → 3:1) to give the title compound as a pale yellow oil (99 mg, 34%). ^{1}H NMR (400 MHz, $CDCl_3$): δ = 9.79 (s, 1H), 7.38 (br, 1H), 7.34– 7.29 (m, 1H), 5.77 (d, *J* = 15.1 Hz, 1H), 5.70 (dd, *J* = 14.1, 11.2 Hz, 1H), 3.73 (s, 3H), 3.58 (t, *J* = 7.4 Hz, 2H), 2.51 (td, *J* = 7.0, 1.0 Hz, 2H), 1.96 – 1.79 (m, 2H), 1.51 (s, 9H); ^{13}C NMR (101 MHz, $CDCl_3$): δ = 201.2, 168.1, 152.3, 145.1, 138.1, 115.9, 106.5, 82.9, 51.5, 43.0, 40.9, 28.3, 19.6; IR (ATR): $\tilde{\nu}$ = 2951, 1711, 1621, 1390, 1312, 1241, 1134, 998 cm^{-1} HRMS (ESI$^+$): *m/z*: calcd. for $C_{15}H_{23}NO_5Na$ [M+Na]$^+$: 320.14684, found: 320.14712.

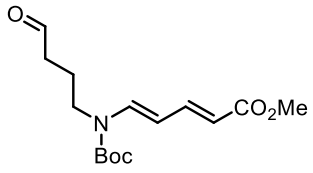

Substrate S44. A solution of compound **S28** (120 mg, 0.42 mmol) in dichloromethane (2.0 mL) was added to a suspension of Dess-Martin periodinane (357 mg, 0.84 mmol) and $NaHCO_3$ (177 mg, 2.10 mmol) in dichloromethane (3.0 mL) at 0 °C (bath temperature). The mixture was stirred at room temperature for 1 h before dichloromethane (5 mL), sat. aq. $NaHCO_3$ (5 mL) and sat. aq. $Na_2S_2O_3$ (5 mL) were added. The resulting mixture was vigorously stirred for 20 min, the organic phase was separated and the aqueous layer was extracted with dichloromethane (3 x 10 mL). The combined organic phases were washed with sat. aq. $Na_2S_2O_3$ (10 mL) and brine (10 mL), dried over $MgSO_4$, and filtered, and the solvent was removed under reduced pressure. The residue was purified by flash chromatography (SiO_2, *n*-pentane/ethyl acetate, 4:1) to give the title compound as a colorless oil (63 mg, 53%). ^{1}H NMR (400 MHz, $CDCl_3$):

δ = 9.81 (s, 1H), 7.41 – 7.37 (m, 1H), 7.31 (ddd, *J* = 15.2, 11.1, 0.7 Hz, 1H), 5.75 (dd, *J* = 15.2, 0.6 Hz, 1H), 5.67 – 5.49 (m, 1H), 3.89 (t, *J* = 7.2 Hz, 2H), 3.73 (s, 3H), 2.73 (td, *J* = 7.2, 1.4 Hz, 2H), 1.51 (s, 9H); ^{13}C NMR (101 MHz, $CDCl_3$): δ = 199.8, 168.0, 152.0, 144.7, 137.7, 116.4, 106.3, 83.3, 51.5, 41.7, 37.7, 28.2; IR (ATR): ṽ = 2980, 1710, 1622, 1387, 1334, 1241, 1134, 1059, 966 cm^{-1} HRMS (ESI$^+$): *m/z*: calcd. for $C_{14}H_{21}NO_5Na$ [M+Na]$^+$: 306.13119, found: 306.13084.

Substrate S45. Diene **88a** (182 mg, 0.80 mmol) was added in portions to a suspension of sodium hydride (25.0 mg, 1.04 mmol) in N,N-dimethylformamide (4.0 mL) at 0 °C (bath temperature). After complete addition, the mixture was stirred at 0 °C for another 10 min. Aldehyde **S23** (264 mg, 1.60 mmol) and tetrabutylammonium iodide (29.5 mg, 0.08 mmol) were added. The mixture was stirred at 80 °C (bath temperature) for 16 h. After cooling to 0 °C, sat. aq. $NaHCO_3$ (5 mL) was carefully added, followed by addition of ethyl acetate (20 mL) and water (10 mL). The mixture was vigorously stirred for 5 min, the organic phase was separated, and the aqueous layer was extracted with ethyl acetate (3 x 20 mL). The combined organic phases were washed with aq. sat. LiCl (5 x 10 mL), dried over $MgSO_4$ and filtered, and the solvent was removed under reduced pressure. The residue was purified by flash chromatography (SiO_2, *n*-hexane/ethyl acetate, 4:1) to give the title compound as a pale yellow oil (192 mg, 77%). ^{1}H NMR (400 MHz, $CDCl_3$): δ = 9.50 (s, 1H), 7.42 (d, *J* = 14.3 Hz, 1H), 7.34 – 7.26 (m, 1H), 5.74 (dt, *J* = 15.2, 0.7 Hz, 1H), 5.63 (dd, *J* = 14.1, 11.0 Hz, 1H), 3.72 (s, 3H), 3.67 (s, 2H), 1.49 (s, 9H), 1.09 (s, 6H); ^{13}C NMR (101 MHz, $CDCl_3$): δ = 203.3, 168.0, 152.6, 144.7, 139.3, 116.4, 107.7, 83.7, 51.5, 49.5, 47.6, 28.1, 20.4; IR (ATR): ṽ = 2977, 1712, 1622, 1435, 1387, 1241, 1133, 997 cm^{-1} HRMS (ESI$^+$): *m/z*: calcd. for $C_{16}H_{25}NO_5Na$ [M+Na]$^+$: 334.16249, found: 334.16237.

Substrate S46. Diene **88a** (159 mg, 0.70 mmol) was added in portions to a suspension of sodium hydride (25.2 mg, 1.05 mmol) in THF (4.0 mL) at 0 °C (bath temperature). After complete addition, the mixture was stirred at 0 °C for another 10 min. Aldehyde **S24** (251 mg, 1.40 mmol) and tetrabutylammonium iodide (25.9 mg, 0.07 mmol) were added and the mixture was stirred at 80 °C (bath temperature) for 6 h. After cooling to 0 °C, sat. aq. $NaHCO_3$ solution (5 mL) was carefully added, followed by addition of ethyl acetate (20 mL) and water (10 mL). The mixture was vigorously stirred for 5 min, the organic phase was separated and the aqueous layer extracted with ethyl acetate (3 x 20 mL). The combined organic phases were washed with brine (20 mL), dried over $MgSO_4$ and filtered, and the solvent was removed under reduced pressure. The residue was purified by flash chromatography (SiO_2, *n*-hexane/ethyl acetate, 1.5:1 → 1:1) to give the title compound as a pale yellow oil (160 mg, 70%). ^{1}H NMR (400 MHz, $CDCl_3$): δ = 9.98 (s, 1H), 7.51 – 7.43 (m, 1H), 7.34 – 7.27 (m, 1H), 5.76 (d, *J* = 15.2 Hz, 1H), 5.58 (ddd, *J* = 14.1, 11.0, 0.6 Hz, 1H), 4.73 (d, *J* = 6.8 Hz, 2H), 4.68 (d, *J* = 6.8 Hz, 2H), 3.99 (s, 2H), 3.73 (s, 3H), 1.52 (s, 9H); ^{13}C NMR (101 MHz, $CDCl_3$): δ = 198.7, 167.8, 152.5, 144.0, 138.7, 117.2, 107.1, 84.1, 73.6, 54.0, 51.5, 43.8, 28.2; IR (ATR): ṽ = 2977, 1706, 1619, 1435, 1385, 1332, 1240, 1127, 992 cm^{-1} HRMS (ESI$^+$): *m/z*: calcd. for $C_{16}H_{23}NO_6Na$ [M+Na]$^+$: 348.14176, found: 348.14165.

Substrate S47/(*E,Z*)-152. A solution of (*E,Z*)-**88a** (136 mg, 0.60 mmol) in N,N-dimethylformamide (2.0 mL) was added to a suspension of sodium hydride (21.6 mg, 0.90 mmol) in N,N-dimethylformamide (2.0 mL) at 0 °C. The mixture was stirred at 0 °C for another 5 min. Aldehyde **151** (239 mg, 1.20 mmol) and tetrabutylammonium iodide (22.2 mg, 0.06 mmol) were added and the mixture was allowed to warm to room temperature. The mixture was stirred at room temperature overnight. The mixture was cooled to 0 °C and sat. aq. $NaHCO_3$ solution (10 mL) was carefully added, followed by addition of ethyl acetate (20 mL) and water (10 mL). The mixture was vigorously stirred for 5 min. The organic phase was separated and the aqueous phase was extracted with ethyl acetate (3 x 20 mL). The combined organic phases were washed with sat. aq. LiCl solution (5 x 10 mL), dried over $MgSO_4$, and filtered, and the solvent was removed under reduced pressure. The crude product was purified by flash chromatography (SiO_2, *n*-hexane/ethyl acetate, 5:1). The title compound was obtained as an orange-brown oil (*Z,E*/*E,E* ≈ 8:1, 157 mg, 76%). ^{1}H NMR (400 MHz, $CDCl_3$): δ = 10.18 (d, *J* = 0.6 Hz, 1H), 7.91 (dd, *J* = 7.5, 1.5 Hz, 1H), 7.61 (td, *J* = 7.6, 1.5 Hz, 1H), 7.52 (td, *J* = 7.5, 1.2 Hz, 1H), 7.28 (d, *J* = 7.8 Hz, 1H), 7.06 (ddd, *J* = 14.9, 12.4, 1.1 Hz, 1H), 6.99 – 6.89 (m, 1H), 5.62 (d, *J* = 14.9 Hz, 1H), 5.39 – 5.32 (m, 3H), 3.55 (s, 3H), 1.45 (s, 9H); ^{13}C NMR (101 MHz, $CDCl_3$): δ = 193.7, 167.3, 153.5, 139.5, 139.0, 135.8, 134.3, 133.3, 133.0, 127.7, 126.1, 119.8, 108.0, 82.8, 51.3, 50.4, 28.2; IR (ATR): $\tilde{\nu}$ = 2979, 1697, 1622, 1434, 1369, 1334, 1277, 1234, 1146, 859, 754 cm^{-1} HRMS (ESI$^+$): *m/z*: calcd. for $C_{19}H_{23}NO_5Na$ [M+Na]$^+$: 368.14684, found: 368.14682.

Substrate S48. *tert*-Butyl (*E*)-buta-1,3-dien-1-ylcarbamate (300 mg, 1.77 mmol) was added in portions to a suspension of sodium hydride (72.0 mg, 3.00 mmol) in THF (18 mL) at 0 °C (bath temperature). After complete addition, the mixture was stirred at 0 °C for 10 min before aldehyde **151** was introduced. The mixture was stirred at 50 °C (bath temperature) for 16 h. After cooling to 0 °C, sat. aq. $NaHCO_3$ solution (5 mL) was carefully added, followed by ethyl acetate (20 mL) and water (10 mL). The mixture was vigorously stirred for 5 min, the organic phase was separated and the aqueous layer was extracted with ethyl acetate (3 x 20 mL). The combined organic phases were washed with brine (20 mL), dried over $MgSO_4$, and filtered, and the solvent was removed under reduced pressure.

In order to remove remaining aldehyde **151**, the crude product was dissolved in dichloromethane, pyridine (0.16 mL, 1.95 mmol) was added, and the resulting mixture was stirred at room temperature for 24 h. The mixture was washed with aq. $CuSO_4$ solution (10% *w/w*, 2 x 10 mL), water (2 x 10 mL) and brine (20 mL) before it was dried over $MgSO_4$ and filtered. The solvent was removed under reduced pressure and the residue purified by flash chromatography (SiO_2, toluene/*tert*-butyl methyl ether, 150:1) to give the title compound as a pale yellow oil (326 mg, 64%). ^{1}H NMR (400 MHz, CD_2Cl_2): δ = 10.18 (s, 1H), 7.88 (dd, *J* = 7.5, 1.5 Hz, 1H), 7.57 (td, *J* = 7.6, 1.5 Hz, 1H), 7.49 (td, *J* = 7.5, 1.2 Hz, 1H), 7.39 – 7.20 (m, 1H), 7.16 (d, *J* = 7.7 Hz, 1H), 6.35 – 6.25 (m, 1H), 5.33 (br, 1H), 5.19 (s, 2H), 4.88 – 4.84 (m, 1H), 4.82 – 4.79 (m, 1H), 1.51 (br, 9H); ^{13}C NMR (101 MHz, CD_2Cl_2): δ = 193.9, 153.2, 139.7, 135.8, 135.6, 134.3, 133.6, 131.7, 127.6, 126.2, 112.9,

111.0, 82.2, 46.4, 28.2; IR (ATR): $\tilde{\nu}$ = 2978, 1706, 1643, 1426, 1373, 1323, 1254, 1154 cm^{-1} HRMS (ESI^+): *m/z*: calcd. for $C_{17}H_{21}NO_3Na$ $[M+Na]^+$: 310.14136, found: 310.14121.

Substrate S49. The title compound was prepared according to the representative procedure **B** using diene **S29** (245 mg, 1.00 mmol) and aldehyde **151** (398 mg, 2.00 mmol). The crude material was purified by flash chromatography (SiO_2, *n*-hexane/ethyl acetate, 10:1 → 4:1) to give the product as a pale yellow solid (288 mg, 79%). ^1H NMR (600 MHz, $[D_6]$-DMSO, 383 K): δ = 10.29 (s, 1H), 7.97 (dd, *J* = 7.6, 1.5 Hz, 1H), 7.64 (td, *J* = 7.6, 1.5 Hz, 1H), 7.56 – 7.49 (m, 1H), 7.38 – 7.31 (m, 3H), 7.30 – 7.22 (m, 2H), 7.19 – 7.11 (m, 2H), 6.90 – 6.75 (m, 1H), 6.31 (d, *J* = 15.6 Hz, 1H), 5.68 (ddd, *J* = 14.2, 10.3, 0.7 Hz, 1H), 5.24 (s, 2H), 1.45 (s, 9H); ^{13}C NMR (151 MHz, $[D_6]$-DMSO, 383 K): δ = 192.9, 151.8, 138.4, 137.2, 133.2, 132.9, 132.8, 130.9, 127.8, 127.6, 127.4, 126.7, 125.9, 125.2, 125.0, 110.4, 81.1, 44.7, 27.3; IR (ATR): $\tilde{\nu}$ = 2977, 1695, 1635, 1390, 1333, 1238, 1147, 973, 749 cm^{-1}; HRMS (ESI^+): *m/z*: calcd. for $C_{23}H_{25}NO_3Na$ $[M+Na]^+$: 386.17266, found: 386.17281.

Substrate S50. Caesium carbonate (135 mg, 0.41 mmol) was added to a solution of 2-(Boc-amino)-benzaldehyde (45.8 mg, 0.21 mmol) in N,N-dimethylformamide (2.0 mL) and the resulting mixture was stirred for 5 min. Tetrabutylammonium iodide (115 mg, 0.31 mmol) and methyl (2*E*,4*E*)-6-bromohexa-2,4-dienoate (63.7 mg, 0.31 mmol) were introduced and the mixture was stirred at 50 °C (bath temperature) for 30 min. After cooling to room temperature, water (10 mL) and ethyl acetate (10 mL) were added, the organic phase was separated and the aqueous layer extracted with ethyl acetate (2 x 10 mL). The combined organic phases were washed with aq. sat. LiCl (3 x 10 mL), dried over $MgSO_4$, and filtered, and the solvent was removed under reduced pressure. The residue was purified by flash chromatography (SiO_2, *n*-pentane/ethyl acetate, 5:1) to give the title compound as a yellow oil (43.8 mg, 61%). ^1H NMR (400 MHz, CD_2Cl_2): δ = 10.05 (s, 1H), 7.85 (dd, *J* = 7.7, 1.7 Hz, 1H), 7.61 (td, *J* = 7.7, 1.7 Hz, 1H), 7.42 (tt, *J* = 7.6, 0.9 Hz, 1H), 7.30 – 7.15 (m, 2H), 6.30 – 6.11 (m, 2H), 5.83 (d, *J* = 15.4 Hz, 1H), 4.35 (s, 2H), 3.70 (s, 3H), 1.32 (s, 9H); ^{13}C NMR (101 MHz, CD_2Cl_2): δ = 190.2, 167.3, 154.6, 144.5, 143.7, 137.6, 135.0, 133.1, 131.1, 129.4, 128.5, 127.8, 121.9, 81.7, 52.6, 51.8, 28.2; IR (ATR): $\tilde{\nu}$ = 2978, 1695, 1598, 1457, 1390, 1367, 1269, 1158, 1001 cm^{-1} HRMS (ESI^+): *m/z*: calcd. for $C_{19}H_{23}NO_5Na$ $[M+Na]^+$: 368.14684, found: 368.14655.

Substrate S51. Potassium carbonate (415 mg, 3.00 mmol) and salicylaldehyde (272 µL, 2.60 mmol) were added to a solution of methyl (2*E*,4*E*)-6-bromohexa-2,4-dienoate (410 mg, 2.00 mmol) in acetonitrile (10 mL) and the resulting mixture was stirred at 65 °C (bath temperature) for 2 h. The solvent was removed under reduced pressure and the residue was dissolved in ethyl acetate (20 mL) and water (20 mL). The organic phase was separated and the aqueous layer was extracted with ethyl acetate (3 x 20 mL). The combined organic phases were washed with brine (20 mL), dried over $MgSO_4$ and filtered, and the solvent was removed under reduced pressure. The residue was purified by flash chromatography (SiO_2, *n*-hexane/ethyl acetate, 5:1) to give the title

compound as an off-white solid (323 mg, 66%). ^{1}H NMR (400 MHz, $CDCl_3$): δ = 10.54 (d, *J* = 0.8 Hz, 1H), 7.86 (dd, *J* = 7.7, 1.8 Hz, 1H), 7.54 (ddd, *J* = 8.5, 7.3, 1.9 Hz, 1H), 7.33 (ddd, *J* = 15.4, 11.0, 0.7 Hz, 1H), 7.06 (tt, *J* = 7.5, 0.9 Hz, 1H), 6.96 (dd, *J* = 8.5, 0.9 Hz, 1H), 6.54 (ddtd, *J* = 15.2, 11.1, 1.7, 0.7 Hz, 1H), 6.30 (dtt, *J* = 15.5, 5.1, 0.8 Hz, 1H), 5.95 (dt, *J* = 15.5, 0.8 Hz, 1H), 4.78 (dd, *J* = 5.1, 1.7 Hz, 2H), 3.76 (s, 3H). The data matched the literature.[244]

Imine 205. A flame-dried two-neck flask under argon was charged with sulfamide (1.00 g, 10.4 mmol), benzaldehyde (1.10 mL, 10.9 mmol), 3 Å molecular sieves (~2g) and dry methanol (10 mL). One drop of sulfuric acid was added, the flask was equipped with a reflux condenser and heated to reflux for 3 d. The mixture was allowed to cool to room temperature and the solids were filtered off. The filtrate was concentrated under reduced pressure and the residue was suspended in diethyl ether (40 mL) and washed with water (5 x 20 mL). The organic layer was separated, dried over $MgSO_4$, filtered, and the solvent was removed under reduced pressure. The obtained solid was recrystallized from *n*-pentane/ethyl acetate and imine **205** was obtained as a colorless solid (700 mg, 37%). ^{1}H NMR (400 MHz, [D_6]-DMSO): δ = 8.92 (s, 1H), 8.03 – 7.90 (m, 2H), 7.75 – 7.66 (m, 1H), 7.63 – 7.55 (m, 2H), 7.41 (s, 2H); IR (ATR): $\tilde{\nu}$ = 3311, 3320, 1599, 1573, 1340, 1153, 913, 689 cm^{-1}; HRMS (ESI$^+$): *m/z*: calcd. for $C_7H_8N_2O_2SNa$ [M+Na]$^+$: 207.01987, found: 207.02010.

Imine 215. A flame-dried two-neck flask under argon was charged with N-propyl-sulfamide (750 mg, 5.43 mmol), benzaldehyde (1.10 mL, 10.9 mmol) and toluene (15 mL). One drop of sulfuric acid was added. The flask was equipped with a Dean-Stark apparatus and the mixture was heated to reflux overnight. The mixture was allowed to cool to room temperature and the solids were filtered off. The filtrate was concentrated under reduced pressure and the residue was suspended in diethyl ether (40 mL) and washed with water (5 x 20 mL). The organic layer was dried over $MgSO_4$, filtered and the solvent was removed under reduced pressure. The residue was washed with *n*-pentane (6 x 20 mL) to remove residual benzaldehyde. After washing, imine **215** was obtained as a colorless solid (600 mg, 49%). ^{1}H NMR (400 MHz, CD_2Cl_2): δ = 8.90 (s, 1H), 8.00 – 7.86 (m, 2H), 7.69 – 7.61 (m, 1H), 7.60 – 7.47 (m, 2H), 4.59 (s, 1H), 3.08 (td, *J* = 7.1, 6.2 Hz, 2H), 1.60 (h, *J* = 7.3 Hz, 3H), 0.94 (t, *J* = 7.4 Hz, 3H); ^{13}C NMR (101 MHz, CD_2Cl_2): δ = 169.7, 134.9, 133.0, 131.2, 129.6, 46.0, 23.4, 11.3; IR (ATR): $\tilde{\nu}$ = 3286, 2967, 1609, 1573, 1452, 1325, 1154, 1075, 789 cm^{-1}; HRMS (ESI$^+$): *m/z*: calcd. for $C_{10}H_{14}N_2O_2SNa$ [M+Na]$^+$: 249.06682, found: 249.06681.

5.3 Enantioselective Nickel-Catalyzed Intermolecular Reductive Couplings

5.3.1 Experimental Procedure, Work-up and Notes

General Procedure I (For Aromatic Aldehydes). A flame-dried Schlenk flask was charged with tris(*trans*-1,2-bis(4-*tert*-butylphenyl)ethene)nickel(0) (Ni($^{t\text{Bu}}$stb)$_3$) (18.7 mg, 0.02 mmol), phosphoramidite **L11** (12.8 mg, 0.02 mmol) and the respective diene (0.40 mmol or 0.60 mmol). The Schlenk flask was evacuated and refilled with argon (3 cycles). THF (0.35 mL) and triethylborane (1 M in THF, 0.30 mL, 0.30 mmol) were added and the resulting solution was stirred for 5 min. The respective aldehyde (0.20 mmol) was added under an argon counterflow, the flask was sealed and the mixture stirred at room temperature for the indicated time. The reaction was quenched *via* the indicated work-up procedure **I** or **II**. Purification of the crude material by flash chromatography furnished the analytically pure vicinal amino alcohol product.

General Procedure II (For Aliphatic Aldehydes). A flame-dried Schlenk flask was charged with tris(*trans*-1,2-bis(4-*tert*-butylphenyl)ethene)nickel(0) (Ni($^{t\text{Bu}}$stb)$_3$) (18.7 mg, 0.02 mmol), phosphoramidite **L11** (12.8 mg, 0.02 mmol) and the respective diene (0.40 mmol). The Schlenk flask was evacuated and refilled with argon (3 cycles). Toluene (1.4 mL) and triethylborane (1 M in toluene, 0.60 mL, 0.60 mmol) were added and the resulting solution was stirred for 5 min. The respective aldehyde (0.20 mmol) was added under an argon counterflow, the flask was sealed and the mixture stirred at room temperature for 72 h. The reaction was quenched *via* the indicated work-up procedure **I** or **II**. Purification of the crude material by flash chromatography furnished the analytically pure vicinal amino alcohol product.

Work-up Procedures

The product initially formed is the corresponding -OBEt$_2$ adduct. The O–B bond is fairly stable towards hydrolysis but can be cleaved under oxidative or basic conditions as described below to give the desired free alcohol. In general, the **oxidative work-up (I)** is preferred, except when functionality sensitive to oxidation is present (*e.g.* the pinacolboronate in product **97**).

The **basic work-up (II)** tends to be less efficient and an extended period of stirring is required to achieve complete cleavage of the O–B bond. It is recommended only for substrates that are sensitive to oxidants.

Oxidative Work-up Procedure (I): The reaction mixture was cooled to 0 °C and pH 7 phosphate buffer solution (1.5 mL) and aq. H_2O_2 (30% *w/w* in water, ≈0.3 mL) were added. The mixture was diluted with ethyl acetate (2 mL) and vigorously stirred for 1 h at 0 °C. Additional ethyl acetate (10 mL) and water (5 mL) were added, the organic phase was separated, and the aqueous layer was extracted with ethyl acetate (2 × 10 mL). The combined organic layers were washed with sat. aq. $Na_2S_2O_3$ (15 mL) and brine (15 mL), dried over $MgSO_4$, filtered and concentrated *in vacuo*.

Basic Work-up Procedure (II): Sat. aq. $NaHCO_3$ (3 mL) and ethyl acetate (2 mL) were added to the reaction mixture and vigorous stirring continued for 3 h at room temperature. The mixture was diluted with ethyl acetate (10 mL) and water (5 mL) and the aqueous phase was extracted with ethyl acetate (2 × 10 mL). The combined organic layers were washed with brine (15 mL), dried over $MgSO_4$, filtered and concentrated *in vacuo*.

Notes

1. THF and toluene were distilled under argon and stored in Schlenk flasks under argon for long-term use. Karl-Fischer-titration was used to check that the water content did not exceed 20 ppm.
2. The presence of residual chlorinated solvents ($CHCl_3$, CH_2Cl_2 etc.) in any of the reaction partners can lead to catalyst deactivation.
3. Liquid aldehydes were distilled under vacuum and stored in the freezer (–18 °C) under argon. Carboxylic acid impurities have a deleterious effect; therefore, the purity of the aldehyde was checked by ^{1}H NMR spectroscopy prior to use.
4. Solid aldehydes were purified by recrystallization prior to use.
5. Triethylborane solutions in THF and toluene were prepared from neat triethylborane and the respective solvent. ***Note***: *Triethylborane is pyrophoric and must be handled carefully under rigorously oxygen-free and water-free conditions*.
6. The amino-pentadienoates showed good stability and were handled and weighed in air. However, partial decomposition was observed when kept in air for extended periods of time (> 3 days). When stored in Schlenk flasks under argon in the freezer (–18 °C), they could be used over extended periods of time (> 6 months) without any notable decomposition.
7. Tris(*trans*-1,2-bis(4-*tert*-butylphenyl)ethene)nickel(0) can be weighed in air, yet is stored in the freezer at –18 °C. The same batch was used for > 1 year without any observable loss of catalytic activity.
8. Although tris(*trans*-1,2-bis(4-*tert*-butylphenyl)ethene)nickel(0) is air-stable in the solid state, care must be taken once it has been dissolved. Therefore, the ligand was always added *before* the solvent as it helps stabilize the nickel(0) complex should residual oxygen be present in solution. Likewise, the diene seems to stabilize the nickel species, while triethylborane quenches any remaining oxygen.
9. Small-scale reactions were carried out in sealed Schlenk flasks. However, ethylene gas is released from reduction of the nickel catalyst by triethylborane and care must be taken to use reaction vessels that can withstand the increase in pressure caused by this gas evolution. ***Note***: *For larger scale reactions, it is essential to use a gas bubbler to prevent build-up of overpressure and possible explosion of the flask*.
10. If the reactions are performed without the addition of any ligand, the mixture immediately turns black, likely because of the formation of nickel black/nickel nanoparticles. The

reaction of an aldehyde with diene **88a** then proceeds exclusively at the π-bond proximal to the ester to give the racemic aldol-type product such as *rac*-**91**.

11. In the presence of the ligand **L11**, the color of the reaction mixture is usually intense orange to yellow. Formation of a dark color or black particles indicates catalyst decomposition and will cause a drop in conversion, regioselectivity and yield presumably due to a competing background reaction.
12. The regioisomeric ratio was determined by ^{1}H NMR analysis of the crude material after the aqueous work-up. Unless stated otherwise, the dr was > 20:1.
13. The use of toluene/*tert*-butyl methyl ether mixtures as the eluent for flash chromatography allowed any regioisomers to be separated from the desired amino alcohol products.
14. Recrystallization was performed to increase the ee of the products. On small scale, the product was simply dissolved by portionwise addition of a solvent and ultrasonication of the sample. An anti-solvent was then added and the vial stored in the freezer at –18 °C until the product had crystallized (at least 1 day).

    For experiments on larger scale, the product was recrystallized by allowing a hot solution of the vicinal amino alcohol derivative to slowly cool to room temperature (see picture below, recrystallization of ca. 900 mg of compound **90a**).

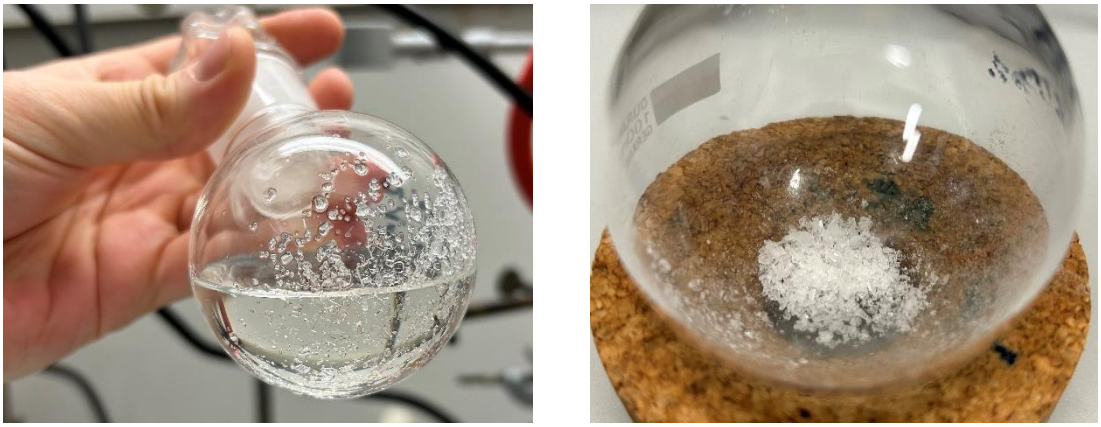

Figure S1: Recrystallization of amino alcohol **90a** on 900 mg scale.

5.3.2 Control Experiments

Amino alcohol 79. A flame dried Schlenk flask under argon was charged with $Ni(cod)_2$ (8.0 mg, 0.03 mmol), phosphoramidite ligand **L11** (18.6 mg, 0.03 mmol), and *tert*-butyl (*E*)-buta-1,3-dien-1-yl carbamate (63.9 mg, 0.38 mmol).[131] The Schlenk flask was evacuated and refilled with argon (3 cycles). THF (0.60 mL), triethylborane (1 M in THF, 0.44 mL, 0.44 mmol) and benzaldehyde (29.6 µL, 0.29 mmol) were added under argon counterflow, the flask was sealed and the mixture was stirred at room temperature for 24 h. The reaction was quenched by addition of sat. aq. $NaHCO_3$ solution (3 mL) and the resulting mixture was stirred for 1 h. The mixture was diluted with ethyl acetate (3 mL) and the organic layer extracted with ethyl acetate (3 x 3 mL). The combined extracts were dried over $MgSO_4$, filtered, and the solvent was removed under reduced pressure. The crude product was purified by flash chromatography (SiO_2, *iso*-hexane/ethyl acetate, 20:1 → 4:1) to give the title compound as an off-white solid (37.0 mg, 46%, > 20:1 dr, 55% ee). mp = 73-75 °C, ^{1}H NMR (400 MHz, $CDCl_3$): δ = 7.38 – 7.27 (m, 5H), 5.79 – 5.69 (m, 1H), 5.09 – 5.02 (m, 2H), 4.90 (s, 1H), 4.54 (br, 1H), 3.96 (br, 1H), 3.36 (s, 1H), 2.24 – 2.17 (m, 1H), 2.10 – 2.02 (m, 1H), 1.44 (s, 9H); ^{13}C NMR (151 MHz, $CDCl_3$): δ = 156.9, 140.8, 134.8, 128.3, 127.7, 126.6, 117.9, 80.0, 76.4, 56.1, 33.9, 28.5; IR (ATR): $\tilde{\nu}$ = 3417, 2978, 1687, 1503, 1366, 1251, 1168, 1023, 702 cm^{-1}; HRMS (ESI$^+$): m/z: calcd. for $C_{16}H_{23}NO_3Na$ $[M+Na]^+$: 300.15701, found: 300.15705.

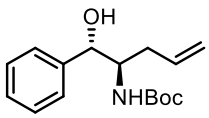

The ee was determined by 2D-HPLC analysis. First dimension = 100 mm Zorbax RX-SIL, 4.6 mm Ø, *n*-heptane/*iso*-propanol = 99:1, v = 1.0 mL/min, λ = 220 nm. Second Dimension = 150 mm Chiralcel OD-3, 4.6 mm Ø, *n*-heptane/*iso*-propanol = 90:10, v = 1.0 ml/min, λ = 220 nm.

First dimension (left) and second dimension (right) of racemic sample:

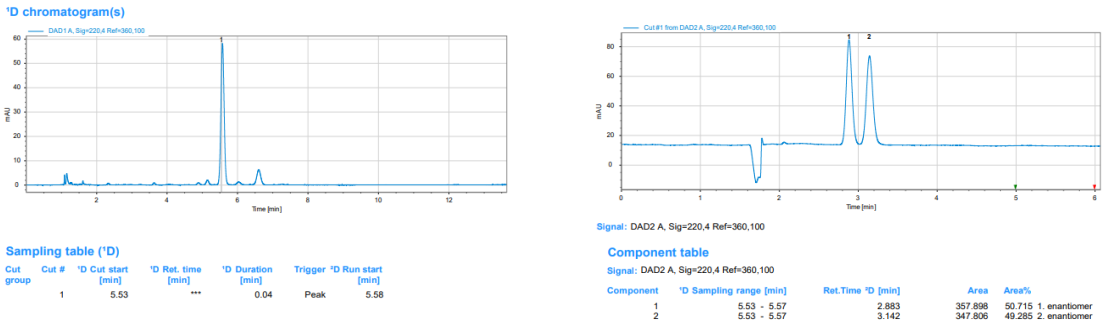

First dimension (left) and second dimension (right) of enantioenriched sample:

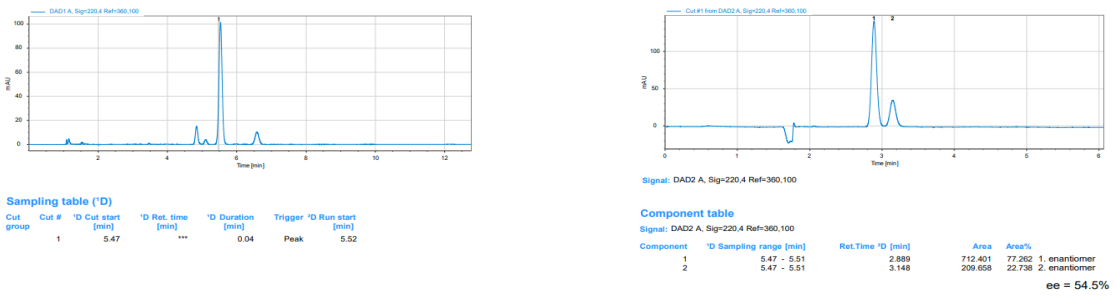

Compound 91. A flame-dried Schlenk flask under argon was charged with tris(*trans*-1,2-bis(4-*tert*-butylphenyl)ethene)nickel(0) (Ni($^{t\text{Bu}}$stb)$_3$) (18.7 mg, 0.02 mmol) and diene **88a** (90.9 mg, 0.40 mmol). The Schlenk flask was evacuated and refilled with argon (3 cycles). THF (0.35 mL) and triethylborane (1 M in THF, 0.30 mL, 0.30 mmol) were added and the resulting solution was stirred for 5 min. Benzaldehyde (20.2 µL, 0.20 mmol) was added under an argon counterflow, the flask was sealed and the mixture stirred at room temperature for 16 h. The reaction was quenched at 0 °C by addition of pH 7 phosphate buffer solution (1.5 mL) and aq. H_2O_2 (30% *w/w* in water, 0.3 mL). Ethyl acetate (2.0 mL) was added and the resulting mixture was vigorously stirred for 1 h. The mixture was diluted with ethyl acetate (10 mL) and water (5 mL) and the aqueous phase was extracted with ethyl acetate (2 x 10 mL). The combined organic layers were washed with sat. aq. $Na_2S_2O_3$ solution (15 mL) and brine (15 mL), dried over $MgSO_4$, and filtered, and the solvent was removed under reduced pressure. The residue was purified by flash chromatography (SiO_2, *iso*-hexane + 1% NEt_3 → *iso*-hexane/ethyl acetate 4:1 + 1% NEt_3) to give the title compound as a colorless oil (63.8 mg, 95%). ^{1}H NMR (400 MHz, CD_2Cl_2): δ = 7.36 – 7.25 (m, 5H), 6.40 (t, *J* = 12.4 Hz, 1H), 6.25 (br, 1H), 4.94 (dd, *J* = 6.1, 2.3 Hz, 1H), 4.89 – 4.81 (m, 1H), 3.55 (s, 3H), 2.85 (s, 1H), 2.77 – 2.72 (m, 1H), 2.43 – 2.27 (m, 2H), 1.43 (s, 9H); ^{13}C NMR (101 MHz, CD_2Cl_2): δ = 174.6, 152.9, 142.2, 128.7, 128.1, 126.6, 126.0, 105.9, 80.5, 74.1, 54.3, 51.9, 28.4, 28.2; IR (ATR): $\tilde{\nu}$ = 3336, 2978, 1701, 1676, 1516, 1367, 1246, 1163, 1019, 702 cm^{-1}; HRMS (ESI$^+$): *m/z*: calcd. for $C_{18}H_{25}NO_5Na$ $[M+Na]^+$: 358.16249, found: 358.16249.

5.3.3 Determination of the Regioisomeric Ratio (rr)

The regioisomeric ratios (rr) were determined by analysis of the ^{1}H NMR spectra of the crude products after the aqueous work-up. Figure S2 shows the ^{1}H NMR spectrum of the crude mixture of the reductive coupling of benzaldehyde with diene **88a** catalyzed by Ni($^{t\text{Bu}}$stb)$_3$/**L11** as well as the ^{1}H NMR spectra of the purified amino alcohol derivative **90a** and its regioisomer **91**. As evident from Figure S2, the ester groups of **90a** and **91** show significant shift differences and hence allow for accurate determination of the rr; this effect is fairly general, see the following representative examples. Likewise, the olefinic protons of the regioisomers are usually well separated and therefore also suitable for the determination of the rr.

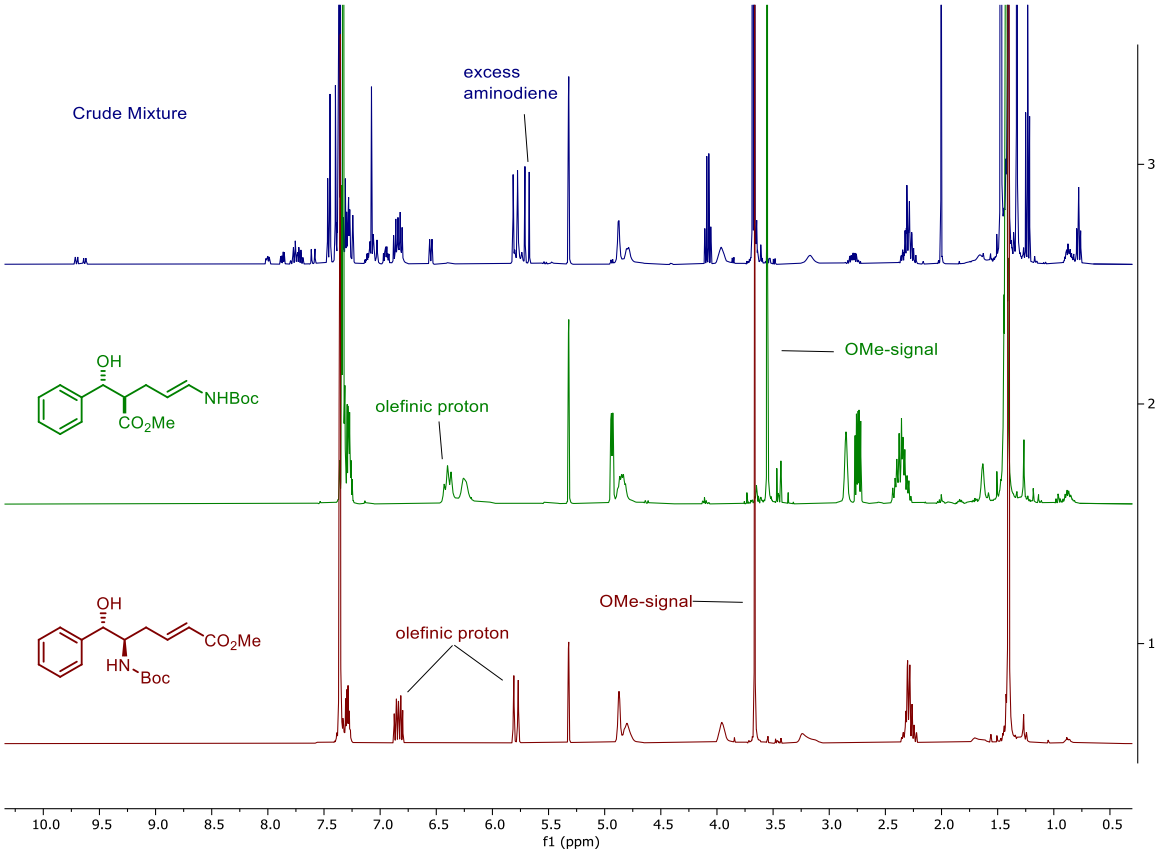

Figure S2: Stacked spectra of the crude mixture of the ligand-controlled reductive coupling of diene **88a** and benzaldehyde (blue), the "Tamaru-type" product **91** (green), and the vicinal amino alcohol **90a** (red).

^{1}H NMR spectrum of the crude reaction mixture obtained in the synthesis of 90a; rr > 20:1

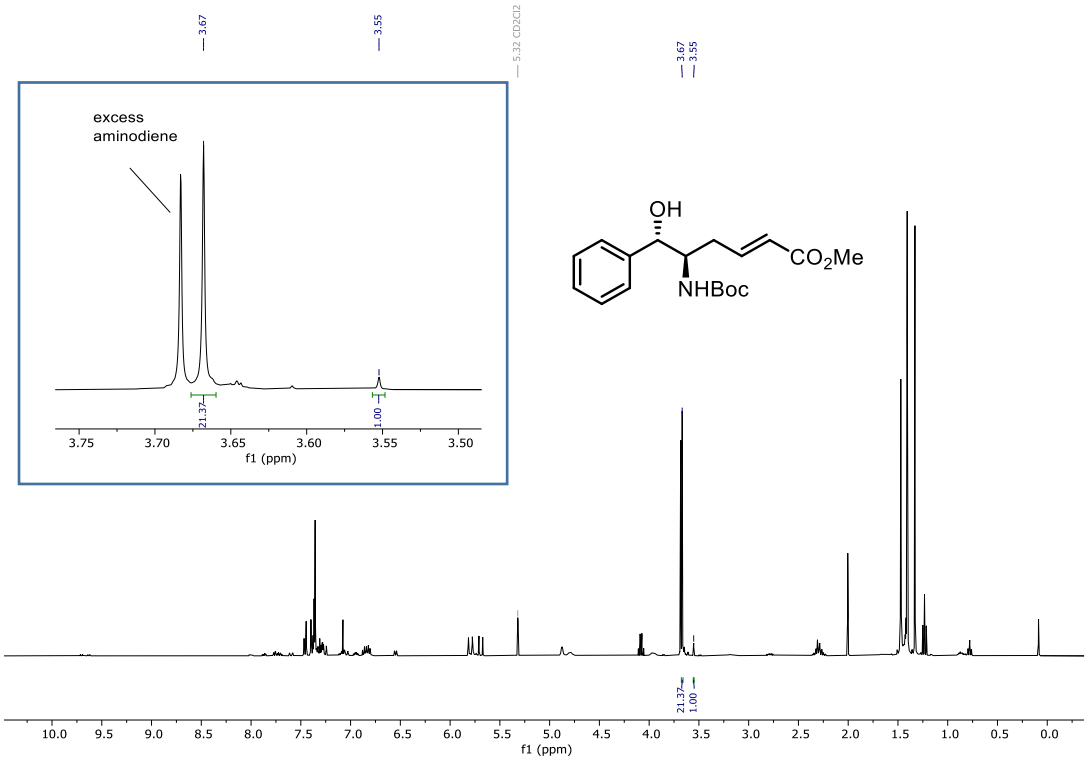

^{1}H NMR spectrum of the crude reaction mixture obtained in the synthesis of 90b; rr ≈ 12:1

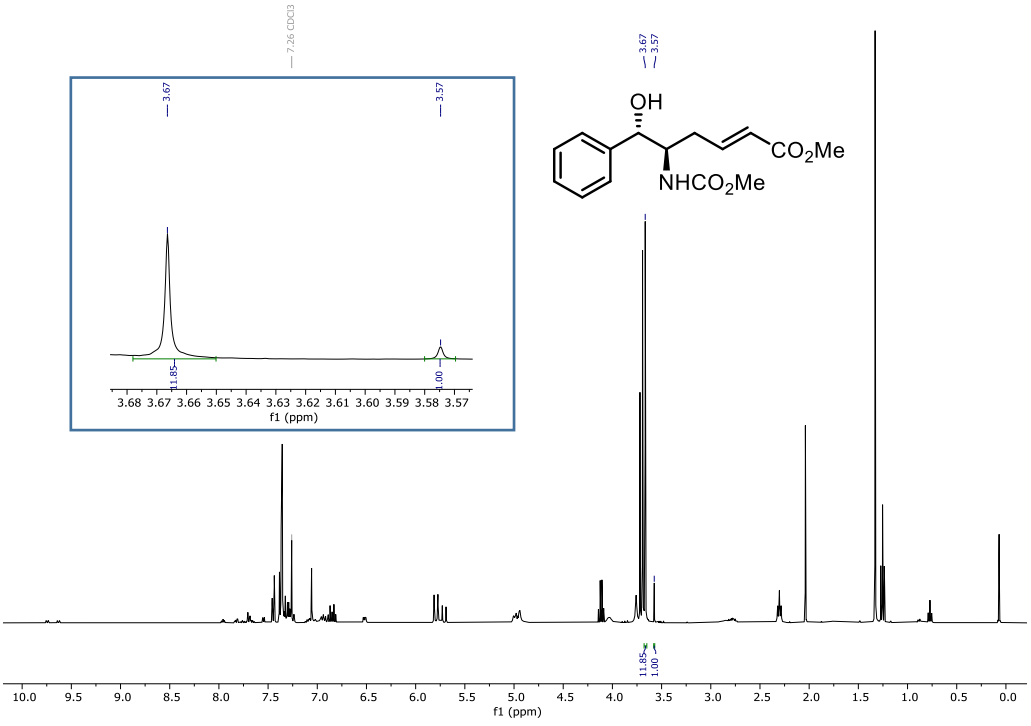

^{1}H NMR spectrum of the crude reaction mixture obtained in the synthesis of 90d; rr > 20:1

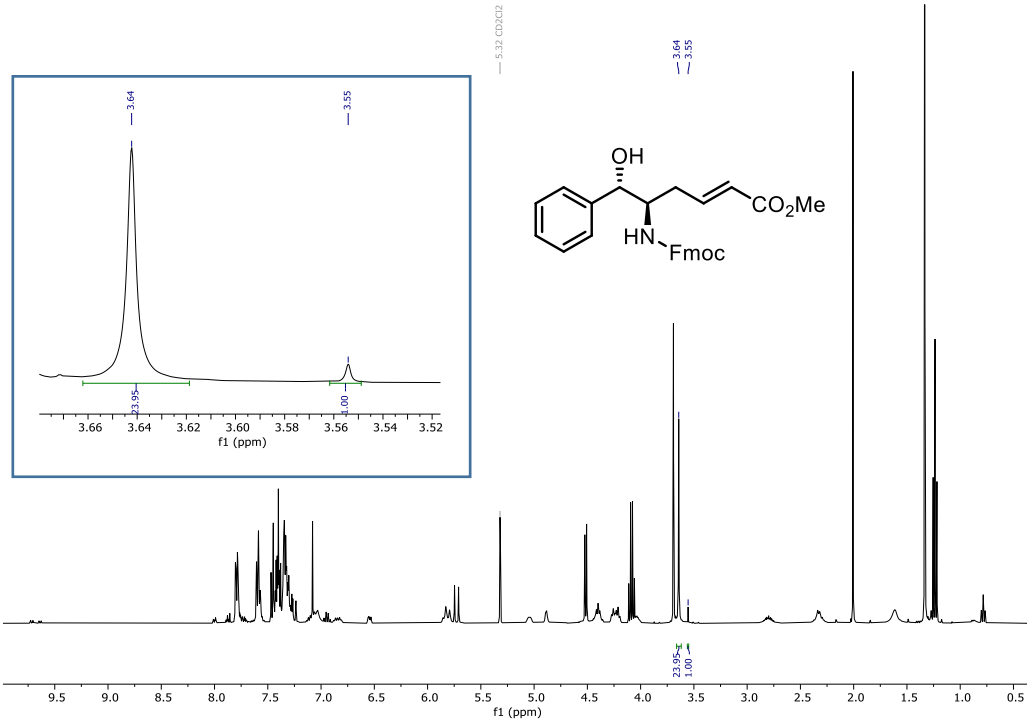

^{1}H NMR spectrum of the crude reaction mixture obtained in the synthesis of 117; rr ≈ 6:1

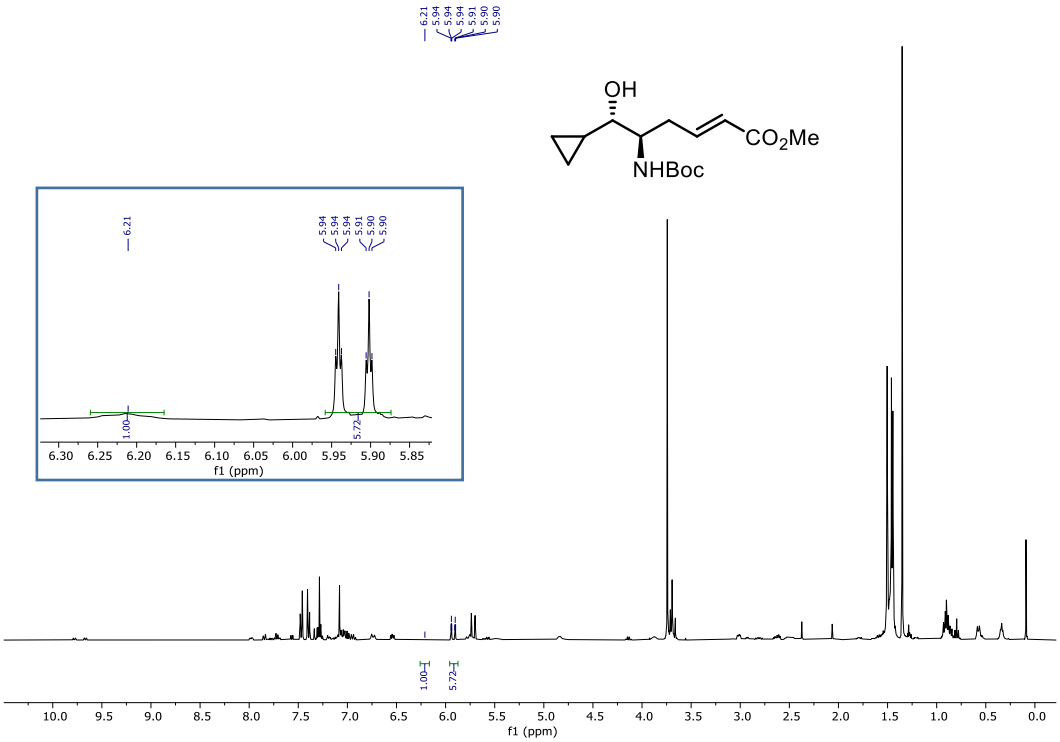

5.3.4 Enantioselective Synthesis of Vicinal Amino Alcohol Derivatives

Amino alcohol 90a. The title compound was prepared according to the general procedure **I** and oxidative work-up **I**, using benzaldehyde (20.3 µL, 0.20 mmol) and diene **88a** (90.9 mg, 0.40 mmol); the reaction time was 24 h. The crude material (rr > 20:1) was purified by flash chromatography (SiO_2, toluene/*tert*-butyl methyl ether, 4:1) and the product was obtained as an off-white solid (61.0 mg, 91%, > 20:1 dr, 91% ee). mp = 112-113 °C; $[\alpha]_D^{20}$ (99% ee, sample after recrystallization) = +14.0 (c = 0.50, $CHCl_3$); ^{1}H NMR (400 MHz, CD_2Cl_2): δ = 7.36 – 7.26 (m, 5H), 6.87 – 6.80 (m, 1H), 5.79 (dt, *J* = 15.6, 1.4 Hz, 1H), 4.87 (s, 1H), 4.80 (s, 1H), 3.95 (s, 1H), 3.66 (s, 3H), 3.24 (br, 1H), 2.36 – 2.22 (m, 2H), 1.40 (s, 9H); ^{13}C NMR (101 MHz, CD_2Cl_2): δ = 166.8, 156.5, 145.9, 141.4, 128.7, 128.1, 126.6, 123.5, 80.1, 76.4, 55.9, 51.7, 32.4, 28.4; IR (ATR): $\tilde{\nu}$ = 3453, 3358, 1689, 1651, 1525, 1323, 1228, 1165, 1016, 701 cm^{-1}; HRMS (ESI$^+$): *m/z*: calcd. for $C_{18}H_{25}NO_5Na$ $[M+Na]^+$: 358.16249, found: 358.16239.

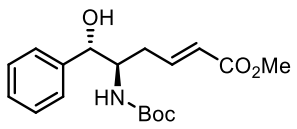

34.0 mg of the product were recrystallized from *tert*-butyl methyl ether/*iso*-hexane to give the enantioenriched product in 99% ee (28.6 mg).

The ee was determined by HPLC analysis: Chiralpak 150 mm IB-N-3, 3 µm, 4.6 mm ∅, *n*-heptane/*iso*-propanol = 95:5, v = 1.0 mL/min, λ = 220 nm, t(major) = 9.15 min, t(minor) = 10.68 min (racemate: top left, enantioenriched sample: top right, recrystallized enantioenriched sample: bottom left).

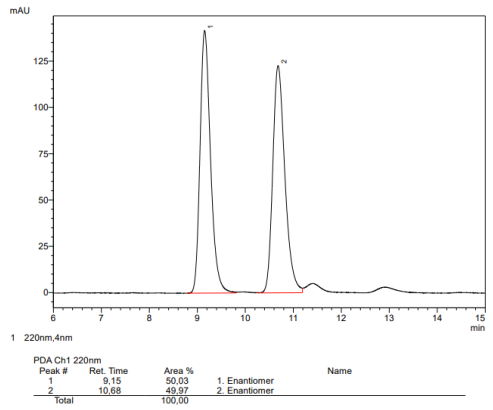

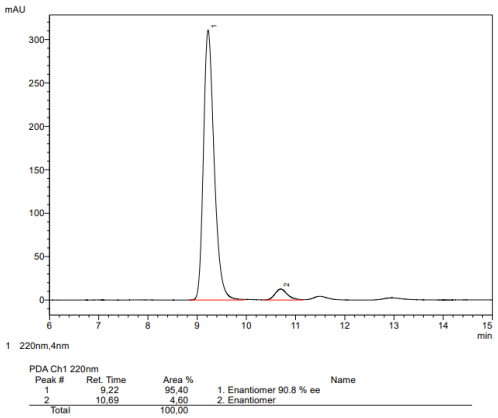

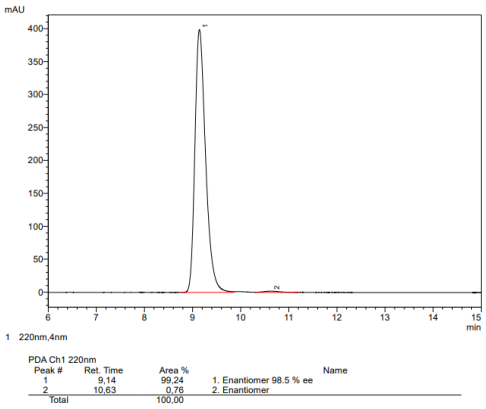

Gram-Scale Reaction. A flame-dried Schlenk flask under argon was charged with tris(*trans*-1,2-bis(4-*tert*-butylphenyl)ethene)nickel(0) (Ni($^{t\text{Bu}}$stb)$_3$) (318 mg, 0.34 mmol), phosphoramidite **L11** (217.5 mg, 0.34 mmol) and diene **88a** (1.55 g, 6.80 mmol). The Schlenk flask was evacuated and refilled with argon (3 cycles). THF (6.0 mL) and triethylborane (1 M in THF, 5.10 mL, 5.10 mmol) were added and the resulting red solution was stirred for 5 minutes. Benzaldehyde (344 µL, 3.40 mmol) was added under an argon counterflow, causing a color change of the mixture to intense orange. After addition of the aldehyde, a gas bubbler was connected to the Schlenk flask and the mixture was stirred under a very gentle flow of argon at room temperature for 24 h. At this point, TLC indicated full conversion of the aldehyde. The mixture was cooled to 0 °C and the reaction was quenched by addition of pH 7 phosphate buffer solution (10 mL) and aq. H_2O_2 (30% *w/w* in water, 4 mL). Ethyl acetate (25 mL) was added and the resulting mixture was vigorously stirred for 1 h. The organic layer was separated and the aqueous phase was extracted with ethyl acetate (3 x 40 mL). The combined organic layers were washed with sat. aq. $Na_2S_2O_3$ (25 mL) and brine (25 mL), dried over $MgSO_4$, filtered, and the solvent was removed under reduced pressure. The residue (rr = 15:1) was purified by flash chromatography (SiO_2, toluene/*tert*-butyl methyl ether, 4:1) to give product **90a** as an off-white solid (1.01 g, 88%, dr > 20:1, 90% ee). For the analytical and spectral data, see above.

A second fraction contained unreacted diene **88a** partly contaminated by the ligand. When this material was subjected to a second flash chromatographic purification using a different eluent (SiO_2, *iso*-hexane/ethyl acetate, 4:1), pure diene **88a** was recovered as a colorless solid (589 mg, 0.76 equiv.).

900 mg of **90a** were recrystallized from *tert*-butyl methyl ether/*iso*-hexane to give the enantioenriched product in 99% ee (707 mg).

Note: Single crystals suitable for X-ray diffraction analysis were obtained in the process of recrystallization and were used to determine the relative and absolute configuration of the vicinal amino alcohol product **90a**.

Amino alcohol 90b. The title compound was prepared according to the general procedure **I** and oxidative work-up **I**, using benzaldehyde (20.3 µL, 0.20 mmol) and diene **88b** (74.1 mg, 0.40 mmol); the reaction time was 24 h. The crude material (rr = 12:1) was purified by flash chromatography (SiO_2, toluene/*tert*-butyl methyl ether, 1.5:1) and the product was obtained as an off-white solid (50.5 mg, 86%, > 20:1 dr, 93% ee). $[\alpha]_D^{20}$ (> 99% ee, sample after recrystallization) = +7.6 (c = 0.50, $CHCl_3$); ^{1}H NMR (400 MHz, CD_2Cl_2): δ = 7.47 – 7.22 (m, 5H), 6.82 (ddd, *J* = 15.6, 7.6, 6.9 Hz, 1H), 5.79 (dt, *J* = 15.6, 1.5 Hz, 1H), 5.06 (d, *J* = 9.1 Hz, 1H), 4.90 (s, 1H), 3.99 (s, 1H), 3.66 (s, 3H), 3.62 (s, 3H), 3.01 (s, 1H), 2.56 – 2.14 (m, 2H); ^{13}C NMR (101 MHz, CD_2Cl_2): δ = 166.8, 157.4, 145.8, 141.2, 128.8, 128.1, 126.5, 123.6, 76.0, 56.3, 52.6, 51.7, 32.0; IR (ATR): $\tilde{\nu}$ = 3496, 3331, 1705, 1687, 1544, 1319, 1229, 1042, 706, 521 cm^{-1}; HRMS (CI): *m/z*: calcd. for $C_{15}H_{20}NO_5$ $[M+H]^+$: 294.13360, found: 294.13363.

19.0 mg of the product were recrystallized from *tert*-butyl methyl ether/*iso*-hexane to give the enantioenriched product in >99% ee (14.6 mg), mp = 101-102 °C. ***Note:*** Single crystals suitable for X-ray diffraction analysis were obtained in the process of recrystallization and were used to determine the relative and absolute configuration of the vicinal amino alcohol product **90b**.

The ee was determined by HPLC analysis: Chiralcel 150 mm IG-3, 3 µm, 4.6 mm ∅, acetonitrile/water = 20:80 → acetonitrile/water = 50:50 (over 10 minutes), v = 1.0 mL/min, λ = 220 nm, t(minor) = 9.12 min, t(major) = 9.87 min (racemate: top left, enantioenriched sample: top right, recrystallized enantioenriched sample: bottom left).

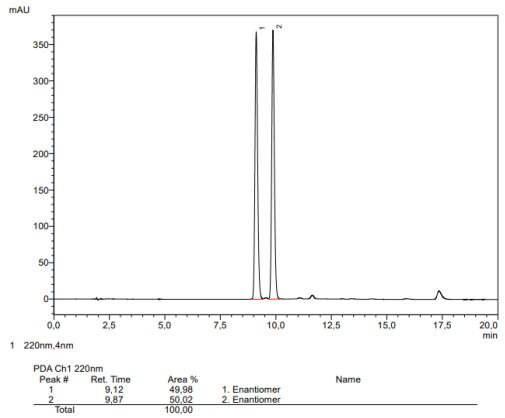

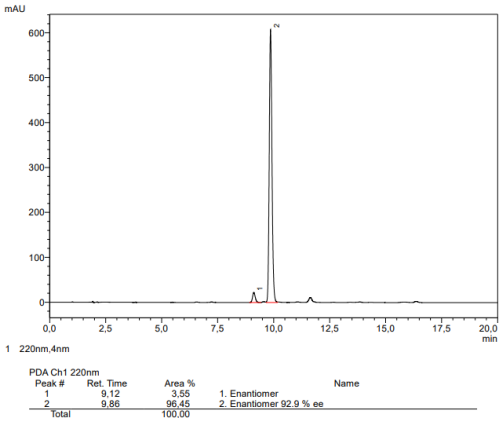

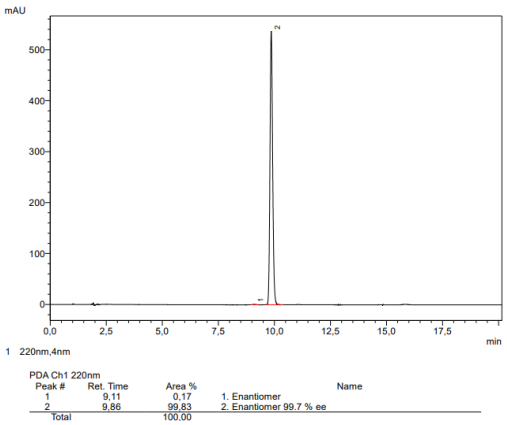

Amino alcohol 90c. The title compound was prepared according to the general procedure **I** and oxidative work-up **I**, using benzaldehyde (20.3 µL, 0.20 mmol) and diene **88c** (104.5 mg, 0.40 mmol); the reaction time was 16 h. The crude material (rr = 14:1) was purified by flash chromatography (SiO_2, toluene/*tert*-butyl methyl ether, 3:1) and the product was obtained as an off-white solid (61.0 mg, 83%, dr > 20:1, 89% ee). mp = 116-117 °C ; $[\alpha]_D^{20}$ (99% ee, sample after recrystallization) = +16.8 (c = 0.50, $CHCl_3$); ^{1}H NMR (400 MHz, CD_2Cl_2): δ = 7.38 – 7.27 (m, 10H), 6.88 – 6.80 (m, 1H), 5.80 (dt, *J* = 15.6, 1.5 Hz, 1H), 5.10 (br, 1H), 5.07 (s, 2H), 4.91 (s, 1H), 4.07 – 4.00 (m, 1H), 3.67 (s, 3H), 2.86 (s, 1H), 2.37 – 2.26 (m, 2H); ^{13}C NMR (101 MHz, CD_2Cl_2): δ = 166.8, 156.7, 145.8, 141.2, 137.1, 128.9, 128.8, 128.4, 128.2 , 128.1, 126.6, 123.6, 76.0, 67.1, 56.3, 51.7, 32.1; IR (ATR): $\tilde{\nu}$ = 3354, 1694, 1653, 1537, 1439, 1321, 1228, 1024, 986, 695 cm^{-1}; HRMS (ESI$^+$): *m/z*: calcd. for $C_{21}H_{23}NO_5Na$ $[M+Na]^+$: 392.14684, found: 392.14717.

18.0 mg of the product were recrystallized from dichloromethane/*iso*-hexane to give the enantioenriched product with 99% ee (13.7 mg).

The ee was determined by HPLC analysis: Chiralpak 150 mm IG-3, 3 µm, 4.6 mm ∅, *n*-heptane/*iso*-propanol = 80:20; v = 1.0 mL/min, λ = 220 nm, t(minor) = 8.28 min, t(major) = 17.11 min (racemate: top left, enantioenriched sample: top right, recrystallized enantioenriched sample: bottom left).

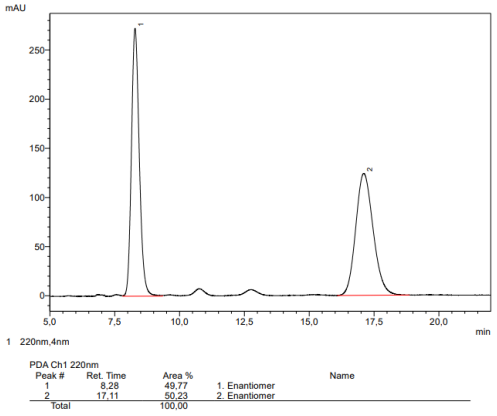

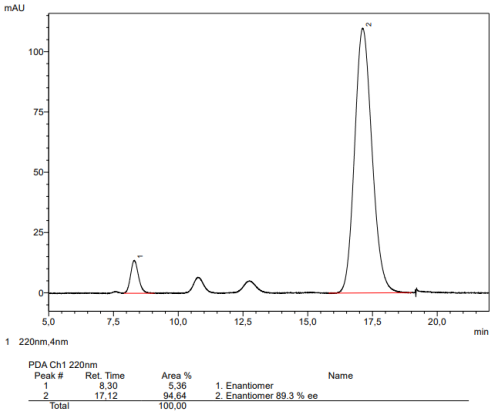

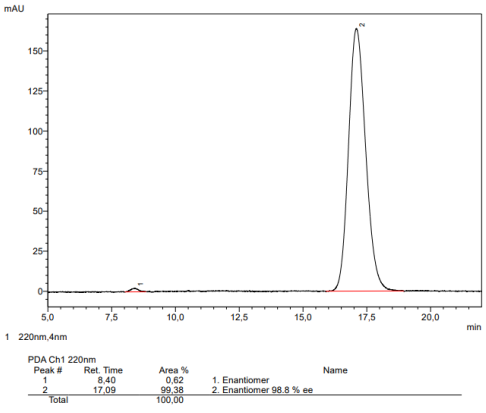

Amino alcohol 90d. The title compound was prepared according to the general procedure **I** and oxidative work-up **I**, using benzaldehyde (20.3 µL, 0.20 mmol) and diene **88d** (139.7 mg, 0.40 mmol). ***Note:*** *because of the low solubility of the diene, the volume of THF was increased to 1.2 mL.* The reaction time was 65 h. The crude material (rr > 20:1) was purified by flash chromatography (SiO_2, toluene/*tert*-butyl methyl ether, 3:1) and the product was obtained as an off-white solid (83.9 mg, 92%, dr > 20:1, 88% ee). mp = 157-158 °C; $[\alpha]_D^{20}$ (88% ee, sample before recrystallization) = +5.0 (c = 0.50, $CHCl_3$); ^{1}H NMR (600 MHz, CD_2Cl_2): δ = 7.79 (d, *J* = 7.5 Hz, 2H), 7.58 (d, *J* = 6.7 Hz, 2H), 7.44 – 7.39 (m, 2H), 7.39 – 7.26 (m, 7H), 6.84 (dt, *J* = 15.1, 7.2 Hz, 1H), 5.81 (d, *J* = 15.6 Hz, 1H), 4.99 (d, *J* = 9.1 Hz, 1H), 4.89 (s, 1H), 4.44 – 4.36 (m, 2H), 4.21 (t, *J* = 6.9 Hz, 1H), 4.05 – 4.02 (m, 1H), 3.64 (s, 3H), 2.71 (d, *J* = 3.7 Hz, 1H), 2.37 – 2.27 (m, 2H); ^{13}C NMR (151 MHz, CD_2Cl_2): δ = 166.7, 156.7, 145.5, 144.5, 144.3, 141.7, 141.7, 141.0, 128.8, 128.2, 128.1, 127.5, 126.6, 125.5, 125.4, 123.8, 120.3, 120.3, 76.1, 67.0, 56.3, 51.7, 47.7, 32.1; IR (ATR): $\tilde{\nu}$ = 3446, 1720, 1687, 1523, 1442, 1333, 1231, 1023, 988, 737 cm^{-1}; HRMS (ESI$^+$): *m/z*: calcd. for $C_{28}H_{28}NO_5Na$ $[M+Na]^+$: 458.19620, found: 458.19665.

20.0 mg of the product were recrystallized from dichloromethane/*iso*-hexane to give the enantioenriched product in 97% ee (14.6 mg).

The ee was determined by HPLC analysis: Chiralpak 150 mm IB-N-3, 3 µm, 4.6 mm ∅, acetonitrile/water = 70:30, v = 1.0 mL/min, λ = 220 nm, t(minor) = 6.20 min, t(major) = 8.84 min (racemate: top left, enantioenriched sample: top right, recrystallized enantioenriched sample: bottom left).

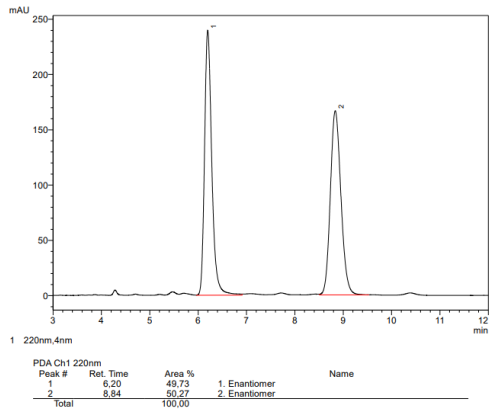

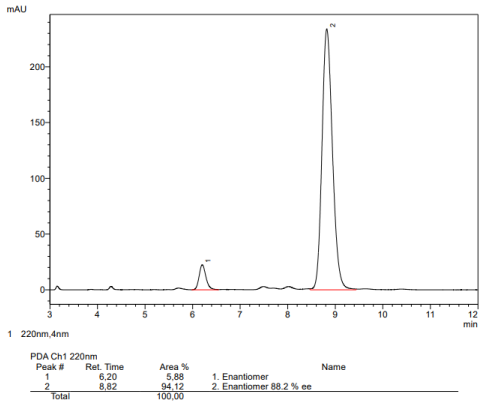

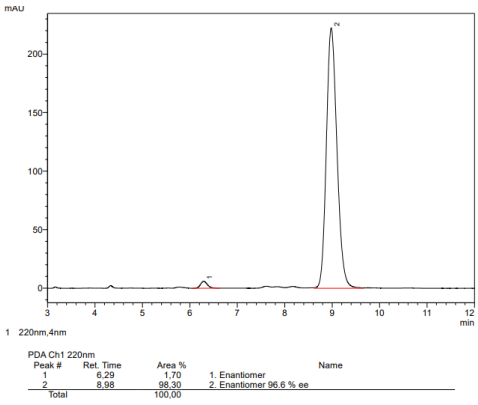

Amino alcohol 92. The title compound was prepared according to the general procedure **I** and oxidative work-up **I**, using methyl 4-formylbenzoate (32.8 mg, 0.20 mmol) and diene **88a** (90.9 mg, 0.40 mmol); the reaction time was 18 h. The crude material (rr > 20:1) was purified by flash chromatography (SiO_2, toluene/*tert*-butyl methyl ether, 3:1) and the product was obtained as an off-white solid (71.5 mg, 91%, dr > 20:1, 91% ee). mp = 128-129 °C; $[\alpha]_D^{20}$ (99% ee, sample after recrystallization) = +7.4 (c = 0.50, $CHCl_3$); ^{1}H NMR (400 MHz, CD_2Cl_2): δ = 8.02 – 7.99 (m, 2H), 7.47 – 7.43 (m, 2H), 6.82 (m, 1H), 5.79 (dt, *J* = 15.6, 1.5 Hz, 1H), 4.96 (t, *J* = 3.9 Hz, 1H), 4.80 (s, 1H), 3.96 (s, 1H), 3.89 (s, 3H), 3.66 (s, 3H), 3.40 (s, 1H), 2.30 – 2.26 (m, 2H), 1.41 (s, 9H); ^{13}C NMR (101 MHz, CD_2Cl_2): δ = 167.1, 166.7, 156.5, 146.5, 145.5, 130.1, 129.9, 126.7, 123.7, 80.3, 76.2, 56.0, 52.4, 51.7, 32.1, 28.4; IR (ATR): $\tilde{\nu}$ = 3368, 1720, 1700, 1679, 1519, 1439, 1276, 1164, 1018, 775 cm^{-1}; HRMS (ESI$^+$): *m/z*: calcd. for $C_{20}H_{27}NO_7Na$ $[M+Na]^+$: 416.16797, found: 416.16840.

62.5 mg of the product were recrystallized from *tert*-butyl methyl ether/*iso*-hexane to give the enantioenriched product in 99% ee (49.5 mg).

The ee was determined by HPLC analysis: Chiralpak 150 mm IC-3, 3 µm, 4.6 mm ∅, *n*-heptane/ethanol = 75:25, v = 1.0 mL/min, λ = 220 nm, t(minor) = 5.44 min, t(major) = 10.98 min (racemate: top left, enantioenriched sample: top right, recrystallized enantioenriched sample: bottom left).

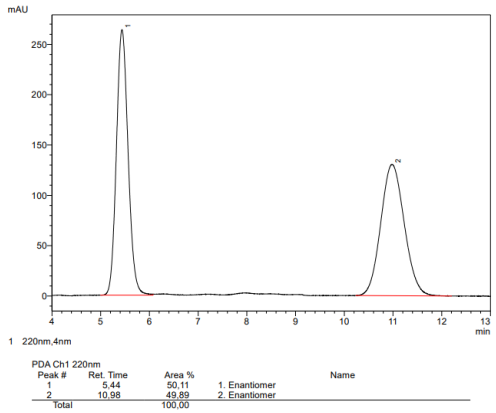

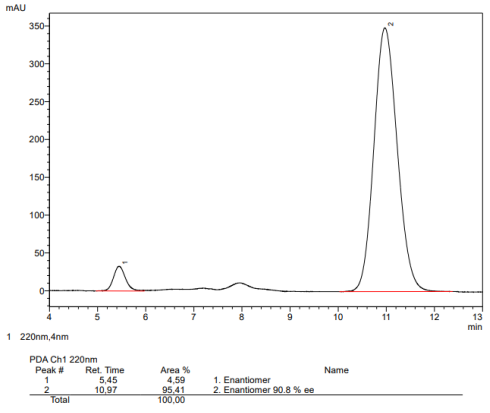

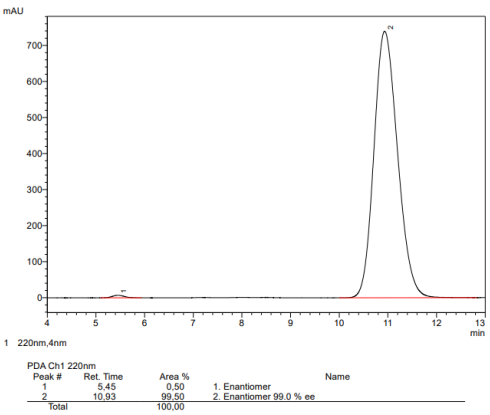

Amino alcohol 93. The title compound was prepared according to the general procedure **I** and

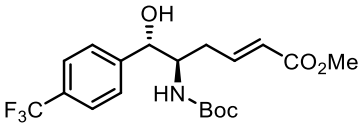

oxidative work-up **I**, using 4-(trifluoromethyl)benzaldehyde (27.3 µL, 0.20 mmol) and diene **88a** (90.9 mg, 0.40 mmol); the reaction time was 17 h. The crude material (rr = 18:1) was purified by flash chromatography (SiO_2, toluene/*tert*-butyl methyl ether, 4:1) and the product was obtained as an off-white solid (67.5 mg, 84%, dr > 20:1, 84% ee). Analytical data see below.

The ee was determined by HPLC analysis: Chiralpak 150 mm IC-3, 3 µm, 4.6 mm ∅, *n*-heptane/ethanol = 95:5, v = 1.0 mL/min, λ = 220 nm, t(minor) = 4.40 min, t(major) = 9.34 min (racemate: left, enantioenriched sample: right).

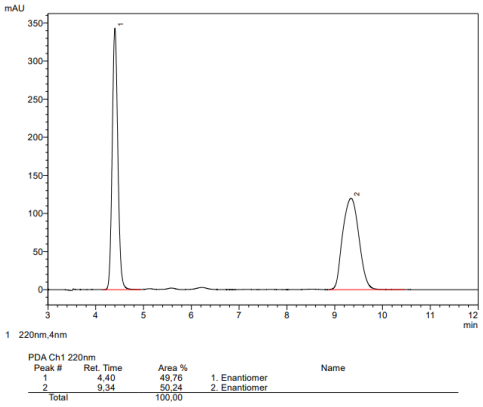

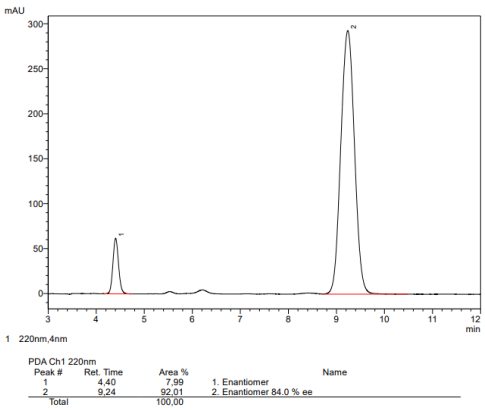

Reaction at –10 °C. The reaction was performed analogously but the reaction mixture was cooled to –10 °C before addition of the aldehyde. The mixture was then stirred at –10°C for 72 h. After work-up, the crude product (rr = 18:1) was purified by flash chromatography (SiO_2, toluene/*tert*-butyl methyl ether, 4:1) and the product was obtained as an off-white solid (61.5 mg, 77%, dr > 20:1, 89% ee). mp = 95-96 °C; $[\alpha]_D^{20}$ (99% ee, sample after recrystallization) = +33.4 (c = 0.50, $CHCl_3$); ^{1}H NMR (400 MHz, CD_2Cl_2): δ = 7.63 (d, *J* = 8.2 Hz, 2H), 7.51 (d, *J* = 8.1 Hz, 2H), 6.85 – 6.78 (m, 1H), 5.79 (dt, *J* = 15.6, 1.5 Hz, 1H), 4.95 (t, *J* = 4.0 Hz, 1H), 4.84 (d, *J* = 8.8 Hz, 1H), 3.96 (s, 1H), 3.66 (s, 3H), 3.59 (s, 1H), 2.32 – 2.28 (m, 2H), 1.39 (s, 9H); ^{13}C NMR (101 MHz, CD_2Cl_2): δ = 166.8, 156.5, 145.7, 145.4, 130.0 (q, $^2J_{CF}$ = 32.2 Hz), 127.2, 125.6 (q, $^3J_{CF}$ = 3.9 Hz), 124.7 (q, $^1J_{CF}$ = 271.8 Hz), 123.8, 80.4, 75.9, 56.0, 51.7, 32.1, 28.4; ^{19}F NMR (282 MHz, CD_2Cl_2): δ = –62.8; IR (ATR): $\tilde{\nu}$ = 3361, 1705, 1678, 1521, 1325, 1161, 1115, 1066, 836 cm^{-1}; HRMS (ESI$^+$): *m/z*: calcd. for $C_{19}H_{24}NO_5F_3Na$ $[M+Na]^+$: 426.14988, found: 426.14999.

37.0 mg of the product were recrystallized from ethyl acetate/*iso*-hexane to give the enantioenriched product in 99% ee (26.9 mg).

The ee was determined by HPLC analysis: Chiralpak 150 mm IC-3, 3 µm, 4.6 mm ∅, *n*-heptane/ethanol = 95:5, v = 1.0 mL/min, λ = 220 nm, t(minor) = 4.40 min, t(major) = 9.34 min (racemate: top left, enantioenriched sample: top right, recrystallized enantioenriched sample: bottom left).

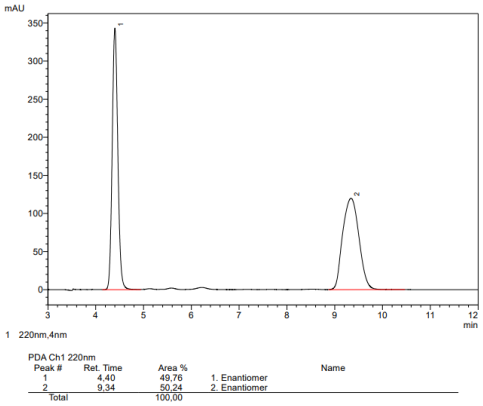

PDA Ch1 220nm

Peak #	Ret. Time	Area %	Name
1	4,40	49,76	1. Enantiomer
2	9,34	50,24	2. Enantiomer
Total		100,00	

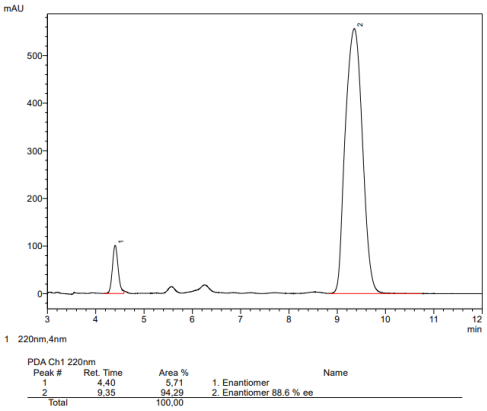

PDA Ch1 220nm

Peak #	Ret. Time	Area %	Name
1	4,40	5,71	1. Enantiomer
2	9,35	94,29	2. Enantiomer 88.6 % ee
Total		100,00	

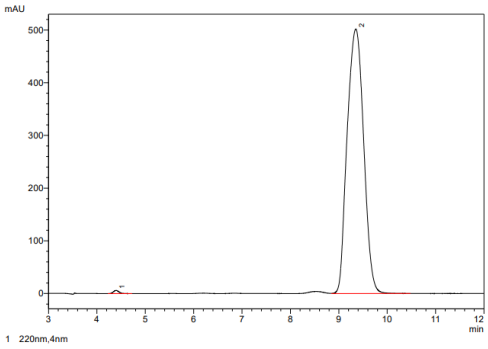

PDA Ch1 220nm

Peak #	Ret. Time	Area %	Name
1	4,39	0,42	1. Enantiomer
2	9,35	99,58	2. Enantiomer 99.2 % ee
Total		100,00	

Amino alcohol 94. The title compound was prepared according to the general procedure **I** and oxidative work-up **I**, using 4-methoxy benzaldehyde (24.3 µL, 0.20 mmol) and diene **88a** (136.4 mg, 0.60 mmol); the reaction time was 48 h. The crude material (rr = 12:1) was purified by flash chromatography (SiO_2, toluene/*tert*-butyl methyl ether, 3:1) and the product was obtained as an off-white solid (61.5 mg, 84%, dr > 20:1, 93% ee). mp = 108-109 °C; $[\alpha]_D^{20}$ (99% ee, sample after recrystallization) = +9.6 (c = 0.50, $CHCl_3$); ^{1}H NMR (400 MHz, CD_2Cl_2): δ = 7.28 – 7.25 (m, 2H), 6.91 – 6.81 (m, 3H), 5.80 (dt, *J* = 15.6, 1.5 Hz, 1H), 4.81 (s, 1H), 4.72 (d, *J* = 8.8 Hz, 1H), 3.92 (s, 1H), 3.79 (s, 3H), 3.67 (s, 3H), 2.98 (s, 1H), 2.38 – 2.20 (m, 2H), 1.40 (s, 9H); ^{13}C NMR (101 MHz, CD_2Cl_2): δ = 166.8, 159.7, 156.5, 145.9, 133.3, 127.8, 123.5, 114.1, 80.0, 76.0, 55.9, 55.6, 51.7, 32.6, 28.4; IR (ATR): $\tilde{\nu}$ = 3363, 1722, 1679, 1512, 1434, 1324, 1248, 1160, 980, 827 cm^{-1}; HRMS (ESI$^+$): *m/z*: calcd. for $C_{19}H_{27}NO_6Na$ [M+Na]$^+$: 388.17306, found: 388.17338.

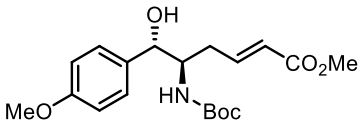

24.0 mg of the product were recrystallized from *tert*-butyl methyl ether/*iso*-hexane to give the enantioenriched product in 99% ee (21.3 mg).

The ee was determined by HPLC analysis: Chiralpak 150 mm IC-3, 3 µm, 4.6 mm ∅, *n*-heptane/ethanol = 90:10, v = 1.0 mL/min, λ = 225 nm, t(minor) = 16.04 min, t(major) = 18.62 min (racemate: top left, enantioenriched sample: top right, recrystallized enantioenriched sample: bottom left).

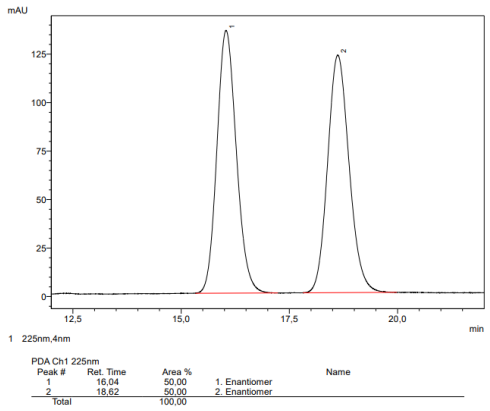

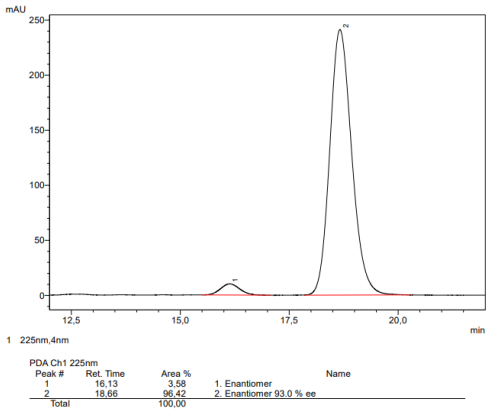

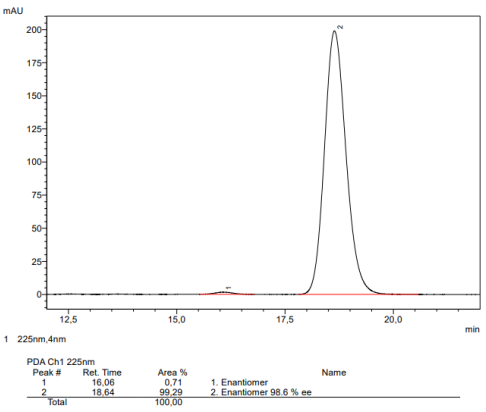

Amino alcohol 95. The title compound was prepared according to the general procedure **I** and oxidative work-up **I**, using 4-fluorobenzaldehyde (21.5 µL, 0.20 mmol) and diene **88a** (90.9 mg, 0.40 mmol); the reaction time was 24 h. The crude material (rr = 10:1) was purified by flash chromatography (SiO_2, toluene/*tert*-butyl methyl ether, 4:1) and the product was obtained as a colorless solid (60.7 mg, 86%, dr > 20:1, 92% ee). mp = 127-128 °C; $[\alpha]_D^{20}$ (99% ee, sample after recrystallization) = +17.6 (c = 0.50, $CHCl_3$); ^{1}H NMR (400 MHz, CD_2Cl_2): δ = 7.37 – 7.32 (m, 2H), 7.09 – 7.03 (m, 2H), 6.87 – 6.79 (m, 1H), 5.80 (dt, *J* = 15.6, 1.5 Hz, 1H), 4.86 (t, *J* = 4.0 Hz, 1H), 4.74 (d, *J* = 8.8 Hz, 1H), 3.92 (s, 1H), 3.67 (s, 3H), 3.23 (s, 1H), 2.36 – 2.22 (m, 2H), 1.40 (s, 9H); ^{13}C NMR (101 MHz, CD_2Cl_2): δ = 166.8, 162.7 (d, $^1J_{CF}$ = 245.0 Hz), 156.5, 145.6, 137.2, 128.4 (d, $^3J_{CF}$ = 8.0 Hz), 123.7, 115.5 (d, $^2J_{CF}$ = 21.5 Hz), 80.2, 75.9, 56.0, 51.7, 32.3, 28.4; ^{19}F NMR (282 MHz, CD_2Cl_2): δ = –115.7; IR (ATR): $\tilde{\nu}$ = 3372, 2951, 1713, 1679, 1523, 1504, 1324, 1217, 1164, 1026, 851 cm^{-1}; HRMS (ESI$^+$): *m/z*: calcd. for $C_{18}H_{24}NO_5FNa$ $[M+Na]^+$: 376.15307, found: 376.15298.

25.0 mg of the product were recrystallized from dichloromethane/*iso*-hexane to give the enantioenriched product in 99% ee (15.3 mg).

The ee was determined by HPLC analysis: Chiralpak 150 mm IC-3, 3 µm, 4.6 mm ∅, *n*-heptane/ethanol = 95:5, v = 1.0 mL/min, λ = 220 nm, t(minor) = 7.09 min, t(major) = 18.20 min (racemate: top left, enantioenriched sample: top right, recrystallized enantioenriched sample: bottom left).

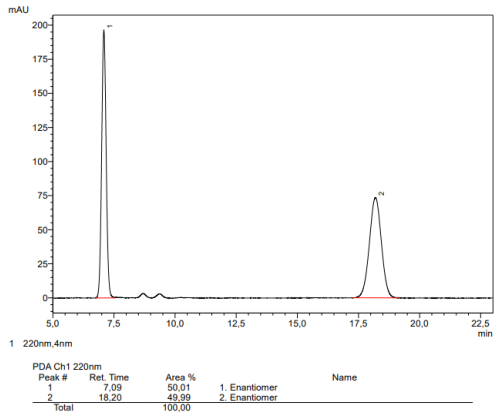

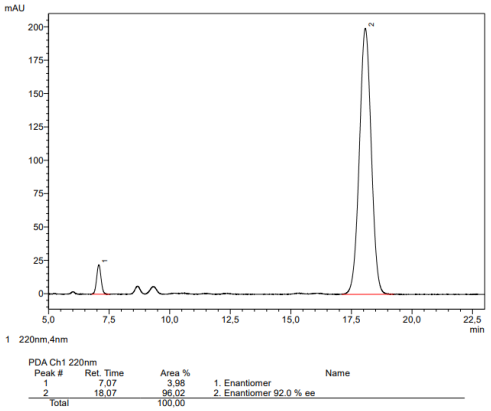

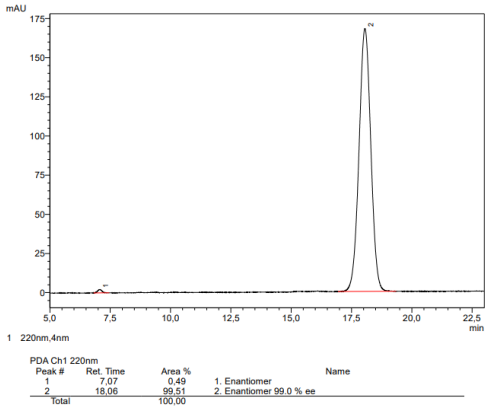

Amino alcohol 96. The title compound was prepared according to the general procedure **I** and oxidative work-up **I**, using 4-chlorobenzaldehyde (28.1 mg, 0.20 mmol) and diene **88a** (90.9 mg, 0.40 mmol); the reaction time was 20 h. The crude material (rr = 17:1) was purified by flash chromatography (SiO_2, toluene/*tert*-butyl methyl ether, 3:1) and the product was obtained as an off-white solid (62.6 mg, 85%, dr > 20:1, 87% ee). mp = 130-131 °C; $[\alpha]_D^{20}$ (99% ee, sample after recrystallization) = +20.8 (c = 0.50, $CHCl_3$); ^{1}H NMR (400 MHz, CD_2Cl_2): δ = 7.37 – 7.30 (m, 4H), 6.86 – 6.78 (m, 1H), 5.80 (dt, *J* = 15.6, 1.5 Hz, 1H), 4.87 (t, *J* = 3.9 Hz, 1H), 4.73 (d, *J* = 8.6 Hz, 1H), 3.92 (s, 1H), 3.67 (s, 3H), 3.23 (s, 1H), 2.35 – 2.22 (m, 2H), 1.40 (s, 9H); ^{13}C NMR (101 MHz, CD_2Cl_2): δ = 166.9, 156.5, 145.7, 140.1, 133.6, 128.8, 128.2, 123.6, 80.2, 75.7, 55.9, 51.7, 32.2, 28.4; IR (ATR): $\tilde{\nu}$ = 3451, 1682, 1526, 1439, 1327, 1282, 1166, 1012, 978, 825 cm^{-1}; HRMS (ESI$^+$): *m/z*: calcd. for $C_{18}H_{24}NO_5ClNa$ [M+Na]$^+$: 392.12352, found: 392.12347.

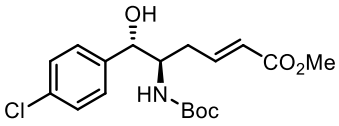

24.0 mg of the product were recrystallized from dichloromethane/*iso*-hexane to give the enantioenriched product in 99% ee (16.1 mg).

The ee was determined by HPLC analysis: Chiralcel 150 mm IG-3, 3 µm, 4.6 mm ∅, acetonitrile/water = 40:60; v = 1.0 mL/min, λ = 220 nm, t(minor) = 7.82 min, t(major) = 8.82 min (racemate: top left, enantioenriched sample: top right, recrystallized enantioenriched sample: bottom left).

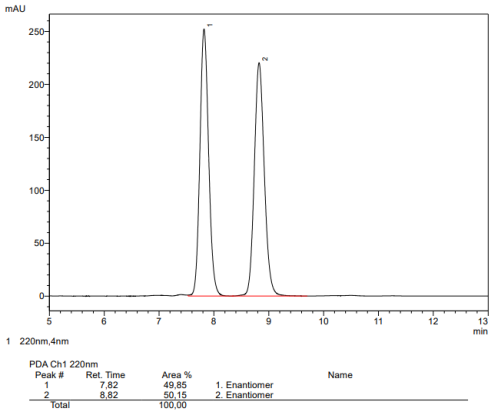

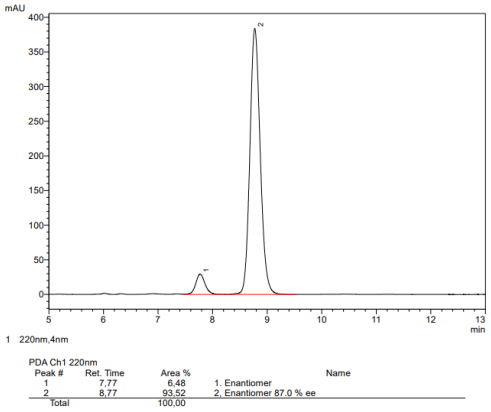

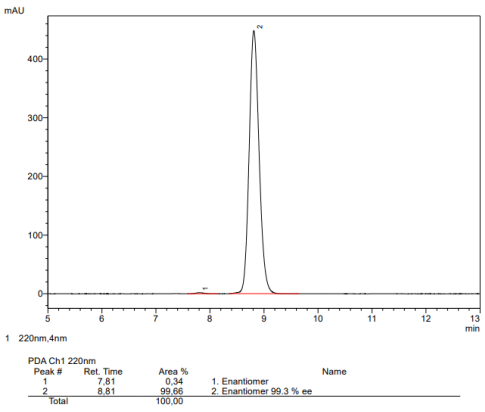

Amino alcohol 97. The title compound was prepared according to the general procedure **I** and basic work-up **II**, using 4-(4,4,5,5-tetramethyl-1,3,2-dioxaborolan-2-yl)benzaldehyde (46.4 mg, 0.20 mmol) and diene **88a** (90.9 mg, 0.40 mmol); the reaction time was 24 h. The crude material (rr = 11:1) was purified by flash chromatography (SiO_2, toluene/*tert*-butyl methyl ether, 4:1) and the product was obtained as an off-white solid (55.7 mg, 0.12 mmol, 60%, dr > 20:1, 90% ee). mp = 90 °C; $[\alpha]_D^{20}$ (90% ee) = +10.6 (c = 0.50, $CHCl_3$); ^{1}H NMR (400 MHz, CD_2Cl_2): δ = 7.76 – 7.74 (m, 2H), 7.37 – 7.35 (m, 2H), 6.86 – 6.79 (m, 1H), 5.78 (dt, *J* = 15.6, 1.5 Hz, 1H), 4.91 (t, *J* = 3.8 Hz, 1H), 4.76 (d, *J* = 8.9 Hz, 1H), 3.96 (s, 1H), 3.66 (s, 3H), 3.20 (s, 1H), 2.28 – 2.20 (m, 2H), 1.41 (s, 9H), 1.33 (s, 12H); ^{13}C NMR (101 MHz, CD_2Cl_2): δ = 166.8, 156.5, 145.8, 144.4, 135.1, 126.0, 123.6, 84.3, 80.1, 76.4, 56.0, 51.7, 32.3, 28.4, 25.1; IR (ATR): $\tilde{\nu}$ = 3360, 1698, 1514, 1358, 1319, 1269, 1143, 1087, 1019, 859 cm^{-1}; HRMS (ESI$^+$): *m/z*: calcd. for $C_{24}H_{36}BNO_7Na$ $[M+Na]^+$: 484.24770, found: 484.24792.

The ee was determined by HPLC analysis: Chiralpak 150 mm IC-3, 3 µm, 4.6 mm ∅, *n*-heptane/ethanol = 95:5, v = 1.0 mL/min, λ = 230 nm, t(minor) = 10.10 min, t(major) = 21.35 min (racemate left, enantioenriched sample right).

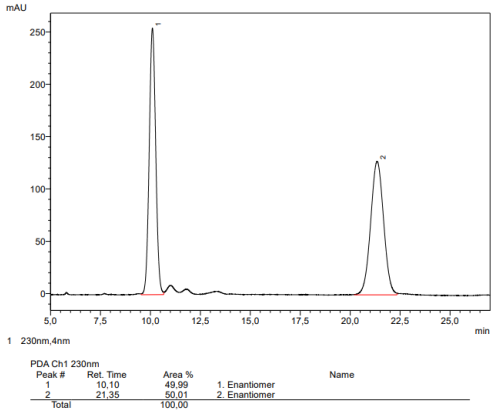

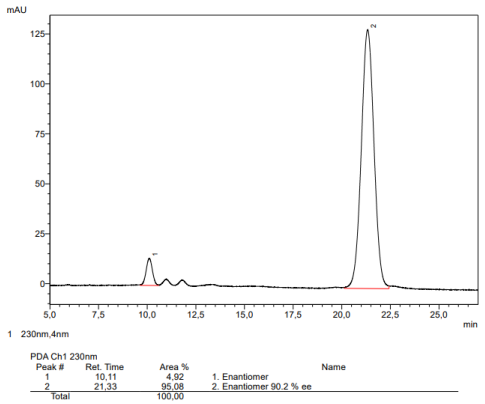

Amino alcohol 98. The title compound was prepared according to the general procedure **I** and oxidative work-up **I**, using 3-methylbenzaldehyde (23.5 µL, 0.20 mmol) and diene **88a** (90.9 mg, 0.40 mmol); the reaction time was 40 h. The crude material (rr = 8:1) was purified by flash chromatography (SiO_2, toluene/*tert*-butyl methyl ether, 4:1) and the product was obtained as an off-white solid (56.0 mg, 80%, dr > 20:1, 87% ee). mp = 95-96 °C; $[\alpha]_D^{20}$ (95% ee, sample after recrystallization) = +17.0 (c = 0.50, $CHCl_3$); ^{1}H NMR (400 MHz, CD_2Cl_2): δ = 7.26 – 7.22 (m, 1H), 7.18 – 7.09 (m, 3H), 6.87 – 6.80 (m, 1H), 5.79 (dt, *J* = 15.6, 1.5 Hz, 1H), 4.85 – 4.81 (m, 2H), 3.94 (s, 1H), 3.66 (s, 3H), 3.18 (s, 1H), 2.35 (s, 3H), 2.33 – 2.21 (m, 2H), 1.41 (s, 9H); ^{13}C NMR (101 MHz, CD_2Cl_2): δ = 166.9, 156.5, 146.1, 141.3, 138.5, 128.7, 128.6, 127.3, 123.6, 123.5, 80.0, 76.3, 56.0, 51.7, 32.3, 28.4, 21.6; IR (ATR): $\tilde{\nu}$ = 3352, 2934, 1723, 1680, 1526, 1433, 1309, 1159, 1013, 974 cm^{-1}; HRMS (ESI$^+$): *m/z*: calcd. for $C_{19}H_{27}NO_5Na$ $[M+Na]^+$: 372.17814, found: 372.17811.

40 mg of the product were recrystallized from *tert*-butyl methyl ether/*iso*-hexane to give the enantioenriched product in 95% ee (19.9 mg).

The ee was determined by HPLC analysis: Chiralpak 150 mm IC-3, 3 µm, 4.6 mm ∅, *n*-heptane/ethanol = 90:10, v = 1.0 mL/min, λ = 220 nm, t(minor) = 4.90 min, t(major) = 13.32 min (racemate: top left, enantioenriched sample: top right, recrystallized enantioenriched sample: bottom left).

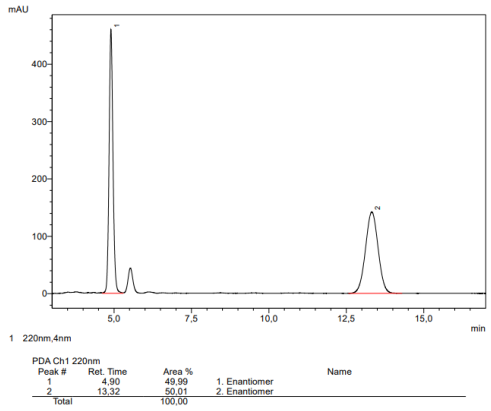

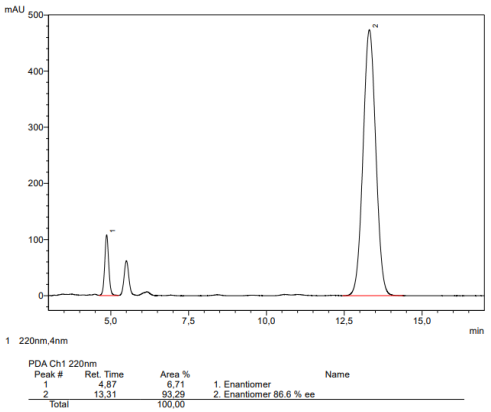

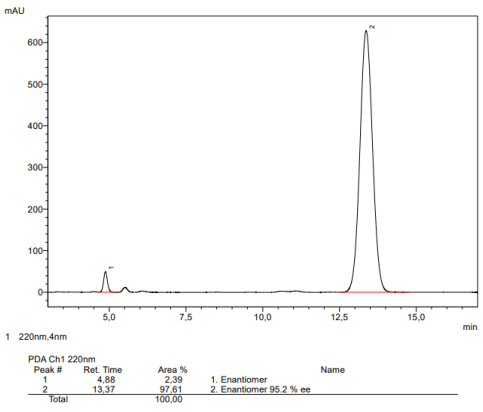

Amino alcohol 99. The title compound was prepared according to the general procedure **I** and

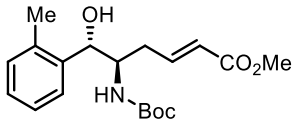

oxidative work-up **I**, using 2-methylbenzaldehyde (23.1 µL, 0.20 mmol) and diene **88a** (90.9 mg, 0.40 mmol); the reaction time was 30 h. The crude material (rr = 5:1) was purified by flash chromatography (SiO_2, toluene/*tert*-butyl methyl ether, 4:1) and the product was obtained as an off-white solid (49.3 mg, 71%, dr > 20:1, 92% ee). mp = 122-123 °C; $[\alpha]_D^{20}$ (99% ee, sample after recrystallization) = +51.8 (c = 0.50, $CHCl_3$); ^{1}H NMR (400 MHz, CD_2Cl_2): δ = 7.51 – 7.49 (m, 1H), 7.24 – 7.14 (m, 3H), 6.85 – 6.78 (m, 1H), 5.78 (dt, *J* = 15.6, 1.5 Hz, 1H), 5.12 (s, 1H), 4.97 (d, *J* = 8.7 Hz, 1H), 3.92 – 3.84 (m, 1H), 3.66 (s, 3H), 2.75 (s, 1H), 2.43 – 2.27 (m, 2H), 2.37 (s, 3H), 1.41 (s, 9H); ^{13}C NMR (101 MHz, CD_2Cl_2): δ = 166.9, 156.1, 146.5, 139.6, 135.3, 130.9, 127.8, 126.4, 126.3, 123.4, 79.9, 73.3, 54.0, 51.6, 31.2, 28.4, 19.2; IR (ATR): $\tilde{\nu}$ = 3359, 1718, 1683, 1657, 1530, 1436, 1317, 1241, 1161, 1023 cm^{-1}; HRMS (ESI$^+$): *m/z*: calcd. for $C_{19}H_{27}NO_5Na$ $[M+Na]^+$: 372.17814, found: 372.17827.

20.5 mg of the product were recrystallized from *tert*-butyl methyl ether/*iso*-hexane to give the enantioenriched product in 99% ee (17.5 mg).

The ee was determined by HPLC analysis: Chiralpak 150 mm IC-3, 3 µm, 4.6 mm ∅, *n*-heptane/ethanol = 95:5, v = 1.0 mL/min, λ = 220 nm, t(minor) = 8.99 min, t(major) = 20.58 min (racemate: top left, enantioenriched sample: top right, recrystallized enantioenriched sample: bottom left).

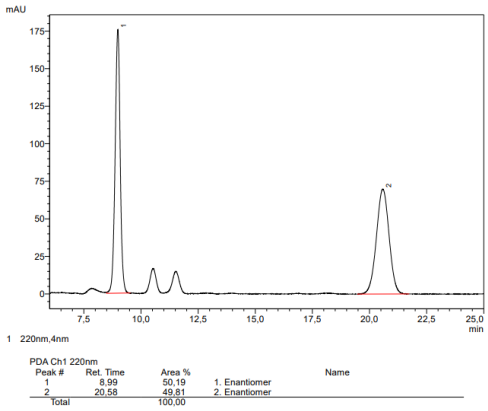

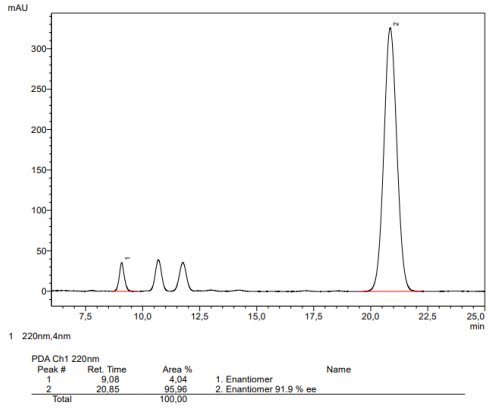

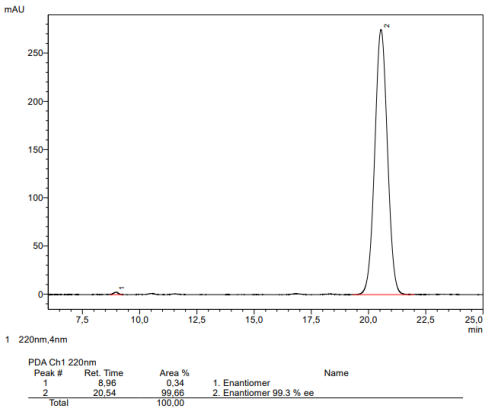

Amino alcohol 100. The title compound was prepared according to the general procedure **I** and oxidative work-up **I**, using 2-naphthaldehyde (31.2 mg, 0.20 mmol) and diene **88a** (90.9 mg, 0.40 mmol); the reaction time was 23 h. The crude material (rr = 14:1) was purified by flash chromatography (SiO_2, toluene/*tert*-butyl methyl ether, 4:1) and the product was obtained as an off-white solid (65.6 mg, 85%, dr > 20:1, 89% ee). mp = 132-133 °C; $[\alpha]_D^{20}$ (99% ee, sample after recrystallization) = +4.2 (c = 0.50, $CHCl_3$); ^{1}H NMR (400 MHz, CD_2Cl_2): δ = 7.86 – 7.83 (m, 4H), 7.52 – 7.46 (m, 3H), 6.87 – 6.79 (m, 1H), 5.77 (dt, *J* = 15.6, 1.5 Hz, 1H), 5.05 (s, 1H), 4.86 (d, *J* = 8.9 Hz, 1H), 4.05 (s, 1H), 3.64 (s, 3H), 3.39 (s, 1H), 2.38 – 2.26 (m, 2H), 1.40 (s, 9H); ^{13}C NMR (101 MHz, CD_2Cl_2): δ =166.8, 156.5, 145.9, 138.9, 133.6, 133.4, 128.4, 128.3, 128.0, 126.6, 126.4, 125.5, 124.7, 123.5, 80.1, 76.5, 56.0, 51.6, 32.3, 28.4; IR (ATR): $\tilde{\nu}$ = 3348, 2926, 1714, 1679, 1503, 1353, 1217, 1153, 1121, 819 cm^{-1}; HRMS (ESI$^+$): *m/z*: calcd. for $C_{22}H_{27}NO_5Na$ $[M+Na]^+$: 408.17814, found: 408.17812.

31.0 mg of the product were recrystallized from *tert*-butyl methyl ether/*iso*-hexane to give the enantioenriched product in 99% ee (23.7 mg).

The ee was determined by HPLC analysis: Chiralpak 150 mm IA-3, 3 µm, 4.6 mm ∅, *n*-heptane/ethanol = 95:5, v = 1.0 mL/min, λ = 225 nm, t(minor) = 13.23 min, t(major) = 16.91 min (racemate: top left, enantioenriched sample: top right, recrystallized enantioenriched sample: bottom left).

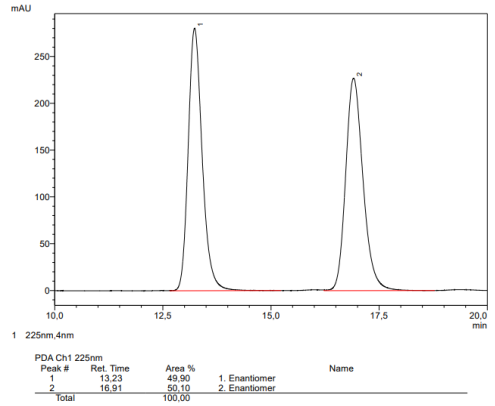

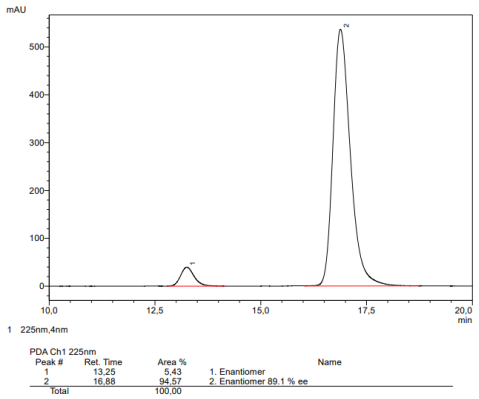

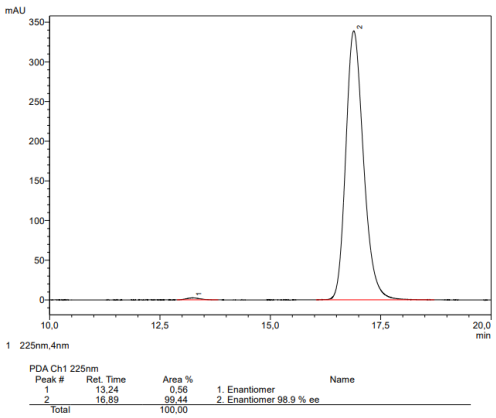

Amino alcohol 101. The title compound was prepared according to the general procedure **I** and oxidative work-up **I**, using furfural (16.6 µL, 0.20 mmol) and diene **88a** (90.9 mg, 0.40 mmol); the reaction time was 23 h. The crude material (rr = 13:1) was purified by flash chromatography (SiO_2, toluene/*tert*-butyl methyl ether, 4:1 → 2:1) and the product was obtained as an off-white solid (55.1 mg, 85%, dr > 20:1, 93% ee). mp = 98-100 °C; $[\alpha]_D^{20}$ (99% ee, sample after recrystallization) = +12.6 (c = 0.50, $CHCl_3$); ^{1}H NMR (400 MHz, $CDCl_3$): δ = 7.39 (dd, *J* = 1.8, 0.9 Hz, 1H), 6.93 – 6.85 (m, 1H), 6.35 (dd, *J* = 3.3, 1.8 Hz, 1H), 6.31 (dt, *J* = 3.3, 0.8 Hz, 1H), 5.84 (dt, *J* = 15.6, 1.4 Hz, 1H), 4.81 (br, 2H), 4.11 (s, 1H), 3.71 (s, 3H), 2.43 – 2.30 (m, 2H), 1.42 (s, 9H); ^{13}C NMR (101 MHz, $CDCl_3$): δ = 166.7, 156.4, 153.6, 144.9, 142.5, 123.7, 110.5, 107.9, 80.3, 70.5, 54.2, 51.6, 33.4, 28.4; IR (ATR): $\tilde{\nu}$ = 3356, 1720, 1682, 1252, 1164, 1007, 976, 736 cm^{-1}; HRMS (ESI$^+$): *m/z*: calcd. for $C_{16}H_{23}NO_6Na$ $[M+Na]^+$: 348.14176, found: 348.14190.

26.0 mg of the product were recrystallized from *tert*-butyl methyl ether/*iso*-hexane to give the enantioenriched product in 99% ee (20.8 mg).

The ee was determined by HPLC analysis: Chiralpak 150 mm IC-3, 3 µm, 4.6 mm ∅, *n*-heptane/ethanol = 90:10, v = 1.0 mL/min, λ = 220 nm, t(minor) = 6.19 min, t(major) = 22.26 min (racemate: top left, enantioenriched sample: top right, recrystallized enantioenriched sample: bottom left).

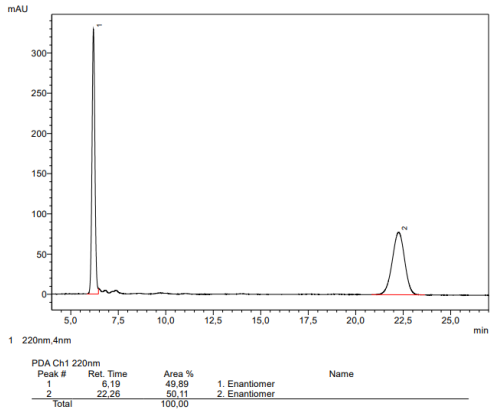

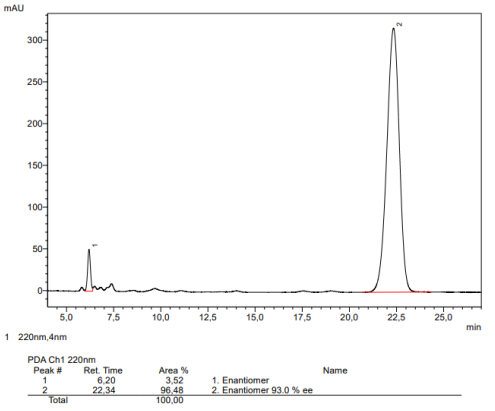

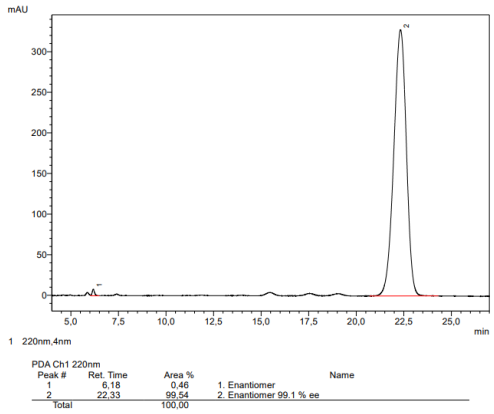

Amino alcohol 102. The title compound was prepared according to the general procedure **I** and

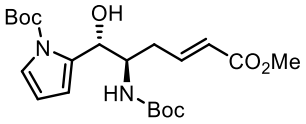

oxidative work-up **I**, using N-Boc-pyrrole-2-carboxaldehyde (39.0 mg, 0.20 mmol) and diene **88a** (136.4 mg, 0.60 mmol); the reaction time was 48 h. The crude material (rr > 20:1) was purified by flash chromatography (SiO_2, toluene/*tert*-butyl methyl ether, 6:1) and the product was obtained as a viscous yellowish oil (65.1 mg, 77%, dr > 20:1, 91% ee). $[\alpha]_D^{20}$ (91% ee) = –7.2 (c = 0.50, $CHCl_3$); ^{1}H NMR (400 MHz, CD_2Cl_2): δ = 7.19 (s, 1H), 6.99 – 6.92 (m, 1H), 6.24 – 6.22 (m, 1H), 6.10 (t, *J* = 3.4 Hz, 1H), 5.89 (dt, *J* = 15.6, 1.5 Hz, 1H), 4.76 (t, *J* = 7.2 Hz, 1H), 4.62 (d, *J* = 9.9 Hz, 1H), 4.18 – 4.08 (m, 2H), 3.69 (s, 3H), 2.76 – 2.69 (m, 1H), 2.48 – 2.40 (m, 1H), 1.60 (s, 9H), 1.32 (s, 9H); ^{13}C NMR (101 MHz, CD_2Cl_2): δ = 166.9, 155.5, 150.9, 146.1, 135.1, 123.6, 122.9, 113.9, 110.5, 85.4, 79.5, 70.9, 52.9, 51.6, 34.5, 28.4, 28.1; IR (ATR): $\tilde{\nu}$ = 3370, 2977, 1710, 1493, 1327, 1248, 1161, 1125, 1042, 725 cm^{-1}; HRMS (ESI$^+$): *m/z*: calcd. for $C_{21}H_{32}N_2O_7Na$ $[M+Na]^+$: 447.21017, found: 447.21050.

The ee was determined by HPLC analysis: Chiralpak 150 mm IC-3, 3 µm, 4.6 mm ∅, *n*-heptane/ethanol = 95:5, v = 1.0 mL/min, λ = 230 nm, t(minor) = 10.69 min, t(major) = 18.45 min (racemate: left, enantioenriched sample: right).

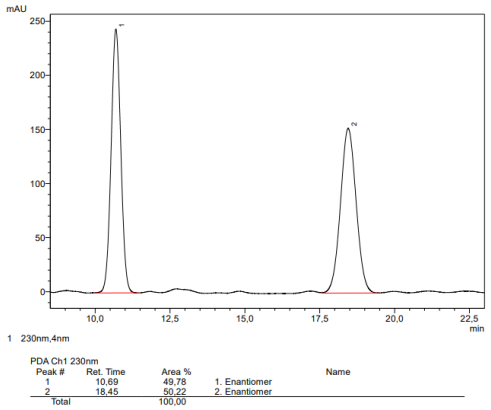

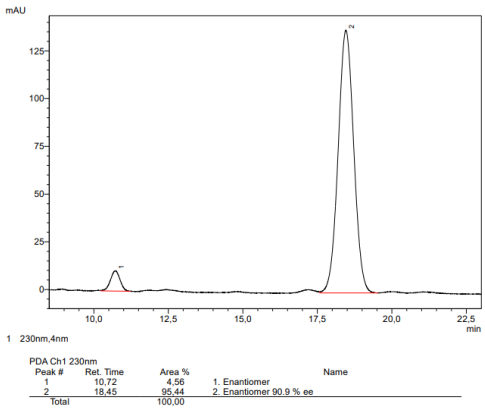

Amino alcohol 103. The title compound was prepared according to the general procedure **I** and

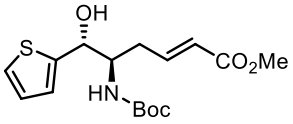

oxidative work-up **I**, using thiophene-2-carbaldehyde (18.7 µL, 0.20 mmol) and diene **88a** (136.4 mg, 0.60 mmol); the reaction time was 48 h. The crude material (rr = 10:1) was purified by flash chromatography (SiO_2, toluene/*tert*-butyl methyl ether, 4:1) and the product was obtained as a pale yellow solid (52.1 mg, 76%, dr > 20:1, 73% ee). mp = 106-108 °C; $[\alpha]_D^{20}$ (99% ee, sample after recrystallization) = +11.2 (c = 0.50, $CHCl_3$); ^{1}H NMR (400 MHz, CD_2Cl_2): δ = 7.28 (dd, *J* = 4.9, 1.3 Hz, 1H), 7.01 – 6.97 (m, 2H), 6.87 (ddd, *J* = 15.6, 7.9, 6.8 Hz, 1H), 5.83 (dt, *J* = 15.6, 1.5 Hz, 1H), 5.08 (s, 1H), 4.85 (d, *J* = 8.8 Hz, 1H), 4.00 (s, 1H), 3.83 (s, 1H), 3.68 (s, 3H), 2.45 – 2.39 (m, 1H), 2.34 – 2.26 (m, 1H), 1.41 (s, 9H); ^{13}C NMR (101 MHz, CD_2Cl_2): δ = 166.8, 156.8, 145.5, 145.0, 127.2, 125.1, 124.7, 123.7, 80.4, 73.4, 56.0, 51.7, 33.0, 28.4; IR (ATR): $\tilde{\nu}$ = 3358, 1691, 1650, 1526, 1322, 1227, 1166, 1048, 979, 639 cm^{-1}; HRMS (ESI$^+$): *m/z*: calcd. for $C_{16}H_{23}NO_5SNa$ $[M+Na]^+$: 364.11892, found: 364.11882.

16.0 mg of the product were recrystallized from *tert*-butyl methyl ether/*iso*-hexane to give the enantioenriched product in 99% ee (7.9 mg).

The ee was determined by HPLC analysis: Chiralpak 150 mm IG-3, 3 µm, 4.6 mm ∅, *n*-heptane/ethanol = 90:10, v = 1.0 mL/min, λ = 230 nm, t(minor) = 12.22 min, t(major) = 21.18 min (racemate: top left, enantioenriched sample: top right, recrystallized enantioenriched sample: bottom left).

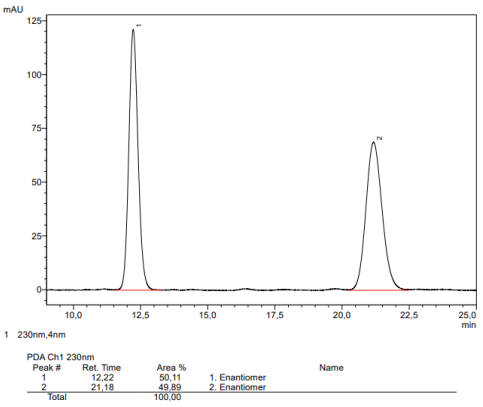

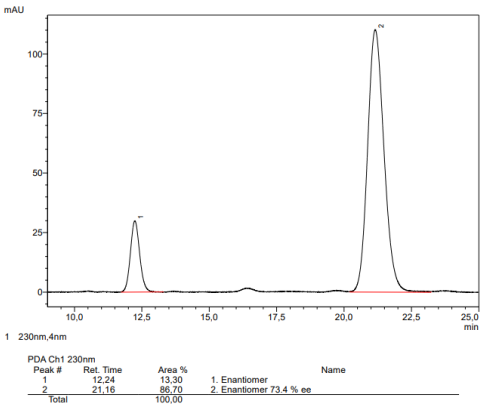

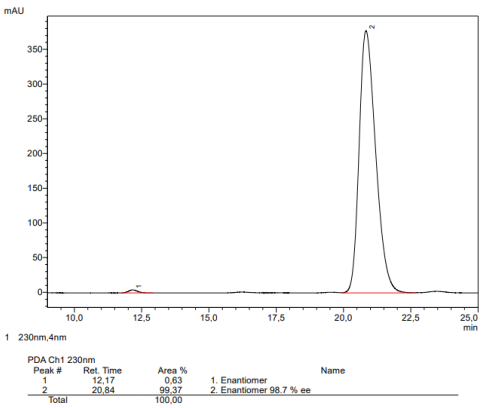

Amino alcohol 104. The title compound was prepared according to the general procedure **I** and oxidative work-up **I**, using 4-cyanobenzaldehyde (26.2 mg, 0.20 mmol) and diene **88a** (90.9 mg, 0.40 mmol); the reaction time was 72 h. The crude material (rr = 8:1) was purified by flash chromatography (SiO_2, toluene/*tert*-butyl methyl ether, 3:1) and the product was obtained as an off-white solid (39.3 mg, 55%, dr > 20:1, 68% ee). mp = 110-113 °C; $[\alpha]_D^{20}$ (88% ee, sample after recrystallization) = +2.6 (c = 0.50, $CHCl_3$); ^{1}H NMR (400 MHz, CD_2Cl_2): δ = 7.68 – 7.64 (m, 2H), 7.52 – 7.49 (m, 2H), 6.84 – 6.77 (m, 1H), 5.80 (dt, *J* = 15.6, 1.5 Hz, 1H), 4.95 (s, 1H), 4.79 (d, *J* = 8.7 Hz, 1H), 3.93 (s, 1H), 3.67 (s, 3H), 3.50 (s, 1H), 2.35 – 2.22 (m, 2H), 1.40 (s, 9H); ^{13}C NMR (101 MHz, CD_2Cl_2): δ = 166.7, 156.5, 146.8, 145.1, 132.6 , 127.5 , 123.9, 119.1, 111.9, 80.5, 76.0, 56.0, 51.7, 32.0, 28.4; IR (ATR): $\tilde{\nu}$ = 3367, 2926, 2229, 1703, 1518, 1367, 1276, 1167, 1044 cm^{-1}; HRMS (ESI$^+$): *m/z*: calcd. for $C_{19}H_{24}N_2O_5Na$ $[M+Na]^+$: 383.15774, found: 383.15758.

35.0 mg of the product were recrystallized from *tert*-butyl methyl ether/*iso*-hexane to give the enantioenriched product in 88% ee (25.0 mg).

The ee was determined by HPLC analysis: Chiralpak 150 mm IB-N-3, 3 µm, 4.6 mm ∅, *n*-heptane/*iso*-propanol = 90:10, v = 1.0 mL/min, λ = 230 nm, t(major) = 7.74 min, t(minor) = 10.94 min (racemate: top left, enantioenriched sample: top right, recrystallized enantioenriched sample: bottom left).

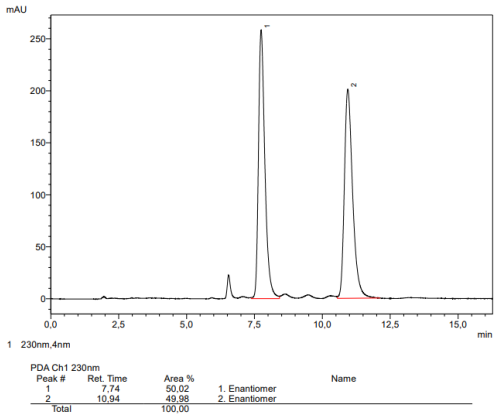

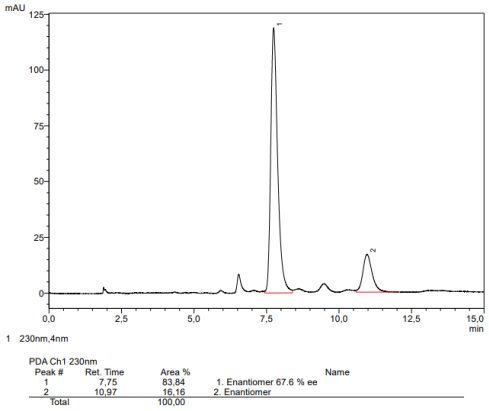

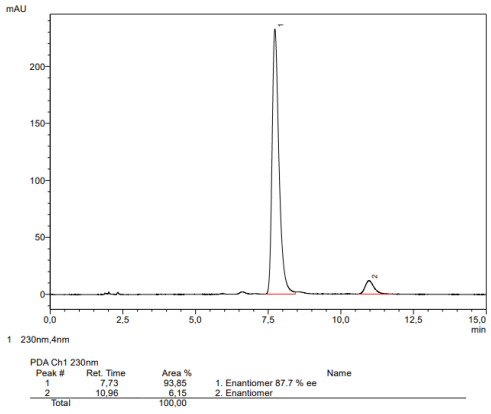

Amino alcohol 106. The title compound was prepared according to the general procedure **I** and

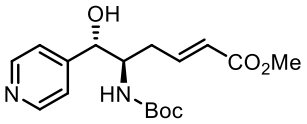

oxidative work-up **I**, using isonicotinaldehyde (21.4 mg, 0.20 mmol) and diene **88a** (90.9 mg, 0.40 mmol); the reaction time was 72 h. The crude material (rr > 8:1) was purified by flash chromatography (SiO_2, *tert*-butyl methyl ether + 2% methanol) and the product was obtained as an off-white solid (29.3 mg, 44%, dr > 20:1, 45% ee). mp = 146-148 °C; $[\alpha]_D^{20}$ (86% ee, sample after recrystallization) = +48.2 (c = 0.76, $CHCl_3$); ^{1}H NMR (400 MHz, CD_2Cl_2): δ = 8.55 – 8.46 (m, 2H), 7.42 – 7.17 (m, 2H), 6.82 (ddd, *J* = 15.7, 7.9, 6.8 Hz, 1H), 5.80 (dt, *J* = 15.6, 1.5 Hz, 1H), 4.90 (d, *J* = 3.2 Hz, 2H), 3.95 (s, 1H), 3.67 (s, 3H), 2.42 – 2.11 (m, 2H), 1.74 (s, 1H), 1.41 (s, 9H); ^{13}C NMR (101 MHz, CD_2Cl_2): δ = 166.7, 156.5, 150.6, 150.0, 145.3, 123.9, 121.8, 80.4, 75.2, 55.7, 51.7, 31.9, 28.4; IR (ATR): $\tilde{\nu}$ = 3353, 1722, 1679, 1521, 1320, 1252, 1162, 1049, 827, 634 cm^{-1}; HRMS (ESI^+): *m/z*: calcd. for $C_{17}H_{25}N_2O_5Na$ $[M+Na]^+$: 337.175797, found: 337.17537.

25.0 mg of the product were recrystallized from *tert*-butyl methyl ether/*iso*-hexane to give the enantioenriched product in 86% ee (8.4 mg).

The ee was determined by HPLC analysis: Chiralpak 150 mm IG-3, 3 µm, 4.6 mm ∅, *n*-heptane/*iso*-propanol = 75:25, v = 1.0 mL/min, λ = 210 nm, t(minor) = 4.33 min, t(major) = 7.24 min (racemate: top left, enantioenriched sample: top right, recrystallized enantioenriched sample: bottom left).

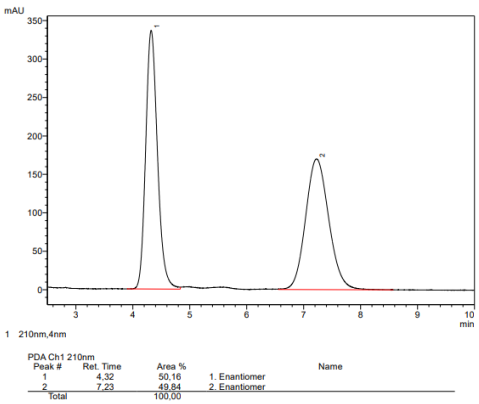

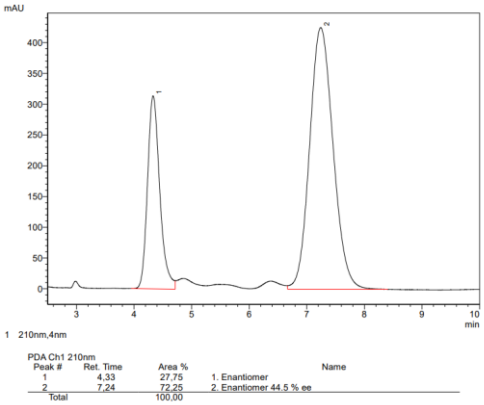

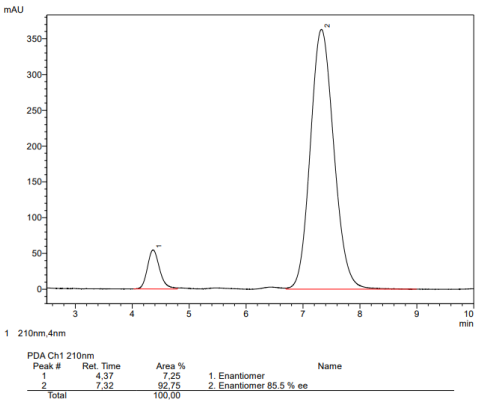

Amino alcohol 107. The title compound was prepared according to the general procedure **I** and

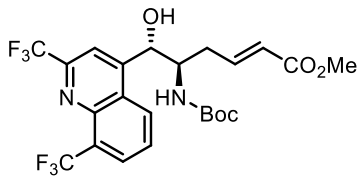

oxidative work-up **I**, using 2,8-bis(trifluoromethyl)quinoline-4-carbaldehyde[140] (14.7 mg, 50.0 µmol) and diene **88a** (22.7 mg, 0.10 mmol); the reaction time was 72 h. The crude material (rr > 20:1) was purified by flash chromatography (SiO_2, toluene/*tert*-butyl methyl ether) and the product was obtained as a pale yellow solid (22.6 mg, 87%, dr > 20:1, 31% ee). mp = 78-80 °C; ^{1}H NMR (600 MHz, CD_2Cl_2): δ = 8.71 (d, *J* = 8.6 Hz, 1H), 8.22 (d, *J* = 7.6 Hz, 1H), 7.85 (t, *J* = 8.0 Hz, 1H), 6.66 (ddd, *J* = 15.6, 8.1, 6.3 Hz, 1H), 5.88 (s, 1H), 5.75 (dt, *J* = 15.6, 1.5 Hz, 1H), 5.04 (d, *J* = 7.7 Hz, 1H), 4.07 (d, *J* = 9.8 Hz, 1H), 3.63 (s, 3H), 3.30 (s, 1H), 2.47 (dt, *J* = 18.1, 9.7 Hz, 1H), 2.33 – 1.98 (m, 1H), 1.47 (s, 9H); ^{13}C NMR (151 MHz, CD_2Cl_2): δ = 166.5, 156.4, 150.6, 148.4 (q, *J* = 35.0 Hz), 144.7, 144.1, 129.6 (q, *J* = 5.5 Hz), 129.3 (q, *J* = 30.0 Hz), 128.5, 128.1, 127.1, 124.2, 124.2 (q, *J* = 273.4 Hz), 121.8 (d, *J* = 275.4 Hz), 115.6, 80.8, 71.9, 55.2, 51.7, 30.1, 28.4; ^{19}F NMR (565 MHz, CD_2Cl_2): δ = –60.6, –68.3; IR (ATR): $\tilde{\nu}$ = 3368, 1699, 1507, 1308, 1141, 1107, 1044, 772 cm^{-1}; HRMS (ESI$^+$): *m/z*: calcd. for $C_{23}H_{24}N_2O_5F_6Na$ [M+Na]$^+$: 545.14816, found: 545.14789.

The ee was determined by HPLC analysis: Chiralpak 150 mm IM-3, 3 µm, 4.6 mm ∅, acetonitrile/water = 40:60, v = 1.0 mL/min, λ = 220 nm, t(minor) = 24.98 min, t(major) = 26.64 min (racemate: left, enantioenriched sample: right).

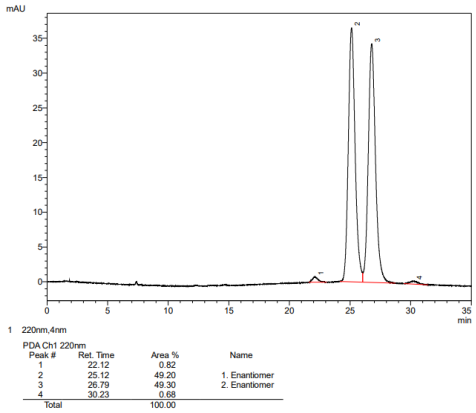

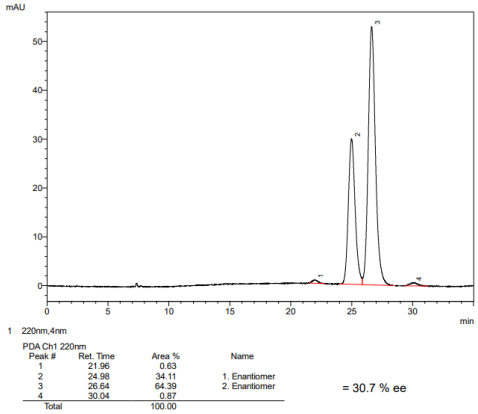

Amino alcohol 112. The title compound was prepared according to the general procedure **II** and oxidative work-up **I**, using hydrocinnamaldehyde (26.3 µL, 0.20 mmol) and diene **88a** (90.9 mg, 0.40 mmol). The crude material (rr = 4:1) was purified by flash chromatography (SiO_2, toluene/*tert*-butyl methyl ether, 4:1) and the product was obtained as an off-white solid (52.4 mg, 72%, dr > 20:1, 95% ee). mp = 122-123 °C; $[\alpha]_D^{20}$ (95% ee, sample before recrystallization) = –2.4 (c = 0.50, $CHCl_3$); ^{1}H NMR (400 MHz, CD_2Cl_2): δ = 7.30 – 7.26 (m, 2H), 7.22 – 7.16 (m, 3H), 6.95 – 6.88 (m, 1H), 5.86 (dt, *J* = 15.6, 1.5 Hz, 1H), 4.80 (d, *J* = 8.7 Hz, 1H), 3.74 – 3.63 (br, 2H), 3.69 (s, 3H), 2.88 – 2.81 (m, 1H), 2.69 – 2.61 (m, 1H), 2.55 (s, 1H), 2.49 – 2.43 (m, 1H), 2.38 – 2.30 (m, 1H), 1.82 – 1.70 (m, 2H), 1.40 (s, 9H); ^{13}C NMR (101 MHz, CD_2Cl_2): δ = 166.8, 156.4, 145.9, 142.3, 128.8, 126.3, 123.6, 80.0, 73.9, 54.8, 51.7, 35.8, 33.0, 32.6, 28.4; IR (ATR): $\tilde{\nu}$ = 3342, 1724, 1681, 1523, 1264, 1166, 1012, 752, 699 cm^{-1}; HRMS (ESI$^+$): *m/z*: calcd. for $C_{20}H_{29}NO_5Na$ $[M+Na]^+$: 386.19379, found: 386.19391.

20.0 mg of the product were recrystallized from *tert*-butyl methyl ether/*iso*-hexane to give the enantioenriched product in >99% ee (15.2 mg).

The ee was determined by HPLC analysis: Chiralpak 150 mm IB-N-3, 3 µm, 4.6 mm ∅, acetonitrile/water = 35:65, v = 1.0 mL/min, λ = 210 nm, t(major) = 31.66 min, t(minor) = 39.17 min (racemate: top left, enantioenriched sample: top right, recrystallized enantioenriched sample: bottom left).

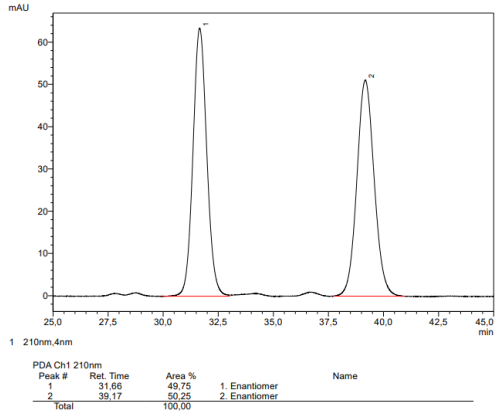

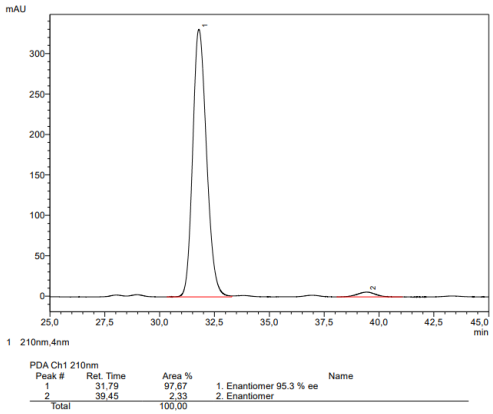

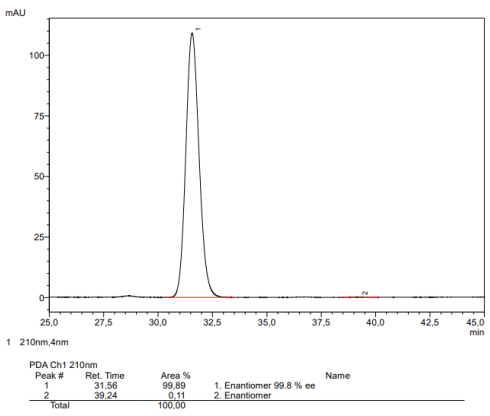

Amino alcohol 113. The title compound was prepared according to the general procedure **II** and oxidative work-up **I**, using octanal (31.2 µL, 0.20 mmol) and diene **88a** (90.9 mg, 0.40 mmol). The crude material (rr = 3:1) was purified by flash chromatography (SiO_2, toluene/*tert*-butyl methyl ether, 4:1) and the product was obtained as an off-white solid (28.6 mg, 40%, dr > 20:1, 94% ee). mp = 112-114 °C; $[\alpha]_D^{20}$ (99% ee, sample after recrystallization) = –4.4 (c = 0.50, $CHCl_3$); ^{1}H NMR (400 MHz, CD_2Cl_2): δ = 6.97 – 6.90 (m, 1H), 5.87 (dt, *J* = 15.6, 1.5 Hz, 1H), 4.80 (d, *J* = 8.8 Hz, 1H), 3.69 (s, 3H), 3.68 – 3.60 (m, 2H), 2.49 – 2.43 (m, 1H), 2.37 – 2.29 (m, 1H), 2.21 (br, 1H), 1.48 – 1.43 (m, 2H), 1.40 (s, 9H), 1.34 – 1.23 (m, 10H), 0.90 – 0.87 (m, 3H); ^{13}C NMR (101 MHz, CD_2Cl_2): δ = 166.8, 156.2, 146.2, 123.5, 79.8, 74.5, 54.5, 51.7, 34.1, 32.8, 32.2, 30.0, 29.6, 28.4, 26.3, 23.1, 14.3; IR (ATR): $\tilde{\nu}$ = 3349, 2923, 2854, 1725, 1680, 1526, 1169 cm^{-1}; HRMS (ESI$^+$): *m/z*: calcd. for $C_{19}H_{35}NO_5Na$ $[M+Na]^+$: 380.24074, found: 380.24087.

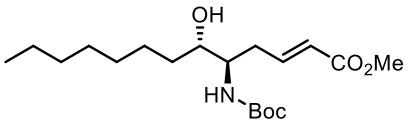

26.3 mg of the product were recrystallized from *tert*-butyl methyl ether/*iso*-hexane to give the enantioenriched product in 99% ee (15.6 mg).

The ee was determined by HPLC analysis: Chiralpak 150 mm IG-3, 3 µm, 4.6 mm ∅, *n*-heptane/ethanol = 95:5, v = 1.0 mL/min, λ = 210 nm, t(major) = 15.12 min, t(minor) = 20.06 min (racemate: top left, enantioenriched sample: top right, recrystallized enantioenriched sample: bottom left).

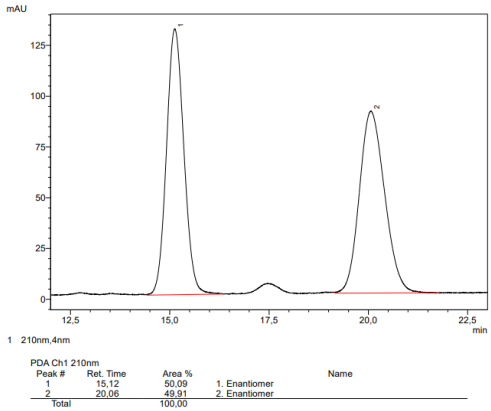

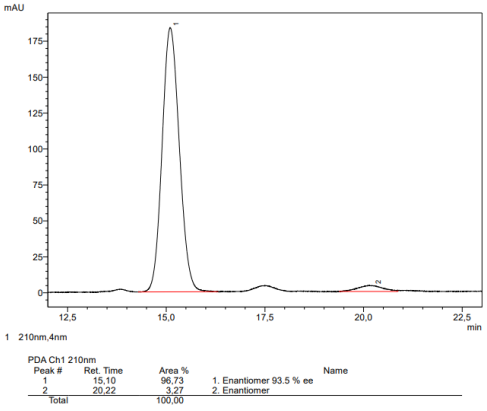

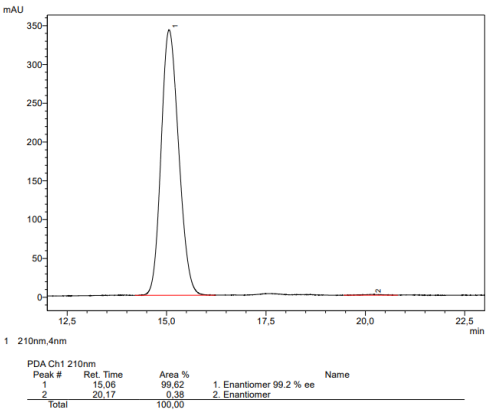

Amino alcohol 114. The title compound was prepared according to the general procedure **II** and oxidative work-up **I**, using *iso*-butyraldehyde (18.3 µL, 0.20 mmol) and diene **88a** (90.9 mg, 0.40 mmol). The crude material (rr = 3:1) was purified by flash chromatography (SiO_2, toluene/*tert*-butyl methyl ether, 3:1) and the product was obtained as an off-white solid (36.5 mg, 61%, dr > 20:1, 94% ee). $[\alpha]_D^{20}$ (94% ee) = –4.0 (c = 0.50, $CHCl_3$); ^{1}H NMR (400 MHz, CD_2Cl_2): δ = 7.00 – 6.92 (m, 1H), 5.87 (dt, *J* = 15.6, 1.5 Hz, 1H), 4.89 (d, *J* = 8.2 Hz, 1H), 3.85 – 3.73 (m, 1H), 3.68 (s, 3H), 3.31 – 3.26 (m, 1H), 2.51 – 2.45 (m, 1H), 2.39 – 2.30 (m, 1H), 2.18 (d, *J* = 5.4 Hz, 1H), 1.74 – 1.66 (m, 1H), 1.40 (s, 9H), 0.97 (d, *J* = 6.6 Hz, 3H), 0.93 (d, *J* = 6.7 Hz, 3H); ^{13}C NMR (101 MHz, CD_2Cl_2): δ = 166.9, 155.8, 146.6, 123.3, 79.6, 51.9, 51.6, 32.5, 31.1, 28.4, 19.2, 18.5; IR (ATR): $\tilde{\nu}$ = 3367, 2959, 1716, 1674, 1522, 1301, 1163, 987, 627 cm^{-1}; HRMS (ESI$^+$): *m/z*: calcd. for $C_{15}H_{27}NO_5Na$ [M+Na]$^+$: 324.17814, found: 324.17831.

The ee was determined by HPLC analysis: Chiralpak 150 mm IC-3, 3 µm, 4.6 mm ∅, *n*-heptane/*iso*-propanol = 90:10, v = 1.0 mL/min, λ = 210 nm, t(minor) = 7.77 min, t(major) = 14.49 min (racemate: left, enantioenriched sample: right).

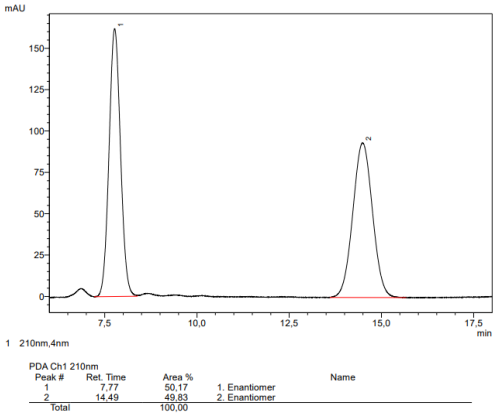

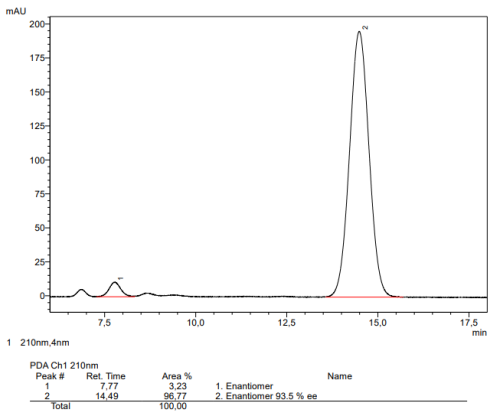

Amino alcohol 116. The title compound was prepared according to the general procedure **II** and oxidative work-up **I**, using propionaldehyde (14.4 µL, 0.20 mmol) and diene **88a** (90.9 mg, 0.40 mmol). The crude material (rr = 2:1) was purified by flash chromatography (SiO_2, toluene/*tert*-butyl methyl ether, 2:1) and the product was obtained as a colorless solid (30.5 mg, 53%, dr > 20:1, 97% ee). mp = 110-113 °C; $[\alpha]_D^{20}$ (97% ee) = –4.4 (c = 0.50, $CHCl_3$); ^{1}H NMR (400 MHz, CD_2Cl_2): δ = 6.97 – 6.90 (m, 1H), 5.87 (dt, *J* = 15.6, 1.5 Hz, 1H), 4.82 (d, *J* = 9.0 Hz, 1H), 3.71 – 3.64 (m, 1H), 3.69 (s, 3H), 3.58 – 3.52 (m, 1H), 2.50 – 2.43 (m, 1H), 2.38 – 2.29 (m, 2H), 1.57 – 1.43 (m, 2H), 1.40 (s, 9H), 0.97 (t, *J* = 7.4 Hz, 3H); ^{13}C NMR (101 MHz, CD_2Cl_2): δ = 166.9, 156.2, 146.3, 123.5, 79.8, 75.9, 54.3, 51.7, 32.8, 28.4, 27.1, 10.5; IR (ATR): $\tilde{\nu}$ = 3351, 2959, 1717, 1673, 1655, 1525, 1302, 1165, 1028, 971, 646 cm^{-1}; HRMS (ESI$^+$): *m/z*: calcd. for $C_{14}H_{25}NO_5Na$ $[M+Na]^+$: 310.16249 , found: 310.16243.

The ee was determined by HPLC analysis: Chiralpak 150 mm IG-3, 3 µm, 4.6 mm ∅, *n*-heptane/ethanol = 90:10, v = 1.0 mL/min, λ = 210 nm, t(minor) = 8.43 min, t(major) = 12.74 min (racemate: left, enantioenriched sample: right).

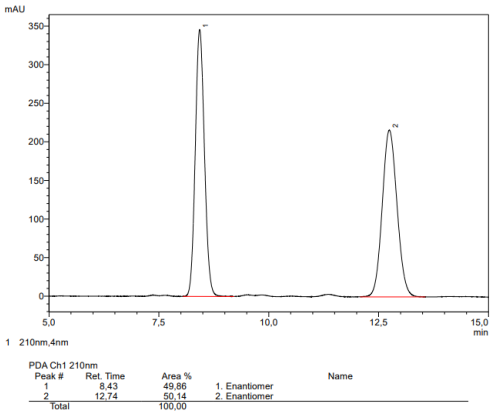

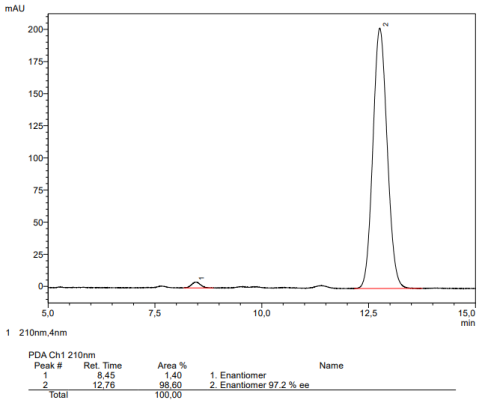

Amino alcohol 117. The title compound was prepared according to the general procedure **II** and

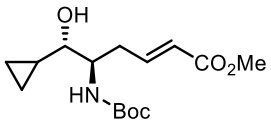

oxidative work-up **I**, using cyclopropanecarboxaldehyde (14.9 µL, 0.20 mmol) and diene **88a** (90.9 mg, 0.40 mmol). The crude material (rr = 6:1) was purified by flash chromatography (SiO_2, toluene/*tert*-butyl methyl ether, 2.5:1) and the product was obtained as an off-white solid (41.8 mg, 70%, dr > 20:1, 94% ee). mp = 108-110 °C, $[\alpha]_D^{20}$ (94% ee) = +5.6 (c = 0.50, $CHCl_3$); ^{1}H NMR (400 MHz, CD_2Cl_2): δ = 7.00 – 6.92 (m, 1H), 5.88 (dt, *J* = 15.6, 1.5 Hz, 1H), 4.84 (br, 1H), 3.86 – 3.76 (m, 1H), 3.69 (s, 3H), 2.99 – 2.95 (m, 1H), 2.63 – 2.56 (m, 1H), 2.48 – 2.40 (m, 1H), 2.34 – 2.24 (m, 1H), 1.40 (s, 9H), 0.93 – 0.85 (m, 1H), 0.59 – 0.49 (m, 2H), 0.36 – 0.24 (m, 2H); ^{13}C NMR (101 MHz, CD_2Cl_2): δ = 166.9, 156.2, 146.3, 123.4, 79.7, 78.6, 54.8, 51.7, 33.2, 28.4, 14.6, 2.8, 2.6; IR (ATR): $\tilde{\nu}$ = 3357, 1724, 1677, 1525, 1311, 1165, 1009, 651 cm^{-1}; HRMS (ESI$^+$): *m/z*: calcd. for $C_{15}H_{25}NO_5Na$ $[M+Na]^+$: 322.16249, found: 322.16256.

The ee was determined by HPLC analysis: Chiralpak 150 mm IG-3, 3 µm, 4.6 mm ∅, *n*-heptane/ethanol = 90:10, v = 1.0 mL/min, λ = 210 nm, t(minor) = 9.99 min, t(major) = 16.75 min (racemate: left, enantioenriched sample: right).

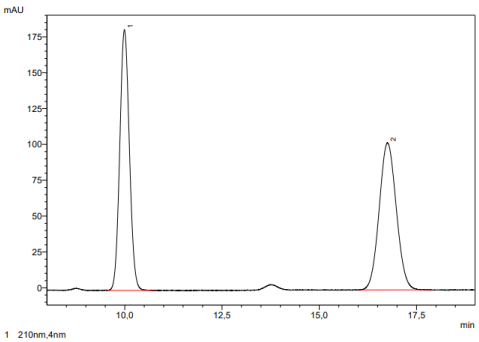

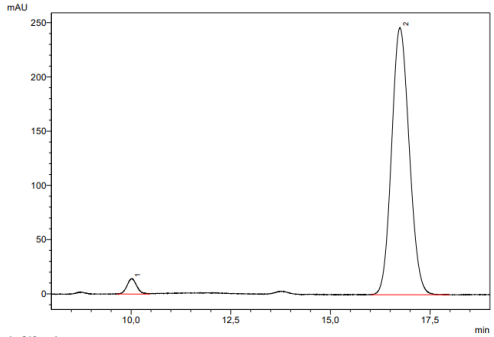

Amino alcohol 118. The title compound was prepared according to the general procedure **II** and oxidative work-up **I**, using cyclobutanecarbaldehyde (18.0 µL, 0.20 mmol) and diene **88a** (90.9 mg, 0.40 mmol). The crude material (rr = 5:1) was purified by flash chromatography (SiO_2, toluene/*tert*-butyl methyl ether, 2.5:1) and the product was obtained as an off-white solid (42.2 mg, 67%, dr > 20:1, 90% ee). mp = 139-140 °C, $[\alpha]_D^{20}$ (90% ee) = –8.4 (c = 0.50, $CHCl_3$); ^{1}H NMR (400 MHz, CD_2Cl_2): δ = 6.95 – 6.88 (m, 1H), 5.85 (dt, *J* = 15.6, 1.5 Hz, 1H), 4.80 (d, *J* = 8.9 Hz, 1H), 3.68 (s, 3H), 3.66 – 3.53 (m, 2H), 2.47 – 2.27 (m, 3H), 2.23 (s, 1H), 2.08 – 1.97 (m, 1H), 1.97 – 1.77 (m, 5H), 1.40 (s, 9H); ^{13}C NMR (101 MHz, CD_2Cl_2): δ = 166.9, 156.1, 146.4, 123.4, 79.7, 78.4, 52.7, 51.7, 38.7, 32.8, 28.4, 25.4, 24.9, 18.6; IR (ATR): $\tilde{\nu}$ = 3356, 2936, 1719, 1675, 1523, 1275, 1163, 985, 646 cm^{-1}; HRMS (ESI$^+$): *m/z*: calcd. for $C_{16}H_{27}NO_5Na$ $[M+Na]^+$: 336.17814, found: 336.17816.

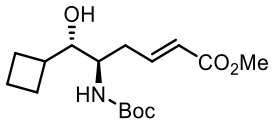

The ee was determined by 2D-HPLC analysis: First dimension = 50 mm RX-SIL, 4.6 mm ∅, *n*-heptane/*iso*-propanol = 99:1, v = 1.0 mL/min, λ = 220 nm; second Dimension = 150 mm Chiralpak IB-N-3, 4.6 mm ∅, *n*-heptane/*iso*-propanol = 98:2, v = 1.0 ml/min, λ = 220 nm.

First dimension (left) and second dimension (right) of the racemic sample:

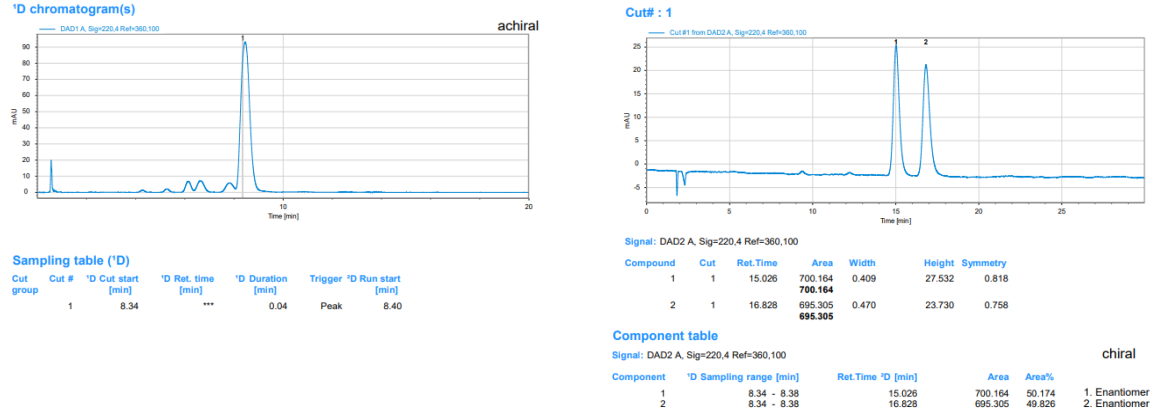

First dimension (left) and second dimension (right) of the enantioenriched sample:

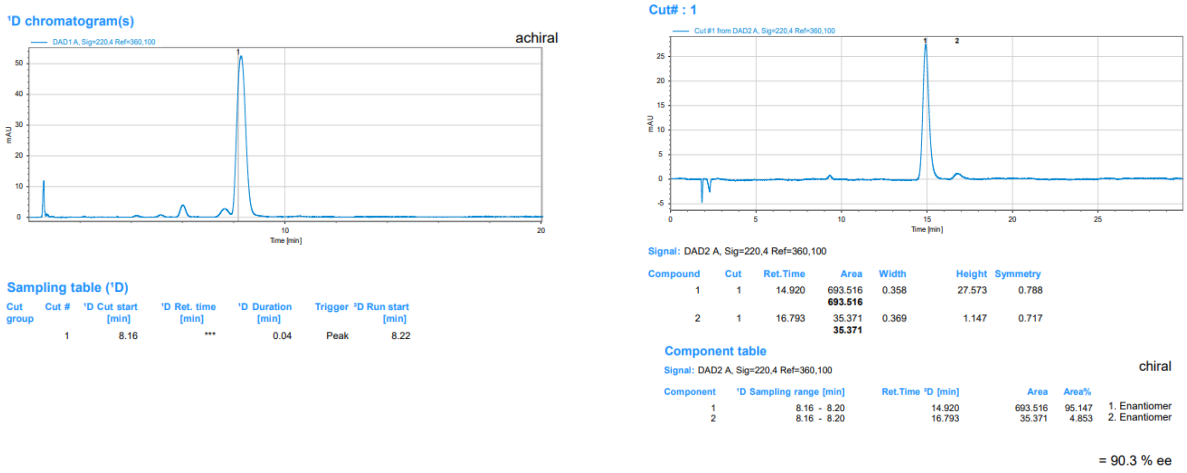

Amino alcohol 119. The title compound was prepared according to the general procedure **II** and

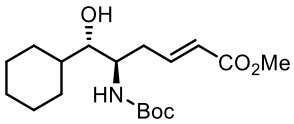

oxidative work-up **I**, using cyclohexanecarbaldehyde (24.2 µL, 0.20 mmol) and diene **88a** (90.9 mg, 0.40 mmol). The crude material (rr = 5:1) was purified by flash chromatography (SiO_2, toluene/*tert*-butyl methyl ether, 4:1) and the product was obtained as an off-white solid (44.3 mg, 65%, dr > 20:1, 88% ee). mp = 96-97 °C; $[\alpha]_D^{20}$ (98% ee, sample after recrystallization) = –11.0 (c = 0.50, $CHCl_3$); ^{1}H NMR (400 MHz, CD_2Cl_2): δ = 6.99 – 6.92 (m, 1H), 5.87 (dt, *J* = 15.6, 1.5 Hz, 1H), 4.91 (d, *J* = 9.4 Hz, 1H), 3.85 – 3.75 (m, 1H), 3.68 (s, 3H), 3.35 – 3.31 (m, 1H), 2.49 – 2.42 (m, 1H), 2.37 – 2.29 (m, 1H), 2.13 (d, *J* = 5.3 Hz, 1H), 1.96 – 1.92 (m, 1H), 1.79 – 1.73 (m, 2H), 1.66 – 1.55 (m, 2H), 1.40 (s, 9H), 1.28 – 0,92 (m, 6H); ^{13}C NMR (101 MHz, CD_2Cl_2): δ = 166.9, 155.8, 146.7, 123.3, 79.5, 78.7, 51.6, 51.4, 40.8, 32.3, 29.5, 29.2, 28.4, 26.7, 26.4, 26.3; IR (ATR): $\tilde{\nu}$ = 3360, 2921, 1725, 1680, 1524, 1252, 1164, 1005, 974, 651 cm^{-1}; HRMS (ESI$^+$): *m/z*: calcd. for $C_{18}H_{31}NO_5Na$ $[M+Na]^+$: 364.20944, found: 364.20946.

36.3 mg of the product were recrystallized from *tert*-butyl methyl ether/*iso*-hexane to give the enantioenriched product in 98% ee (24.4 mg).

The ee was determined by HPLC analysis: Chiralpak 150 mm IG-3, 3 µm, 4.6 mm ∅, acetonitrile/water = 40:60, v = 1.0 mL/min, λ = 210 nm, t(major) = 18.01 min, t(minor) = 20.67 min (racemate: top left, enantioenriched sample: top rigt, recrystallized enantioenriched sample: bottom left).

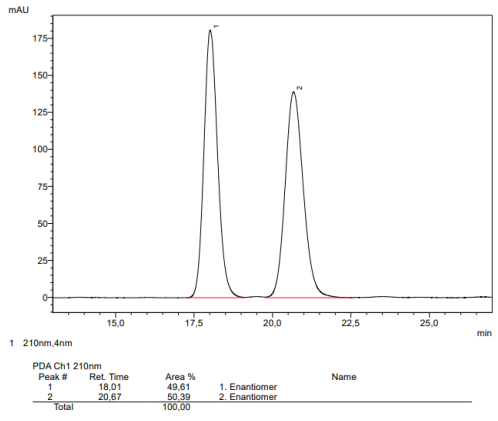

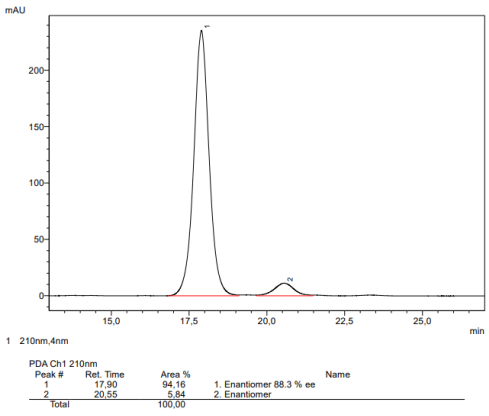

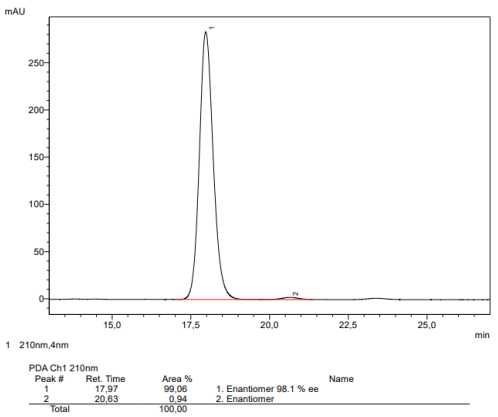

Amino alcohol 120. The title compound was prepared according to the general procedure **II** and oxidative work-up **I**, using tetrahydropyran-4-carbaldehyde (21.7 µL, 0.20 mmol) and diene **88a** (90.9 mg, 0.40 mmol). The crude material (rr = 4:1) was purified by flash chromatography (SiO_2, toluene/*tert*-butyl methyl ether, 1:2) and the product was obtained as a colorless, sticky oil (44.1 mg, 64%, dr > 20:1, 87% ee). $[\alpha]_D^{20}$ (87% ee) = –5.4 (c = 0.53, $CHCl_3$); ^{1}H NMR (400 MHz, CD_2Cl_2): δ = 6.99 – 6.91 (m, 1H), 5.88 (dt, *J* = 15.6, 1.5 Hz, 1H), 4.89 (d, *J* = 9.3 Hz, 1H), 3.99 – 3.91 (m, 2H), 3.83 – 3.73 (m, 1H), 3.69 (s, 3H), 3.40 – 3.30 (m, 3H), 2.50 – 2.43 (m, 1H), 2.42 – 2.29 (m, 2H), 1.83 – 1.77 (m, 1H), 1.65 – 1.59 (m, 1H, overlaps with H_2O signal), 1.46 – 1.42 (m, 2H), 1.40 (s, 9H), 1.36 – 1.32 (m, 1H); ^{13}C NMR (101 MHz, CD_2Cl_2): δ = 166.9, 155.9, 146.2, 123.5, 79.8, 78.1, 68.1, 67.7, 51.7, 51.3, 38.2, 32.3, 29.5, 29.2, 28.4; IR (ATR): $\tilde{\nu}$ = 3368, 2926, 1705, 1700, 1517, 1366, 1165, 1091, 710 cm^{-1}; HRMS (ESI$^+$): *m/z*: calcd. for $C_{17}H_{29}NO_6Na$ [M+Na]$^+$: 366.18871, found: 366.18879.

The ee was determined by HPLC analysis: Chiralpak 150 mm IB-N-3, 3 µm, 4.6 mm ∅, *n*-heptane/ethanol = 95:5, v = 1.0 mL/min, λ = 210 nm, t(major) = 22.99 min, t(minor) = 24.82 min (racemate: left, enantioenriched sample: right).

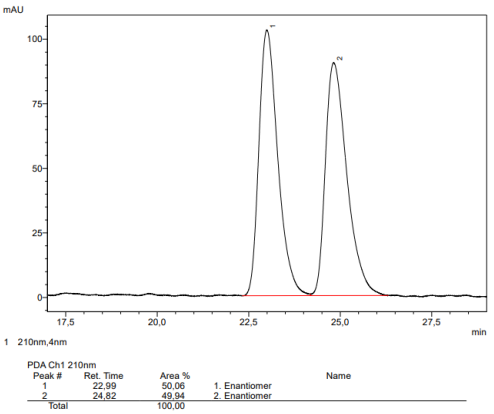

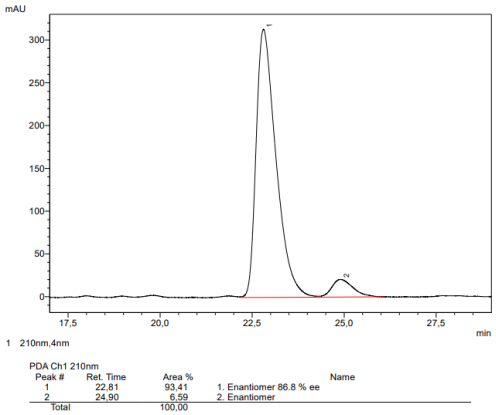

Amino alcohol 121. The title compound was prepared according to the general procedure **II** and oxidative work-up **I**, using (*R*)-citronellal (36.3 µL, 0.20 mmol) and diene **88a** (90.9 mg, 0.40 mmol). The crude material (rr = 2:1, dr = 11:1) was purified by flash chromatography (SiO_2, toluene/*tert*-butyl methyl ether, 4:1) to give the product as a colorless solid (41.0 mg, 53%, dr = 11:1). The product was carefully washed with cold pentane (2 x 1 mL) to obtain the product in an improved diastereomeric ratio (32.2 mg, 42%, dr = 20:1). mp = 101-103 °C; $[\alpha]_D^{20}$= −13.4 (c = 0.50, $CHCl_3$); ^{1}H NMR (400 MHz, CD_2Cl_2): δ = 6.97 – 6.89 (m, 1H), 5.87 (dt, *J* = 15.6, 1.4 Hz, 1H), 5.13 – 5.08 (m, 1H), 4.78 (d, *J* = 8.9 Hz, 1H), 3.77 – 3.71 (m, 1H), 3.69 (s, 3H), 3.66 – 3.62 (br, 1H), 2.49 – 2.43 (m, 1H), 2.37 – 2.29 (m, 1H), 2.24 (s, 1H), 2.07 – 1.92 (m, 2H), 1.68 (d, *J* = 1.4 Hz, 3H), 1.60 (s, 3H), 1.48 – 1.44 (m, 1H), 1.41 (s, 9H), 1.36 – 1.12 (m, 4H), 0.90 (d, *J* = 6.5 Hz, 3H); ^{13}C NMR (101 MHz, CD_2Cl_2): δ = 166.8, 156.3, 146.1, 131.6, 125.0, 123.5, 79.8, 72.1, 55.2, 51.7, 41.1, 38.3, 33.1, 29.3, 28.4, 25.8, 19.1, 17.8; IR (ATR): $\tilde{\nu}$ = 3370, 2920, 1691, 1509, 1437, 1366, 1249, 1166, 1042 cm^{-1}; HRMS (ESI$^+$): *m/z*: calcd. for $C_{21}H_{37}NO_5Na$ $[M+Na]^+$: 406.25639, found: 406.25645.

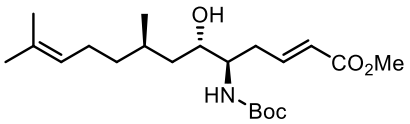

Amino alcohol 122a. The title compound was prepared according to the general procedure **II** and oxidative work-up **I**, using 2-((*tert*-butyldiphenylsilyl)oxy)acetaldehyde (59.7 mg, 0.20 mmol)[236] and diene **88a** (90.9 mg, 0.40 mmol). The crude material (rr = 1.5:1) was purified by flash chromatography (SiO_2, toluene/*tert*-butyl methyl ether, 8:1 → 6:1) and the product was obtained as a colorless sticky oil (56.2 mg, 53%, dr > 20:1, 97% ee). $[\alpha]_D^{20}$ (97% ee) = +4.2 (c = 0.50, $CHCl_3$); ^{1}H NMR (400 MHz, CD_2Cl_2): δ = 7.68 – 7.64 (m, 4H), 7.48 – 7.39 (m, 6H), 6.94 – 6.87 (m, 1H), 5.84 (dt, *J* = 15.6, 1.5 Hz, 1H), 4.89 (d, *J* = 9.4 Hz, 1H), 3.86 – 3.76 (m, 1H), 3.72 – 3.66 (m, 3H), 3.68 (s, 3H), 2.82 (s, 1H), 2.51 – 2.35 (m, 2H), 1.37 (s, 9H), 1.07 (s, 9H); ^{13}C NMR (101 MHz, CD_2Cl_2): δ = 166.8, 156.0, 145.7, 136.0, 135.9, 133.3, 133.2, 130.3, 128.3, 123.7, 79.7, 73.5, 65.7, 52.4, 51.7, 34.2, 28.4, 27.0, 19.4; IR (ATR): $\tilde{\nu}$ = 3367, 2930, 1709, 1503, 1166, 1111, 701 cm^{-1}; HRMS (ESI$^+$): *m/z*: calcd. for $C_{29}H_{41}NO_6SiNa$ $[M+Na]^+$: 550.25954 , found: 550.25932.

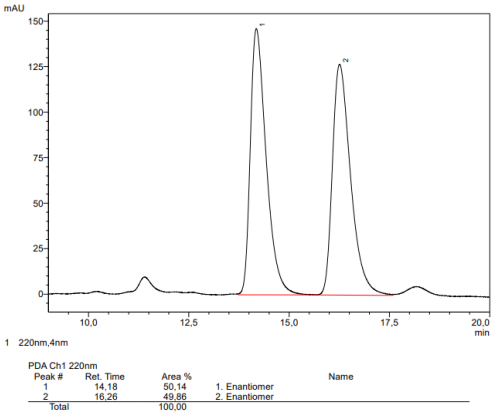

The ee was determined by HPLC analysis: Chiralpak 150 mm IB-N-3, 3 µm, 4.6 mm ∅, *n*-heptane/*iso*-propanol = 98:2, v = 1.0 mL/min, λ = 220 nm, t(minor) = 14.18 min, t(major) = 16.26 min (racemate: left, enantioenriched sample: right).

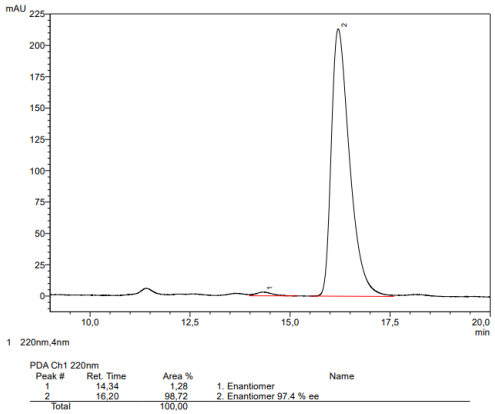

Amino alcohol 122b. The title compound was prepared according to the general procedure **II** and

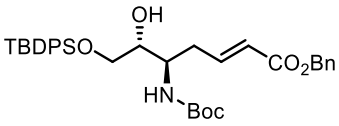

oxidative work-up **I**, using 2-((*tert*-butyldiphenylsilyl)oxy)acetaldehyde (20.9 mg, 70.0 µmol)[236] and diene **S3** (42.5 mg, 140 µmol). The crude material (rr = 2:1) was purified by flash chromatography (SiO_2, toluene/*tert*-butyl methyl ether, 8:1 → 7:1) and the product was obtained as a pale yellow sticky oil (24.6 mg, 58%, dr > 20:1, 97% ee). $[\alpha]_D^{20}$ (97% ee) = –10.4 (c = 0.25, $CHCl_3$); ^{1}H NMR (400 MHz, CD_2Cl_2): δ = 7.68 – 7.65 (m, 4H), 7.47 – 7.30 (m, 11H), 6.95 (dt, *J* = 15.2, 7.4 Hz, 1H), 5.89 (dt, *J* = 15.6, 1.5 Hz, 1H), 5.15 (s, 2H), 4.89 (d, *J* = 9.2 Hz, 1H), 3.85 – 3.75 (m, 1H), 3.73 – 3.65 (m, 3H), 2.81 (br, 1H), 2.52 – 2.37 (m, 2H), 1.35 (s, 9H), 1.07 (s, 9H); ^{13}C NMR (101 MHz, CD_2Cl_2): δ = 166.1, 156.0, 146.1, 136.8, 135.97, 135.95, 133.3, 133.2, 130.3, 128.9, 128.5, 128.4, 128.3, 123.7, 79.7, 73.5, 66.4, 65.7, 52.4, 34.3, 28.4, 27.0, 19.4; IR (ATR): $\tilde{\nu}$ = 3400, 2930, 1711, 1499, 1365, 1250, 1165, 1111, 1009, 739, 699 cm^{-1}; HRMS (ESI$^+$): *m/z*: calcd. for $C_{35}H_{45}NO_6SiNa$ $[M+Na]^+$: 626.29084, found: 626.29075.

The ee was determined by HPLC analysis: Chiralpak 150 mm IB-N-3, 3 µm, 4.6 mm ∅, *n*-heptane/ethanol = 98:2, v = 1.0 mL/min, λ = 210 nm, t(minor) = 11.30 min, t(major) = 12.55 min (racemate: left, enantioenriched sample: right).

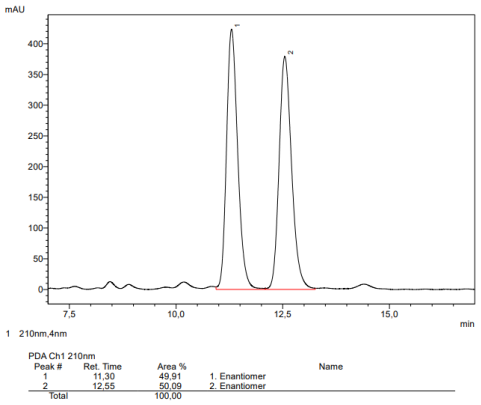

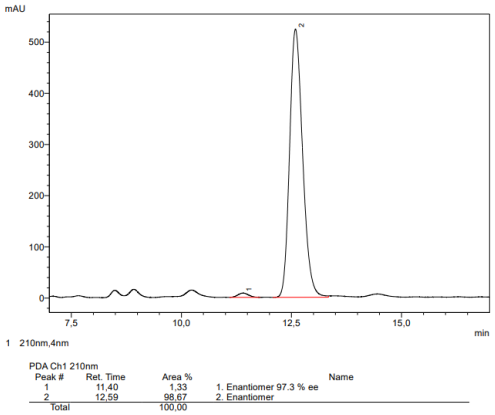

Amino alcohol 123. The title compound was prepared according to the general procedure **II** and oxidative work-up **I**, using 2-(4-methoxyphenoxy)-acetaldehyde (33.2 mg, 0.20 mmol)[237] and diene **88a** (90.9 mg, 0.40 mmol). The crude material (rr = 2:1) was purified by flash chromatography (SiO_2, toluene/*tert*-butyl methyl ether, 4:1 → 3:1) and the product was obtained as an off-white solid (40.2 mg, 51%, dr > 20:1, 96% ee). mp = 110-112 °C; $[\alpha]_D^{20}$ (96% ee) = −15.8 (c = 0.50, $CHCl_3$); ^{1}H NMR (400 MHz, CD_2Cl_2): δ = 6.99 – 6.91 (m, 1H), 6.87 – 6.81 (m, 4H), 5.90 (dt, *J* = 15.6, 1.5 Hz, 1H), 4.89 (d, *J* = 9.1 Hz, 1H), 4.01 – 3.84 (m, 4H), 3.75 (s, 3H), 3.69 (s, 3H), 3.06 (s, 1H), 2.62 – 2.55 (m, 1H), 2.52 – 2.44 (m, 1H), 1.41 (s, 9H); ^{13}C NMR (101 MHz, CD_2Cl_2): δ = 166.8, 156.2, 154.7, 152.9, 145.5, 123.9, 115.9, 115.0, 80.1, 72.4, 70.7, 56.0, 52.4, 51.7, 33.8, 28.4; IR (ATR): $\tilde{\nu}$ = 3370, 2928, 1710, 1509, 1231, 1169, 1041, 826 cm^{-1}; HRMS (ESI$^+$): *m/z*: calcd. for $C_{20}H_{29}NO_7Na$ $[M+Na]^+$: 418.18362 , found: 418.18376.

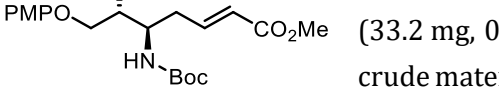

The ee was determined by HPLC analysis: Chiralpak 150 mm IG-3, 3 µm, 4.6 mm ∅, *n*-heptane/*iso*-propanol = 85:15, v = 1.0 mL/min, λ = 225 nm, t(major) = 15.45 min, t(minor) = 20.95 min (racemate: left, enantioenriched sample: right).

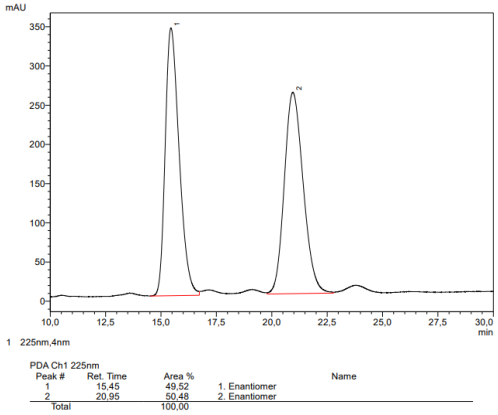

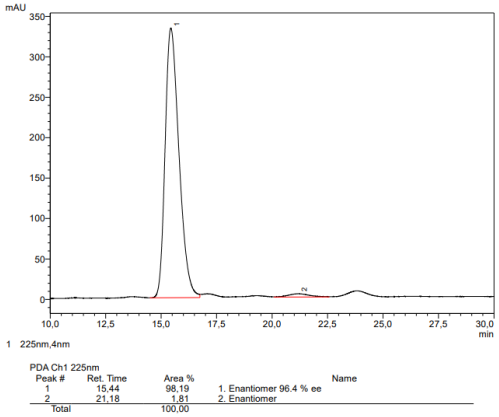

Amino alcohol 129a. A flame-dried Schlenk flask under argon was charged with tris(*trans*-1,2-bis(4-*tert*-butylphenyl)ethene)nickel(0) ($Ni(^{t}Bustb)_3$) (14.0 mg, 0.015 mmol) and phosphoramidite ligand **L11** (9.6 mg, 0.015 mmol). The Schlenk flask was evacuated and refilled with argon (3 cycles). A solution of diene **127a** (109 mg, 0.45 mmol) in THF (0.10 mL) and triethylborane (1 M in THF, 0.45 mL, 0.45 mmol) were successively added and the resulting solution was stirred for 5 min before benzaldehyde (15.2 µL, 0.15 mmol) was added under an argon counterflow. The flask was sealed and the mixture stirred at room temperature for 40 h. The reaction was quenched at 0 °C by addition of pH 7 phosphate buffer solution (1.5 mL) followed by aq. H_2O_2 (30% *w/w* in water, 0.3 mL). Ethyl acetate (2 mL) was added and the resulting mixture was vigorously stirred for 1 h. The mixture was diluted with ethyl acetate (10 mL) and water (5 mL) and the organic phase was separated. The aqueous layer was extracted with ethyl acetate (2 x 10 mL), the combined organic phases were washed with sat. aq. $Na_2S_2O_3$ solution (15 mL) and brine (15 mL), dried over $MgSO_4$, and filtered, and the solvent was removed under reduced pressure. The residue (rr > 20:1) was purified by flash chromatography (SiO_2, toluene/*tert*-butyl methyl ether, 4:1) to give the title compound as a colorless solid (44.1 mg, 84%, > 20:1 dr, 91% ee). mp = 106-107 °C, $[\alpha]_D^{20}$ (91% ee) = +5.9 (c = 0.65, $CHCl_3$); ***Note:*** *Rotamers were observed at RT, hence characterization by NMR had to be performed at elevated temperature.* ^{1}H NMR (600 MHz, [D_6]-DMSO, 393 K): δ = 7.35 – 7.33 (m, 2H), 7.29 (dd, *J* = 8.4, 6.8 Hz, 2H), 7.24 – 7.21 (m, 1H), 6.83 (ddd, *J* = 15.7, 7.9, 6.2 Hz, 1H), 5.87 (dt, *J* = 15.7, 1.6 Hz, 1H), 5.15 (d, *J* = 5.2 Hz, 1H), 4.64 – 4.62 (m, 1H), 4.17 – 4.13 (m, 1H), 3.65 (s, 3H), 2.77 – 2.73 (m, 1H), 2.66 – 2.60 (m, 1H), 2.57 (s, 3H), 1.30 (s, 9H); ^{13}C NMR (151 MHz, [D_6]-DMSO, 393 K): δ = 165.2, 154.0, 145.9, 142.7, 127.0, 126.3, 125.9, 121.4, 77.9, 73.6, 60.3, 50.1, 30.1, 29.5, 27.4; IR (ATR): $\tilde{\nu}$ = 3438, 2972, 1725, 1694, 1667, 1438, 1393, 1325, 1160, 1043 cm^{-1}; HRMS (ESI$^+$): m/z: calcd. for $C_{19}H_{27}NO_5Na$ $[M+Na]^+$: 372.17814, found: 372.17834.

The ee was determined by HPLC analysis: Chiralpak 150 mm IG-3, 3 µm, Ø = 4.6 mm, acetonitrile/water = 40:60, v = 1.0 mL/min, v = 1.0 mL/min, λ = 210 nm, t(minor) = 8.26 min, t(major) = 10.13 min (racemate left, enantioenriched sample right).

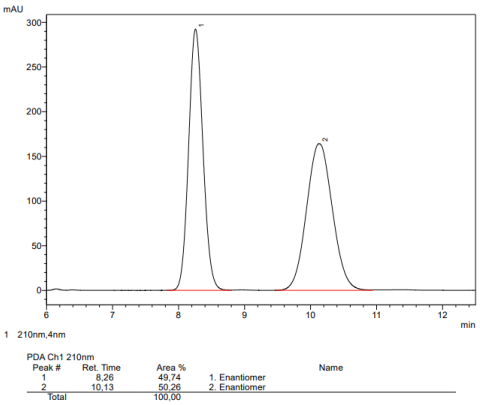

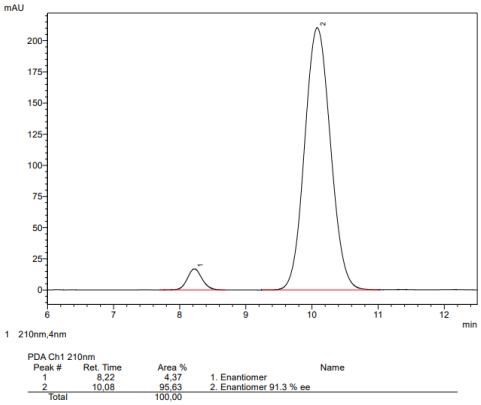

Amino alcohol 129b. A flame-dried Schlenk flask under argon was charged with tris(*trans*-1,2-bis(4-*tert*-butylphenyl)ethene)nickel(0) (14.0 mg, 0.015 mmol), phosphoramidite ligand **L11** (9.6 mg, 0.015 mmol) and diene **127b** (142.8 mg, 0.45 mmol). The Schlenk flask was evacuated and refilled with argon (3 cycles). Triethylborane (1 M in THF, 0.45 mL, 0.45 mmol) was added and the resulting solution was stirred for 5 min before benzaldehyde (15.2 µL, 0.15 mmol) was added under an argon counterflow. The flask was sealed and the mixture stirred at room temperature for 42 h. The mixture was cooled to 0 °C before the reaction was quenched by addition of pH 7 phosphate buffer solution (1.5 mL) followed by aq. H_2O_2 (30% *w/w* in water, 0.3 mL). Ethyl acetate (2 mL) was introduced and the mixture was vigorously stirred for 1 h. The mixture was diluted with additional ethyl acetate (10 mL) and water (5 mL) and the organic phase was separated. The aqueous layer was extracted with ethyl acetate (2 x 10 mL), the combined organic phases were washed with sat. aq. $Na_2S_2O_3$ solution (15 mL) and brine (15 mL), dried over $MgSO_4$, and filtered, and the solvent was removed under reduced pressure. The residue (rr > 20:1) was purified by flash chromatography (SiO_2, toluene/*tert*-butyl methyl ether, 15:1 → 10:1) to furnish the title compound as a colorless oil (56.4 mg, 88%, > 20:1 dr, 86% ee). $[\alpha]_D^{20}$ (86% ee) = +4.4 (c = 0.55, $CHCl_3$); ***Note:*** *Rotamers were observed at RT, hence characterization by NMR had to be performed at elevated temperature.* ^{1}H NMR (600 MHz, [d^6]-DMSO, 393 K): δ = 7.34 – 7.28 (m, 4H), 7.26 – 7.23 (m, 1H), 7.22 – 7.16 (m, 3H), 7.10 – 7.08 (m, 2H), 6.62 (ddd, *J* = 15.7, 7.8, 6.6 Hz, 1H), 5.63 (dt, *J* = 15.7, 1.5 Hz, 1H), 5.18 (s, 1H), 4.84 (d, *J* = 7.6 Hz, 1H), 4.24 (d, *J* = 15.6 Hz, 1H), 3.93 – 3.90 (m, 1H), 3.87 (d, *J* = 15.7 Hz, 1H), 3.62 (s, 3H), 2.75 – 2.71 (m, 1H), 2.69 – 2.63 (m, 1H), 1.35 (s, 9H); ^{13}C NMR (151 MHz, [d^6]-DMSO, 393 K): δ = 165.0, 154.4, 146.1, 142.8, 138.3, 127.2, 127.1, 127.0, 126.4, 126.0, 125.9, 121.2, 78.7, 73.7, 62.5, 50.0, 49.3, 31.3, 27.4 (3CIR (ATR): ṽ = 3462, 2974, 1724, 1691, 1663, 1454, 1366, 1163, 701 cm^{-1}; HRMS (ESI$^+$): m/z: calcd. for $C_{25}H_{31}NO_5Na$ [M+Na]$^+$: 448.20944, found: 448.20897.

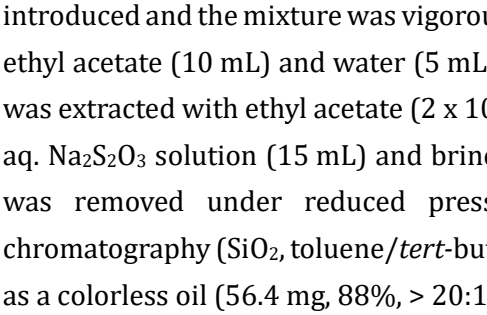

The ee was determined by HPLC analysis: Chiralpak 150 mm IG-3, 3 µm, Ø = 4.6 mm, acetonitrile/water = 50:50, v = 1.0 mL/min, v = 1.0 mL/min, λ = 210 nm, t(minor) = 8.95 min, t(major) = 9.90 min (racemate left, enantioenriched sample right).

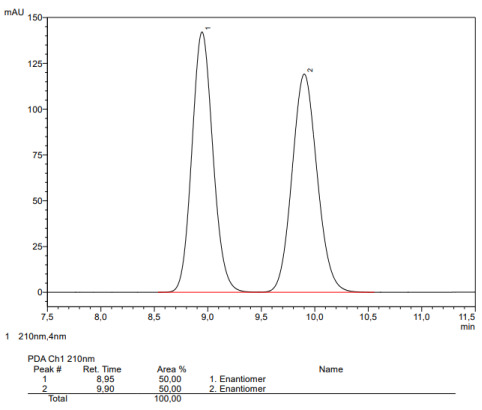

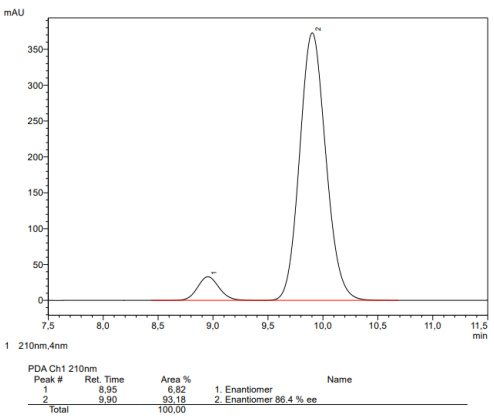

Amino alcohol 130a. A flame-dried Schlenk flask under argon was charged with tris(*trans*-1,2-bis(4-*tert*-butylphenyl)ethene)nickel(0) (9.4 mg, 0.01 mmol), phosphoramidite ligand **L11** (6.4 mg, 0.01 mmol) and diene **128a** (48.1 mg, 0.20 mmol). The Schlenk flask was evacuated and refilled with argon (3 cycles). THF (0.7 mL) and triethylborane (1 M in THF, 0.30 mL, 0.30 mmol) were added and the resulting mixture was stirred for 5 min before benzaldehyde (10.1 µL, 0.10 mmol) was added under argon counterflow. The flask was sealed and the mixture stirred at room temperature for 48 h. The mixture was cooled to 0 °C before the reaction was quenched by addition of pH 7 phosphate buffer solution (1.5 mL) followed by aq. H_2O_2 (30% *w/w* in water, 0.2 mL). Ethyl acetate (2 mL) was introduced and the resulting mixture was vigorously stirred for 1 h. The mixture was diluted with additional ethyl acetate (5 mL) and water (5 mL) and the organic phase was separated. The aqueous layer was extracted with ethyl acetate (3 x 5 mL), the combined organic phases were washed with sat. aq. $Na_2S_2O_3$ solution (5 mL) and brine (5 mL), dried over $MgSO_4$, and filtered, and the solvent was removed under reduced pressure. The residue was purified by flash chromatography (SiO_2, toluene/acetone, 2.5:1) to give the title compound as a colorless oil (23.4 mg, 67%, ≈ 14:1 dr, 95% ee). $[\alpha]_D^{20}$ (95% ee) = +29.9 (c = 0.72, $CHCl_3$); ^{1}H NMR (400 MHz, CD_2Cl_2): δ = 7.38 – 7.32 (m, 4H), 7.29 – 7.25 (m, 1H), 6.71 (dt, *J* = 15.2, 7.1 Hz, 1H), 6.25 (d, *J* = 15.1 Hz, 1H), 4.99 (d, *J* = 8.9 Hz, 1H), 4.85 (d, *J* = 4.0 Hz, 1H), 3.95 (br, 1H), 3.72 (br, 1H), 3.00 (s, 3H), 2.90 (s, 3H), 2.34 – 2.29 (m, 2H), 1.39 (s, 9H); ^{13}C NMR (101 MHz, CD_2Cl_2): δ = 166.6, 156.5, 142.0, 141.7, 128.6, 127.8, 126.8, 123.1, 79.8, 76.5, 56.1, 37.5, 35.7, 32.3, 28.5; IR (ATR): $\tilde{\nu}$ = 3338, 2929, 1699, 1659, 1603, 1496, 1394, 1251, 1168, 703 cm^{-1}; HRMS (ESI^+): m/z: calcd. for $C_{19}H_{28}N_2O_4Na$ $[M+Na]^+$: 371.19413, found: 371.19411.

The ee was determined by HPLC analysis: Chiralpak 150 mm IG-3, 3 µm, Ø = 4.6 mm, acetonitrile/H_2O = 30:70, v = 1.0 mL/min, λ = 220 nm, t(minor) = 11.34 min, t(major) = 19.71 min (racemate left, enantioenriched sample right). The diastereomeric ratio of the enantioenriched sample was determined as dr ≈ 13.8:1.0.

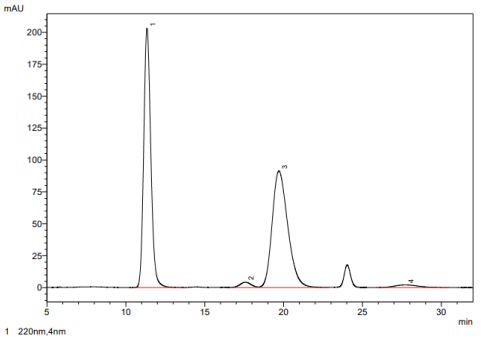

PDA Ch1 220nm

Peak #	Ret. Time	Area %	Name
1	11,34	48,58	1. enantiomer major diastereomer
2	17,58	1,60	1. enantiomer minor diastereomer
3	19,71	48,16	2. enantiomer major diastereomer
4	27,71	1,65	2. enantiomer minor diastereomer
Total		100,00	

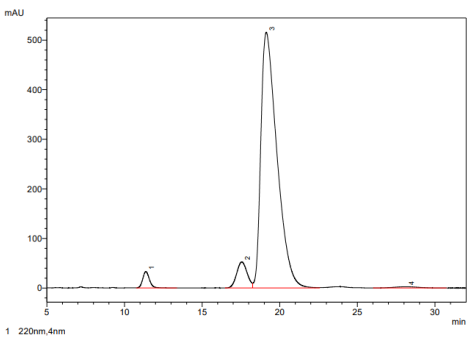

PDA Ch1 220nm

Peak #	Ret. Time	Area %	Name
1	11,38	2,44	1. enantiomer major diastereomer
2	17,55	6,07	1. enantiomer minor diastereomer 79.9 % ee
3	19,14	90,81	2. enantiomer major diastereomer 94.8 % ee
4	28,12	0,68	2. enantiomer minor diastereomer
Total		100,00	

Amino alcohol 130b. A flame-dried Schlenk flask under argon was charged with tris(*trans*-1,2-bis(4-*tert*-butylphenyl)ethene)nickel(0) (9.4 mg, 0.01 mmol), phosphoramidite ligand **L11** (6.4 mg, 0.01 mmol) and diene **128b** (51.3 mg, 0.20 mmol). The Schlenk flask was evacuated and refilled with argon (3 cycles). Triethylborane (1 M in THF, 0.30 mL, 0.30 mmol) was added and the resulting solution was stirred for 5 min before benzaldehyde (10.1 µL, 0.10 mmol) was added under an argon counterflow. The flask was sealed and the mixture stirred at room temperature for 72 h. The mixture was cooled to 0 °C before the reaction was quenched by addition of pH 7 phosphate buffer solution (1.5 mL) followed by aq. H_2O_2 (30% *w/w* in water, 0.2 mL). Ethyl acetate (2 mL) was introduced and the resulting mixture vigorously stirred for 1 h. The mixture was diluted with additional ethyl acetate (5 mL) and water (5 mL) and the organic phase was separated. The aqueous layer was extracted with ethyl acetate (3 x 5 mL), the combined organic phases were washed with sat. aq. $Na_2S_2O_3$ solution (5 mL) and brine (5 mL), dried over $MgSO_4$, and filtered, and the solvent was removed under reduced pressure. The residue was purified by flash chromatography (SiO_2, toluene/*tert*-butyl methyl ether, 2:1 → 1:1.5) to give the title compound as a colorless oil (26.0 mg, 71%, > 20:1 dr, 96% ee). $[\alpha]_D^{20}$(96% ee) = +35.2 (c = 0.65, $CHCl_3$); ^{1}H NMR (400 MHz, CD_2Cl_2): δ = 7.38 – 7.26 (m, 5H), 6.81 (dt, *J* = 15.4, 7.2 Hz, 1H), 6.40 (dt, *J* = 15.5, 1.5 Hz, 1H), 4.87 (t, *J* = 3.9 Hz, 1H), 4.79 (d, *J* = 8.6 Hz, 1H), 3.97 (br, 1H), 3.66 (s, 3H), 3.37 (s, 1H), 3.17 (s, 3H), 1.40 (s, 9H); ^{13}C NMR (101 MHz, CD_2Cl_2): δ = 166.6, 156.6, 143.5, 141.5, 128.6, 128.0, 126.8, 121.7, 80.0, 76.6, 62.1, 56.2, 32.5, 28.4; IR (ATR): $\tilde{\nu}$ = 3338, 2929, 1699, 1659, 1603, 1496, 1394, 1365, 1251, 1168, 703 cm^{-1}; HRMS (ESI$^+$): m/z: calcd. for $C_{19}H_{28}N_2O_4Na$ [M+Na]$^+$: 371.19413, found: 371.19411.

The ee was determined by HPLC analysis: Chiralpak 150 mm IG-3, 3 µm, Ø = 4.6 mm, acetonitrile/20mM NH_4CO_3 (pH = 9) = 30:70, v = 1.0 mL/min, λ = 210 nm, t(minor) = 16.01 min, t(major) = 18.96 min (racemate left, enantioenriched sample right).

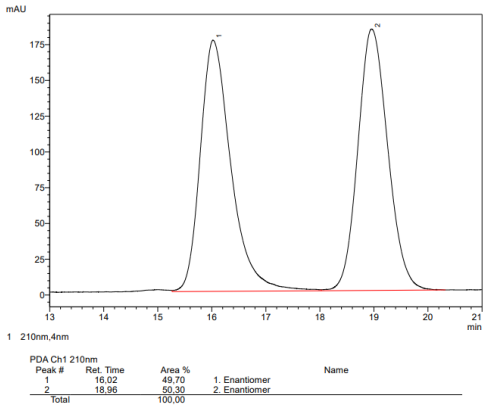

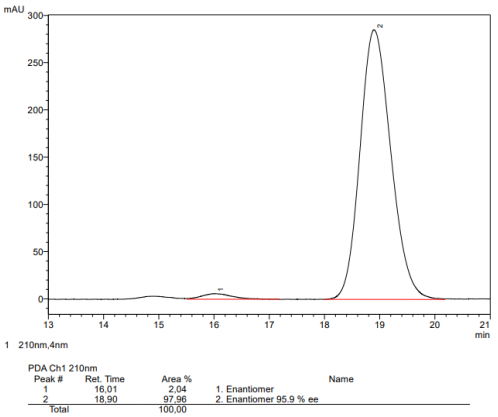

Amino alcohol 134. A flame-dried Schlenk flask was charged with tris(*trans*-1,2-bis(4-*tert*-butylphenyl)ethene)nickel(0) (Ni($^{t\text{Bu}}$stb)$_3$) (7.0 mg, 7.5 µmol), phosphoramidite ligand **L11** (4.8 mg, 7.5 µmol) and diene **133** (30.9 mg, 0.10 mmol). The Schlenk flask was evacuated and refilled with argon (3 cycles). Triethylborane (1 M in THF, 0.15 mL, 0.15 mmol) was added and the resulting solution was stirred for 5 min. Benzaldehyde (5.1 µL, 0.05 mmol) was added under an argon counterflow, the flask was sealed and the mixture stirred at room temperature for 72 h. The reaction was cooled to 0 °C and was quenched by addition of pH 7 phosphate buffer solution (1.0 mL) and aq. H_2O_2 (30% in water, ~0.15 mL). Ethyl acetate (2.0 mL) was added and the resulting mixture was vigorously stirred for 1 h. The mixture was diluted with ethyl acetate (5 mL) and water (5 mL) and was transferred into a separatory funnel. The organic layer was separated and the aqueous layer was extracted with ethyl acetate (2 x 5 mL). The combined organic layers were washed with sat. aq. $Na_2S_2O_3$ solution (5 mL) and brine (5 mL), dried over $MgSO_4$, and filtered, and the solvent was removed under reduced pressure. The crude product (rr > 20:1, 85% conversion) was purified by flash chromatography (SiO_2, toluene/*tert*-butyl methyl ether, 4:1) and the title compound was obtained as a colorless oil (15.3 mg, 73%, dr = 15:1, 56% ee). ^{1}H NMR (400 MHz, CD_2Cl_2): δ = 7.86 – 7.74 (m, 2H), 7.66 – 7.57 (m, 1H), 7.57 – 7.44 (m, 2H), 7.41 – 7.21 (m, 5H), 6.87 (dt, *J* = 15.1, 7.1 Hz, 1H), 6.31 (dt, *J* = 15.1, 1.5 Hz, 1H), 4.86 (d, *J* = 12.6 Hz, 2H), 3.95 (s, 1H), 2.86 (s, 1H), 2.52 – 2.22 (m, 2H), 1.39 (s, 9H); ^{13}C NMR (101 MHz, CD_2Cl_2): δ = 155.7, 143.8, 140.8, 140.7, 133.2, 132.1, 129.2, 128.4, 127.8, 127.5, 79.7, 75.9, 55.0, 31.0, 28.0; IR (ATR): $\tilde{\nu}$ = 3369, 2977, 1689, 1497, 1306, 1163, 1143 cm^{-1}; HRMS (ESI$^+$): *m/z*: calcd. for $C_{22}H_{27}NO_5SNa$ $[M+Na]^+$: 440.15021, found: 440.15065.

The ee was determined by HPLC analysis: Chiralpak 150 mm IG-3, 3 µm, 4.6 mm ∅, acetonitrile/water = 40:60, v = 1.0 mL/min, λ = 220 nm, t(minor) = 16.57 min, t(minor) = 20.53 min (racemate: left, enantioenriched sample: right)

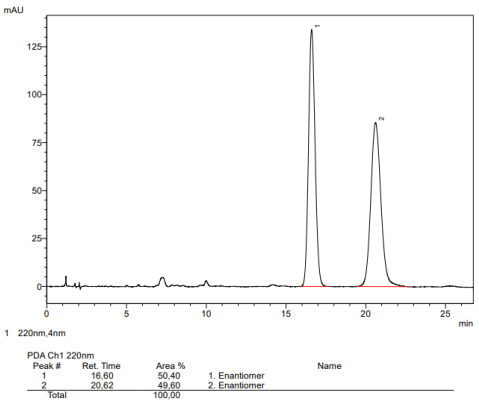

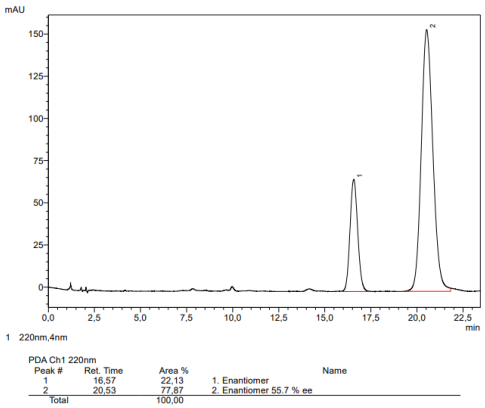

Amino alcohol 145. A flame-dried Schlenk flask under argon was charged with tris(*trans*-1,2-bis(4-*tert*-butylphenyl)ethene)nickel(0) ($Ni(^{t\text{Bu}}stb)_3$) (18.7 mg, 0.02 mmol) and phosphoramidite ligand **L11** (12.8 mg, 0.02 mmol). The Schlenk flask was evacuated and refilled with argon (3 cycles). A solution of diene (*E,Z*)**-88a** (90.9 mg, 0.40 mmol) in THF (0.35 mL) and triethylborane (1 M in THF, 0.30 mL, 0.30 mmol) were successively added and the resulting mixture was stirred for 5 min. Benzaldehyde (20.2 µL, 0.20 mmol) was added under an argon counterflow, the flask was sealed and the mixture stirred at room temperature for 48 h. The reaction was quenched at 0 °C by addition of pH 7 phosphate buffer solution (1.5 mL) and aq. H_2O_2 (30% *w/w* in water, 0.3 mL). Ethyl acetate (2.0 mL) was added and the resulting mixture was vigorously stirred for 1 h. The mixture was diluted with ethyl acetate (10 mL) and water (5 mL) and the aqueous phase was extracted with ethyl acetate (2 x 10 mL). The combined organic layers were washed with sat. aq. $Na_2S_2O_3$ solution (15 mL) and brine (15 mL), dried over $MgSO_4$, filtered, and the solvent was removed under reduced pressure. The crude material (rr > 20:1) was purified by flash chromatography (SiO_2, toluene/*tert*-butyl methyl ether, 3:1) and the product was obtained as a colorless solid (62.6 mg, 93%, dr > 20:1, 40% ee). mp = 85-87 °C; $[\alpha]_D^{20}$ (98% ee, sample after recrystallization) = + 7.1 (c = 0.56, $CHCl_3$); ^{1}H NMR (400 MHz, CD_2Cl_2): δ = 7.29 – 7.17 (m, 5H), 6.83 (dt, *J* = 15.1, 7.4 Hz, 1H), 5.78 (dt, *J* = 15.6, 1.5 Hz, 1H), 4.76 (d, *J* = 7.2 Hz, 1H), 4.62 (t, *J* = 4.1 Hz, 1H), 3.79 – 3.72 (m, 1H), 3.60 (s, 3H), 3.03 (s, 1H), 2.47 – 2.40 (m, 1H), 2.32 – 2.24 (m, 1H), 1.25 (s, 9H); ^{13}C NMR (101 MHz, CD_2Cl_2): δ = 166.9, 156.4, 145.6, 142.1, 128.7, 128.1, 126.7, 123.7, 79.9, 75.7, 56.0, 51.7, 35.3, 28.4; IR (ATR): $\tilde{\nu}$ = 3402, 2976, 1712, 1673, 1513, 1356, 1221, 1166, 1107, 1043, 696 cm^{-1}; HRMS (ESI^+): *m/z*: calcd. for $C_{18}H_{25}NO_5Na$ $[M+Na]^+$: 358.16249, found: 358.16250.

55.0 mg of the product were recrystallized from *tert*-butyl methyl ether/*iso*-hexane to yield the enantioenriched product from the mother liquor in 98% ee (25.2 mg).

The ee was determined by HPLC analysis: Chiralpak 150 mm IG-3, 3 µm, 4.6 mm ∅, *n*-heptane/*iso*-propanol = 90:10, v = 1.0 mL/min, λ = 210 nm, t(minor) = 16.11 min, t(major) = 19.80 min (racemate: top left, enantioenriched sample: top right, recrystallized enantioenriched sample: bottom left).

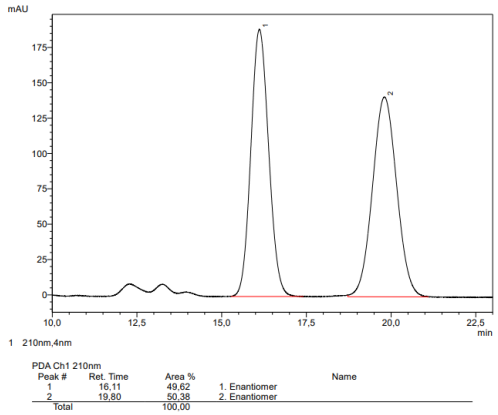

PDA Ch1 210nm

Peak #	Ret. Time	Area %	Name
1	16,11	49,62	1. Enantiomer
2	19,80	50,38	2. Enantiomer
Total		100,00	

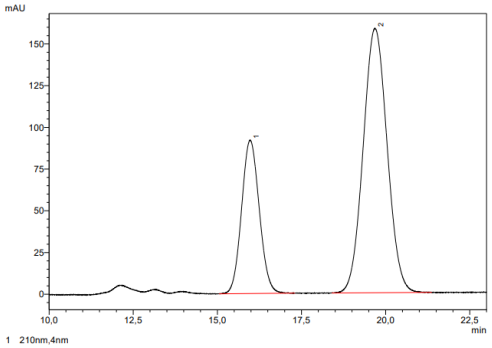

PDA Ch1 210nm

Peak #	Ret. Time	Area %	Name
1	15,97	29,98	1. Enantiomer
2	19,68	70,02	2. Enantiomer 40.0 % ee
Total		100,00	

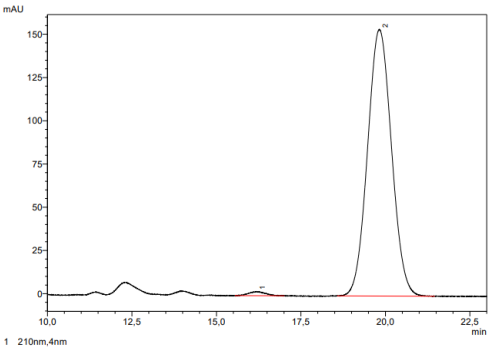

PDA Ch1 210nm

Peak #	Ret. Time	Area %	Name
1	16,18	1,05	1. Enantiomer
2	19,82	98,95	2. Enantiomer 97.9 % ee
Total		100,00	

Amino alcohol 146. A flame-dried Schlenk flask under argon was charged with tris(*trans*-1,2-bis(4-*tert*-butylphenyl)ethene)nickel(0) (Ni($^{t\text{Bu}}$stb)$_3$) (18.7 mg, 0.02 mmol) and phosphoramidite ligand **L11** (12.8 mg, 0.02 mmol). The Schlenk flask was evacuated and refilled with argon (3 cycles). A solution of diene *(E,Z)*-**88a** (90.9 mg, 0.40 mmol) in toluene (1.40 mL) and triethylborane (1 M in toluene, 0.60 mL, 0.60 mmol) were successively added and the resulting mixture was stirred for 5 min. Hydrocinnamaldehyde (26.3 µL, 0.20 mmol) was added under an argon counterflow, the flask was sealed and the mixture stirred at room temperature for 72 h. The reaction was quenched at 0 °C by addition of pH 7 phosphate buffer solution (1.5 mL) and aq. H_2O_2 (30% *w/w* in water, 0.3 mL). Ethyl acetate (2.0 mL) was added and the resulting mixture was vigorously stirred for 1 h. The mixture was diluted with ethyl acetate (10 mL) and water (5 mL) and the aqueous phase was extracted with ethyl acetate (2 x 10 mL). The combined organic layers were washed with sat. aq. $Na_2S_2O_3$ solution (15 mL) and brine (15 mL), dried over $MgSO_4$, and filtered, and the solvent was removed under reduced pressure. The crude material was purified by flash chromatography (SiO_2, toluene/*tert*-butyl methyl ether, 3:1) and the product was obtained as a colorless solid (40.8 mg, 56%, dr > 20:1, 53% ee). mp = 99-101 °C; ^{1}H NMR (400 MHz, CD_2Cl_2): δ = 7.31 – 7.24 (m, 2H), 7.21 – 7.13 (m, 3H), 6.91 (dt, *J* = 15.2, 7.4 Hz, 1H), 5.87 (dt, *J* = 15.6, 1.4 Hz, 1H), 4.86 (d, *J* = 9.5 Hz, 1H), 3.69 (s, 3H), 3.75 – 3.65 (m, 1H), 3.61 (qd, *J* = 6.5, 2.3 Hz, 1H), 2.71 (qt, *J* = 13.7, 7.8 Hz, 2H), 2.45 (t, *J* = 7.3 Hz, 2H), 2.22 (s, 1H), 1.78 (q, *J* = 7.6 Hz, 2H), 1.41 (s, 9H); ^{13}C NMR (101 MHz, CD_2Cl_2): δ = 166.9, 156.4, 145.8, 142.3, 128.8, 126.3, 123.5, 79.7, 72.7, 51.7, 36.6, 36.0, 32.3, 28.4; IR (ATR): $\tilde{\nu}$ = 3406, 2926, 1714, 1678, 1515, 1434, 1318, 1226, 1161, 1119, 1035, 696 cm^{-1}; HRMS (ESI$^+$): *m/z*: calcd. for $C_{20}H_{29}NO_5Na$ [M+Na]$^+$: 386.19379, found: 386.19385.

The ee was determined by HPLC analysis: Chiralpak 150 mm IG-3, 3 µm, 4.6 mm ∅, *n*-heptane/ethanol = 95:5, v = 1.0 mL/min, λ = 210 nm, t(major) = 31.54 min, t(minor) = 43.75 min (racemate: left, enantioenriched sample: right).

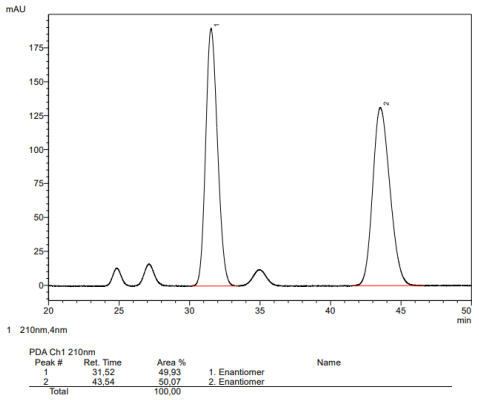

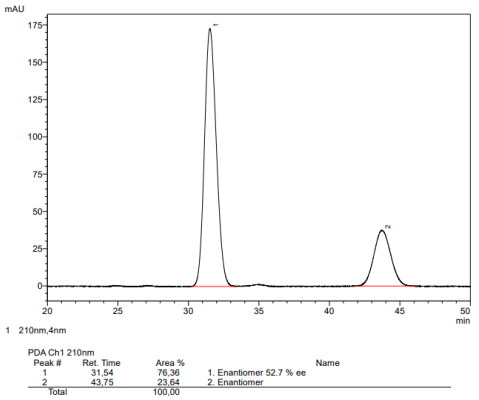

Mosher Ester Analysis

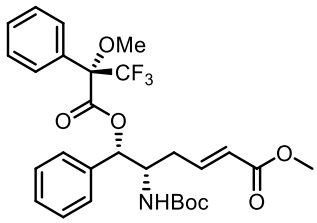

Mosher Ester S52a. DMAP (0.6 mg, 4.8 µmol), triethylamine (10.0 µL, 71.6 µmol) and (*R*)-Mosher's acid chloride (5.00 µL, 26.7 µmol) were added to a solution of amino alcohol **145** (8.0 mg, 23.9 µmol, 98% ee) in dichloromethane (0.5 mL) and the resulting mixture was stirred at room temperature overnight. Dichloromethane (2 mL) and sat. aq. NH_4Cl solution (2 mL) were added and the resulting mixture was vigorously stirred for 5 min. The organic layer was separated and the aqueous layer was extracted with dichloromethane (2 x 5 mL). The combined organic phases were dried over $MgSO_4$ and filtered, and the solvent was removed under reduced pressure. The residue was purified by flash chromatography (SiO_2, pentane/ethyl acetate, 7:1 → 4:1) to give the title compound as a colorless oil (7.5 mg, 57%). $[\alpha]_D^{20}$= + 7.7 (c = 0.70, $CHCl_3$); ^{1}H NMR (600 MHz, $CDCl_3$): δ = 7.41 – 7.33 (m, 5H), 7.33 – 7.29 (m, 3H), 7.21 – 7.18 (m, 2H), 6.83 (dt, *J* = 15.6, 7.7 Hz, 1H), 5.92 (d, *J* = 6.6 Hz, 1H), 5.79 (d, *J* = 15.5 Hz, 1H), 4.53 (d, *J* = 9.4 Hz, 1H), 4.18 (br, 1H), 3.72 (s, 3H), 3.50 (s, 3H), 2.39 – 2.31 (m, 1H), 2.20 – 2.12 (m, 1H), 1.38 (s, 9H); ^{13}C NMR (151 MHz, $CDCl_3$): δ = 166.5, 165.6, 155.1, 143.6, 135.7, 131.8, 129.8, 129.1, 128.8, 128.6, 127.6, 127.3, 124.4, 123.4 (q, $^1J_{CF}$ = 288.7 Hz), 84.9 (q, $^2J_{CF}$ = 27.9 Hz), 80.2, 78.6, 55.7, 53.4, 51.7, 34.4, 28.4; ^{19}F NMR (565 MHz, $CDCl_3$): δ = –71.5; IR (ATR): $\tilde{\nu}$ = 3363, 2979, 1749, 1707, 1518, 1249, 1162, 1016, 721, 699 cm^{-1}; HRMS (ESI$^+$): *m/z*: calcd. for $C_{28}H_{32}F_3NO_7Na$ $[M+Na]^+$: 574.20231, found: 574.20279.

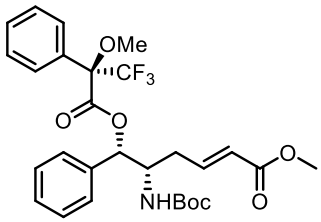

The diasteromeric Mosher ester **S52b**, was prepared analogously using (*S*)-Mosher's acid chloride as a colorless oil (10.4 mg, 61%). $[\alpha]_D^{20}$= + 32.2 (c = 0.90, $CHCl_3$); ^{1}H NMR (600 MHz, $CDCl_3$): δ = 7.44 – 7.38 (m, 3H), 7.37 – 7.33 (m, 5H), 7.31 – 7.27 (m, 2H), 6.81 (dt, *J* = 15.1, 7.3 Hz, 1H), 6.02 (d, *J* = 6.0 Hz, 1H), 5.76 (dt, *J* = 15.6, 1.5 Hz, 1H), 4.47 (d, *J* = 9.4 Hz, 1H), 4.12 (br, 1H), 3.71 (s, 3H), 3.47 (s, 3H), 2.35 – 2.25 (m, 1H), 2.18 – 2.10 (m, 1H), 1.35 (s, 9H); ^{13}C NMR (151 MHz, $CDCl_3$): δ = 166.5, 165.8, 155.0, 143.7, 135.8, 132.0, 129.9, 129.2, 128.9, 128.6, 127.6, 127.4, 124.2, 123.6 (q, $^1J_{CF}$ = 288.9 Hz), 84.7 (q, $^2J_{CF}$ = 27.8 Hz), 80.1, 78.2, 55.6, 53.6, 51.7, 34.4, 28.3; ^{19}F NMR (565 MHz, $CDCl_3$): δ = –71.1; IR (ATR): $\tilde{\nu}$ = 3363, 2953, 1749, 1715, 1499, 1250, 1167, 1015, 730, 699 cm^{-1}; HRMS (ESI$^+$): *m/z*: calcd. for $C_{28}H_{32}F_3NO_7Na$ $[M+Na]^+$: 574.20231, found: 574.20255.

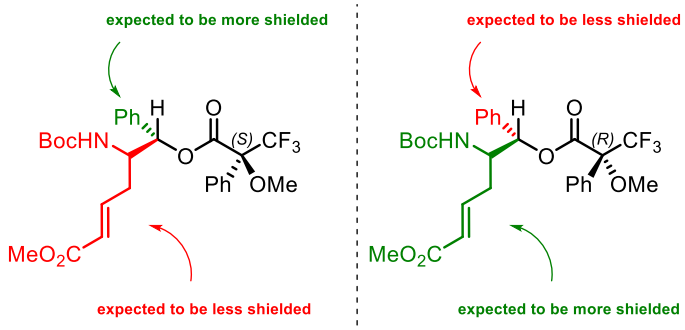

negative $\Delta\delta_{SR}$ expected for resonances of the phenyl group

positive $\Delta\delta_{SR}$ expected for resonances of the chain bearing the amino group and acrylate handle

Observed $\Delta\delta_{SR}$ values (Hz):

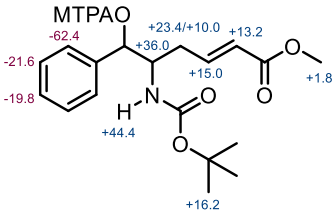

Stereocenter bearing the alcohol group assigned as (*S*). Due to the *syn*-configuration, the absolute configuration on the stereocenter bearing the amino group could be determined as (*S*) as well.

Scheme S1: Mosher ester analysis of compound **S52**.[245]

5.3.5 Downstream Derivatization

Compound 147. A Schlenk flask under argon was charged with the recrystallized amino alcohol derivative **90a** (67.5 mg, 0.20 mmol, 99% ee), Pd/C (15 mg, 14.1 µmol) and ethyl acetate (2 mL). The mixture was purged with H_2 from a balloon for 1 min and was then stirred under H_2-atmosphere for 30 min at room temperature. The mixture was filtered through a plug of Celite and the filtrate was evaporated under reduced pressure. The hydrogenated product was obtained as an off-white solid (quant.) and was directly used in the next step without further purification.

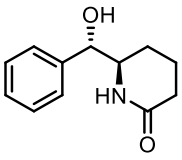

HCl in dioxane (4 M, 1 mL) was added to a solution of the crude product in 1,4-dioxane (2 mL). The mixture was stirred at 50 °C for 16 h. The solvent was removed under reduced pressure and the hydrochloride salt was obtained as a colorless solid (quant.), which was directly used in the next step without further purification.

The hydrochloride salt was dissolved in ethanol (3 mL). NEt_3 (112 µL, 0.81 mmol) was added and the resulting mixture was stirred at 65 °C for 17 h. The solvent was removed under reduced pressure and the residue was purified by flash chromatography (SiO_2, ethyl acetate/methanol, 100:6) to give the title compound as a colorless solid (36.7 mg, 89%, >99% ee). mp = 111-113 °C; $[\alpha]_D^{20}$ (>99% ee) = +65.8 (c = 0.50, $CHCl_3$); ^{1}H NMR (400 MHz, CD_2Cl_2): δ = 7.40 – 7.30 (m, 5H), 5.98 (s, 1H), 4.59 (d, *J* = 5.5 Hz, 1H), 3.65 – 3.60 (m, 1H), 3.15 (s, 1H), 2.28 – 2.21 (m, 1H), 2.14 – 2.05 (m, 1H), 1.86 – 1.76 (m, 2H), 1.66 – 1.55 (m, 1H), 1.51 – 1.41 (m, 1H); ^{13}C NMR (101 MHz, CD_2Cl_2): δ = 173.0, 140.6, 128.9, 128.6, 127.3, 76.4, 58.6, 31.9, 24.1, 19.8; IR (ATR): $\tilde{\nu}$ = 3392, 1645, 1451, 1410, 1329, 1305, 1192, 1065, 704 cm^{-1}; HRMS (ESI$^+$): *m/z*: calcd. for $C_{12}H_{15}NO_2Na$ $[M+Na]^+$: 228.09950, found: 228.09927.

The ee was determined by HPLC analysis: Chiralpak 150 mm IC-3, 3 µm, 4.6 mm ∅, *n*-heptane/*iso*-propanol = 60:40, v = 1.0 mL/min, λ = 210 nm, t(minor) = 9.72 min, t(major) = 12.67 min (racemate: left, enantioenriched sample: right).

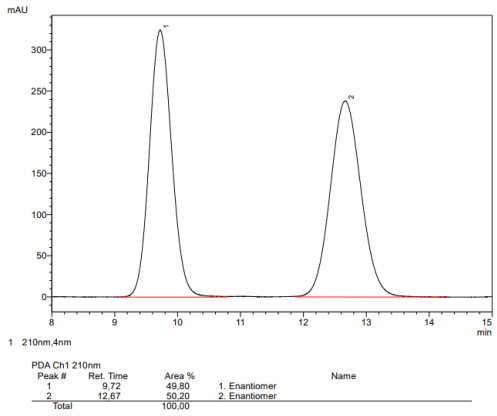

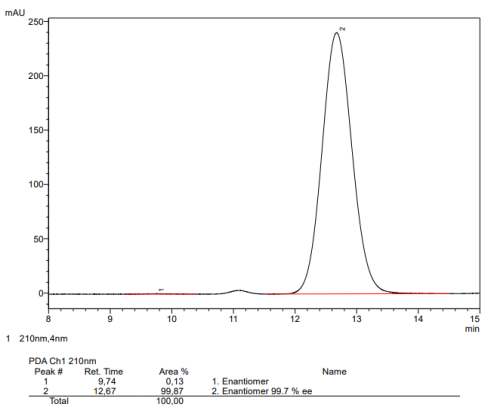

Compound 148. A flame dried pressure flask was charged with a solution of lithium aluminum hydride (1.0 M in THF, 0.90 mL, 0.90 mmol). A solution of lactam **147** (57.7 mg, 0.28 mmol, >99% ee) in THF (2 mL) was added dropwise at 0 °C. After complete addition, the mixture was stirred at 65 °C (bath temperature) for 90 min. The mixture was cooled to 0 °C and the reaction carefully quenched by dropwise addition of sat. aq. Rochelle salt solution (3 mL). The mixture was diluted with dichloromethane (5 mL) and was vigorously stirred for 30 min. The organic phase was separated and the aqueous layer extracted with dichloromethane (4 x 10 mL). The combined organic phases were washed with brine (10 mL), dried over $MgSO_4$, and filtered, and the solvent was removed under reduced pressure to give the title compound as an off-white solid that needed no further purification (53.4 mg, quant., >99% ee). mp = 124-126 °C; $[\alpha]_D^{20}$ (>99% ee) = +42.8 (c = 0.50, $CHCl_3$); ^{1}H NMR (400 MHz, CD_2Cl_2): δ = 7.36 – 7.23 (m, 5H), 4.69 (d, *J* = 4.4 Hz, 1H), 3.21 (br, 2H), 3.11 – 3.06 (m, 1H), 2.82 – 2.77 (m, 1H), 2.64 (td, *J* = 12.0, 2.9 Hz, 1H), 1.79 – 1.69 (m, 1H), 1.57 – 1.53 (m, 1H), 1.45 – 1.17 (m, 4H); ^{13}C NMR (101 MHz, CD_2Cl_2): δ = 141.9, 128.5, 127.6, 126.8, 76.1, 62.5, 47.0, 26.2, 25.9, 24.5; IR (ATR): $\tilde{\nu}$ = 3287, 2926, 1448, 1432, 1262, 1108, 997, 899, 817, 701 cm^{-1}; HRMS (ESI$^+$): *m/z*: calcd. for $C_{12}H_{18}NO$ $[M+H]^+$: 192.13829, found: 192.13845.

The ee was determined by HPLC analysis: Chiralpak 150 mm IG-3, 3 µm, 4.6 mm ∅, *n*-heptane + 0.05% DEA/*iso*-propanol = 95:5, v = 1.0 mL/min, λ = 210 nm, t(minor) = 7.62 min, t(major) = 8.46 min (racemate: left, enantioenriched sample: right).

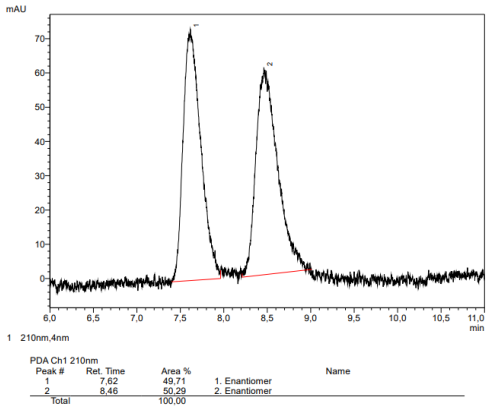

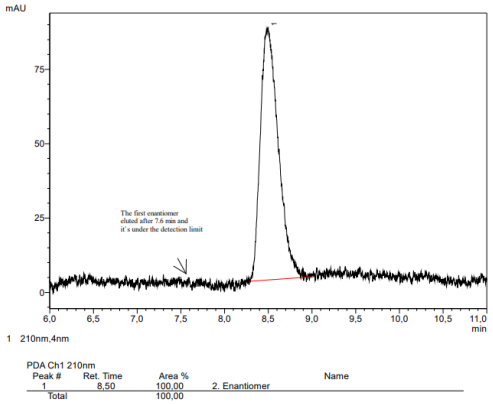

Compound 149. DBU (2.5 µL, 16.7 µmol, 0.22 eq.) was added to a solution of the recrystallized amino alcohol **90a** (25.5mg, 76.0 µmol, 99% ee) in THF (0.75 mL) and the resulting mixture was stirred at room temperature for 16 h. The solvent was evaporated and the residue purified by flash chromatography (SiO_2, *iso*-hexane/ethyl acetate, 2:1) to give the title compound as a colorless solid (24.8 mg, 73.9 µmol, 97%, 2:1 dr). *Note: The compound shows partially broadened signals in NMR at room temperature and was therefore analyzed at 263 K. The dr was determined as 2:1, with one rotamer present for each diastereomer. The ratio of rotamer pairs to each other was ~ 4:1.* mp = 100-102 °C; ^{1}H NMR (600 MHz, 263 K, $CDCl_3$): δ = 7.42 – 7.39 (m, 2H), 7.36 – 7.32 (m, 2H), 7.29 – 7.24 (m, 1H), 5.00 (d, *J* = 7.4 Hz, 1H), 4.83 (d, *J* = 3.7 Hz, 1H), 4.66 – 4.58 (m, 1H), 4.14 – 4.10 (m, 1H), 3.72 (3H), 2.84 (dd, *J* = 15.8, 7.4 Hz, 1H), 2.67 (dd, *J* = 15.8, 5.8 Hz, 1H), 2.03 (ddd, *J* = 13.1, 5.9, 3.0 Hz, 1H), 1.93 (ddd, *J* = 13.1, 9.5, 7.2 Hz, 1H), 1.43 (s, 9H); ^{13}C NMR (151 MHz, 263 K, $CDCl_3$): δ =171.6, 155.2, 140.5, 128.4, 127.7, 125.7, 86.6, 79.9, 75.0, 59.0, 52.2, 40.4, 37.3, 28.4; IR (ATR): ṽ =3354, 2977, 1737, 1708, 1521, 1366, 1249, 1168, 1062, 701 cm^{-1}; HRMS (ESI$^+$): *m/z*: calcd. for $C_{18}H_{26}NO_5$ [M+H]$^+$: 336.18055, found: 336.18032.

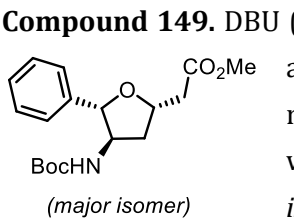

(major isomer)

The diastereomers were assigned based on NOESY data:

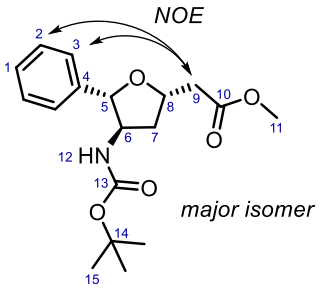

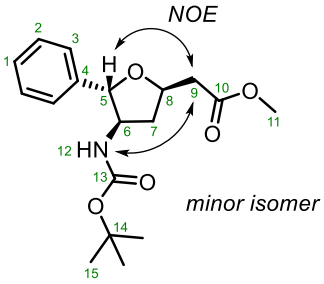

Compound 150. A flame dried Schlenk flask under argon was charged with the recrystallized amino alcohol derivative **90a** (41.0 mg, 0.12 mmol, 99% ee) and diethyl ether (1.0 mL). The mixture was cooled to 0 °C before $SOCl_2$ (89.0 µL, 1.23 mmol) was added dropwise. The mixture was allowed to warm to room temperature and stirred for 2 h. The reaction was carefully quenched at 0 °C by dropwise addition of sat. aq. $NaHCO_3$ (2.0 mL). Ethyl acetate (2 mL) was added, the organic phase was separated and the aqueous phase was extracted with ethyl acetate (3 x 5 mL). The combined organic phases were washed with brine (5 mL), dried over $MgSO_4$, and filtered, and the solvent was removed under reduced pressure. The residue was purified by flash chromatography (SiO_2, pentane/ethyl acetate, 3:1 → 1:2) to give the title compound as a colorless solid (27.9 mg, 87%, >99% ee). mp = 129-131 °C; $[\alpha]_D^{20}$ (>99% ee) = +52.8 (c = 0.50, $CHCl_3$); ^{1}H NMR (400 MHz, $CDCl_3$): δ = 7.43 – 7.32 (m, 5H), 6.86 (ddd, *J* = 15.7, 7.8, 6.9 Hz, 1H), 6.00 (br, 1H), 5.99 (dt, *J* = 15.6, 1.4 Hz, 1H), 5.15 (d, *J* = 6.2 Hz, 1H), 3.87 (dddd, *J* = 7.2, 6.2, 5.2, 1.1 Hz, 1H), 3.74 (s, 3H), 2.69 – 2.53 (m, 2H); ^{13}C NMR (101 MHz, $CDCl_3$): δ = 166.2, 158.6, 141.9, 137.7, 129.4, 129.2, 126.0, 125.5, 82.8, 59.5, 51.9, 37.5; IR (ATR): $\tilde{\nu}$ =3305, 2923, 1752, 1720, 1436, 1278, 1224, 1167, 1010, 699 cm^{-1}; HRMS (ESI$^+$): *m/z*: calcd. for $C_{14}H_{15}NO_4Na$ $[M+Na]^+$: 284.08933, found: 284.08920.

The ee was determined by HPLC analysis: Chiralpak 150 mm IG-3, 3 µm, 4.6 mm ∅, acetonitrile/water = 50:50, v = 1.0 mL/min, λ = 220 nm, t(major) = 4.89 min, t(minor) = 5.63 min (racemate: left, enantioenriched sample: right).

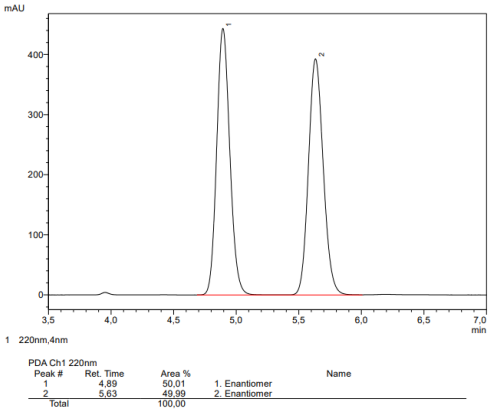

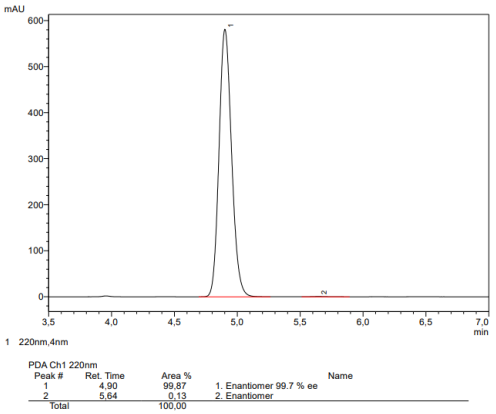

Note: Single crystals suitable for X-ray diffraction analysis were obtained by recrystallization from cyclohexane/ethyl acetate, which were used to confirm the cyclization proceeds with inversion of the alcohol center to give the *syn*-configured product **150**.

5.4 Enantioselective Nickel-Catalyzed Intramolecular Reductive Couplings

5.4.1 Experimental Procedure and Work-up

General Procedure III (for solid aldehydes)

A flame-dried Schlenk flask was charged under argon with tris(*trans*-1,2-bis(4-*tert*-butylphenyl)ethene)nickel(0) (Ni($^{t\text{Bu}}$stb)$_3$) (9.4 mg, 10.0 μmol) and (*S*)-AntPhos **L29** (4.1 mg, 11.0 μmol). The flask was evacuated and refilled with argon (3 cycles). THF (0.75 mL) and triethylborane (1.0 M in THF, 0.25 mL, 0.25 mmol) were added and the resulting solution was cooled to 0 °C and stirred for 2 min before the respective substrate (0.10 mmol) was introduced under an argon counterflow. The flask was sealed and the mixture stirred at 0 °C (bath temperature) for the indicated time. The reaction was quenched *via* the work-up procedure **III** or **IV** as specified in each case.

General Procedure IV (for liquid aldehydes)

A flame-dried Schlenk flask was charged under argon with tris(*trans*-1,2-bis(4-*tert*-butylphenyl)ethene)nickel(0) (Ni($^{t\text{Bu}}$stb)$_3$) (9.4 mg, 10.0 μmol) and (*S*)-AntPhos **L29** (4.1 mg, 11.0 μmol). The flask was evacuated and refilled with argon (3 cycles). THF (0.25 mL) and triethylborane (1.0 M in THF, 0.25 mL, 0.25 mmol) were added and the resulting solution was cooled to 0 °C and stirred for 2 min. A solution of the respective substrate (0.10 mmol) in THF (0.50 mL) was introduced under an argon counterflow, the flask was sealed and the mixture stirred at 0 °C (bath temperature) for the indicated time. The reaction was quenched *via* the work-up procedure **III** or **IV** as specified in each case.

General Procedure V (using Et_2Zn)

A flame-dried Schlenk flask under argon was charged with tris(*trans*-1,2-bis(4-*tert*-butylphenyl)ethene)nickel(0) (Ni($^{t\text{Bu}}$stb)$_3$) (9.4 mg, 10.0 μmol) and (*S*)-AntPhos **L29** (4.1 mg, 11.0 μmol). The flask was evacuated and refilled with argon (3 cycles) before THF (0.25 mL) and diethylzinc (1.0 M in hexane, 0.25 mL, 0.25 mmol) were added, and the resulting solution was cooled to 0 °C and stirred for 2 min. A solution of the respective substrate (0.10 mmol) in THF (0.50 mL) was introduced under an argon counterflow, the flask was sealed and the mixture stirred at 0 °C (bath temperature) for the indicated time. The reaction was quenched *via* the work-up procedure **III** or **IV** as specified in each case.

Work-up Procedures

Oxidative Work-up Procedure (III): The reaction mixture was cooled to 0 °C and pH 7 phosphate buffer solution (1.0 mL), aq. H_2O_2 (30% *w/w*, ≈0.1 mL) and ethyl acetate (2.0 mL) were added. The mixture was vigorously stirred at room temperature for 30 min. Additional ethyl acetate (10 mL) and water (5 mL) were introduced, the organic phase was separated, and the aqueous layer was extracted with ethyl acetate (2 × 10 mL). The combined organic phases were washed with sat. aq. $Na_2S_2O_3$ (10 mL) and brine (10 mL), dried over $MgSO_4$, and filtered, and then concentrated *in vacuo*. The residue was purified as specified for each compound.

Basic Work-up Procedure (IV): The reaction mixture was cooled to 0 °C and sat. aq. $NaHCO_3$ solution (2.0 mL) and ethyl acetate (2.0 mL) were added. The mixture was vigorously stirred at room temperature for 30 min. The mixture was diluted with ethyl acetate (10 mL) and water (5 mL) and the aqueous layer was extracted with ethyl acetate (2 × 10 mL). The combined organic layers were washed with brine (15 mL), dried over $MgSO_4$, and filtered, and then concentrated *in vacuo*. The residue was purified as specified for each compound.

5.4.2 Enantioselective Synthesis of Tetrahydroisoquinoline Derivatives and Related Heterocycles

Tetrahydroisoquinoline Derivative 153. The title compound was prepared according to the general procedure **III** followed by oxidative work-up **III**, using substrate **152** (34.5 mg, 0.10 mmol); the reaction time was 24 h. The crude material was purified by flash chromatography (SiO_2, *n*-pentane/*tert*-butyl methyl ether, 1:1) to give the product as a colorless oil (30.7 mg, 88%, 92% ee). $[\alpha]_D^{20}$ = +60.6 (c = 0.50, $CHCl_3$); ^{1}H NMR (600 MHz, [D_6]-DMSO, 383 K): δ = 7.31 (dd, *J* = 7.3, 1.6 Hz, 1H), 7.28 (td, *J* = 7.4, 1.6 Hz, 1H), 7.27 – 7.21 (m, 1H), 7.20 (d, *J* = 7.4 Hz, 1H), 6.83 (dt, *J* = 15.6, 7.8 Hz, 1H), 5.81 (dt, *J* = 15.6, 1.5 Hz, 1H), 4.77 (d, *J* = 17.1 Hz, 1H), 4.47 (d, *J* = 2.7 Hz, 1H), 4.46 (ddd, *J* = 8.9, 5.4, 2.7 Hz, 1H), 4.19 (d, *J* = 17.1 Hz, 1H), 3.65 (s, 3H), 2.24 (dddd, *J* = 14.6, 6.9, 5.4, 1.6 Hz, 1H), 2.10 (dddd, *J* = 14.6, 8.8, 7.8, 1.5 Hz, 1H), 1.45 (s, 9H); ^{13}C NMR (151 MHz, [D_6]-DMSO, 383 K): δ = 165.1, 154.3, 144.9, 134.3, 132.3, 128.9, 127.1, 125.9, 125.4, 121.9, 78.5, 68.3, 55.4, 50.2, 41.8, 32.9, 27.5; IR (ATR): $\tilde{\nu}$ = 3433, 2925, 1722, 1688, 1406, 1365, 1241, 1160, 1123, 1031, 732 cm^{-1}; HRMS (ESI$^+$): *m/z*: calcd. for $C_{19}H_{25}NO_5Na$ [M+Na]$^+$: 370.16249, found: 370.16251.

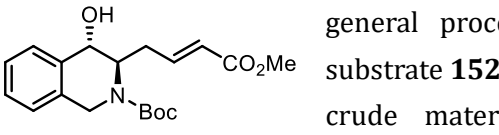

The ee was determined by HPLC analysis: Chiralpak 150 mm IB-N-3, 3 µm, 4.6 mm ∅, acetonitrile/water = 30:70, v = 1.0 mL/min, λ = 220 nm, t(minor) = 20.00 min, t(major) = 25.06 min, (racemic sample: left, enantioenriched sample: right).

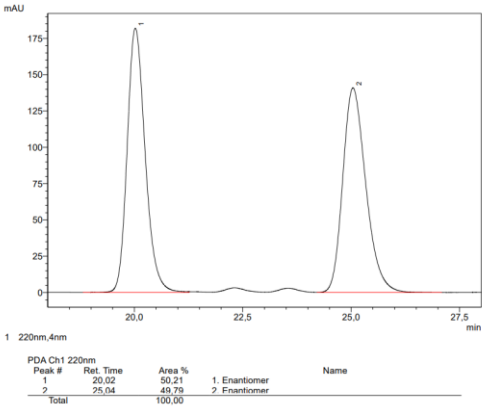

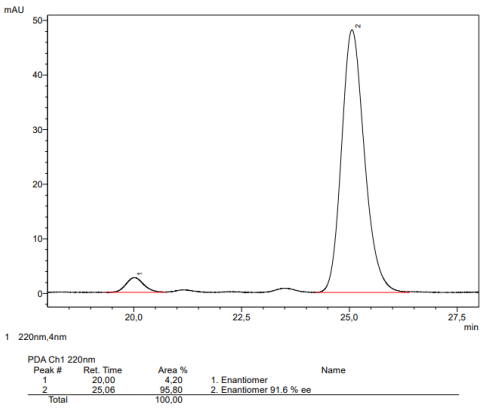

Scale-Up Experiment:

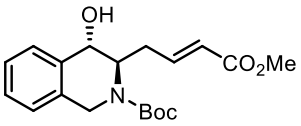

A flame-dried Schlenk flask was charged under argon with tris(*trans*-1,2-bis(4-*tert*-butylphenyl)ethene)nickel(0) (Ni($^{t\text{Bu}}$stb)$_3$) (93.6 mg, 0.10 mmol) and (*S*)-AntPhos (40.7 mg, 0.11 mmol). The flask was evacuated and refilled with argon (3 cycles) before THF (7.5 mL) and triethylborane (1.0 M in THF, 2.50 mL, 2.50 mmol) were added. The resulting solution was cooled to 0 °C (bath temperature) and stirred for 2 min before substrate **152** (345 mg, 1.00 mmol) was introduced under an argon counterflow. A gas bubbler was connected to the Schlenk flask and the mixture was stirred under a very gentle flow of argon at 0 °C (bath temperature) for 16 h. pH 7 Phosphate buffer solution (10 mL), aq. H_2O_2 (30% *w/w* in water, ≈1.0 mL) and ethyl acetate (20 mL) were successively added at 0 °C and the mixture was allowed to reach room temperature while vigorously stirring for 30 min. Additional ethyl acetate (20 mL) and water (10 mL) were introduced, the organic phase was separated, and the aqueous layer was extracted with ethyl acetate (2 × 20 mL). The combined organic layers were washed with sat. aq. $Na_2S_2O_3$ (20 mL) and brine (20 mL), dried over $MgSO_4$, filtered and concentrated *in vacuo*. The residue was purified by flash chromatography (SiO_2, *n*-pentane/*tert*-butyl methyl ether, 1:1) to give the title compound as a colorless oil (302 mg, 87%, 92% ee).

Tetrahydroisoquinoline Derivative 154. The title compound was prepared according to the general procedure **III** followed by oxidative work-up **III**, using substrate **S30** (75.9 mg, 0.20 mmol); the reaction time was 16 h. The crude material was purified by flash chromatography (SiO_2, *n*-pentane/ethyl acetate, 1.5:1) to give the product as a colorless oil (68.3 mg, 90%, 93% ee). $[\alpha]_D^{20}$ = +22.5 (c = 0.48, $CHCl_3$); ^{1}H NMR (600 MHz, [D_6]-DMSO, 383 K): δ = 7.41 – 7.35 (m, 4H), 7.34 – 7.30 (m, 2H), 7.29 (dd, *J* = 7.4, 1.6 Hz, 1H), 7.27 – 7.24 (m, 1H), 7.23 – 7.21 (m, 1H), 6.82 (ddd, *J* = 15.6, 7.7, 7.0 Hz, 1H), 5.81 (dt, *J* = 15.7, 1.5 Hz, 1H), 5.17 (d, *J* = 12.7 Hz, 1H), 5.16 – 5.11 (m, 1H), 5.06 (br, 1H), 4.87 (d, *J* = 17.3 Hz, 1H), 4.55 (ddd, *J* = 8.5, 6.0, 2.6 Hz, 1H), 4.50 (d, *J* = 2.6 Hz, 1H), 4.30 (d, *J* = 17.0 Hz, 1H), 3.65 (s, 3H), 2.25 (dddd, *J* = 14.7, 6.9, 6.0, 1.6 Hz, 1H), 2.17 (dddd, *J* = 14.8, 8.4, 7.6, 1.5 Hz, 1H); ^{13}C NMR (151 MHz, [D_6]-DMSO, 383 K): δ = 165.1, 155.0, 144.4, 136.5, 134.2, 131.9, 129.0, 127.7, 127.2, 127.0, 126.7, 126.1, 125.4, 122.1, 68.1, 65.9, 55.7, 50.3, 42.0, 32.7; IR (ATR): $\tilde{\nu}$ = 3410, 1699, 1420, 1322, 1272, 1227, 1123, 1032, 742 cm^{-1}; HRMS (ESI$^+$): *m/z*: calcd. for $C_{22}H_{23}NO_5Na$ [M+Na]$^+$: 404.14684, found: 404.14694.

The ee was determined by HPLC analysis: Chiralpak 150 mm IG-N-3, 3 µm, 4.6 mm ∅, acetonitrile/water = 45:55, v = 1.0 mL/min, λ = 215 nm, t(minor) = 17.66 min, t(major) = 22.89 min (racemic sample: left, enantioenriched sample: right).

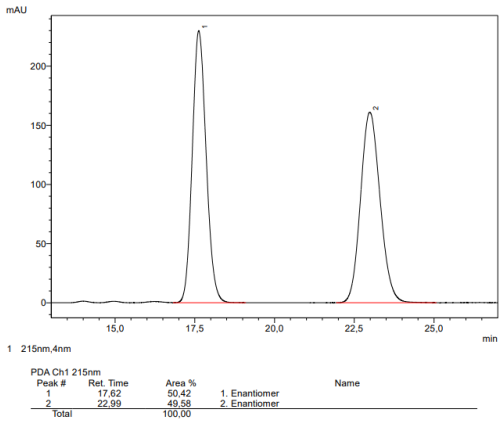

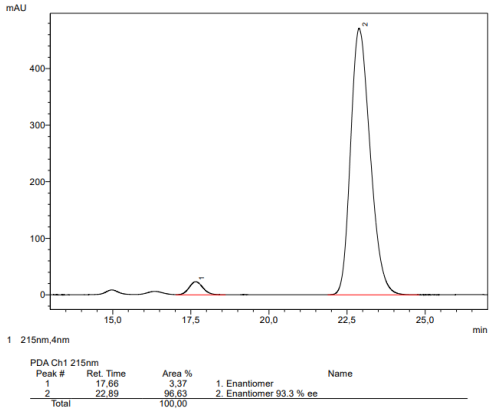

Tetrahydroisoquinoline Derivative 155. The title compound was prepared according to the general procedure **IV** followed by oxidative work-up **III**, using substrate **S31** (36.3 mg, 0.10 mmol); the reaction time was 16 h. The crude material was purified by flash chromatography (SiO_2, *n*-pentane/ethyl acetate, 1.5:1) to give the product as a colorless oil (27.6 mg, 76%, 92% ee). $[\alpha]_D^{20}$ = +46.3 (c = 0.54, $CHCl_3$); ^{1}H NMR (600 MHz, [D$_6$]-DMSO, 383 K): δ = 7.35 – 7.27 (m, 1H), 7.20 – 7.15 (m, 1H), 7.10 (ddd, *J* = 10.1, 8.2, 1.1 Hz, 1H), 6.83 (ddd, *J* = 15.6, 7.9, 6.8 Hz, 1H), 5.84 (dt, *J* = 15.6, 1.5 Hz, 1H), 5.10 (d, *J* = 4.5 Hz, 1H), 4.80 (d, *J* = 17.6 Hz, 1H), 4.51 (d, *J* = 4.0 Hz, 1H), 4.49 (dd, *J* = 5.3, 2.5 Hz, 1H), 4.14 (d, *J* = 17.8 Hz, 1H), 3.65 (s, 3H), 2.26 (dddd, *J* = 14.7, 6.8, 5.3, 1.6 Hz, 1H), 2.12 (dddd, *J* = 14.8, 9.2, 7.9, 1.4 Hz, 1H), 1.46 (s, 9H); ^{13}C NMR (151 MHz, [D$_6$]-DMSO, 383 K): δ = 165.1, 157.9 (d, *J* = 244.4 Hz), 154.2, 144.6, 136.9 (d, *J* = 3.5 Hz), 127.4 (d, *J* = 8.3 Hz), 125.0 (d, *J* = 3.2 Hz), 122.0, 119.6 (d, *J* = 15.5 Hz), 113.3 (d, *J* = 20.7 Hz), 78.8, 67.6 (d, *J* = 2.7 Hz), 55.1, 50.2, 36.1 (d, *J* = 6.1 Hz), 32.3, 27.5; ^{19}F NMR (585 MHz, [D$_6$]-DMSO, 383 K): δ = –120.4 (dd, *J* = 10.3, 5.8 Hz); IR (ATR): $\tilde{\nu}$ = 3433, 2977, 1722, 1692, 1409, 1366, 1319, 1244, 1162, 1120, 1039, 978 cm^{-1}; HRMS (ESI$^+$): *m/z*: calcd. for $C_{19}H_{24}FNO_5Na$ $[M+Na]^+$: 388.15307, found: 388.15309.

The ee was determined by HPLC analysis: Chiralpak 150 mm IG-3, 3 µm, 4.6 mm ∅, acetonitrile/water = 45:55, v = 1.0 mL/min, λ = 220 nm, t(minor) = 7.18 min, t(major) = 12.56 min (racemic sample: left, enantioenriched sample: right).

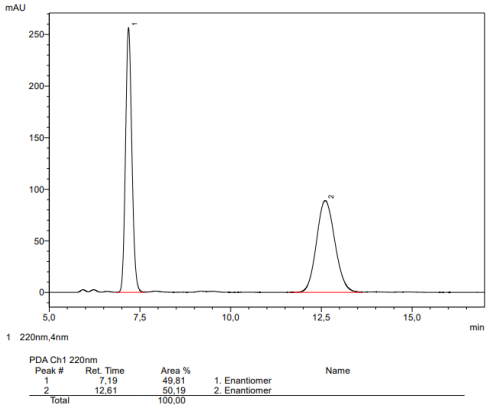

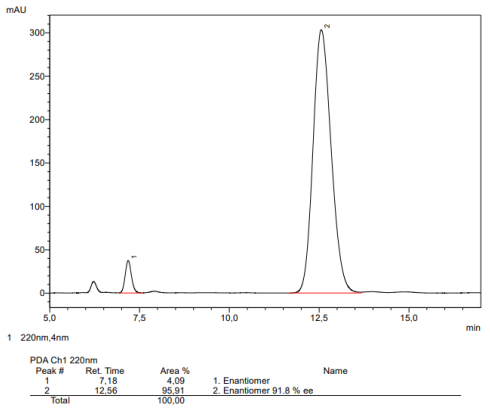

Tetrahydroisoquinoline Derivative 156. The title compound was prepared according to the general procedure **III** followed by oxidative work-up **III**, using substrate **S32** (36.3 mg, 0.10 mmol); the reaction time was 16 h. The crude material was purified by flash chromatography (SiO_2, *n*-pentane/ethyl acetate, 2:1) to give the product as a colorless oil (28.0 mg, 77%, 93% ee). $[\alpha]_D^{20}$ = +42.2 (c = 0.40, $CHCl_3$); ^{1}H NMR (600 MHz, [D_6]-DMSO, 383 K): δ = 7.38 – 7.32 (m, 1H), 7.05 – 7.01 (m, 2H), 6.82 (ddd, *J* = 15.6, 7.8, 6.8 Hz, 1H), 5.82 (dt, *J* = 15.7, 1.5 Hz, 1H), 4.99 (br, 1H), 4.78 (d, *J* = 17.4 Hz, 1H), 4.47 (d, *J* = 1.8 Hz, 1H), 4.47 – 4.44 (m, 1H), 4.18 (d, *J* = 17.6 Hz, 1H), 3.65 (s, 3H), 2.23 (dddd, *J* = 14.7, 6.9, 5.4, 1.6 Hz, 1H), 2.16 – 2.04 (m, 1H), 1.45 (s, 9H); ^{13}C NMR (151 MHz, [D_6]-DMSO, 383 K): δ = 165.1, 161.1 (d, *J* = 243.8 Hz), 154.2, 144.7, 134.9 (d, *J* = 8.1 Hz), 131.1 (d, *J* = 8.4 Hz), 130.6 (d, *J* = 2.9 Hz), 121.9, 112.9 (d, *J* = 21.4 Hz), 111.9 (d, *J* = 22.1 Hz), 78.6, 67.6, 55.4, 50.3, 41.7, 32.7, 27.5; ^{19}F NMR (585 MHz, [D_6]-DMSO, 383 K): δ = –114.6 (m); IR (ATR): $\tilde{\nu}$ = 3422, 2926, 1723, 1694, 1410, 1367, 1251, 1163, 1121, 1042 cm^{-1}; HRMS (ESI$^+$): *m/z*: calcd. for $C_{19}H_{24}FNO_5Na$ $[M+Na]^+$: 388.15307, found: 388.15287.

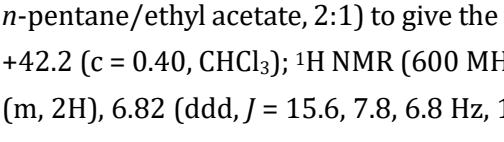

The ee was determined by HPLC analysis: Chiralpak 150 mm IG-3, 3 µm, 4.6 mm ∅, acetonitrile/water = 40:60, v = 1.0 mL/min, λ = 220 nm, t(minor) = 8.32 min, t(major) = 9.30 min (racemic sample: left, enantioenriched sample: right).

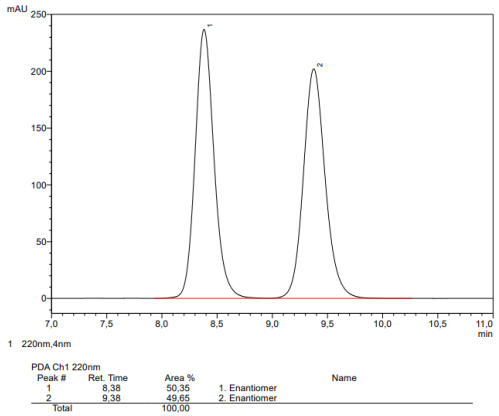

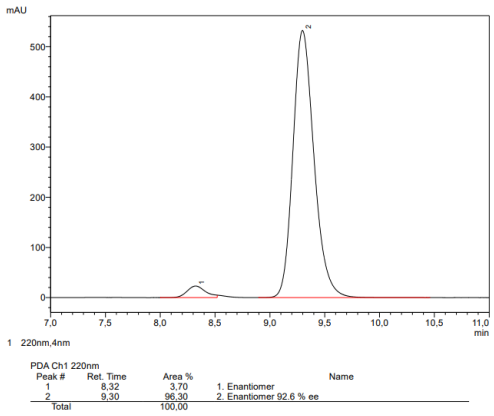

Tetrahydroisoquinoline Derivative 157. The title compound was prepared according to the general procedure **III** followed by oxidative work-up **III**, using substrate **186** (36.3 mg, 0.10 mmol); the reaction time was 16 h. The crude material was purified by flash chromatography (SiO_2, *n*-pentane/ethyl acetate, 2:1) to give the product as a colorless oil (32.8 mg, 90%, 97% ee). $[\alpha]_D^{20}$ = +60.2 (c = 0.56, $CHCl_3$); ^{1}H NMR (600 MHz, [D_6]-DMSO, 383 K): δ = 7.25 (ddt, *J* = 8.4, 5.5, 0.4 Hz, 1H), 7.11 (ddt, *J* = 9.4, 2.8, 0.5 Hz, 1H), 7.10 – 7.05 (m, 1H), 6.83 (ddd, *J* = 15.6, 7.9, 6.8 Hz, 1H), 5.83 (dt, *J* = 15.6, 1.5 Hz, 1H), 5.14 (br, 1H), 4.74 (dt, *J* = 16.9, 1.3 Hz, 1H), 4.47 (d, *J* = 2.8 Hz, 1H), 4.42 (ddd, *J* = 8.6, 5.5, 2.8 Hz, 1H), 4.15 (d, *J* = 16.8 Hz, 1H), 3.65 (s, 3H), 2.27 (dddd, *J* = 14.7, 7.0, 5.5, 1.6 Hz, 1H), 2.12 (dddd, *J* = 14.7, 9.1, 7.9, 1.4 Hz, 1H), 1.45 (s, 9H); ^{13}C NMR (151 MHz, [D_6]-DMSO, 383 K): δ = 165.1, 160.4 (d, *J* = 242.9 Hz), 154.2, 144.7, 136.9 (d, *J* = 7.0 Hz), 128.5 (d, *J* = 2.9 Hz), 127.4 (d, *J* = 8.0 Hz), 122.0, 114.9 (d, *J* = 21.1 Hz), 114.0 (d, *J* = 21.6 Hz), 78.6, 68.0 (d, *J* = 1.5 Hz), 55.2, 50.3, 41.3, 32.8, 27.5; ^{19}F NMR (585 MHz, [D_6]-DMSO, 383 K): δ = −116.4 (m); IR (ATR): $\tilde{\nu}$ = 3425, 2977, 1722, 1690, 1409, 1367, 1254, 1163, 1041, 873 cm^{-1}; HRMS (ESI$^+$): *m/z*: calcd. for $C_{19}H_{24}FNO_5Na$ $[M+Na]^+$: 388.15307, found: 388.15286.

The ee was determined by HPLC analysis: Chiralpak 150 mm IG-3, 3 µm, 4.6 mm ∅, acetonitrile/water = 45:55, v = 1.0 mL/min, λ = 220 nm, t(minor) = 8.87 min, t(major) = 15.79 min (racemic sample: left, enantioenriched sample: right).

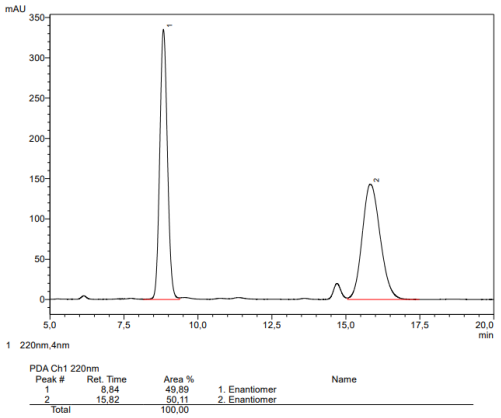

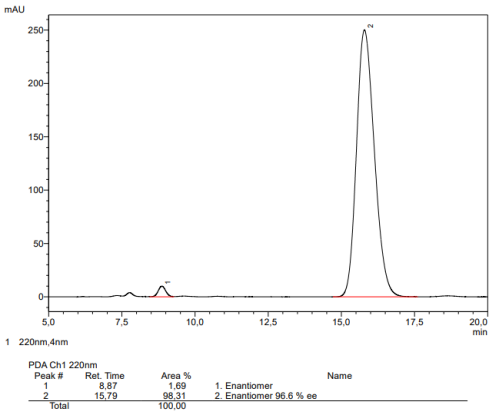

Tetrahydroisoquinoline Derivative 158a and Double Bond Isomer 158b. The title compound

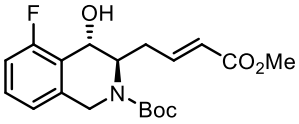

was prepared according to the general procedure **III** (reaction was performed at room temperature) followed by oxidative work-up **III,** using substrate **S33** (36.3 mg, 0.10 mmol); the reaction time was 16 h. The crude material was purified by flash chromatography (SiO_2, *n*-pentane/ethyl acetate, 2:1) to give the product as a colorless oil (31.5 mg, 86%, 55% ee, rr ≈ 4:1). ***Note:*** *The product was obtained as a ~4:1 mixture of alkene isomers that could not be separated.*

$[\alpha]_D^{20}$ = +55.0 (c = 0.40, $CHCl_3$); ^{1}H NMR (600 MHz, [D_6]-DMSO, 383 K): δ = 7.32 (ddd, *J* = 8.2, 7.7, 5.8 Hz, 1H), 7.10 – 7.05 (m, 1H), 7.05 – 6.99 (m, 1H), 6.81 (ddd, *J* = 15.7, 7.8, 6.8 Hz, 1H), 5.82 (dt, *J* = 15.6, 1.5 Hz, 1H), 4.81 (d, *J* = 17.8 Hz, 1H), 4.77 (d, *J* = 2.2 Hz, 1H), 4.55 (t, *J* = 7.2 Hz, 1H), 4.22 (d, *J* = 17.8 Hz, 1H), 3.65 (s, 3H), 2.22 (dddd, *J* = 14.7, 6.9, 5.5, 1.6 Hz, 1H), 2.06 (dddd, *J* = 14.7, 9.3, 7.8, 1.4 Hz, 1H), 1.46 (s, 9H); ^{13}C NMR (151 MHz, [D_6]-DMSO, 383 K): δ = 165.1, 160.4 (d, *J* = 246.3 Hz), 154.2, 144.5, 135.0 (d, *J* = 4.7 Hz), 128.6 (d, *J* = 8.9 Hz), 122.0, 121.6, 121.6 – 121.4 (m), 112.3 (d, *J* = 21.7 Hz), 78.7, 61.5 (d, *J* = 3.6 Hz), 55.0, 50.3, 41.2, 32.3, 27.5; ^{19}F NMR (585 MHz, [D_6]-DMSO, 383 K): δ = –121.6 (dd, *J* = 9.7, 5.8 Hz); IR (ATR): $\tilde{\nu}$ = 3436, 2976, 1723, 1689, 1408, 1366, 1249, 1165, 1117, 1040, 783 cm^{-1}; HRMS (ESI$^+$): *m/z*: calcd. for $C_{19}H_{24}FNO_5Na$ $[M+Na]^+$: 388.15307, found: 388.15285.

The ee was determined by HPLC analysis: Chiralpak 150 mm IA-3, 3 µm, 4.6 mm ∅, *n*-heptane/ethanol = 90:10, v = 1.0 mL/min, λ = 210 nm, **for major regioisomer:** t(minor) = 8.05 min, t(major) = 12.88 min, **for minor regioisomer:** t(minor) = 6.11 min, t(major) = 9.53 min, (racemic sample: left, enantioenriched sample: right).

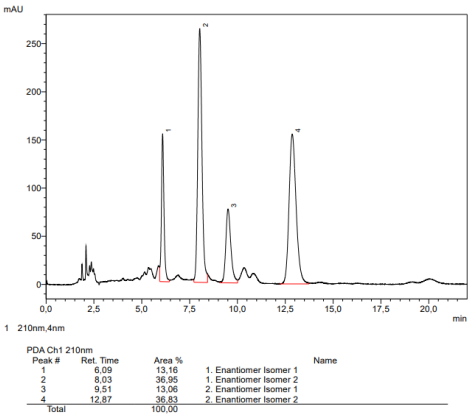

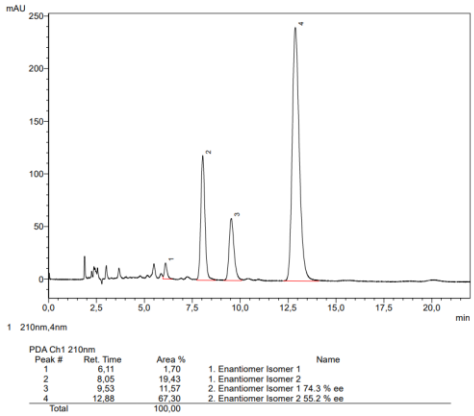

Tetrahydroisoquinoline Derivative 159. The title compound was prepared according to the general procedure **III** followed by oxidative work-up **III**, using substrate **S37** (48.6 mg, 0.10 mmol); the reaction time was 16 h. The crude material was purified by flash chromatography (SiO_2, *n*-pentane/ethyl acetate, 1:1) to give the product as an off-white solid (41.3 mg, 85%, 97% ee). mp = 195-196 °C; $[\alpha]_D^{20}$ = +23.1 (c = 0.51, $CHCl_3$); ^{1}H NMR (600 MHz, [D_6]-DMSO, 383 K): δ = 7.97 – 7.92 (m, 2H), 7.83 – 7.82 (m, 1H), 7.80 – 7.76 (m, 1H), 7.70 – 7.65 (m, 1H), 7.64 – 7.60 (m, 2H), 7.55 (dt, *J* = 8.0, 0.5 Hz, 1H), 6.81 (ddd, *J* = 15.6, 7.9, 6.8 Hz, 1H), 5.83 (dt, *J* = 15.6, 1.5 Hz, 1H), 5.26 (br, 1H), 4.86 (d, *J* = 17.5 Hz, 1H), 4.52 (d, *J* = 2.8 Hz, 1H), 4.44 (ddd, *J* = 9.1, 5.4, 2.8 Hz, 1H), 4.24 (d, *J* = 17.7 Hz, 1H), 3.64 (s, 3H), 2.26 (dddd, *J* = 14.7, 6.8, 5.4, 1.6 Hz, 1H), 2.11 (dddd, *J* = 14.7, 9.2, 7.9, 1.4 Hz, 1H), 1.44 (s, 9H); ^{13}C NMR (151 MHz, [D_6]-DMSO, 383 K): δ = 165.1, 154.1, 144.5, 141.0, 140.2, 140.1, 134.3, 132.8, 130.2, 129.0, 126.7, 124.9, 124.6, 122.1, 78.8, 67.8, 55.2, 50.3, 41.6, 32.5, 27.5; IR (ATR): $\tilde{\nu}$ = 3459, 2977, 1722, 1693, 1406, 1324, 1154, 1092, 725 cm^{-1}; HRMS (ESI$^+$): *m/z*: calcd. for $C_{25}H_{29}NO_7SNa$ $[M+Na]^+$: 510.15569, found: 510.15598.

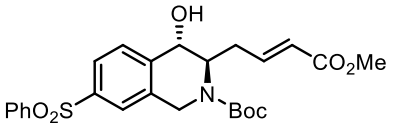

Note: Single crystals suitable for X-ray diffraction analysis were obtained in the process of recrystallization *via* vapor diffusion using *n*-pentane and ethyl acetate.

The ee was determined by HPLC analysis: Chiralpak 150 mm IB-N-3, 3 µm, 4.6 mm ∅, acetonitrile/water = 45:55, v = 1.0 mL/min, λ = 220 nm, t(minor) = 9.10 min, t(major) = 10.92 min, (racemic sample: left, enantioenriched sample: right).

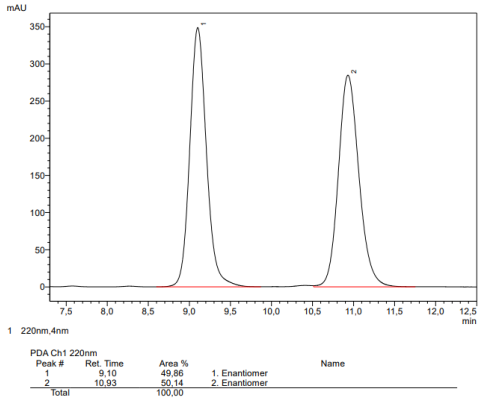

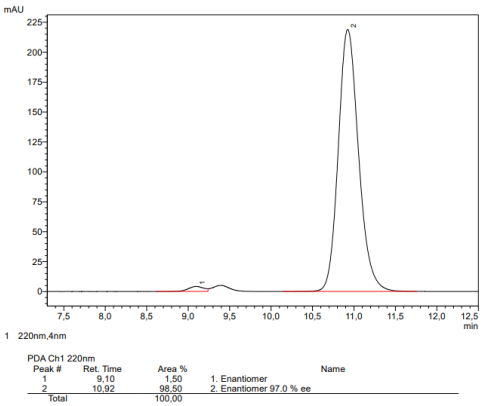

Tetrahydroisoquinoline Derivative 160. The title compound was prepared according to the general procedure **III** followed by oxidative work-up **III**, using substrate **S35** (42.1 mg, 0.10 mmol); the reaction time was 16 h. The crude material was purified by flash chromatography (SiO_2, *n*-hexane/ethyl acetate, 1.5:1) to give the product as an off-white solid (38.0 mg, 90%, 91% ee). $[\alpha]_D^{20}$ = +56.2 (c = 0.50, $CHCl_3$); ^{1}H NMR (600 MHz, [D_6]-DMSO, 383 K): δ = 7.68 – 7.64 (m, 2H), 7.53 (ddt, *J* = 7.9, 1.6, 0.7 Hz, 1H), 7.50 – 7.49 (m, 1H), 7.46 (dddd, *J* = 7.8, 6.7, 1.4, 0.8 Hz, 1H), 7.40 (d, *J* = 7.8 Hz, 1H), 7.38 – 7.34 (m, 1H), 6.85 (ddd, *J* = 15.6, 7.8, 6.8 Hz, 1H), 5.83 (dt, *J* = 15.6, 1.5 Hz, 1H), 5.01 (d, *J* = 4.9 Hz, 1H), 4.86 (d, *J* = 17.3 Hz, 1H), 4.52 (d, *J* = 2.5 Hz, 1H), 4.50 (dq, *J* = 5.5, 2.7 Hz, 1H), 4.27 (d, *J* = 17.2 Hz, 1H), 3.65 (s, 3H), 2.28 (dddd, *J* = 14.7, 6.9, 5.5, 1.6 Hz, 1H), 2.15 (dddd, *J* = 14.7, 9.1, 7.9, 1.4 Hz, 1H), 1.47 (s, 9H); ^{13}C NMR (151 MHz, [D_6]-DMSO, 383 K): δ = 165.2, 154.3, 144.9, 139.5, 139.3, 133.5, 132.9, 129.6, 128.2, 126.8, 126.1, 124.4, 123.7, 121.9, 78.5, 68.1, 55.5, 50.3, 42.0, 32.8, 27.6; IR (ATR): $\tilde{\nu}$ = 3428, 2925, 1723, 1691, 1407, 1366, 1270, 1168, 1040, 767 cm^{-1}; HRMS (ESI$^+$): *m/z*: calcd. for $C_{25}H_{29}NO_5Na$ [M+Na]$^+$: 446.19379, found: 446.19370.

The ee was determined by HPLC analysis: Chiralpak 150 mm IA-3, 3 µm, 4.6 mm ∅, *n*-heptane/ethanol = 90:10, v = 1.0 mL/min, λ = 254 nm, t(minor) = 11.35 min, t(major) = 14.03 min, (racemic sample: left, enantioenriched sample: right).

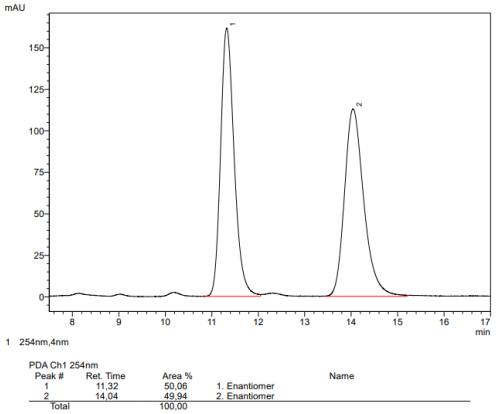

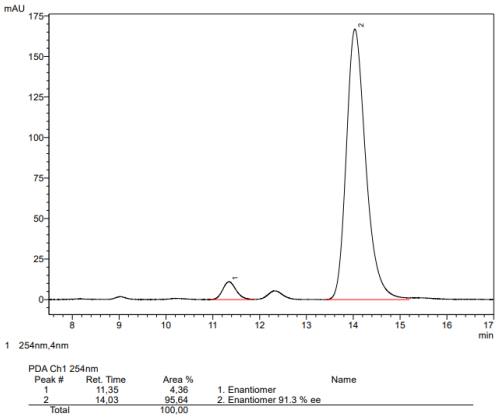

Tetrahydroisoquinoline Derivative 161. The title compound was prepared according to the general procedure **V** (the reaction was performed at 0 °C) followed by a basic work-up **IV**, using substrate **S36** (42.4 mg, 0.10 mmol); the reaction time was 24 h. The crude material was purified by flash chromatography (SiO_2, *n*-pentane/ethyl acetate, 1:1) to give the product as a colorless solid (29.8 mg, 70%, 93% ee). $[\alpha]_D^{20}$ = +75.3 (c = 0.45, $CHCl_3$); ^{1}H NMR (600 MHz, [D_6]-DMSO, 383 K): δ = 7.44 – 7.43 (m, 1H), 7.43 – 7.39 (m, 1H), 7.27 (d, *J* = 8.1 Hz, 1H), 6.82 (ddd, *J* = 15.6, 7.9, 6.8 Hz, 1H), 5.82 (dt, *J* = 15.6, 1.5 Hz, 1H), 5.08 (d, *J* = 5.1 Hz, 1H), 4.78 (d, *J* = 17.3 Hz, 1H), 4.45 (d, *J* = 4.7 Hz, 1H), 4.44 (dd, *J* = 5.3, 2.7 Hz, 1H), 4.17 (d, *J* = 17.5 Hz, 1H), 3.65 (s, 3H), 2.25 (dddd, *J* = 14.7, 6.8, 5.3, 1.6 Hz, 1H), 2.09 (dddd, *J* = 14.7, 9.1, 7.9, 1.4 Hz, 1H), 1.45 (s, 9H); ^{13}C NMR (151 MHz, [D_6]-DMSO, 383 K): δ = 165.1, 154.1, 144.7, 135.1, 133.8, 131.1, 128.9, 128.2, 122.0, 120.2, 78.7, 67.7, 55.3, 50.3, 41.3, 32.6, 27.5; IR (ATR): $\tilde{\nu}$ = 3425, 2978, 1723, 1693, 1405, 1366, 1321, 1271, 1164, 1041 cm^{-1}; HRMS (ESI$^+$): *m/z*: calcd. for $C_{19}H_{24}NO_5BrNa$ $[M+Na]^+$: 448.07301, found: 448.07288.

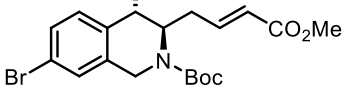

The ee was determined by HPLC analysis: Chiralpak 150 mm OJ-3R, 3 µm, 4.6 mm ∅, acetonitrile/water = 35:65, v = 1.0 mL/min, λ = 220 nm, t(major) = 23.90 min, t(minor) = 26.83 min, (racemic sample: left, enantioenriched sample: right).

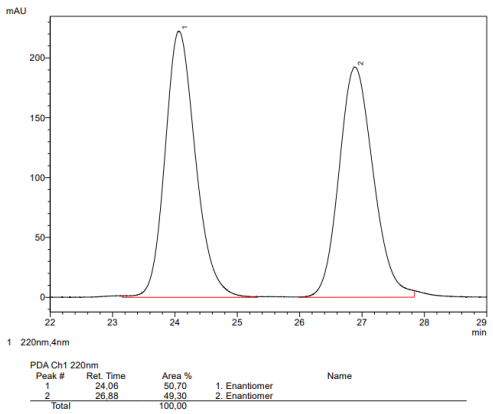

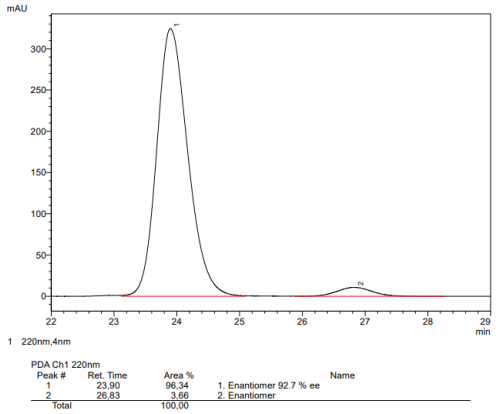

Tetrahydroisoquinoline Derivative 162. The title compound was prepared according to the general procedure **III** and basic work-up **IV**, using substrate **S38** (47.1 mg, 0.10 mmol); the reaction time was 16 h. The crude material was purified by flash chromatography (SiO_2, *n*-pentane/ethyl acetate, 2:1) to give the product as a colorless oil (40.4 mg, 85%, 95% ee). $[\alpha]_D^{20}$ = +48.7 (c = 0.46, $CHCl_3$); ^{1}H NMR (600 MHz, [D_6]-DMSO, 383 K): δ = 7.56 (dd, *J* = 7.4, 1.2 Hz, 1H), 7.51 (s, 1H), 7.32 (d, *J* = 7.5 Hz, 1H), 6.82 (ddd, *J* = 15.7, 7.8, 6.8 Hz, 1H), 5.81 (dt, *J* = 15.7, 1.5 Hz, 1H), 5.03 (d, *J* = 5.3 Hz, 1H), 4.78 (d, *J* = 17.0 Hz, 1H), 4.48 (dd, *J* = 5.3, 2.8 Hz, 1H), 4.45 (ddd, *J* = 8.5, 5.5, 2.8 Hz, 1H), 4.19 (d, *J* = 17.1 Hz, 1H), 3.65 (s, 3H), 2.24 (dddd, *J* = 14.7, 6.9, 5.4, 1.6 Hz, 1H), 2.10 (dddd, *J* = 14.7, 9.1, 7.8, 1.4 Hz, 1H), 1.45 (s, 9H), 1.33 (s, 12H); ^{13}C NMR (151 MHz, [D_6]-DMSO, 383 K): δ = 165.1, 154.2, 144.8, 137.5, 131.8 (2 x), 131.5, 128.3, 121.9, 83.1, 78.5, 68.3, 55.4, 50.2, 41.7, 32.8, 27.5, 24.1; (the C-Bpin signal is broad and could only be assigned based on the 2D HMBC (~127.7 ppm)); IR (ATR): $\tilde{\nu}$ = 3436, 2977, 1723, 1692, 1393, 1360, 1270, 1164, 1144, 1105, 1040, 854 cm^{-1}; HRMS (ESI$^+$): *m/z*: calcd. for $C_{25}H_{36}BNO_7Na$ [M+Na]$^+$: 496.24770, found: 496.24760.

The ee was determined by HPLC analysis: Chiralpak 150 mm IA-3, 3 µm, 4.6 mm ∅, *n*-heptane/*iso*-propanol = 95:5, v = 1.0 mL/min, λ = 225 nm, t(major) = 11.37 min, t(minor) = 15.93 min, (racemic sample: left, enantioenriched sample: right).

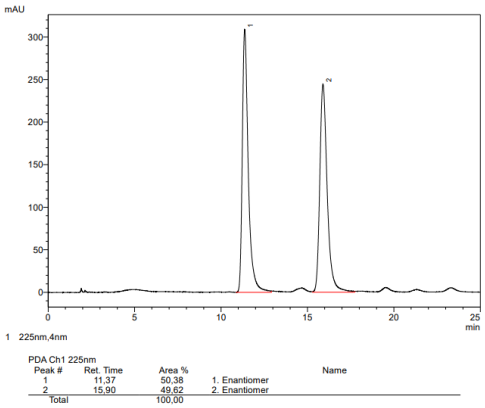

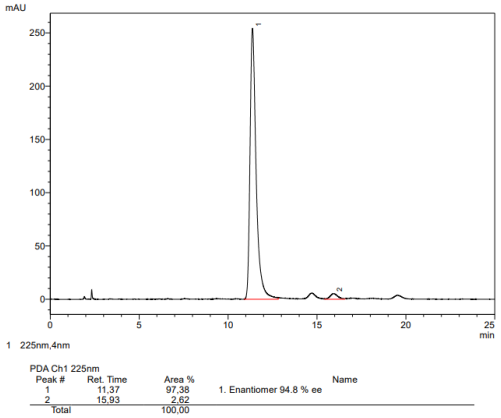

Tetrahydroisoquinoline Derivative 163. The title compound was prepared according to the general procedure **III** followed by oxidative work-up **III**, using substrate **S34** (37.5 mg, 0.10 mmol); the reaction time was 48 h. The crude material was purified by flash chromatography (SiO_2, *n*-pentane/ethyl acetate, 1.5:1) to give the product as a colorless sticky solid (25.3 mg, 67%, 71% ee). $[\alpha]_D^{20}$ = +33.6 (c = 0.58, $CHCl_3$); ^{1}H NMR (600 MHz, [D_6]-DMSO, 383 K): δ = 7.21 (dt, *J* = 8.3, 0.5 Hz, 1H), 6.86 – 6.75 (m, 3H), 5.80 (dt, *J* = 15.6, 1.5 Hz, 1H), 4.79 (s, 1H), 4.74 (d, *J* = 17.1 Hz, 1H), 4.47 – 4.44 (m, 1H), 4.42 (d, *J* = 2.5 Hz, 1H), 4.15 (d, *J* = 17.3 Hz, 1H), 3.78 (s, 3H), 3.65 (s, 3H), 2.21 (dddd, *J* = 14.7, 7.0, 5.5, 1.6 Hz, 1H), 2.08 (dddd, *J* = 14.7, 9.2, 7.8, 1.4 Hz, 1H), 1.45 (s, 9H); ^{13}C NMR (151 MHz, [D_6]-DMSO, 383 K): δ = 165.1, 158.6, 154.3, 144.9, 133.6, 130.3, 126.7, 121.8, 112.5, 110.5, 78.4, 67.9, 55.6, 54.7, 50.2, 42.0, 32.8, 27.6; IR (ATR): $\tilde{\nu}$ = 3425, 2974, 1723, 1690, 1613, 1406, 1365, 1270, 1162, 1126, 1063 cm^{-1}; HRMS (ESI$^+$): *m/z*: calcd. for $C_{20}H_{27}NO_6Na$ $[M+Na]^+$: 400.17306, found: 400.17307.

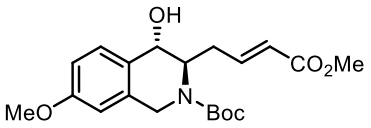

The ee was determined by HPLC analysis: Chiralpak 150 mm IG-3, 3 µm, 4.6 mm ∅, acetonitrile/water = 45:55, v = 1.0 mL/min, λ = 220 nm, t(minor) = 11.01 min, t(major) = 16.37 min, (racemic sample: left, enantioenriched sample: right).

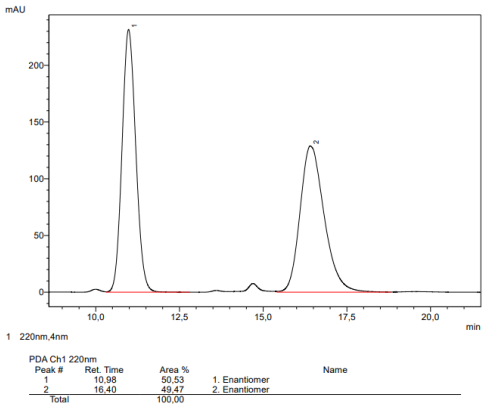

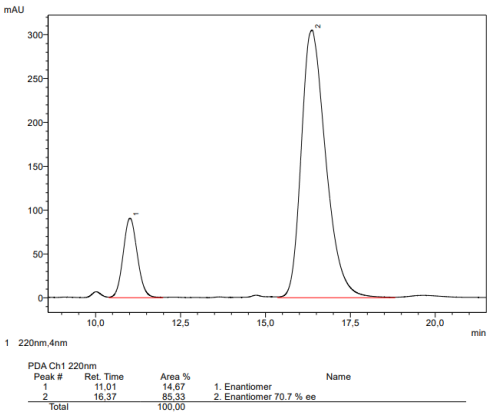

Tetrahydroisoquinoline Derivative 164. The title compound was prepared according to the general procedure **III** followed by basic work-up **IV**, using substrate **S38** (47.1 mg, 0.10 mmol); the reaction time was 16 h. The crude material was then dissolved in THF (1.0 mL). pH 7 Phosphate buffer solution (1.0 mL) and aq. H_2O_2 (30% *w/w*, ≈0.1 mL) were added and the resulting mixture was stirred at room temperature for 18 h. Additional ethyl acetate (10 mL) and water (5 mL) were introduced, the organic phase was separated, and the aqueous layer was extracted with ethyl acetate (2 × 10 mL). The combined organic phases were washed with sat. aq. $Na_2S_2O_3$ (10 mL) and brine (10 mL), dried over $MgSO_4$, filtered and concentrated *in vacuo*. The residue was purified by flash chromatography (SiO_2, toluene/*tert*-butyl methyl ether, 1:2) to give the product as a colorless solid (30.8 mg, 85%, 95% ee). $[\alpha]_D^{20}$ = +63.8 (c = 0.48, $CHCl_3$); ^{1}H NMR (600 MHz, [D_6]-DMSO, 383 K): δ = 8.96 (s, 1H), 7.09 (d, *J* = 8.2 Hz, 1H), 6.82 (ddd, *J* = 15.6, 7.8, 6.9 Hz, 1H), 6.66 (ddd, *J* = 8.2, 2.0, 1.2 Hz, 1H), 6.61 – 6.54 (m, 1H), 5.80 (dt, *J* = 15.6, 1.5 Hz, 1H), 4.67 (d, *J* = 17.1 Hz, 1H), 4.43 (ddd, *J* = 8.5, 5.5, 2.5 Hz, 1H), 4.37 (d, *J* = 2.5 Hz, 1H), 4.09 (d, *J* = 17.2 Hz, 1H), 3.65 (s, 3H), 2.20 (dddd, *J* = 14.7, 7.0, 5.5, 1.6 Hz, 1H), 2.08 (dddd, *J* = 14.7, 9.1, 7.8, 1.4 Hz, 1H), 1.45 (s, 9H); ^{13}C NMR (151 MHz, [D_6]-DMSO, 383 K): δ = 165.2, 156.5, 154.3, 145.0, 133.3, 130.2, 125.0, 121.8, 113.6, 111.7, 78.4, 67.9, 55.7, 50.2, 41.9, 32.8, 27.6; IR (ATR): $\tilde{\nu}$ = 3340, 2977, 1695, 1660, 1410, 1367, 1291, 1163, 1126, 1039, 861 cm^{-1}; HRMS (ESI$^+$): *m/z*: calcd. for $C_{19}H_{25}NO_6Na$ [M+Na]$^+$: 386.15741, found: 386.15755.

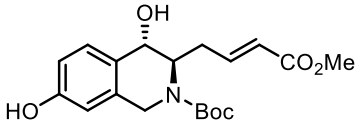

The ee was determined by HPLC analysis: Chiralpak 150 mm IB-N-3, 3 µm, 4.6 mm ∅, *n*-heptane/ethanol = 95:5, v = 1.0 mL/min, λ = 220 nm, t(minor) = 16.13 min, t(major) = 25.65 min, (racemic sample: left, enantioenriched sample: right).

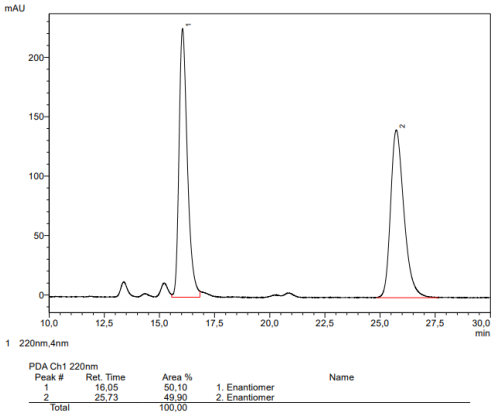

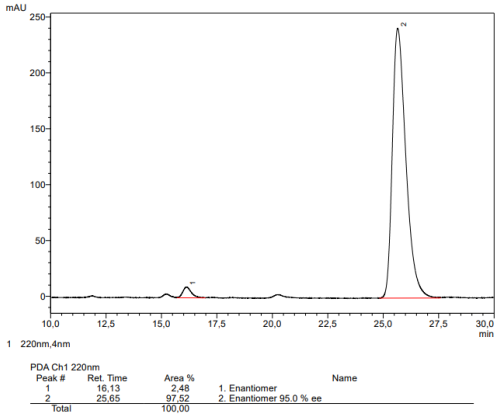

Tetrahydroisoquinoline Derivative 165. The title compound was prepared according to the general procedure **IV** followed by oxidative work-up **III**, using substrate **S39** (38.0 mg, 0.10 mmol); the reaction time was 20 h. The crude material was purified by flash chromatography (SiO_2, *n*-pentane/ethyl acetate, 2:1) to give the product as a colorless oil (30.7 mg, 80%, 98% ee). $[\alpha]_D^{20}$ = +50.2 (c = 0.56, $CHCl_3$); ^{1}H NMR (600 MHz, [D_6]-DMSO, 383 K): δ = 7.38 – 7.35 (m, 1H), 7.31 (dd, *J* = 8.2, 2.3 Hz, 1H), 7.24 (d, *J* = 8.2 Hz, 1H), 6.83 (ddd, *J* = 15.6, 7.9, 6.8 Hz, 1H), 5.83 (dt, *J* = 15.6, 1.5 Hz, 1H), 5.15 (d, *J* = 5.1 Hz, 1H), 4.75 (d, *J* = 17.3 Hz, 1H), 4.47 (br, 1H), 4.43 (ddd, *J* = 8.5, 5.4, 2.8 Hz, 1H), 4.15 (d, *J* = 17.4 Hz, 1H), 3.65 (s, 3H), 2.27 (dddd, *J* = 14.7, 6.9, 5.4, 1.6 Hz, 1H), 2.11 (dddd, *J* = 14.7, 9.1, 7.9, 1.4 Hz, 1H), 1.45 (s, 9H); ^{13}C NMR (151 MHz, [D_6]-DMSO, 383 K): δ = 165.1, 154.2, 144.7, 136.7, 131.4, 130.5, 128.5, 127.4, 127.0, 122.0, 78.7, 67.9, 55.2, 50.2, 41.4, 32.7, 27.5; IR (ATR): $\tilde{\nu}$ = 3414, 2977, 1722, 1691, 1408, 1366, 1249, 1164, 1040, 881 cm^{-1}; HRMS (ESI$^+$): *m/z*: calcd. for $C_{19}H_{24}NO_5ClNa$ $[M+Na]^+$: 404.12352, found: 404.12358.

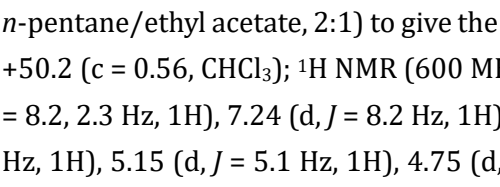

The ee was determined by HPLC analysis: Chiralpak 150 mm IG-3, 3 µm, 4.6 mm ∅, acetonitrile/water = 45:55, v = 1.0 mL/min, λ = 220 nm, t(minor) = 17.46 min, t(major) = 29.16 min, (racemic sample: left, enantioenriched sample: right).

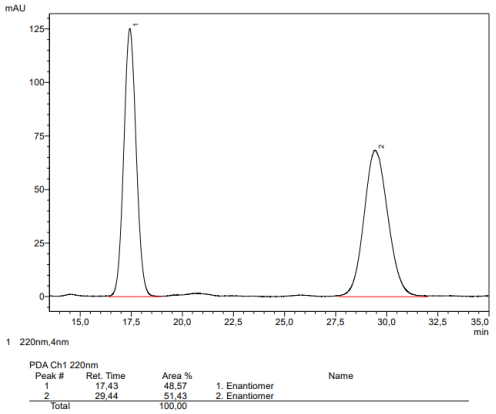

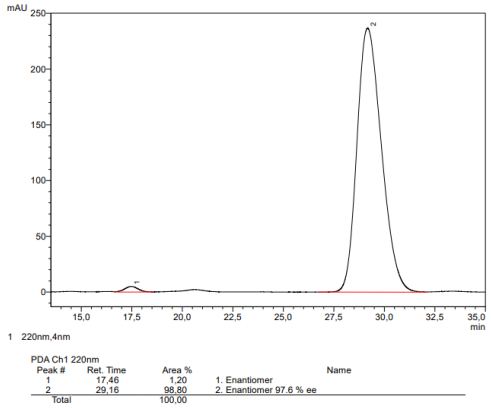

Tetrahydroisoquinoline Derivative 166. The title compound was prepared according to the general procedure **III** followed by oxidative work-up **III**, using substrate **S40** (42.9 mg, 0.10 mmol); the reaction time was 16 h. The crude material was purified by flash chromatography (SiO_2, *n*-pentane/ethyl acetate, 2.5:1) to give the product as a colorless oil (34.3 mg, 80%, 97% ee). $[\alpha]_D^{20}$ = +53.7 (c = 0.65, $CHCl_3$); ^{1}H NMR (600 MHz, [D_6]-DMSO, 383 K): δ = 7.35 (ddt, *J* = 8.6, 1.2, 0.6 Hz, 1H), 7.27 (dq, *J* = 1.6, 0.5 Hz, 1H), 7.23 (ddt, *J* = 8.3, 2.6, 1.0 Hz, 1H), 6.83 (ddd, *J* = 15.6, 7.9, 6.8 Hz, 1H), 5.83 (dt, *J* = 15.7, 1.5 Hz, 1H), 5.23 (d, *J* = 5.4 Hz, 1H), 4.79 (d, *J* = 17.4 Hz, 1H), 4.51 (dd, *J* = 5.3, 2.8 Hz, 1H), 4.44 (ddd, *J* = 9.0, 5.4, 2.8 Hz, 1H), 4.19 (d, *J* = 17.1 Hz, 1H), 3.65 (s, 3H), 2.29 (dddd, *J* = 14.7, 6.9, 5.4, 1.6 Hz, 1H), 2.13 (dddd, *J* = 14.7, 9.2, 7.9, 1.4 Hz, 1H), 1.45 (s, 9H); ^{13}C NMR (151 MHz, [D_6]-DMSO, 383 K): δ = 165.1, 154.1, 146.6 (q, *J* = 1.9 Hz), 144.6, 136.9, 131.8, 127.4, 122.0, 120.6, 119.6 (q, *J* = 256.5 Hz), 119.4, 78.7, 67.9, 55.2, 50.2, 41.3, 32.7, 27.5; ^{19}F NMR (585 MHz, [D_6]-DMSO, 383 K): δ = −56.6; IR (ATR): $\tilde{\nu}$ = 3427, 2978, 1724, 1692, 1410, 1257, 1211, 1161, 1042 cm^{-1}; HRMS (ESI$^+$): *m/z*: calcd. for $C_{20}H_{24}NO_6F_3Na$ [M+Na]$^+$: 454.14479, found: 454.14452.

The ee was determined by HPLC analysis: Chiralpak 150 mm IG-3, 3 µm, 4.6 mm ∅, acetonitrile/water = 45:55, v = 1.0 mL/min, λ = 220 nm, t(minor) = 11.84 min, t(major) = 16.64 min, (racemic sample: left, enantioenriched sample: right).

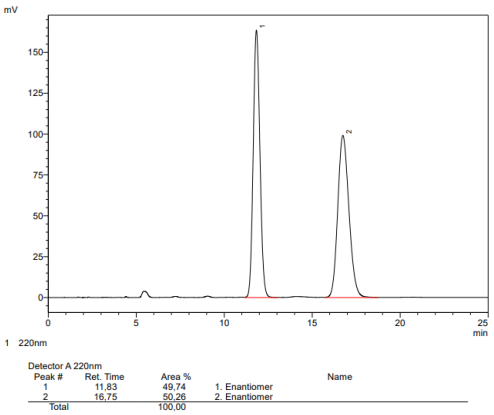

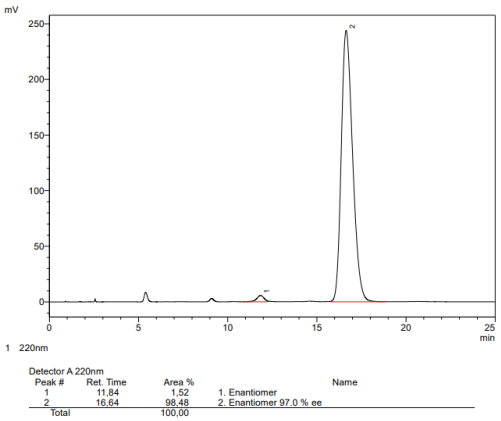

Compound 167. The title compound was prepared according to the general procedure **V** and basic work-up **IV**, using substrate **S41** (35.1 mg, 0.10 mmol); the reaction time was 16 h. The crude material was purified by flash chromatography (SiO_2, *n*-pentane/ethyl acetate, 1:1) to give the product as a colorless oil (23.7 mg, 67%, 70% ee). $[\alpha]_D^{20}$ = +36.4 (c = 0.45, $CHCl_3$); ^{1}H NMR (600 MHz, [D_6]-DMSO, 383 K): δ = 7.42 (d, *J* = 3.0 Hz, 1H), 7.25 – 7.18 (m, 1H), 6.81 (ddd, *J* = 15.6, 7.8, 6.8 Hz, 1H), 5.82 (dt, *J* = 15.7, 1.5 Hz, 1H), 4.86 (br, 1H), 4.80 (dd, *J* = 16.5, 1.4 Hz, 1H), 4.58 (d, *J* = 2.5 Hz, 1H), 4.50 (ddd, *J* = 9.2, 5.5, 2.5 Hz, 1H), 4.16 (d, *J* = 17.1 Hz, 1H), 3.65 (s, 3H), 2.26 – 2.16 (m, 1H), 2.07 (dddd, *J* = 14.8, 9.2, 7.8, 1.4 Hz, 1H), 1.44 (s, 9H); ^{13}C NMR (151 MHz, [D_6]-DMSO, 383 K): δ = 165.1, 154.4, 144.8, 136.8, 132.7, 123.4, 121.9, 118.2, 78.5, 65.1, 55.9, 50.3, 39.9, 32.4, 27.5; IR (ATR): $\tilde{\nu}$ = 3427, 2976, 1721, 1685, 1395, 1366, 1236, 1163, 1094, 1039, 731 cm^{-1}; HRMS (ESI$^+$): *m/z*: calcd. for $C_{17}H_{23}NO_5SNa$ $[M+Na]^+$: 376.11891, found: 376.11902.

The ee was determined by HPLC analysis: Chiralpak 150 mm IG-3, 3 µm, 4.6 mm ∅, acetonitrile/water = 50:50, v = 1.0 mL/min, λ = 220 nm, t(minor) = 6.43 min, t(major) = 14.45 min, (racemic sample: left, enantioenriched sample: right).

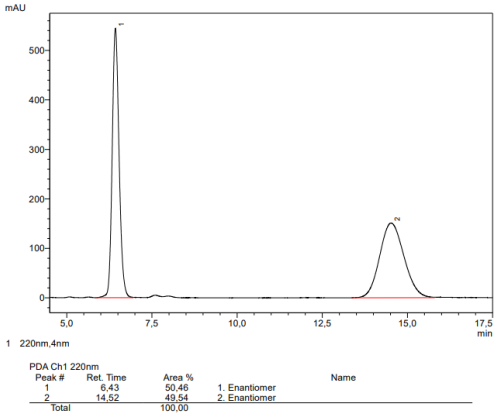

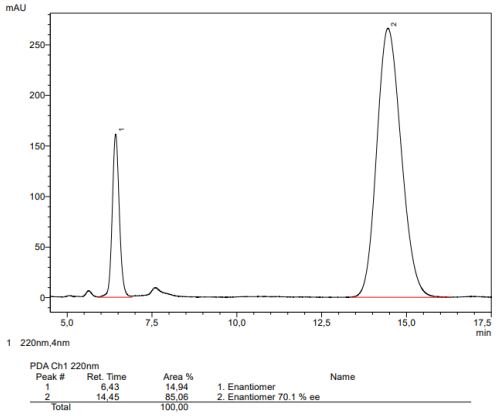

Compound 168. A flame-dried Schlenk flask was charged under argon with tris(*trans*-1,2-bis(4-*tert*-butylphenyl)ethene)nickel(0) (Ni($^{t\text{Bu}}$stb)$_3$) (9.4 mg, 10.0 µmol) and (*S*)-AntPhos (4.1 mg, 11.0 µmol). The flask was evacuated and refilled with argon (3 cycles) before THF (0.25 mL) and triethylborane (1.0 M in THF, 0.25 mL, 0.25 mmol) were added. The resulting solution was stirred for 2 min before substrate **S42** (33.5 mg, 0.10 mmol) was introduced as a solution in THF (0.50 mL). The flask was placed in a preheated metal block at 60 °C. The reaction mixture was stirred at 60 °C for 18 h. Reaction control by thin layer chromatography indicated incomplete conversion of the starting material; therefore, more (*S*)-AntPhos (4.1 mg, 11.0 µmol) and (Ni($^{t\text{Bu}}$stb)$_3$) (9.4 mg, 10.0 µmol) were added. The mixture was stirred at 60 °C for another 18 h before it was subjected to oxidative work-up **III**. The crude product (dr ≈ 2:1) was purified by flash chromatography (SiO_2, *n*-pentane/ethyl acetate, 3:1) to give the title compound as a colorless oil (14.7 mg, 44%, 86% ee, single diastereomer). $[\alpha]_D^{20}$ = +25.8 (c = 0.65, $CHCl_3$); ^{1}H NMR (600 MHz, [D$_6$]-DMSO, 383 K): δ = 7.52 (dd, *J* = 1.9, 0.9 Hz, 1H), 6.87 (ddd, *J* = 15.7, 8.5, 6.1 Hz, 1H), 6.37 – 6.33 (m, 1H), 5.92 (ddd, *J* = 15.6, 1.8, 1.2 Hz, 1H), 5.52 (d, *J* = 5.4 Hz, 1H), 4.83 (d, *J* = 5.6 Hz, 1H), 4.64 (ddd, *J* = 10.4, 6.3, 3.7 Hz, 1H), 4.55 (dd, *J* = 16.4, 1.9 Hz, 1H), 3.86 (dd, *J* = 16.5, 2.4 Hz, 1H), 3.65 (s, 3H), 2.65 (dddd, *J* = 15.3, 6.0, 3.8, 1.8 Hz, 1H), 2.22 – 2.13 (m, 1H), 1.42 (s, 9H); ^{13}C NMR (151 MHz, [D$_6$]-DMSO, 383 K): δ = 165.2, 153.6, 148.4, 146.0, 142.0, 122.0, 114.3, 107.5, 79.0, 62.7, 53.7, 50.2, 37.2, 27.43, 27.41; IR (ATR): $\tilde{\nu}$ = 3436, 2926, 1723, 1693, 1398, 1316, 1227, 1168, 1141, 1044, 733 cm^{-1}; HRMS (ESI$^+$): *m/z*: calcd. for $C_{17}H_{23}NO_6Na$ [M+Na]$^+$: 360.14176, found: 360.14163.

The ee was determined by HPLC analysis: Chiralpak 150 mm IG-3, 3 µm, 4.6 mm ∅, acetonitrile/water = 40:60, v = 1.0 mL/min, λ = 220 nm, t(minor) = 7.00 min, t(major) = 8.04 min, (racemic sample: left, enantioenriched sample: right).

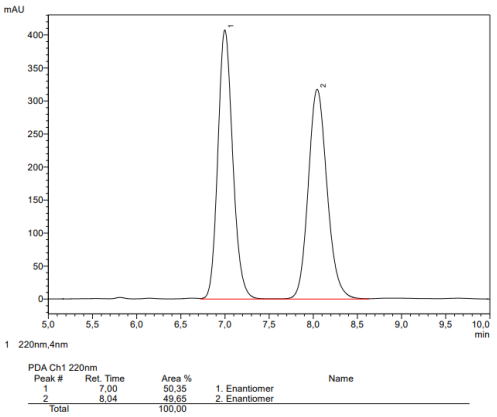

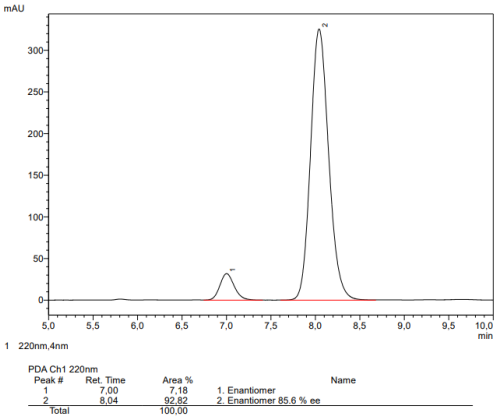

Piperidine Derivative 169. A flame-dried Schlenk flask was charged under argon with tris(*trans*-1,2-bis(4-*tert*-butylphenyl)ethene)nickel(0) ($Ni(^{tBu}stb)_3$) (9.4 mg, 10.0 µmol) and (*S*)-AntPhos (4.1 mg, 11.0 µmol) and was then evacuated and refilled with argon (3 cycles). THF (0.25 mL) and diethylzinc (1.0 M in hexane, 0.25 mL, 0.25 mmol) were introduced and the resulting solution was stirred for 2 min before a solution of substrate **S43** (29.7 mg, 0.10 mmol) in THF (0.50 mL) was added dropwise over 5 h via syringe pump. After complete addition, the mixture was stirred for another 16 h at room temperature. The reaction was subjected to basic work-up **IV**. The crude product (dr ≈ 1.2:1) was purified by flash chromatography (SiO_2, toluene/*tert*-butyl methyl ether, 1:1 → 1:2) to give the title compound as a colorless oil (10.1 mg, 34%, 90% ee, dr > 20:1). $[\alpha]_D^{20}$ = –16.7 (c = 0.75, $CHCl_3$); ^{1}H NMR (600 MHz, [D_6]-DMSO, 383 K): δ = 6.85 (ddd, *J* = 15.6, 8.4, 6.4 Hz, 1H), 5.88 (dt, *J* = 15.6, 1.7 Hz, 1H), 4.67 (br, 1H), 4.32 (dt, *J* = 10.5, 4.7 Hz, 1H), 3.79 (dd, *J* = 13.5, 4.9 Hz, 1H), 3.64 (s, 3H), 3.59 (dt, *J* = 11.5, 5.5 Hz, 1H), 2.67 (td, *J* = 13.3, 3.1 Hz, 1H), 2.54 (dddd, *J* = 15.1, 6.4, 4.1, 1.7 Hz, 1H), 2.47 (dddd, *J* = 15.1, 10.5, 8.4, 1.3 Hz, 1H), 1.66 (dq, *J* = 11.9, 3.9 Hz, 1H), 1.64 – 1.59 (m, 1H), 1.46 (tdd, *J* = 13.0, 12.0, 3.6 Hz, 1H), 1.39 (s, 9H), 1.36 (qt, *J* = 13.0, 4.9 Hz, 1H); ^{13}C NMR (151 MHz, [D_6]-DMSO, 383 K): δ = 165.3, 153.5, 146.6, 121.3, 78.2, 67.2, 54.5, 50.1, 36.7, 27.4, 26.9, 26.1, 23.2; IR (ATR): $\tilde{\nu}$ = 3429, 2938, 1723, 1689, 1666, 1415, 1272, 1214, 1154, 750, 688 cm^{-1}; HRMS (ESI$^+$): *m/z*: calcd. for $C_{15}H_{25}NO_5Na$ $[M+Na]^+$: 322.162493, found: 322.16266.

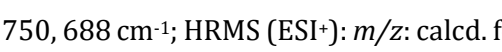

The ee was determined by HPLC analysis: Chiralpak 150 mm IG-3, 3 µm, 4.6 mm ∅, acetonitrile/water = 35:65, v = 1.0 mL/min, λ = 220 nm, t(minor) = 5.71 min, t(major) = 15.11 min, (racemic sample: left, enantioenriched sample: right).

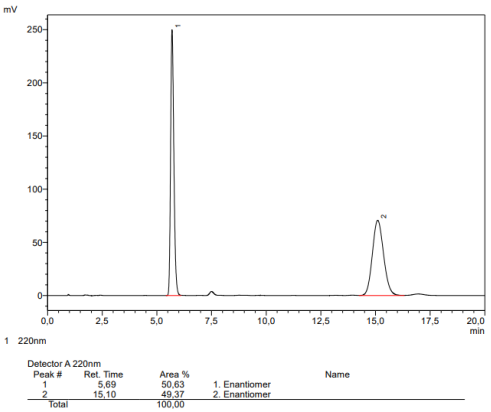

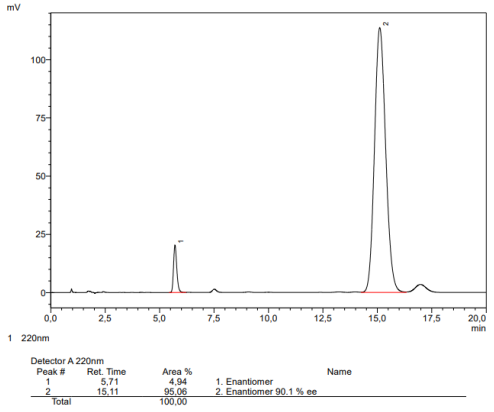

Pyrrolidine Derivative 170. A flame-dried Schlenk flask was charged under argon with

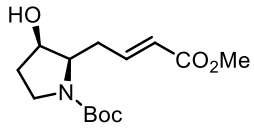

tris(*trans*-1,2-bis(4-*tert*-butylphenyl)ethene)nickel(0) (Ni($^{t\text{Bu}}$stb)$_3$) (9.4 mg, 10.0 µmol) and (*S*)-AntPhos (4.1 mg, 11.0 µmol) and was then evacuated and refilled with argon (3 cycles). THF (0.25 mL) and diethylzinc (1.0 M in hexane, 0.25 mL, 0.25 mmol) were added and the resulting solution was stirred for 2 min before a solution of substrate **S44** (28.3 mg, 0.10 mmol) in THF (0.50 mL) was added dropwise over 5 h via syringe pump. After complete addition, the reaction mixture was stirred for another 16 h at room temperature. The reaction was subjected to basic work-up **IV**. The residue was purified by flash chromatography (SiO_2, *n*-pentane/ethyl acetate, 1:1.5) to give the title compound as a colorless oil (14.2 mg, 50%, 96% ee). $[\alpha]_D^{20}$ = –18.3 (c = 0.60, $CHCl_3$); ^{1}H NMR (600 MHz, [D$_6$]-DMSO, 373 K): δ = 6.98 (ddd, *J* = 15.7, 7.8, 7.2 Hz, 1H), 5.83 (dt, *J* = 15.6, 1.5 Hz, 1H), 4.86 (br, 1H), 4.24 (dt, *J* = 7.9, 6.4 Hz, 1H), 3.77 (q, *J* = 6.3 Hz, 1H), 3.65 (s, 3H), 3.29 (dt, *J* = 10.8, 7.7 Hz, 1H), 3.24 (ddd, *J* = 10.8, 8.4, 4.9 Hz, 1H), 2.58 (dtd, *J* = 13.9, 6.9, 1.6 Hz, 1H), 2.45 – 2.40 (m, 1H), 1.95 (dddd, *J* = 12.6, 7.9, 6.3, 4.9 Hz, 1H), 1.72 (dq, *J* = 12.4, 7.9 Hz, 1H), 1.41 (s, 9H); ^{13}C NMR (151 MHz, [D$_6$]-DMSO, 373 K): δ = 165.5, 153.3, 147.1, 121.2, 77.9, 69.7, 58.8, 50.3, 42.6, 31.1, 30.6, 27.6; IR (ATR): $\tilde{\nu}$ = 3410, 2973, 1723, 1694, 1688, 1395, 1266, 1170, 1131 cm^{-1}; HRMS (ESI$^+$): *m/z*: calcd. for $C_{14}H_{23}NO_5Na$ [M+Na]$^+$: 308.14684, found: 308.14642.

The ee was determined by HPLC analysis: Chiralpak 150 mm IG-3, 3 µm, 4.6 mm ∅, acetonitrile/water = 20:80 → 30:70 (over 19 min), then 30:70 → 60:30 (over 5 min), v = 1.0 mL/min, λ = 220 nm, t(minor) = 21.66 min, t(major) = 31.28 min, (racemic sample: left, enantioenriched sample: right).

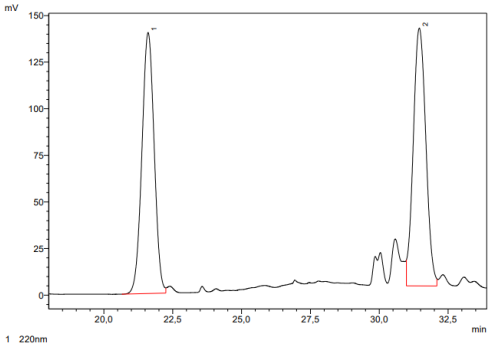

Detector A 220nm

Peak #	Ret. Time	Area %	Name
1	21,61	49,70	1. Enantiomer
2	31,45	50,30	2. Enantiomer
Total		100,00	

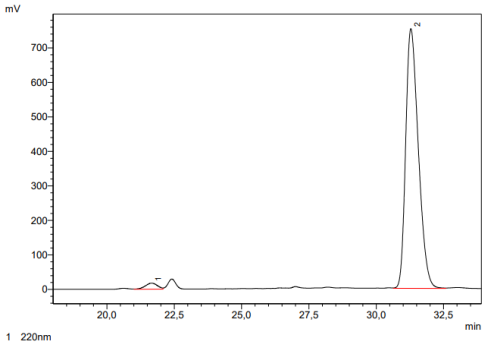

Detector A 220nm

Peak #	Ret. Time	Area %	Name
1	21,66	2,22	1. Enantiomer
2	31,28	97,78	2. Enantiomer 95,6 % ee
Total		100,00	

Pyrrolidine Derivative 171. The title compound was prepared according to the general procedure **IV** (reaction performed at room temperature) followed by oxidative work-up **III**, using substrate **S45** (31.1 mg, 0.10 mmol); the reaction time was 18 h. The crude material was purified by flash chromatography (SiO_2, *n*-pentane/ethyl acetate, 3:1) to give the product as a colorless oil (22.3 mg, 71%, 86% ee). $[\alpha]_D^{20}$ = –29.4 (c = 0.50, $CHCl_3$); ^{1}H NMR (600 MHz, [D_6]-DMSO, 373 K): δ = 6.97 (dt, *J* = 15.7, 7.2 Hz, 1H), 5.85 (dt, *J* = 15.7, 1.5 Hz, 1H), 4.82 (d, *J* = 5.7 Hz, 1H), 3.83 (dt, *J* = 7.7, 5.5 Hz, 1H), 3.66 (s, 3H), 3.63 (t, *J* = 5.3 Hz, 1H), 3.19 (d, *J* = 10.5 Hz, 1H), 3.01 (d, *J* = 10.4 Hz, 1H), 2.69 – 2.58 (m, 2H), 1.41 (s, 9H), 0.99 (s, 3H), 0.88 (s, 3H); ^{13}C NMR (151 MHz, [D_6]-DMSO, 373 K): δ = 165.5, 154.0, 147.0, 121.1, 78.0, 76.9, 59.8, 56.1, 50.3, 40.4, 31.0, 27.6, 24.4, 19.5; IR (ATR): $\tilde{\nu}$ = 3438, 2973, 1725, 1694, 1666, 1401, 1367, 1267, 1162, 1114 cm^{-1}; HRMS (ESI$^+$): *m/z*: calcd. for $C_{16}H_{27}NO_5Na$ $[M+Na]^+$: 336.17814, found: 336.17807.

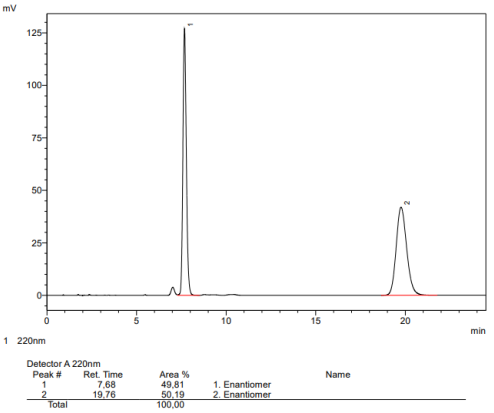

The ee was determined by HPLC analysis: Chiralpak 150 mm IG-3, 3 µm, 4.6 mm ∅, acetonitrile/water = 40:60, v = 1.0 mL/min, λ = 220 nm, t(minor) = 7.70 min, t(major) = 19.73 min, (racemic sample: left, enantioenriched sample: right).

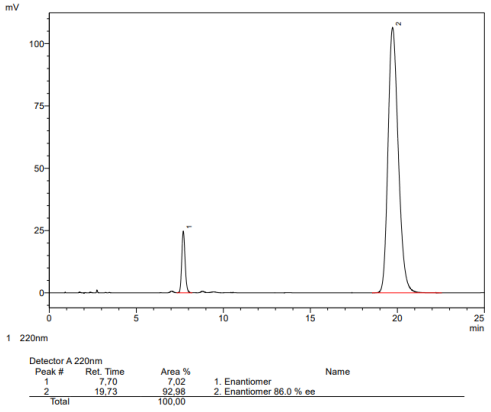

Pyrrolidine Derivative 172. The title compound was prepared according to the general procedure **IV** followed by oxidative work-up **III**, using substrate **S46** (32.5 mg, 0.10 mmol); the reaction time was 18 h. The crude material was purified by flash chromatography (SiO_2, *n*-pentane/ethyl acetate, 1:2) to give the product as a colorless oil (21.8 mg, 67%, 95% ee). $[\alpha]_D^{20}$ = +3.8 (c = 0.48, $CHCl_3$); ^{1}H NMR (600 MHz, [D_6]-DMSO, 383 K): δ = 6.91 (ddd, *J* = 15.8, 7.7, 7.0 Hz, 1H), 5.82 (dt, *J* = 15.6, 1.5 Hz, 1H), 5.38 (br, 1H), 4.85 (d, *J* = 5.9 Hz, 1H), 4.51 (d, *J* = 5.9 Hz, 1H), 4.35 (d, *J* = 5.9 Hz, 1H), 4.31 (d, *J* = 5.9 Hz, 1H), 4.14 (d, *J* = 6.2 Hz, 1H), 3.77 (q, *J* = 6.3 Hz, 1H), 3.66 (s, 3H), 3.63 (d, *J* = 11.4 Hz, 1H), 3.58 (d, *J* = 11.3 Hz, 1H), 2.55 – 2.51 (m, 1H), 2.32 – 2.21 (m, 1H), 1.41 (s, 9H); ^{13}C NMR (151 MHz, [D_6]-DMSO, 383 K): δ = 165.4, 153.3, 146.3, 121.3, 78.3, 76.9, 74.2, 72.7, 58.7, 52.8, 50.2, 46.8, 31.1, 27.5; IR (ATR): $\tilde{\nu}$ = 3403, 2951, 1722, 1694, 1664, 1395, 1268, 1166, 1100, 979 cm^{-1}; HRMS (ESI$^+$): *m/z*: calcd. for $C_{16}H_{25}NO_6Na$ [M+Na]$^+$: 350.15741, found: 350.15752.

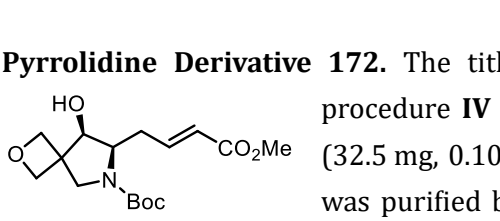

The ee was determined by HPLC analysis: Chiralpak 150 mm IG-3, 3 µm, 4.6 mm ∅, acetonitrile/water = 40:60, v = 1.0 mL/min, λ = 220 nm, t(minor) = 5.92 min, t(major) = 10.87 min, (racemic sample: left, enantioenriched sample: right).

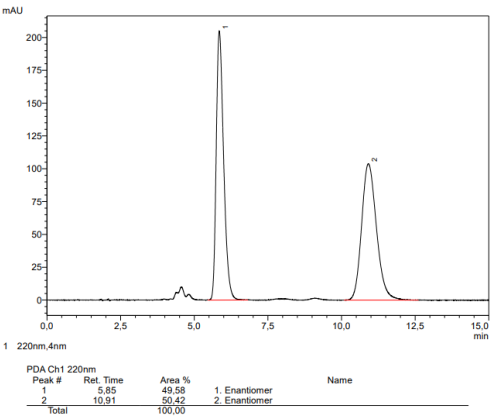

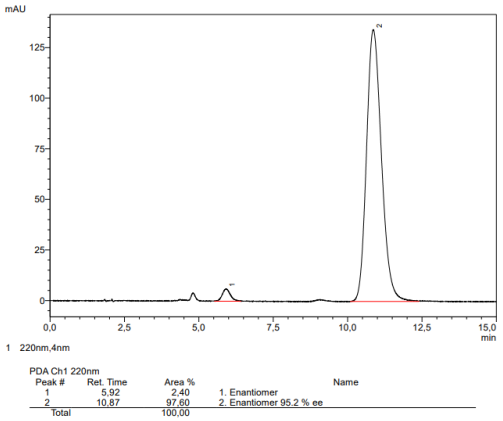

Tetrahydroisoquinoline Derivative 173. The title compound was prepared according to the general procedure **IV** and oxidative work-up **III**, using substrate **S47** (34.5 mg, 0.10 mmol); the reaction time was 16 h. The crude material was purified by flash chromatography (SiO_2, *n*-pentane/ethyl acetate, 2.5:1) and the product was obtained as an offwhite solid (25.1 mg, 72%, 41% ee). ***Note:*** *Due to the insufficient ee of the product, the absolute configuration has not been rigorously proven by Mosher ester analysis or X-Ray diffraction analysis.* $[\alpha]_D^{20}$ = –59.2 (c = 0.51, $CHCl_3$); ^{1}H NMR (600 MHz, [D_6]-DMSO, 383K): δ = 7.56 (dddd, *J* = 7.5, 1.6, 1.1, 0.5 Hz, 1H), 7.31 – 7.20 (m, 2H), 7.18 – 7.12 (m, 1H), 6.85 (ddd, *J* = 15.6, 8.4, 6.4 Hz, 1H), 5.81 (ddd, *J* = 15.6, 1.7, 1.3 Hz, 1H), 5.55 (d, *J* = 5.0 Hz, 1H), 4.82 (t, *J* = 5.2 Hz, 1H), 4.73 – 4.64 (m, 1H), 4.55 (dt, *J* = 10.1, 4.9 Hz, 1H), 4.22 (d, *J* = 17.4 Hz, 1H), 3.64 (s, 3H), 2.47 (dddd, *J* = 15.0, 6.4, 3.9, 1.8 Hz, 1H), 1.93 (dddd, *J* = 15.1, 10.3, 8.4, 1.3 Hz, 1H), 1.45 (s, 9H); ^{13}C NMR (151 MHz, [D_6]-DMSO, 383K): δ = 165.2, 153.6, 146.1, 136.2, 131.1, 126.0, 125.8, 124.9, 124.6, 121.6, 78.9, 66.4, 53.3, 50.2, 42.1, 28.3, 27.5; IR (ATR): $\tilde{\nu}$ = 3443, 2977, 1723, 1694, 1667, 1405, 1366, 1318, 1238, 1160, 1095, 737 cm^{-1}; HRMS (ESI$^+$): *m/z*: calcd. for $C_{19}H_{25}NO_5Na$ $[M+Na]^+$: 370.16249, found: 370.16257.

The ee was determined by HPLC analysis: Chiralpak 150 mm IB-N-3, 3 µm, 4.6 mm ∅, acetonitrile/water = 40:60, v = 1.0 mL/min, λ = 220 nm, t(major) = 9.50 min, t(minor) = 11.70 min, (enantioenriched sample: left, racemic sample: right).

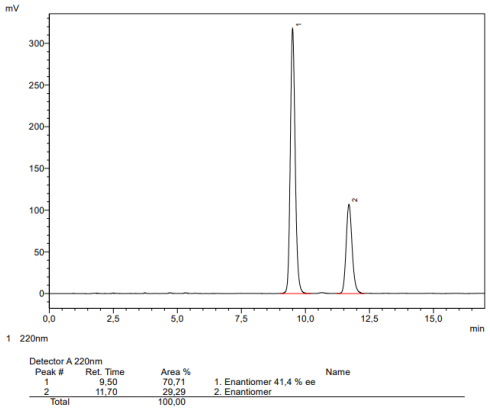

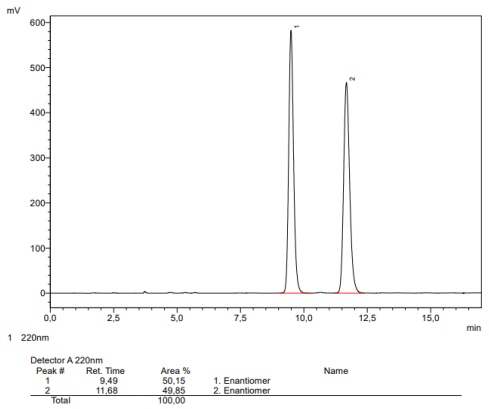

Tetrahydroisoquinoline Derivative 174. The title compound was prepared according to the general procedure **IV** (the reaction was performed at room temperature) followed by oxidative work-up **III**, using substrate **S48** (28.7 mg, 0.10 mmol); the reaction time was 20 h. The crude material was purified by flash chromatography (SiO_2, *n*-pentane/ethyl acetate, 2:1) to give the product as a pale yellow oil (25.1 mg, 87%, 28% ee, rr ≈ 11:1). ***Note:*** *The product was obtained as a ~11:1 mixture of regioisomers that could not be separated.*

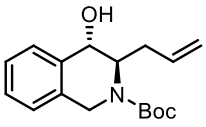

^{1}H NMR (600 MHz, [D$_6$]-DMSO, 373 K): δ = 7.33 – 7.21 (m, 3H), 7.21 – 7.17 (m, 1H), 5.83 – 5.67 (m, 1H), 5.01 – 4.92 (m, 2H), 4.76 (d, *J* = 17.1 Hz, 1H), 4.48 (d, *J* = 2.6 Hz, 1H), 4.39 (td, *J* = 7.4, 2.5 Hz, 1H), 4.17 (d, *J* = 17.1 Hz, 1H), 2.08 – 1.89 (m, 2H), 1.47 (s, 9H); ^{13}C NMR (151 MHz, [D$_6$]-DMSO, 373 K): δ = 154.4, 134.6, 134.6, 132.5, 129.1, 127.0, 125.9, 125.3, 116.0, 78.2, 67.9, 55.8, 41.9, 34.5, 27.7; IR (ATR): $\tilde{\nu}$ = 3404, 2976, 1690, 1410, 1366, 1244, 1169, 1019, 767 cm^{-1}; HRMS (ESI$^+$): *m/z*: calcd. for $C_{17}H_{23}NO_3Na$ [M+Na]$^+$: 312.15701, found: 312.15658.

The ee was determined by 2D-HPLC analysis. First dimension = 50 mm Nucleodur C18 Gravity SB 1.8 µm, 4.6 mm Ø, methanol/water = 50:50 → 10:90, v = 1.0 mL/min, λ = 220 nm. Second Dimension = 150 mm Chiralpak IG-3, 4.6 mm Ø, acetonitrile/water = 50:50, v = 1.0 ml/min, λ = 220 nm, t(major) = 5.57 min, t(minor) = 8.25 min.

First dimension (racemic sample: left, enantioenriched sample: right):

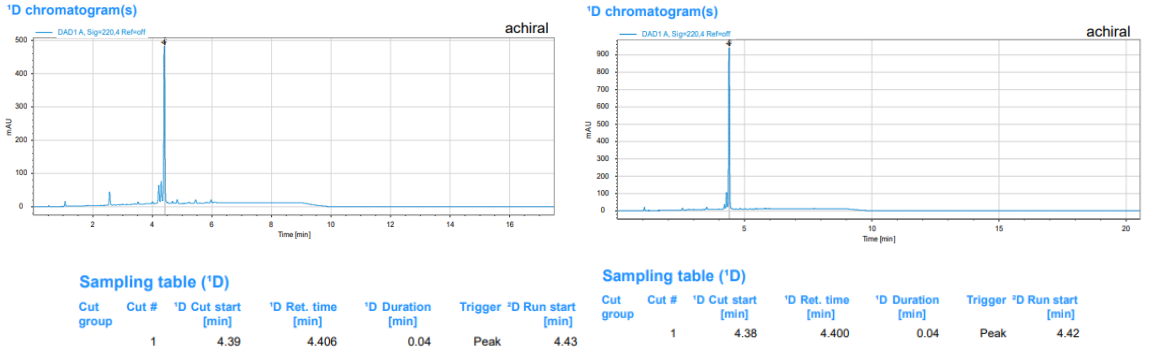

Sampling table (^{1}D)

Cut group	Cut #	^{1}D Cut start [min]	^{1}D Ret. time [min]	^{1}D Duration [min]	Trigger	^{2}D Run start [min]
	1	4.39	4.406	0.04	Peak	4.43

Sampling table (^{1}D)

Cut group	Cut #	^{1}D Cut start [min]	^{1}D Ret. time [min]	^{1}D Duration [min]	Trigger	^{2}D Run start [min]
	1	4.38	4.400	0.04	Peak	4.42

Second dimension (racemic sample: left, enantioenriched sample: right):

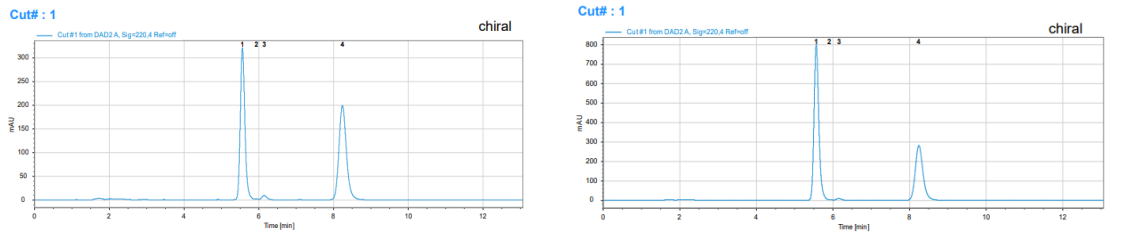

Component table

Signal: DAD2 A, Sig=220,4 Ref=off

Component	^{1}D Sampling range [min]	Ret.Time ^{2}D [min]	Area	Area%	
1	4.39 - 4.43	5.568	2742.215	49.064	Hauptisomer 1. Enantiomer
2	4.39 - 4.43	5.935	13.831	0.247	
3	4.39 - 4.43	6.149	80.307	1.437	
4	4.39 - 4.43	8.243	2752.680	49.251	Hauptisomer 2. Enantiomer

Component table

Signal: DAD2 A, Sig=220,4 Ref=off

ee = 28.4%

Component	^{1}D Sampling range [min]	Ret.Time ^{2}D [min]	Area	Area%	
1	4.38 - 4.42	5.568	6982.553	63.618	Hauptisomer 1. Enantiomer
2	4.38 - 4.42	5.902	15.398	0.140	
3	4.38 - 4.42	6.155	81.027	0.738	
4	4.38 - 4.42	8.248	3896.843	35.504	Hauptisomer 2. Enantiomer

Tetrahydroisoquinoline Derivative 175. The title compound was prepared according to the general procedure **III** followed by oxidative work-up **III**, substrate **S49** (36.3 mg, 0.10 mmol); the reaction time was 72 h. The crude material was purified by flash chromatography (SiO_2, *n*-pentane/ethyl acetate, 2:1) to give the product as colorless solid (28.6 mg, 78%, 14% ee). ^{1}H NMR (600 MHz, [D_6]-DMSO, 383 K): δ = 7.36 – 7.23 (m, 7H), 7.22 – 7.17 (m, 2H), 6.34 (dt, *J* = 15.9, 1.5 Hz, 1H), 6.16 (ddd, *J* = 15.8, 7.5, 6.9 Hz, 1H), 4.88 (br, 1H), 4.78 (d, *J* = 17.1 Hz, 1H), 4.54 (d, *J* = 2.6 Hz, 1H), 4.47 (ddd, *J* = 8.6, 6.4, 2.5 Hz, 1H), 4.24 (d, *J* = 17.1 Hz, 1H), 2.25 – 2.15 (m, 1H), 2.13 (dddd, *J* = 14.3, 8.2, 7.5, 1.4 Hz, 1H), 1.42 (s, 9H); ^{13}C NMR (151 MHz, [D_6]-DMSO, 383 K): δ = 154.4, 136.8, 134.6, 132.5, 130.9, 129.0, 127.7, 127.0, 126.5, 126.3, 125.9, 125.3(1), 125.2(6), 78.2, 68.1, 56.2, 42.0, 33.7, 27.6; IR (ATR): $\tilde{\nu}$ = 3414, 2976, 1688, 1410, 1365, 1243, 1167, 1125, 1014, 966, 746 cm^{-1}; HRMS (ESI$^+$): *m/z*: calcd. for $C_{23}H_{27}NO_3Na$ $[M+Na]^+$: 388.18831, found: 388.18816.

The ee was determined by HPLC analysis: Chiralpak 150 mm IG-3, 3 µm, 4.6 mm ∅, acetonitrile/water = 55:45, v = 1.0 mL/min, λ = 254 nm, t(minor) = 12.22 min, t(major) = 28.68 min, (racemic sample: left, enantioenriched sample: right).

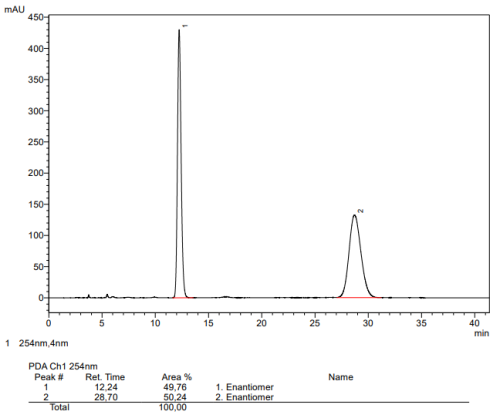

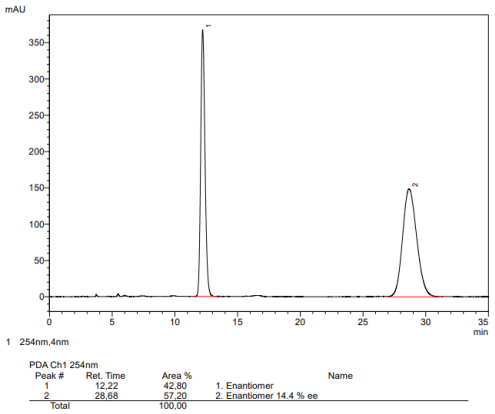

Tetrahydroquinoline Derivative 176. The title compound was prepared according to the general procedure **IV** followed by oxidative work-up **III**, using substrate **S50** (34.5 mg, 0.10 mmol); the reaction time was 18 h. The crude material (dr ≈ 3:1) was purified by flash chromatography (SiO_2, *n*-pentane/ethyl acetate, 3:1) to give the product as a colorless oil (20.0 mg, 58%, 5% ee, dr > 20:1). ^{1}H NMR (400 MHz, $CDCl_3$): δ = 7.83 (dd, *J* = 8.5, 1.1 Hz, 1H), 7.38 (dd, *J* = 7.7, 1.7 Hz, 1H), 7.29 – 7.23 (m, 1H), 7.14 – 6.92 (m, 2H), 5.87 (dt, *J* = 15.5, 1.4 Hz, 1H), 4.43 (d, *J* = 4.6 Hz, 1H), 3.82 (dd, *J* = 13.4, 5.6 Hz, 1H), 3.77 (d, *J* = 3.4 Hz, 1H), 3.74 (s, 3H), 2.31 (dddd, *J* = 14.0, 6.8, 5.6, 1.5 Hz, 1H), 2.23 – 2.05 (m, 2H), 1.78 (br, 1H), 1.53 (s, 9H); ^{13}C NMR (101 MHz, $CDCl_3$): δ = 166.8, 153.7, 146.1, 137.7, 129.1, 129.0, 128.4, 123.9, 123.4, 123.3, 81.7, 70.3, 51.7, 44.5, 40.4, 32.2, 28.4; IR (ATR): $\tilde{\nu}$ = 3450, 2925, 1701, 1660, 1489, 1367, 1248, 1161, 1147, 1020, 757 cm^{-1}; HRMS (ESI$^+$): *m/z*: calcd. for $C_{19}H_{25}NO_5Na$ [M+Na]$^+$: 370.162493, found: 370.16240.

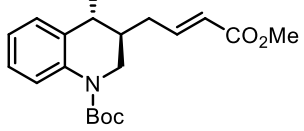

The ee was determined by HPLC analysis: Chiralpak 150 mm IB-N-3, 3 µm, 4.6 mm ∅, acetonitrile/water = 40:60, v = 1.0 mL/min, λ = 240 nm, t(major) = 12.35 min, t(minor) = 13.09 min, (racemic sample: left, enantioenriched sample: right).

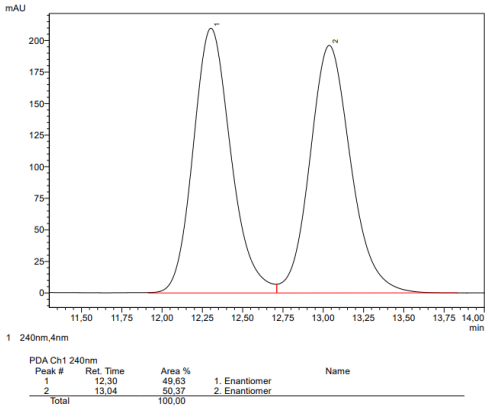

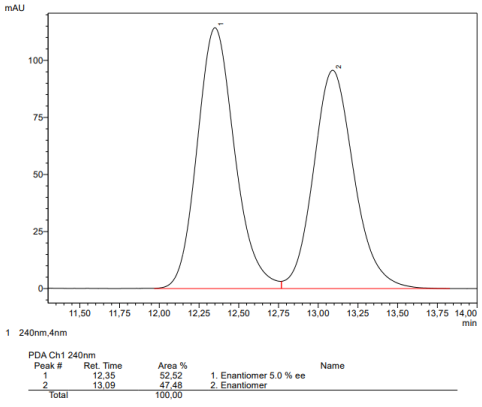

Chromanol Derivative 177. The title compound was prepared according to the general procedure **IV** followed by oxidative work-up **III**, using substrate **S51** (17.2 mg, 0.07 mmol); the reaction time was 24 h. The crude material (dr ≈ 5:1) was purified by flash chromatography (SiO_2, *n*-pentane/*tert*-butyl methyl ether, 1.5:1 → 1:1) to give the product as a yellow oil (14.0 mg, 81%, 2% ee, dr > 20:1). ^{1}H NMR (400 MHz, $CDCl_3$): δ = 7.31 (dd, *J* = 7.6, 1.7 Hz, 1H), 7.23 (ddd, *J* = 8.2, 7.2, 1.7 Hz, 1H), 7.07 – 6.91 (m, 2H), 6.85 (dd, *J* = 8.3, 1.2 Hz, 1H), 5.87 (dt, *J* = 15.6, 1.5 Hz, 1H), 4.47 (d, *J* = 4.1 Hz, 1H), 4.28 (dd, *J* = 11.3, 2.6 Hz, 1H), 4.03 (ddd, *J* = 11.3, 4.5, 1.1 Hz, 1H), 3.74 (s, 3H), 2.34 – 2.16 (m, 2H), 2.12 (dtd, *J* = 9.1, 4.0, 2.5 Hz, 1H); ^{13}C NMR (101 MHz, $CDCl_3$): δ = 166.8, 154.2, 146.0, 130.1, 130.0, 123.4, 123.1, 121.2, 117.1, 67.7, 65.0, 51.7, 39.1, 31.2; IR (ATR): $\tilde{\nu}$ = 3438, 2926, 1722, 1707, 1654, 1610, 1488, 1456, 1319, 1267, 1225, 1038, 759 cm^{-1}; HRMS (ESI$^+$): *m/z*: calcd. for $C_{14}H_{16}O_4Na$ $[M+Na]^+$: 271.09408, found: 271.09376.

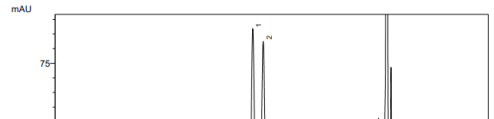

The ee was determined by HPLC analysis: Chiralpak 150 mm IB-N-3, 3 µm, 4.6 mm ∅, acetonitrile/water = 30:70, v = 1.0 mL/min, λ = 220 nm, t(minor) = 13.75 min, t(major) = 14.47 min (racemic sample: left, enantioenriched sample: right).

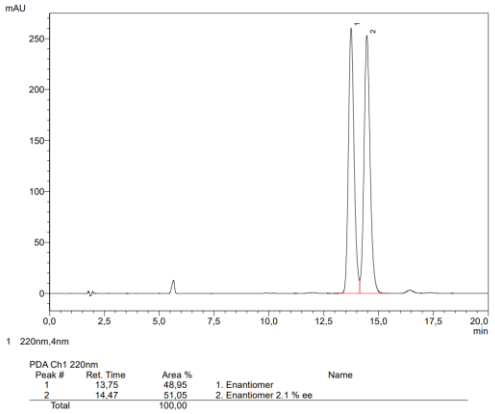

5.4.3 Downstream Derivatization

Compound 178. A solution of diethylaminosulfur trifluoride (DAST) (20.0 µL, 0.15 mmol) in dichloromethane (0.1 mL) was added dropwise to a solution of **153** (40.0 mg, 0.12 mmol, 92% ee) in dichloromethane (0.3 mL) at –78 °C (bath temperature). After complete addition, the reaction mixture was stirred at this temperature for 2 h. The mixture was warmed to 0 °C before sat. aq. $NaHCO_3$ (0.5 mL) was carefully added. The mixture was vigorously stirred for 5 min, water (5 mL) and dichloromethane (5 mL) were introduced, the organic phase was separated, and the aqueous layer was extracted with dichloromethane (3 x 5 mL). The combined organic phases were washed with brine (10 mL), dried over $MgSO_4$ and filtered, and the solvent was removed under reduced pressure. The residue was purified by flash chromatography (*n*-pentane/ethyl acetate, 5:1) to give the title compound as a colorless oil (25.9 mg, 64%, 90% ee). $[\alpha]_D^{20}$ = +42.0 (c = 0.49, $CHCl_3$); ^{1}H NMR (600 MHz, [D_6]-DMSO, 383 K): δ = 7.49 – 7.41 (m, 2H), 7.36 – 7.30 (m, 2H), 6.83 (ddd, *J* = 15.6, 8.0, 6.6 Hz, 1H), 5.88 (dt, *J* = 15.6, 1.5 Hz, 1H), 5.48 (dd, *J* = 49.4, 2.3 Hz, 1H), 4.89 (dd, *J* = 17.8, 3.6 Hz, 1H), 4.83 (dddd, *J* = 14.7, 10.0, 5.0, 2.3 Hz, 1H), 4.26 (dd, *J* = 17.8, 5.2 Hz, 1H), 3.66 (s, 3H), 2.34 (dddd, *J* = 14.8, 6.6, 5.0, 1.7 Hz, 1H), 2.10 (dddd, *J* = 14.8, 10.0, 8.0, 1.3 Hz, 1H), 1.46 (s, 9H); ^{13}C NMR (151 MHz, [D_6]-DMSO, 383 K): δ = 165.0, 153.9, 143.7, 133.3 (d, *J* = 3.3 Hz), 130.3 (d, *J* = 3.4 Hz), 129.3 (d, *J* = 4.2 Hz), 128.1 (d, *J* = 17.6 Hz), 126.4 (d, *J* = 3.3 Hz), 125.8 (d, *J* = 3.0 Hz), 122.5, 87.5 (d, *J* = 170.9 Hz), 79.1, 52.6, 50.3, 41.0, 30.8 (d, *J* = 6.9 Hz), 27.4; ^{19}F NMR (585 MHz, [D_6]-DMSO, 383 K): δ = –151.5; IR (ATR): $\tilde{\nu}$ = 2976, 1722, 1689, 1407, 1366, 1326, 1160, 1124, 977, 769, 744 cm^{-1}; HRMS (EI): *m/z*: calcd. for $C_{19}H_{24}NO_4F$ $[M]^{+\cdot}$: 372.15816, found: 372.15829. ***Note:*** *The relative configuration was assigned based on NOESY data and the ^3J(H8,H9) coupling constant.*

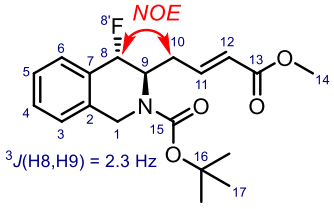

The ee was determined by HPLC analysis: Chiralpak 150 mm IG-3, 3 µm, 4.6 mm ∅, acetonitrile/water = 60:40, v = 1.0 mL/min, λ = 210 nm, t(minor) = 4.88 min, t(major) = 5.60 min, (racemic sample: left, enantioenriched sample: right).

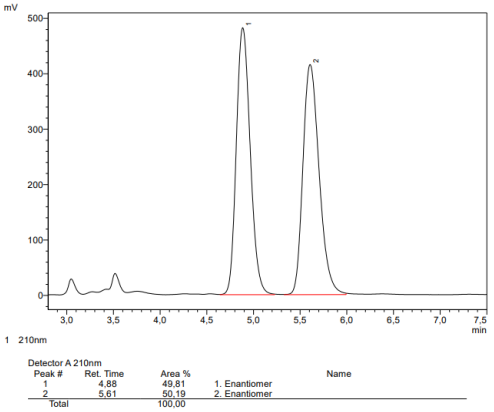

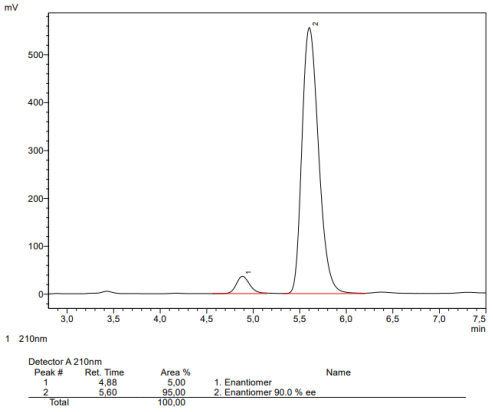

Compound 181. DBU (2.0 µL, 13.4 µmol) was added to a solution of **172** (17.0 mg, 51.9 µmol, 95% ee) in THF (0.5 mL) and the resulting mixture was stirred at room temperature for 16 h. The solvent was evaporated and the residue purified by flash chromatography (SiO_2, *n*-pentane/ethyl acetate, 1:2) to give the title compound as a colorless oil (14.0 mg, 82%, 94% ee, dr ≈ 4:1). $[\alpha]_D^{20}$= –56.9 (c = 0.70, $CHCl_3$); ^{1}H NMR (600 MHz, [D_6]-DMSO, 373 K): δ = 4.70 (d, *J* = 4.8 Hz, 1H), 4.61 (d, *J* = 6.4 Hz, 1H), 4.46 (d, *J* = 6.4 Hz, 1H), 4.41 (d, *J* = 5.7 Hz, 1H), 4.34 (d, *J* = 5.9 Hz, 1H), 4.30 (ddd, *J* = 5.7, 4.8, 1.3 Hz, 1H), 4.15 (dtd, *J* = 9.3, 6.3, 5.6 Hz, 1H), 3.89 (d, *J* = 11.3 Hz, 1H), 3.62 (s, 3H), 3.29 (d, *J* = 11.3 Hz, 1H), 2.61 – 2.51 (m, 2H), 2.27 (ddd, *J* = 13.4, 5.6, 1.3 Hz, 1H), 1.83 (ddd, *J* = 13.4, 9.3, 5.7 Hz, 1H), 1.43 (s, 9H); ^{13}C NMR (151 MHz, [D_6]-DMSO, 373 K): δ = 170.1, 152.5, 86.0, 79.4, 78.5, 74.9, 72.5, 61.3, 53.1, 50.5, 47.3, 39.0, 38.7, 27.7; IR (ATR): $\tilde{\nu}$ = 2974, 2872, 1738, 1694, 1398, 1175, 1151, 1069, 905, 730 cm^{-1}; HRMS (ESI$^+$): *m/z*: calcd. for $C_{16}H_{25}NO_6Na$ $[M+Na]^+$: 350.15741, found: 350.15743. ***Note:*** *The diastereomers were assigned based on NOESY data.*

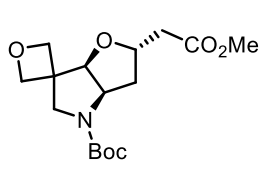

(major isomer)

The ee was determined by HPLC analysis: Chiralpak 150 mm IB-N-3, 3 µm, 4.6 mm ∅, *n*-heptane/*iso*-propanol = 95:5, v = 1.0 mL/min, λ = 205 nm, **for major diastereomer:** t(major) = 9.57 min, t(minor) = 12.57 min, **for minor diastereomer:** t(major) = 11.18 min, t(minor) = 13.86 min, (racemic sample: left, enantioenriched sample: right).

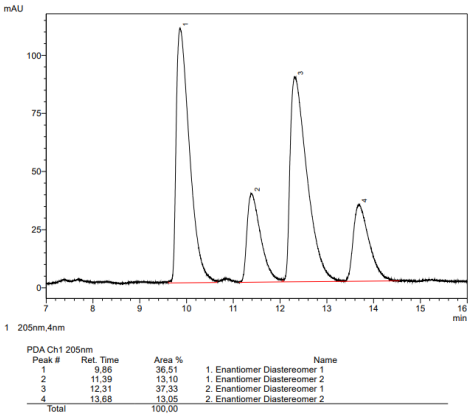

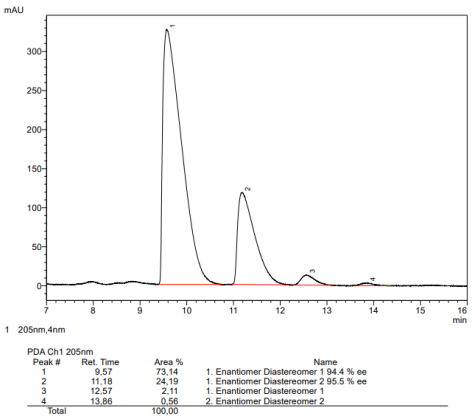

Assignment of Diastereomers by NOESY Data:

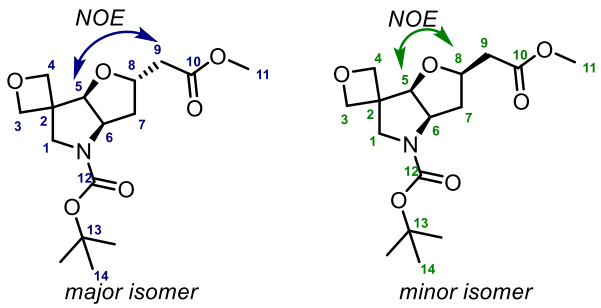

Compound 182. A Schlenk flask was charged under argon with a solution of **154** (34.5 mg, 90.5 µmol, 93% ee) in ethyl acetate (1.0 mL). Methanol (1.0 mL) and Pd/C (9.6 mg, 9.05 µmol) were added and the mixture was purged with H_2 from a balloon for 1 min. The mixture was then stirred under a H_2-atmosphere for 16 h at room temperature. The suspension was filtered through a plug of Celite, thoroughly rinsing with methanol (20 mL). The combined filtrates were evaporated under reduced pressure to give an off-white solid, which was used in the next step without further purification.

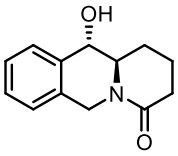

The solid was dissolved in ethanol (3.0 mL) and triethylamine (126 µL, 0.90 mmol) was added. The mixture was stirred at reflux temperature for 24 h. The volatiles were removed under reduced pressure and the residue was purified by flash chromatography (SiO_2, ethyl acetate) to give the title compound as a colorless oil (15.7 mg, 80%, 94% ee). $[\alpha]_D^{20}$= –143.7 (c = 0.75, $CHCl_3$); ^{1}H NMR (400 MHz, CD_3OD): δ = 7.61 – 7.53 (m, 1H), 7.29 – 7.22 (m, 2H), 7.17 – 7.13 (m, 1H), 5.31 (d, *J* = 17.2 Hz, 1H), 4.57 (d, *J* = 9.8 Hz, 1H), 4.18 (d, *J* = 17.2 Hz, 1H), 3.44 (dt, *J* = 10.1, 5.2 Hz, 1H), 2.42 (t, *J* = 6.4 Hz, 2H), 2.15 (dt, *J* = 7.2, 5.2 Hz, 2H), 2.02 – 1.87 (m, 1H), 1.90 – 1.70 (m, 1H); ^{13}C NMR (101 MHz, CD_3OD): δ = 172.2, 139.4, 133.3, 128.5, 127.9, 127.5, 126.7, 70.1, 60.6, 45.8, 33.2, 25.2, 18.4; IR (ATR): $\tilde{\nu}$ = 3341, 2947, 2874, 1611, 1580, 1445, 1415, 1251, 1186, 1054, 747 cm^{-1}; HRMS (EI): *m/z*: calcd. for $C_{13}H_{15}NO_2$ $[M]^{+\cdot}$: 217.10973, found: 217.10983.

The ee was determined by HPLC analysis: Chiralpak 150 mm IB-N-3, 3 µm, 4.6 mm ∅, acetonitrile/water = 20:80, v = 1.0 mL/min, λ = 220 nm, t(major) = 6.23 min, t(minor) = 7.86 min, (racemic sample: left, enantioenriched sample: right).

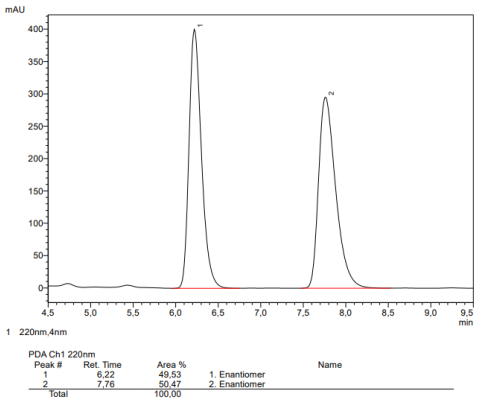

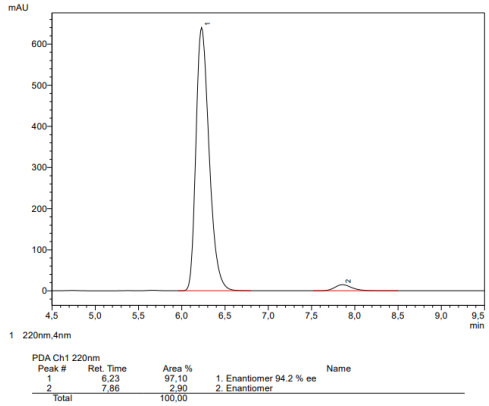

Compound 183. A solution of compound **182** (15.0 mg, 69.0 µmol) in THF (0.3 mL) was added dropwise to a solution of lithium aluminum hydride (7.9 mg, 0.21 mmol) in THF (0.3 mL) at 0 °C (bath temperature). After complete addition, the mixture was stirred at 50 °C (bath temperature) for 1 h. The mixture was cooled to 0 °C before sat. aq. NH_4Cl solution (1 mL) was added dropwise, followed by sat. aq. Rochelle salt solution (1 mL). The mixture was diluted with dichloromethane (2 mL) and was vigorously stirred for 10 min. The organic phase was separated and the aqueous layer was extracted with dichloromethane (4 x 8 mL). The combined organic phases were washed with brine (5 mL), dried over $MgSO_4$, and filtered, and the solvent was removed under reduced pressure. The residue was purified by flash chromatography (*n*-pentane/ethyl acetate, 1:2 + 3% NEt_3) to give the title compound as an off-white solid (10.3 mg, 73%, 94% ee). $[\alpha]_D^{20} = -23.6$ (c = 0.50, MeOH); ^{1}H NMR (400 MHz, CD_3OD): δ = 7.59 – 7.40 (m, 1H), 7.34 – 7.16 (m, 2H), 7.13 – 6.96 (m, 1H), 4.38 (d, *J* = 8.7 Hz, 1H), 3.81 (d, *J* = 15.2 Hz, 1H), 3.52 – 3.38 (m, 1H), 3.19 – 2.94 (m, 1H), 2.40 – 2.32 (m, 1H), 2.23 (ddd, *J* = 12.5, 11.6, 3.1 Hz, 1H), 2.13 (ddd, *J* = 10.1, 8.7, 3.2 Hz, 1H), 1.92 – 1.82 (m, 1H), 1.79 – 1.70 (m, 1H), 1.62 (dtt, *J* = 13.3, 12.4, 3.7 Hz, 1H), 1.47 – 1.21 (m, 2H); ^{13}C NMR (101 MHz, CD_3OD): δ = 138.5, 134.6, 128.2, 128.0, 127.9, 126.4, 73.3, 66.8, 58.9, 57.0, 31.3, 26.2, 24.7; IR (ATR): $\tilde{\nu}$ = 3340, 2929, 2853, 2811, 1451, 1350, 1124, 1031, 747 cm^{-1}; HRMS (EI): *m/z*: calcd. for $C_{13}H_{17}NO$ $[M]^{+\cdot}$: 203.13046, found: 203.13045.

The ee was determined by HPLC analysis: Chiralpak 150 mm OJ-3R, 3 µm, 4.6 mm ∅, acetonitrile/aq. NH_4HCO_3 (pH 9) = 30:70, v = 1.0 mL/min, λ = 220 nm, t(minor) = 3.64 min, t(major) = 3.97 min, (racemic sample: left, enantioenriched sample: right).

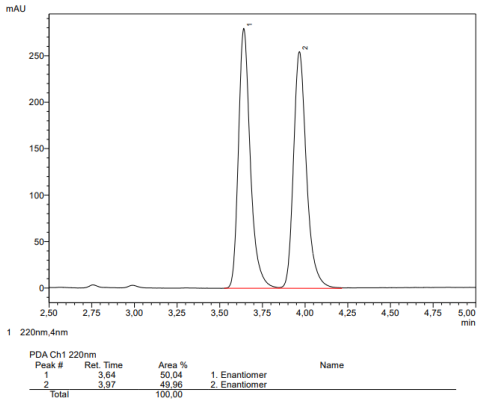

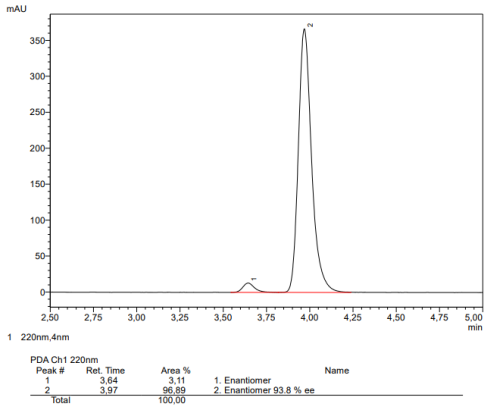

Compound 184. Tetrahydroisoquinoline derivative **154** (34.3 mg, 0.09 mmol, 93% ee) was added to a solution of $K_3[Fe(CN)_6]$ (89.0 mg, 0.27 mmol), K_2CO_3 (37.3 mg, 0.27 mmol), $K_2OsO_4 \cdot 2H_2O$ (1.0 mg, 2.7 µmol), $(DHQ)_2PHAL$ (4.2 mg, 5.4 µmol) and methanesulfonamide (17.1 mg, 0.18 mmol) in 1:1 *tert*-butanol/water (2 mL) at 0 °C (bath temperature). The mixture was stirred at 0 °C for 24 h. Sat. aq. $Na_2S_2O_3$ (5 mL) was added and the mixture was vigorously stirred for 10 min before it was diluted with ethyl acetate (10 mL). The organic phase was separated, the aqueous layer was extracted with ethyl acetate (3 x 10 mL). The combined organic phases were washed with brine (10 mL), dried over $MgSO_4$, and filtered, and the solvent was removed under reduced pressure.

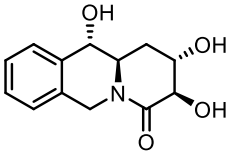

major isomer

The residue was dissolved in methanol (2 mL) and the solution transferred into a Schlenk flask under argon. Pd/C (9.6 mg, 9.0 µmol) was added, the mixture was purged with H_2 from a balloon for 1 min, and was then stirred under H_2 atmosphere for 20 h. The suspension was filtered through a plug of Celite and the filtrate was evaporated under reduced pressure. The residue was purified by flash chromatography (SiO_2, dichloromethane + 5% methanol → dichloromethane + 10% methanol → acetone + 30% methanol) to furnish the title compound as a pale brown solid (18.3 mg, 82% over 2 steps, dr ≈ 10:1). $[\alpha]_D^{20} = -11.8$ (c = 0.85, MeOH); ^{1}H NMR (600 MHz, CD_3OD): δ = 7.57 (dt, *J* = 7.5, 1.2 Hz, 1H), 7.30 – 7.20 (m, 2H), 7.15 (dd, *J* = 7.3, 1.1 Hz, 1H), 5.30 (d, *J* = 16.9 Hz, 1H), 4.57 (d, *J* = 10.0 Hz, 1H), 4.21 (d, *J* = 16.9 Hz, 1H), 3.98 (ddd, *J* = 10.1, 7.8, 3.9 Hz, 1H), 3.89 (dd, *J* = 7.9, 1.0 Hz, 1H), 3.53 (ddd, *J* = 9.9, 6.1, 3.8 Hz, 1H), 2.54 (dt, *J* = 13.9, 3.9 Hz, 1H), 2.13 (ddd, *J* = 13.9, 10.1, 6.2 Hz, 1H); ^{13}C NMR (151 MHz, CD_3OD): δ = 171.6, 139.2, 133.4, 128.6, 128.0, 127.8, 126.6, 75.0, 70.4, 67.7, 58.1, 45.7, 30.0; IR (ATR): $\tilde{\nu}$ = 3317, 1636, 1443, 1249, 1053, 753 cm^{-1}; HRMS (ESI$^+$): *m/z*: calcd. for $C_{13}H_{15}NO_4Na$ $[M+Na]^+$: 272.08933, found: 272.08950.

The selectivity of the dihydroxylation was assigned by the established stereochemical model[195] and the assignment confirmed by NOE-data:

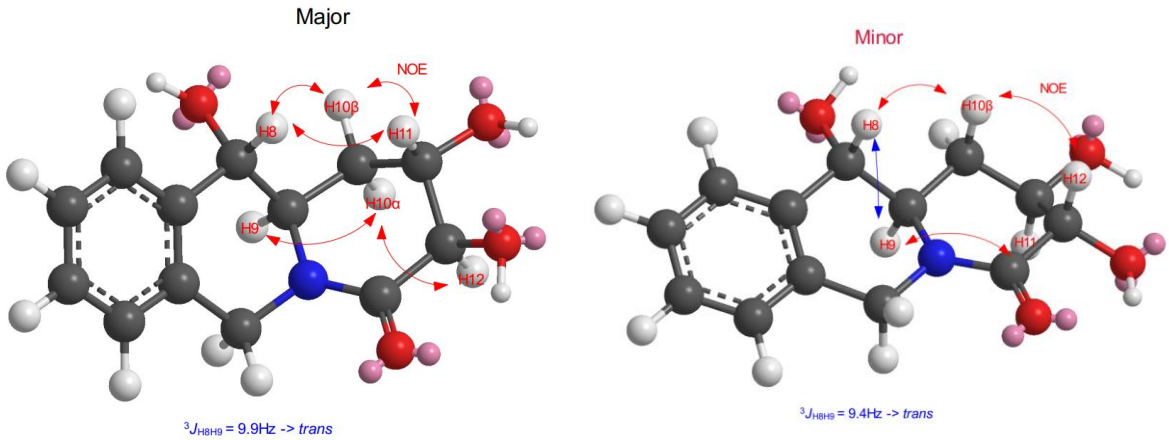

Compound 185. $BH_3 \cdot SMe_2$ (44.1 µL, 0.44 mmol) was added dropwise to a solution of compound

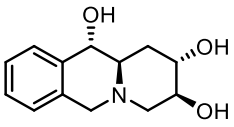

184 (11.0 mg, 44.1 µmol) in THF at 0 °C (bath temperature). After complete addition, the mixture was stirred at reflux temperature for 5 h. The mixture was cooled to 0 °C before ethanol (2 mL) was added dropwise, and the resulting mixture was vigorously stirred for 10 min. The solvent was removed under reduced pressure and the residue was dissolved in ethanol (2 mL). After stirring of the solution at reflux temperature for 2 h, the solvent was removed under reduced pressure and the residue was purified by flash chromatography (SiO_2, ethyl acetate/methanol, 20:3 + 2% NEt_3) to give the title compound as a colorless solid (8.1 mg, 78%). $[\alpha]_D^{20} = -17.2$ (c = 0.40, MeOH); ^{1}H NMR (400 MHz, CD_3OD): δ = 7.51 (dt, *J* = 7.5, 1.1 Hz, 1H), 7.27 – 7.14 (m, 2H), 7.08 – 7.01 (m, 1H), 4.44 (d, *J* = 8.9 Hz, 1H), 3.87 (q, *J* = 3.5 Hz, 1H), 3.80 (d, *J* = 15.4 Hz, 1H), 3.72 – 3.69 (m, 1H), 3.56 (d, *J* = 15.3 Hz, 1H), 2.89 (dd, *J* = 12.3, 3.1 Hz, 1H), 2.78 (dd, *J* = 12.3, 2.4 Hz, 1H), 2.58 (ddd, *J* = 10.7, 8.9, 3.4 Hz, 1H), 2.26 (dtd, *J* = 14.1, 3.6, 1.3 Hz, 1H), 2.00 – 1.88 (m, 1H); ^{13}C NMR (101 MHz, CD_3OD): δ = 138.6, 134.5, 128.2, 127.8, 126.4, 72.3, 69.5, 68.2, 60.5, 58.5, 56.3, 32.8; IR (ATR): $\tilde{\nu}$ = 3396, 2923, 1632, 1438, 1353, 1273, 1066, 1033, 746 cm^{-1}; HRMS (ESI^+): *m/z*: calcd. for $C_{13}H_{18}NO_3$ $[M+H]^+$: 236.12812, found: 236.12799.

5.4.4 Rotamer Formation

Rotamer Formation

While the products of the nickel-catalyzed reductive cyclization reactions could typically be isolated in high purity, many signals in the ^{1}H, ^{13}C and ^{19}F NMR spectra recorded at room temperature were significantly broadened or even doubled. In the ^{1}H NMR spectra, many characteristic signals and ^{n}J-couplings could not be resolved and the obtained spectra were rather complex (see below). Therefore, it was decided to characterize compounds affected by massive rotamer formation at elevated temperatures, which resulted in significantly simpler spectra.

^{1}H NMR (600 MHz, $CDCl_3$, 298 K) of compound 156

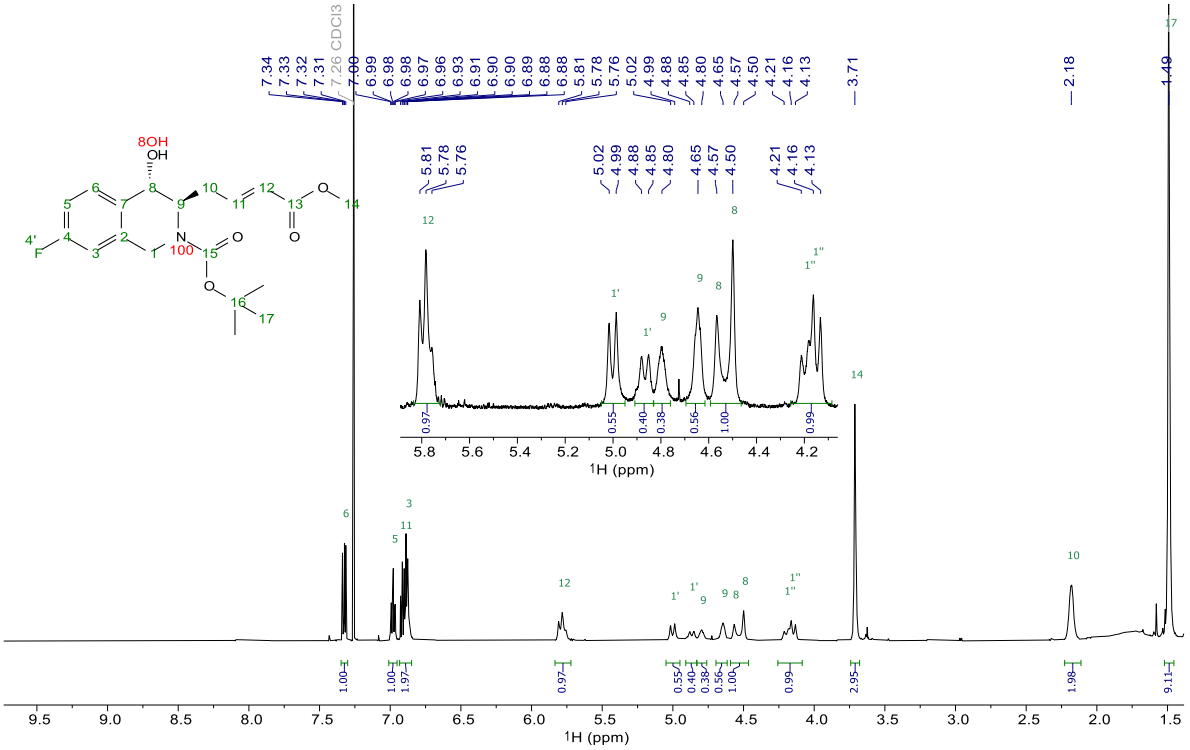

^{13}C NMR (151 MHz, $CDCl_3$, 298 K) of compound 156

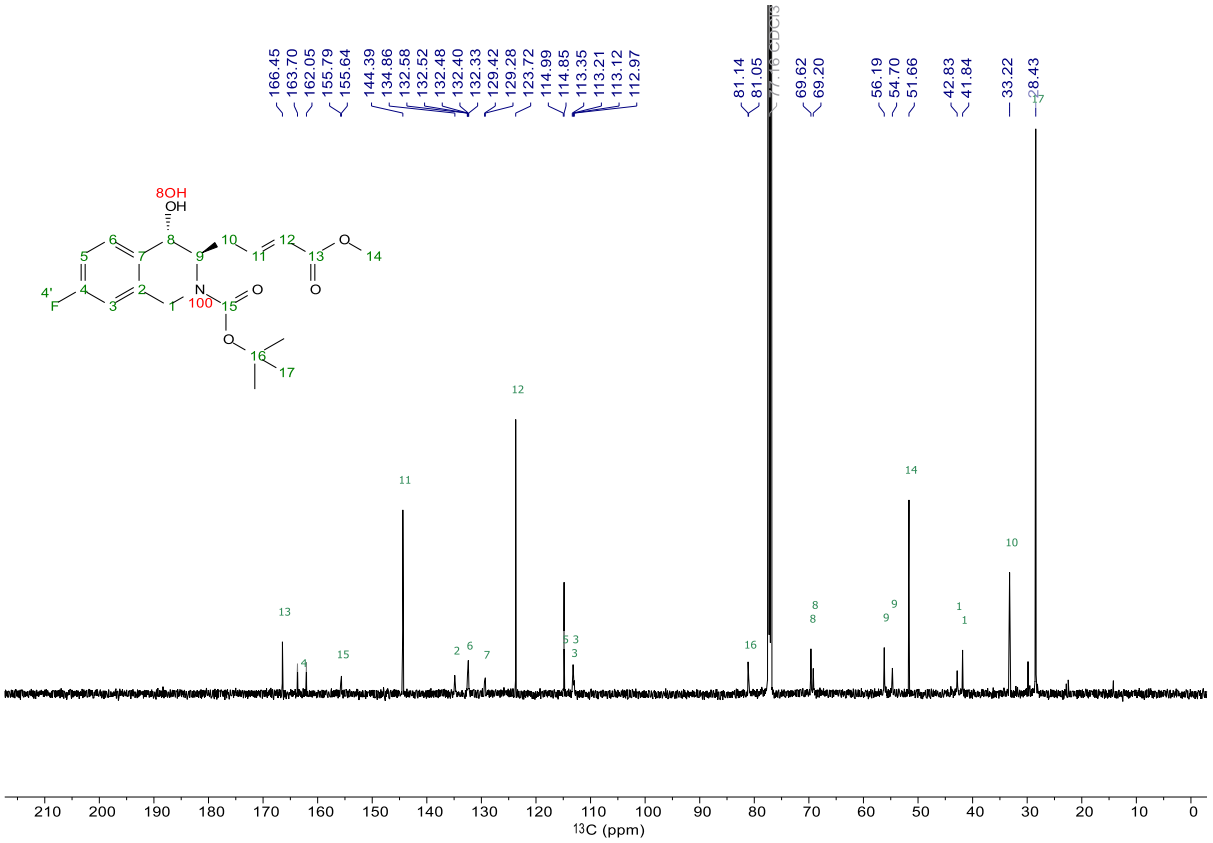

^{19}F NMR (585 MHz, $CDCl_3$, 298 K) of compound 156

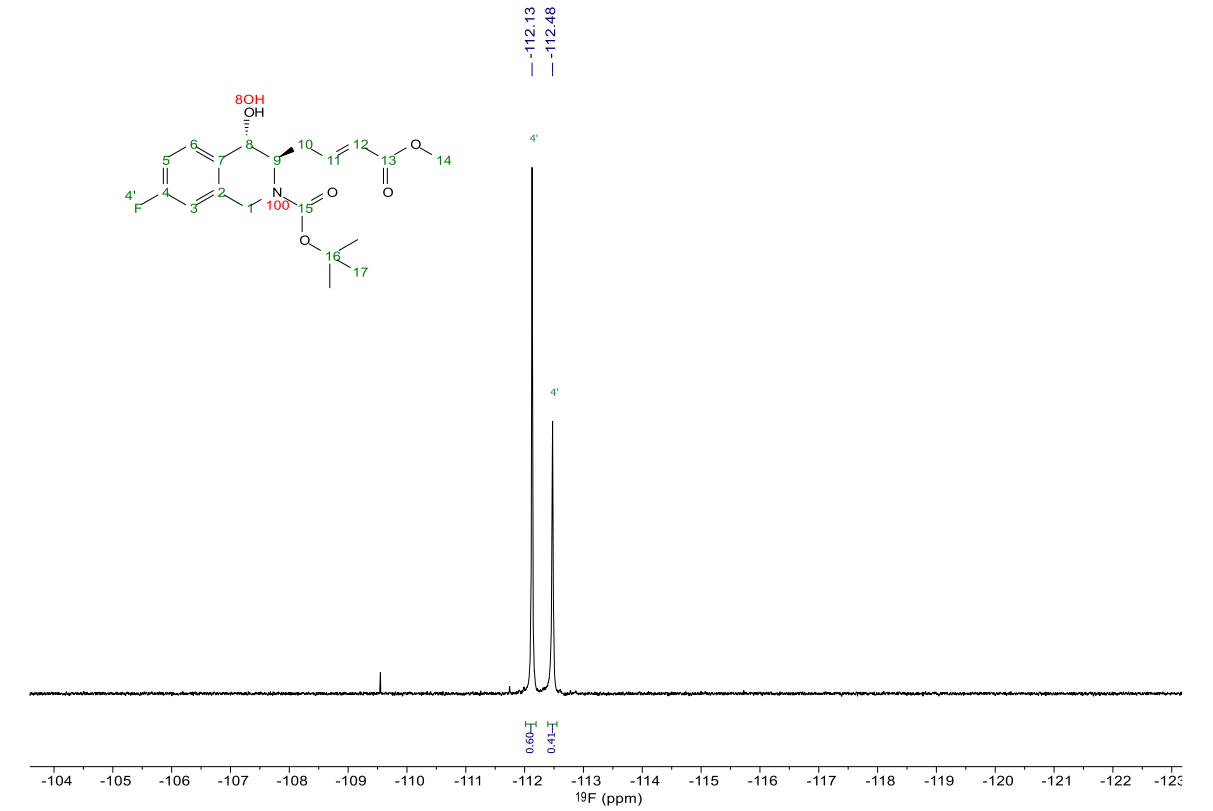

Temperature effect on rotamer formation as observed in the ^{1}H NMR spectrum of compound 153 ([D_6]-DMSO, 600 MHz)

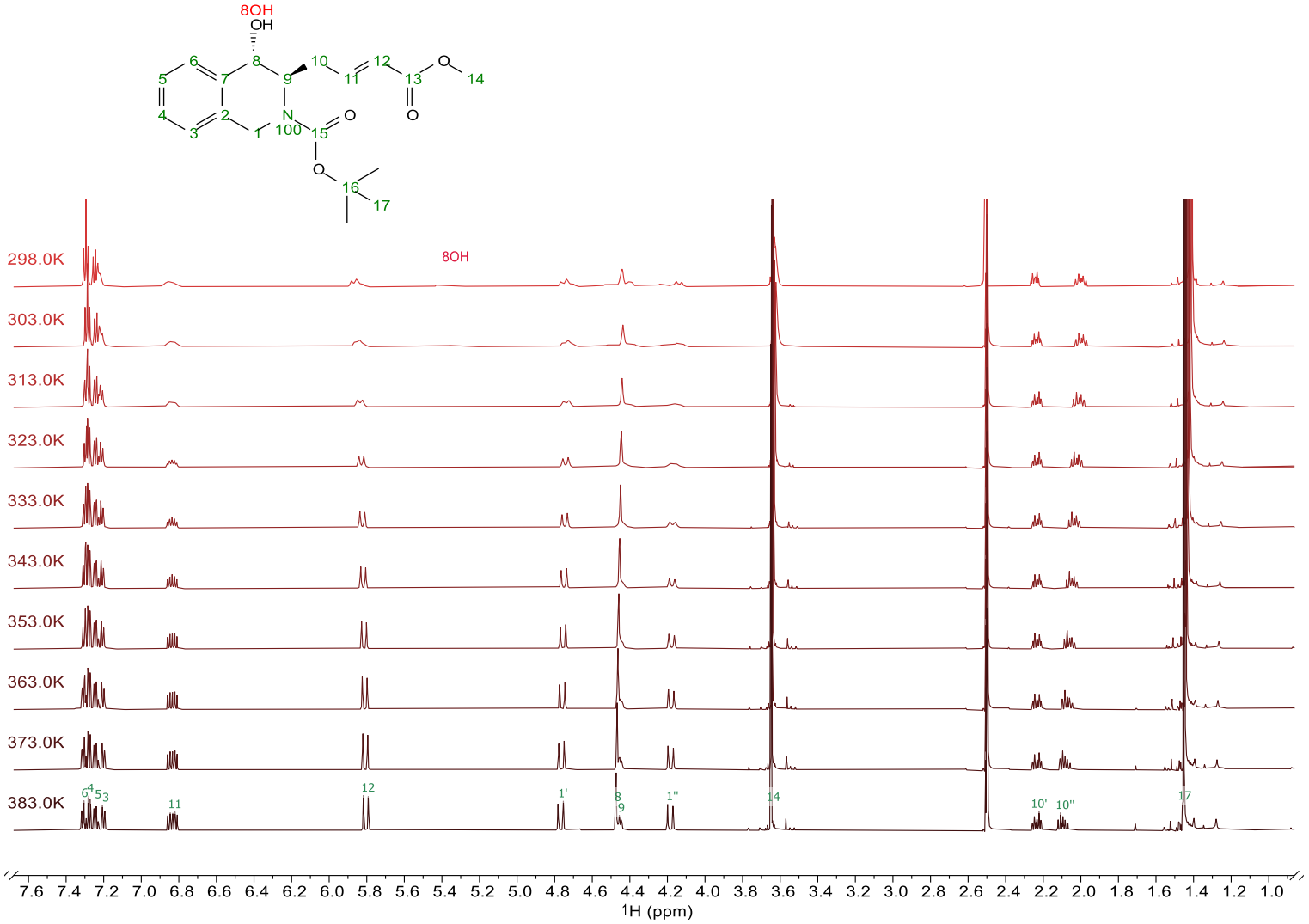

5.4.5 Preliminary Data on Nickel-Catalyzed Synthesis of Chromanol Derivatives

Since the attempted enantioselective synthesis of chromanol **177** in the presence of P-chiral (*S*)-AntPhos exhibited only limited diastereoselectivity and virtually no enantiocontrol (see Chapter 3.4), a range of achiral and chiral ligands was screened to further investigate this reaction. Under most conditions, however, substantial formation of the head-to-tail dimer **[177]$_2$** was observed, further complicating reaction optimization. This outcome was unexpected, as no dimerization had been detected in the presence of (*S*)-AntPhos for this model reaction or any other substrate. Importantly, **177** and **[177]$_2$** cannot be efficiently separated by flash chromatography. Consequently, complete suppression of dimer formation is desired.

Table S1: Selected optimization experiments for the racemic intramolecular reductive cyclization of **S51**.

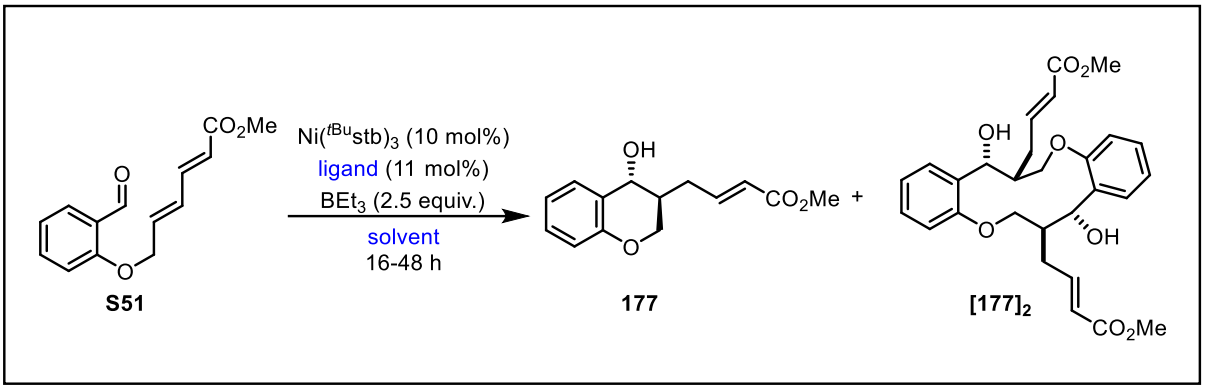

Entry	Solvent	Ligand	dr	177/[177]$_2$	Conversion
1	THF	---	5:1	100:0	quant.
2	toluene	---	2:1	100:0	quant.
3	DMA	---	10:1	100:0	quant.[a]
4	THF	PCy_3	1:2	1.3:1	quant.
5	THF	PPh_3	n.d.	n.d.	<10%
6	THF	SIPr·HCl	n.d.	n.d.	<10% [a,b]
7	THF	P(O-2,4-*t*-$Bu_2C_6H_3)_3$	4:1	11:1	quant.
8	THF	$P(TMS)_3$	20:1	>20:1	quant.[a]

[a] = unknown byproducts observed in crude NMR / messy reaction profile; [b] = 1:1 ratio of ligand and LiO^tBu used

In contrast to the reductive cyclization of amino-pentadienoate derived substrates, the diastereoselectivity of the present model reaction appears to be highly dependent on the choice of solvent (Table S1, entries 1 to 3). Moreover, the ligand cone angle may influence both the diastereoselectivity and the extent of dimer formation, as suggested by the improved results obtained with the sterically demanding phosphines P(O-2,4-*t*-$Bu_2C_6H_3)_3$ (θ = 215°)[246] and $P(TMS)_3$ (θ = 179°)[247] (Table S1, entries 7 and 8). This interpretation is, however, somewhat contradicted by the excellent diastereoselectivity and clean reaction profile observed under ligand-free conditions, as well as the poor performance obtained with the bulky phosphine PCy_3 (Table S1, entry 4).[248]

Given the increased complexity of the system, attention was subsequently shifted toward chiral ligands to assess whether the development of an enantioselective variant might even be feasible at all. To this end, a selection of ligand candidates commonly employed in nickel-catalyzed diene coupling reactions was evaluated in the model reaction (Figure S3 and Table S2). The introduction of a chiral ligand added an additional level of complexity, as enantioinduction was generally poor. Among the ligands tested, only the VAPOL-derived phosphoramidite **L11** delivered a promising result, affording the product with an enantiomeric excess of 40%. In contrast, TADDOL-derived phosphoramidites and phosphonites effectively suppressed dimer formation but failed to induce significant enantioselectivity.

Although the evaluation of additional ligand classes may provide the data necessary for a more systematic assessment of ligand effects, the considerable complexity of the transformation has become apparent. Consequently, the development of a robust and enantioselective protocol will likely require substantial further optimization and mechanistic investigation.

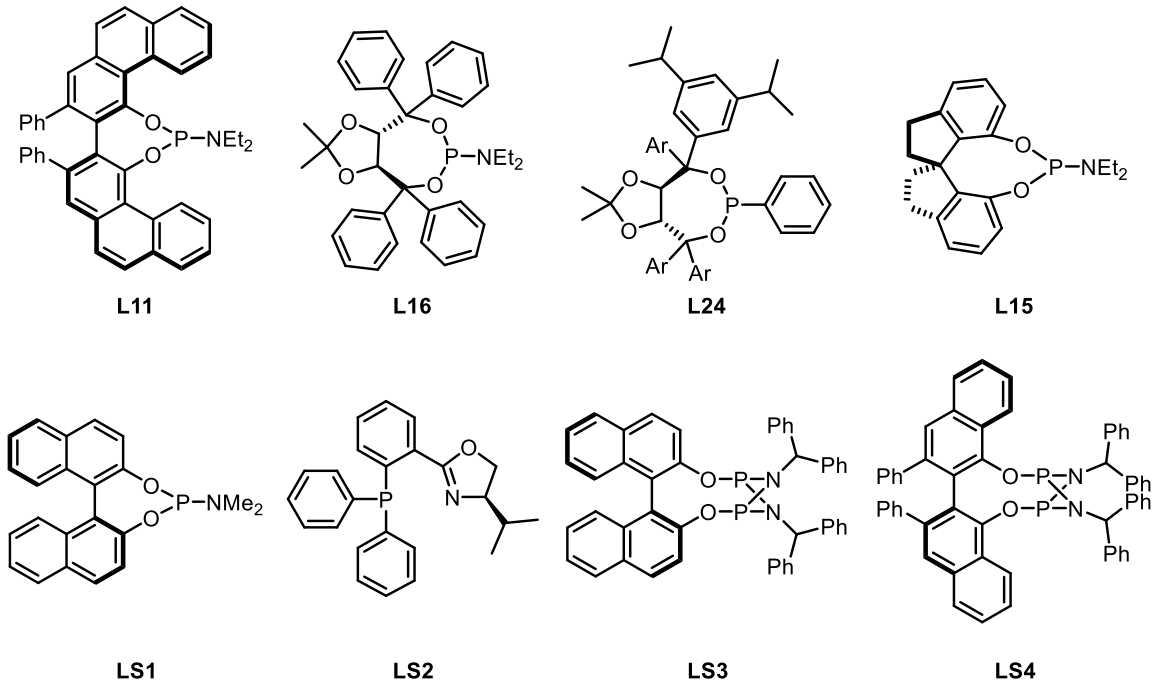

Figure S3: Chiral ligand candidates for the attempted optimization of the enantioselective reductive cyclization of **S51**.

Table S2: Selected optimization experiments for the enantioselective intramolecular reductive cyclization of **S51**.

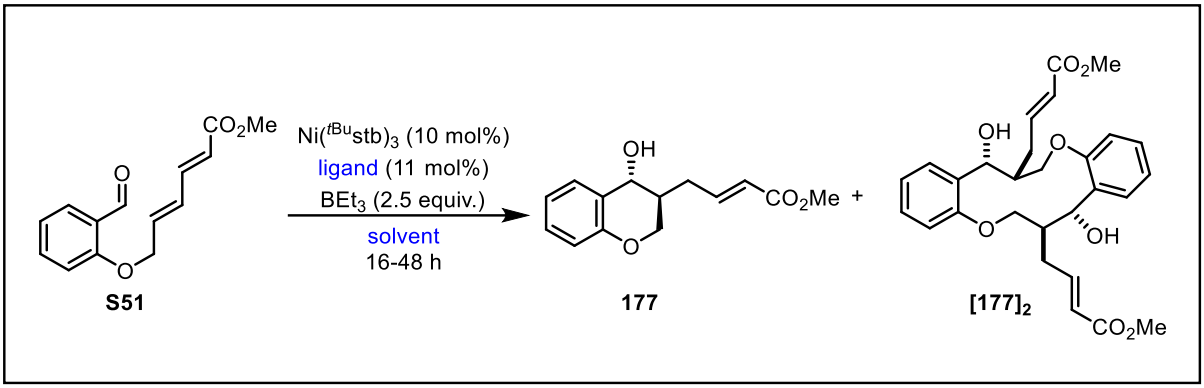

Entry	Solvent	Ligand	dr	ee	177/$[177]_2$	Conversion
1	THF	**L11**	8:1	40%	3:1	quant.
2	THF	**L16**	7:1	2%	19:1	quant.
3	THF	**L24**	8:1	2%	100:0	quant.
4	THF	**L15**	n.d.	n.d.	n.d.	<10%
5	THF	**LS1**	n.d.	n.d.	n.d.	0%
6	THF	**LS2**	n.d.	n.d.	n.d.	0%
7	THF	**LS3**	3:1	13%	6:1	quant.
8	THF	**LS4**	6:1	7%	11:1	quant.

5.4.6 Preparation and Analysis of Allyl-Oxanickelacycle Complexes

***Note**: Ni(cod)$_2$ was chosen instead of Ni(^{tBu}stb)$_3$ because the substituted stilbene ligands of the latter are the least soluble component and crystallize before any complex could be obtained. In the NMR studies, they obscure the aromatic/olefinic region of the spectra and hence render the interpretation even more challenging.*

Crystallization of Complex 187

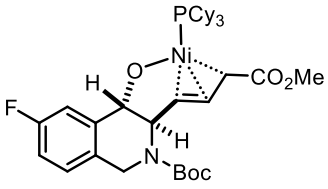

A solution of tricyclohexylphosphine (43.2 mg, 0.15 mmol) in THF (1.5 mL) was added to bis-(1,5-cyclooctadiene)-nickel(0) (38.5 mg, 0.14 mmol) and the resulting yellow-orange solution was stirred at room temperature for 3 min. Substrate **186** (50.9 mg, 0.14 mmol) was added, causing a color change to dark red. The mixture was stirred at room temperature for 1 h before all volatiles were removed *in vacuo* and the residue was suspended in pentane (2.0 mL). After stirring at room temperature for 5 min, the solvent was removed again *in vacuo;* this step was repeated twice. The obtained red solid was dissolved in diethylether (2.0 mL) and pentane (2.0 mL), the solution was filtered *via* cannula, and the filtrate was stored at −20 °C for 2 d, leading to the formation of red-brown crystals suitable for X-ray diffraction analysis.

Crystallization of Complex 190

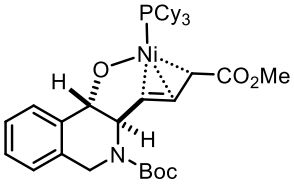

A solution of tricyclohexylphosphine (39.3 mg, 0.14 mmol) in THF (4.5 mL) was added to bis-(1,5-cyclooctadiene)-nickel(0) (35.0 mg, 0.13 mmol) and the resulting yellow-orange solution was stirred at room temperature for 3 min. Substrate **152** (44.0 mg, 0.13 mmol) was added, causing a color change to red-brown. The mixture was stirred at room temperature for 1 h before all volatiles were removed *in vacuo* and the residue was suspended in pentane (2 mL). After stirring at room temperature for 5 min, the solvent was removed *in vacuo*. The resulting red solid was dissolved in diethylether (0.5 mL) and pentane (4.0 mL), the solution was filtered *via* cannula, and the filtrate was stored at −20 °C for 5 weeks, leading to the formation of red-brown crystals suitable for X-ray diffraction analysis.

NMR Analysis of Complex 190

A solution of tricyclohexylphosphine (9.2 mg, 32.6 µmol) in [D_8]-THF (0.6 mL) was added to bis-(1,5-cyclooctadiene)nickel(0) (8.8 mg, 32.0 µmol) and the resulting yellow-orange mixture was stirred at room temperature for 3 min. Substrate **152** (11.1 mg, 32.0 µmol) was added, causing a color change to red-brown. The mixture was stirred at room temperature for 1 h before the solution was transferred into a J-Young NMR tube using a syringe filter. The spectra of the filtrate were recorded at 298 K. ^{1}H NMR (600 MHz, [D_8]-THF): δ = 7.33 (d, *J* = 7.4 Hz, 1H), 7.15 (ddd, *J* = 7.4, 6.3, 2.4 Hz, 1H), 7.08 – 7.02 (m, 2H), 6.43 (t, *J* = 12.9 Hz, 1H), 5.33 (d, *J* = 9.5 Hz, 1H), 4.85 (br, 1H), 4.72 (ddd, *J* = 12.9, 9.9, 3.2 Hz, 1H), 4.10 (s, 1H), 3.56 (s, 3H), 3.15 (t, *J* = 9.7 Hz, 1H), 2.06 – 1.99 (m, 9H), 1.88 (dd, *J* = 11.2, 2.3 Hz, 1H), 1.86 – 1.75 (m, 6H), 1.76 – 1.65 (m, 9H), 1.43 (s, 9H), 1.37 – 1.20 (m, 9H); ^{13}C NMR (151 MHz, [D_8]-THF): δ = 174.6 (d, *J* = 1.6 Hz), 155.9, 148.2, 132.6, 127.5, 126.1, 125.3, 122.6, 109.5, 103.8 (d, *J* = 11.4 Hz), 92.0 (d, *J* = 8.2 Hz), 79.9, 51.2, 45.7, 36.9, 30.8, 30.7, 28.7, 28.6 (d, *J* = 10.9 Hz), 28.6 (d, *J* = 10.5 Hz), 27.4 (d, *J* = 1.3 Hz); ^{31}P NMR (243 MHz, [D_8]-THF): δ = 28.3.

^{1}H NMR (600 MHz, [D_8]-THF, 298 K) of complex 190

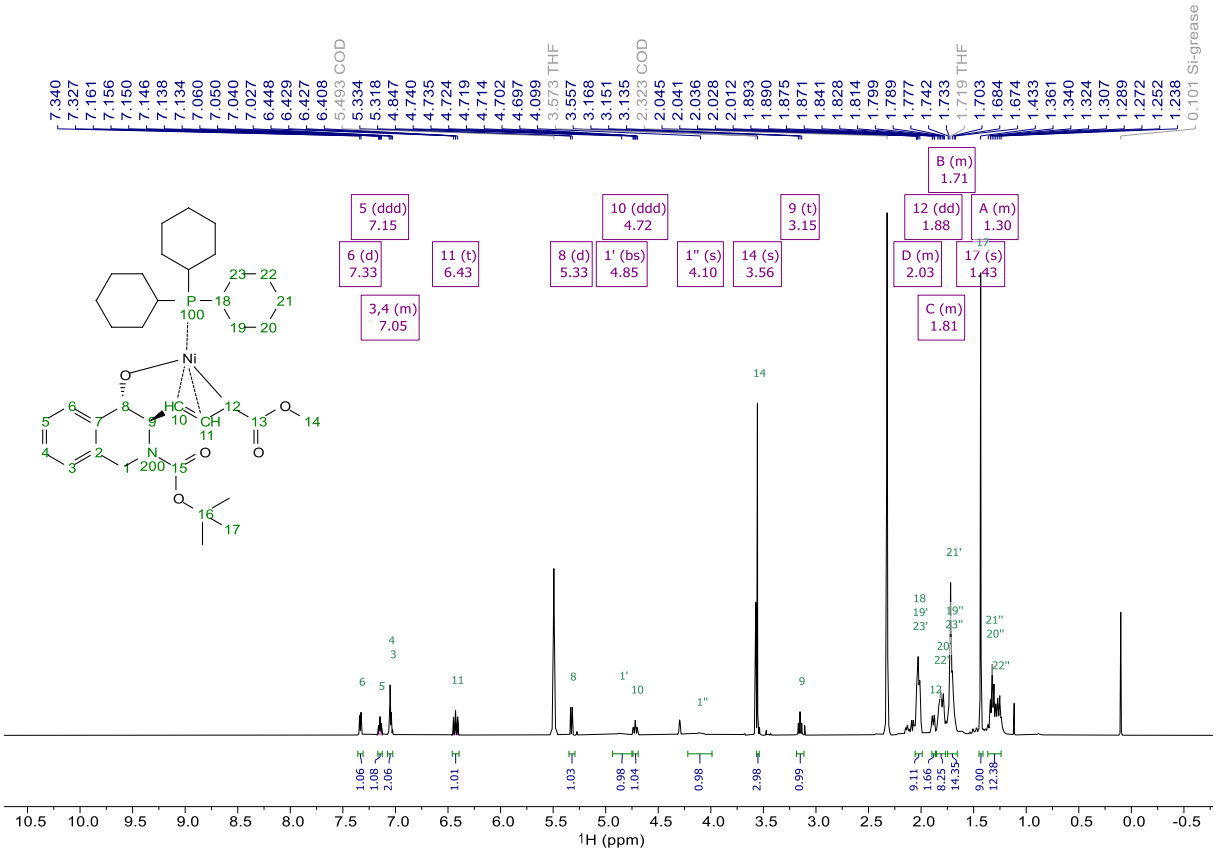

^{13}C NMR (151 MHz, [D$_8$]-THF, 298 K) of complex 190

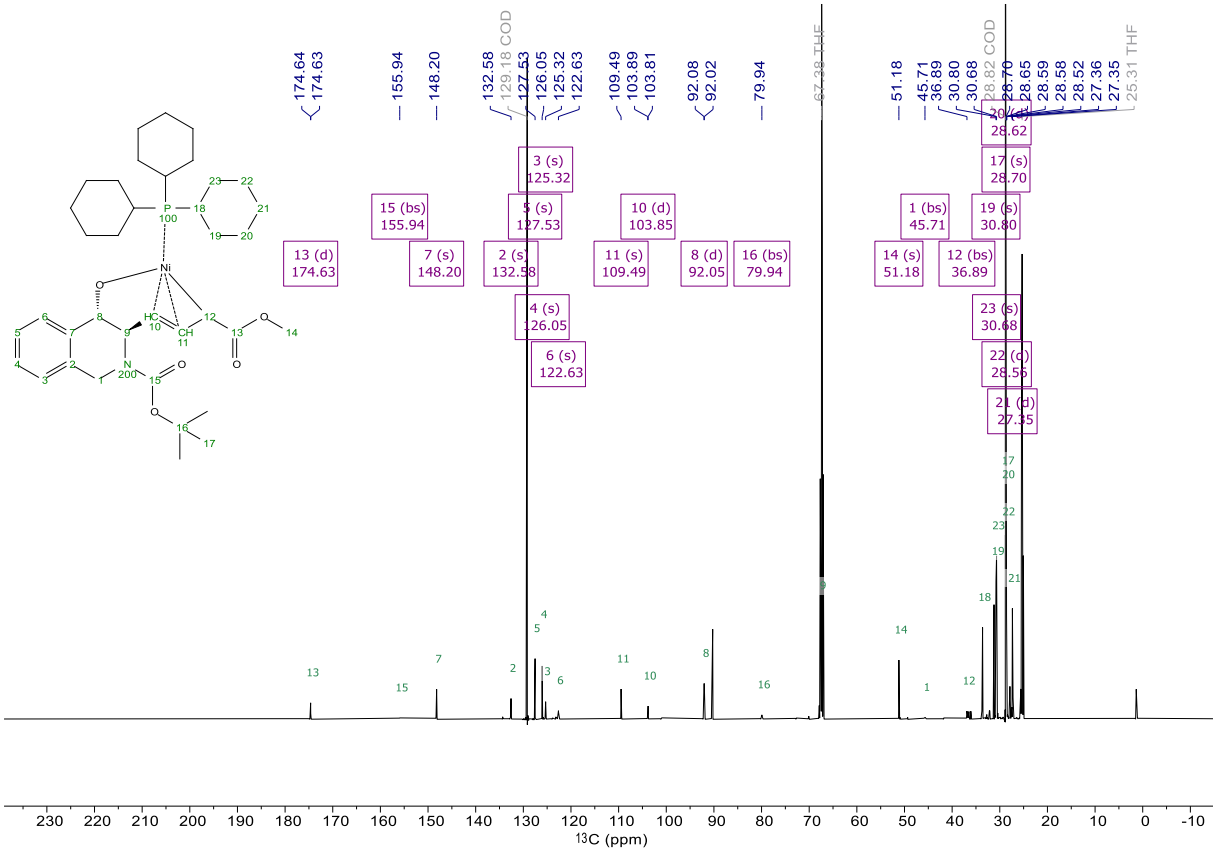

^{1}H-^{13}C HSQC NMR (600 MHz, 151 MHz, [D$_8$]-THF, 298 K) of complex 190

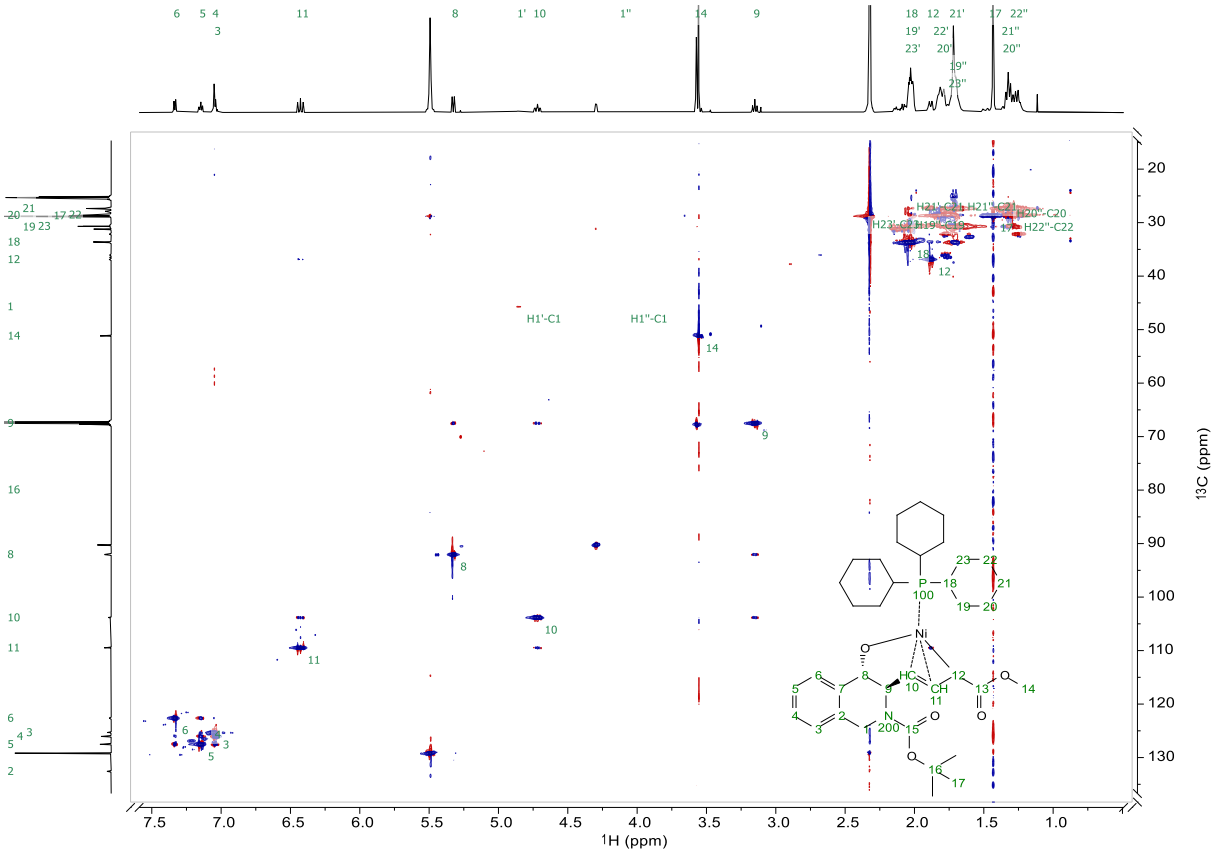

^{1}H-^{13}C HMBC NMR (600 MHz, 151 MHz, [D_8]-THF, 298 K) of complex 190

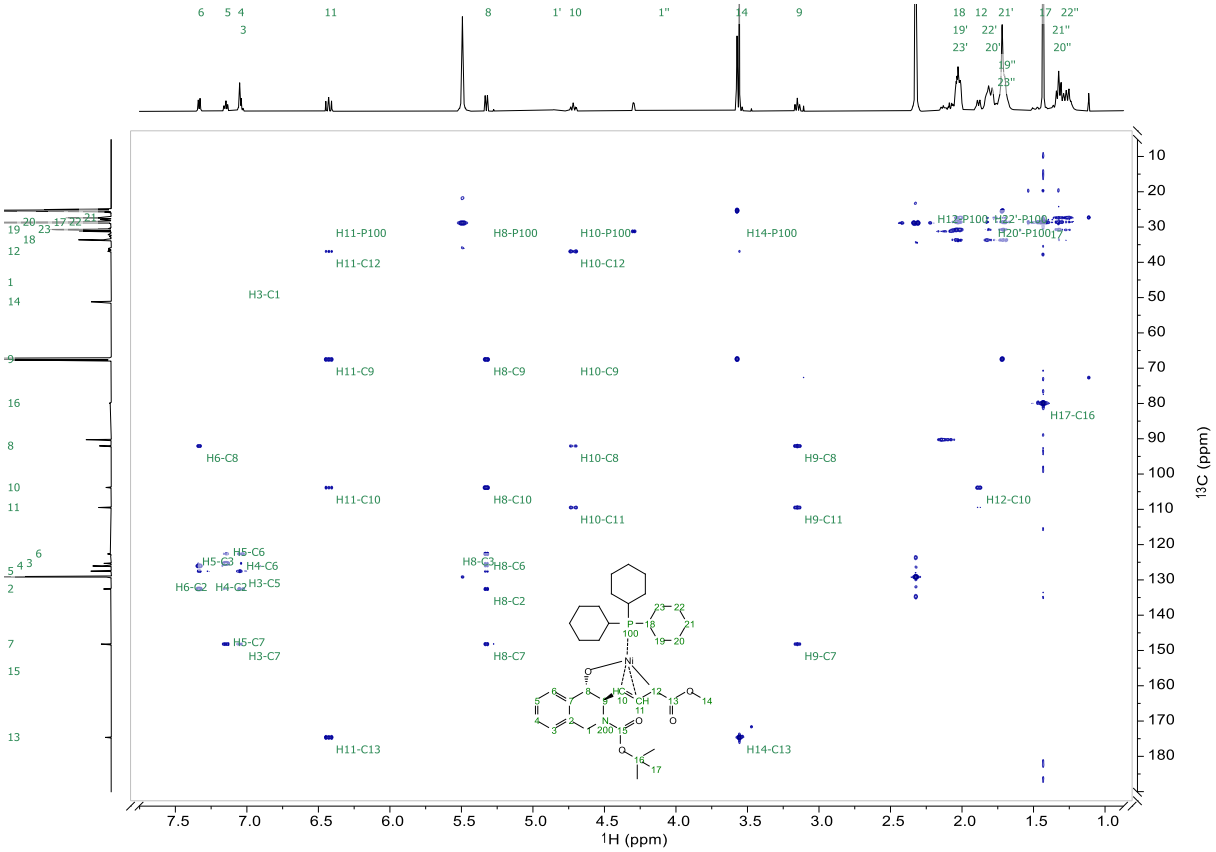

^{1}H-^{1}H COSY NMR (600 MHz, [D_8]-THF, 298 K) of complex 190

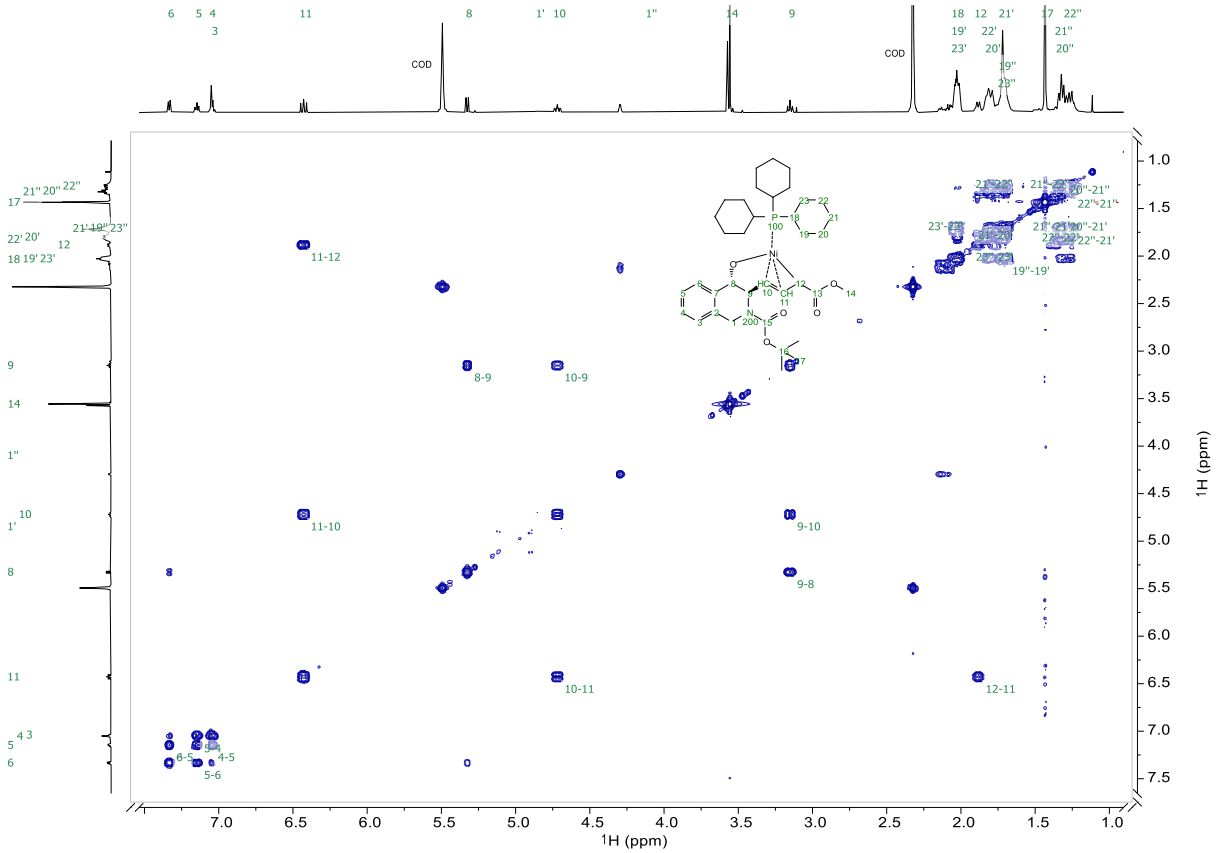

^{1}H-^{1}H NOESY NMR (600 MHz, [D$_8$]-THF, 298 K) of complex 190

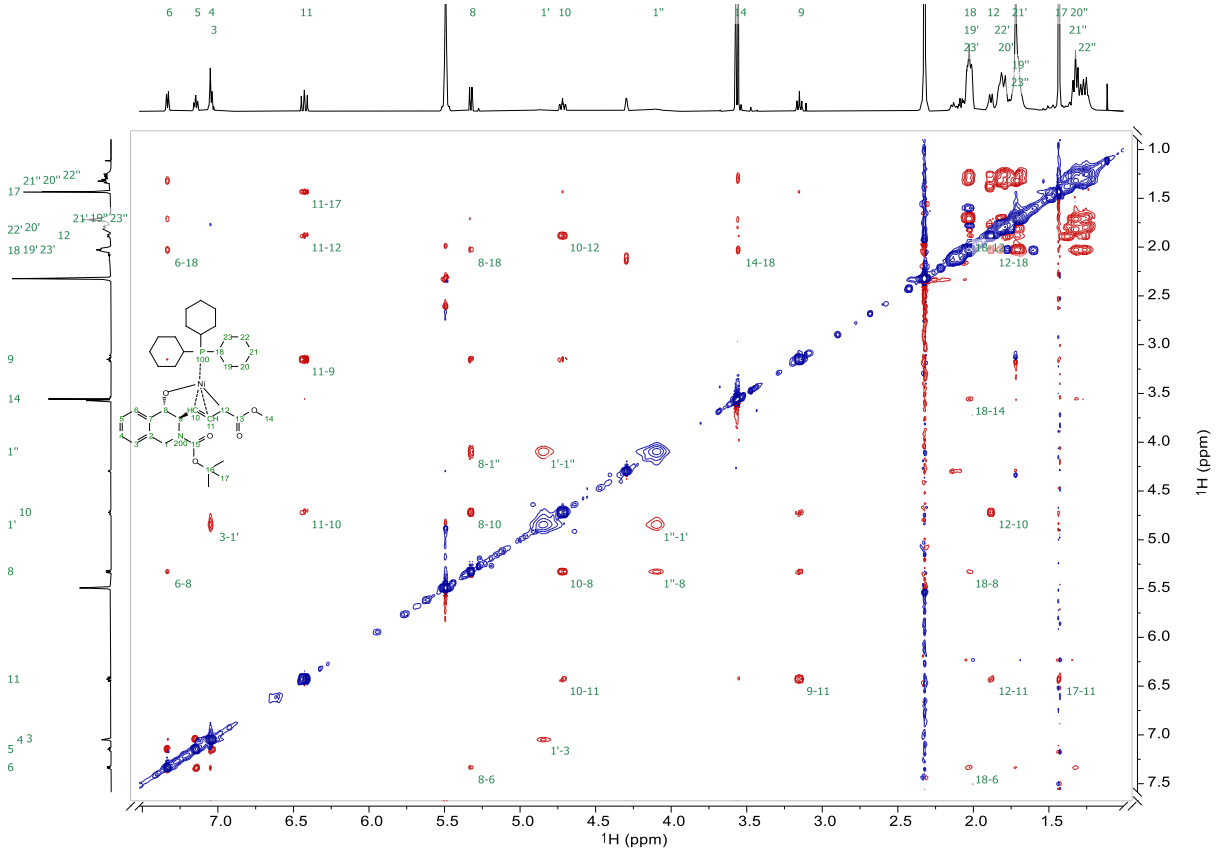

^{31}P NMR (243 MHz, [D$_8$]-THF, 298 K) and ^{1}H-^{31}P HMBC (600 MHz, 243 MHz, [D$_8$]-THF, 298 K) of complex 190

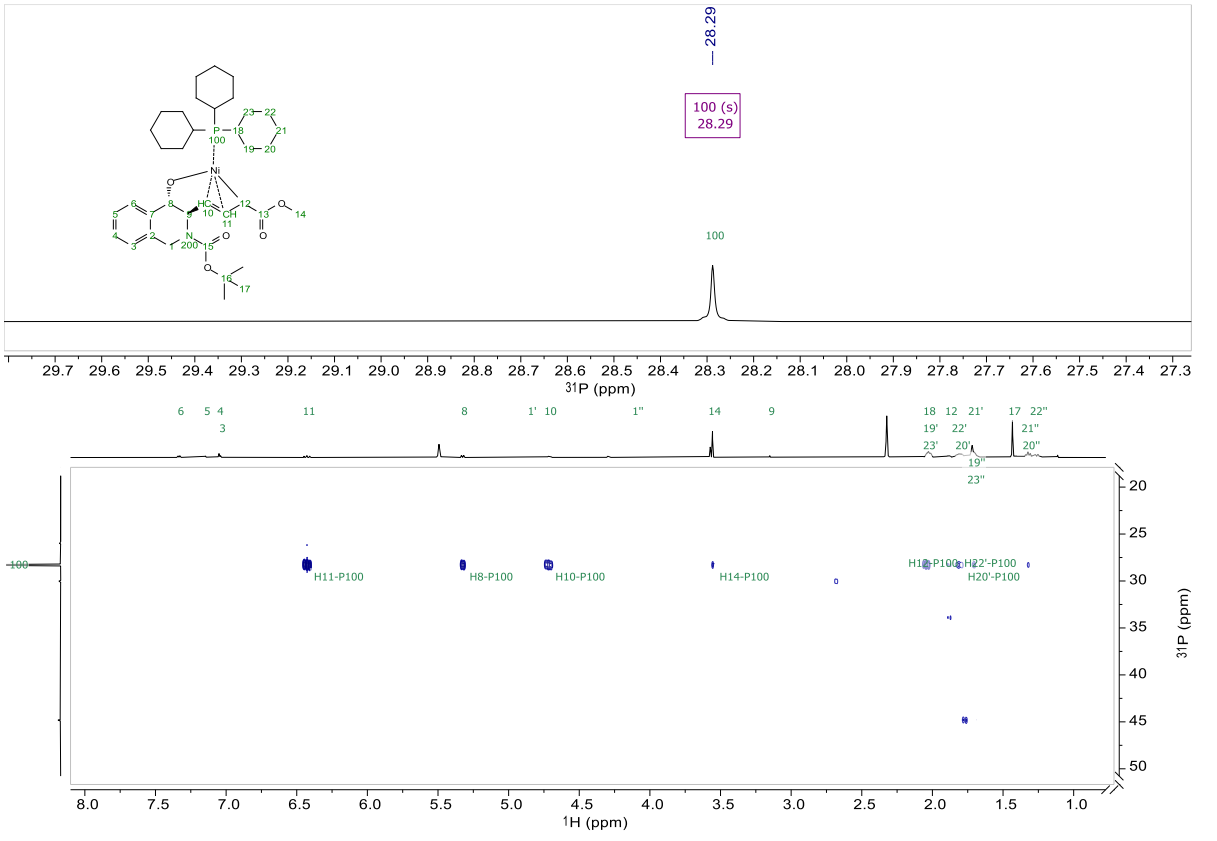

^{1}H-^{15}N HMBC (600 MHz, 62 MHz, [D$_8$]-THF, 298 K) of complex 190

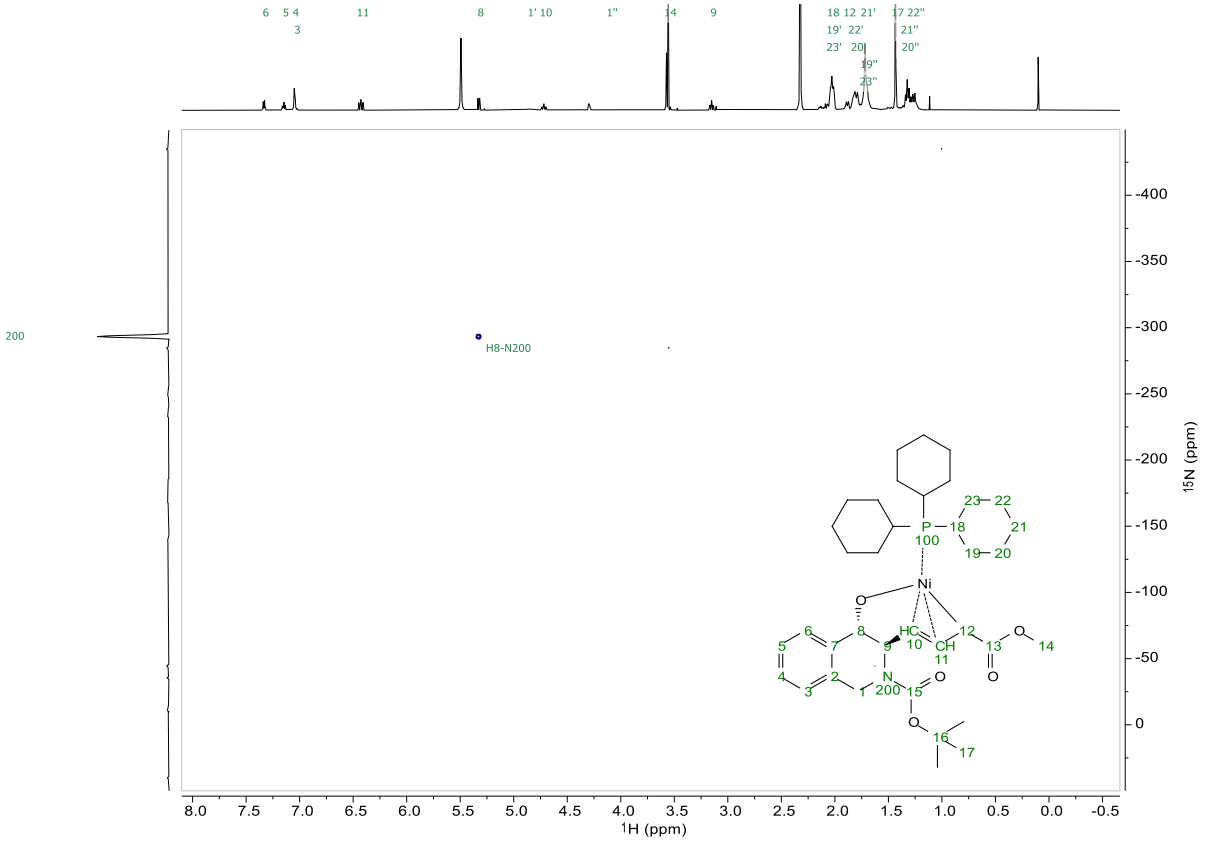

NMR analysis of Complexes 192 and 193

A solution of (*S*)-AntPhos **L29** (24.0 mg, 65.0 µmol) in [D_8]-THF (0.8 mL) was added to bis-(1,5-cyclooctadiene)nickel(0) (17.0 mg, 61.8 µmol) and the resulting yellow-orange mixture was stirred at room temperature for 3 min. The solution was cooled to –40 °C (bath temperature) before substrate **152** (21.3 mg, 61.8 µmol) was added, causing a color change to red-brown. The mixture was stirred for 20 min at –40 °C and then transferred into a J-Young NMR tube using a syringe filter and NMR spectra were recorded at 233 K. Pertinent spectra and their analysis are shown below.

The sample also contained free ligand **L29**, residual starting material **152**, and a complex of type [(**L29**)$_2$Ni(0)] in addition to two reactive intermediates **192** and **193**. The concentration of the metallacycle intermediates (Int = combined concentration) increased with time, whereas the amount of [(**L29**)$_2$Ni(0)] as well as of the starting material **152** decreased (Figure S4, also see Figure 14 in the main text).

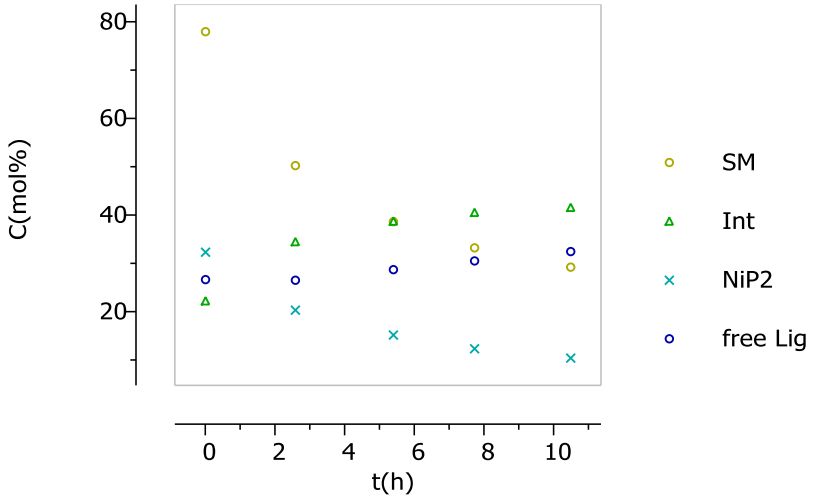

Figure S4: Time-dependent concentration profiles of different species observed in the NMR experiment (SM = substrate **152**, Int = allyl-oxanickelacycle (**192**+**193**), NiP_2 = Ni(**L29**)$_2$, free Lig = **L29**).

The most relevant signals of the isomeric reactive intermediates could be assigned based on the 1D and 2D NMR data. In regions of complex overlaps, signals were assigned based on 1D selective TOCSYs or the 2D NMR correlation experiments.

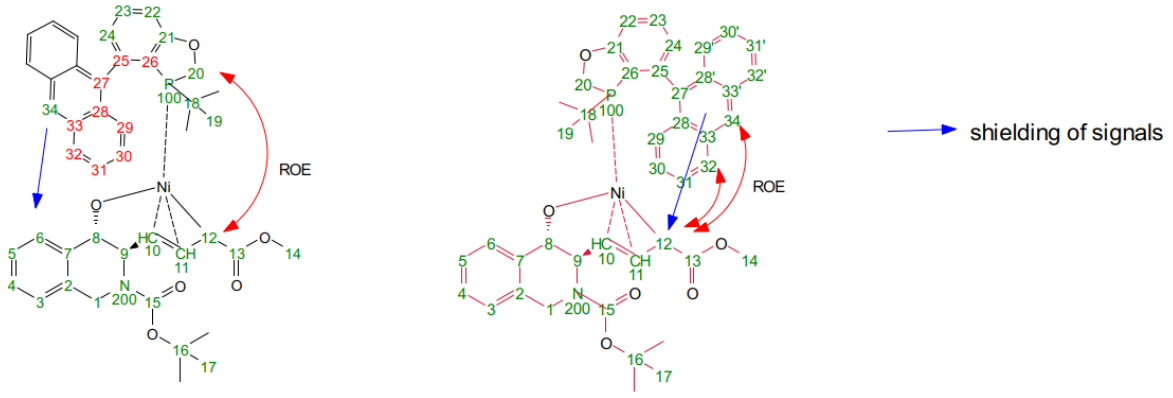

Figure S5: ROE and shielding effects observed for the two atropisomers.

Arbitrary numbering scheme of the minor isomer **193** (left) and the major isomer **192** (right); relevant ROEs and shielding effects.

The ^{13}C NMR chemical shifts of C8-C12 of both diastereomers were very similar to those observed for complex **190** carrying a PCy_3 ligand (see above). It was therefore concluded that the coordination of the allyl subunit is basically identical. Additionally, the coupling between H8 and H9 is large in both cases (~9.8 Hz), supporting the *trans*-configuration. Two large ^3J couplings between H11 on the one hand and H10 as well as H12a (~12±1 Hz) are also in good agreement with what had been observed for **190**.

However, certain signals, most notably H12, differ significantly from each other in the two diastereomers **192** and **193**. H12 is shifted from 1.90 ppm in the minor isomer to −0.44 ppm in the major isomer. Based on an ROE from H12 to H34 and H32 this effect is attributed to a different spatial positioning of the ligand's anthracene unit. The anisotropy caused by the aromatic ring current results in a drastic shielding of this nucleus in the major isomer **192**, which must be positioned exactly above the ring. A similar, but less drastic, effect is observed for H6 of the minor isomer **193** (6.25 ppm vs 7.26 ppm).

Additionally, H10 and H12 show significantly different ^3J couplings to P-100 in the two isomers. In the major diastereomer, H10 has a large ^{31}P coupling constant of 5.4 Hz; in the minor diastereomer, it is H12 in which shows a ^{31}P coupling constant of 3.6 Hz.

Major Atropisomer (192): Signal Assignments

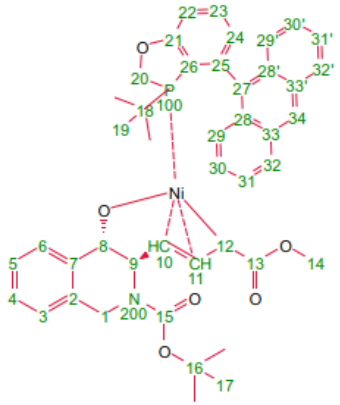

Atom	δ (ppm)	J	COSY	HSQC	HMBC	ROESY
1 C	45.194			1', 1''	3	
H'	4.907	14.50(1'')	1''	1	2, 3, 7, 9, 15	1''
H''	4.153	14.50(1')	1'	1	2, 3, 7, 15	1', 8
2 C	132.549				1', 1'', 4, 6, 8	
3 C	125.573			3	1', 1'', 5	
H	7.127		4	3	1, 5, 7	
4 C	126.381			4	6	
H	7.095		3, 5	4	2, 6	
5 C	127.571			5	3	
H	7.215		4, 6	5	3, 7	
6 C	122.477			6	4, 8	
H	7.257		5	6	2, 4, 8	
7 C	147.314				1', 1'', 3, 5, 8, 9	
8 C	90.780	10.60(100)		8	6, 9, 10	
H	5.436	9.80(9)	9	8	2, 6, 7, 9, 10	1'', 10, 30
9 C	66.645	2.40(100)		9	1', 8, 10, 11	
H	2.988	9.80(8), 10.10(10)	8, 10	9	7, 8, 11, 200	11
10 C	101.012	13.10(100)		10	8, 11, 12	
H	3.544	5.40(100P), 10.10(9), 1.60(12), 12.20(11)	9, 11	10	8, 9, 11, 12, 200	8, 11, 12, 30, 31
11 C	111.576			11	9, 10	
H	6.256	12.20(10), 11.90(12)	10, 12	11	9, 10, 13, 200	9, 10, 17
12 C	40.573	4.20(100)		12	10	
H	-0.442	0.90(100P), 1.60(10), 11.90(11)	11	12	10	10, 32, 34
13 C	174.137	1.40(100)			11, 14	

Atom	δ (ppm)	J	COSY	HSQC	HMBC	ROESY
14 C	50.481			14		
H3	2.794			14	13	
15 C	155.781				1', 1''	
16 C	80.089				17	
17 C	28.489			17	17	
H3	1.345			17	16, 17	11
18 C	33.113	15.00(100)			19, 20', 20''	
19 C	25.585			19	19	
H3	0.537			19	18, 19, 200	20'', 29'
20 C	65.654	13.20(100)		20', 20''		
H'	5.644	3.40(100P), 12.50(20'')	20''	20	18, 200	
H''	4.802	1.30(100P), 12.50(20')	20'	20	18, 21, 200	19
21 C	165.850	5.00(100)			20'', 22, 23	
22 C	112.461			22		
H	7.216		23	22	21, 24, 26, 200	
23 C	134.099			23		
H	7.693		22, 24	23	21, 25, 200	
24 C	126.493	6.10(100)			22	
H	7.110		23		27, 200	
25 C					23	
26 C	119.363	29.70(100)			22	
27 C	135.733	1.90(100)			24, 29, 29'	
28 C	130.903				30, 32	
28' C	131.367				30', 32'	

Atom	δ (ppm)	J	COSY	HSQC	HMBC	ROESY
29 C	127.970			29	31	
H	8.359		30	29	27, 31, 33, 200	
29' C	129.296			29'	31'	
H	7.912		30'	29'	27, 31', 33'	19
30 C	127.613			30		
H	7.859		29, 31	30	28, 32	8, 10
30' C	126.578			30'		
H	7.434		29', 31'	30'	28', 32'	
31 C	126.136			31	29	
H	7.669		30, 32	31	29, 33	10
31' C	125.965			31'	29'	
H	7.490		30', 32'	31'	29', 33'	
32 C	130.146			32	30	
H	8.170		31	32	28, 33	12, 34
32' C	129.663			32'	30'	
H	8.155		31'	32'	28', 33'	34
33 C	132.267				29, 31, 32	
33' C	132.904				29', 31', 32'	
34 C	129.278			34		
H	8.691			34		12, 32, 32'
100 P	27.686	1.40(13), 5.00(21), 1.90(27), 4.20(12), 15.00(18), 13.20(20), 2.40(9), 10.60(8), 29.70(26), 6.10(24), 13.10(10), 0.90(12H), 3.40(20'), 1.30(20''), 5.40(10H)				
200 N	-293.594				9, 10, 11, 19, 20', 20'', 22, 23, 24, 29	

Minor Atropisomer (193): Signal Assignments

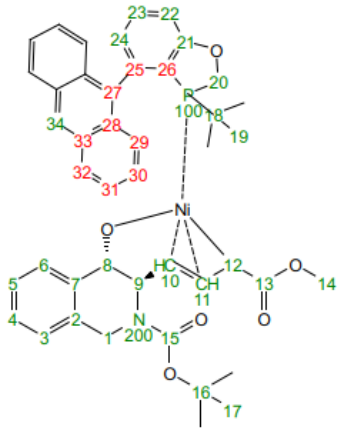

Atom	δ (ppm)	J	COSY	HSQC	HMBC	ROESY
1 C	45.150			1', 1"	3	
H'	4.764	14.80(1")	1"	1	2, 3, 7, 9, 15	1"
H"	3.841	14.80(1')	1'	1	2, 3, 7, 9, 15	1', 8
2 C	131.908				1', 1", 4, 6, 8	
3 C	124.938			3	1', 1", 5	
H	7.011		4	3	1, 5, 7	
4 C	125.952			4	6	
H	7.091		3, 5	4	2, 6	
5 C	127.078			5	3	
H	7.264		4, 6	5	3, 7	
6 C	123.440			6	4, 8	
H	6.253		5	6	2, 4, 8	8
7 C	147.176				1', 1", 3, 5, 8, 9	
8 C	90.844	8.50(100)		8	6, 9, 10	
H	4.754	9.80(9)	9	8	2, 6, 7, 9, 10, 100, 200	1", 6, 10
9 C	65.664	1.30(100)		9	1', 1", 8, 10, 11	
H	2.441	9.80(8), 9.90(10)	8, 10	9	7, 8, 11	11
10 C	103.342	10.70(100)		10	8, 11, 12	
H	4.764	12.90(11), 1.00(12), 9.90(9)	9, 11	10	8, 9, 12	8, 11, 12
11 C	112.878			11	9	
H	6.461	1.60(100P), 12.90(10), 11.20(12)	10, 12	11	9, 10, 13, 100	9, 10, 17
12 C	39.173	4.30(100)		12	10	
H	1.900	3.60(100P), 1.00(10), 11.20(11)	11	12	10, 100	10, 20"
13 C	173.754	1.40(100)			11, 14	
14 C	51.772			14		
H3	3.417			14	13	
15 C	155.839				1', 1"	
16 C	80.013				17	
17 C	28.697			17	17	
H3	1.492			17	16, 17	11

Atom	δ (ppm)	J	COSY	HSQC	HMBC	ROESY
18 C	35.410	12.90(100)			20', 20"	
19 C	25.616			19		
H3	0.687			19		20'
20 C	69.974	16.20(100)		20', 20"		
H'	5.237			20	18, 21, 100	19
H"	5.086			20	18, 100	12
21 C	165.685				20'	
22 C						
H	7.132		23		100	
23 C						
H	7.643		22, 24		100	
24 C						
H	7.074		23		100	
25 C						
26 C						
27 C						
28 C						
29 C						
H						
30 C						
H						
31 C						
H						
32 C						
H						
33 C						
34 C						
H	8.532					
100 P	17.927	1.60(11H), 1.40(13), 4.30(12), 10.70(10), 8.50(8), 16.20(20), 1.30(9), 3.60(12H), 12.90(18)			8, 11, 12, 20', 20", 22, 23, 24	
200 N	-293.594				8	

Analysis of the reaction mixture by ^{1}H NMR (600 MHz, [D_8]-THF, 233 K)

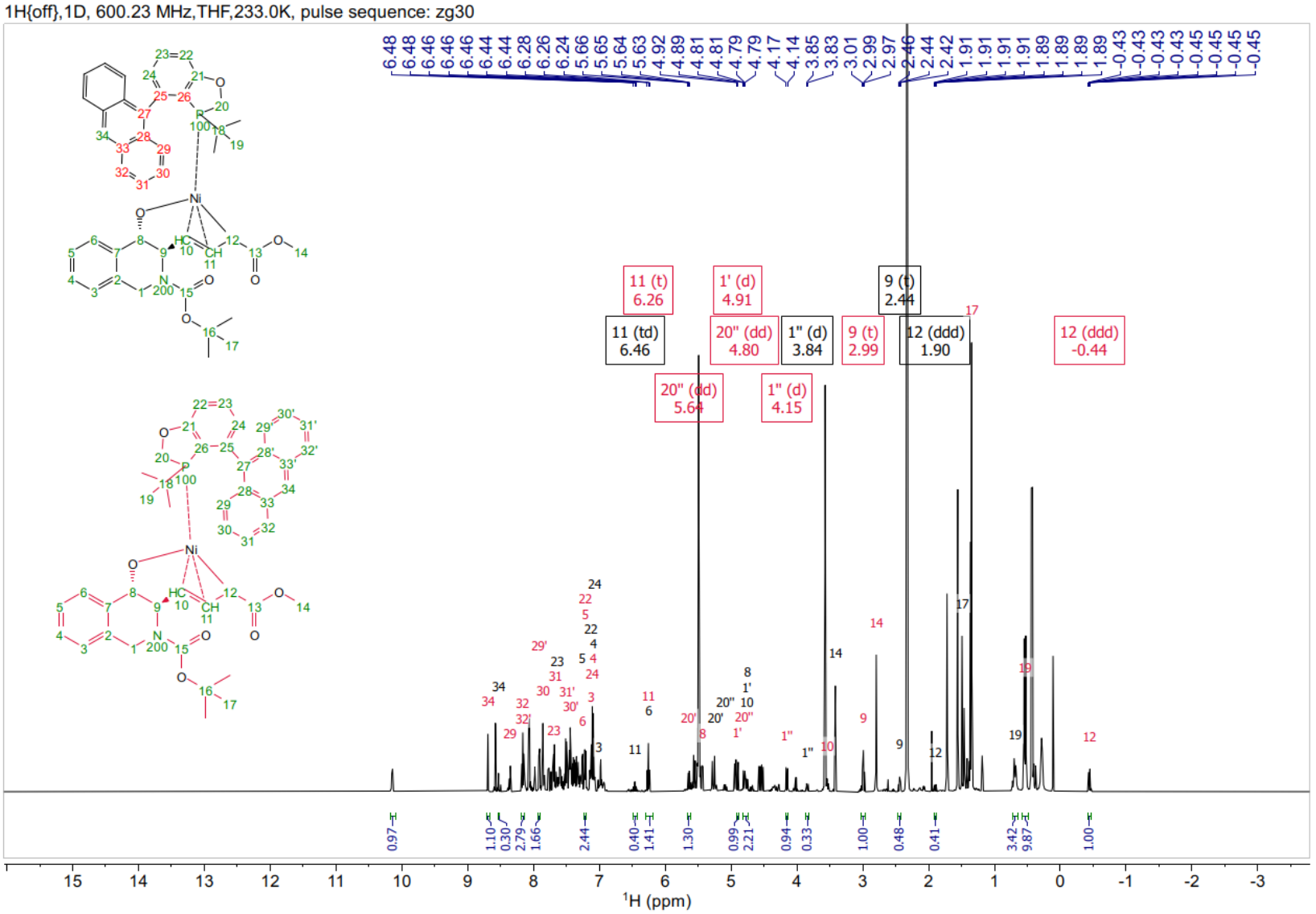

Analysis of the reaction mixture by ^{13}C NMR (151 MHz, [D_8]-THF, 233 K)

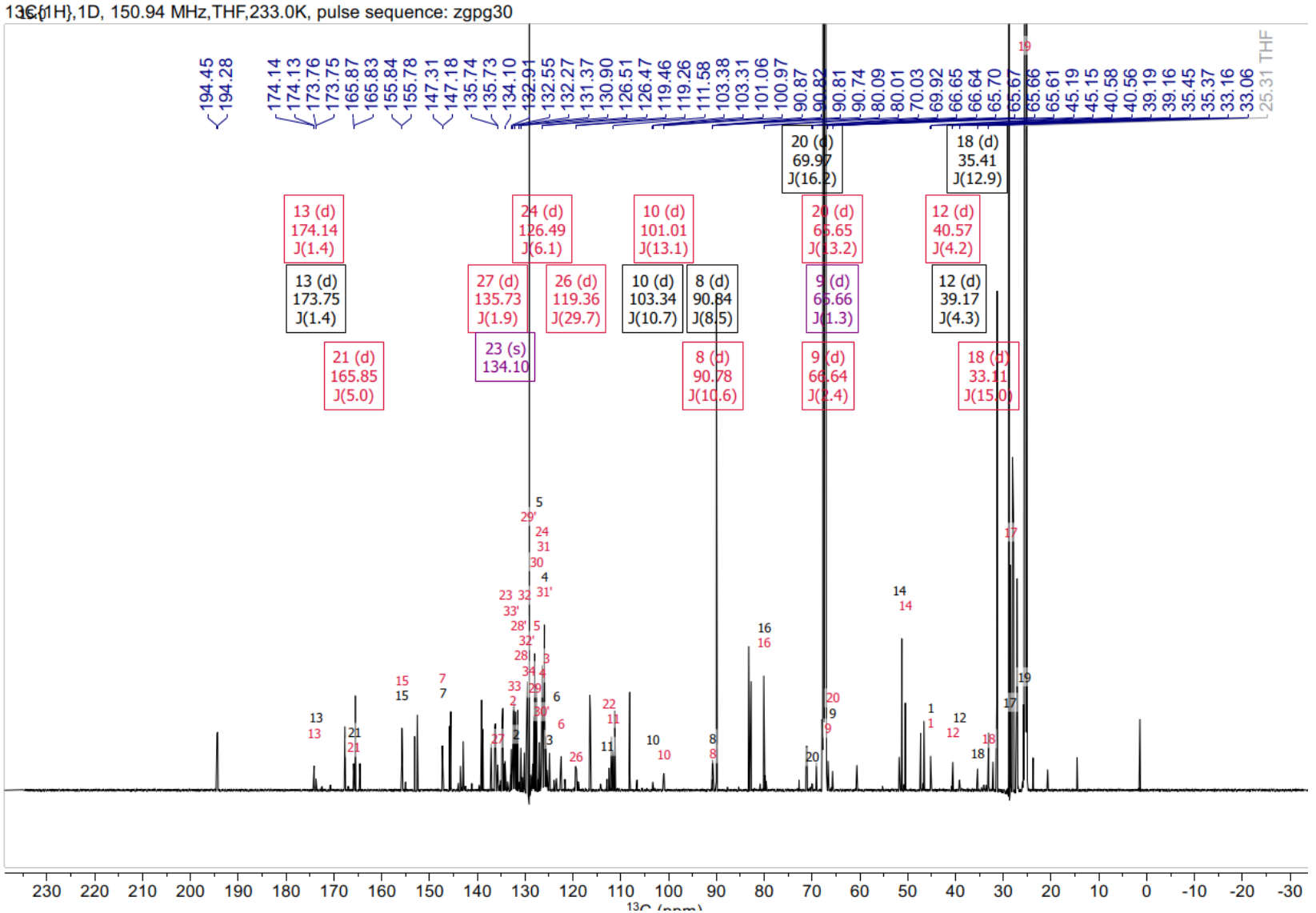

Analysis of the reaction mixture by ^{1}H-^{13}C HSQC NMR (600 MHz, 151 MHz, [D_8]-THF, 233 K)

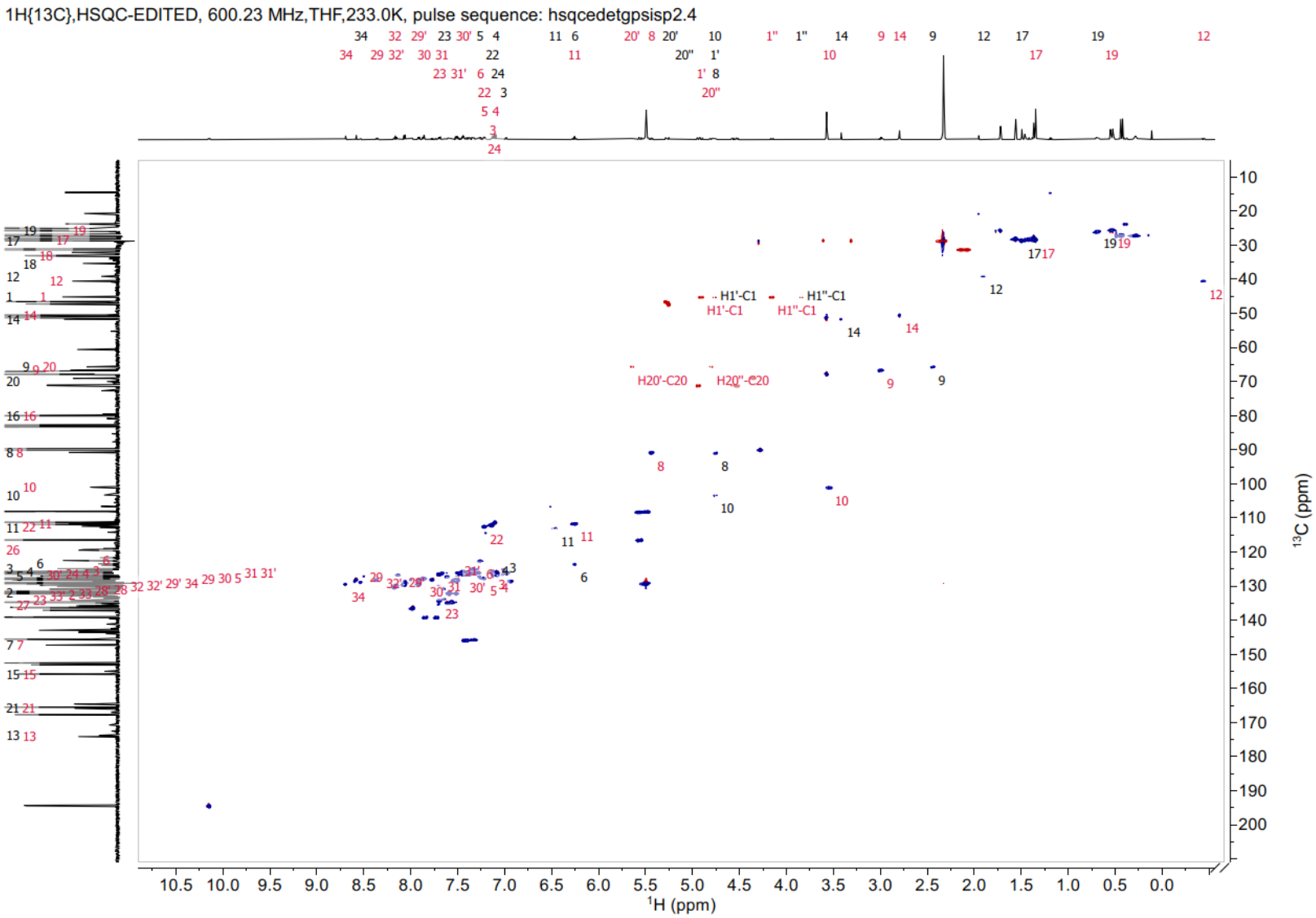

Analysis of the reaction mixture by ^{1}H-^{13}C HMBC NMR (600 MHz, 151 MHz, [D_8]-THF, 233 K)

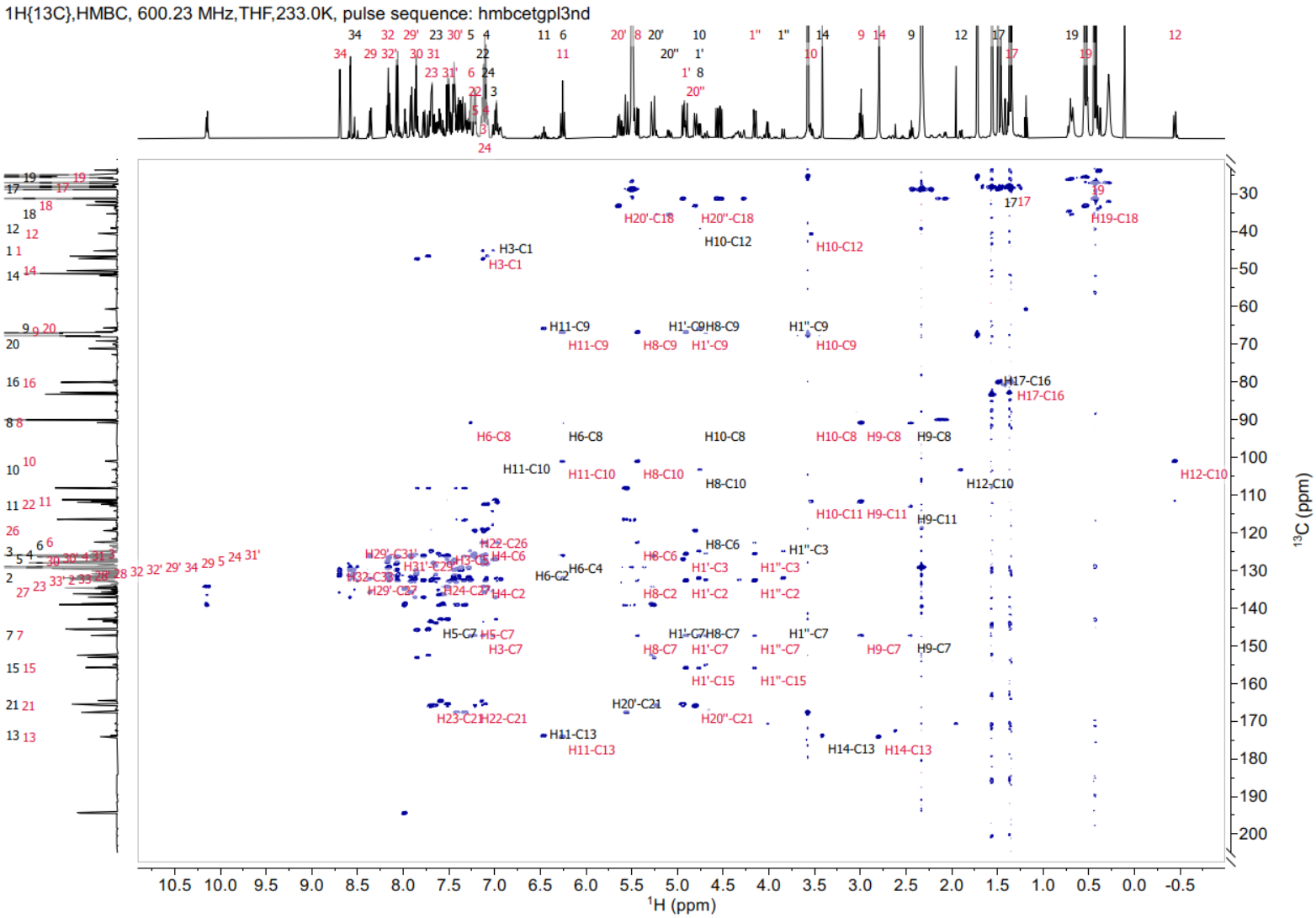

Analysis of the reaction mixture by ^{31}P (243 MHz, [D_8]-THF, 233 K) and ^{1}H-^{31}P HMBC NMR (600 MHz, 243 MHz, [D_8]-THF, 233 K)

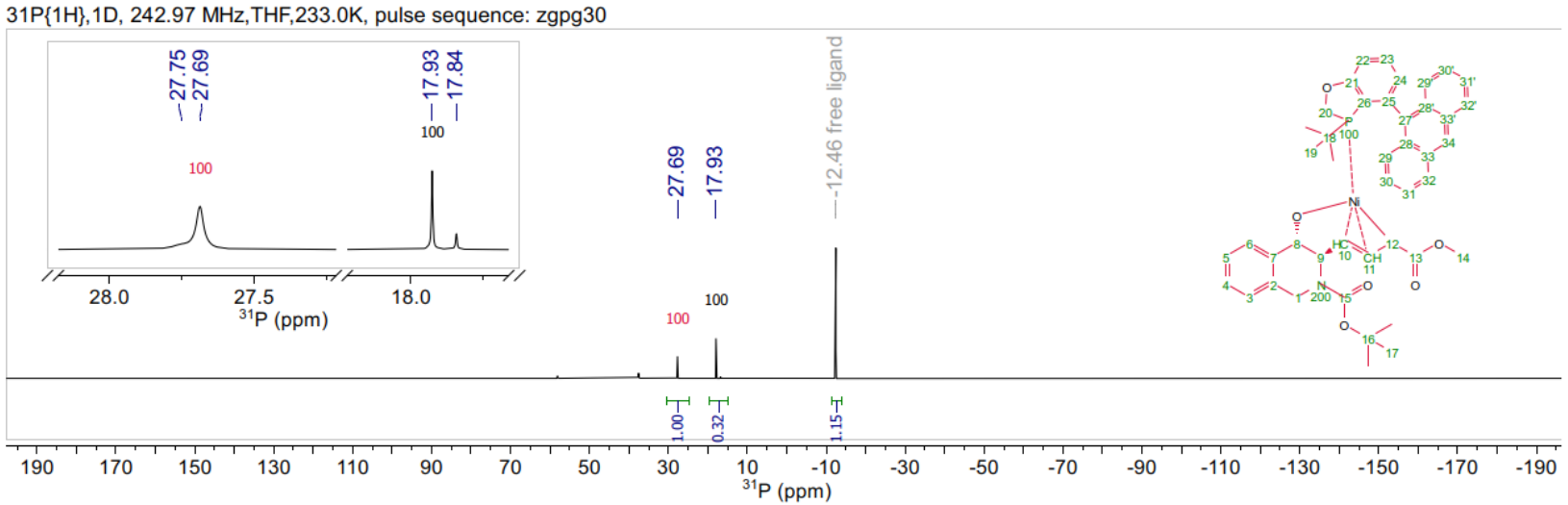

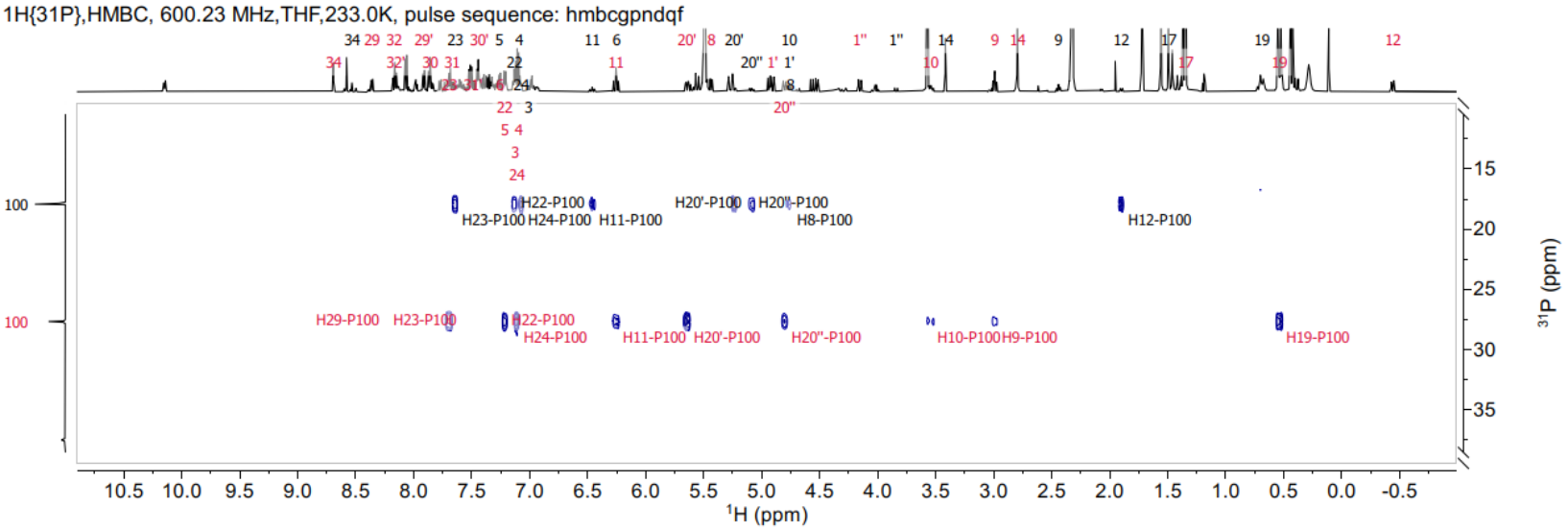

Analysis of the reaction mixture by ^{1}H-^{1}H COSY NMR (600 MHz, [D_8]-THF, 233 K)

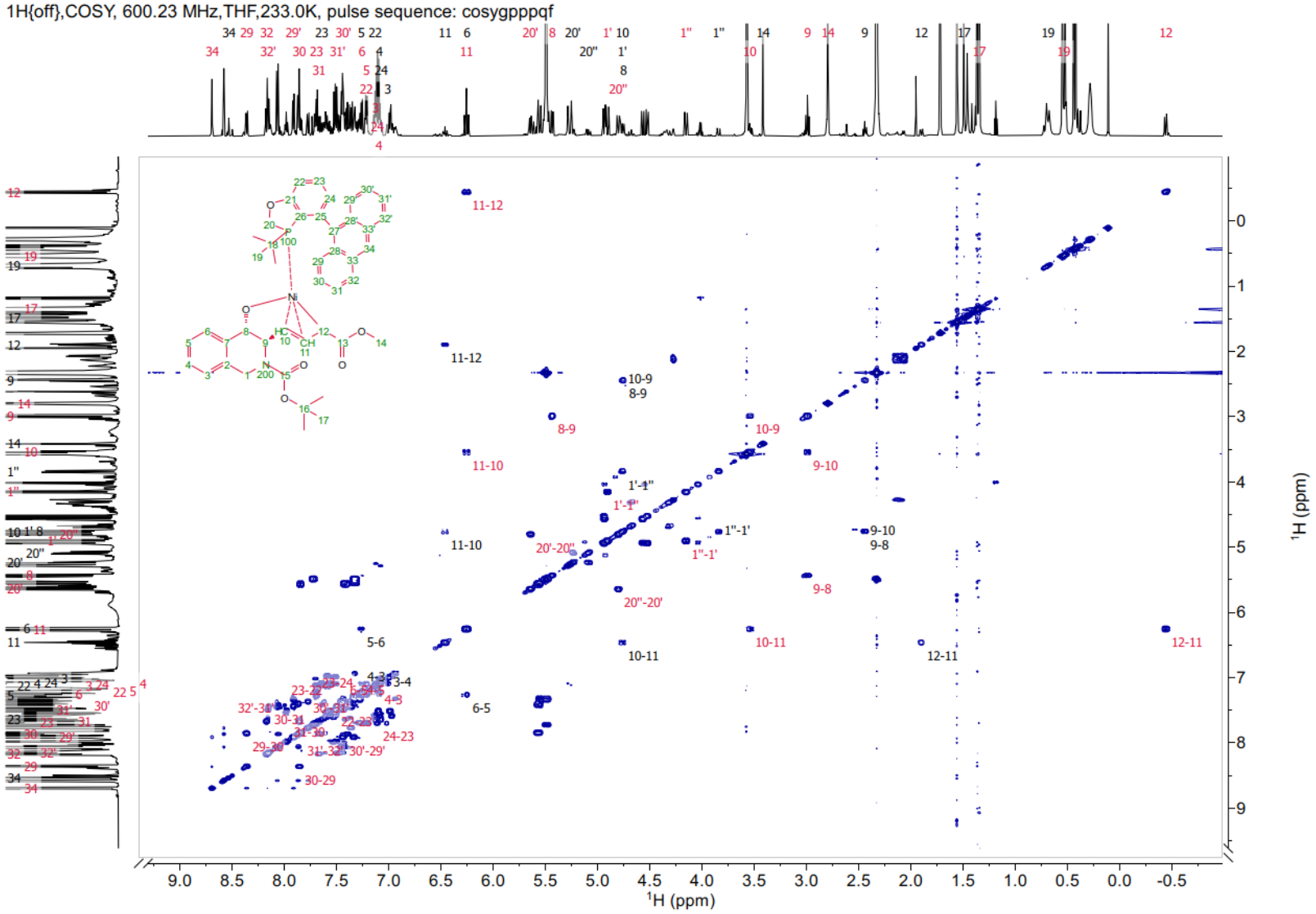

Analysis of the reaction mixture by ^{1}H-^{1}H ROESY NMR (600 MHz, [D$_8$]-THF, 233 K)

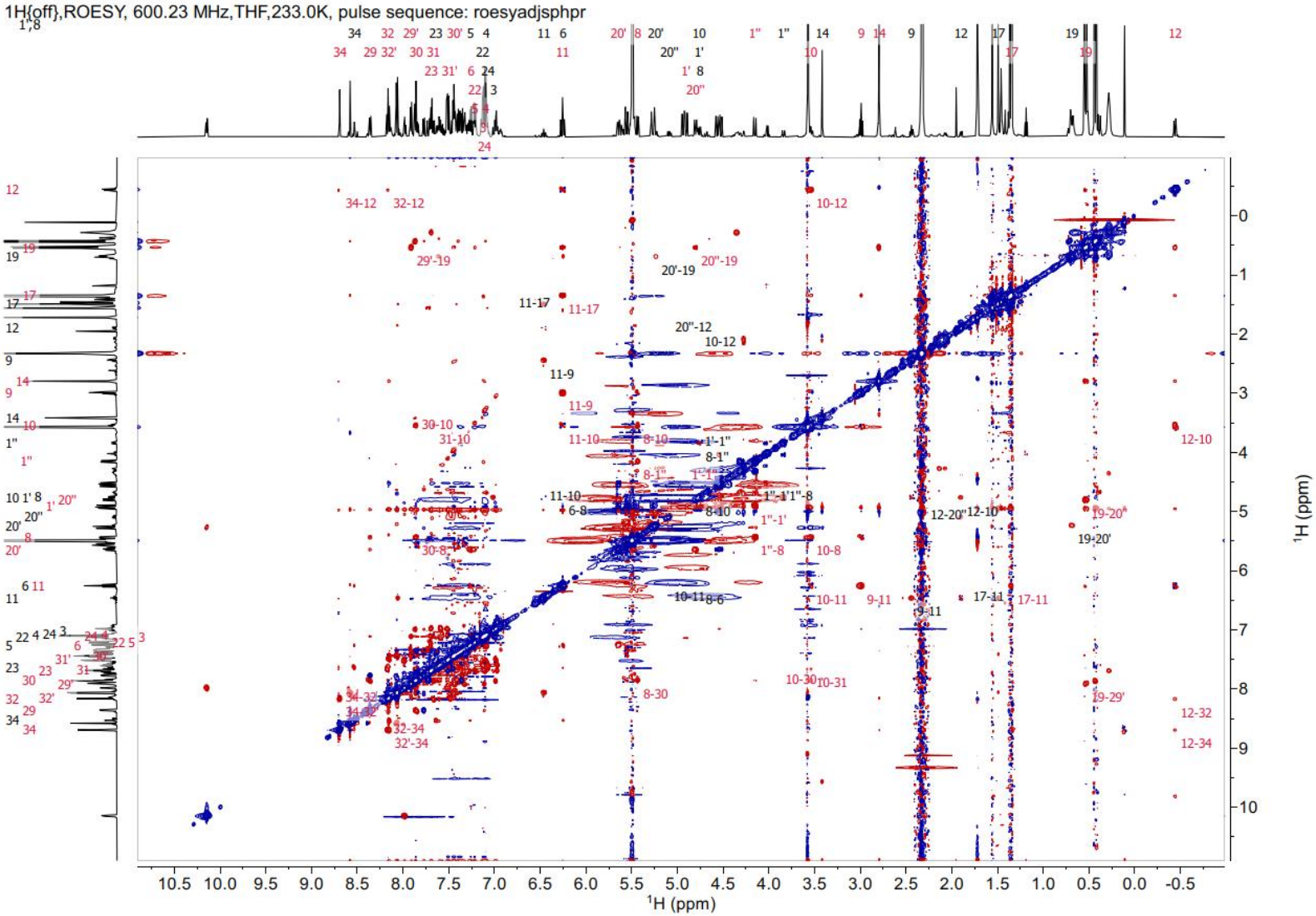

Analysis of the reaction mixture by ^{13}C DEPT-135 NMR (151 MHz, [D_8]-THF, 233 K)

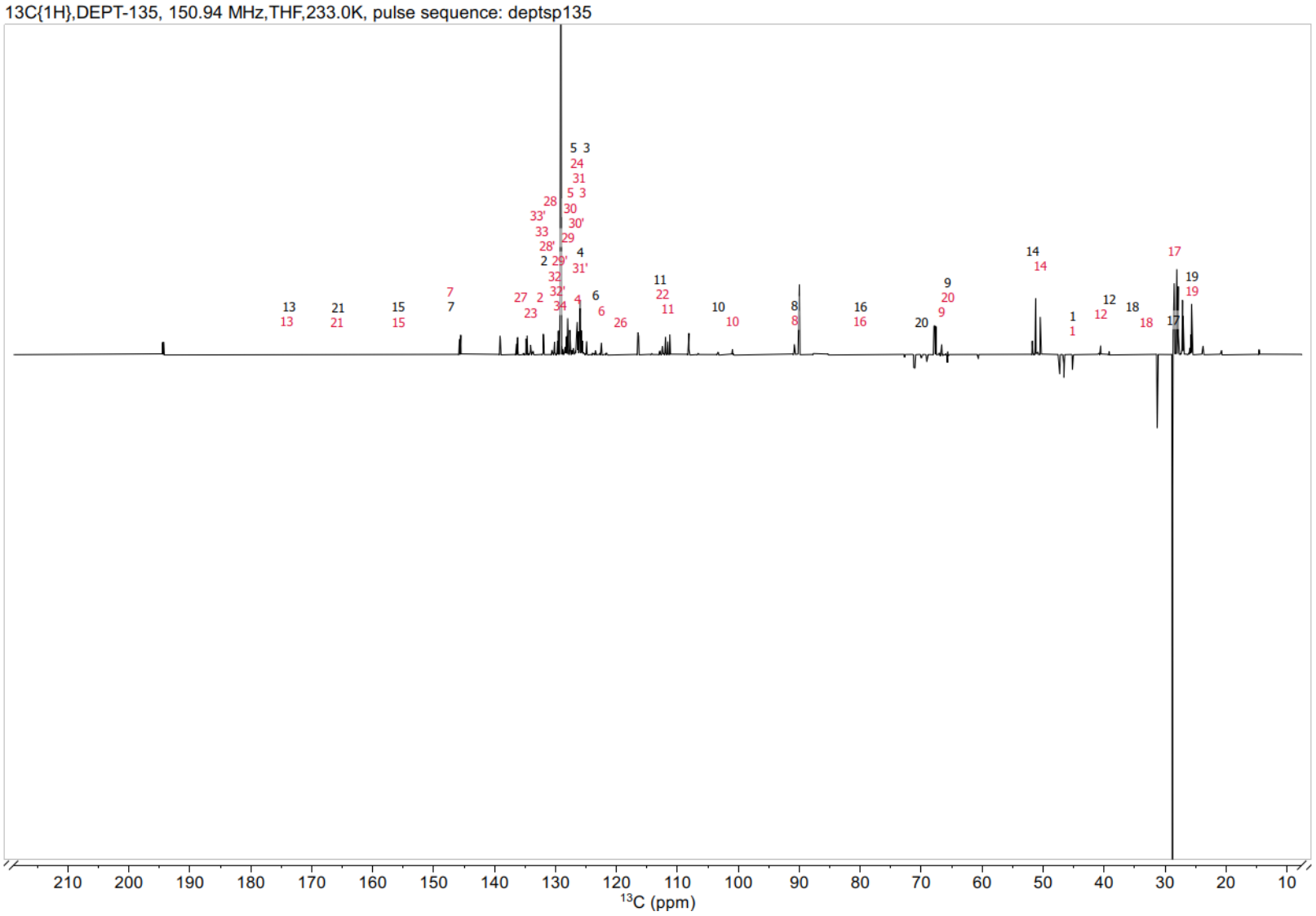

Analysis of the reaction mixture by comparison of coupled and ^{31}P-decoupled ^{1}H NMR spectra (600 MHz, [D_8]-THF, 233 K)

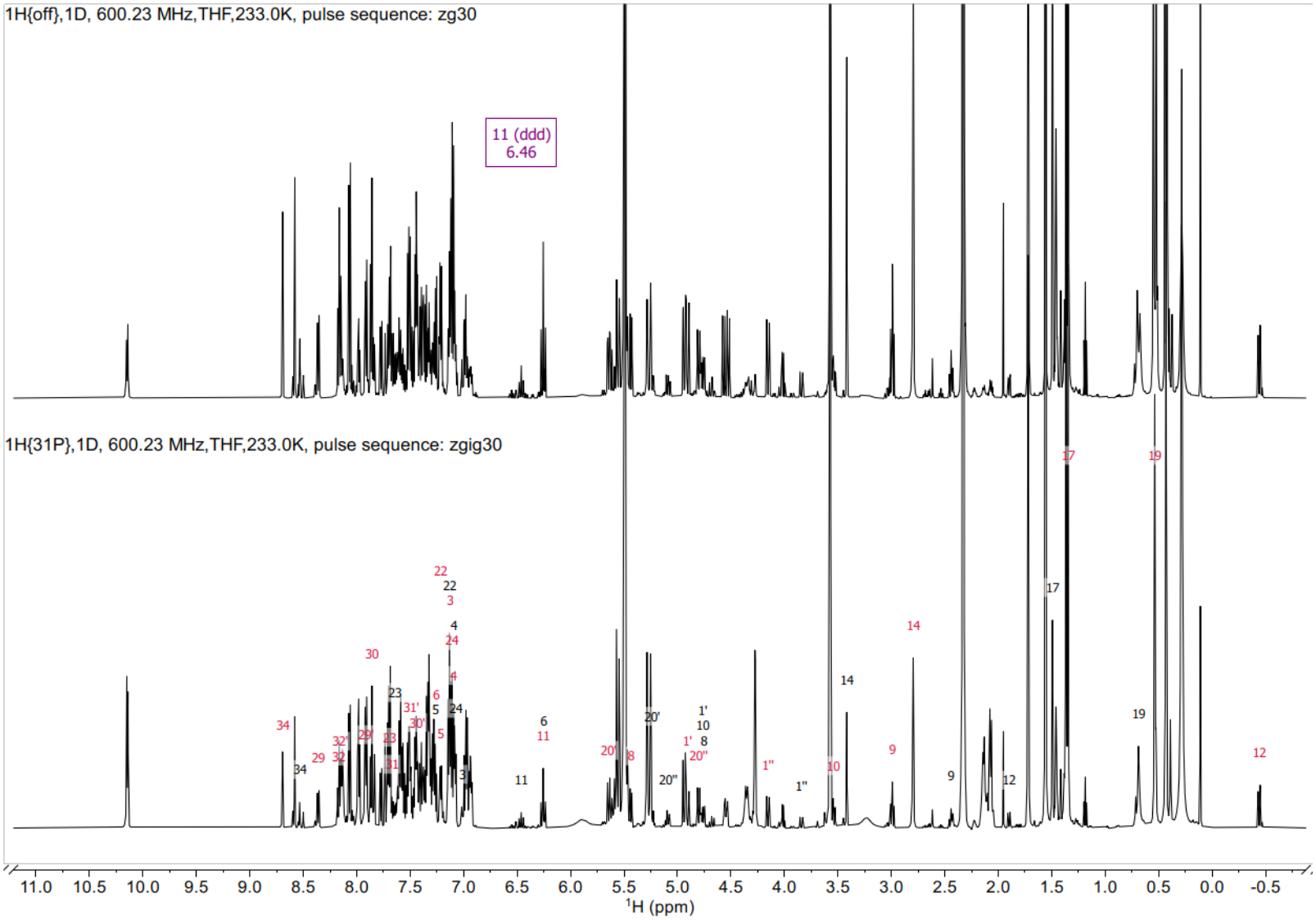

Analysis of the minor atropisomer by 1D-selective TOCSY from excitation of H11 (600 MHz, [D_8]-THF, 233 K)

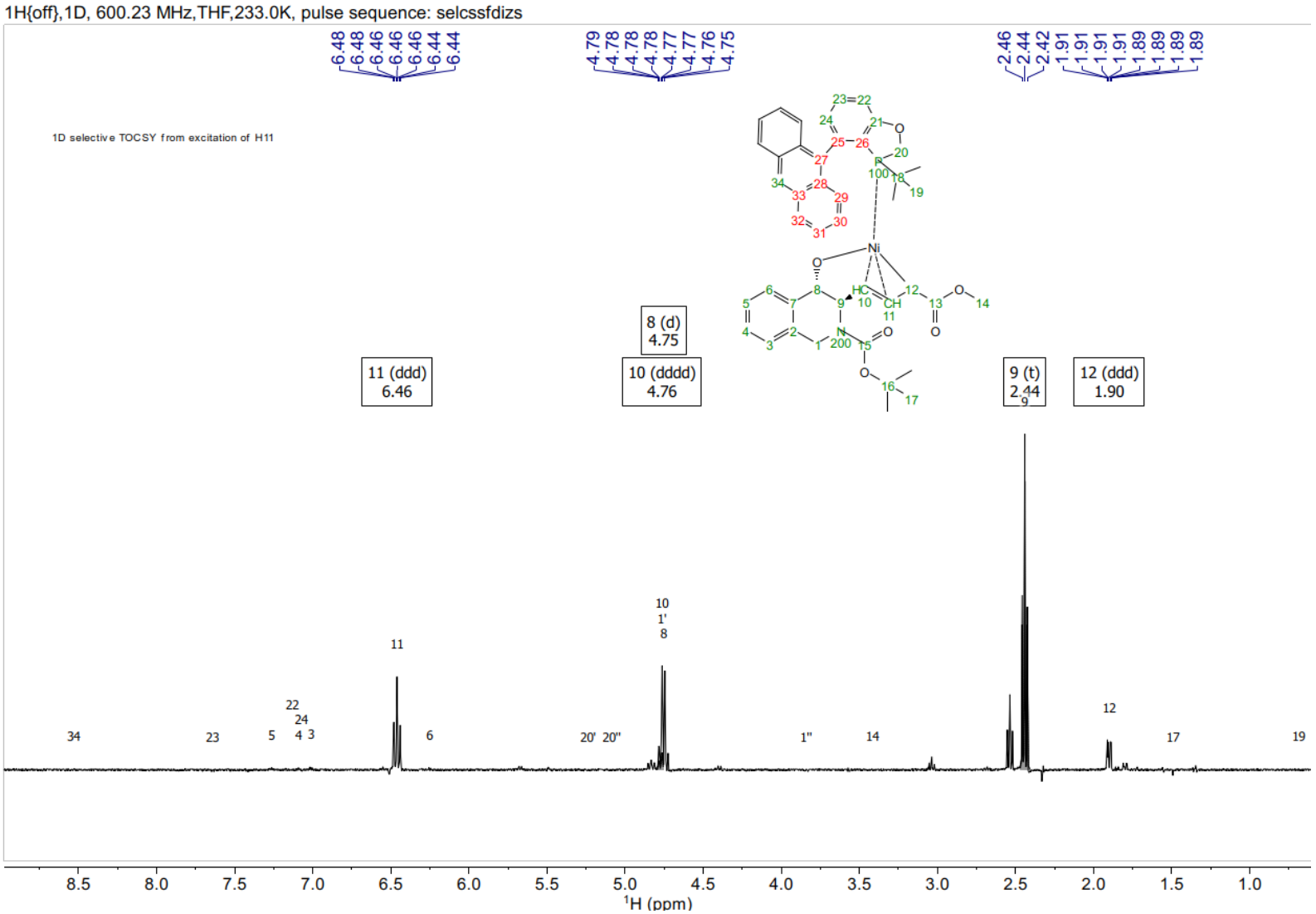

Analysis of the major atropisomer by 1D-selective TOCSY from excitation of H11/H6 (600 MHz, [D_8]-THF, 233 K)

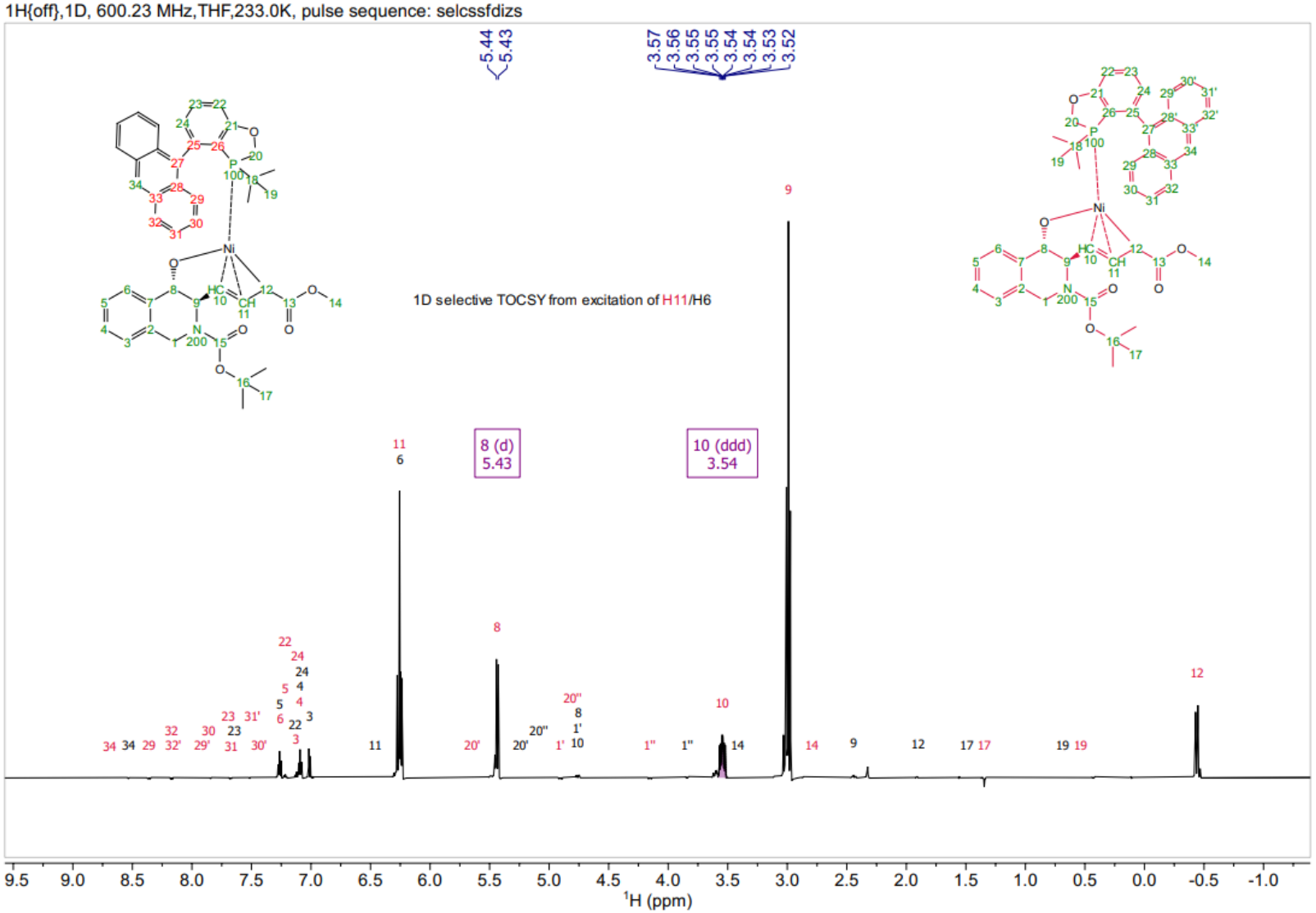

5.4.7 Kinetic Reaction Profile of a Reductive Cyclization Reaction and Speciation of the Crude Reaction Mixture

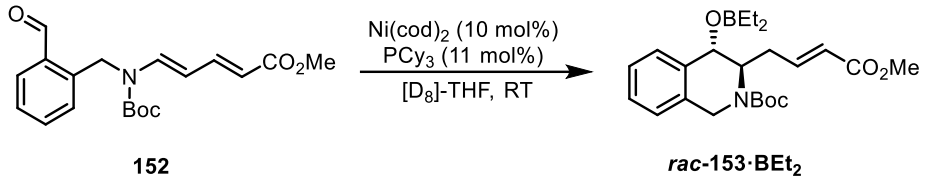

152 ***rac*-153·BEt$_2$**

A flame-dried Schlenk flask under argon was charged with solutions of Ni(cod)$_2$ (2.8 mg, 10.0 µmol) in [D$_8$]-THF (0.4 mL) and PCy$_3$ (3.1 mg, 11.0 µmol) in [D$_8$]-THF (0.35 mL). Triethylborane (1.0 M in [D$_8$]-THF, 0.25 mL, 0.25 mmol) and 1,3,5-trimethoxybenzene (5.1 mg, 30.0 µmol) were added and the resulting solution was stirred for 2 min at room temperature before substrate **152** (34.5 mg, 0.10 mmol) was introduced under an argon counterflow. The resulting mixture was stirred for ≈30 s until a clear brown solution was obtained and was subsequently transferred into a J-Young tube under argon. The reaction was monitored by NMR spectroscopy (^{1}H and ^{31}P NMR), with the first data point acquired ≈3 min after the reaction was initiated.

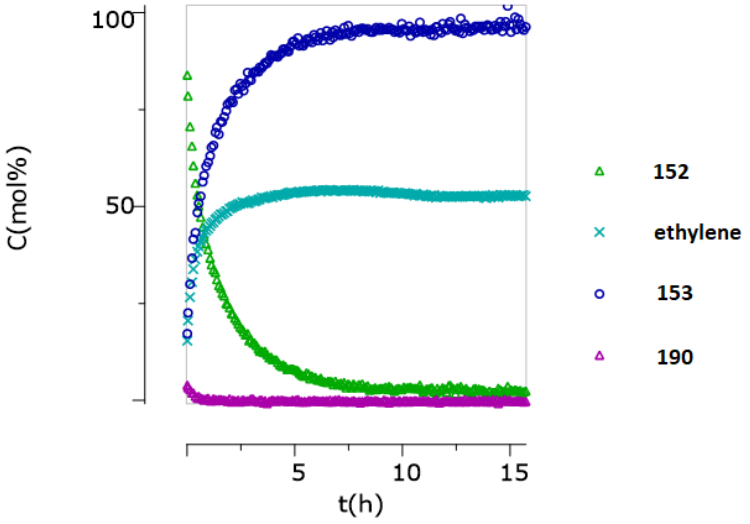

Figure S6: Time-dependent concentration profile of the reductive cyclization reaction; the conversion was determined using 1,3,5-trimethoxybenzene as internal standard.

The reaction profile shown in Figure S6 illustrates the conversion of **152** and the simultaneous formation of the borinate ester of **153** as the primary product of the reaction. Likewise, the formation of an equimolar amount of ethylene relative to the converted substrate was observed by ^{1}H NMR spectroscopy, which is formed by β-hydride elimination of the nickel-alkyl intermediate after transmetalation within the catalytic cycle. The ethylene concentration reaches a plateau due to saturation of the THF used as the solvent. After complete conversion of substrate **152**, the reaction mixture was further analyzed. Specifically, an ^{11}B NMR spectrum showed the signals of residual triethylborane (δ_B = 73.5 ppm, br), which was used in excess; in addition, the signal of the expected borinate ester of **153** (δ_B = 53.6 ppm, br) was detected, which is the primary product of the reaction prior to hydrolytic work-up.

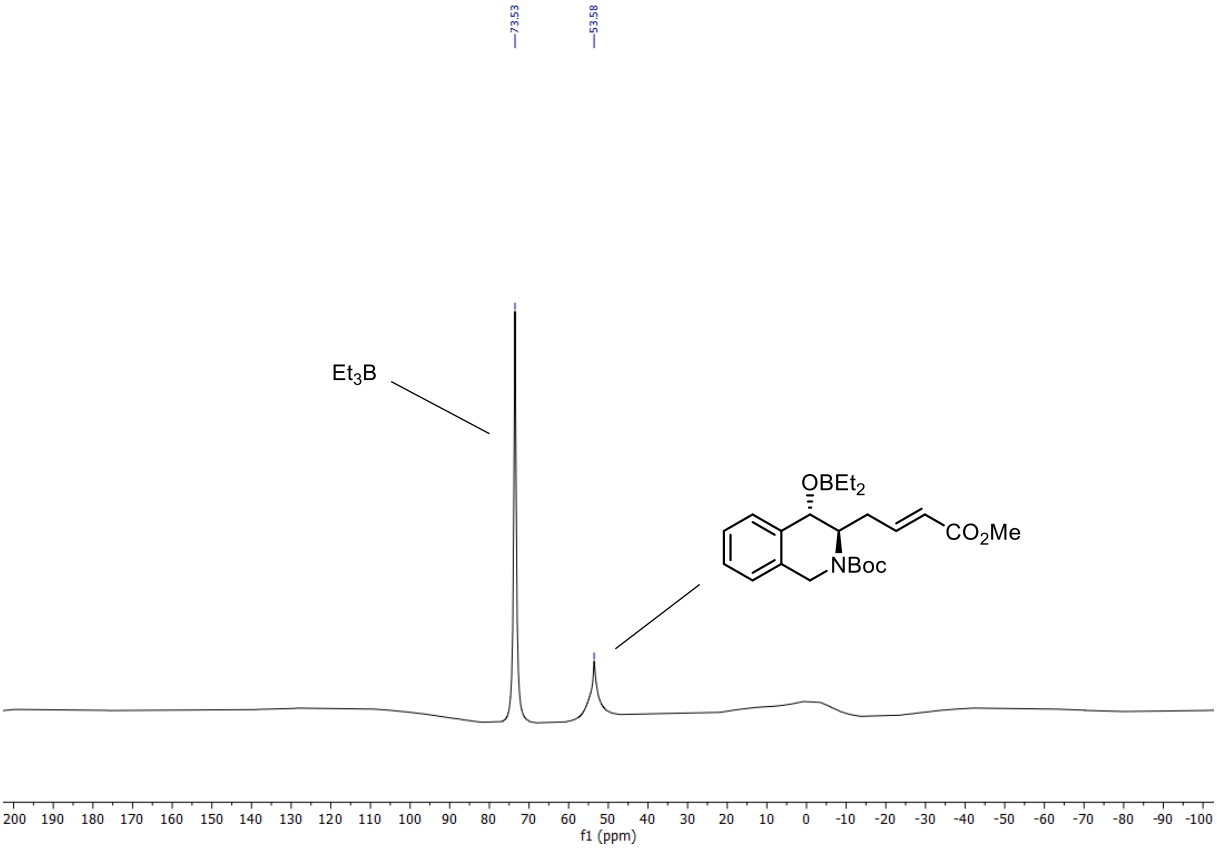

Figure S7: ^{11}B NMR (193 MHz, [D$_8$]-THF, 298 K) of the reaction mixture after complete substrate conversion.

Furthermore, ^{31}P NMR analysis of the reaction mixture was performed both during the catalytic reaction and after its completion. Importantly, the signal of the allyl-oxanickelacycle intermediate **190** was clearly detected at the beginning of the reaction but lost intensity; in any case, it was detected during the entire course of the reaction, where it accounts for ca. 1 mol% of the total of 11 mol% of PCy_3 initially added to the reaction mixture. In addition, several other phosphorous-containing species were observed. Besides $OPCy_3$ ($\delta_P \approx 46.6$ ppm), which is likely formed by oxidation of PCy_3 by trace amounts of oxygen in the NMR tube, several new species were formed during the reductive coupling reaction. The signal at $\delta_P = 39.4$ ppm can be assigned to [Ni(PCy_3)(ethylene)$_2$] by comparison with an authentic sample. This assignment is further supported by 1D and 2D experiments revealing the significantly upfield-shifted resonances of the nickel-bound ethylene ($\delta_H = 2.41$ ppm; $\delta_C = 50.3$ ppm). A more complex signal pattern consisting of four resonances was observed in the range of $\delta_P = 33.8–34.5$ ppm. Based on fact that these P-containing products were gradually formed during the course of the reaction and the close shift range, these signals were tentatively assigned to a species of the type [Ni(PCy_3)(ethylene)(**153**·BEt_2)] in which the borinate ester primarily formed coordinates to the nickel center by its alkene moiety. The presence of two different signals was attributed to different relative orientations of the coordinated reductive coupling product with respect to the remaining ligands, while additional splitting likely arises from rotamer formation of the N-Boc group, resulting in the observed total of four ^{31}P NMR signals. This assignment is supported by the

observation of exchange peaks between two of the four signals (tentatively ascribed to the rotamers) in a ^{31}P-^{1}H EXSY experiment.

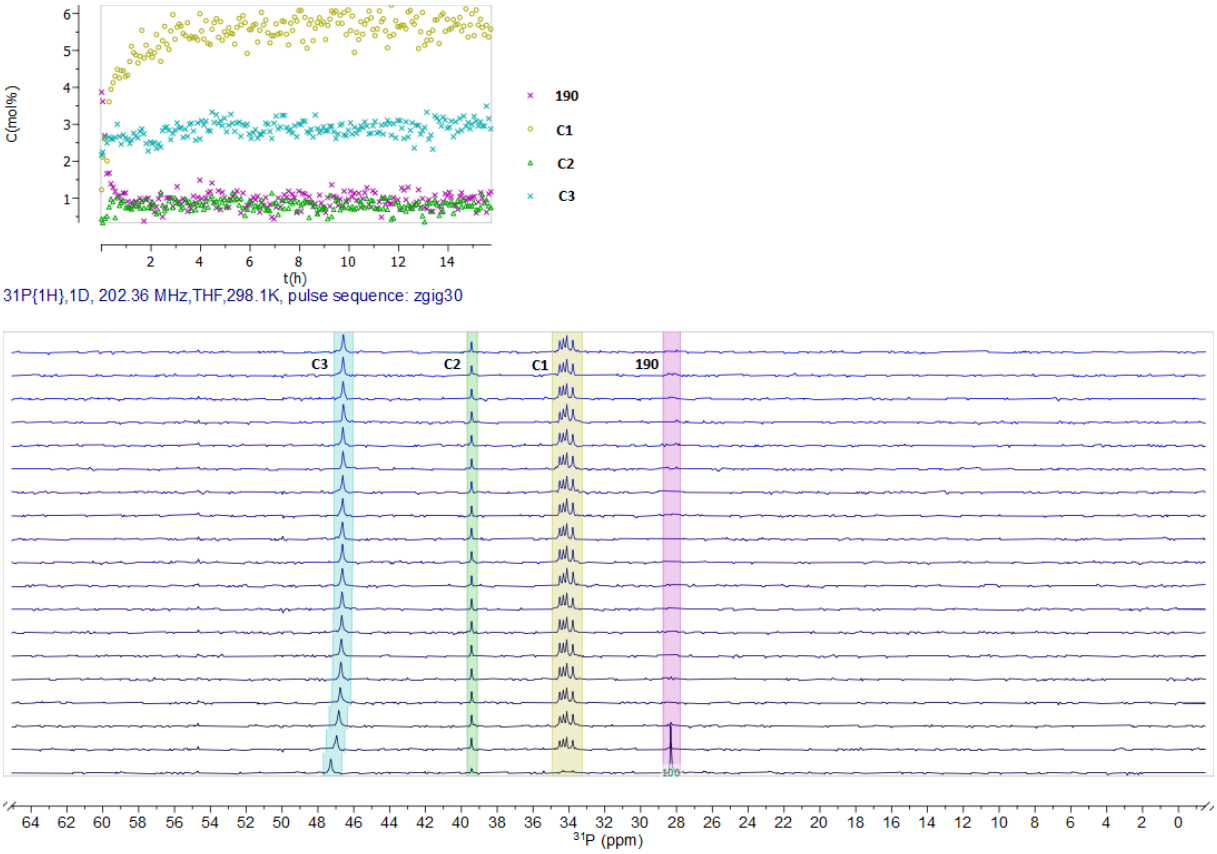

Figure S8: Time-dependent concentration profile of phosphorus-containing species observed during and after the nickel-catalyzed reductive cyclization (202 MHz, [D8]-THF, 298 K); **C1:** [Ni(PCy_3)(ethylene)(**153**·BEt_2)] (see Text); **C2:** [Ni(PCy_3)(ethylene)$_2$]; **C3:** Cy_3P=O.

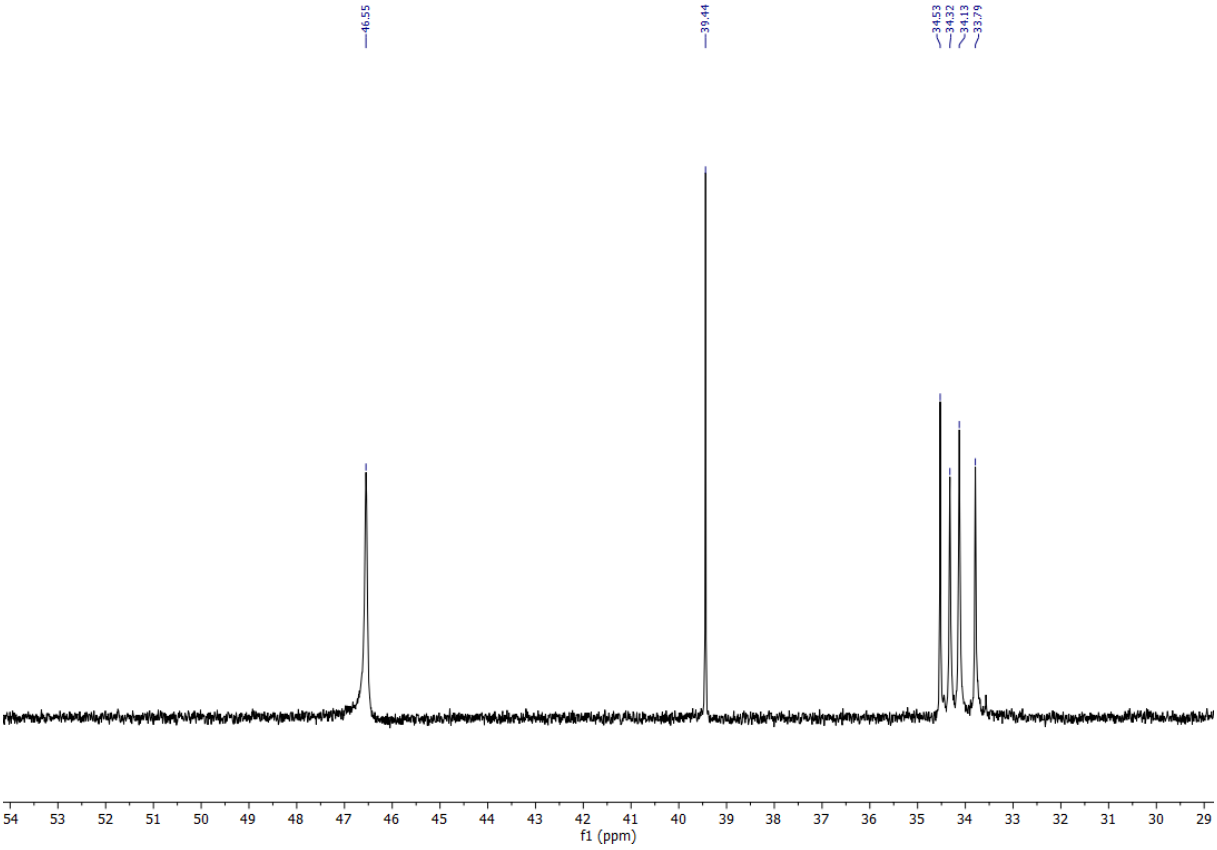

Figure S9: ^{31}P NMR spectrum (243 MHz, [D$_8$]-THF, 298 K) of the reaction mixture after full conversion of substrate **152**.

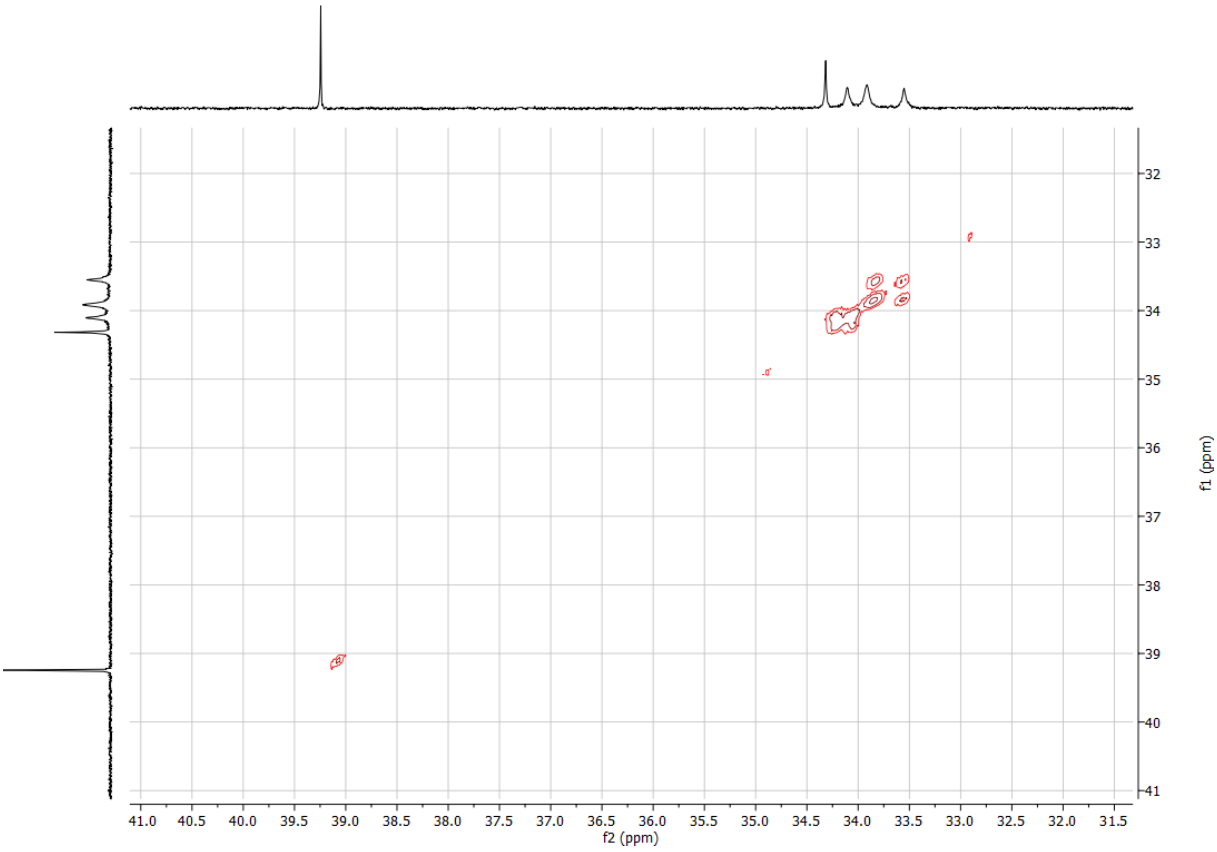

Figure S10: ^{31}P-^{1}H EXSY NMR spectrum (243/600 MHz, [D$_8$]-THF, 323 K) of the reaction mixture after full conversion of substrate **152**.

Control Experiment with Triethylsilane

A flame-dried Schlenk flask under argon was charged with $Ni(cod)_2$ (15.4 mg, 56.0 µmol) and a solution of PCy_3 (17.3 mg, 61.6 µmol) in [D_8]-THF (0.6 mL). Substrate **152** (19.3 mg, 56.0 µmol) was introduced under an argon counterflow and the resulting mixture was stirred at room temperature for 1 h to ensure quantitative formation of allyl-oxanickelacycle **190**. Triethylsilane (8.9 µL, 56.0 µmol) was then added and the resulting mixture was stirred at room temperature for 5 min before it was transferred into a J-Young tube under argon. Analysis of the mixture by ^{1}H, ^{29}Si and ^{31}P NMR after 30 min and 20 h after addition of the silane showed the allyl-oxanickelacycle **190** and unreacted Et_3SiH as the virtually only detectable species in solution. The nickelacycle obviously does not react with the silane. These data indicate that a productive turnover via σ-bond metathesis, as previously proposed by Mori *et al.*,[27] does not occur to any significant extent under the chosen conditions. Since substrate **152** does not succumb to cyclization when exposed to [Ni($^{t\text{Bu}}$stb)$_3$] (10 mol%), ligand **L29** (11 mol%) and excess Et_3SiH (see main text), a conceivable alternative pathway involving oxidative addition of the silane to nickel(0), followed by migratory insertion of the resulting nickel(II) hydride complex with formation of an allylnickel species, and subsequent cyclization with formation of a nickelacylce is not operative either; such a mechanism has also been proposed in the literature.[21]

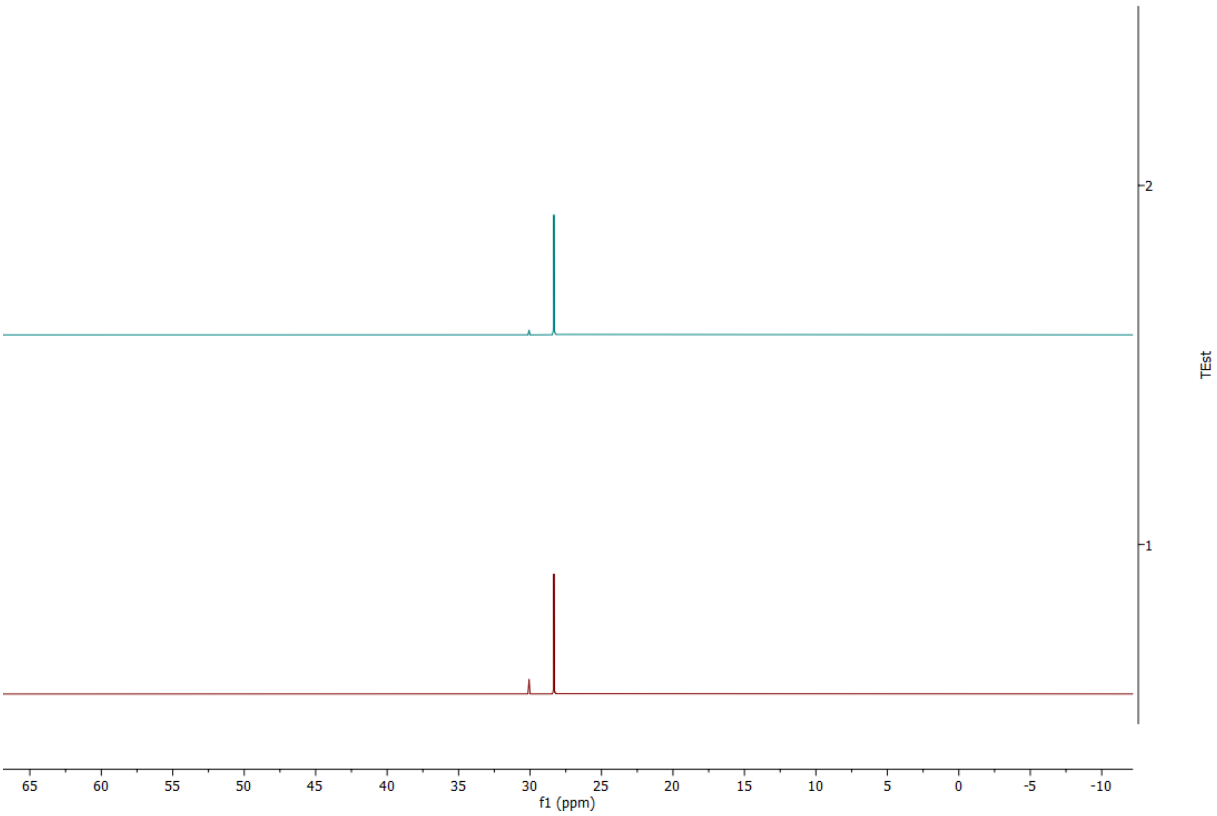

Figure S11: ^{31}P NMR spectrum (243 MHz; [D_8]-THF, 298 K) of the reaction mixture recorded after 30 min (top) and after 20 h (bottom) following the addition of Et_3SiH to the nickelacycle **190** (δ_P = 28.3 ppm).

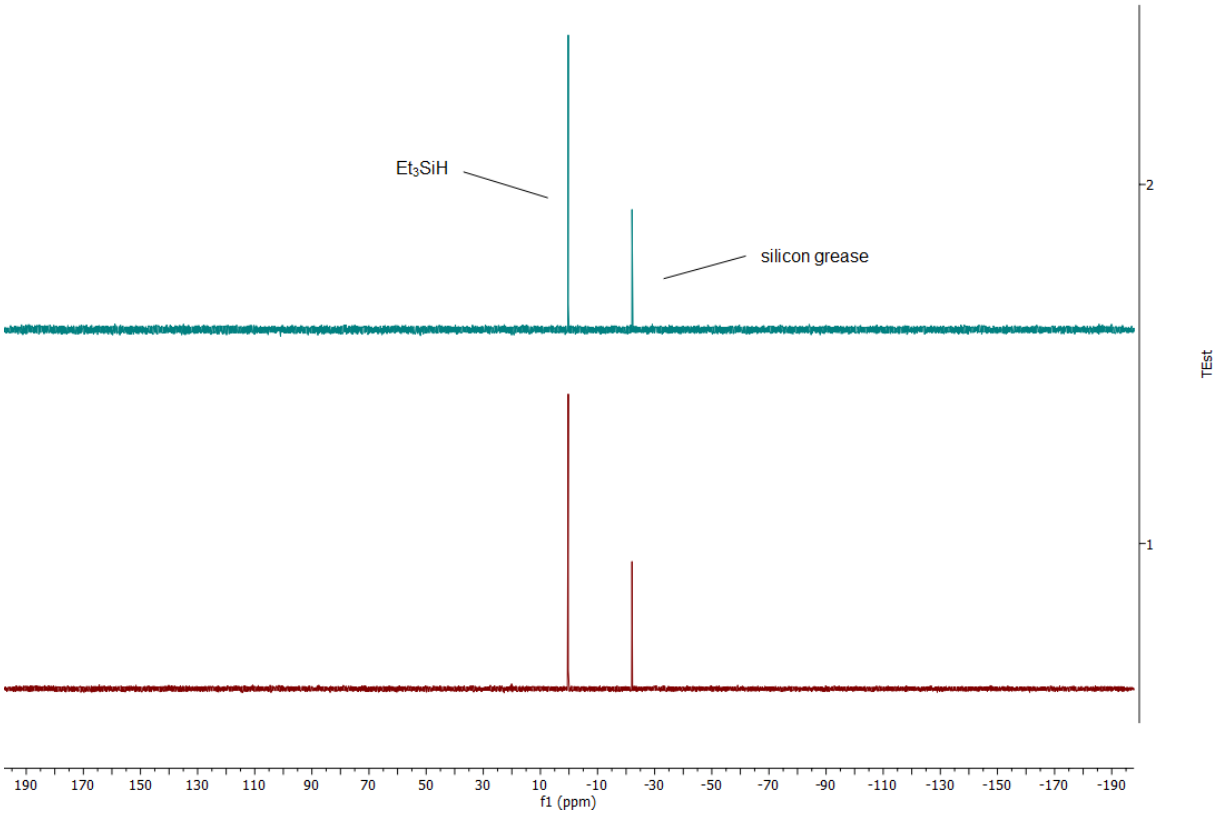

Figure S12: ^{29}Si-refocussed INEPT NMR spectrum (119 MHz, [D_8]-THF, 298 K) of the reaction mixture; top = 30 min after addition of Et_3SiH, bottom = 20 h after addition of Et_3SiH to the allyl-oxanickelacycle **190**.

5.4.8 Determination of the Relative and Absolute Configuration of the Reductive Cyclization Products

The stereoconfiguration of product **159** determined by X-ray diffraction analysis served as point of reference (Figure S13). The relative configuration of this compound is also clearly reflected in characteristic NOEs as observed by NMR. Moreover, the $^{3}J_{HH}$ coupling constants of the H-atoms at the two stereocenters show a coupling constant of $^{3}J_{HH} \approx 2.7$ Hz in the ^{1}H NMR, which confirms a *gauche* orientation, which is again in line with the structure in the solid state (Figure S14; also see main text).

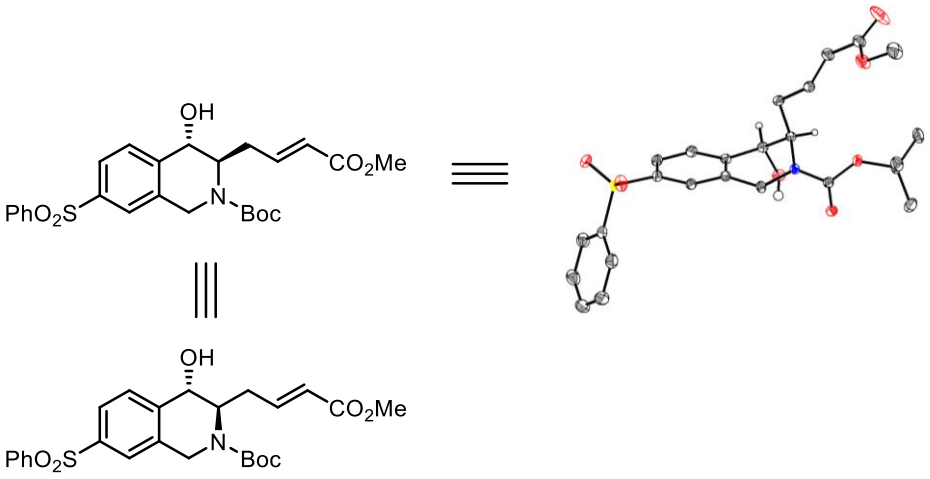

Figure S13: Determination of the absolute configuration of **159** by X-ray diffraction analysis.

All products showing the same pattern and data were hence assigned in analogy.

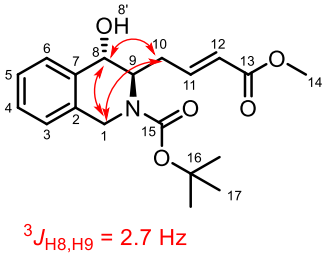

Figure S14: Diagnostic NOESY data and $^{3}J_{HH}$ coupling constant observed in the tetrahydroisoquinoline products.

In the cases compiled below, the relative and absolute configuration was apparently different.

NOESY Data and Mosher Ester Analysis of 168

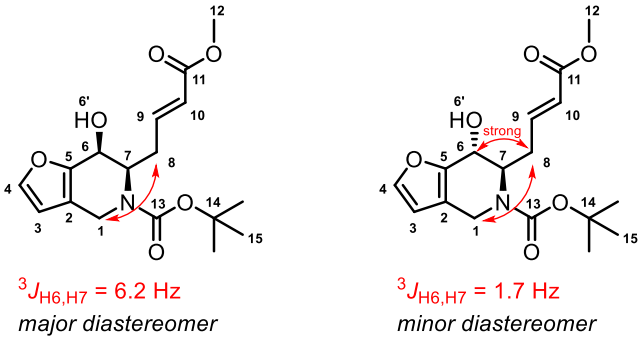

Figure S15: Major and minor diastereomer observed for the furane-derived tetrahydroisoquinoline.

In order to verify the relative configuration of **168**, the NMR data of the major and the minor diastereomer were compared. The minor *trans*-diastereomer shows a strong NOE between H6 and H8'/H8'', while the major diastereomer does not. Moreover, the $^3J_{H6,H7}$ coupling constant of the minor diastereomer was 1.7 Hz, which speaks for a *gauche*-orientation of the pertinent protons. The major diastereomer on the other hand showed a $^3J_{H6,H7}$ = 6.2 Hz, which corroborates the proposed *cis*-configuration.

The Mosher ester analysis showed that the C6 stereocenter of the major isomer bearing the alcohol group is (*S*)-configured and hence inverted compared to that in the tetrahydroisoquinoline derivative **159**. The configuration of the second stereocenter could be deduced from this.

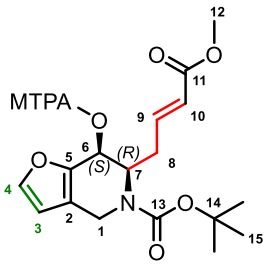

Table S3: Analysis of the Mosher esters according to Hoye and co-workers.[245, 249]

Atom number	(*S*)-MTPA-Ester δ (ppm)	(*R*)-MTPA-Ester δ (ppm)	δ*S* – δ*R* (ppm)
1'	3.94	3.95	-0.01
1''	4.59	4.60	-0.01
3	6.48	6.46	+0.02
4	7.67	7.62	+0.05
6	6.23	6.22	+0.01
7	4.92	5.02	-0.10
8'	2.25	2.37	-0.12
8''	1.98	2.32	-0.34
9	6.69	6.79	-0.10
10	5.85	5.94	-0.09

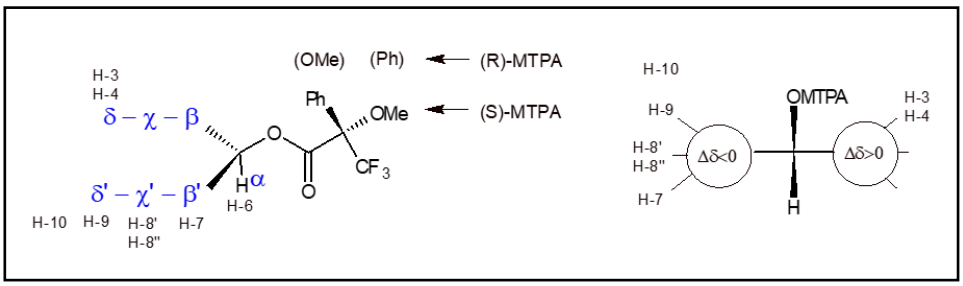

NOESY Data and Mosher Ester Analysis of 169

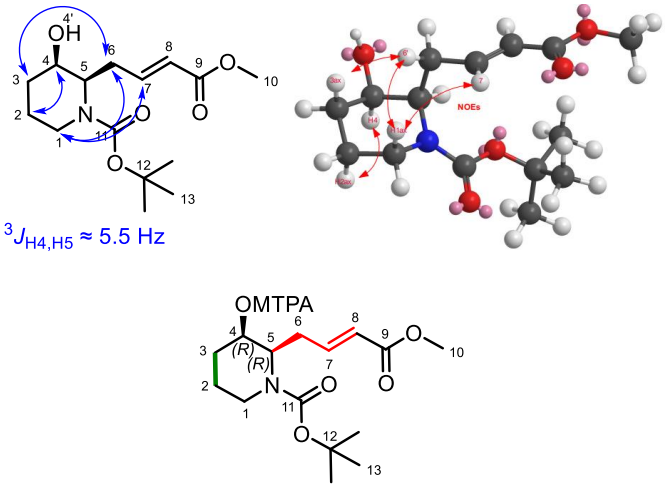

Table S4: Analysis of the Mosher esters according to Hoye and co-workers.[245]

Atom number	(*S*)-MTPA-Ester δ (ppm)	(*R*)-MTPA-Ester δ (ppm)	δ*S* – δ*R* (ppm)
1'	2.76	2.78	-0.02
1''	3.80	3.80	0
2'	1.51	1.50	0.01
2''	1.72	1.69	0.03
3'	1.76	1.65	0.11
3''	1.90	1.83	0.07
4	5.04	5.04	0
5'	4.49	4.58	-0.09
6'	2.64	2.71	-0.07
6''	1.87	2.19	-0.32
7	6.63	6.74	-0.11
8	5.78	5.87	-0.09

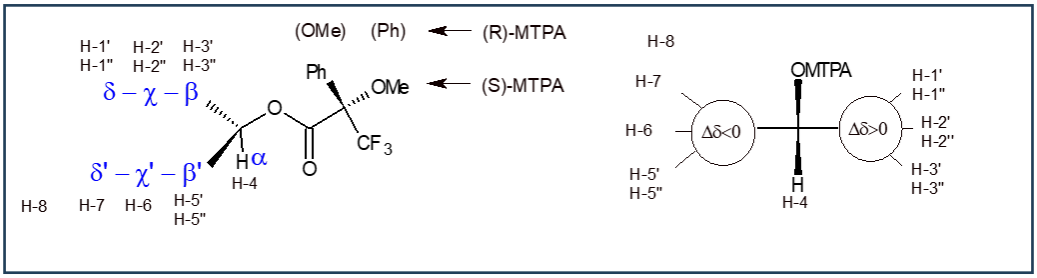

The stereocenter bearing the alcohol group was assigned as (*R*) by the Mosher ester analysis.[245]Due to the *cis*-configuration, the absolute configuration on the second stereocenter could be assigned as (*R*).

NOESY Data and Mosher Ester Analysis of 170

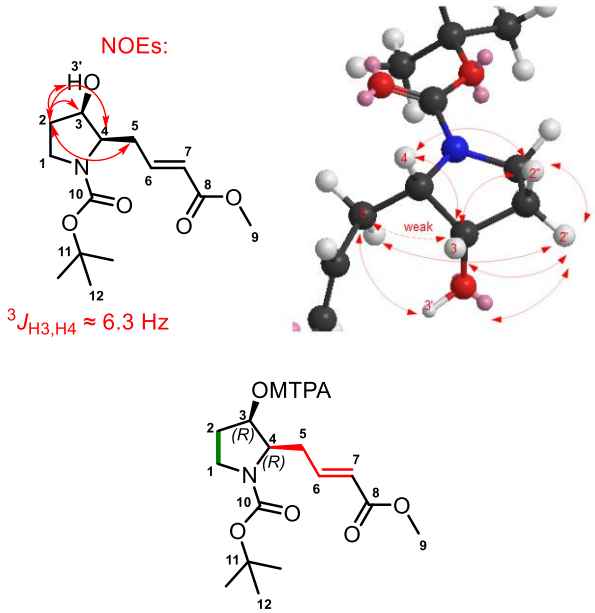

Table S5: Analysis of the Mosher esters according to Hoye and co-workers.[245]

Atom number	(*S*)-MTPA-Ester δ (ppm)	(*R*)-MTPA-Ester δ (ppm)	δ*S* – δ*R* (ppm)
1'	3.25	3.14	+0.11
1''	3.50	3.46	+0.04
2'	1.95	1.84	+0.11
2''	2.28	2.26	+0.02
3	5.50	5.50	0
4	4.13	4.19	-0.06
5'	2.24	2.39	-0.15
5''	2.38	2.51	-0.13
6	6.70	6.79	-0.09
7	5.68	5.77	-0.09

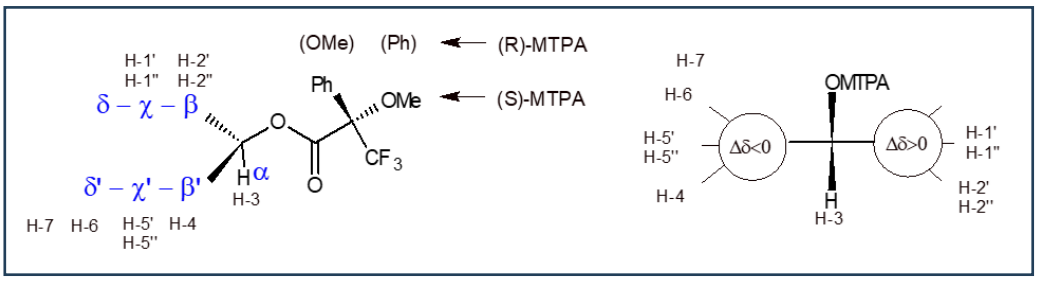

The stereocenter bearing the alcohol group was assigned as (*R*) by the Mosher ester analysis.[245] Due to the *cis*-configuration, the absolute configuration on the second stereocenter could be assigned as (*R*).

The Mosher Ester Derivatives

Mosher Ester S53a. (*R*)-Mosher's acid chloride (4.3 µL, 22.8 µmol), DMAP (0.5 mg, 4.1 µmol) and triethylamine (8.7 µL, 62.2 µmol) were added to a solution of **168** (7.0 mg, 20.7 µmol) in dichloromethane (0.5 mL) and the resulting mixture was stirred at room temperature for 2 h. Dichloromethane (2 mL) and sat. aq. NH_4Cl (2 mL) were added and the resulting mixture was vigorously stirred for 5 min. The organic layer was separated and the aqueous layer was extracted with dichloromethane (2 x 5 mL). The combined organic phases were dried over $MgSO_4$ and filtered, and the solvent was removed under reduced pressure. The residue was purified by flash chromatography (SiO_2, *n*-pentane/ethyl acetate, 4:1) to give the title compound as a colorless oil (5.0 mg, 44%). ^{1}H NMR (600 MHz, [D_6]-DMSO, 353 K): δ = 7.67 (dd, *J* = 1.9, 0.9 Hz, 1H), 7.60 – 7.57 (m, 2H), 7.52 – 7.49 (m, 3H), 6.69 (ddd, *J* = 15.6, 8.6, 5.9 Hz, 1H), 6.48 (d, *J* = 1.9 Hz, 1H), 6.25 – 6.20 (m, 1H), 5.85 (ddd, *J* = 15.6, 1.8, 1.1 Hz, 1H), 4.92 (ddd, *J* = 11.6, 6.4, 3.5 Hz, 1H), 4.59 (dd, *J* = 16.8, 1.9 Hz, 1H), 3.94 (dd, *J* = 16.8, 2.4 Hz, 1H), 3.64 (s, 3H), 3.61 (q, *J* = 1.0 Hz, 3H), 2.25 (dddd, *J* = 15.0, 11.6, 8.6, 1.1 Hz, 1H), 1.98 (dddd, *J* = 15.0, 5.9, 3.6, 1.8 Hz, 1H), 1.41 (s, 9H); IR (ATR): ṽ = 2952, 1756, 1725, 1698, 1396, 1227, 1169, 1122, 1021, 720 cm^{-1}; HRMS (ESI$^+$): *m/z*: calcd. for $C_{27}H_{30}NO_8F_3Na$ [M+Na]$^+$: 576.18157, found: 576.18233.

Mosher Ester S53b. (*S*)-Mosher's acid chloride (3.6 µL, 19.2 µmol), DMAP (0.5 mg, 4.1 µmol) and triethylamine (6.2 µL, 44.4 µmol) were added to a solution of **168** (5.0 mg, 14.8 µmol) in dichloromethane (0.5 mL) and the resulting mixture was stirred at room temperature for 2 h. Dichloromethane (2 mL) and sat. aq. NH_4Cl (2 mL) were added and the resulting mixture was vigorously stirred for 5 min. The organic layer was separated and the aqueous layer was extracted with dichloromethane (2 x 5 mL). The combined organic phases were dried over $MgSO_4$ and filtered, and the solvent was removed under reduced pressure. The residue was purified by flash chromatography (SiO_2, *n*-pentane/ethyl acetate, 4:1) to give the title compound as a colorless oil (4.8 mg, 59%). ^{1}H NMR (600 MHz, [D_6]-DMSO, 353 K): δ = 7.62 (dd, *J* = 1.9, 0.9 Hz, 1H), 7.59 – 7.56 (m, 2H), 7.52 – 7.49 (m, 3H), 6.79 (ddd, *J* = 15.6, 8.5, 6.0 Hz, 1H), 6.46 (d, *J* = 1.9 Hz, 1H), 6.22 (dm, *J* = 6.3 Hz, 1H), 5.94 (ddd, *J* = 15.7, 1.7, 1.2 Hz, 1H), 5.02 (dt, *J* = 10.7, 6.3 Hz, 1H), 4.60 (dd, *J* = 16.7, 1.6 Hz, 1H), 3.95 (dd, *J* = 16.7, 2.3 Hz, 1H), 3.64 (s, 3H), 3.53 (q, *J* = 1.0 Hz, 3H), 2.37 (dddd, *J* = 15.2, 10.7, 8.5, 1.2 Hz, 1H), 2.32 (dddd, *J* = 15.3, 6.0, 4.3, 1.7 Hz, 1H), 1.42 (s, 9H); IR (ATR): ṽ = 2951, 1756, 1726, 1699, 1396, 1228, 1170, 1018, 720 cm^{-1}; HRMS (ESI$^+$): *m/z*: calcd. for $C_{27}H_{30}NO_8F_3Na$ [M+Na]$^+$: 576.18157, found: 576.18179.

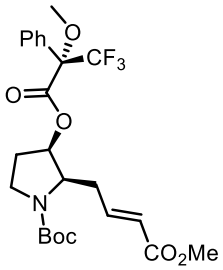

Mosher Ester 54a. (*R*)-Mosher's acid chloride (5.4 µL, 28.9 µmol), DMAP (0.5 mg, 4.1 µmol) and triethylamine (8.1 µL, 57.8 µmol) were added to a solution of **170** (5.5 mg, 19.3 µmol) in dichloromethane (0.5 mL) and the resulting mixture was stirred at room temperature for 18 h. Dichloromethane (2 mL) and sat. aq. NH_4Cl (2 mL) were added and the resulting mixture was vigorously stirred for 5 min. The organic layer was separated and the aqueous layer was extracted with dichloromethane (2 x 5 mL). The combined organic phases were dried over $MgSO_4$ and filtered, and the solvent was removed under reduced pressure. The residue was purified by flash chromatography (SiO_2, *n*-pentane/ethyl acetate, 3:1) to give the title compound as a colorless oil (6.5 mg, 67%). ^{1}H NMR (600 MHz, [D$_6$]-DMSO, 353 K): δ = 7.50 – 7.46 (m, 5H), 6.70 (dt, *J* = 15.7, 7.2 Hz, 1H), 5.68 (dt, *J* = 15.7, 1.5 Hz, 1H), 5.50 (q, *J* = 6.2 Hz, 1H), 4.13 (q, *J* = 6.3 Hz, 1H), 3.64 (s, 3H), 3.52 (q, *J* = 1.1 Hz, 3H), 3.50 (ddd, *J* = 10.8, 8.2, 5.9 Hz, 1H), 3.25 (ddd, *J* = 10.9, 7.9, 6.6 Hz, 1H), 2.38 (dt, *J* = 15.0, 6.6 Hz, 1H), 2.28 (ddt, *J* = 13.2, 8.2, 6.6 Hz, 1H), 2.23 (dtd, *J* = 15.0, 7.2, 1.5 Hz, 1H), 1.95 (ddt, *J* = 13.8, 7.9, 6.0 Hz, 1H), 1.40 (s, 9H); IR (ATR): $\tilde{\nu}$ = 2979, 1750, 1724, 1696, 1394, 1257, 1167, 1122, 1023, 720 cm^{-1}; HRMS (ESI$^+$): *m/z*: calcd. for $C_{24}H_{30}NO_7F_3Na$ [M+Na]$^+$: 524.18666, found: 524.18636.

Mosher Ester 54b. (*S*)-Mosher's acid chloride (7.2 µL, 38.6 µmol), DMAP (0.5 mg, 4.1 µmol) and triethylamine (8.1 µL, 57.8 µmol) were added to a solution of **170** (5.5 mg, 19.3 µmol) in dichloromethane (0.5 mL) and the resulting mixture was stirred at room temperature for 18 h. Dichloromethane (2 mL) and sat. aq. NH_4Cl (2 mL) were added and the resulting mixture was vigorously stirred for 5 min. The organic layer was separated and the aqueous layer was extracted with dichloromethane (2 x 5 mL). The combined organic phases were dried over $MgSO_4$ and filtered, and the solvent was removed under reduced pressure. The residue was purified by flash chromatography (SiO_2, *n*-pentane/ethyl acetate, 3:1) to give the title compound as a colorless oil (6.6 mg, 68%). ^{1}H NMR (600 MHz, [D$_6$]-DMSO, 353 K): δ = 7.51 – 7.46 (m, 5H), 6.79 (dt, *J* = 15.7, 7.2 Hz, 1H), 5.77 (dt, *J* = 15.7, 1.5 Hz, 1H), 5.50 (q, *J* = 6.2 Hz, 1H), 4.18 (q, *J* = 6.2 Hz, 1H), 3.65 (s, 3H), 3.47 (q, *J* = 1.1 Hz, 3H), 3.46 (ddd, *J* = 10.8, 8.2, 5.9 Hz, 1H), 3.13 (dt, *J* = 10.8, 7.8 Hz, 1H), 2.51 (dt, *J* = 15.0, 6.6 Hz, 1H), 2.39 (dtd, *J* = 15.0, 7.1, 1.5 Hz, 1H), 2.26 (ddt, *J* = 13.2, 8.2, 6.6 Hz, 1H), 1.84 (ddt, *J* = 13.2, 7.8, 6.2 Hz, 1H), 1.40 (s, 9H); IR (ATR): $\tilde{\nu}$ = 2979, 1751, 1723, 1695, 1395, 1255, 1168, 1121, 1043, 762 cm^{-1}; HRMS (ESI$^+$): *m/z*: calcd. for $C_{24}H_{30}NO_7F_3Na$ [M+Na]$^+$: 524.18666, found: 524.18642.

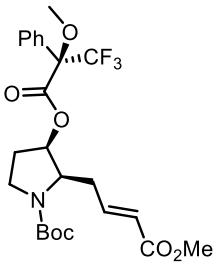

Mosher Ester S55a. (*R*)-Mosher's acid chloride (4.8 µL, 25.4 µmol), DMAP (0.3 mg, 2.5 µmol) and triethylamine (5.3 µL, 38.1 µmol) were added to a solution of **169** (3.8 mg, 12.7 µmol) in dichloromethane (0.5 mL) and the resulting mixture was stirred at room temperature for 18 h. Dichloromethane (2 mL) and sat. aq. NH_4Cl (2 mL) were added and the resulting mixture was vigorously stirred for 5 min. The organic layer was separated and the aqueous layer was extracted with dichloromethane (2 x 5 mL). The combined organic phases were dried over $MgSO_4$ and filtered, and the solvent was removed under reduced pressure. The residue was purified by flash chromatography (SiO_2, toluene/*tert*-butyl methyl ether, 10:1) to give the title compound as a colorless oil (4.2 mg, 64%). ^{1}H NMR (600 MHz, [D_6]-DMSO, 353 K): δ = 7.52 – 7.47 (m, 5H), 6.63 (ddd, *J* = 15.5, 8.5, 6.2 Hz, 1H), 5.78 (dt, *J* = 15.5, 1.4 Hz, 1H), 5.04 (ddd, *J* = 12.0, 5.5, 4.6 Hz, 1H), 4.49 (ddd, *J* = 12.0, 5.5, 3.7 Hz, 1H), 3.80 (dd, *J* = 13.7, 5.0 Hz, 1H), 3.63 (s, 3H), 3.53 (q, *J* = 1.0 Hz, 3H), 2.76 (td, *J* = 13.3, 2.9 Hz, 1H), 2.64 (dddd, *J* = 14.9, 11.3, 8.5, 1.3 Hz, 1H), 1.93 – 1.83 (m, 2H), 1.81 – 1.68 (m, 2H), 1.51 (qt, *J* = 13.1, 4.5 Hz, 1H), 1.39 (s, 9H); IR (ATR): ṽ = 2925, 1750, 1725, 1693, 1411, 1243, 1156, 1020, 722 cm^{-1}; HRMS (ESI$^+$): *m/z*: calcd. for $C_{25}H_{32}NO_7F_3Na$ [M+Na]$^+$: 538.20231, found: 538.20272.

Mosher Ester S55b. (*S*)-Mosher's acid chloride (4.8 µL, 25.4 µmol), DMAP (0.3 mg, 2.5 µmol) and triethylamine (5.3 µL, 38.1 µmol) were added to a solution of **169** (3.8 mg, 12.7 µmol) in dichloromethane (0.5 mL) and the resulting mixture was stirred at room temperature for 18 h. Dichloromethane (2 mL) and sat. aq. NH_4Cl (2 mL) were added and the resulting mixture was vigorously stirred for 5 min. The organic layer was separated and the aqueous layer was extracted with dichloromethane (2 x 5 mL). The combined organic phases were dried over $MgSO_4$ and filtered, and the solvent was removed under reduced pressure. The residue was purified by flash chromatography (SiO_2, toluene/*tert*-butyl methyl ether, 10:1) to give the title compound as a colorless oil (4.5 mg, 69%). ^{1}H NMR (600 MHz, [D_6]-DMSO, 353 K): δ = 7.49 (s, 5H), 6.74 (ddd, *J* = 15.6, 8.5, 6.2 Hz, 1H), 5.87 (dt, *J* = 15.6, 1.4 Hz, 1H), 5.04 (ddd, *J* = 11.6, 5.5, 4.5 Hz, 1H), 4.58 (ddd, *J* = 11.3, 5.5, 3.8 Hz, 1H), 3.80 (dd, *J* = 13.6, 5.0 Hz, 1H), 3.63 (s, 3H), 3.48 (q, *J* = 1.0 Hz, 3H), 2.77 (td, *J* = 13.6, 2.9 Hz, 1H), 2.71 (dddd, *J* = 14.9, 11.3, 8.5, 1.3 Hz, 1H), 2.19 (dddd, *J* = 14.9, 6.2, 3.8, 1.7 Hz, 1H), 1.87 – 1.80 (m, 1H), 1.73 – 1.61 (m, 2H), 1.54 – 1.46 (m, 1H), 1.39 (s, 9H); IR (ATR): ṽ = 2953, 1750, 1726, 1694, 1412, 1272, 1249, 1158, 1022 cm^{-1}; HRMS (ESI$^+$): *m/z*: calcd. for $C_{25}H_{32}NO_7F_3Na$ [M+Na]$^+$: 538.20231, found: 538.20222.

5.5 Nickel-Catalyzed Redox-Neutral Tandem Reactions

Control Experiment

Compound 203. A flame-dried Schlenk flask was charged with bis-(1,5-cyclooctadien)-nickel(0) (3.8 mg, 13.8 µmol) and phosphoramidite ligand **L11** (9.7 mg, 15.2 µmol). The Schlenk flask was evacuated and refilled with argon (3 cycles). THF (0.25 mL), triethylborane (1 M in THF, 0.15 mL, 0.15 mmol) and silyl dienol ether **31** (93.6 mg, 0.41 mmol) were added and the resulting solution was stirred for 5 min. Imine **197** (40.0 mg, 0.14 mmol) and degassed water (7.45 µL, 0.41 mmol) were added under an argon counterflow, the flask was sealed and the mixture stirred at room temperature for 18 h. The reaction was cooled to 0 °C and was quenched by addition of sat. aq. $NaHCO_3$ solution (2 mL). Ethyl acetate (2 mL) was added and the resulting mixture was vigorously stirred for 30 min. The mixture was diluted with ethyl acetate (5 mL) and water (5 mL) and was transferred into a separatory funnel. The organic layer was separated and the aqueous layer was extracted with ethyl acetate (2 x 5 mL). The combined organic layers were washed with brine (5 mL), dried over $MgSO_4$, and filtered, and the solvent was removed under reduced pressure. The crude product (rr > 20:1) was purified by flash chromatography (SiO_2, *n*-pentane/*tert*-butyl methyl ether, 10:1 → 5:1) and the title compound was obtained as a colorless solid (55.0 mg, 77%, 87% ee). ^{1}H NMR (400 MHz, $CDCl_3$): δ = 7.23 – 7.17 (m, 3H), 7.13 – 7.07 (m, 2H), 6.88 – 6.79 (m, 2H), 6.76 – 6.68 (m, 2H), 5.99 – 5.70 (m, 2H), 5.46 (d, *J* = 6.6 Hz, 1H), 5.29 – 5.02 (m, 2H), 4.51 (dd, *J* = 6.6, 3.4 Hz, 1H), 3.92 (dt, *J* = 9.1, 3.3 Hz, 1H), 3.77 (s, 3H), 2.48 (dddt, *J* = 14.1, 9.3, 7.1, 1.2 Hz, 1H), 2.19 (dddt, *J* = 14.1, 7.1, 3.0, 1.3 Hz, 1H), 1.00 – 0.87 (m, 21H); ^{13}C NMR (101 MHz, $CDCl_3$): δ = 156.9, 139.7, 133.2, 130.0, 128.3, 127.7, 127.5, 122.5, 119.2, 114.4, 76.9, 59.4, 55.6, 38.7, 18.2, 18.0, 12.8; IR (ATR): $\tilde{\nu}$ = 3275, 2943, 2866, 1510, 1461, 1246, 1154, 1090, 957, 883 cm^{-1}; HRMS (ESI$^-$): *m/z*: calcd. for $C_{27}H_{41}N_2O_4SiS$ [M-H]$^-$: 517.25618, found: 517.25678.

The ee was determined by HPLC analysis: Chiralpak 150 mm IG-3, 3 µm, 4.6 mm ∅, acetonitrile/water = 55:45, v = 1.0 mL/min, λ = 230 nm, t(major) = 30.23 min, t(minor) = 33.24 min (racemate: left, enantioenriched sample: right).

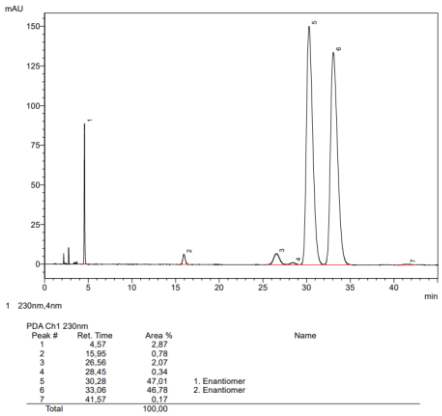

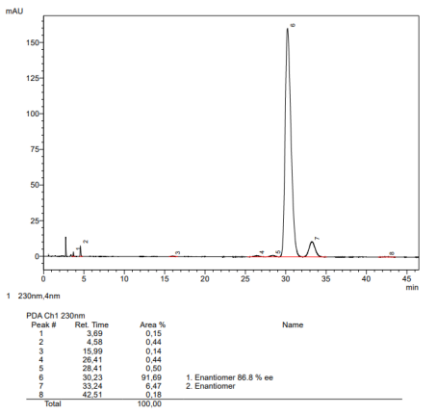

Redox-Neutral Tandem Reactions

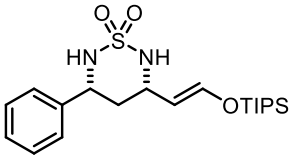

Sulfamide Derivative 214. A flame-dried Schlenk flask was charged with $NiCl_2$(dme) (4.4 mg, 20.2 µmol) and zinc powder (2.6 mg, 15.2 µmol). The Schlenk flask was evacuated and refilled with argon (3 cycles). THF (0.4 mL) was added and the mixture was stirred at room temperature for 5 min. Silyl dienol ether **31** (61.1 mg, 0.27 mmol) and imine **205** (24.9 mg, 0.14 mmol) were added and the resulting suspension was stirred vigorously (1250 rpm) for 65 h. The mixture was diluted with *tert*-butyl methyl ether (10 mL), filtered over a silica plug and the solvent was removed under reduced pressure. The crude product (~80% conversion) was purified by column chromatography (SiO_2, *n*-pentane/*tert*-butyl methyl ether, 4:1 → 3:1) and compound **214** (42.7 mg, 77%) was obtained as a colorless solid. ^{1}H NMR (400 MHz, $CDCl_3$): δ = 7.45 – 7.31 (m, 5H), 6.68 (dd, *J* = 11.8, 0.8 Hz, 1H), 4.98 (dd, *J* = 11.8, 8.1 Hz, 1H), 4.71 (ddd, *J* = 12.1, 7.1, 2.7 Hz, 1H), 4.29 – 4.17 (m, 1H), 4.14 (d, *J* = 7.2 Hz, 1H), 3.93 (d, *J* = 7.5 Hz, 1H), 2.02 (dt, *J* = 14.0, 2.7 Hz, 1H), 1.68 (dt, *J* = 14.1, 11.9 Hz, 1H), 1.22 – 1.10 (m, 3H), 1.09 – 0.99 (m, 18H); ^{13}C NMR (101 MHz, $CDCl_3$): δ = 145.5, 139.5, 129.2, 128.8, 126.6, 109.3, 59.0, 54.7, 38.9, 17.8, 12.0; IR (ATR): $\tilde{\nu}$ = 3362, 2945, 2867, 1664, 1171, 1064, 883, 694 cm^{-1}; HRMS (ESI$^+$): *m/z*: calcd. for $C_{20}H_{34}N_2O_3SiSNa$ $[M+Na]^+$: 433.19516, found: 433.19503.

The relative configuration of **214** was determined based on NOESY data and diagnostic ^3J coupling constants:

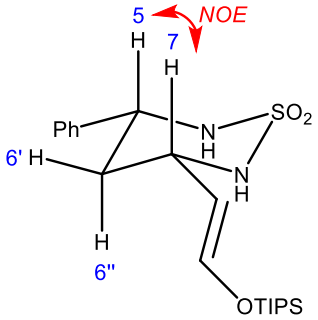

^3J(H6"-H5/H7) = 11.9 Hz -> *trans*

Sulfamide Derivative 216. A flame-dried Schlenk flask was charged with $NiCl_2$(dme) (8.9 mg, 40.5 µmol) and zinc powder (5.3 mg, 80.1 µmol). The Schlenk flask was evacuated and refilled with argon (3 cycles). THF (0.4 mL) was added and the mixture was stirred at room temperature for 5 min. Silyl dienol ether **31** (61.1 mg, 0.27 mmol) and imine **215** (30.6 mg, 0.14 mmol) were added and the resulting suspension was stirred vigorously (1250 rpm) for 5 d. The mixture was diluted with *tert*-butyl methyl ether (10 mL), filtered over a silica plug and the solvent was removed under reduced pressure. The crude product (~70% conversion, dr = 11:1) was purified by column chromatography (SiO_2, *n*-pentane/*tert*-butyl methyl ether, 12:1 → 6:1) and compound **216** (40.0 mg, 65%) was obtained as a colorless solid. ^{1}H NMR (400 MHz, $CDCl_3$): δ = 7.41 – 7.29 (m, 5H), 6.62 (dd, *J* = 11.8, 0.7 Hz, 1H), 4.96 (dd, *J* = 11.8, 9.0 Hz, 1H), 4.71 (ddd, *J* = 11.4, 7.8, 3.3

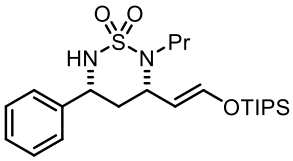

Hz, 1H), 4.34 – 4.19 (m, 1H), 4.05 (d, *J* = 7.8 Hz, 1H), 3.17 (ddd, *J* = 14.3, 9.7, 5.9 Hz, 1H), 3.05 (ddd, *J* = 14.3, 9.6, 6.2 Hz, 1H), 2.01 – 1.78 (m, 2H), 1.76 – 1.58 (m, 2H), 1.24 – 1.10 (m, 3H), 1.07 (d, *J* = 6.5 Hz, 18H), 0.87 (t, J = 7.4 Hz, 3H); ^{13}C NMR (101 MHz, $CDCl_3$): δ = 145.5, 139.6, 129.1, 128.6, 126.4, 108.8, 58.8, 58.2, 47.3, 37.9, 23.2, 17.8, 12.0, 11.3; IR (ATR): $\tilde{\nu}$ = 3251, 2943, 2866, 1651, 1462, 1331, 1166, 1065, 882, 695 cm^{-1}; HRMS (ESI$^+$): *m/z*: calcd. for $C_{23}H_{40}N_2O_3SiSNa$ [M+Na]$^+$: 475.24211, found: 475.24220.

Sulfamide Derivative 218. A flame-dried Schlenk flask was charged with $NiCl_2$(dme) (8.9 mg, 40.5 µmol) and zinc powder (5.3 mg, 80.1 µmol). The Schlenk flask was evacuated and refilled with argon (3 cycles). THF (0.4 mL) was added and the mixture was stirred at room temperature for 5 min. Silyl dienolether **31** (*E*,*E*/*Z*,*E* = 2.3:1, 65.0 mg, 0.27 mmol) and imine **205** (24.9 mg, 0.14 mmol) were added and the resulting suspension was stirred vigorously (1250 rpm) for 72 h. The mixture was diluted with *tert*-butyl methyl ether (10 mL), filtered over a silica plug and the solvent was removed under reduced pressure. The crude product (~70% conversion, dr = 11:1) was purified by column chromatography (SiO_2, *n*-pentane/*tert*-butyl methyl ether, 10:1 → 3:1) and compound **218** (29.0 mg, 51%, dr = 1.2:1) was obtained as a colorless solid. ***Note:*** The relative configuration of the two diastereomers was confirmed by NOESY data.

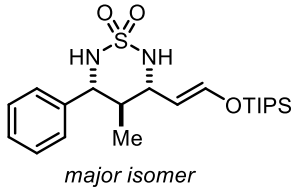

major isomer

for major 1,2-anti-isomer: ^{1}H NMR (400 MHz, $CDCl_3$): δ = 7.40 – 7.36 (m, 2H), 7.36 – 7.32 (m, 1H), 7.32 – 7.29 (m, 2H), 6.67 (dd, *J* = 11.7, 0.5 Hz, 1H), 4.89 (dd, *J* = 11.7, 9.3 Hz, 1H), 4.31 – 4.26 (m, 2H), 4.12 (d, *J* = 6.9 Hz, 1H), 3.87 – 3.79 (m, 1H), 1.80 – 1.72 (m, 1H), 1.21 – 1.12 (m, 3H), 1.10 – 1.05 (m, 18H), 0.69 (d, *J* = 6.7 Hz, 3H); ^{13}C NMR (101 MHz, $CDCl_3$): δ = 146.6, 138.9, 129.2, 128.9, 127.6, 108.8, 65.9, 61.0, 40.6, 17.8, 17.8, 14.2, 12.0; *for minor 1,2-syn-isomer:* ^{1}H NMR (400 MHz, $CDCl_3$): δ = 7.40 – 7.36 (m, 2H), 7.32 – 7.29 (m, 1H), 7.25 – 7.20 (m, 2H), 6.68 (dd, *J* = 11.8, 1.0 Hz, 1H), 5.01 (dd, *J* = 11.8, 7.9 Hz, 1H), 4.96 (dd, *J* = 8.0, 2.7 Hz, 1H), 4.42 (tdd, *J* = 7.8, 2.7, 1.0 Hz, 1H), 4.33 (d, *J* = 8.0 Hz, 1H), 4.02 (d, *J* = 7.7 Hz, 1H), 1.96 (qt, *J* = 7.0, 2.7 Hz, 1H), 1.21 – 1.12 (m, 3H); 1.10 – 1.05 (m, 18H), 0.75 (d, *J* = 7.0 Hz, 3H); ^{13}C NMR (101 MHz, $CDCl_3$): δ = 145.4, 138.1, 128.9, 128.0, 125.9, 107.6, 62.3, 58.4, 37.5, 17.8, 12.1, 4.5; IR (ATR): $\tilde{\nu}$ = 3263, 2944, 2867, 1663, 1457, 1339, 1174, 938, 883, 687 cm^{-1}; HRMS (ESI$^+$): *m/z*: calcd. for $C_{21}H_{36}N_2O_3SiSNa$ [M+Na]$^+$: 447.21081, found: 447.21073.

6 Bibliography

[1] P. Sabatier, *Catalysis in Organic Chemistry*, **1922**.
[2] V. P. Ananikov, *ACS Catal.* **2015**, *5*, *3*, 1964–1971.
[3] N. Hazari, P. R. Melvin, M. M. Beromi, *Nat. Rev. Chem.* **2017**, *1*, *3*, 0025.
[4] K. Ziegler, *Angew. Chem.* **1952**, *64*, *12*, 323–329.
[5] K. Ziegler, E. Holzkamp, H. Breil, H. Martin, *Angew. Chem.* **1955**, *67*, *19-20*, 541–547.
[6] M. W. Haenel, *Karl Ziegler: Historical Landmarks of Chemistry; Max-Planck-Institut für Kohlenforschung: Mülheim an der Ruhr*, **2008**.
[7] K. Fischer, K. Jonas, P. Misbach, R. Stabba, G. Wilke, *Angew. Chem.* **1973**, *85*, *23*, 1001–1012.
[8] K. Fischer, K. Jonas, G. Wilke, *Angew. Chem. Int. Ed.* **1973**, *12*, *7*, 565–566.
[9] L. Nattmann, R. Saeb, N. Nöthling, J. Cornella, *Nat. Catal.* **2020**, *3*, *1*, 6–13.
[10] L. Nattmann, J. Cornella, *Organometallics* **2020**, *39*, *18*, 3295–3300.
[11] V. T. Tran, Z.-Q. Li, O. Apolinar, J. Derosa, M. V. Joannou, S. R. Wisniewski, M. D. Eastgate, K. M. Engle, *Angew. Chem. Int. Ed.* **2020**, *59*, *19*, 7409–7413.
[12] V. T. Tran, N. Kim, C. Z. Rubel, X. Wu, T. Kang, T. C. Jankins, Z.-Q. Li, M. V. Joannou, S. Ayers, M. Gembicky, J. Bailey, E. J. Sturgell, B. B. Sanchez, J. S. Chen, S. Lin, M. D. Eastgate, S. R. Wisniewski, K. M. Engle, *Angew. Chem. Int. Ed.* **2023**, *62*, *9*, e202211794.
[13] C. Z. Rubel, W.-J. He, S. R. Wisniewski, K. M. Engle, *Acc. Chem. Res.* **2024**, *57*, *3*, 312–326.
[14] J. Li, P. Wang, B. Bai, Y. Xiao, Y.-F. Wan, Y. Yan, F. Li, G. Song, G. Li, C. Wang, X.-P. Zhang, J. Dong, T. Kang, D. Xue, *J. Am. Chem. Soc.* **2025**, *147*, *7*, 5851–5859.
[15] F. Flecken, S. Hanf, *Eur. J. Inorg. Chem.* **2026**, *29*, *10*, e202500564.
[16] B. Bogdanović, P. Heimbach, M. Kröner, G. Wilke, J. Brandt, *Justus Liebigs Ann. Chem.* **1969**, *727*, *1*, 143–160.
[17] R. Benn, B. Büssemeier, S. Holle, P. W. Jolly, R. Mynott, I. Tkatchenko, G. Wilke, *J. Organomet. Chem.* **1985**, *279*, *1*, 63–86.
[18] Y. Tamaru, *Modern Organonickel Chemistry*, **2005**, Wiley-VCH Verlag GmbH & Co. KGaA.
[19] R. Baker, B. N. Blackett, R. C. Cookson, R. C. Cross, D. P. Madden, *J. Chem. Soc., Chem. Commun.* **1972**, *6*, 343–344.
[20] R. Baker, M. J. Crimmin, *J. Chem. Soc., Perkin Trans. 1* **1979**, *0*, 1264–1267.
[21] Y. Sato, M. Takimoto, K. Hayashi, T. Katsuhara, K. Takagi, M. Mori, *J. Am. Chem. Soc.* **1994**, *116*, *21*, 9771–9772.
[22] M.-C. P. Yeh, J.-H. Liang, Y.-L. Jiang, M.-S. Tsai, *Tetrahedron* **2003**, *59*, *19*, 3409–3415.
[23] Y. Sato, N. Saito, M. Mori, *Chem. Lett.* **2002**, *31*, *1*, 18–19.
[24] N. Saito, M. Mori, Y. Sato, *J. Organomet. Chem.* **2007**, *692*, *1*, 460–471.
[25] K. Shibata, M. Kimura, M. Shimizu, Y. Tamaru, *Org. Lett.* **2001**, *3*, *14*, 2181–2183.
[26] Y. Sato, N. Saito, M. Mori, *Tetrahedron* **1998**, *54*, *7*, 1153–1168.
[27] Y. Sato, N. Saito, M. Mori, *J. Am. Chem. Soc.* **2000**, *122*, *10*, 2371–2372.
[28] Y. Sato, N. Saito, M. Mori, *J. Org. Chem.* **2002**, *67*, *26*, 9310–9317.
[29] S. Ogoshi, *Nickel Catalysis in Organic Synthesis: Methods and Reactions*, **2019**, Wiley-VCH Verlag GmbH & Co. KGaA.
[30] E. Oblinger, J. Montgomery, *J. Am. Chem. Soc.* **1997**, *119*, *38*, 9065–9066.
[31] X.-Q. Tang, J. Montgomery, *J. Am. Chem. Soc.* **1999**, *121*, *25*, 6098–6099.
[32] W.-S. Huang, J. Chan, T. F. Jamison, *Org. Lett.* **2000**, *2*, *26*, 4221–4223.
[33] E. A. Colby, T. F. Jamison, *J. Org. Chem.* **2003**, *68*, *1*, 156–166.
[34] K. M. Miller, W.-S. Huang, T. F. Jamison, *J. Am. Chem. Soc.* **2003**, *125*, *12*, 3442–3443.
[35] K. M. Miller, T. F. Jamison, *Org. Lett.* **2005**, *7*, *14*, 3077–3080.
[36] M. R. Chaulagain, G. J. Sormunen, J. Montgomery, *J. Am. Chem. Soc.* **2007**, *129*, *31*, 9568–9569.
[37] Y. Yang, S.-F. Zhu, C.-Y. Zhou, Q.-L. Zhou, *J. Am. Chem. Soc.* **2008**, *130*, *43*, 14052–14053.
[38] C.-Y. Zhou, S.-F. Zhu, L.-X. Wang, Q.-L. Zhou, *J. Am. Chem. Soc.* **2010**, *132*, *32*, 10955–10957.
[39] W. Fu, M. Nie, A. Wang, Z. Cao, W. Tang, *Angew. Chem. Int. Ed.* **2015**, *54*, *8*, 2520–2524.
[40] G. Liu, W. Fu, X. Mu, T. Wu, M. Nie, K. Li, X. Xu, W. Tang, *Commun. Chem.* **2018**, *1*, *1*, 90.
[41] W. Chen, Y. Cheng, T. Zhang, Y. Mu, W. Jia, G. Liu, *J. Org. Chem.* **2021**, *86*, *7*, 5166–5182.

[42] Y. Hayashi, Y. Hoshimoto, R. Kumar, M. Ohashi, S. Ogoshi, *Chem. Commun.* **2016**, *52*, *37*, 6237–6240.
[43] Y. Hayashi, Y. Hoshimoto, R. Kumar, M. Ohashi, S. Ogoshi, *Chem. Lett.* **2017**, *46*, *8*, 1096–1098.
[44] X.-Y. Sun, X.-R. Liu, Y.-W. Huang, Q.-L. Zhou, L.-J. Xiao, *Org. Lett.* **2026**, *28*, *7*, 2512–2517.
[45] Y.-Q. Li, J.-M. Liu, X. Liu, L.-X. Ruan, S.-L. Shi, *Org. Lett.* **2026**, *28*, *7*, 2460–2464.
[46] S. Ghosh, A. Rooj, R. Chakrabortty, V. Ganesh, *Org. Lett.* **2024**, *26*, *18*, 4024–4029.
[47] S. Ghosh, A. Khamrai, V. Ganesh, *Org. Lett.* **2025**, *27*, *45*, 12549–12554.
[48] M. Takimoto, Y. Hiraga, Y. Sato, M. Mori, *Tetrahedron Lett.* **1998**, *39*, *25*, 4543–4546.
[49] R. Sawaki, Y. Sato, M. Mori, *Org. Lett.* **2004**, *6*, *7*, 1131–1133.
[50] M. Kimura, A. Ezoe, K. Shibata, Y. Tamaru, *J. Am. Chem. Soc.* **1998**, *120*, *16*, 4033–4034.
[51] M. Kimura, A. Ezoe, M. Mori, K. Iwata, Y. Tamaru, *J. Am. Chem. Soc.* **2006**, *128*, *26*, 8559–8568.
[52] M. Kimura, H. Fujimatsu, A. Ezoe, K. Shibata, M. Shimizu, S. Matsumoto, Y. Tamaru, *Angew. Chem. Int. Ed.* **1999**, *38*, *3*, 397–400.
[53] T.-P. Loh, H.-Y. Song, Y. Zhou, *Org. Lett.* **2002**, *4*, *16*, 2715–2717.
[54] P. R. McCarren, P. Liu, P. H.-Y. Cheong, T. F. Jamison, K. N. Houk, *J. Am. Chem. Soc.* **2009**, *131*, *19*, 6654–6655.
[55] S. Ogoshi, K.-i. Tonomori, M.-a. Oka, H. Kurosawa, *J. Am. Chem. Soc.* **2006**, *128*, *21*, 7077–7086.
[56] Y. Sato, R. Sawaki, N. Saito, M. Mori, *J. Org. Chem.* **2002**, *67*, *3*, 656–662.
[57] M. Kimura, A. Ezoe, S. Tanaka, Y. Tamaru, *Angew. Chem. Int. Ed.* **2001**, *40*, *19*, 3600–3602.
[58] M. Kimura, A. Miyachi, K. Kojima, S. Tanaka, Y. Tamaru, *J. Am. Chem. Soc.* **2004**, *126*, *44*, 14360–14361.
[59] T. Mori, Y. Akioka, G. Onodera, M. Kimura, *Molecules* **2014**, *19*, *7*, 9288–306.
[60] M. Kimura, K. Shibata, Y. Koudahashi, Y. Tamaru, *Tetrahedron Lett.* **2000**, *41*, *35*, 6789–6793.
[61] M. Kimura, S. Matsuo, K. Shibata, Y. Tamaru, *Angew. Chem. Int. Ed.* **1999**, *38*, *22*, 3386–3388.
[62] K. Shibata, M. Kimura, K. Kojima, S. Tanaka, Y. Tamaru, *J. Organomet. Chem.* **2001**, *624*, *1*, 348–353.
[63] A. Ezoe, M. Kimura, T. Inoue, M. Mori, Y. Tamaru, *Angew. Chem. Int. Ed.* **2002**, *41*, *15*, 2784–2786.
[64] M. Kimura, K. Kojima, Y. Tamaru, *Synthesis* **2004**, *18*, 3089–3091.
[65] M. Kimura, A. Ezoe, M. Mori, Y. Tamaru, *J. Am. Chem. Soc.* **2005**, *127*, *1*, 201–209.
[66] H. Y. Cho, J. P. Morken, *J. Am. Chem. Soc.* **2008**, *130*, *48*, 16140–16141.
[67] H. Y. Cho, J. P. Morken, *J. Am. Chem. Soc.* **2010**, *132*, *22*, 7576–7577.
[68] S. Jiang, T. Zhang, X.-Y. Luo, S. Dong, J.-T. Ma, L.-J. Xiao, *Angew. Chem. Int. Ed.* **2025**, *64*, *24*, e202504494.
[69] N. Saito, T. Yamazaki, Y. Sato, *Tetrahedron Lett.* **2008**, *49*, *34*, 5073–5076.
[70] D. T. Mickles, C. Westlund, J. S. Marcum, S. J. Meek, *Org. Lett.* **2025**, *27*, *50*, 13886–13891.
[71] Y.-Q. Li, G. Chen, S.-L. Shi, *Org. Lett.* **2021**, *23*, *7*, 2571–2577.
[72] X.-W. Han, T. Zhang, W.-W. Yao, H. Chen, M. Ye, *CCS Chemistry* **2020**, *3*, *3*, 955–963.
[73] M. Holmes, L. A. Schwartz, M. J. Krische, *Chem. Rev.* **2018**, *118*, *12*, 6026–6052.
[74] Y. Yang, S.-F. Zhu, H.-F. Duan, C.-Y. Zhou, L.-X. Wang, Q.-L. Zhou, *J. Am. Chem. Soc.* **2007**, *129*, *8*, 2248–2249.
[75] Y. Sato, Y. Hinata, R. Seki, Y. Oonishi, N. Saito, *Org. Lett.* **2007**, *9*, *26*, 5597–5599.
[76] K.-X. Zhang, M.-Y. Liu, B.-Y. Yao, Q.-L. Zhou, L.-J. Xiao, *J. Am. Chem. Soc.* **2024**, *146*, *32*, 22157–22165.
[77] M. Zhang, M. Luo, G. Zhao, H. Wang, *Angew. Chem. Int. Ed.* **2025**, *64*, *37*, e202510690.
[78] N. Saito, A. Kobayashi, Y. Sato, *Angew. Chem. Int. Ed.* **2012**, *51*, *5*, 1228–1231.
[79] J.-T. Ma, T. Zhang, B.-Y. Yao, L.-J. Xiao, Q.-L. Zhou, *J. Am. Chem. Soc.* **2023**, *145*, *35*, 19195–19201.
[80] J. S. Marcum, S. J. Meek, *J. Am. Chem. Soc.* **2022**, *144*, *42*, 19231–19237.
[81] J.-T. Ma, B.-Y. Yao, T. Zhang, S.-H. Cheng, B. Xuan, M. Ye, Q.-L. Zhou, L.-J. Xiao, *J. Am. Chem. Soc.* **2025**, *147*, *49*, 45648–45659.

[82] X.-R. Liu, X.-Y. Luo, Y.-Q. Wang, W.-J. Nan, M.-Y. Liu, W.-G. Xiao, M. Ye, Q.-L. Zhou, L.-J. Xiao, *Angew. Chem. Int. Ed.* **2026**, *n/a*, *n/a*, e2370635.
[83] M. Heinrich, J. J. Murphy, M. K. Ilg, A. Letort, J. Flasz, P. Philipps, A. Fürstner, *Angew. Chem. Int. Ed.* **2018**, *57*, *41*, 13575–13581.
[84] M. Heinrich, J. J. Murphy, M. K. Ilg, A. Letort, J. T. Flasz, P. Philipps, A. Fürstner, *J. Am. Chem. Soc.* **2020**, *142*, *13*, 6409–6422.
[85] M. P. Paudyal, N. P. Rath, C. D. Spilling, *Org. Lett.* **2010**, *12*, *13*, 2954–2957.
[86] J. J. Murphy, *Final Research Report* **2019**, Max-Planck-Institut für Kohlenforschung.
[87] T. Mukaiyama, H. Uchiro, I. Shiina, S. Kobayashi, *Chem. Lett.* **1990**, *19*, *6*, 1019–1022.
[88] T. Mukaiyama, I. Shiina, H. Uchiro, S. Kobayashi, *Bull. Chem. Soc. Jpn.* **1994**, *67*, *6*, 1708–1716.
[89] S. E. Denmark, W.-j. Chung, *Angew. Chem. Int. Ed.* **2008**, *47*, *10*, 1890–1892.
[90] T. Q. Davies, J. J. Murphy, M. Dousset, A. Fürstner, *J. Am. Chem. Soc.* **2021**, *143*, *34*, 13489–13494.
[91] T. Roth, H. Wadepohl, D. S. Wright, L. H. Gade, *Chem. Eur. J.* **2013**, *19*, *41*, 13823–13837.
[92] J. Bao, W. D. Wulff, J. B. Dominy, M. J. Fumo, E. B. Grant, A. C. Rob, M. C. Whitcomb, S.-M. Yeung, R. L. Ostrander, A. L. Rheingold, *J. Am. Chem. Soc.* **1996**, *118*, *14*, 3392–3405.
[93] Z. Ding, W. E. G. Osminski, H. Ren, W. D. Wulff, *Org. Process Res. Dev.* **2011**, *15*, *5*, 1089–1107.
[94] H. Harada, R. K. Thalji, R. G. Bergman, J. A. Ellman, *J. Org. Chem.* **2008**, *73*, *17*, 6772–6779.
[95] A. Z. González, D. Benitez, E. Tkatchouk, W. A. Goddard, III, F. D. Toste, *J. Am. Chem. Soc.* **2011**, *133*, *14*, 5500–5507.
[96] F. Verdugo, L. Villarino, J. Durán, M. Gulías, J. L. Mascareñas, F. López, *ACS Catal.* **2018**, *8*, *7*, 6100–6105.
[97] S. Zhang, S. Zhang, Y. Fan, X. Zhang, J. Chen, C. Jin, S. Chen, L. Wang, Q. Zhang, Y. Chen, *Angew. Chem. Int. Ed.* **2023**, *62*, *51*, e202313186.
[98] J. Y. Kim, T. Q. Davies, A. Fürstner, *Chem. Commun.* **2023**, *59*, *84*, 12613–12616.
[99] T. Q. Davies, J. Y. Kim, A. Fürstner, *J. Am. Chem. Soc.* **2022**, *144*, *41*, 18817–18822.
[100] X. Yan, W. Feng, J. X. Ng, J. Li, Y. Liu, B. Zhang, P.-L. Shao, Y. Zhao, *Chem. Soc. Rev.* **2025**, *54*, *17*, 7966–8018.
[101] S. C. Bergmeier, *Tetrahedron* **2000**, *56*, *17*, 2561–2576.
[102] D. J. Ager, I. Prakash, D. R. Schaad, *Chem. Rev.* **1996**, *96*, *2*, 835–876.
[103] According to a Reaxys search conducted on 30 July 2026 using the generic vicinal amino alcohol motif as the query structure.
[104] T. S. Kaufman, E. A. Rúveda, *Angew. Chem. Int. Ed.* **2005**, *44*, *6*, 854–885.
[105] N. D. Ridgway, R. S. McLeod, *Biochemistry of Lipids, Lipoproteins and Membranes*, **2021**.
[106] Y. A. Hannun, L. M. Obeid, *Nat. Rev. Mol. Cell Biol.* **2008**, *9*, *2*, 139–150.
[107] Y. A. Hannun, L. M. Obeid, *Nat. Rev. Mol. Cell Biol.* **2018**, *19*, *3*, 175–191.
[108] K. Radkowski, A. Fürstner, *Adv. Synth. Catal.* **2022**, *364*, *19*, 3342–3347.
[109] H. Umezawa, T. Aoyagi, H. Morishima, M. Matsuzaki, M. Hamada, T. Takeuchi, *J. Antibiot.* **1970**, *23*, *5*.
[110] J. Marciniszyn, J. A. Hartsuck, J. Tang, *J. Biol. Chem.* **1976**, *251*, *22*, 7088–7094.
[111] S. Sritharan, N. Sivalingam, *Life Sci.* **2021**, *278*, 119527.
[112] D. S. Goldstein, *Cardiovasc. Drug Rev.* **2006**, *24*, *3-4*, 189–203.
[113] K. J. Palmer, S. M. Holliday, R. N. Brogden, *Drugs* **1993**, *45*, *3*, 430–75.
[114] L. A. F. Andrade, J. M. Silla, M. P. Freitas, *J. Mol. Struct.* **2014**, *1072*, 203–207.
[115] D. E. Frantz, R. Fässler, E. M. Carreira, *J. Am. Chem. Soc.* **2000**, *122*, *8*, 1806–1807.
[116] F. González-Bobes, G. C. Fu, *J. Am. Chem. Soc.* **2006**, *128*, *16*, 5360–5361.
[117] G. Desimoni, G. Faita, P. Quadrelli, *Chem. Rev.* **2003**, *103*, *8*, 3119–3154.
[118] Y. Hayashi, H. Gotoh, T. Hayashi, M. Shoji, *Angew. Chem. Int. Ed.* **2005**, *44*, *27*, 4212–4215.
[119] M. Marigo, T. C. Wabnitz, D. Fielenbach, K. A. Jørgensen, *Angew. Chem. Int. Ed.* **2005**, *44*, *5*, 794–797.
[120] K. L. Jensen, G. Dickmeiss, H. Jiang, Ł. Albrecht, K. A. Jørgensen, *Acc. Chem. Res.* **2011**, *45*, *2*, 248–264.
[121] L. Deloux, M. Srebnik, *Chem. Rev.* **1993**, *93*, *2*, 763–784.
[122] P. Gupta, N. Mahajan, *New J. Chem.* **2018**, *42*, *15*, 12296–12327.

[123] K. Spielmann, M. Xiang, L. A. Schwartz, M. J. Krische, *J. Am. Chem. Soc.* **2019**, *141*, *36*, 14136–14141.
[124] S. L. Gargaro, R. K. Klake, K. L. Burns, S. O. Elele, S. L. Gentry, J. D. Sieber, *Org. Lett.* **2019**, *21*, *23*, 9753–9758.
[125] R. K. Klake, M. D. Edwards, J. D. Sieber, *Org. Lett.* **2021**, *23*, *16*, 6444–6449.
[126] S. Collins, J. D. Sieber, *Org. Lett.* **2023**, *25*, *9*, 1425–1430.
[127] R. K. Klake, J. D. Sieber, *Org. Lett.* **2023**, *25*, *25*, 4730–4734.
[128] S. L. Gargaro, R. K. Klake, J. D. Sieber, *Org. Lett.* **2023**, *25*, *25*, 4644–4649.
[129] K. Li, X. Shao, L. Tseng, S. J. Malcolmson, *J. Am. Chem. Soc.* **2018**, *140*, *2*, 598–601.
[130] J. Zhu, F. Rahim, P. Zhou, A. Zhang, S. J. Malcolmson, *J. Am. Chem. Soc.* **2024**, *146*, *29*, 20270–20278.
[131] T. Hashimoto, H. Nakatsu, K. Maruoka, *Angew. Chem. Int. Ed.* **2015**, *54*, *15*, 4617–4621.
[132] T. Q. Davies, *Unpublished Results* **2021**.
[133] N. Gauvry, F. Huet, *J. Org. Chem.* **2001**, *66*, *2*, 583–588.
[134] T. Bender, A. Fürstner, *J. Am. Chem. Soc.* **2024**, *146*, *49*, 33295–33301.
[135] H. Shimasaki, H. Kagechika, H. Fukasawa, E. Kawachi, K. Shudo, *Chem. Pharm. Bull.* **1995**, *43*, *1*, 100–107.
[136] T. Varlet, M. Matišić, E. Van Elslande, L. Neuville, V. Gandon, G. Masson, *J. Am. Chem. Soc.* **2021**, *143*, *30*, 11611–11619.
[137] S. Bräse, C. Gil, K. Knepper, V. Zimmermann, *Angew. Chem. Int. Ed.* **2005**, *44*, *33*, 5188–5240.
[138] Y. Guan, Z. Ding, W. D. Wulff, *Chem. Eur. J.* **2013**, *19*, *46*, 15565–15571.
[139] X. Yin, L. Zheng, A. Mohammadlou, B. R. Cagnon, W. D. Wulff, *J. Org. Chem.* **2020**, *85*, *16*, 10432–10450.
[140] E. Milner, W. McCalmont, J. Bhonsle, D. Caridha, D. Carroll, S. Gardner, L. Gerena, M. Gettayacamin, C. Lanteri, T. Luong, V. Melendez, J. Moon, N. Roncal, J. Sousa, A. Tungtaeng, P. Wipf, G. Dow, *Bioorg. Med. Chem. Lett.* **2010**, *20*, *4*, 1347–1351.
[141] Z.-X. Xie, L.-Z. Zhang, X.-J. Ren, S.-Y. Tang, Y. Li, *Chin. J. Chem.* **2008**, *26*, *7*, 1272–1276.
[142] E. J. Rastelli, D. M. Coltart, *Angew. Chem. Int. Ed.* **2015**, *54*, *47*, 14070–14074.
[143] I. Kreituss, K.-Y. Chen, S. H. Eitel, J.-M. Adam, G. Wuitschik, A. Fettes, J. W. Bode, *Angew. Chem. Int. Ed.* **2016**, *55*, *4*, 1553–1556.
[144] A. H. J. Engwerda, R. Maassen, P. Tinnemans, H. Meekes, F. P. J. T. Rutjes, E. Vlieg, *Angew. Chem. Int. Ed.* **2019**, *58*, *6*, 1670–1673.
[145] R. Ohta, Y. Shio, T. Akiyama, M. Yamada, K. Harada, M. Arisawa, *New J. Chem.* **2023**, *47*, *16*, 7694–7700.
[146] A. Berlie, I. Terry, M. Szablewski, *J. Clust. Sci.* **2013**, *24*, *4*, 1057–1066.
[147] S. Balasubramaniam, I. S. Aidhen, *Synthesis* **2008**, *23*, 3707–3738.
[148] T. Koike, M. Tanabe, N. Takeuchi, S. Tobinaga, *Chem. Pharm. Bull.* **1997**, *45*, *2*, 243–248.
[149] M. Mąkosza, *Chem. Eur. J.* **2014**, *20*, *19*, 5536–5545.
[150] L. E. Overman, C. B. Petty, T. Ban, G. T. Huang, *J. Am. Chem. Soc.* **1983**, *105*, *20*, 6335–6337.
[151] S. R. Pollack, A. Dion, *J. Org. Chem.* **2021**, *86*, *17*, 11748–11762.
[152] J. E. Mathieson, J. J. Crawford, M. Schmidtmann, R. Marquez, *Org. Biomol. Chem.* **2009**, *7*, *10*, 2170–2175.
[153] A. E. Pasqua, F. D. Ferrari, J. J. Crawford, R. Marquez, *Tetrahedron Lett.* **2014**, *55*, *44*, 6042–6043.
[154] T. R. Hoye, C. S. Jeffrey, F. Shao, *Nat. Protoc.* **2007**, *2*, *10*, 2451–8.
[155] J. L. García Ruano, J. Alemán, M. B. Cid, *Synthesis* **2006**, *4*, 687–691.
[156] Y. Yang, D. P. Phillips, S. Pan, *Tetrahedron Lett.* **2011**, *52*, *14*, 1549–1552.
[157] C. Bhat, S. T. Bugde, S. G. Tilve, *Synthesis* **2014**, *46*, *19*, 2551–2573.
[158] C. K. W. Lai, O. P. Twentyman, S. T. Holgate, *Am. Rev. Respir. Dis.* **1989**, *140*, *4*, 917–923.
[159] S. Kano, Y. Yuasa, T. Yokomatsu, S. Shibuya, *Heterocycles* **1988**, *27*, 1241–1248.
[160] E. A. Standley, S. Z. Tasker, K. L. Jensen, T. F. Jamison, *Acc. Chem. Res.* **2015**, *48*, *5*, 1503–1514.
[161] Y. Hoshimoto, M. Ohashi, S. Ogoshi, *Acc. Chem. Res.* **2015**, *48*, *6*, 1746–1755.
[162] J. Y. Kim, *Final Research Report* **2024**.
[163] M. E. Jung, G. Piizzi, *Chem. Rev.* **2005**, *105*, *5*, 1735–1766.

[164] P. Gabko, M. Kalník, M. Bella, *Beilstein J. Org. Chem.* **2025**, *21*, 1324–1373.
[165] M. E. Jung, J. Gervay, *J. Am. Chem. Soc.* **1991**, *113*, *1*, 224–232.
[166] Y. Ji, Q. Gao, W. Han, B. Fang, *Catalysts* **2024**, *14*, *12*, 884.
[167] M. Chrzanowska, M. D. Rozwadowska, *Chem. Rev.* **2004**, *104*, *7*, 3341–3370.
[168] J. D. Scott, R. M. Williams, *Chem. Rev.* **2002**, *102*, *5*, 1669–1730.
[169] W. Liu, S. Liu, R. Jin, H. Guo, J. Zhao, *Org. Chem. Front.* **2015**, *2*, *3*, 288–299.
[170] M. Chrzanowska, A. Grajewska, M. D. Rozwadowska, *Chem. Rev.* **2016**, *116*, *19*, 12369–12465.
[171] M. M. A. Asif, S. R. Lisa, N. Qais, *RSC Adv.* **2023**, *13*, *16*, 11010–11036.
[172] E. Anakabe, Jose L. Vicario, D. Badía, L. Carrillo, V. Yoldi, *Eur. J. Org. Chem.* **2001**, *2001*, *22*, 4343–4352.
[173] K. W. Bentley, *Nat. Prod. Rep.* **2006**, *23*, *3*, 444–63.
[174] S. Purser, P. R. Moore, S. Swallow, V. Gouverneur, *Chem. Soc. Rev.* **2008**, *37*, *2*, 320–330.
[175] T. Liang, C. N. Neumann, T. Ritter, *Angew. Chem. Int. Ed.* **2013**, *52*, *32*, 8214–8264.
[176] N. A. Meanwell, *J. Med. Chem.* **2018**, *61*, *14*, 5822–5880.
[177] J. Ranjith, H.-J. Ha, *Molecules* **2021**, *26*, *6*, 1774.
[178] R.-N. Guo, X.-F. Cai, L. Shi, Z.-S. Ye, M.-W. Chen, Y.-G. Zhou, *Chem. Commun.* **2013**, *49*, *76*, 8537–8539.
[179] M.-W. Chen, Y. Ji, J. Wang, Q.-A. Chen, L. Shi, Y.-G. Zhou, *Org. Lett.* **2017**, *19*, *18*, 4988–4991.
[180] Y. Zheng, C. M. Tice, S. B. Singh, *Bioorg. Med. Chem. Lett.* **2014**, *24*, *16*, 3673–3682.
[181] E. V. Litskan, S. V. Lynnyk, R. H. Shypov, B. V. Vashchenko, A. Y. Hoida, O. O. Klymenko-Ulianov, A. O. Gorlova, D. S. Granat, O. O. Grygorenko, D. M. Volochnyuk, S. V. Ryabukhin, *Chem. Eur. J.* **2025**, *31*, *51*, e00940.
[182] V. Kubyshkin, P. K. Mykhailiuk, *Chem. Rev.* **2026**, *126*, *6*, 3829–3882.
[183] S. R. Chemler, *Curr. Bioact. Compd.* **2009**, *5*, *1*, 2–19.
[184] Z. Li, Z. Jin, R. Huang, *Synthesis* **2001**, *16*, 2365–2378.
[185] X. Yang, Q. Shi, S.-C. Yang, C.-Y. Chen, S.-L. Yu, K. F. Bastow, S. L. Morris-Natschke, P.-C. Wu, C.-Y. Lai, T.-S. Wu, S.-L. Pan, C.-M. Teng, J.-C. Lin, P.-C. Yang, K.-H. Lee, *J. Med. Chem.* **2011**, *54*, *14*, 5097–5107.
[186] For a synthetic study into this family from our laboratory, see: Kennedy, J. W. J; Fürstner, A. *Chem. Eur. J.* **2006**, *12*, 7398-7410.
[187] Z. Wang, M. Wu, Y. Wang, Z. Li, L. Wang, G. Han, F. Chen, Y. Liu, K. Wang, A. Zhang, L. Meng, Q. Wang, *Eur. J. Med. Chem.* **2012**, *51*, 250–258.
[188] For an early study into the antifungal properties of hydroxylated phenanthroquinolizidines, see: Foldeak, S. *Tetrahedron* **1971**, *27*, 3465-3476.
[189] W. Gao, A. P.-C. Chen, C.-H. Leung, E. A. Gullen, A. Fürstner, Q. Shi, L. Wei, K.-H. Lee, Y.-C. Cheng, *Bioorg. Med. Chem. Lett.* **2008**, *18*, *2*, 704–709.
[190] P. Šafář, Š. Marchalín, B. Balónová, M. Šoral, J. Moncol, A. Ghinet, B. Rigo, A. Daïch, *Eur. J. Org. Chem.* **2018**, *2018*, *40*, 5499–5511.
[191] T. Pagáč, P. Šafář, Š. Marchalín, Z. Ježíková, B. Balónová, M. Šupolíková, E. Nováková, J. Kubíčková, M. Šoral, J. Sivý, P. Olejníková, *Monatsh. Chem.* **2018**, *149*, *10*, 1865–1876.
[192] J. Kubíčková, K. Elefantová, L. Pavlikova, M. Cagala, M. Šereš, P. Šafář, Š. Marchalín, K. Ďurišová, V. Boháčová, Z. Sulova, B. Lakatoš, A. Breier, P. Olejníková, *Molecules* **2019**, *24*, *11*, 2127.
[193] M. Suffness, J. Douros, *Med. Chem.* **1980**, *16*, 465 – 487.
[194] For an inital study on hydroxylated Antofine and Cryptopleurine analogs see: Yang, X.; Shi, Q.; Lai, C.-Y.; Chen, C.-Y.; Ohkoshi, E.; Yang, S.-C., *et al*. *Journal of Medicinal Chemistry* **2012**, *55*, *15*, 6751–6761.
[195] H. C. Kolb, M. S. VanNieuwenhze, K. B. Sharpless, *Chem. Rev.* **1994**, *94*, *8*, 2483–2547.
[196] M. Kimura, D. Nojiri, M. Fukushima, S. Oi, Y. Sonoda, Y. Inoue, *Org. Lett.* **2009**, *11*, *17*, 3794–3797.
[197] M. Fukushima, D. Takushima, M. Kimura, *J. Am. Chem. Soc.* **2010**, *132*, *46*, 16346–16348.
[198] Z.-C. Chen, Q. Ouyang, W. Du, Y.-C. Chen, *J. Am. Chem. Soc.* **2024**, *146*, *10*, 6422–6437.
[199] B.-X. Xiao, B. Jiang, R.-J. Yan, J.-X. Zhu, K. Xie, X.-Y. Gao, Q. Ouyang, W. Du, Y.-C. Chen, *J. Am. Chem. Soc.* **2021**, *143*, *12*, 4809–4816.

[200] R.-R. Liu, D.-J. Wang, L. Wu, B. Xiang, G.-Q. Zhang, J.-R. Gao, Y.-X. Jia, *ACS Catal.* **2015**, *5*, *11*, 6524–6528.
[201] L.-J. Xiao, C.-Y. Zhao, L. Cheng, B.-Y. Feng, W.-M. Feng, J.-H. Xie, X.-F. Xu, Q.-L. Zhou, *Angew. Chem. Int. Ed.* **2018**, *57*, *13*, 3396–3400.
[202] W.-G. Xiao, B. Xuan, L.-J. Xiao, Q.-L. Zhou, *Chem. Sci.* **2023**, *14*, *32*, 8644–8650.
[203] Y.-W. Huang, T. Zhang, S.-H. Cheng, Q.-L. Zhou, L.-J. Xiao, *J. Am. Chem. Soc.* **2025**, *147*, *39*, 35675–35683.
[204] Y. Du, L. Zhang, S. Duan, X. Yang, S. Liu, H. Zhang, P. J. Walsh, X. Yang, *J. Am. Chem. Soc.* **2025**, *147*, *33*, 30190–30198.
[205] J.-X. Zhu, Z.-C. Chen, W. Du, Y.-C. Chen, *Angew. Chem. Int. Ed.* **2022**, *61*, *17*, e202200880.
[206] J.-B. Lu, S.-Y. Liang, W.-T. Gui, Z.-C. Chen, W. Du, Y.-C. Chen, *Org. Lett.* **2023**, *25*, *4*, 576–580.
[207] J. Pan, T. O. Ho, Y.-C. Chen, B.-M. Yang, Y. Zhao, *Angew. Chem. Int. Ed.* **2024**, *63*, *6*, e202317703.
[208] Y.-F. Li, W.-T. Gui, F. Pi, Z. Chen, L. Zhu, Q. Ouyang, W. Du, Y.-C. Chen, *Angew. Chem. Int. Ed.* **2024**, *63*, *44*, e202407682.
[209] B. Jiang, H.-T. Wang, Z.-C. Chen, W. Du, Y.-C. Chen, *ACS Catal.* **2024**, *14*, *2*, 628–636.
[210] A. Saint Pol, M. Roger, A. Mifleur, P. Loxq, L. Chausset-Boissarie, A. Béthegnies, M. Penhoat, I. Suisse, M. Sauthier, *Adv. Synth. Catal.* **2026**, *368*, *2*, e70183.
[211] S. A. Macgregor, G. W. Neave, C. Smith, *Faraday Discuss.* **2003**, *124*, *0*, 111–127.
[212] E. B. Corcoran, M. T. Pirnot, S. Lin, S. D. Dreher, D. A. DiRocco, I. W. Davies, S. L. Buchwald, D. W. C. MacMillan, *Science* **2016**, *353*, *6296*, 279–283.
[213] K. Koo, G. L. Hillhouse, *Organometallics* **1995**, *14*, *9*, 4421–4423.
[214] B. L. Lin, C. R. Clough, G. L. Hillhouse, *J. Am. Chem. Soc.* **2002**, *124*, *12*, 2890–2891.
[215] R. Sun, Y. Qin, D. G. Nocera, *Angew. Chem. Int. Ed.* **2020**, *59*, *24*, 9527–9533.
[216] C. L. L. C. Wilfred L. E Armarego, *Purification of Laboratory Chemicals, Sixth Edition*, **2009**.
[217] D. R. Lide, *CRC Handbook of Chemistry and Physics*, **2005**.
[218] L. L. Anka-Lufford, K. M. M. Huihui, N. J. Gower, L. K. G. Ackerman, D. J. Weix, *Chem. Eur. J.* **2016**, *22*, *33*, 11564–11567.
[219] A. García-Domínguez, Z. Li, C. Nevado, *J. Am. Chem. Soc.* **2017**, *139*, *20*, 6835–6838.
[220] D. J. Charboneau, N. Hazari, H. Huang, M. R. Uehling, S. L. Zultanski, *J. Org. Chem.* **2022**, *87*, *12*, 7589–7609.
[221] T. Kurokawa, M. Kim, J. Du Bois, *Angew. Chem. Int. Ed.* **2009**, *48*, *15*, 2777–2779.
[222] N. R. Babij, G. M. McKenna, R. M. Fornwald, J. P. Wolfe, *Org. Lett.* **2014**, *16*, *12*, 3412–3415.
[223] C. Li, K. Lang, H. Lu, Y. Hu, X. Cui, L. Wojtas, X. P. Zhang, *Angew. Chem. Int. Ed.* **2018**, *57*, *51*, 16837–16841.
[224] K. Kiyokawa, S. Nakamura, K. Jou, K. Iwaida, S. Minakata, *Chem. Commun.* **2019**, *55*, *78*, 11782–11785.
[225] S. Lee, D. M. Kim, J.-S. Ryu, *Adv. Synth. Catal.* **2024**, *366*, *15*, 3379–3386.
[226] C. S. Day, R. Martin, *Chem. Soc. Rev.* **2023**, *52*, *19*, 6601–6616.
[227] C.-Y. Lin, P. P. Power, *Chem. Soc. Rev.* **2017**, *46*, *17*, 5347–5399.
[228] B. R. Dible, M. S. Sigman, A. M. Arif, *Inorg. Chem.* **2005**, *44*, *11*, 3774–3776.
[229] K. Matsubara, Y. Fukahori, T. Inatomi, S. Tazaki, Y. Yamada, Y. Koga, S. Kanegawa, T. Nakamura, *Organometallics* **2016**, *35*, *19*, 3281–3287.
[230] R. J. Somerville, C. Odena, M. F. Obst, N. Hazari, K. H. Hopmann, R. Martin, *J. Am. Chem. Soc.* **2020**, *142*, *25*, 10936–10941.
[231] M. M. Schwab, D. Himmel, S. Kacprzak, D. Kratzert, V. Radtke, P. Weis, K. Ray, E.-W. Scheidt, W. Scherer, B. de Bruin, S. Weber, I. Krossing, *Angew. Chem. Int. Ed.* **2015**, *54*, *49*, 14706–14709.
[232] A. Bismuto, P. Müller, P. Finkelstein, N. Trapp, G. Jeschke, B. Morandi, *J. Am. Chem. Soc.* **2021**, *143*, *28*, 10642–10648.
[233] P. Müller, P. Finkelstein, N. Trapp, A. Bismuto, G. Jeschke, B. Morandi, *Inorg. Chem.* **2023**, *62*, *41*, 16661–16668.
[234] S. Ni, J. Yan, S. Tewari, E. J. Reijerse, T. Ritter, J. Cornella, *J. Am. Chem. Soc.* **2023**, *145*, *18*, 9988–9993.
[235] N. Eid, I. Karamé, B. Andrioletti, *Eur. J. Org. Chem.* **2018**, *2018*, *36*, 5016–5022.

[236] J. I. Bowen, L. Wang, M. P. Crump, C. L. Willis, *Org. Biom. Chem.* **2021**, *19*, *28*, 6210–6215.
[237] N. Guimond, M. J. MacDonald, V. Lemieux, A. M. Beauchemin, *J. Am. Chem. Soc.* **2012**, *134*, *40*, 16571–16577.
[238] L. Boisvert, F. Beaumier, C. Spino, *Org. Lett.* **2007**, *9*, *26*, 5361–5363.
[239] N. Aljaar, J. Conrad, U. Beifuss, *J. Org. Chem.* **2013**, *78*, *3*, 1045–1053.
[240] S. Wang, Y. Zhou, H. Huang, *Org. Lett.* **2021**, *23*, *6*, 2125–2129.
[241] D. Janssen-Müller, S. Singha, T. Olyschläger, C. G. Daniliuc, F. Glorius, *Org. Lett.* **2016**, *18*, *17*, 4444–4447.
[242] J. Jauch, *J. Prakt. Chem.* **2000**, *342*, *1*, 100–101.
[243] S. Hitosugi, D. Tanimoto, W. Nakanishi, H. Isobe, *Chem. Lett.* **2012**, *41*, 972–973.
[244] K. R. Law, C. S. P. McErlean, *Chem. Eur. J.* **2013**, *19*, *47*, 15852–15855.
[245] T. R. Hoye, C. S. Jeffrey, F. Shao, *Nat. Protocols* **2007**, *2*, *10*, 2451–2458.
[246] R. Crous, M. Datt, D. Foster, L. Bennie, C. Steenkamp, J. Huyser, L. Kirsten, G. Steyl, A. Roodt, *Dalton Trans.* **2005**, *6*, 1108–1116.
[247] J. Bruckmann, C. Kruger, *Acta Cryst. C* **1995**, *51*, *6*, 1152–1155.
[248] J. Jover, J. Cirera, *Dalton Trans.* **2019**, *48*, *40*, 15036–15048.
[249] S. Berger, S. Braun, *200 and More NMR Experiments*, **2004**, Wiley-VCH Verlag GmbH & Co. KGaA.

7 Appendix

7.1 List of Abbreviations

Å	Ångstrom, 1 Å = 10^{-10} m
Ac	acetyl
acac$^-$	acetylacetonate
AD	asymmetric dihydroxylation
Ar	aryl
ATR	attenuated total reflectance
Bn	benzyl
Boc	*tert*-butyloxycarbonyl
BPin	pinacolboronate ester
Bu	butyl
Cbz	benzyloxycarbonyl
cdt	1,5,9-cyclododecatriene
CNS	central nervous system
cod	1,5-cyclooctadiene
COSY	correlation spectroscopy
Cy	cyclohexyl
d	day(s)
DABCO	1,4-diazabicyclo[2.2.2]octane
DAST	diethylaminosulfur trifluoride
dba	dibenzylideneacetone
DBU	1,8-diazabicyclo(5.4.0)undec-7-ene
DEPT	distortionless enhancement by polarization transfer
DFT	density functional theory
DIPEA	*N*,*N*-diisopropylethylamine (Hünig's base)
DMA	*N*,*N*-dimethylacetamide

dme	1,2-dimethoxyethane
DMF	*N*,*N*-dimethylformamide
DMSO	dimethyl sulfoxide
dppe	1,2-bis(diphenylphosphino)ethane
dr	diastereomeric ratio
ee	enantiomeric excess
EI	electron ionization
equiv.	equivalents
ESI	electrospray ionization
Et	ethyl
Fc	ferrocenium
Fmoc	fluorenylmethoxycarbonyl
GC	gas chromatography
h	hour(s)
Hept	heptyl
HMBC	heteronuclear multiple bond correlation
HOMO	highest occupied molecular orbital
HPLC	high performance liquid chromatography
HRMS	high resolution mass spectrometry
HSQC	heteronuclear single quantum coherence
IR	infrared
K	Kelvin
L	ligand
LC	liquid chromatography
LED	light-emitting diode
LUMO	lowest unoccupied molecular orbital
Me	methyl
MOM	methoxymethyl

MS	mass spectrometry *or* molecular sieves (pore size given in Å)
MTBE	*tert*-butyl methyl ether
NHC	N-heterocyclic carbene
NMR	nuclear magnetic resonance
NOESY	nuclear Overhauser enhancement spectroscopy
PG	protecting group
Ph	phenyl
Phth	phthalimido
PMP	*para*-methoxy phenyl
ppm	parts per million
rac	racemic
ROESY	rotating frame Overhauser effect spectroscopy
rr	regioisomeric ratio
RT	room temperature
$^{t\text{Bu}}$stb	4,4'-di-*tert*-butylstilbene
TBAB	tetrabutylammonium bromide
TBAF	tetrabutylammonium fluoride
TBAI	tetrabutylammonium iodide
TBDPS	*tert*-butyldiphenylsilyl
TBS	*tert*-butyldimethylsilyl
TDAE	tetrakis(dimethylamino)ethylene
TES	triethylsilyl
THF	tetrahydrofuran
TIPS	triisopropylsilyl
TLC	thin layer chromatography
TOCSY	total correlation spectroscopy
Ts	tosyl
UV	ultraviolet

7.2 Overview of Tools

This thesis was independently written by the author. The language tools DeepL and ChatGPT were used to assist with language proofreading, grammar corrections, and occasional minor textual revisions.

7.3 Supporting Crystallographic Information

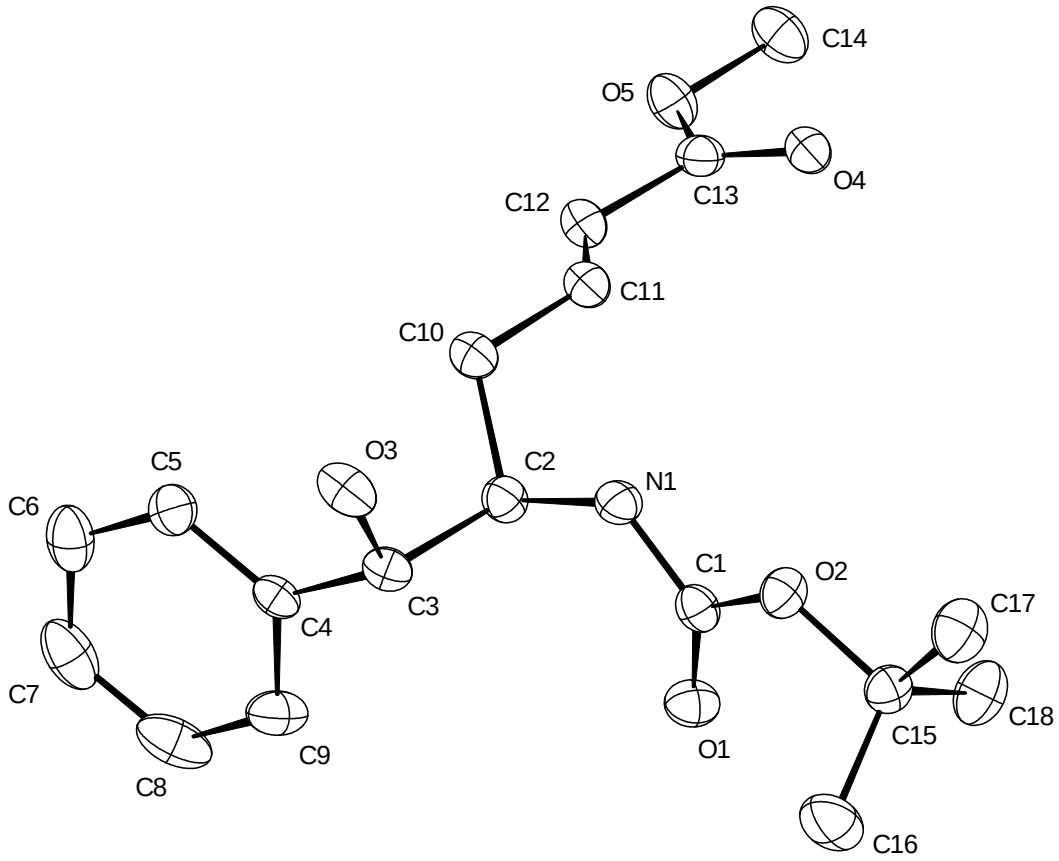

Figure S16: The structure of compound **90a** in the solid state; H-atoms omitted for clarity.

X-ray crystal structure analysis of 90a:

C_{18} H_{25} N O_5, M_r = 335.39 g · mol^{-1}, colorless prism, crystal size 0.131 x 0.066 x 0.051 mm^3, orthorhombic, space group $P2_12_12_1$[19], a = 9.0951(3) Å, b = 9.5582(3) Å, c = 18.4316(7) Å, V = 1548.82(11) Å^3, T = 100(2) K, Z = 4, D_{calc} = 1.218 g · cm^3, λ = 1.54178 Å, μ(*Cu-K*$_\alpha$) = 0.728 mm^{-1}, analytical absorption correction (T_{min} = 0.95, T_{max} = 0.98), Bruker AXS Enraf-Nonius KappaCCD diffractometer with a FR591 rotating Cu-anode X-ray source, 4.204 < θ < 71.807°, 62197 measured reflections, 3520 independent reflections, 3214 reflections with $I > 2\sigma(I)$, R_{int} = 0.0626, 222 parameters, S = 1.062, absolute structure parameter = 0.00(7), residual electron density +0.1 (0.70 Å from H1) / -0.2 e · Å^{-3} (0.78 Å from C1). The structure was solved by *SHELXT* and refined by full-matrix least-squares (*SHELXL*) against F^2 to R_1 = 0.030 [$I > 2\sigma(I)$], wR_2 = 0.072. **CCDC-2377029**

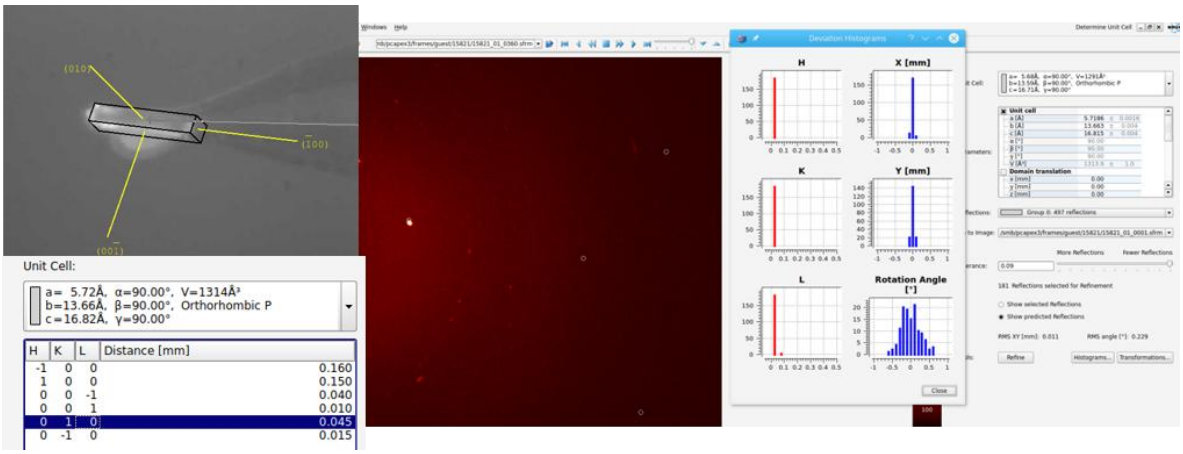

Figure S17: Crystal faces and unit cell determination/refinement of compound **90a**.

INTENSITY STATISTICS FOR DATASET # 1

Resolution	#Data	#Theory	%Complete	Redundancy	Mean I	Mean I/s	Rmerge	Rsigma
Inf - 3.29	57	57	100.0	18.49	164.00	105.36	0.0278	0.0087
3.29 - 2.22	124	124	100.0	18.13	50.84	92.96	0.0284	0.0093
2.22 - 1.77	174	174	100.0	19.90	38.69	76.0[1]	0.0367	0.0105
1.77 - 1.54	180	180	100.0	18.68	20.85	56.53	0.0458	0.0134
1.54 - 1.40	177	177	100.0	16.94	12.63	40.70	0.0632	0.0196
1.40 - 1.30	176	176	100.0	13.48	12.74	33.11	0.0666	0.0240
1.30 - 1.22	185	185	100.0	22.07	12.74	39.40	0.0728	0.0224
1.22 - 1.16	166	166	100.0	27.81	10.52	39.20	0.0854	0.0214
1.16 - 1.11	182	182	100.0	26.92	9.67	35.57	0.0897	0.0234
1.11 - 1.06	205	205	100.0	26.39	10.62	37.30	0.0867	0.0223
1.06 - 1.03	143	143	100.0	23.64	7.45	28.30	0.1124	0.0306
1.03 - 0.99	223	223	100.0	22.26	5.41	22.58	0.1341	0.0390
0.99 - 0.97	139	139	100.0	21.35	6.23	26.34	0.1046	0.0332
0.97 - 0.94	190	190	100.0	19.72	3.91	18.90	0.1507	0.0511
0.94 - 0.91	239	239	100.0	18.32	3.28	16.90	0.1699	0.0553
0.91 - 0.90	94	94	100.0	18.64	3.66	19.44	0.1378	0.0467
0.90 - 0.88	176	176	100.0	18.69	2.97	17.06	0.1846	0.0537
0.88 - 0.86	205	210	97.6	9.32	2.38	10.46	0.1998	0.0992
0.86 - 0.84	217	220	98.6	3.05	2.00	6.51	0.1633	0.1542
0.84 - 0.82	221	229	96.5	2.87	2.26	7.71	0.1367	0.1247
0.82 - 0.81	71	121	58.7	1.12	1.61	4.42	0.1979	0.2182
0.91 - 0.81	984	1050	93.7	8.06	2.44	10.58	0.1697	0.1027
Inf - 0.81	3544	3610	98.2	17.29	12.90	31.79	0.0622	0.0213

Table S6: Crystal data and structure refinement of compound **90a**.

Identification code	15500	
Empirical formula	$C_{18}H_{25}NO_5$	
Color	colorless	
Formula weight	335.39 g·mol^{-1}	
Temperature	100(2) K	
Wavelength	1.54178 Å	
Crystal system	Orthorhombic	
Space group	$P2_12_12_1$, (no. 19)	
Unit cell dimensions	a = 9.0951(3) Å	α = 90°.
	b = 9.5582(3) Å	β = 90°.
	c = 21.0340(7) Å	γ = 90°.
Volume	1828.54(10) Å^3	
Z	4	
Density (calculated)	1.218 Mg·m^{-3}	
Absorption coefficient	0.728 mm^{-1}	
F(000)	720 e	
Crystal size	0.131 x 0.066 x 0.051 mm^3	
θ range for data collection	4.204 to 71.807°.	
Index ranges	-11 ≤ h ≤ 11, -10 ≤ k ≤ 11, -25 ≤ l ≤ 25	
Reflections collected	62197	
Independent reflections	3520 [R_{int} = 0.0626]	
Reflections with I>2σ(I)	3214	
Completeness to θ = 67.679°	99.6 %	
Absorption correction	Gaussian	
Max. and min. transmission	0.98055 and 0.94823	
Refinement method	Full-matrix least-squares on F^2	
Data / restraints / parameters	3520 / 0 / 222	
Goodness-of-fit on F^2	1.062	
Final R indices [I>2σ(I)]	R_1 = 0.0300	wR^2 = 0.0706
R indices (all data)	R_1 = 0.0350	wR^2 = 0.0724
Absolute structure parameter	0.00(7)	
Extinction coefficient	n/a	
Largest diff. peak and hole	0.115 and -0.148 e·Å^{-3}	

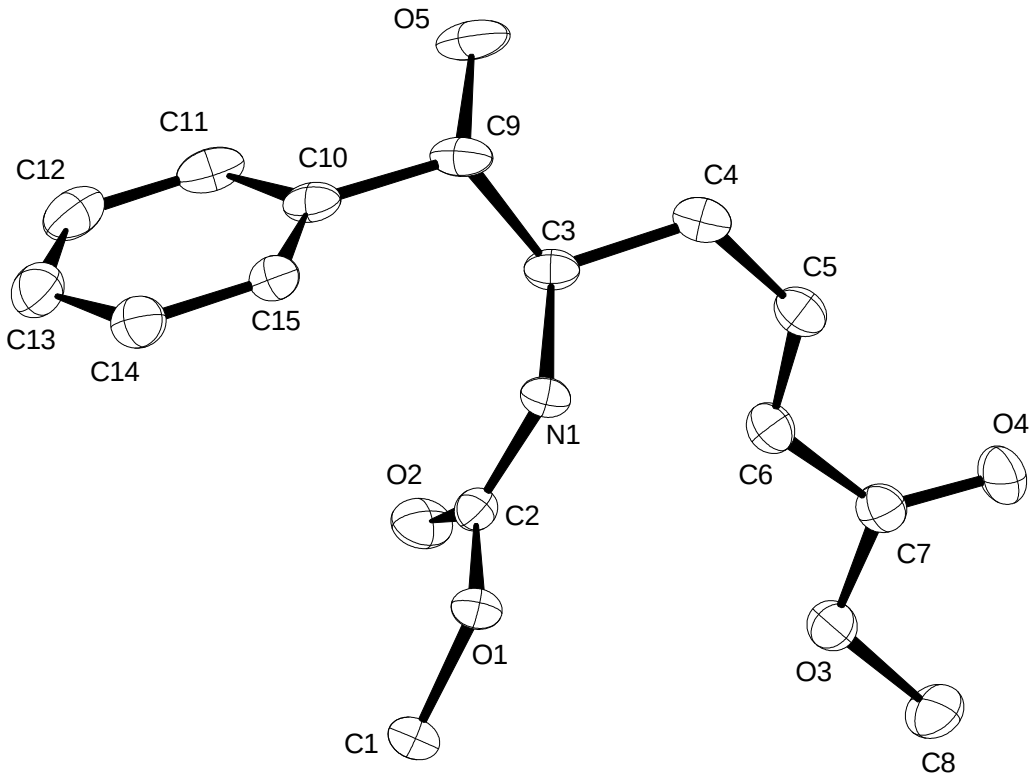

Figure S18: The structure of compound **90b** in the solid state; H-atoms omitted for clarity.

X-ray crystal structure analysis of 90b:

C_{15} H_{19} N O_5, M_r = 293.31 g · mol^{-1}, colorless prism, crystal size 0.28 x 0.24 x 0.05 mm^3, orthorhombic, space group $P2_12_12_1$[19], a = 5.0555(2) Å, b = 16.6216(7) Å, c = 21.0340(7) Å, V = 1828.54(10) Å^3, T = 100(2) K, Z = 4, D_{calc} = 1.258 g · cm^3, λ = 1.54178 Å, $\mu(Cu\text{-}K_\alpha)$ = 0.789 mm^{-1}, analytical absorption correction (T_{min} = 0.84, T_{max} = 0.96), Bruker AXS Enraf-Nonius KappaCCD diffractometer with a FR591 rotating Cu-anode X-ray source, 3.581 < θ < 71.542°, 54998 measured reflections, 2912 independent reflections, 2848 reflections with $I > 2\sigma(I)$, R_{int} = 0.0294, 213 parameters, S = 1.173, absolute structure parameter = 0.05(4), residual electron density +0.2 (2.22 Å from H1A) / -0.2 e · Å^{-3} (0.93 Å from N1). The structure was solved by *SHELXT* and refined by full-matrix least-squares (*SHELXL*) against F^2 to R_1 = 0.035 [$I > 2\sigma(I)$], wR_2 = 0.087. **CCDC-2377028**

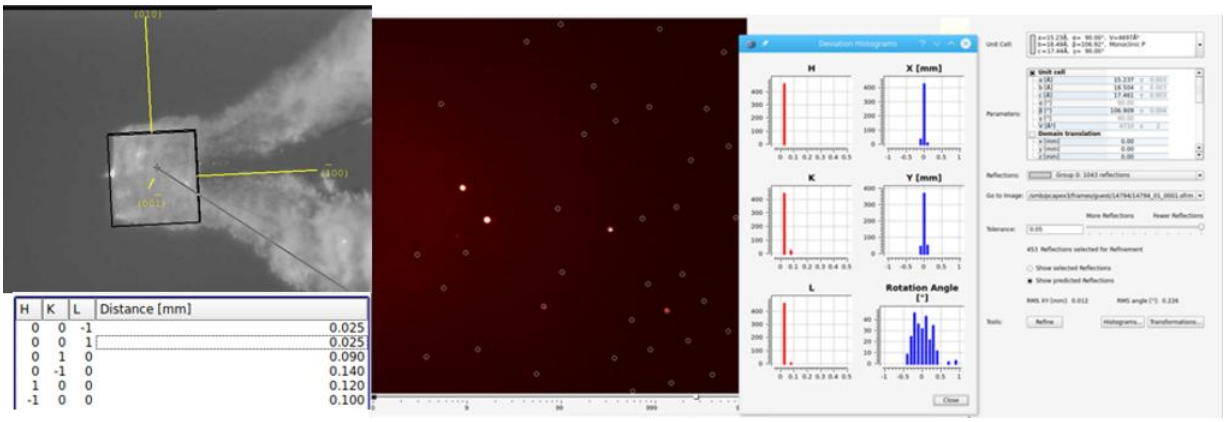

Figure S19: Crystal faces and unit cell determination/refinement of compound **90b**.

INTENSITY STATISTICS FOR DATASET # 1

Resolution	#Data	#Theory	%Complete	Redundancy	Mean I	Mean I/s	Rmerge	Rsigma
Inf - 4.05	27	27	100.0	17.22	139.86	100.07	0.0258	0.0086
4.05 - 2.46	60	60	100.0	27.00	87.95	133.13	0.0260	0.0069
2.46 - 1.90	89	89	100.0	29.25	43.25	136.23	0.0263	0.0070
1.90 - 1.63	86	86	100.0	31.99	26.51	123.94	0.0267	0.0069
1.63 - 1.47	91	91	100.0	29.57	19.19	111.92	0.0257	0.0077
1.47 - 1.35	89	89	100.0	28.81	13.17	101.98	0.0302	0.0094
1.35 - 1.26	82	85	96.5	25.33	10.69	96.37	0.0341	0.0098
1.26 - 1.19	91	95	95.8	45.48	12.55	141.74	0.0310	0.0075
1.19 - 1.14	86	86	100.0	48.05	12.57	148.68	0.0315	0.0058
1.14 - 1.09	89	89	100.0	52.19	11.52	150.77	0.0308	0.0057
1.09 - 1.05	83	83	100.0	50.59	8.52	138.84	0.0315	0.0060
1.05 - 1.01	92	93	98.9	48.67	7.39	133.44	0.0347	0.0065
1.01 - 0.97	101	125	80.8	32.82	4.74	102.61	0.0407	0.0082
0.97 - 0.95	70	70	100.0	34.20	5.92	100.31	0.0363	0.0120
0.95 - 0.92	113	113	100.0	33.81	4.82	90.26	0.0407	0.0104
0.92 - 0.90	85	85	100.0	32.36	3.74	92.02	0.0403	0.0091
0.90 - 0.88	81	81	100.0	33.59	3.27	92.07	0.0469	0.0099
0.88 - 0.86	96	96	100.0	14.78	2.67	42.78	0.0834	0.0340
0.86 - 0.84	91	95	95.8	5.80	2.60	14.00	0.1635	0.0568
0.84 - 0.83	52	62	83.9	5.32	1.45	11.81	0.1882	0.0712
0.83 - 0.81	95	116	81.9	3.62	1.82	11.37	0.2445	0.0784
0.91 - 0.81	465	500	93.0	14.19	2.55	40.79	0.0679	0.0383
Inf - 0.81	1749	1816	96.3	30.38	15.08	99.19	0.0301	0.0089

Table S7: Crystal data and structure refinement of compound **90b**.

Identification code	14794	
Empirical formula	$C_{15}H_{19}NO_5$	
Color	colorless	
Formula weight	293.31 $g \cdot mol^{-1}$	
Temperature	100(2) K	
Wavelength	1.54178 Å	
Crystal system	ORTHORHOMBIC	
Space group	**$P2_12_12_1$, (no. 19)**	
Unit cell dimensions	a = 5.0555(2) Å	α = 90°.
	b = 16.6216(7) Å	β = 90°.
	c = 18.4316(7) Å	γ = 90°.
Volume	1548.82(11) $Å^3$	
Z	4	
Density (calculated)	1.258 $Mg \cdot m^{-3}$	
Absorption coefficient	0.789 mm^{-1}	
F(000)	624 e	
Crystal size	0.28 x 0.24 x 0.05 mm^3	
θ range for data collection	3.581 to 71.542°.	
Index ranges	$-4 \le h \le 5$, $-20 \le k \le 20$, $-22 \le l \le 22$	
Reflections collected	54998	
Independent reflections	2912 [R_{int} = 0.0294]	
Reflections with I>2σ(I)	2848	
Completeness to θ = 67.679°	97.5 %	
Absorption correction	Gaussian	
Max. and min. transmission	0.96 and 0.84	
Refinement method	Full-matrix least-squares on F^2	
Data / restraints / parameters	2912 / 0 / 213	
Goodness-of-fit on F^2	1.173	
Final R indices [I>2σ(I)]	R_1 = 0.0353	wR^2 = 0.0865
R indices (all data)	R_1 = 0.0361	wR^2 = 0.0868
Absolute structure parameter	0.05(4)	
Largest diff. peak and hole	0.2 and -0.2 $e \cdot Å^{-3}$	

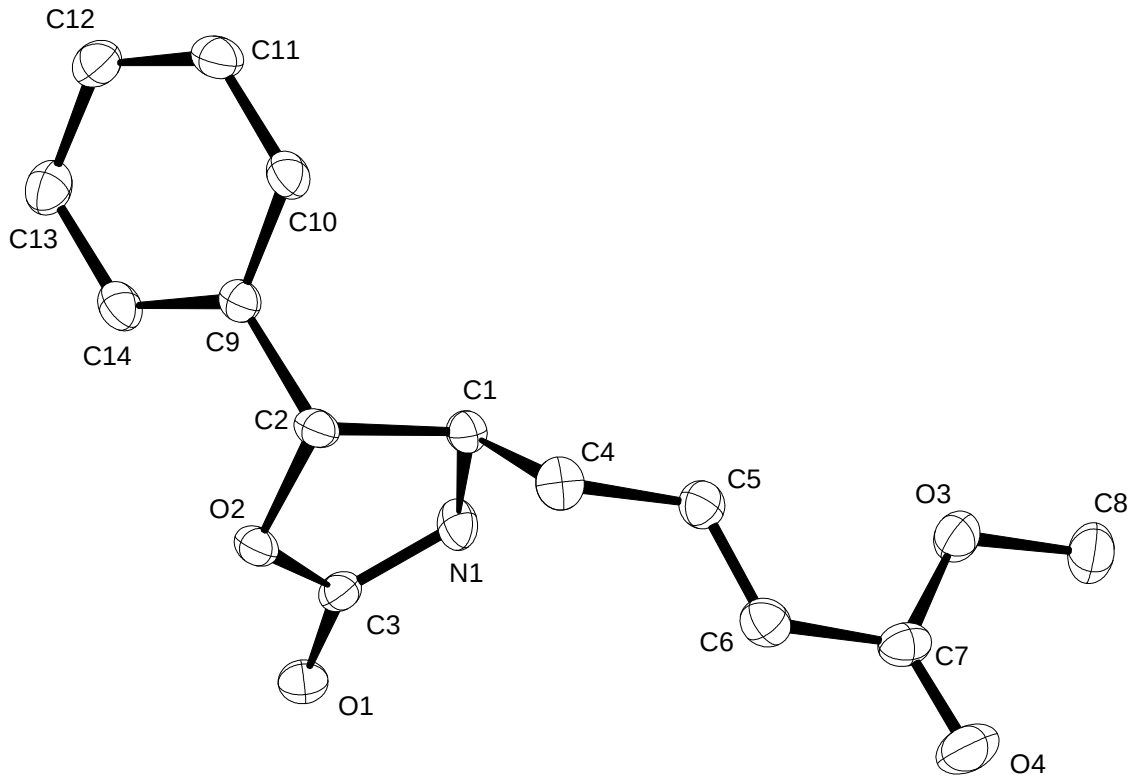

Figure S20: The structure of compound **150** in the solid state; H-atoms omitted for clarity.

X-ray crystal structure analysis of 150:

C_{14} H_{15} N O_4, M_r = 261.27 g · mol^{-1}, colorless needles, crystal size 0.401 x 0.087 x 0.07 mm^3, orthorhombic, space group $P2_12_12_1$[19], a = 5.6941(6) Å, b = 13.5841(14) Å, c = 16.7511(18) Å, V = 1295.7(2) Å^3, T = 100(2) K, Z = 4, D_{calc} = 1.339 g · cm^3, λ = 1.54178 Å, μ(Cu-K_α) = 0.820 mm^{-1}, analytical absorption correction (T_{min} = 0.82, T_{max} = 0.96), Bruker AXS Enraf-Nonius KappaCCD diffractometer with a FR591 rotating Cu-anode X-ray source, 4.190 < θ < 71.897°, 46340 measured reflections, 2506 independent reflections, 2338 reflections with $I > 2\sigma(I)$, R_{int} = 0.0494, 173 parameters, S = 1.283, absolute structure parameter = -0.18(5), residual electron density +0.2 (0.88 Å from O4) / -0.2 e · Å^{-3} (0.85 Å from C2). The structure was solved by *SHELXT* and refined by full-matrix least-squares (*SHELXL*) against F^2 to R_1 = 0.032 [$I > 2\sigma(I)$], wR_2 = 0.08. **CCDC-2377038**.

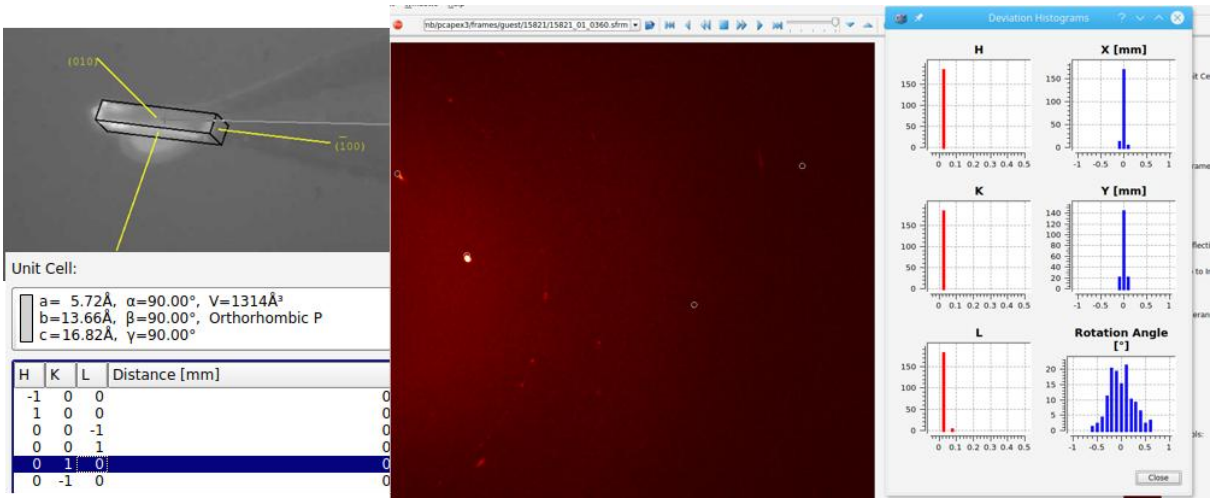

Figure S21: Crystal faces and unit cell determination/refinement of compound **150**.

INTENSITY STATISTICS FOR DATASET # 1

Resolution	#Data	#Theory	%Complete	Redundancy	Mean I	Mean I/s	Rmerge	Rsigma
Inf - 4.00	23	23	100.0	17.30	69.62	77.92	0.0302	0.0229
4.00 - 2.45	52	52	100.0	27.10	84.48	117.37	0.0317	0.0077
2.45 - 1.87	75	75	100.0	28.97	31.40	110.72	0.0305	0.0076
1.87 - 1.62	76	76	100.0	31.72	20.44	110.12	0.0324	0.0074
1.62 - 1.45	75	75	100.0	30.07	15.30	91.37	0.0327	0.0087
1.45 - 1.34	76	76	100.0	27.18	9.57	81.43	0.0356	0.0099
1.34 - 1.25	80	80	100.0	26.76	9.06	74.35	0.0525	0.0112
1.25 - 1.18	74	74	100.0	49.50	10.37	100.44	0.0574	0.0079
1.18 - 1.12	82	82	100.0	47.50	10.39	97.13	0.0529	0.0081
1.12 - 1.08	72	72	100.0	46.71	9.22	92.05	0.0603	0.0086
1.08 - 1.04	73	73	100.0	45.90	9.12	92.76	0.0587	0.0085
1.04 - 1.01	66	66	100.0	43.20	5.93	75.71	0.0733	0.0106
1.01 - 0.97	93	93	100.0	37.01	5.26	62.82	0.1094	0.0130
0.97 - 0.94	81	81	100.0	37.33	3.51	54.03	0.1063	0.0152
0.94 - 0.92	67	67	100.0	36.30	3.52	45.04	0.1029	0.0154
0.92 - 0.90	72	72	100.0	34.11	5.12	60.19	0.0854	0.0131
0.90 - 0.88	80	80	100.0	33.20	2.55	45.64	0.1384	0.0176
0.88 - 0.86	77	77	100.0	17.03	2.65	28.84	0.1518	0.0392
0.86 - 0.84	79	79	100.0	7.11	1.86	9.97	0.2613	0.1179
0.84 - 0.82	98	98	100.0	6.42	1.60	9.45	0.2248	0.1145
0.82 - 0.81	37	47	78.7	2.38	1.95	7.29	0.1877	0.2323
0.91 - 0.81	406	416	97.6	15.44	2.42	25.26	0.1307	0.0670
Inf - 0.81	1508	1518	99.3	30.70	11.94	68.15	0.0490	0.0131

Table S8: Crystal data and structure refinement of compound **150**.

Identification code	15834	
Empirical formula	$C_{14}H_{15}NO_4$	
Color	colorless	
Formula weight	261.27 $g \cdot mol^{-1}$	
Temperature	100(2) K	
Wavelength	1.54178 Å	
Crystal system	ORTHORHOMBIC	
Space group	**$P2_12_12_1$, (no. 19)**	
Unit cell dimensions	a = 5.6941(6) Å	α = 90°.
	b = 13.5841(14) Å	β = 90°.
	c = 16.7511(18) Å	γ = 90°.
Volume	1295.7(2) $Å^3$	
Z	4	
Density (calculated)	1.339 $Mg \cdot m^{-3}$	
Absorption coefficient	0.820 mm^{-1}	
F(000)	552 e	
Crystal size	0.401 x 0.087 x 0.07 mm^3	
θ range for data collection	4.190 to 71.897°.	
Index ranges	$-7 \le h \le 6$, $-16 \le k \le 16$, $-20 \le l \le 20$	
Reflections collected	46340	
Independent reflections	2506 [R_{int} = 0.0494]	
Reflections with I>2σ(I)	2338	
Completeness to θ = 67.679°	99.9 %	
Absorption correction	Gaussian	
Max. and min. transmission	0.96 and 0.82	
Refinement method	Full-matrix least-squares on F^2	
Data / restraints / parameters	2506 / 0 / 173	
Goodness-of-fit on F^2	1.109	
Final R indices [I>2σ(I)]	R_1 = 0.0316	wR^2 = 0.0747
R indices (all data)	R_1 = 0.0417	wR^2 = 0.0785
Absolute structure parameter	0.18(5)	
Largest diff. peak and hole	0.2 and -0.2 $e \cdot Å^{-3}$	

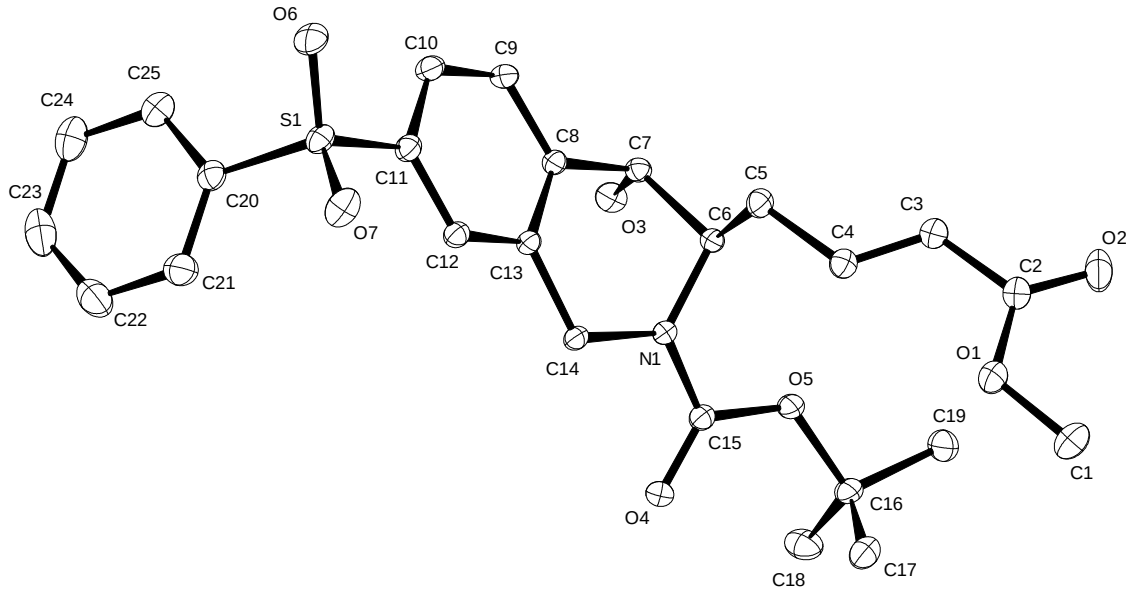

Figure S22: Structure of compound **159** in the solid state; H-atoms omitted for clarity.

X-ray crystal structure analysis of 159:

C_{25} H_{29} N O_7 S, M_r = 487.55 g·mol^{-1}, colorless plate, crystal size 0.280 x 0.063 x 0.041 mm^3, monoclinic, space group $P2_1$ [4], a = 12.9929(17) Å, b = 6.1545(6) Å, c = 15.306(2) Å, β = 94.309(5)°, V = 1220.5(3) Å^3, T = 100(2) K, Z = 2, D_{calc} = 1.327 g·cm^3, λ = 0.71073 Å, μ(*Mo-K*$_\alpha$) = 0.178 mm^{-1}, Gaussian absorption correction (T_{min} = 0.98, T_{max} = 0.99), Bruker AXS D8-Venture diffractometer with IμS Diamond Mo-anode X-ray source and PHOTON III detector, 1.984 < θ < 30.930°, 178581 measured reflections, 7694 independent reflections, 7334 reflections with $I > 2\sigma(I)$, R_{int} = 0.0684, Absolute structure parameter =-0.009(16). The structure was solved by *SHELXT* and refined by full-matrix least-squares (*SHELXL*) against F^2 to R_1 = 0.0288 [$I > 2\sigma(I)$], wR_2 = 0.0769, 323 parameters. **CCDC-2552556**

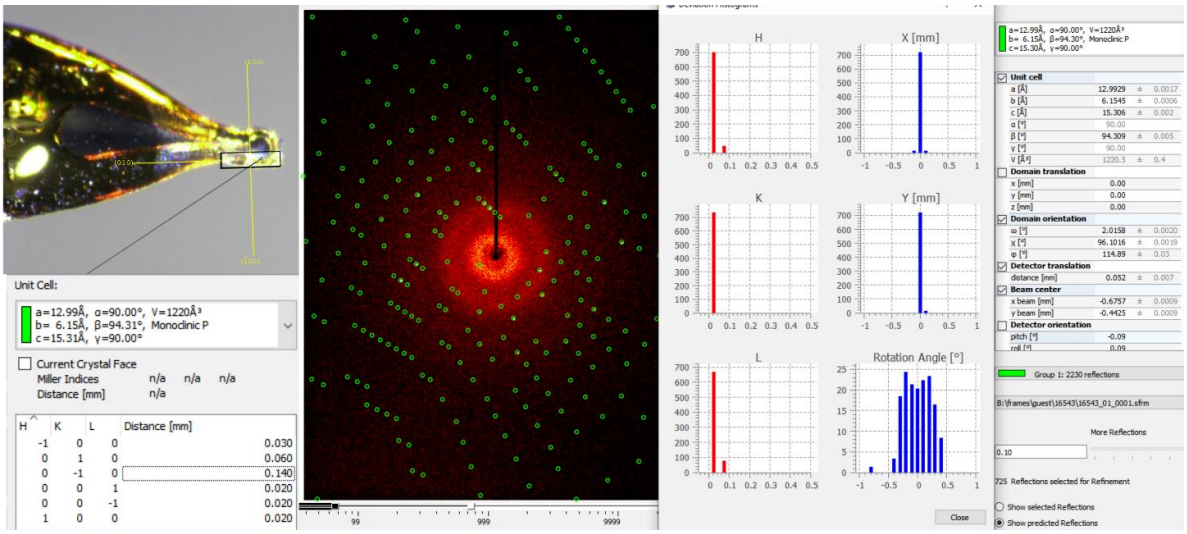

Figure S23: Crystal faces and unit cell determination/refinement of compound **159**.

INTENSITY STATISTICS FOR DATASET

Resolution	#Data	#Theory	%Complete	Redundancy	Mean I	Mean I/s	Rmerge	Rsigma
Inf - 2.63	136	143	95.1	23.28	88.05	106.90	0.0333	0.0167
2.63 - 1.77	322	322	100.0	31.31	38.40	113.94	0.0297	0.0075
1.77 - 1.41	453	453	100.0	31.76	15.90	82.20	0.0468	0.0097
1.41 - 1.23	445	445	100.0	30.29	15.72	74.37	0.0512	0.0106
1.23 - 1.12	457	457	100.0	28.83	12.95	64.61	0.0595	0.0121
1.12 - 1.03	479	479	100.0	28.88	10.43	57.89	0.0724	0.0142
1.03 - 0.97	502	502	100.0	27.70	7.17	46.09	0.0915	0.0177
0.97 - 0.93	370	370	100.0	27.21	5.75	40.16	0.1066	0.0205
0.93 - 0.88	549	549	100.0	27.53	4.52	35.03	0.1279	0.0243
0.88 - 0.85	415	415	100.0	25.69	4.19	31.80	0.1329	0.0260
0.85 - 0.82	499	499	100.0	22.94	3.76	28.43	0.1432	0.0299
0.82 - 0.79	539	539	100.0	21.45	3.28	25.56	0.1561	0.0337
0.79 - 0.77	392	392	100.0	20.32	3.04	23.42	0.1685	0.0383
0.77 - 0.75	460	460	100.0	17.90	3.04	21.95	0.1615	0.0406
0.75 - 0.73	535	535	100.0	15.44	2.96	20.06	0.1624	0.0469
0.73 - 0.72	260	260	100.0	14.06	2.60	16.93	0.1727	0.0569
0.72 - 0.70	601	604	99.5	11.24	2.49	15.35	0.1785	0.0804
0.70 - 0.69	289	299	96.7	9.22	2.63	14.66	0.1700	0.0928
0.69 - 0.67	645	739	87.3	7.59	2.07	12.75	0.1883	0.0928
0.67 - 0.66	336	378	88.9	6.67	2.23	11.97	0.1893	0.1053
0.66 - 0.65	363	484	75.0	5.29	1.68	10.06	0.2107	0.1207
0.75 - 0.65	3029	3299	91.8	9.75	2.38	14.69	0.1760	0.0804
Inf - 0.65	9047	9324	97.0	20.31	8.05	37.69	0.0695	0.0218

Table S9: Crystal data and structure refinement of compound **159**.

Identification code	16543	
Empirical formula	$C_{25}H_{29}NO_7S$	
Color	colourless	
Formula weight	487.55 $g \cdot mol^{-1}$	
Temperature	100(2) K	
Wavelength	0.71073 Å	
Crystal system	MONOCLINIC	
Space group	**$P2_1$, (no. 4)**	
Unit cell dimensions	a = 12.9929(17) Å	α = 90°.
	b = 6.1545(6) Å	β = 94.309(5)°.
	c = 15.306(2) Å	γ = 90°.
Volume	1220.5(3) $Å^3$	
Z	2	
Density (calculated)	1.327 $Mg \cdot m^{-3}$	
Absorption coefficient	0.178 mm^{-1}	
F(000)	516 e	
Crystal size	0.280 x 0.063 x 0.041 mm^3	
θ range for data collection	1.984 to 30.930°.	
Index ranges	$-18 \le h \le 18, -8 \le k \le 8, -22 \le l \le 22$	
Reflections collected	178581	
Independent reflections	7694 [R_{int} = 0.0684]	
Reflections with I>2σ(I)	7334	
Completeness to θ = 25.242°	99.8 %	
Absorption correction	Gaussian	
Max. and min. transmission	0.99 and 0.98	
Refinement method	Full-matrix least-squares on F^2	
Data / restraints / parameters	7694 / 1 / 323	
Goodness-of-fit on F^2	1.055	
Final R indices [I>2σ(I)]	R_1 = 0.0288	wR^2 = 0.0752
R indices (all data)	R_1 = 0.0315	wR^2 = 0.0769
Absolute structure parameter	-0.009(16)	
Largest diff. peak and hole	0.3 and -0.2 $e \cdot Å^{-3}$	

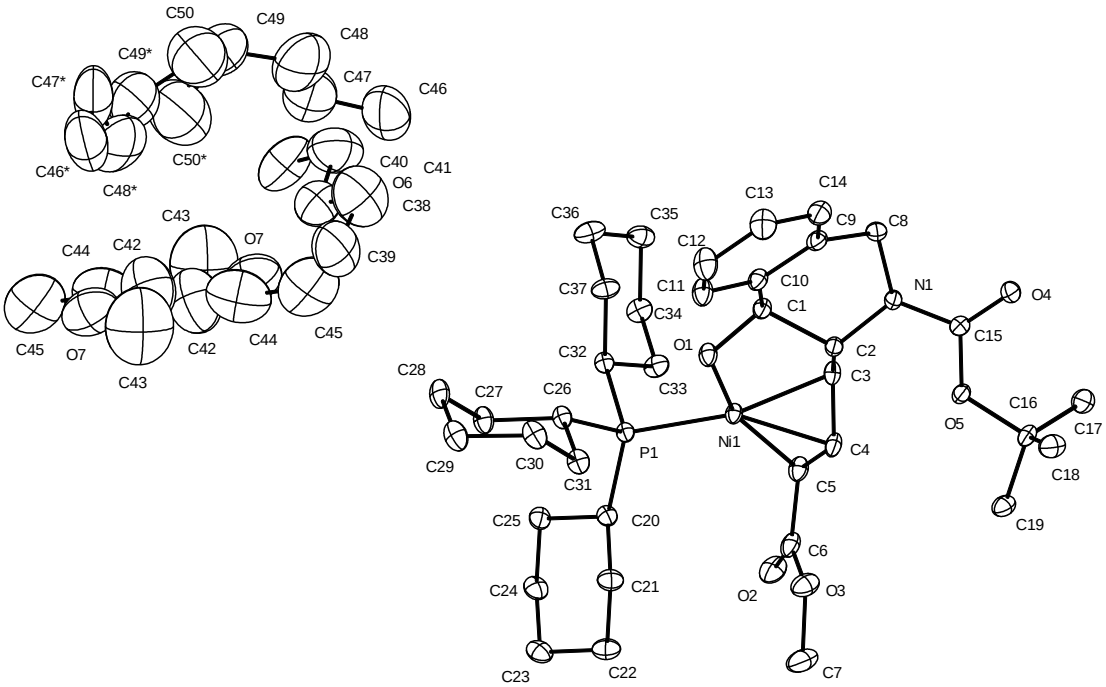

Figure S24: The asymmetric unit of complex **190**; H-atoms omitted for clarity.

X-ray crystal structure analysis of 190:

$C_{87}\ H_{144}\ N_2\ Ni_2\ O_{12}\ P_2$, M_r = 1589.39 g·mol^{-1}, orange block, crystal size 0.196 x 0.114 x 0.092 mm^3, monoclinic, space group $C2/c$ [15], a = 39.083(4) Å, b = 13.6370(12) Å, c = 18.1640(16) Å, β = 115.551(4)°, V = 8734.1(14) Å^3, T = 100(2) K, Z = 4, D_{calc} = 1.209 g·cm^3, λ = 0.71073 Å, $\mu(Mo\text{-}K_\alpha)$ = 0.526 mm^{-1}, Gaussian absorption correction (T_{min} = 0.93764, T_{max} = 0.97015), Bruker-AXS Kappa Mach3 APEX-II diffractometer with IμS Mo-anode X-ray source, 1.155 < θ < 33.142°, 159662 measured reflections, 16630 independent reflections, 11645 reflections with $I > 2\sigma(I)$, R_{int} = 0.0797. The structure was solved by *SHELXT* and refined by full-matrix least-squares (*SHELXL*) against F^2 to R_1 = 0.0463 [$I > 2\sigma(I)$], wR_2 = 0.1279, 564 parameters. **CCDC-2552555**

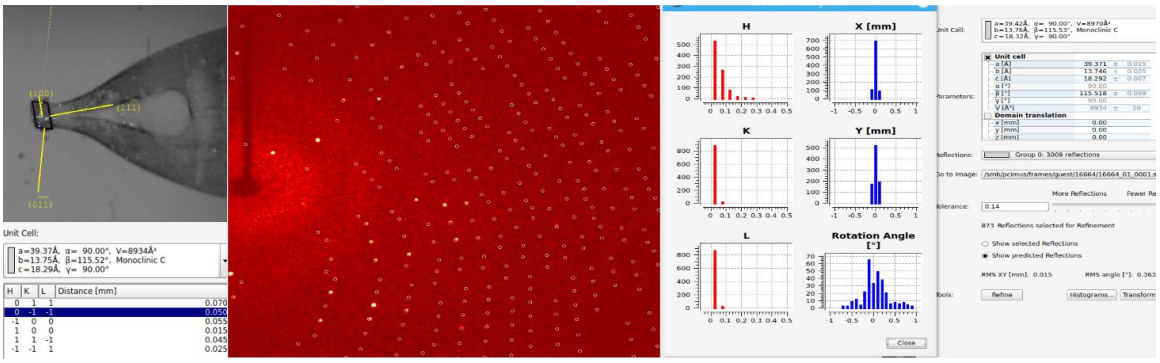

Figure S25: Crystal faces and unit cell determination/refinement of complex **190**.

INTENSITY STATISTICS FOR DATASET

Resolution	#Data	#Theory	%Complete	Redundancy	Mean I	Mean I/s	Rmerge	Rsigma
Inf - 2.61	292	292	100.0	16.81	84.59	69.61	0.0257	0.0093
2.61 - 1.72	685	685	100.0	18.07	43.43	59.51	0.0334	0.0110
1.72 - 1.36	973	973	100.0	18.23	26.63	47.84	0.0472	0.0143
1.36 - 1.18	1020	1020	100.0	17.77	18.15	34.49	0.0628	0.0189
1.18 - 1.07	990	990	100.0	15.32	14.50	27.19	0.0782	0.0259
1.07 - 0.99	1013	1013	100.0	11.27	11.14	18.30	0.0999	0.0397
0.99 - 0.93	1015	1015	100.0	9.38	9.56	14.61	0.1182	0.0518
0.93 - 0.89	824	824	100.0	8.16	8.31	11.53	0.1325	0.0646
0.89 - 0.85	985	985	100.0	7.70	6.95	9.57	0.1577	0.0796
0.85 - 0.81	1190	1190	100.0	7.31	6.06	8.07	0.1807	0.0957
0.81 - 0.78	1074	1074	100.0	6.99	5.41	6.82	0.2053	0.1130
0.78 - 0.76	773	773	100.0	6.72	4.55	5.59	0.2358	0.1375
0.76 - 0.74	922	922	100.0	6.57	4.15	5.25	0.2630	0.1564
0.74 - 0.72	981	983	99.8	6.27	3.63	4.37	0.2965	0.1860
0.72 - 0.70	1112	1112	100.0	6.12	3.35	4.04	0.3149	0.2119
0.70 - 0.68	1245	1248	99.8	5.84	3.22	3.64	0.3412	0.2360
0.68 - 0.67	670	672	99.7	5.66	2.90	3.22	0.3624	0.2734
0.67 - 0.65	1461	1467	99.6	5.49	2.76	2.96	0.3936	0.3001
0.65 - 0.64	821	826	99.4	5.32	2.24	2.36	0.4468	0.3847
0.64 - 0.63	846	853	99.2	5.21	2.11	2.12	0.4761	0.4209
0.63 - 0.62	532	609	87.4	3.22	1.92	1.54	0.4946	0.6315
0.72 - 0.62	6687	6787	98.5	5.42	2.75	3.00	0.3786	0.3041
Inf - 0.62	19424	19526	99.5	8.91	9.79	14.03	0.0800	0.0645

Table S10: Crystal data and structure refinement of complex **190**.

Empirical formula	$C_{87}H_{144}N_2Ni_2O_{12}P_2$	
Color	orange	
Formula weight	1589.39 g·mol^{-1}	
Temperature	100(2) K	
Wavelength	0.71073 Å	
Crystal system	Monoclinic	
Space group	$C2/c$, (no. 15)	
Unit cell dimensions	a = 39.083(4) Å	α = 90°
	b = 13.6370(12) Å	β = 115.551(4)°
	c = 18.1640(16) Å	γ = 90°
Volume	8734.1(14) Å^3	
Z	4	
Density (calculated)	1.209 Mg·m^{-3}	
Absorption coefficient	0.526 mm^{-1}	
F(000)	3448 e	
Crystal size	0.196 x 0.114 x 0.092 mm^3	
θ range for data collection	1.155 to 33.142°.	
Index ranges	-59 ≤ h ≤ 60, -20 ≤ k ≤ 20, -27 ≤ l ≤ 27	
Reflections collected	159662	
Independent reflections	16630 [R_{int} = 0.0797]	
Reflections with I>2σ(I)	11645	
Completeness to θ = 25.242°	100.0 %	
Absorption correction	Gaussian	
Max. and min. transmission	0.97015 and 0.93764	
Refinement method	Full-matrix least-squares on F^2	
Data / restraints / parameters	16630 / 259 / 564	
Goodness-of-fit on F^2	1.045	
Final R indices [I>2σ(I)]	R_1 = 0.0463	wR^2 = 0.1125
R indices (all data)	R_1 = 0.0811	wR^2 = 0.1279
Largest diff. peak and hole	0.711 and -0.575 e·Å^{-3}	

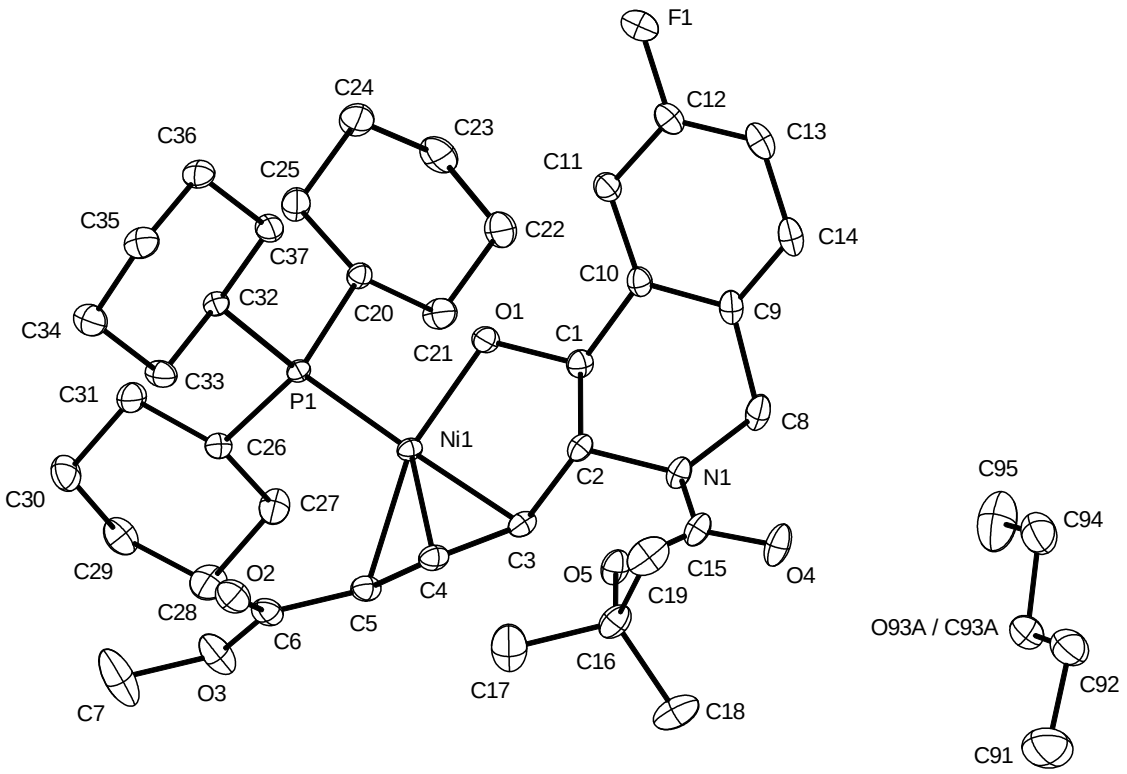

Figure S26: The asymmetric unit of complex **187**; H-atoms omitted for clarity.

X-ray crystal structure analysis of 187:

$C_{41.36}$ $H_{65.72}$ F N Ni $O_{5.64}$ P, M_r = 775.932 g·mol^{-1}, orange prism, crystal size 0.226 x 0.191 x 0.103 mm^3, triclinic, space group *P*-1 [2], a = 10.4154(7) Å, b = 11.7385(8) Å, c = 17.3245(11) Å, α = 96.390(2)°, β = 99.258(2)°, γ = 95.742(3)°, V = 2062.5(2) Å^3, T = 100(2) K, Z = 2, D_{calc} = 1.249 g·cm^3, λ = 0.71073 Å, μ(*Mo-K*$_\alpha$) = 0.558 mm^{-1}, Gaussian absorption correction ($T_{\min}$ = 0.91542, $T_{\max}$ = 0.95970), Bruker-AXS Kappa Mach3 APEX-II diffractometer with IμS Mo-anode X-ray source, 1.20 < θ < 34.91°, 81912 measured reflections, 17697 independent reflections, 14482 reflections with $I > 2\sigma(I)$, R_{int} = 0.0353. The structure was solved by *SHELXT* and refined by full-matrix least-squares (*SHELXL*). The final structure refinement was performed by olex2.refine 1.5 (L-M) together with NoSpherA2 (atomic form factors) against F^2 to R_1 = 0.0267 [$I > 2\sigma(I)$], wR_2 = 0.0529, 679 parameters. **CCDC-2552554**

The final structure refinement was carried out using aspherical scattering factors with NoSpherA2. NoSpherA2 implementation of Hirshfeld Atom Refinement (HAR) makes use of tailor-made aspherical atomic form factors calculated on-the-fly from a Hirshfeld-partitioned electron density (ED) - not from spherical-atom form factors. The ED is calculated from a Gaussian basis set single determinant SCF wave function for a fragment of the crystal. This fragment can be embedded in an electrostatic crystal field by employing cluster charges or modelled using implicit solvation models, depending on the software used. The following options were chosen:

SOFTWARE: ORCA 6.0; PARTITIONING: NoSpherA2; INT ACCURACY: Normal; METHOD: PBE; BASIS SET: def2-TZVPP; CHARGE: 0; MULTIPLICITY: 1.

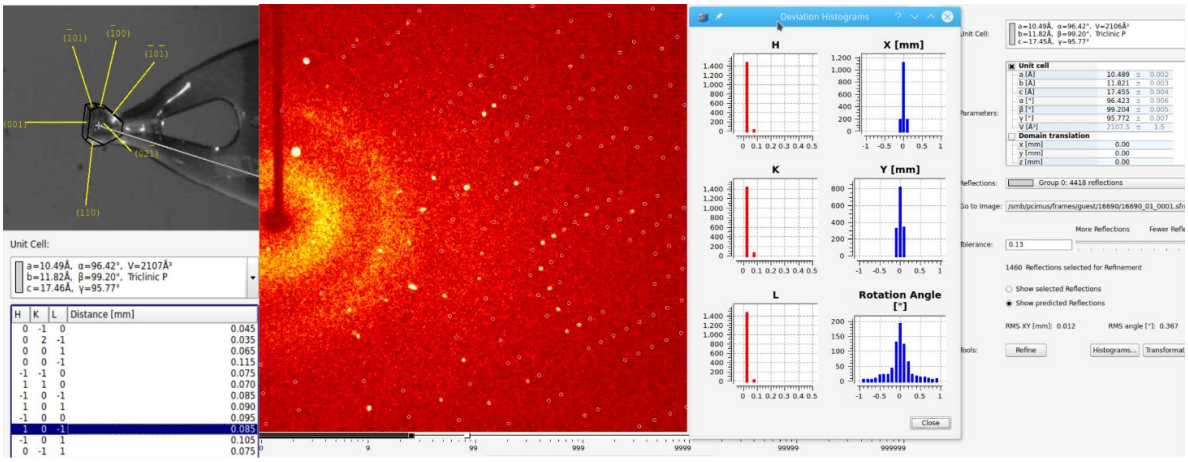

Figure S27: Crystal faces and unit cell determination/refinement of complex **187**.

INTENSITY STATISTICS FOR DATASET

Resolution	#Data	#Theory	%Complete	Redundancy	Mean I	Mean I/s	Rmerge	Rsigma
Inf - 2.54	266	266	100.0	9.41	55.69	78.53	0.0210	0.0104
2.54 - 1.69	620	620	100.0	9.59	27.85	69.83	0.0232	0.0109
1.69 - 1.34	904	904	100.0	9.52	16.45	59.34	0.0251	0.0123
1.34 - 1.17	894	894	100.0	9.20	11.54	48.71	0.0302	0.0145
1.17 - 1.06	944	944	100.0	7.69	8.98	38.47	0.0360	0.0184
1.06 - 0.99	818	818	100.0	5.78	6.73	28.49	0.0432	0.0251
0.99 - 0.93	926	926	100.0	4.78	6.34	25.03	0.0467	0.0293
0.93 - 0.88	967	967	100.0	4.22	5.13	20.61	0.0487	0.0361
0.88 - 0.84	960	960	100.0	3.84	4.10	16.65	0.0600	0.0443
0.84 - 0.81	831	831	100.0	3.80	3.98	15.79	0.0598	0.0477
0.81 - 0.78	963	963	100.0	3.57	3.32	13.36	0.0685	0.0574
0.78 - 0.76	753	753	100.0	3.47	2.96	11.90	0.0754	0.0641
0.76 - 0.74	813	815	99.8	3.38	2.67	10.70	0.0827	0.0722
0.74 - 0.72	920	922	99.8	3.20	2.54	9.66	0.0855	0.0801
0.72 - 0.70	1013	1020	99.3	3.12	2.27	8.97	0.0966	0.0884
0.70 - 0.68	1137	1148	99.0	2.97	2.18	8.06	0.1070	0.0989
0.68 - 0.67	621	625	99.4	2.92	2.16	7.77	0.1069	0.1026
0.67 - 0.65	1302	1327	98.1	2.82	1.87	6.83	0.1259	0.1189
0.65 - 0.64	751	764	98.3	2.61	1.72	5.97	0.1278	0.1387
0.64 - 0.63	812	833	97.5	2.65	1.45	5.45	0.1519	0.1556
0.63 - 0.62	482	716	67.3	1.63	1.28	4.58	0.1626	0.1842
0.72 - 0.62	6118	6433	95.1	2.73	1.90	7.04	0.1169	0.1161
Inf - 0.62	17697	18016	98.2	4.55	6.27	21.23	0.0350	0.0331

Table S11: Crystal data and structure refinement of complex **187**.

Empirical formula	$C_{41.36}H_{65.72}FNNiO_{5.64}P$	
Color	orange	
Formula weight	775.932 $g \cdot mol^{-1}$	
Temperature	100(2) K	
Wavelength	0.71073 Å	
Crystal system	Triclinic	
Space group	*P*-1, (no. 2)	
Unit cell dimensions	a = 10.4154(7) Å	α = 96.390(2)°.
	b = 11.7385(8) Å	β = 99.258(2)°.
	c = 17.3245(11) Å	γ = 95.742(3)°.
Volume	2062.5(2) $Å^3$	
Z	2	
Density (calculated)	1.249 $Mg \cdot m^{-3}$	
Absorption coefficient	0.558 mm^{-1}	
F(000)	837.430 e	
Crystal size	0.226 x 0.191 x 0.103 mm^3	
θ range for data collection	1.20 to 34.91°.	
Index ranges	$-16 \le h \le 16, -18 \le k \le 18, -27 \le l \le 27$	
Reflections collected	81912	
Independent reflections	17697 [R_{int} = 0.0353]	
Reflections with I>2σ(I)	14482	
Completeness to θ = 25.2417°	100.00 %	
Absorption correction	Gaussian	
Max. and min. transmission	0.95970 and 0.91542	
Refinement method	Full-matrix least-squares on F^2	
Data / restraints / parameters	17697 / 0 / 679	
Goodness-of-fit on F^2	1.0216	
Final R indices [I>2σ(I)]	R_1 = 0.0267	wR^2 = 0.0494
R indices (all data)	R_1 = 0.0400	wR^2 = 0.0529
Largest diff. peak and hole	0.4022 and -0.3483 $e \cdot Å^{-3}$	